NASA LaRC Workshop on Guidance, Navigation, Controls, and Dynamics for Atmospheric Flight 1993

Carey S. Buttrill, *Editor*
NASA Langley Research Center
Hampton, Virginia

Proceedings of a workshop sponsored by the
Aircraft Working Group of the NASA LaRC Guidance,
Navigation, and Control Technical Committee and held at
NASA Langley Research Center
March 18–19, 1993

(NASA-CP-10127) NASA LARC WORKSHOP
ON GUIDANCE, NAVIGATION, CONTROLS,
AND DYNAMICS FOR ATMOSPHERIC
FLIGHT, 1993 (NASA) 565 p

N94-25096
--THRU--
N94-25115
Unclas

DECEMBER 1993

G3/01   0206574

JASA

National Aeronautics and
Space Administration

Langley Research Center
Hampton, Virginia 23681-0001

PREFACE

A Guidance, Navigation, Controls, and Dynamics for Atmospheric Flight Workshop was held at the NASA Langley Research Center on March 18-19, 1993. The workshop was sponsored and co-chaired by the members of the Aircraft Working Group of the Langley Guidance, Navigation, and Controls Technical Committee. The objectives of the workshop were to discuss the status of current research in this area at Langley Research Center, create an awareness of work going on over a broad cross-spectrum of research branches, and to provide a forum for researchers to express ideas on where future research should be directed. To meet these objectives, over 30 presentations were made, largely describing LaRC research.

The workshop was organized in 8 sessions as follows:

- Overviews
- General
- Controls
- Military Aircraft
- Dynamics
- Guidance
- Systems
- Panel Discussion

A highlight of the workshop was the panel discussion which addressed the following issue: "Direction of Guidance, Navigation and Controls research to insure U.S. competitiveness and leadership in aerospace technologies." The panel consisted of Dave Leggett of Wright Labs, Clint Browning of Honeywell, Tom Richardson of Boeing, and John Hodgkinson of McDonnell Douglas. In addition to the panelists, visitors from Calspan, Honeywell, and Martin Marietta were present. The outside interest to what was intended to be an in-house, informal workshop, was significant.

The workshop was designed to be an informal exchange of ideas and an update on current research endeavors, therefore no formal written papers were required. The proceedings are a compilation of the materials used by the workshop presenters for their presentations. Appreciation is expressed to those presenters who provided formal papers or facing page text to accompany the slides in this volume. A list of attendees is included in this document.

The Guidance, Navigation and Controls Technical Committee Aircraft Working Group:

Jay Brandon
Carey Buttrill
Vivek Mukhopadhyay
Dan Moerder
Howard Stone

CONTENTS

Session 1: Overviews
Chair: Carey Buttrill

Session 2: General
Chair: Jay Brandon

Session 3: Controls
Chair: Dr. Vivek Mukhopadhyay

iii

Session 4: Military Aircraft
Chair: Jay Brandon

Session 5: Dynamics
Chair: Carey Buttrill

Session 6: Guidance
Chair: Dr. Dan Moerder

Session 7: Systems
Chair: Howard Stone

Session 8: Panel Discussion
Moderator: Howard Stone

ATTENDEES

Lt. Richard Adams
WL/FIGC
WPAFB, OH 45433

Mr. William Adams Jr.
NASA/Langley Research Ctr
MS 489
Hampton, VA 23681-0001

Mr. Phillip. C. Arcara, Jr.
NASA/Langley Research Ctr
MS 412
Hampton, VA 23681-0001

Dr. Ernest Armstrong
NASA/Langley Research Ctr
MS 230
Hampton, VA 23681-0001

Mr. Melvin L. Bailey
Lockheed Engineering &
Sciences Co.
NASA/Langley Research Ctr
MS 489
Hampton, VA 23681-0001

Mr. Randall Bailey
Calspan Corp / Flight
Research Dept.
P. O. Box 400
Buffalo, NY 14225

Mr. Daniel G. Baize
NASA/Langley Research Ctr
MS 412
Hampton, VA 23681-0001

Mr. John D. W. Barrick
NASA/Langley Research Ctr
MS 483
Hampton, VA 23681-0001

Mr. James G. Batterson
NASA/Langley Research Ctr
MS 161
Hampton, VA 23681-0001

Mr. Salvatore J. Bavuso
NASA/Langley Research Ctr
MS 478
Hampton, VA 23681-0001

Mr. Fred L. Beissner, Jr.
Lockheed Engineering &
Sciences Co.
MS 489
Hampton, VA 23666

Ms. Celeste Belcastro
NASA/Langley Research Ctr
MS 130
Hampton, VA 23681-0001

Ms. Christine Belcastro
NASA/Langley Research Ctr
MS 489
Hampton, VA 23681-0001

Mr. Robert R. Bless, Jr.
NASA/Langley Research Ctr
MS 161
Hampton, VA 23681-0001

Mr. Jay Brandon
NASA/Langley Research Ctr
MS 355
Hampton, VA 23681-0001

Mr. Clint Browning
Honeywell
3350 US HWY 19 N
Clearwater, FL

Mr. Carey Buttrill
NASA/Langley Research Ctr
MS 489
Hampton, VA 23681-0001

Ms. Susan Carzoo
Unisys Corp.
NASA/Langley Research Ctr
MS 169
Hampton, VA 23681-0001

Mr. Phil Chandler
WL/FIGD
WPAFB, OH 45433

Mr. David Christhilf
Lockheed Engineering &
Sciences Co.
NASA/Langley Research Ctr
MS 489
Hampton, VA 23681-0001

Mr. Peter G. Coen
NASA/Langley Research Ctr
MS 412
Hampton, VA 23681-0001

Ms. Lucille H. Crittenden
Research Triangle Institute
NASA/Langley Research Ctr
MS 490
Hampton, VA 23681-0001

Mr. Kevin Cunningham
Unisys Corp.
NASA/Langley Research Ctr
MS 169
Hampton, VA 23681-0001

Mr. Jonathan D'Cruz
NASA/Langley Research Ctr
MS 243
Hampton, VA 23681-0001

Mr. Vic Delnore
NASA/Langley Research Ctr
MS 490
Hampton, VA 23681-0001

Mr. S. Derry
NASA/Langley Research Ctr
MS 125B
Hampton, VA 23681-0001

Mr. Ed Dickes
NASA/Langley Research Ctr
MS 343
Hampton, VA 23681-0001

Mr. Kevin Dutton
NASA/Langley Research Ctr
MS 161
Hampton, VA 23681-0001

Mr. Carl Elks
NASA/Langley Research Ctr
MS 130
Hampton, VA 23681-0001

Mr. Jerry Elliott
NASA/Langley Research Ctr
MS 489
Hampton, VA 23681-0001

vii

Mr. Walt Engelund
NASA/Langley Research Ctr
MS 365
Hampton, VA 23681-0001

Mr. Bob Fairbairn
NASA/Langley Research Ctr
MS 356
Hampton, VA 23681-0001

Mr. John Feather
McDonnell Douglas
3855 Lakewood Blvd
Long Beach, CA 90846

Ms. Lynda Foernsler
NASA/Langley Research Ctr
MS 161
Hampton, VA 23681-0001

Mr. Mike Fox
NASA/Langley Research Ctr
MS 413
Hampton, VA 23681-0001

Mr. H. D. Garner
NASA/Langley Research Ctr
MS 470
Hampton, VA 23681-0001

Dr. Dan Giesy
Lockheed
MS 230
Hampton, VA 23681-0001

Mr. Oscar Gonzolez
NASA/Langley Research Ctr
MS 230
Hampton, VA 23681-0001

Mr. Ken Goodrich
NASA/Langley Research Ctr
MS 489
Hampton, VA 23681-0001

Ms. Irene Gregory
NASA/Langley Research Ctr
MS 489
Hampton, VA 23681-0001

Mr. Todd Hodges
NASA/Langley Research Ctr
MS 286
Hampton, VA 23681-0001

Mr. John Hodgkinson
McDonnell Douglas
3855 Lakewood Blvd
Long Beach, CA 90846

Ms. Mary Jo Hoffman
Honeywell
Systems & Research Ctr
3660 Technology Drive
Mpls, MN 55418

Dr. Bruce Holmes
NASA/Langley Research Ctr
MS 116
Hampton, VA 23681-0001

Mr. Warren Hoskins
LMSC
MS 297
Hampton, VA 23681-0001

Capt. Jim Hubert
AF Liaison
MS 221
Hampton, VA 23681-0001

Mr. George Hunt
NASA/Langley Research Ctr
MS 169
Hampton, VA 23681-0001

Mr. Bruce Jackson
NASA/Langley Research Ctr
MS 489
Hampton, VA 23681-0001

Mr. Mahesh Jeerage
Honeywell, Inc.
Systems & Research Ctr
3660 Technology Drive
Mpls, MN 55418

Mr. Eric Johnson
NASA/Langley Research Ctr
MS 489
Hampton, VA 23681-0001

Mr. Richard P. Joques
Martin Maretta
2101 Executive Drive
Tower Box 81
Hampton, VA 23666

Mr. Jacob Kay
BIHRIZ Applied Research

Dr. V. Klein
NASA/Langley Research Ctr
MS 489
Hampton, VA 23681-0001

Mr. Alex Kokolios
NASA/Langley Research Ctr
MS 489
Hampton, VA 23681-0001

Mr. Renjith Kumar
NASA/Langley Research Ctr
MS 288
Hampton, VA 23681-0001

Mr. Ralph E. Lambert
McDonnell Douglas
Aerospace
P. O. Box 516
MC 034-1300
St. Louis, MO 63166

Mr. David Larrelli
NASA/Langley Research Ctr
MS 471
Hampton, VA 23681-0001

Mr. Dave Leggett
Wright Lab/WL/FIGC
Wright Patterson AFB 45433

Mr. Richard Leslie
NASA/Langley Research Ctr
MS 169
Hampton, VA 23681-0001

Mr. Kyong Lim
NASA/Langley Research Ctr
MS 161
Hampton, VA 23681-0001

Mr. M. J. Logan
NASA/Langley Research Ctr
MS 412
Hampton, VA 23681-0001

Mr. Zoran Martinovic
AMA
MS 288
Hampton, VA 23681-0001

Mr. Marcus McElry
NASA/Langley Research Ctr
MS 412
Hampton, VA 23681-0001

Mr. J. Dana McMinn
NASA/Langley Research Ctr
MS 489
Hampton, VA 23681-0001

Mr. Mike Messina
NASA/Langley Research Ctr
MS 489
Hampton, VA 23681-0001

Mr. David Middleton
NASA/Langley Research Ctr
MS 489
Hampton, VA 23681-0001

Dr. Dan Moerder
NASA/Langley Research Ctr
MS 161
Hampton, VA 23681-0001

Dr. Ray Montgomery
NASA/Langley Research Ctr
MS 161
Hampton, VA 23681-0001

Dr. Gene Morelli
NASA/Langley Research Ctr
MS 489
Hampton, VA 23681-0001

Mr. Fred Morrell
NASA/Langley Research Ctr
MS 489
Hampton, VA 23681-0001

Mr. Jack Morris
NASA/Langley Research Ctr
MS 406
Hampton, VA 23681-0001

Dr. Vivik Mukhopadhyay
NASA/Langley Research Ctr
MS 243
Hampton, VA 23681-0001

Mr. Keith Noderer
NASA/Langley Research Ctr
MS 489
Hampton, VA 23681-0001

Ms. Marilyn Ogburn
NASA/Langley Research Ctr
MS 355
Hampton, VA 23681-0001

Mr. Aaron J. Ostroff
NASA/Langley Research Ctr
MS 489
Hampton, VA 23681-0001

Mr. Bruce Outlaw
NASA/Langley Research Ctr
MS 256
Hampton, VA 23681-0001

Dr. Bandu Pamadi
Vigyan, Inc.
MS 161
Hampton, VA 23681-0001

Mr. Lee Person
NASA/Langley Research Ctr
MS 255A
Hampton, VA 23681-0001

Mr. W. H. Phillips
NASA/Langley Research Ctr
MS 489
Hampton, VA 23681-0001

Ms. Jennifer Pinkeron
NASA/Langley Research Ctr
MS 412
Hampton, VA 23681-0001

Mr. Felix Pitts
NASA/Langley Research Ctr
MS 130
Hampton, VA 23681-0001

Mr. Tony Pototzky
NASA/Langley Research Ctr
MS 905
Hampton, VA 23681-0001

Dr. Doug Price
NASA/Langley Research Ctr
MS 161
Hampton, VA 23681-0001

Mr. W. A. Ragsdale
Unisys
MS 169
Hampton, VA 23681-0001

Mr. Dave Raney
NASA/Langley Research Ctr
MS 489
Hampton, VA 23681-0001

Dr. D. M. Rao
Vigyan, Inc.
MS 912
Hampton, VA 23681-0001

Mr. Tom Richardson
Boeing
P. O. Box 3707
M/S 4C-70
Seattle, WA 98124-2207

Dr. John Ritter
NASA/Langley Research Ctr
MS 483
Hampton, VA 23681-0001

Mr. Rob Rivers
NASA/Langley Research Ctr
MS 255A
Hampton, VA 23681-0001

Mr. Hans Seywald
AMA
MS 161
Hampton, VA 23681-0001

Mr. Gautam Sharma
Vigyan, Inc.
MS 912
30 Research Drive
Hampton, VA 23666

Dr. John Shaughnessy
NASA/Langley Research Ctr
MS 489
Hampton, VA 23681-0001

Mr. Floyd Shipman
NASA/Langley Research Ctr
MS 478
Hampton, VA 23681-0001

Mr. Walter Silva
NASA/Langley Research Ctr
MS 173
Hampton, VA 23681-0001

U.S. GENERAL AVIATION:
THE INGREDIENTS FOR A RENAISSANCE

A Vision and Technology Strategy

for

U.S. Industry
NASA
FAA
Universities

January, 1993

U.S. GENERAL AVIATION:
THE INGREDIENTS FOR A RENAISSANCE

A Vision and Technology Strategy

for

U.S. Industry
NASA
FAA
Universities

January, 1993

Title

- In the Nation today, General Aviation
  - Is a **vital** component in the nation's air transportation system
  - Is **threatened** for survival
  - Has enormous **potential** for expansion in utility and use

- This potential for expansion is fueled by **new** satellite navigation and communication, small computers, flat panel displays, and **advanced** aerodynamics, materials and manufacturing methods, and propulsion technologies which create opportunities for new levels of environmental and economic acceptability.

- Expanded general aviation utility and use could have a large **impact** on the nation's jobs, commerce, industry, airspace capacity, trade balance, and quality of life.

3
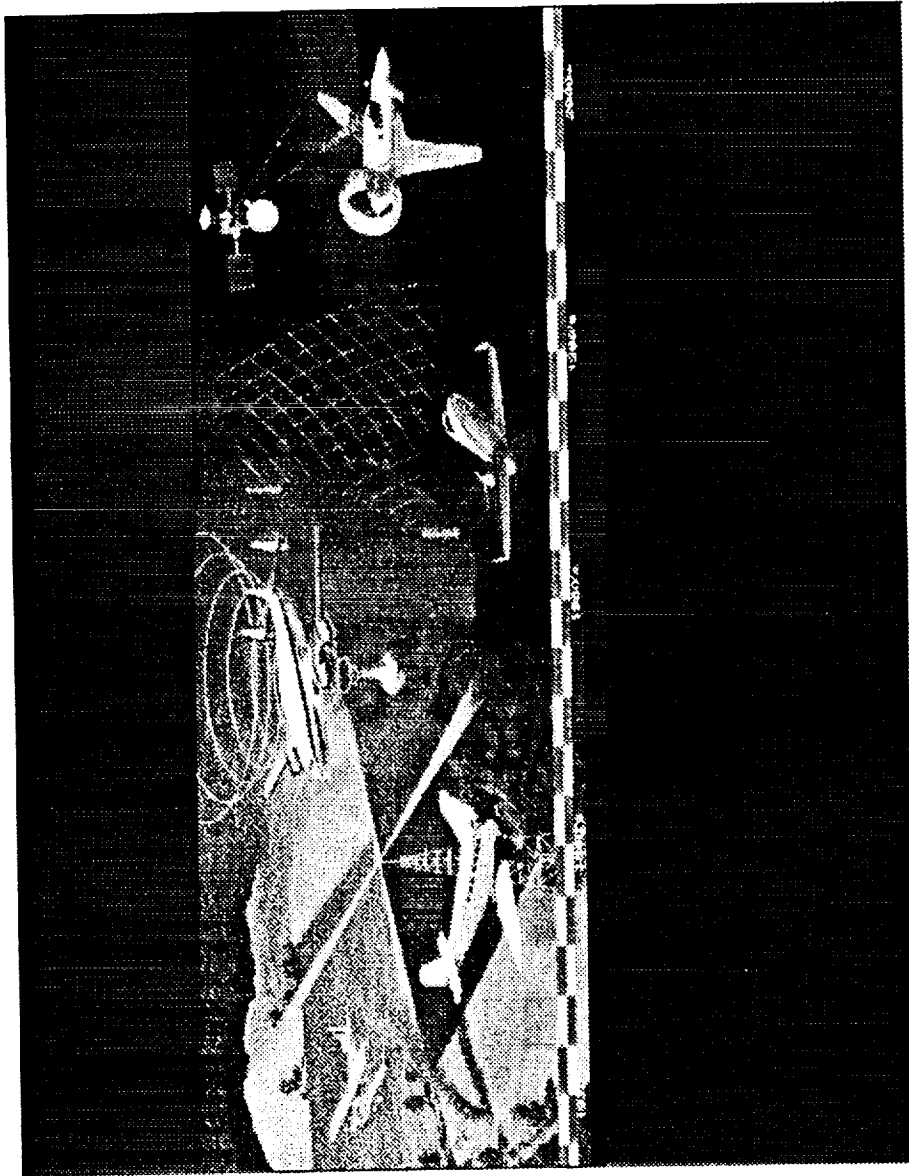
Panorama

- Nation's economic strength and quality of life depend on the **utility, capacity, safety, and efficiency** of transportation and communications systems.

- In the U.S., **Three waves of expansion** have occurred in transportation and communications. These three waves have fueled the nation's economic growth through the emigration of industries out of the cities, into the country.

  1. The first wave occurred earlier than aviation, with the development of canals, rural electrification, and railroads;

  2. The second wave occurred in the 1950's with the development of the Interstate Highways and Hub/Spoke air travel, as well as nation-wide telecommunications;

  3. We are in the beginnings of the third wave, with the implementation of Fiber-optics, satellite communications and navigation, and new air and ground transportation modes

  - On the **ground**, new high-speed and light rail will serve a few hub cities; we could see the introduction of Intelligent Vehicle/Highway Systems.

  - In the **air**, we will see a new generation of supersonic transport airplanes for transoceanic travel; very large (600 to 800 passenger) subsonic jet transports; fast commuter aircraft (perhaps including tilt-rotors); and, potentially, expanded general aviation to more completely serve the "off-airways" population in the nation.

I want to leave you today with an vision of how expanded general aviation transportation could **contribute** to the nation's future transportation infrastructure, **why now** is the time for action; and **how** we can make it happen

5

GENERAL AVIATION SHIPMENT AND BILLINGS
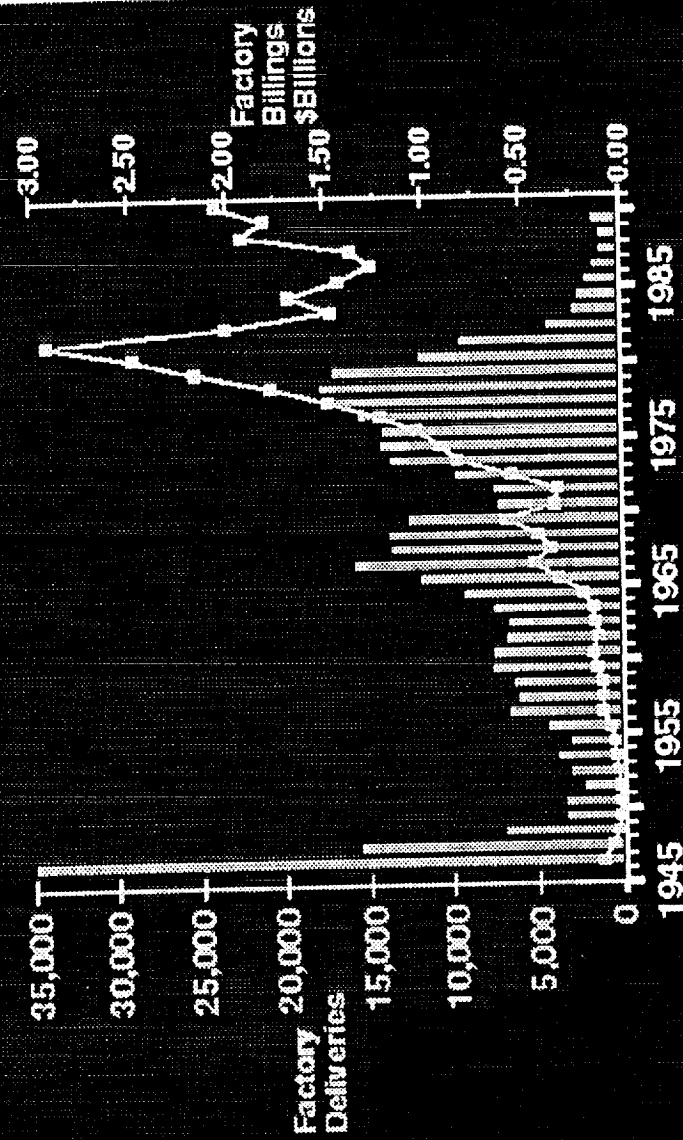
General Aviation Shipment and Billings

- The opportunities facing us are exciting, but the threats are serious:
  - Active **pilots** down 15% in last 10 years
  - Active GA **fleet** contracting, down 10%/10yrs; 3% last year; 75% fly <100 hrs/yr
  - Public use **airports** down 15%/10yrs; 43% **FBOs** operate at loss
  - Aircraft **production** at 3% of 1978 peak; average **age** = 25 years; **technology** > 30 yrs.
  - **Jobs** down over 50% in last 10 years from 43,000 to 20,000 in general aviation
  - **Imports** today = exports of 1978
  - Public **misperceptions** of G.A.'s role in the air transportation system,
  - A broad range of inhibitors to **utility**;
  - The absence of a **national technology strategy** for general aviation.

- Before 1978, GA billings tracked the GNP/GDP. Decoupled in 1978; reasons?:
  - Product Liability
  - Tax code changes
  - GI Bill ended
  - Availability of cheap, used airplanes to satisfy the "enthusiast" market
  - Most important from a technology strategy standpoint, after 1978 we no longer invested in the development of technologies for utility. That is, the lower-end airplanes became out-of-date with the increasingly complex airspace system. In contrast, the higher-end airplanes did keep pace, and they are selling today.

7

MARKET DEMAND

27 Air Traffic Hubs
(65% of Passengers)
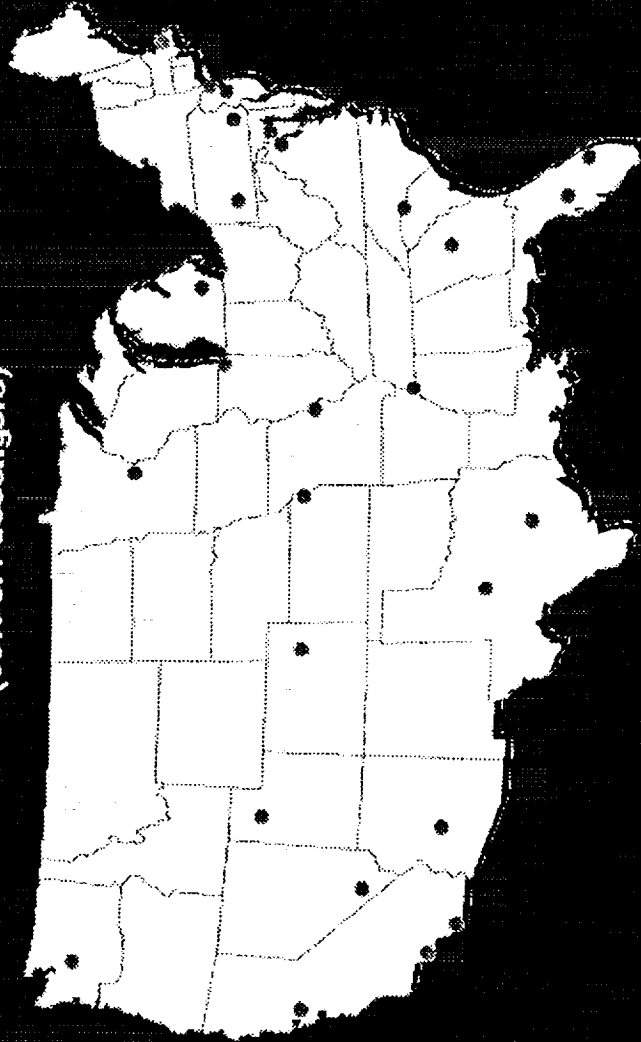
Airport Infrastructure (Hubs)

- The Nation's 27 largest air traffic hubs serve about 65 percent of the total scheduled air carrier passengers.

- These long-haul route hubs are supported by the next level of service:

MARKET DEMAND

Top71 Large and Medium Hubs
(89% of Passengers)
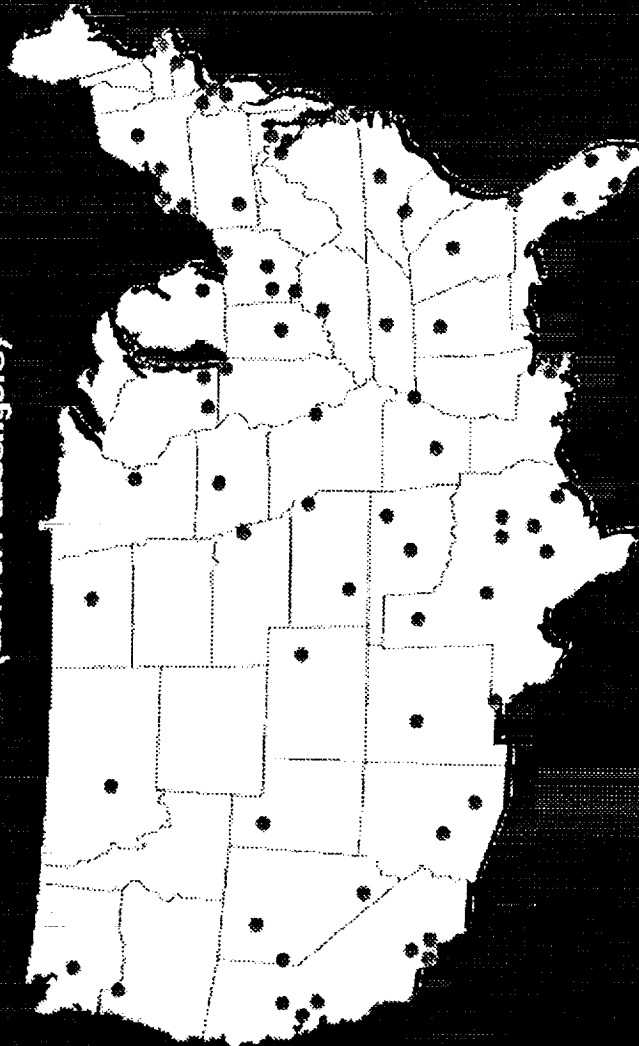
Airport Infrastructure (Hubs + Spokes)

- The top 71 largest and medium hubs serve almost **90%** of the nation's total scheduled air carrier passengers.

- In total, the current hub-spoke system serves **483 cities with 582 airports**. However, this hub-spoke system does not efficiently serve the nation's population which lives further than one-hour's drive from those 582 airports. This part of the nation's population is without scheduled (or even readily available, affordable, non-scheduled) air service, and is therefore out of the country's economic mainstream.

- These data beg the **question**: "How can the nation's air transportation infrastructure be expanded to provide air service to the rest of the population?" This presentation will suggest that the answer lies in general aviation.

- The **good news** is that we already have invested in the ground and air traffic management infrastructure needed to expand air transportation to the rest of the nation:
  - FAA Capital Investment Plan ($32B) for communications, navigation, surveillance
  - And the rest of the infrastructure consists of the nation's general aviation airport system:

GENERAL AVIATION INFRASTRUCTURE

17,000 FACILITIES (5200 PUBLIC-USE)

General Aviation Infrastructure

- This is the **general aviation component** of the nation's air transportation infrastructure
  - Very under-utilized
  - Threatened
  - Need aircraft and airspace systems with higher utility to make full use of this national asset.

- The general aviation airport infrastructure consists of over **17,000 facilities, 13,000 airports, 5200 public-use** airports.

- These airports provide many small and medium industries with transportation to their customers, **rapid, on-demand, random-access transportation** for parts delivery, aerial ambulance services, and organ donor flight support. It is because of the availability of air transportation that these airports help **spread industry and commerce** throughout the nation.

- Even small public-use airports contribute significant **economic benefits.** In **Virginia,** for example, the **average** public-use airport has only 23 aircraft based, and contributes **1.6 million per year** in economic activity, most of which is spent locally.

- What you see here is the rest of the nation's air transportation infrastructure which we already own and which **could be** even more important, economically, in the future.

1 3

Technology Ingredients

- Let's look at the technology ingredients which can enable the development of a new generation of general aviation aircraft. Specifically, Cockpit/Airspace/Airplane Technologies have matured in 1980's and which will mature in the 1990's, enable the potential for an expansion in the utility, safety, and use of general aviation airplanes in the U.S. air transportation system

1 5

COCKPIT 2000

- Ease in Learning/Relearning
- Autonomous Operations
- Intuitive Controls / Displays

16
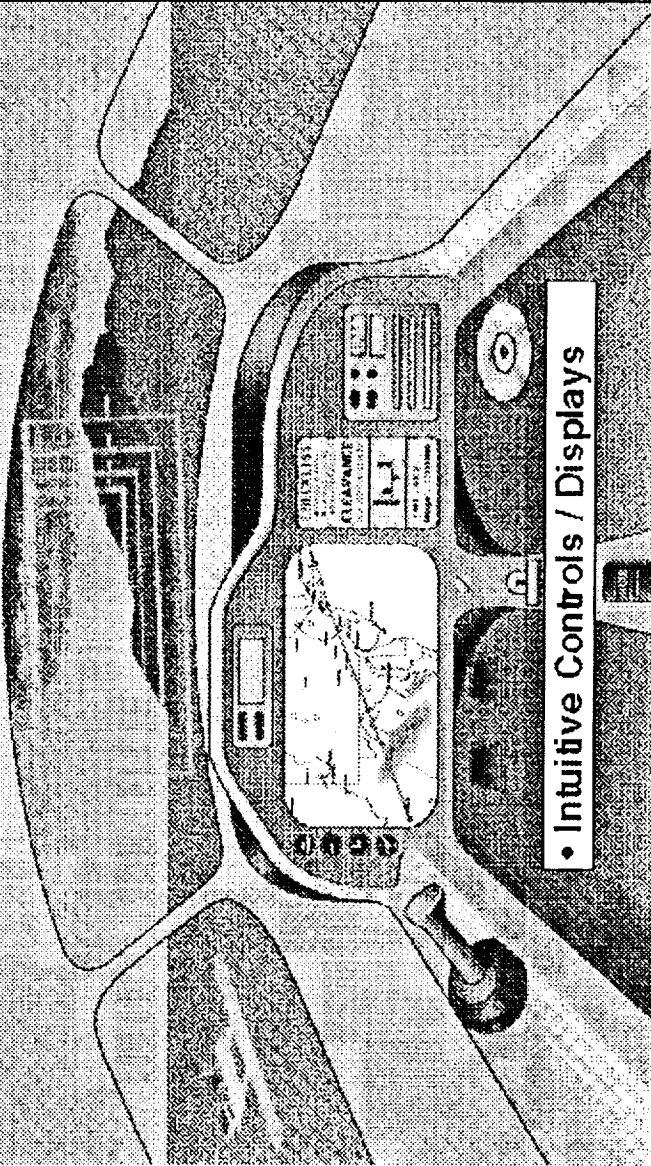
Cockpit 2000

The development of low cost, small computers and flat panel displays have created the opportunity to apply human-centered automation technologies which can enable the development of systems for controls, navigation, communication, and operations which are easier to learn and relearn, and systems which can provide for computer aided decision-making for simplified operations in future aircraft. These systems can also have embedded instruction capabilities; in fact, the cockpits in these future aircraft could have dual use as simulators on the ground for training purposes.
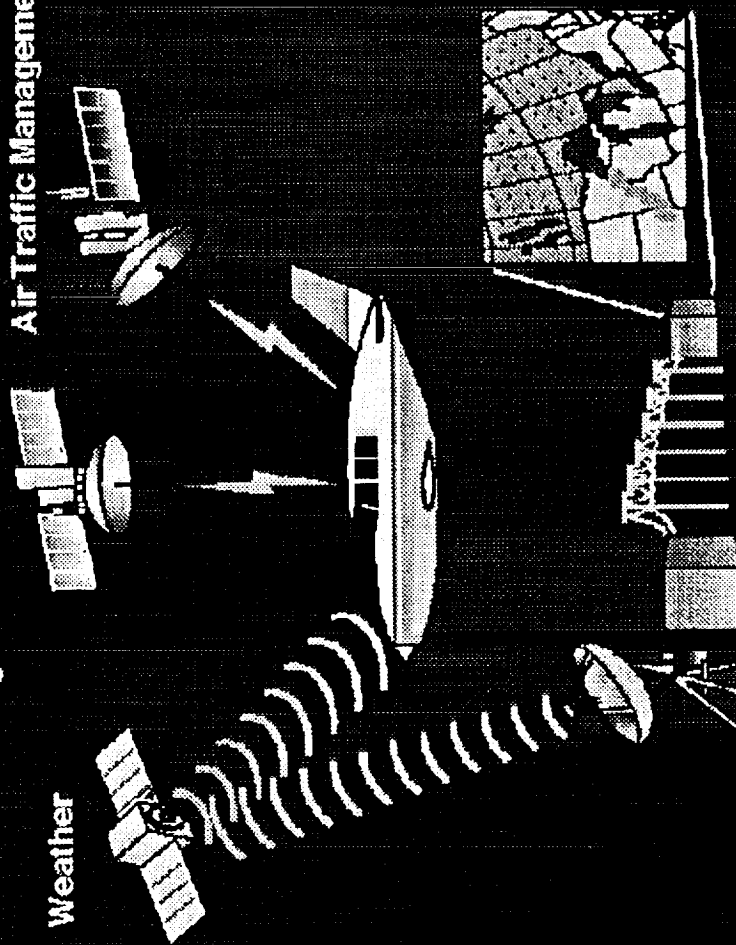
Airspace 2000

- Within the past several years we have seen a **migration** of weather information centers out of the **flight service** weather bureau stations into briefing rooms at local airports. The next logical step in the migration is for weather information to be provided in the **cockpit**. In fact such a system was test flown in a Piper Malibu under a NASA SBIR research contract in the Summer of 1990, in Wisconsin. With today's communications and sensor capabilities, it is even possible have general aviation airplanes report meteorological data to other aircraft and ground stations, much the way the transport operators have started doing today.

- The development of **GPS** and other global navigation satellite systems is the most significant revolution since the **advent of radio navigation**. This technology will provide the **accuracy** to make every landing sight at least a Category I Precision Approach. The accuracy is only half the story, the **cost** is the other half. As the use of GPS navigators spreads throughout the world for both air and ground vehicles, economies of scale will drive costs down.

- The final part of the Airspace story is the future air traffic management system. The The FAA has been provided with $32 billion **Capital Investment Plan** to modernize the navigation, communication, surveillance, and control systems for our nation's next generation airspace system. This system has the potential to support the General Aviation Vision and strategy in this presentation.

19

AIRPLANE 2000 (Roskam, et.al., 1990)
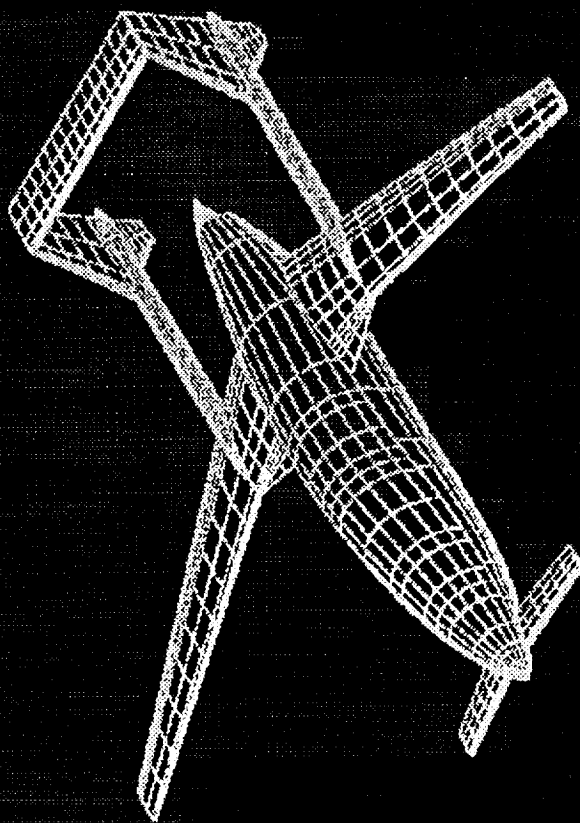
Airplane 2000

- In order for the next generation of general aviation airplanes to be environmentally and economically acceptable, they need to take the fullest possible advantage of advancements in

  - acoustics,
  - materials and manufacturing methods,
  - aerodynamics,
  - and propulsion.

- As the world's aircraft companies have learned to squeeze every last drop of performance out of airplane designs, the competition has moved from performance to product development cycle times. This means that significant competitive advantage is gained by investing in the development of advanced computational design tools, improved testing techniques, and lower cost manufacturing technologies.

- These advancements need to be incorporated in order to "pay the way," so to speak, for the investment in the cockpit technologies which expand the utility and safety.

2 1

MARKET DEMAND

Air Transportation System Growth Forecasts

HSCT

U.S. Carriers

General Aviation

International Carriers

Commuter

Enplanements, Millions

1000

100

10

1990   1995   2000   2005

Year
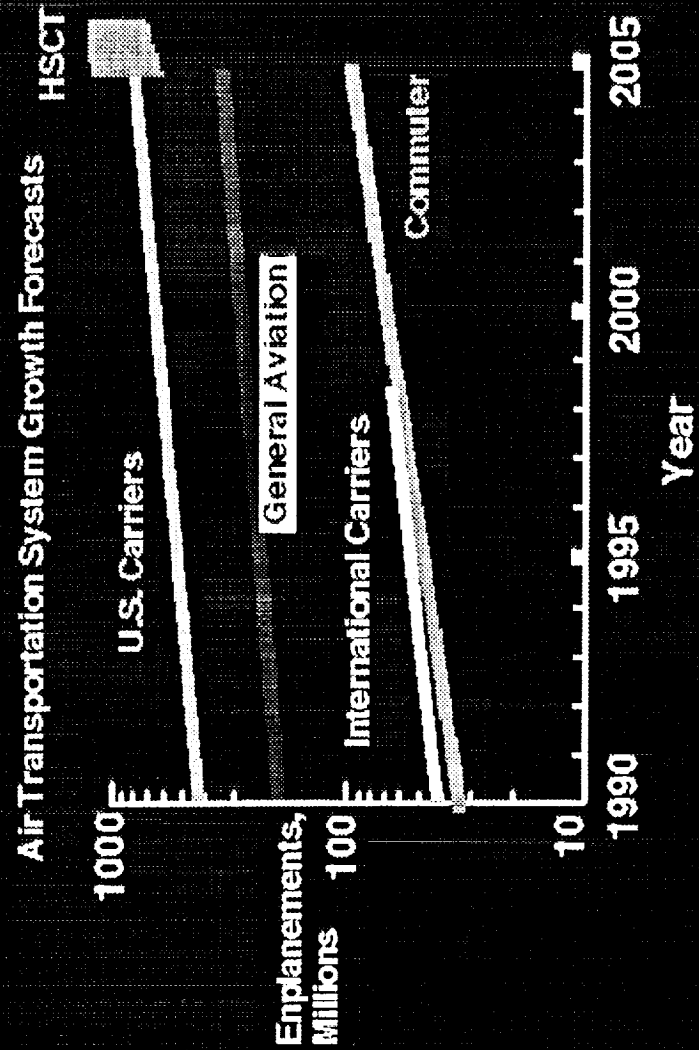
Market Demand

- General Aviation enplanements = 1/3 of U.S. Air Carriers, 3 times commuter & Int'l Carriers General Aviation **miles flown** (4.5578 billion) = Air Carrier (4.9478 billion miles)
  - In terms of enplanements, General Aviation is the **nation's largest airline!**
  - important to look at P-Ms for 150 to 700 mile trips:
    GA is 1/3 of those air trips, 4% of total air and ground
  - for shorter trips, <150 m., cars serve most of need
  - for longer trips, >700 m., long haul scheduled air carriers serve most of need
  - General Aviation could expand to fulfill more of the nation's need for the intermediate routes.

- **What's wrong** with this picture is that the **growth rate** forecast for general aviation is only 0.3%, or one-tenth of the growth rate of a healthy GDP growth rate. In comparison, the other modes of air travel are forecast to grow at rates of 4 to 7 percent.

- From the perspective of **people served**, G.A. is a large part of the national air transportations system, is underutilitized, and can contribute in our efforts to improve airspace capacity and congestion.

2 3

GENERAL AVIATION AIRCRAFT USE 1989
TOTAL = 35,012,000 HOURS

Personal, 29.5%

Instructional, 18.5%

Aerial Application, 5.8%

Observation, 5.3%

Commuter, 4.3%

Air Taxi, 9.3%

Other, 3.2%

Corporate, 10.7%

Business, 13.4%

2 4
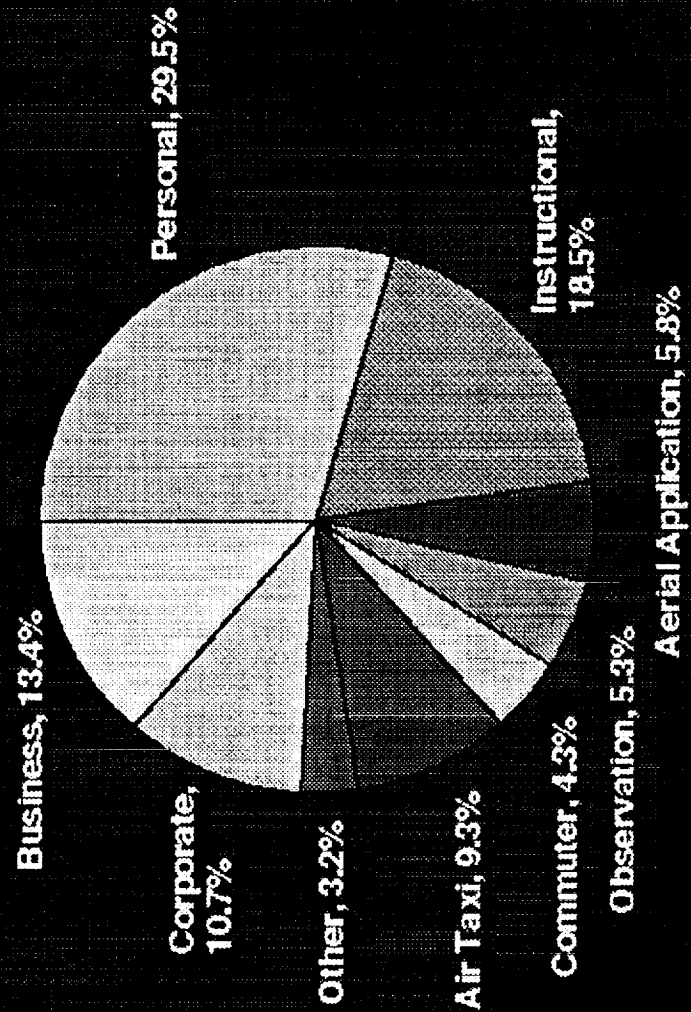
General Aviation Aircraft Use

- G.A. flew 35M hours in 1989, twice the Air Carrier hours; 62% for cross-country

- 30% Personal Flying is the GA equivalent of tourist flying on the airlines (54% of Air Carrier flying is "personal"). Even the 30% personal use is important to the economic health of FBO's so that they will be able to serve the commercial users (47% of nation's FBO's lost money last year)

- By the measure of **value of usage**, technology development for expanded use of General Aviation would be a wise investment for the future U.S. Air Transportation System infrastructure

U.S. ANNUAL AIR TRAFFIC OPERATIONS
1987-1989 AVERAGE

Total

75.6%

21%

4%

IFR

48%

37%

14%

Air Carrier

Military

General Aviation
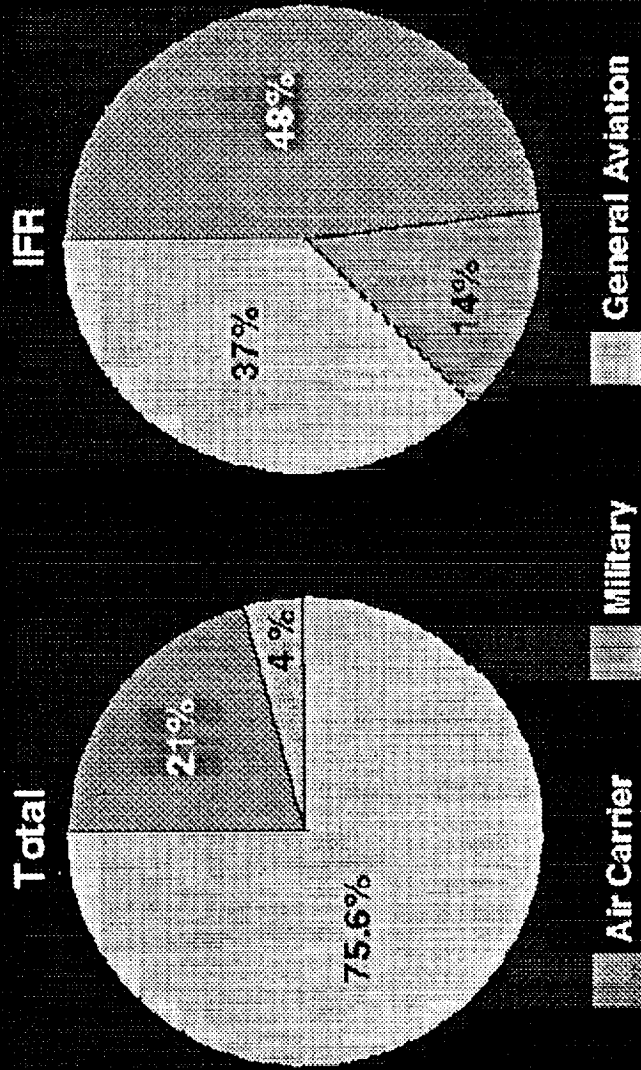
U.S. Total Annual Air Traffic Operations, 1987-1989 Average

- An operation is an arrival or a departure.

- Total U.S. operations comprised of 75% G.A. aircraft;
  G.A. departures are nearly 4 times the rate of Air Carriers

- There are important **differences** between the two kinds of pilots and operations.
  GA pilots tend to be part time, fly into **strange airports** more frequently than scheduled
  air carrier pilots, have less time to invest in **initial and recurrency training**, and have
  less capable **equipment** both in terms of aircraft and systems performance, and
  in cockpit flight systems.

- For maximum impact, research to improve the **operational
  capacity** of the national air transportation system should
  address the **cockpit and airspace** technologies specific to G.A.
  airplanes and pilots in addition to our current efforts for transport aircraft.

2 7

GENERAL AVIATION FATAL ACCIDENTS 1982-1988

Human Factors

By Cause
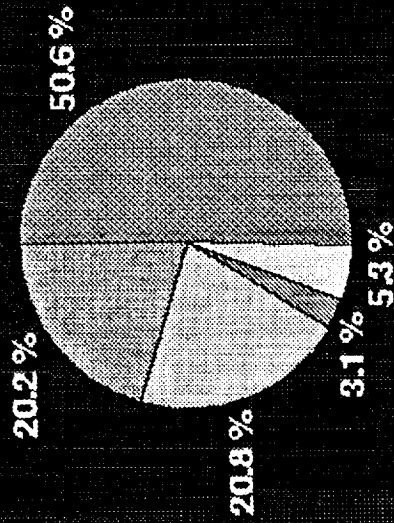
50.6 %
20.2 %
20.8 %
3.1 %
5.3 %

Terminal (Weather, Stall/Spin, Other)
Power/Propeller/Systems
Fuel Management
Weather, Cruise
Other & Undetermined

General Aviation Accidents (1982-1988, AOPA/ASF)

- Enormous improvements over the past decades for G.A. accidents; **current fatalities/100 Khrs is 1/2 of 1975 rate; During past 4 years**, G.A. acft flown by salaried crews had fewer accidents/100Khrs than scheduled air carriers

- The message in these accident statistics is that newly maturing technologies can significantly impact nearly all of the kinds of accidents occurring today.

- The general aviation safety **goal** should be established by studying the reasons for the outstanding record for corporate aviation safety, understand the differences between the pilots, equipment, and operations, then apply the lessons to all of general aviation.

- Terminal operations accidents include taxi, takeoff, climb, descent, IFR and VFR approach, and landing. The casual factors in these accidents include stall/spin or other loss of control, attempted VFR into IFR conditions, improper operations, and mid-air collisions (which represent 0.5% of all accidents).

- Cruise weather accidents are 4.7% of total, but 20.8% of fatal accidents. New technologies are particularly relevant to this kind of accident. If pilots can be aware on a near real time basis of their position, the relative location of weather and terrain, this kind of accident would greatly decrease. We have most of these technologies ready for integration today. The challenges are human factors engineering of the displays, and certification.

GENERAL AVIATION FATAL ACCIDENTS 1982-1988

By Cause

50.6 %
20.2 %
20.8 %
3.1 %
5.3 %

Terminal (Weather, Stall/Spin, Other)
Power/Propeller/Systems
Fuel Management
Weather, Cruise
Other & Undetermined

Human Factors

16.3 %
83.7 %

Other Than Pilot Human Factors
Pilot Human Factors
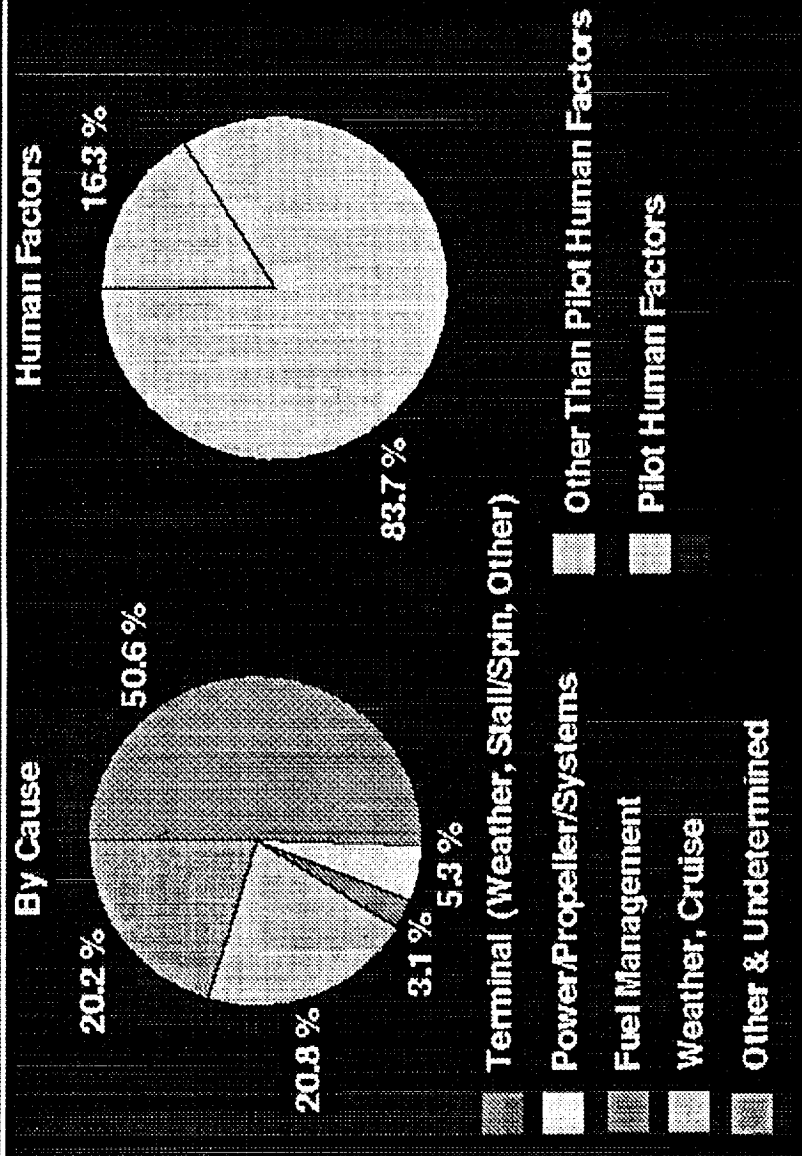
General Aviation Human Factors Accidents   (1982 - 1988)

- Overwhelming proportion: Human Factors
  - Involving flight deck;, ATC-flight deck interactions; aircraft maintenance; and airways maintenance

- The airframe/engine/systems play a decreasing role in accidents.

- Definition of "Human Factors" related accidents
  - Judgment
  - Man-machine interface
  - Need to include other than "Pilot-Error" in this category, Numerous casual factors include:
    - improper maintenance
    - improper installation
    - improper overhaul
    - improper part
    - improper assembly

- Technology offers to greatly alleviate many "Human Factors" accidents

- We need to expand General Aviation activities in the National Human Factors Research Program

FUEL EFFICIENCY COMPARISONS
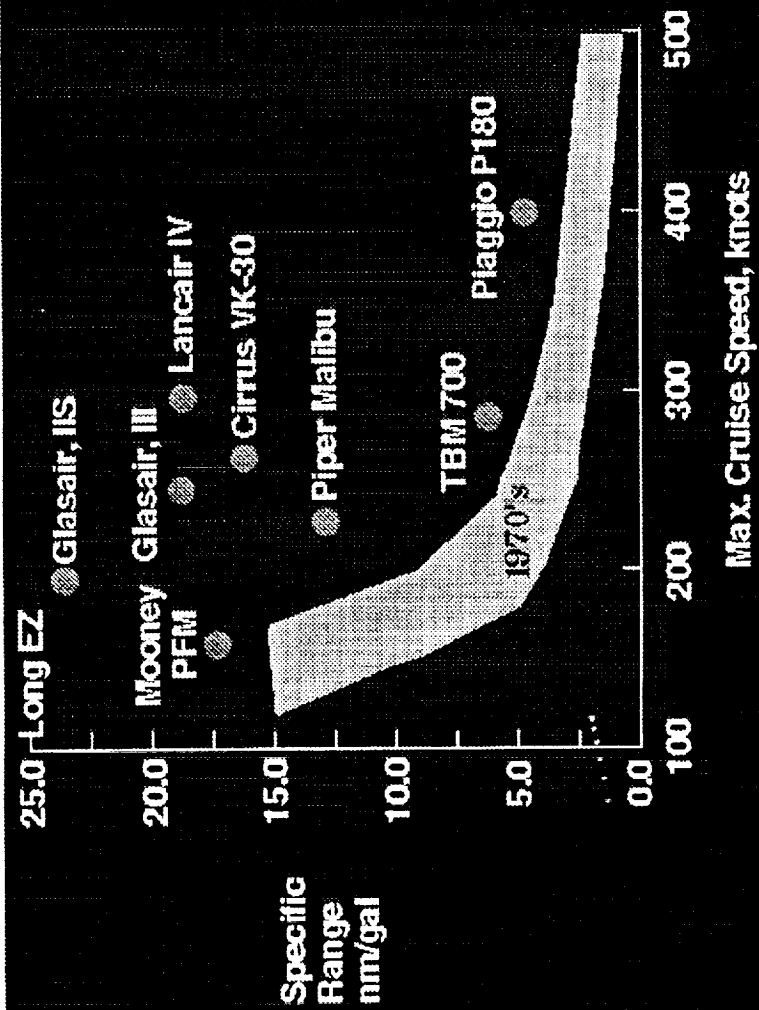
Fuel Efficiency Comparisons

- This figure illustrates the **strides** of the past two decades in airplane performance We have seen a doubling of the fuel efficiency at a given speed; conversely, we have seen a doubling of the speed at a given fuel efficiency.

- While these gains are impressive, even **further gains** are possible from advancements in:
  - Drag reduction aerodynamics, including laminar flow control
  - Lighter weight structures and materials
  - Improved engines with lower power-to-weight ratios and fuel burn

- As the world's airplane manufacturers continue to take advantage of these advancements, a new driver for competition is emerging: product **development cycle time**. The ability of U.S. manufacturers to compete in the future will increasingly depend on their ability to reduce the time required to design, test, and certify new aircraft and systems. Aeronautics research can contribute to reduced cycle times by improving the speed and accuracy of computational design tools, testing techniques, and certification processes.

OBSTACLES TO UTILITY

USER ACCEPTANCE

- Cost/Performance
- Time for learning/relearning
- Safety
- Comfort

Obstacles to Utility

- The **critical question** is, "What obstacles inhibit the expanded use of General Aviation aircraft?"
  This is an important question because the **solutions** lie in the answers.

- Cost of ownership / operation / nearly all-weather systems performance
  - Product liability adds to the purchase price
  - Current production rates of 1500 aircraft do not command economy of scale
  - Tax laws, Airline competition, Reliability
  - Both **technology and volume** are required to bring costs down.

- Proficiency requirements
  - Learning and re-learning to fly airplanes requires expensive time/cost
  - Airplanes must be made **easier** to learn and re-learn how to fly

- General Aviation fleet safety is not yet competitive with automobiles
  - The goal for G.A. should be to achieve corporate levels of safety; It will be difficult to achieve, but **technology** offers significant help.

- Ride comfort
  - Gust response
  - Interior noise: without headphones;
  - Features: air-conditioning; audio systems; flight phones.

3 5

OBSTACLES TO UTILITY

USER ACCEPTANCE

- Cost/Performance
- Time for learning/relearning
- Safety
- Comfort

COMMUNITY ACCEPTANCE

- Noise
- Safety
- Emissions
- Elitist Image

Utilization Inhibitors, (Concluded)

- Airport noise concerns top the list. The threat of **curtailed, curfewed, and and outright banning** of aircraft operations at many of the world's airports is increasing.
  - Advanced **acoustics technologies** have improved our ability to to deal with these threats.

- Until **safety** improves for the entire General Aviation fleet, the community acceptance for this mode of travel will remain low.
  - The safety goals previously discussed can be sought after through the application of **cockpit information and display technologies.**

- **Emissions** are becoming an increasing concern as subsonic fleet sizes increase.
  - From a technology standpoint, we need to look at the application of advanced electronic engine **controls** and alternative engine **cycles** and fuels on future fleet emissions.

- The elitist **image** which many in the public have for General Aviation is a result of the fact that a relatively small part of the population makes direct use of this mode of travel. As an increasing part of the population comes to experience the benefits of General Aviation, either **directly, or indirectly**, this image should change.

3 7

PROGRESS IN TECHNOLOGY

Non - Aeronautical

- airbags
- anti-lock brakes (in 1.7 million 1992 cars)
- CD-ROM
- cellular telephone
- cruise control
- electronic ignition
- electronic moving maps
- infrared remote controls
- interior noise control
- displays
- micro computers
- radial tires
- reliable powered subsystems
- smart "idiot" lights
- smart suspension system

3 8

Progress in Technology

- Since the last applications of significant technical advancements in G.A., numerous technologies have become a part of **everyday life** in mass markets and presumably could contribute to the development of new airplanes.

- These non-aeronautical technologies have established the **level of expectation** of the marketplace for future airplanes which would be marketed to travelers beyond the historical "enthusiast" market.

PROGRESS IN TECHNOLOGY

Aeronautical

- ACARS
- Active Noise Control
- Advanced Metallics
- CAD/CAM
- Computational Fluid Dynamics (CFD)
- Fault-tolerance
- Fiber-optics
- Lightning Protected Composites
- Crash-worthiness
- Computational Structural Mechanics (CSM)
- Enhanced Visual Systems (EVS)
- GPS
- LORAN
- NLF/HLFC
- Molded Phenolic Composite Engines

Progress in Technology. (Concluded)

- During the past decade aeronautics technologies have advanced significantly.

- Many of these technologies have been incorporated into the modern fleet of **business jet and turboprop aircraft** built and selling in the U.S. today. However, these technologies have not been incorporated into the smaller aircraft which have **less and less of the utility needed** for safe, comfortable, economical operation in today's increasingly complex airspace system.

41

FUTURE TECHNOLOGY DRIVERS

Advanced Airspace System

ATC
Datalink

GPS

Real Time
Cockpit
Weather

Direct
Broadcast
Satellites

Advanced
Engines

Satellite Based
Cellular Telephones

1990   1995   2000
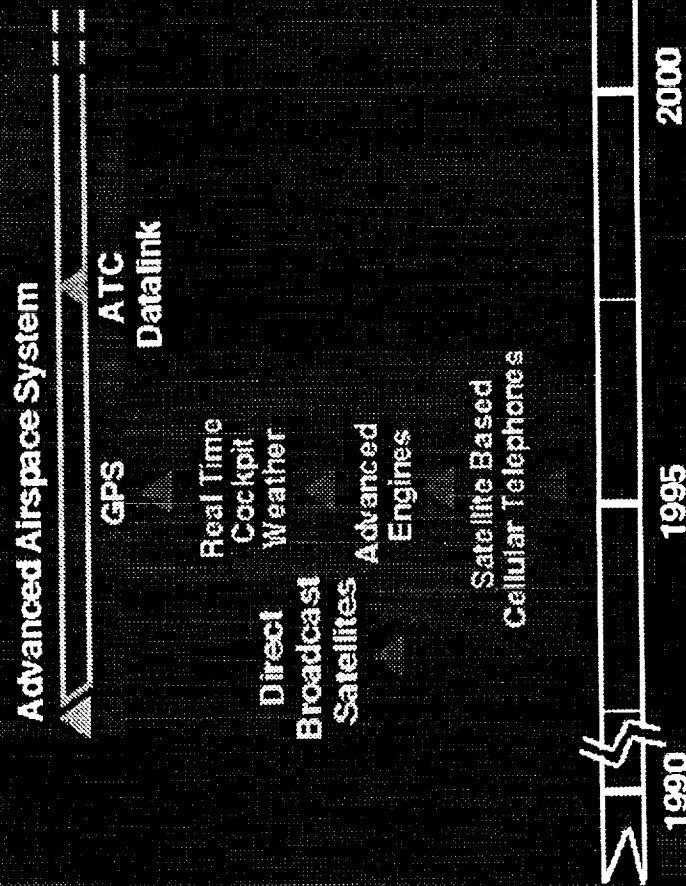
Future Technology Drivers

- Direct broadcast satellites may be commercially operationally before 1994 to carry both voice and video information

- The first GPS precision approach is planned to be operational this summer for the Experimental Aircraft Association convention in Oshkosh, Wisconsin.

- Near real-time weather products in the cockpit could be available on a subscription basis by 1995.

- Advanced engine activities which are underway at NASA could result in a rotary engine flight evaluation in the 1995 time frame.

- The advent of satellite based cellular telephones could add a new dimension of creature comfort and convenience to all air transportation.

- The U.S. $32 billion investment in the FAA Advanced Airspace System has the potential to support the next generation general aviation transportation safety, utility, and expansion goals. ATC Datalink, as part of the communications system improvements, could be on line before 1998).

4 3

FUTURE TECHNOLOGY DRIVERS

Advanced Airspace System

GPS

ATC Datalink

Real Time Cockpit Weather

Advanced Engines

Direct Broadcast Satellites

Satellite Based Cellular Telephones

Advanced Weather Measurements and Forecasting

TeraFlops Parallel Computing

FBL/PBW

IV/HS

1990

1995

2000

44
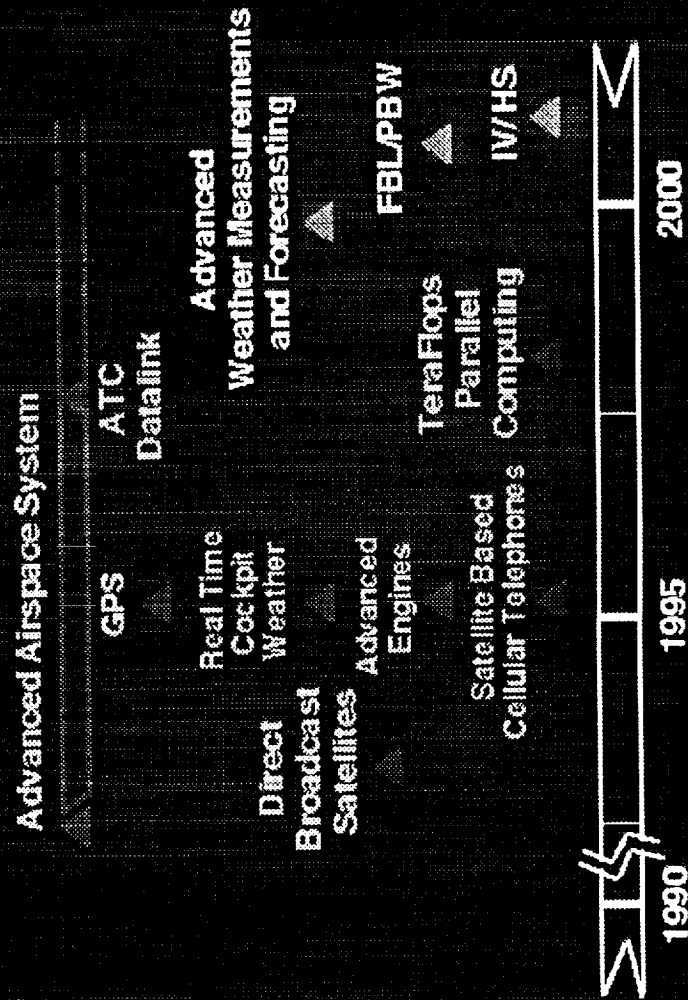
Future Technology Drivers (cont'd)

- TerraFlops computing will increase speed 1000-fold and decrease cost of high-performance computing.

- Fly-by Light/Power-by-wire will come into maturity in the next decade

- Intelligent Vehicle/ Highway System may provide for crucial economies of scale for GPS components and flat panels when produced at the level of millions of units/year for automobiles.

- Advanced Weather Measurements
  - ASOS: (NWS, 537 units, 1992 - 1996)
  - AWOS: (FAA, 40 units, 1992 - 1993)
  - NEXRAD: (NWS, 113 sites, 1993 - 1996?)
  - TDWR (FAA, 47 sites, 1993 - 1995)
  - Profilers (NWS: Block 1, mid U.S. today
    Block 2, 200-300 units nationwide about 2000 a.d.)
  - MAPS (NCAR/NWS, Aviation Gridded Forecast System, 1998)

4 5

FINDINGS

- **General aviation situation:**
  - Major segment of the national air transportation system
    - Threatened
    - Potential for expansion in safety, utility, performance, use

- **Potential for expansion enabled by new technologies:**
  - Navigation
  - Communications
    - Controls
    - Information systems

- **Environmental and economic acceptability enabled by technical advancements:**
  - Aerodynamics
  - Acoustics
    - Propulsion
    - Materials

- **General Aviation mission requirements are under-represented in national technology strategies.**

- **U.S. research planning cannot wait for product liability resolution.**

Findings

- General Aviation's capability to serve the U.S. transportation needs is **threatened**, but GA can be **revitalized** with vastly greater safety, capacity, utility and efficiency to contribute fully to U.S. economic growth.

- Newly maturing technologies have laid the **foundations** for general aviation to expand, not only to meet **U.S. needs**, but to meet **foreign market** needs (especially third world) as well.

- As international aeronautical **competition** has squeezed nearly ever last mile-per-gallon out of technologies, the **competitive playing field** of the future will be dominated by who can move the fastest through **product development cycles.** This means that to be competitive, the U.S. must invest in the development of technologies affecting faster, more accurate **computational design tools,** advanced **testing** techniques, lower cost, faster **manufacturing** techniques, and more rapid **certification** processes.

- The primary task of the NASA Advisory Council, Aeronautics Advisory Committee, **Task Force** on General Aviation Transportation is to address the last point concerning a national technology strategy to define what technologies are needed to enable general aviation to contribute to the national airspace **capacity** issues and **revitalize** the U.S. general aviation industry through expanded use and volume of production. While product liability is still critical, research planning must begin now.

47

GENERAL AVIATION GOALS

- Safe, high utility airplanes

- Electronic VFR

- Decision-Aided Flight Planning and Operations

- Electronic Cockpit Libraries

- Dual-Use Cockpits

- Environmentally, economically acceptable airplanes:
  - Acoustics
  - Propulsion
  - Materials and Manufacturing Methods
  - Aerodynamics

<u>GA Goals</u>

- The General Aviation Safety goals could be established by translating the lessons from the ultra-safe corporate operations, where feasible, to the General Aviation fleet.

- Electronic VFR: means minimize the IFR/VFR distinction
  - Wide field of view displays
  - Single, GPS-based universal approach procedures and systems
  - Near real-time weather in the cockpit

- Decision-Aided Flight Planning and Operations
  - increased autonomy, transparent to operator
  - Integrated weather, traffic information in the cockpit for preflight, enroute operations
  - GPS-based random access, point-to-point navigation

- Electronic Cockpit Libraries
  - Optical storage of enroute and terminal navigation information
  - Datalink for comm and clearance information
  - Electronically stored and displayed aircraft performance data

Technology Goals (concluded)

- Dual-Use Cockpits
  - Embedded Flight Training (recurrent and, ultimately, initial)
  - Intuitive (decoupled) flight controls and displays
  - Flight envelope protection systems
  - Self-teaching simulators and onboard flight systems

- Aircraft for expanded general aviation utility must meet community environmental expectations, and user expectations for utility and cost.

50

NATIONAL TECHNOLOGY STRATEGY PROPOSAL

- Establish viability of General Aviation expansion.

- Establish public constituency in support of expanded General Aviation utility and use.

- Integrate research with aircraft & airman certification processes for new technologies.

- Coordinate cockpit & airplane technology planning with FAA Capital Investment Plan.

- Strengthen avenues for technology transfer to U.S. industry.

Technology Strategy

- Establish viability of a new transportation mode:
  - Environmental
  - Economic
  - Technical
  - Political and social

- Establish public constituency in support of a new air transportation mode
  - In "off-airways" communities throughout the nation
  - G.A. is today where the automobile was in the 1930's before the Interstate Highway System
  - Educate public about the future G.A. role

- Integrate research with certification processes for new technologies.
  - Predictable cost to certify
  - Predictable time to certify
  - Use of simulation for advanced flight systems certification (systems reliability, compatibility, interoperability)

- Work to assure that the capabilities in the Automated Airspace System will fully enable and support this general aviation vision.

5 2

<u>**Technology Strategy**</u> <u>**(continued)**</u>

- Capitalize on new capabilities for technology development and transfer involving cooperative-proprietary government/industry efforts
  - New ways for Industry/Government to collaborate for **competitiveness**
  - Strengthen weak link in the technology development chain: **validation**
  - NASA / FAA/ Universities/**SBIR**

FUTURE SPACE TRANSPORTATION SYSTEM ARCHITECTURE AVIONICS REQUIREMENTS

Presented to
NASA LaRC Workshop on Guidance,
Navigation, Controls, and Dynamics for
Atmospheric Flight
March 18, 1993
by
Howard Stone
and
Walt Engelund

NASA STRATEGY FOR ACCESS TO SPACE

Access to Space Vision

Space Transportation
Requirements 1993-2030
- NASA
- DOD
- Commercial

Option 1
Space Shuttle
to 2030

Option 2
Space Shuttle
Phasedown
starting in 2005

Option 3
Space Shuttle
Phasedown
starting in 2008

Study A
Shuttle
Improvements
to 2005

Study B
New Transportation
System
Conventional
Technology

Study C
Shuttle
Improvements
to 2008

Study D
New Transportation
System
Advanced
Technology

NASA Strategy for Access to Space

The agency began a multi-center study in January 1993 to examine options for providing the most cost effective space transportation system in the future. The Space Shuttle will be the primary transportation system for the near future and throughout the deployment of the Space Station Freedom later in this decade. Future options are to replace the Space Shuttle in 2005 to 2008 or improve the Space Shuttle and keep it flying to about 2030. If the Space Shuttle is replaced in 2005, more conventional technology systems would be used such as spacecraft deployed by an expendable launch vehicle. If the replacement is delayed until about 2008, it is believed that advanced technology concepts could be used such as fully reusable systems.

In the current study which is due to end this summer, many concepts will be examined, and preliminary cost numbers will be generated to see which option is the most cost effective. Technology requirements and plans will be defined to chart the path for the agency program in the next several years.

ACCESS TO SPACE EVALUATION CRITERIA

Fundamental Requirement	Key Requirement (Mandatory)	Essential Characteristics (Highly Desirable)	Desired Features (Nice to Have)
1.1 Satisfy the National Launch needs • Commercial • DOD • NASA unmanned • NASA manned Includes definition of payloads from small to exploration class, and destinations at all inclinations	2.1 Improve crew safety (crew survivability ≥ 0.999) 2.2 Acceptable life cycle cost: Affordable DDT&E and annual operations cost 50% or less over current systems 2.3 Vehicle reliability at least 0.98 2.4 Growth capabilities 2.5 Environmental – meet all requirements planned for year 2002 2.6 Good operability (flexibility, availability, responsiveness)	3.1 Acceptable program schedule 3.2 Acceptable program risks (technical, cost, schedule) 3.3 Improves commercial competitiveness of launch vehicles 3.4 Contributes to industrial economy (dual-use technology and processes) 3.5 Helps maintain industrial base	4.1 Maintain (or improve) national prestige 4.2 Promote science and education 4.3 Enable incremental development or improvements 4.4 Enhance international relationships 4.5 Improve capability relative to current systems (including STS)

Access to Space Evaluation Criteria

The fundamental requirement of the new space transportation options is to satisfy the national launch needs. In the current study, the needs are dominated by the Space Station Freedom crew rotation and resupply requirements.

Mandatory requirements include a high probability of crew survivability which drives the vehicle design to provide for abort, particularly during the critical ascent phase. The cost requirements imply that new ways of doing business must be found for future systems.

SERVICER VEHICLE OPTION FOR UNPRESSURIZED STATION CARGO

Carry unpressurized cargo for space station inside adapter

O2 carrier

O2 carrier goes up in adapter
Returns empty in payload bay

RMS stowed in payload bay

Payload bay

N2 carrier

Radiator in payload bay door

Airlock hatch
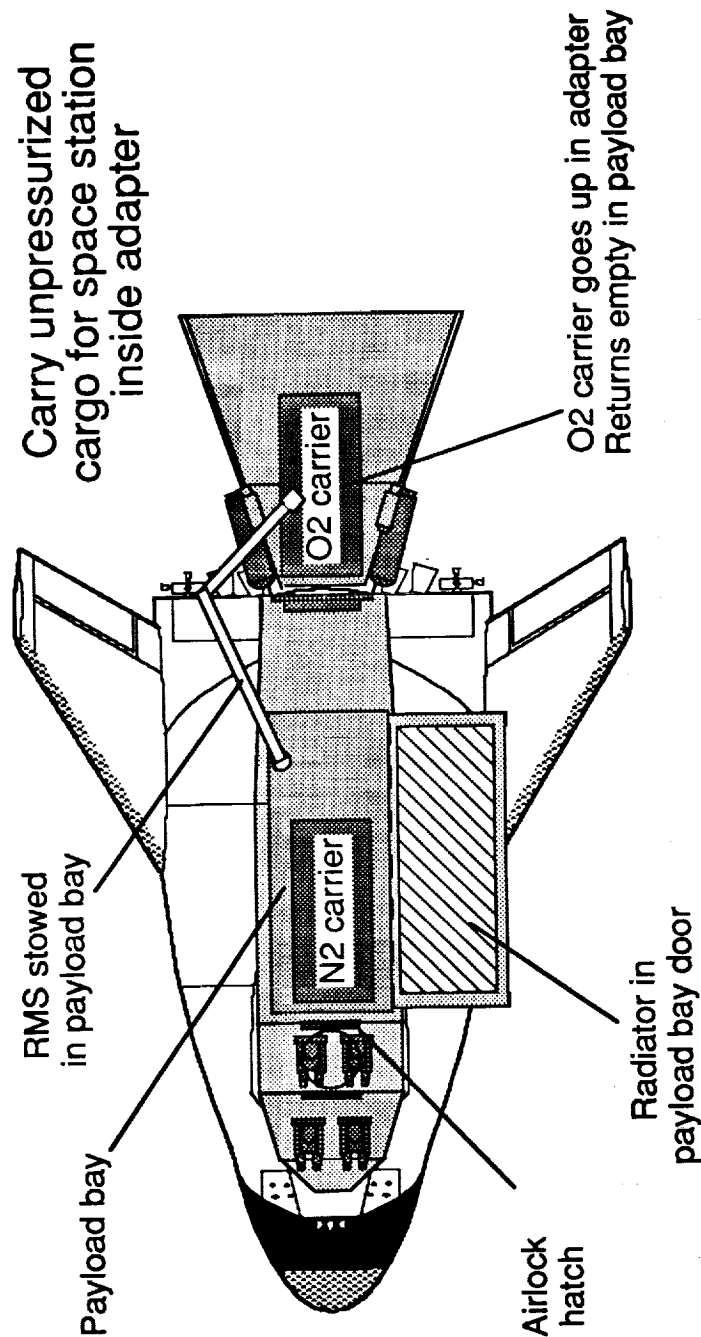
Split HL-42 adapter jettisoned at booster separation exposing unpressurized cargo -- RMS on HL-42 servicer version places cargo on station

Servicer Vehicle Option for
Unpressurized Station Cargo

In the conventional technology option, 2B, the Langley-developed, lifting-body concept, the HL-20 Personnel Launch System, is a candidate concept for carrying personnel and cargo requiring late access to the Space Station. Since cargo delivery requirements are being included in the current study, the HL-20 has been enlarged to a 42-ft length to allow for additional payload capability. This concept, which has been designated the HL-42, will also provide a satellite servicing capability as shown in the figure.

CLV Configuration Options

Crew Logistics Vehicle In-House Study
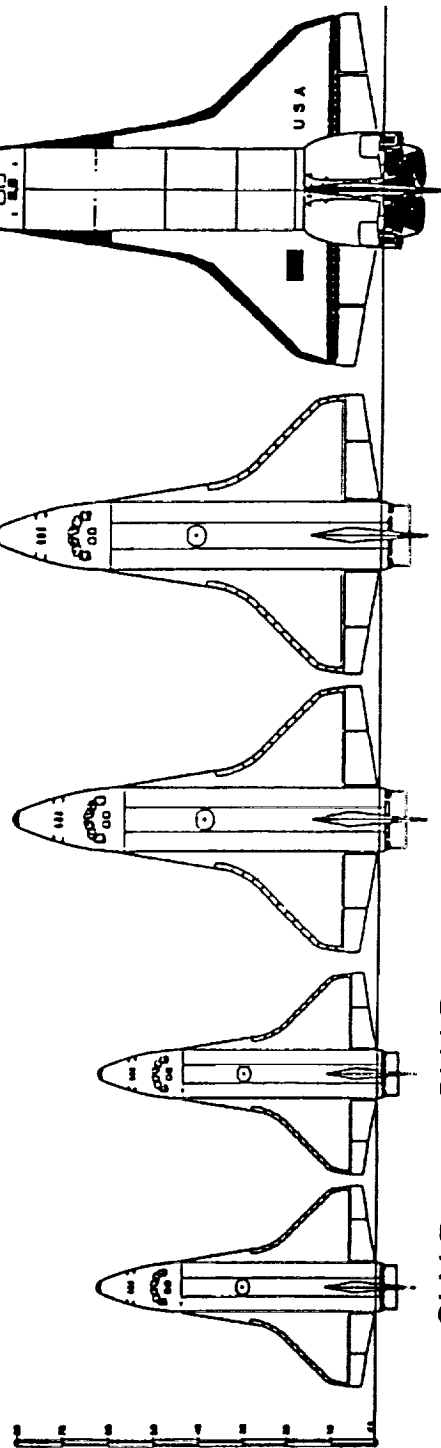
	CLV-B	CLV-P	CLV-UP	CLV-C	STS Orbiter
Linear Scale Factor (CLV/STS)	.50	.61	.79	.83	1.00
Payload Mass (kg)					
Pressurized	3908	7710	7710	7710	19,278
Unpressurized	0	0	3175	5512	104,350
Gross Mass (kg)	32,495	43,200	59,700	66,550	
Flts/Year	4	6	6	6	
Additional Flight Spt					
Pressurized	4 Titan IV/PLM/C	0	0	0	
Unpressurized	2 Titan IV/CTV	2 Titan IV/CTV	1 Titan IV/CTV	0	
Comments	No EVA or Sat Serv. No Unpressurized Return	No EVA or Sat Serv. No Unpressurized Return			

Systems Engineering Division
Systems Definition Branch

Lyndon B. Johnson Space Center

CLV Configuration Options

Also in option 2B, the Johnson Space Center team has been examining several photographically reduced Space Shuttle concepts for launch on an expendable booster. These concepts have no main propulsion systems since the booster supplies all the ascent propulsion. These concepts referred to as the Crew Logistics Vehicle (CLV), have varying cargo capability depending upon vehicle size. The largest concept, CLV-C, can carry the Space Station logistics and the station crew on a single flight, and therefore has the lowest flight rate of all the concepts. Its size and weight are also very nearly the shuttle orbiter values, and the concept would have to be side mounted on the expendable booster.

There are several other concepts being examined including a winged payload carrier, defined by the Marshall Space Flight Center, and an Apollo capsule concept which is advocated by the Johnson Space Center.

LANGLEY SINGLE STAGE ROCKET
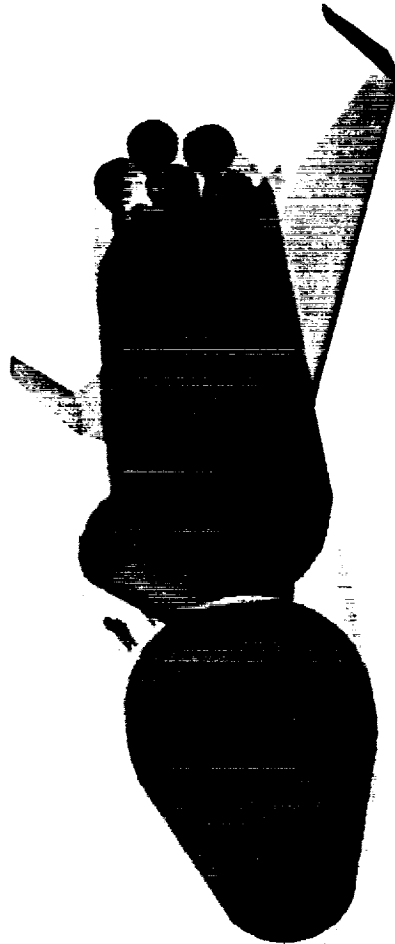
Mission: DRM-1 Space Station Freedom Resupply
Deliver and return 20 klb PLH & 16 (.964) cu. ft. to SSF to
KSC with hard docking capability

Langley Single Stage Rocket Vehicle

The advanced technology concepts in option 3D include rocket and airbreathing concepts. An example of an all-rocket concept is the Single Stage Vehicle (SSV) shown in the figure. This concept is fully reusable with internal cryogenic LOX and LH2 tanks and seven rocket engines in the base. Carrying all the propellant onboard results in a 171-ft long vehicle, about 50 percent larger than the Space Shuttle Orbiter. It is vertically launched and landed on a runway like the Space Shuttle.

6 5

DELTA CLIPPER PROVIDES MULTIMISSION CAPABILITY

VCZ25980.4 M5EG

DELTA Clipper

Takeoff

On-Orbit

Mission Phase

Reentry

Landing

Space Lift/Logistics

☐ Space Support
☐ Force Enhancement

Space Sortie/Test

☐ Space Control
☐ Force Application
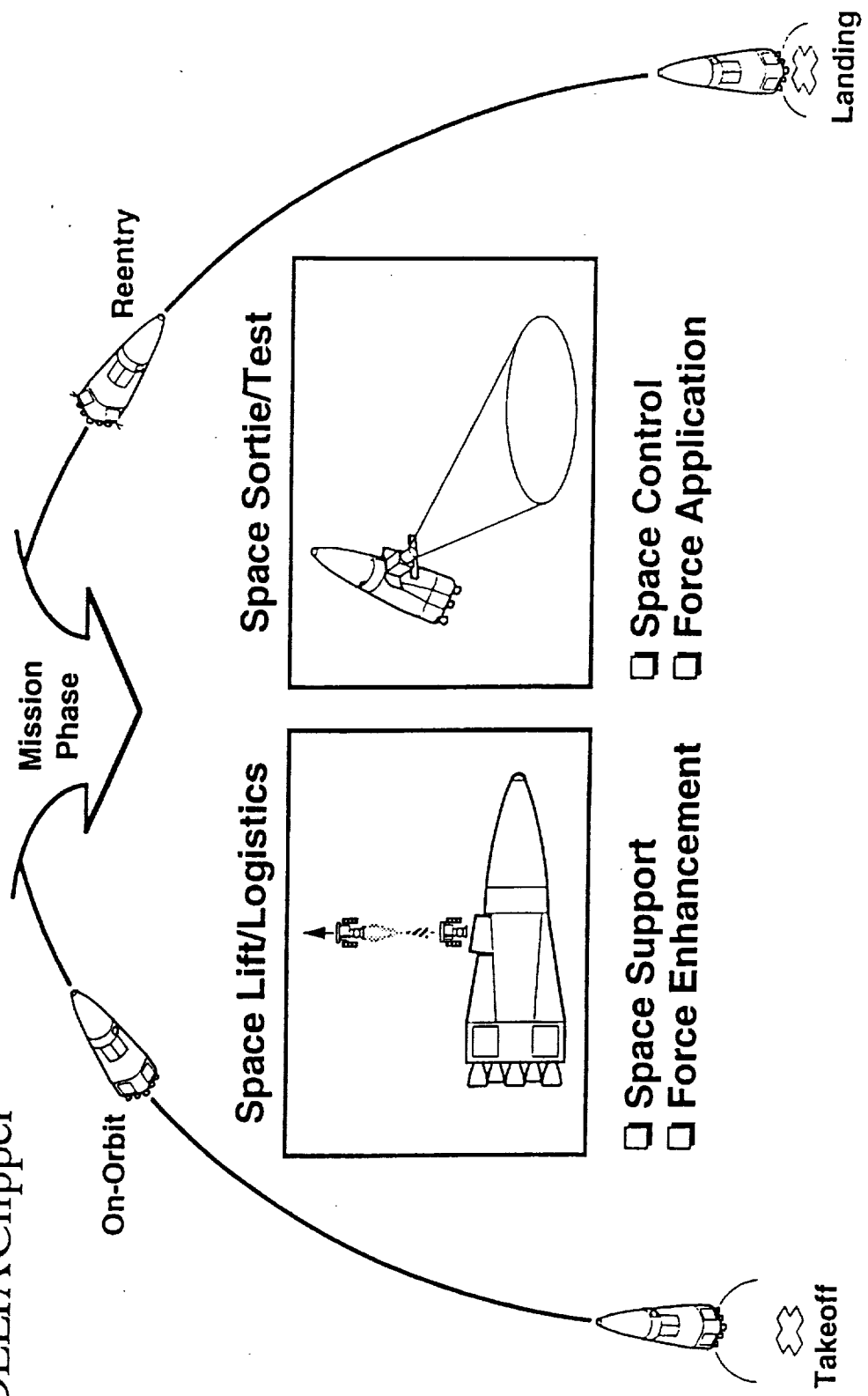
Delta Clipper Provides
Multimission Capability

Another all rocket concept known as the Delta Clipper is being developed for the Strategic Defense Initiative Office by McDonnell-Douglas. This vehicle lifts-off vertically in a conventional manner but lands vertically using the rocket engines to achieve a soft landing. After mission completion, the vehicle enters the earth atmosphere nose first, and just before touchdown a turnaround maneuver is executed and the engines started for landing on the base. A scaled version of this vehicle has been constructed and a flight test program is due to start in a few months.

BETA III MODULAR BUILDING BLOCK ARCHITECTURE
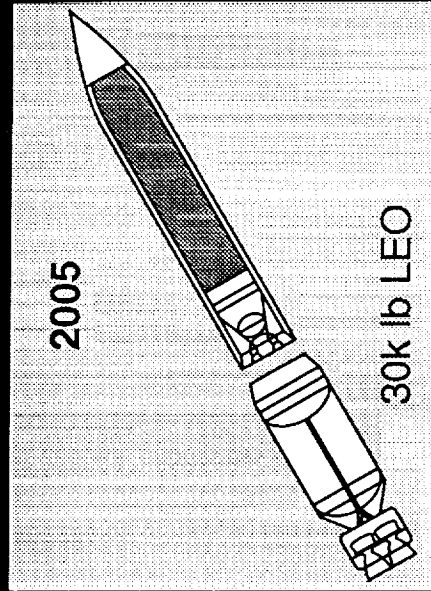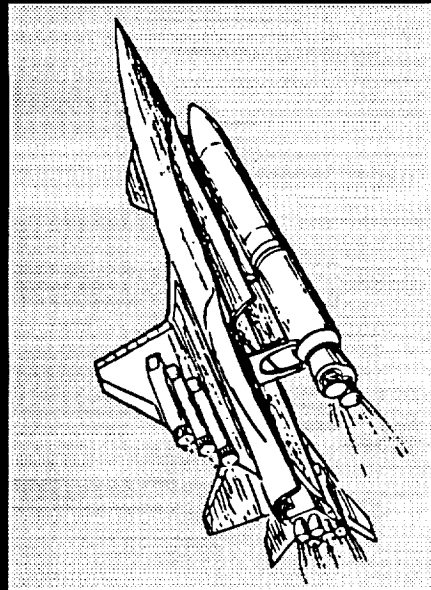
2005

30k lb LEO
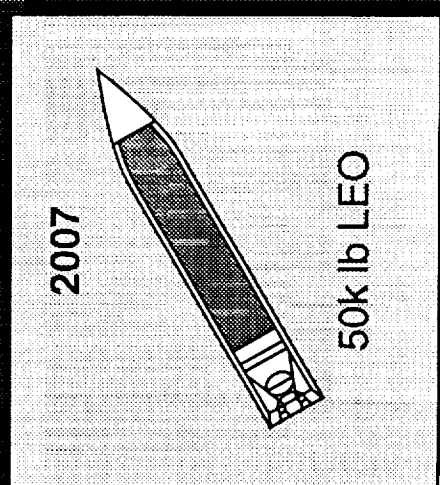
2007

50k lb LEO
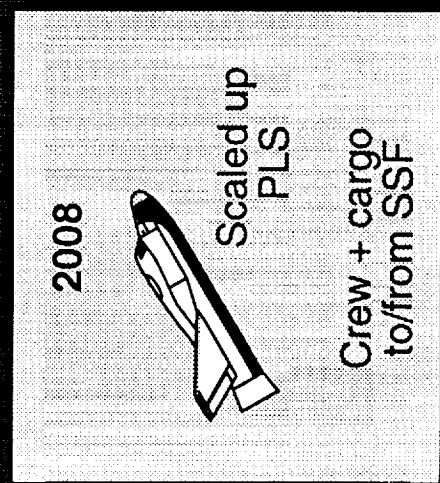
2008

Scaled up PLS

Crew + cargo to/from SSF
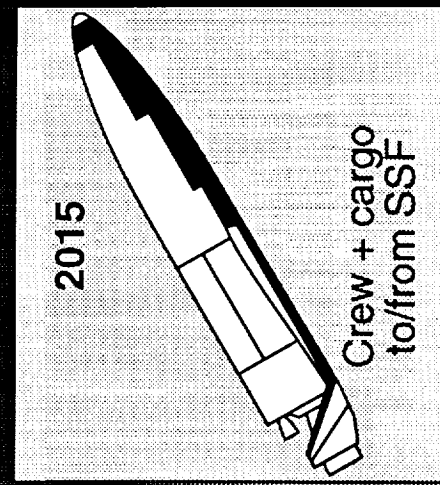
2015

Crew + cargo to/from SSF

Beta III Modular Building Block Architecture

A two-stage airbreather/rocket has been studied by the Boeing Company for the NASA Lewis Research Center and the Air Force Wright Field Laboratory. This concept uses six large jet turbofan engines to lift off the runway. At a suitable altitude and speed, rocket engines on the booster and the second stage are ignited. At Mach 3 to 4 and approximately 100,000-ft of altitude, the second stage separates and goes into orbit while the booster rocket engines shut down, and the booster returns to the launch site. Several different combinations of spacecraft and upper stages could be used with this booster system.

REFERENCE RBCC SSTO DESIGN
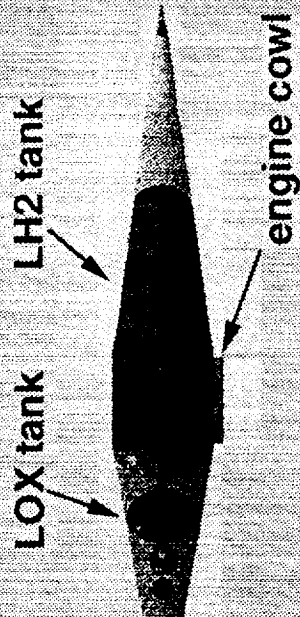
Conical RBCC SSTO
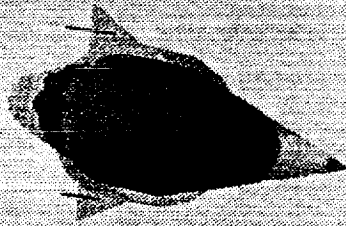
GLOW	721,520 lbs
dry weight	136,400
mass ratio	3.918
LH2 prop wt./total prop	.356
payload bay volume	5300 ft³
payload to 51.6° 220 Nm	25 klbs
vehicle length	288.1 ft
max. body diameter	31.0 ft
wingspan	63.2 ft

Side View

LOX tank

LH2 tank

engine cowl

Top View

payload bay

crew cabin

3 93 - JRO

Reference RBCC SSTO Design

A Single-Stage-to-Orbit (SSTO) airbreather/rocket concept known as the Rocket Based Combined Cycle (RBCC) vehicle has also been defined. This concept could be horizontally or vertically launched. The vehicle shown here is designed to be vertically launched. In this design, the rocket engines located within the cowl supply the initial thrust. As the speed increases, air is ducted into the cowl, and at Mach 3 the airbreathing engine system takes over. At Mach 15, the rocket engines are re-ignited for orbital insertion. This system is designed to complete the ascent trajectory quickly and not for airbreathing cruise. At the completion of the mission, this vehicle lands horizontally.

There is also a National Aerospace Plane concept being examined in this study. Thus, the potential space transportation concepts range from being rather simple and near-term technology to the more complex, far-term technology, large systems.

7 1

SPACE TRANSPORTATION SYSTEM VEHICLE
AVIONICS REQUIREMENTS

- All weather operation

- Autonomous operations/on-board checkout

- Health monitoring

- Multifunction display and controls system

- Autoland, autorendezvous/docking

- Reliable multiple communications channels

Space Transportation System Vehicle
Avionics Requirements

The key advanced avionics requirements for these vehicle concepts are envisioned to provide significantly improved operational efficiency and effectiveness. It is very desirable to have adaptive guidance, navigation, and control approaches that will allow launch and return in almost any weather condition. The vehicles must be able to accommodate atmospheric density variations and winds without software changes. The flight operations must become much more autonomous in all flight regimes like an aircraft, and preflight checkout should make use of the onboard systems. When the vehicle returns to the launch site, subsystem health must be known and maintenance tasks scheduled accordingly. Ground testing of most subsystems must be eliminated. Also, the health monitoring system must be designed to enhance the ability to abort the mission significantly and save the crew and the vehicle. The displays and controls must be much less complex than current systems and must significantly reduce pilot work load. It is important to have low power, light weight displays and controls. Rendezvous and docking and all flight phases must have autopilot capability to reduce pilot work load for routine operations and in abort situations The vehicles must have the demonstrated ability to return to the launch site. Abort from all mission phases can put additional demands on the communications system.

INERTIAL NAVIGATION SYSTEM WITH INTEGRATED GPS

- Improved location capability
- Flight control outputs
- Very low life cycle costs
- No scheduled maintenance
- No re-calibration
- Extensive BIT
- No flight line test equipment
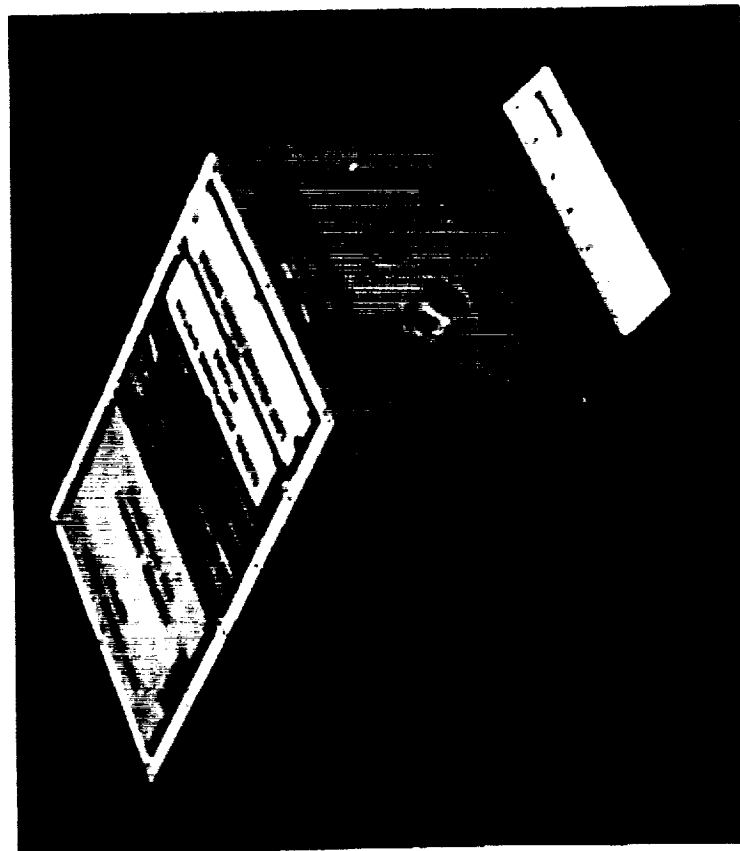
Honeywell Small Lightweight GPS/INS

Inertial Navigation System with Integrated GPS

In order to package, weigh, and cost advanced vehicle concepts, individual subsystem components must be defined. Generally, new technology systems with some demonstrated capability are assumed except where an advanced technology will be mission enabling. In the avionics arena, the new technology components are being developed in several ongoing programs. Honeywell has developed a ring laser inertial system with a tightly coupled Global Positioning System (GPS) receiver integrated in a small, lightweight package. This package requires 65 watts power and has several operationally attractive features which are listed on the figure.

Honeywell

ASCM

Advanced Spaceborne Computer Module
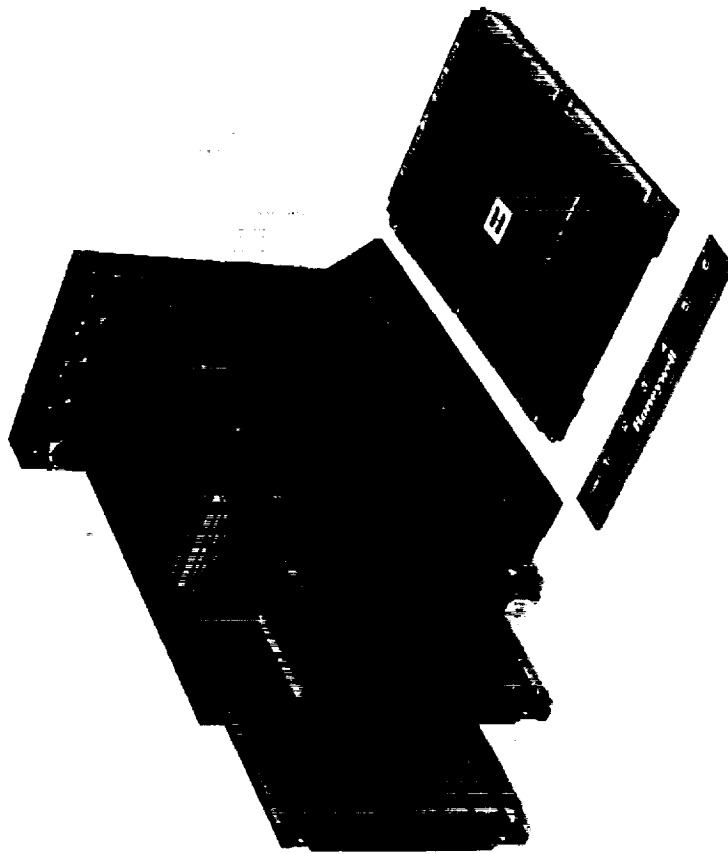
Features

CPM-Control
Processor Module

- MIL-STD 1750A processor
- 1 MBYTES main memory (8Kx8)
- 3-5 MIPS operation
- 10 MBIT/sec serial data bus
- MIL-STD 1553B serial data bus

7 6

ASCM

Advanced Spaceborne Computer Module

A Department of Defense program is funding the development of this computer package. It is a MIL-STD-1750A processor that is small, light weight, and low power with good performance and radiation hardening. At the present time, software is being developed for a self-checking pair architecture. To achieve the fail operational/fail operational/fail safe redundancy requirement generally required for manned space transportation systems, a triplex or quad system will be required. There is also an Advanced Technology Insertion Module for the processor that provides optical data bus ports.

HEADS UP DISPLAY/CLASS COCKPIT CONTROL PANEL

Honeywell Multifunction Electronic Display (MED) to replace electromechanical cockpit instruments and training simulator.

Heads Up Display/Glass Cockpit Control Panel

A new Space Shuttle Orbiter display and control panel shown in the figure is being developed by the Honeywell Satellite Systems Operation as a subcontractor to Rockwell International. The panel has flat panel liquid crystal displays (LCD) that are programmed for several functions depending upon flight regime. These LCD panels are 6.7-in square, weigh about 16 lbs, and require about 90 watts.

VHMS ELEMENTS

Vehicle Health Monitoring System (VHMS)

Flight & maintenance management

Vehicle

Information processing

VHM

Mass storage

Built-in test

Built-in test stimulus

Ground harness

Telemetry link

Ground

GHM

Mass storage

Ground based test

Ground test stimulus

Built-in monitoring

Structures

TVC

Valve

Engine

RCS

Motor

Tank

Power

Sensors

8 0
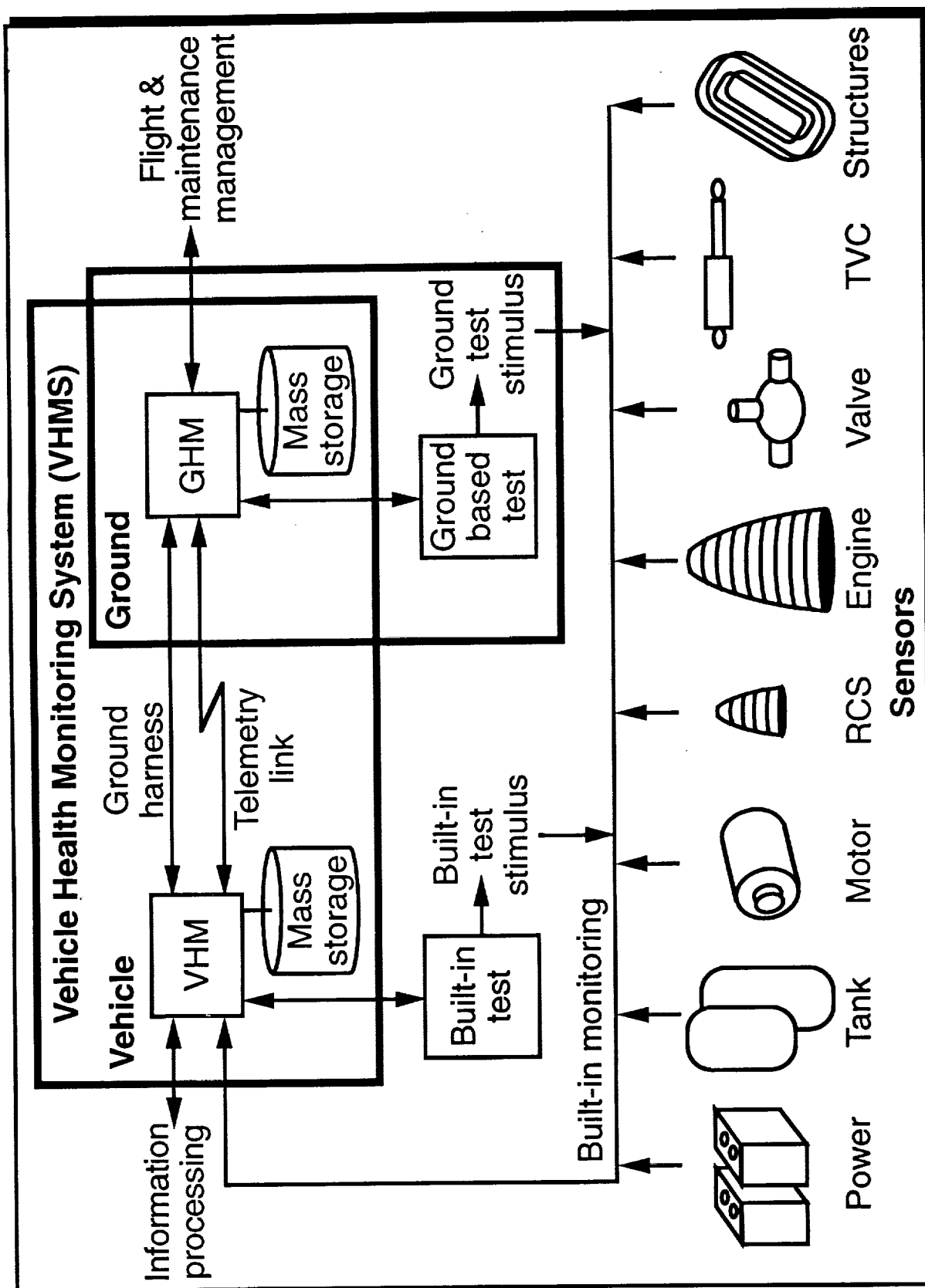
VHMS Elements

The baseline Vehicle Health Monitoring System (VHMS) elements shown in the figure are based on a Boeing design for the Air Force/NASA Advanced Launch System (ALS) program that was developed 3 years ago. The ALS vehicle had a recoverable propulsion/avionics module that was to be reused. The total system has an onboard element and a ground element. The onboard element records data during the flight from the subsystems and sends notification of any potential critical failure to the vehicle information processing system. The ground element analyzes the recorded flight data for use in the ground maintenance procedures and the prelaunch checkout.

AVIONICS TECHNOLOGY FOR FUTURE SPACE TRANSPORTATION SYSTEM VEHICLES

- Demonstrate integrated health monitoring system (including reusable cryogenic tanks)

- Develop and test fault tolerant architecture (hardware and software)

- Develop and demonstrate integrated GNC system for all weather/flight condition operations

Avionics Technology for Future
Space Transportation System Vehicles

In studying advanced space transportation concepts and defining the required avionics system attributes, it appears that the current advanced systems have or will soon have sufficient capability to meet the needs. The next step in technology development is to define representative systems, assemble the hardware, develop the software, and test /demonstrate the systems. An integrated health monitoring system design must be demonstrated including a viable approach for monitoring the health status of reusable cryogenic tanks flight after flight. The fault tolerant processing system development area has issues such as software testing and certification methods and dissimilar backup system requirements that must be addressed. An integrated guidance, navigation, and control system for nearly all weather operations and a viable abort capability also need further definition and demonstration.

HIGHLY-RELIABLE
FLY-BY-LIGHT/POWER-BY-WIRE
TECHNOLOGY
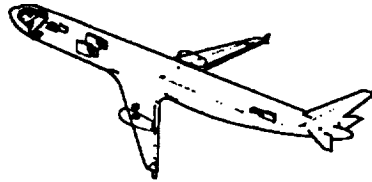
Felix L. Pitts

NASA Langley Research Center

Workshop on Guidance, Navigation, Controls, and
Dynamics for Atmospheric Flight

March 18, 1993

FLY-BY-LIGHT/
POWER-BY-WIRE
TECHNOLOGY

OUTLINE

PROGRAM OVERVIEW
Background
Goals/Objectives
Approach / Milestones
Deliverables

FY 92 PROGRAM ACCOMPLISHMENTS
Workshop Summary
Optical Sensors
EME

FY 93 Plans

ELECTROMAGNETIC MODELING VIDEO

PROGRAM OVERVIEW

FLY-BY-LIGHT/
POWER-BY-WIRE
TECHNOLOGY

PROGRAM HISTORY

- Suggested By Industry In Civil Aeronautics Technology Development and Validation Plan
- NASA AAC Reviews: 11/88-LaRC; 1/90-ARC; 11/91-LeRC
- Non-Advocate Review 8/90 @ NASA HQ
- Draft Working Plan 7/91; Draft Program Plan 9/91
- Requirements Workshop @ LaRC 3/92
- NASA Red/Blue Team: Circa 1992

- APPROXIMATE CURRENT BUDGET (NET $M)

FY 93	FY94	FY95	FY96	FY97	FY98
4	6	7	8	9	10

FBL/PBW

FLY-BY-LIGHT/
POWER-BY-WIRE
TECHNOLOGY

WHAT IS IT?

- REPLACEMENT OF ELECTRONIC DATA TRANSMISSION, MECHANICAL CONTROL LINKAGES, AND ELECTRONIC SENSORS WITH OPTICAL COMPONENTS AND SUBSYSTEMS

- ELIMINATION OF HYDRAULICS, VARIABLE ENGINE BLEED AIR, AND THE CONSTANT SPEED DRIVE FOR POWER GENERATION THROUGH ADVANCES IN AEROSPACE POWER SYSTEM TECHNOLOGY

  - ELECTRONIC MOTOR CONTROLLERS

  - POWER SYSTEM DISTRIBUTION AND CONTROL

BENEFITS

- CIRCUMVENT EMI CONCERNS IN APPLYING DIGITAL CONTROL
  - Intrinsic EMI Immunity and Lifetime Immunity to Signal EMI of Optics
  - Simplify Certification
- ELIMINATE HYDRAULICS, ENGINE BLEED AIR, VSCF DRIVE
- WEIGHT AND VOLUME REDUCTION

ENHANCE DIGITAL CONTROL ACCEPTANCE

FBL/PBW WORK BREAKDOWN STRUCTURE

FLY-BY-LIGHT/
POWER-BY-WIRE
TECHNOLOGY

**HIGHLY RELIABLE FLY-BY-LIGHT/POWER-BY-WIRE
SYSTEMS TECHNOLOGY**

GOAL: Develop the Technology Base for Confident Application of Integrated FBL/PBW Systems to Transport Aircraft

OBJECTIVES:

- 1.0 Requirements and Preliminary Design
- 2.0 Develop and Flight Test Optical Sensors and Electro-Optical Converters
- 3.0 Develop and Ground Test a Power Management and Distribution System and Flight Test an Electrical Actuator
- 4.0 Demonstrate Architecture Design and Validation Appropriate for Certification of FBL/PBW Systems
- 5.0 Develop Validated Analytical and Experimental Assessment Methodologies for Electromagnetic Environment Effects
- 6.0 Demonstrate End-to-End FBL/PBW Systems in Ground Tests and Partial Flight Test

C1-2

FLY-BY-LIGHT/ POWER-BY-WIRE TECHNOLOGY — LaRC FBL/PBW APPROACH LeRC
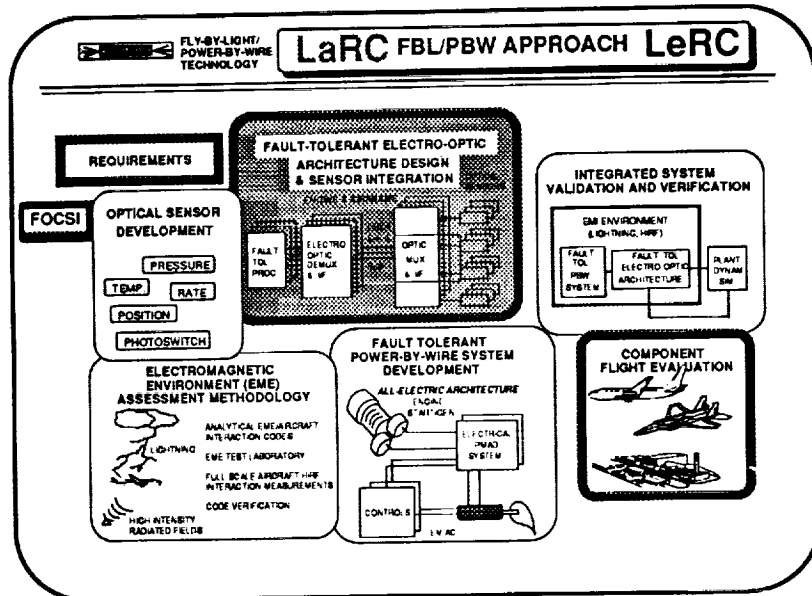
FY 92 ACCOMPLISHMENTS

FLY-BY-LIGHT/ POWER-BY-WIRE TECHNOLOGY

- 1.0 Requirements

  - Conducted Requirements and Technology Workshop at LaRC
  - 160 Participants / NASA CP 10108 Published 9/92
  - Many Open Issues / Few Detailed Requirements Established
  - Recommend System Requirements Study

- 2.0 Develop / Flight Test Optical Sensors and Electro-Optic Converters

  - Functional and Environmental Testing of Optical Sensors and
    Electro-Optics Complete (Pressure, Temp, Pos, RPM, Light-Off)

- 5.0 Develop Validated Analytical and Experimental Assessment
  Methodologies for Electromagnetic Environment Effects

  - HIRF Lab Requirements Defined / Documented
  - Gigahertz Transverse Electromagnetic Chamber Procured
  - EM Modeling of HIRF with 737 Aircraft and Video

ELECTROMAGNETIC ENVIRONMENTAL EFFECTS
SUMMARY

FLY-BY-LIGHT/ POWER-BY-WIRE TECHNOLOGY | **HIGH INTENSITY RADIATED FIELDS (HIRF)**

• **The man-made electromagnetic threat to critical electronic systems aboard advanced aircraft**

- Radars

- Radio Broadcast Transmitters

- Other Emitters of Electromagnetic Energy

HIRF THREAT to ADVANCED AIRCRAFT

- **Composite Structures**
  - Less Shielding than All Metal

- **Flight-Critical Controls**
  - Higher Reliability Requirements than Non-Critical Controls

- **Digital Control Systems**
  - More Sensitive to Transients than Analog
  - Can Cease Correct Operation without Component Damage

*Upsets Cannot Be Tolerated
In Advanced Aircraft Systems*

HIRF OVERVIEW

- FAA Commissioned SAE-AE-4R Committee 12/88
  - Advisory Circular and Users Manual for Hazards of Electromagnetic
    Radiation to Aircraft
- Chair: Stan Schneider, Boeing Military Airplane Co.
  - Secretary: Noel Sargent, LeRC
  - -Three Sub-Committees
    - Environment (Chair: Ron Rodgers, ALPA)
    - Advisory Circular (Chair: Chris Kendall, CKC Consultants)
    - Users Manual (Chair: Fred Heather, Patuxent River NAS)
- Status: Final Meeting 1/92
  - SAE Report Spring 1992
- Problems
  - How to Use and Apply, How to Treat Critical versus Essential Systems
  - Need Lab/Bench Tests
- Research Opportunities
  - Modeling and Test Techniques

DIGITAL SYSTEM UPSET

FLY-BY-LIGHT/
POWER-BY-WIRE
TECHNOLOGY

- **Functional Error Mode**
  - System/Subsystem Level
  - Caused by Electrical Transient
    - Lightning
    - HIRF
    - NEMP
    - SEU / Inter-Galactic Particles
  - No Component Damage
- **Corrective Action**
  - Reset/Reload Software
  - Internal Recovery Mechanism
- **No Standard Guidelines/Criteria**
  - Upset Detection
  - Designing Reliable Upset Recovery Mechanisms
  - Performing Tests/Analyses for Upset Susceptibility/Reliability

CURRENT EME ACTIVITIES

FLY-BY-LIGHT/
POWER-BY-WIRE
TECHNOLOGY

- Lawrence Livermore Transport Aircraft Internal EME

- LaRC Lab HIRF Assessment

  - AIRLAB HIRF Test Facility
  - Bendix Quad Flight Control System (Loan)

INTERNAL EME

OBJECTIVE:

Develop a baseline internal Electromagnetic Environment (EME) assessment methodology for the proposed Fly-By-Light/Power-By-Wire augmentation

APPROACH:

Apply Lawrence Livermore National Laboratory (LLNL) weapons system High Power Microwave EME assessment technology to transport aircraft

- Model EM interactions using LLNL codes
- Validate model with experimental data
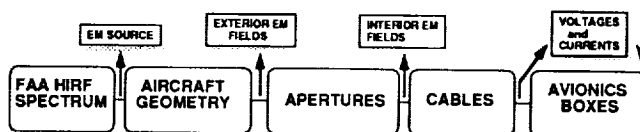
EM MODELING

TEMPORAL SCATTERING & RESPONSE EM MODELING

LAWRENCE LIVERMORE EM CODES

PRE-PROCESSING   PHYSICS   POST-PROCESSING

HIRF LABORATORY

FLY-BY-LIGHT/
POWER-BY-WIRE
TECHNOLOGY

Test Cell or
Reverberation Chamber

Bendix
Flight
Control
Computer

EM
Source

EM
Field

The flight control computer
is subjected to EM fields
within a test cell.

Simulation of
Aircraft, Engines,
Sensors, Actuators

The flight control computer is
connected to a simulation
of the aircraft, engines,
sensors, and actuators.

Laboratory
Instruments

EM field data, operational
data from the flight control
computer, and the effect of
the control computer on
the simulated aircraft are
collected for analysis.

AIRLAB HIRF EM TEST LAB

FLY-BY-LIGHT/
POWER-BY-WIRE
TECHNOLOGY

- GIGAHERTZ TRANSVERSE ELECTROMAGNETIC CELL (GTEM)
  - High Field Levels (1 kV/m CW) Testing DC to 1 GHz
  - Moderate Field Levels (<400 V/m CW) Testing DC to 10 GHz
  - High Field Levels Pulse Testing (40 kV/m) from DC to 10 GHz
  - Instrument Calibration Capability DC and 10 GHz

- REVERBERATION CHAMBERS
  - Low Power (0.9kW vs 65kW @ 1kV/m, 1GHz for GTEM)
  - No Test Article Re-orientation
  - RC1 Coverage >87MHz, RC2 Coverage >141MHz
  - Random Field Polarization and Large Number of Modes
    Necessitate Separate Sensor Calibration Facility such as GTEM

FLY-BY-LIGHT/
POWER-BY-WIRE
TECHNOLOGY

EM TEST LAB FREQUENCY COVERAGE

GIGAHERTZ TRANSVERSE
ELECTROMAGNETIC CELL (GTEM)

RADIO FREQUENCY
ABSORBER

1 m TEST SECTION

1 kV/m @ 65kW
200 V/m @ 800W

REVERBERATION CHAMBERS (RCs)

RC1: 47'X23'X9.5' 60 MODES @ 87MHz 860V/m		
RC2: 60 MODES @141 MHz 1420 V/m	AMPLIFIER ROOM SHIELD ROOM	CONTROL ROOM

Frequency
GHz 100
GHz 10
GHz 1
MHz 100
MHz 10
MHz 1
kHz 100
kHz 10

RCs
GTEM

FY 93 PLANS

9 4
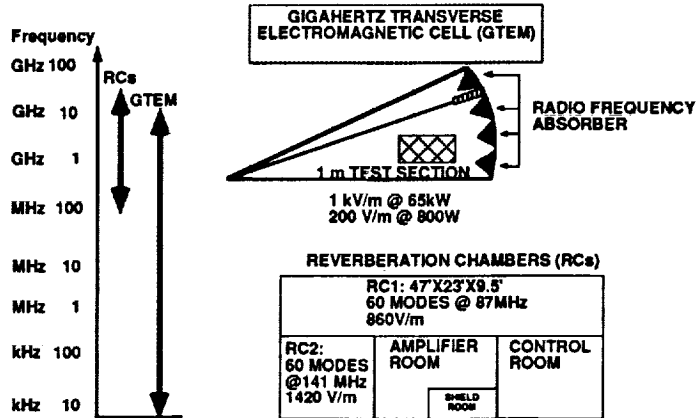
FY 93 PLANS

- • 1.0 Requirements
- - Integrated Requirements Analysis and Preliminary Design Studies
- • 2.0 Develop and Flight Test Optical Sensors and Electro-Optical Converters
- - Flight Test FOCSI Optical Sensors on F-18 SRA
- - Competitive Procurement of Task Assignment Contract
- • 3.0 Develop and Ground Test a Power Management and Distribution System and Flight Test an Electrical Actuator
- - Competitive Procurement of Task Assignment Contract
- • 4.0 Demonstrate Architecture Design and Validation Appropriate for Certification of FBL/PBW Systems (Prelim Design under 1.0)
- • 5.0 Develop Validated Analytical and Experimental Assessment Methodologies for Electromagnetic Environment Effects
- - Validate Code with ATOPS 737 Aircraft, HIRF 400Hz Protection Study
- - Build HIRF Lab

Integrated Requirements Analysis
and Preliminary Design Studies

- • REQUIREMENTS GENERATION
  - - Aircraft Specification
  - - Most Aircraft Systems-Priority to Flight Critical Systems
  - - Sensors, Actuators, Computation, Power, Pneumatics
- • TECHNOLOGY ASSESSMENTS
  - - Photonics, Sensor Encoding, Various Electrical Actuators, Power, Pneumatics,

    Data Comm, Systems Technologies/Integration
- • ARCHITECTURE TRADES
  - - Centralized/Distributed, Dumb/Smart Actuators, Integrated/Stand Alone Power Mgt, Integration/Separation of Critical and Non-Critical Tasks
- • SYSTEM DESIGN and ANALYSIS
  - - Preliminary Design of Candidate Architecture
  - - Recommend Flight Configuration for 1996 and 1998 Demo

DIFFERENTIAL GPS FOR AIR TRANSPORT - STATUS

RICHARD M. HUESCHEN

OF

LANGLEY RESEARCH CENTER
FLIGHT SYSTEMS DIRECTORATE
GUIDANCE AND CONTROL DIVISION
AIRCRAFT GUIDANCE AND CONTROLS BRANCH

MARCH 18, 1993

OUTLINE

BACKGROUND

- Global Navigation Satellite System (GNSS)

- Initial Operational Capability for Various Transport Aircraft Operations

- Differential GPS

LARC/HONEYWELL FLIGHT TESTS

- Description of System and Tests

- Test Results

OHIO UNIVERSITY GRANT

- GPS Interferometry

- Attitude & Heading Determination

- Precision DGPS Navigation

- Status

AGCB Aircraft Guidance & Controls Branch   2

The presentation presents background on what the Global Navigation Satellite System (GNSS) is, desired target dates for initial GNSS capabilities for aircraft operations, and a description of differential GPS (Global Positioning System).

The presentation also presents an overview of joint flight tests conducted by LaRC and Honeywell on an integrated differential GPS/inertial reference unit (IRU) navigation system. The overview describes the the system tested and the results of the the flight tests.

The last item presented is an overview of a current grant with Ohio University from LaRC which has the goal of developing a precision DGPS navigation system based on interferometry techniques. The fundamentals of GPS interferometry are presented and its application to determine attitude and heading and precision positioning are shown. The presentation concludes with the current status of the grant.
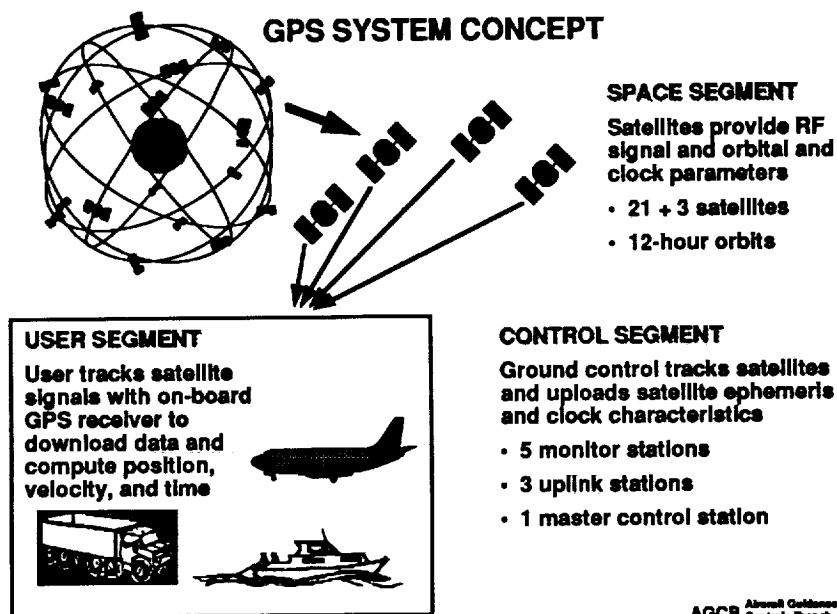
GNSS (GLOBAL NAVIGATION SATELLITE SYSTEM)

- GNSS, Defined by ICAO, Encompasses All Current and Future Satellites that will be Available for Global Aircraft Navigation

- Currently, Navstar GPS and GLONASS are Providing Global Navigation Signals in a Pre-Operational Mode

- The GPS (Global Positioning System) is Scheduled to be Operational Late '93 or Early '94 and GLONASS '95 (?)

- Expect in the Future that GPS like Signals will be Available on Geostationary Inmarsat Satellites

AGCB Aircraft Guidance & Controls Branch

The Global Navigation Satellite System (GNSS) is the name adopted for world-wide satellite navigation by the International Civil Aviation Organization (ICAO). Two global satellite navigation systems are currently under development and both are currently providing signals for use in a pre-operational mode. One is the Global Positioning System (GPS) being developed in the United States by the DOD and the other is the Global Orbiting Navigation Satellite System (GLONASS) being developed by Commonwealth of Independent States (CIS and formerly the Soviet Union). The GPS is expected to achieve full operational capability by late 1993 or early 1994 and GLONASS in 1995. Substantial uncertainty exists for the operational date of GLONASS due to the current instability in the CIS. Plans are underway to provide GPS-like signals on the geostationary Inmarsat satellites. These signals will provide redundant coverage for increased reliability. In addition, Inmarsat is being considered for transmission of a health/status message for GPS called the GPS Integrity Channel (GIC). In summary, GNSS encompasses all satellite systems providing navigation information including integrity messages regarding the navigation information.

GPS SYSTEM CONCEPT

SPACE SEGMENT

Satellites provide RF signal and orbital and clock parameters

- 21 + 3 satellites
- 12-hour orbits

USER SEGMENT

User tracks satellite signals with on-board GPS receiver to download data and compute position, velocity, and time

CONTROL SEGMENT

Ground control tracks satellites and uploads satellite ephemeris and clock characteristics

- 5 monitor stations
- 3 uplink stations
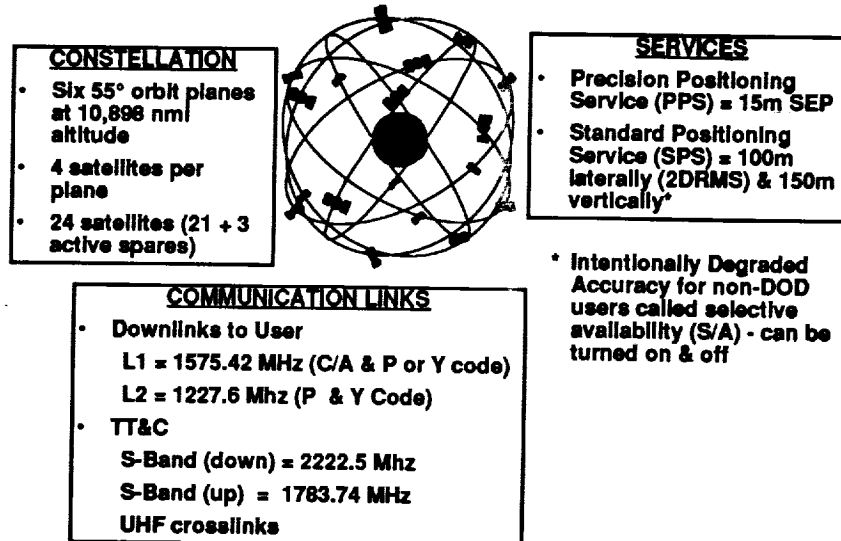- 1 master control station

AGCB Aircraft Guidance & Controls Branch

There are three major segments for a global satellite navigation system – the space segment, the user segment, and the control segment. This viewgraph depicts these segments and gives some general information about them for the GPS. The GPS space segment will contain 24 satellites – 21 will be activity and 3 will be spares to replace a malfunctioning or failed satellite. The space segment provides an RF signal which contains orbital and precision clock parameters for the satellite. The RF signal is also modulated by a unique digital bit-pattern sequence or code.

The user segment consists of those entities (airplanes, ships, trains, cars, trucks, boats, surveyors) which have a GPS receiver. The GPS receiver also contains a precision clock and generates the same unique bit patterns as the satellites. The receiver downloads the orbital data and clock parameters of the satellite and correlates the received bit pattern with the receiver bit pattern to determine signal transmission time. Given this time, the range (commonly referred to as the pseudorange) to the satellite is computed using the speed of light and compensation for ionospheric and tropospheric bending. From four pseudoranges the three-dimensional position of the vehicle is determined given the satellite positions (determined from transmitted orbital parameters). Four pseudoranges are required because there are four unknowns (3 position dimensions and the receiver clock bias). The receiver also computes the vehicle velocity from Doppler measurements and provides a precision time measurement.

The control segment tracks the satellites. From tracking measurements the control segment computes the ephemeris and clock parameters of each satellite and then uploads this data to the satellites. The GPS has 5 monitor stations, 3 uplink stations, one master control station, and one backup control station.

GPS BLOCK II SATELLITES

CONSTELLATION

- Six 55° orbit planes at 10,898 nmi altitude
- 4 satellites per plane
- 24 satellites (21 + 3 active spares)

SERVICES

- Precision Positioning Service (PPS) = 15m SEP
- Standard Positioning Service (SPS) = 100m laterally (2DRMS) & 150m vertically*

* Intentionally Degraded Accuracy for non-DOD users called selective availability (S/A) - can be turned on & off

COMMUNICATION LINKS

- Downlinks to User

  L1 = 1575.42 MHz (C/A & P or Y code)

  L2 = 1227.6 Mhz (P & Y Code)
- TT&C

  S-Band (down) = 2222.5 Mhz

  S-Band (up) = 1783.74 MHz

  UHF crosslinks

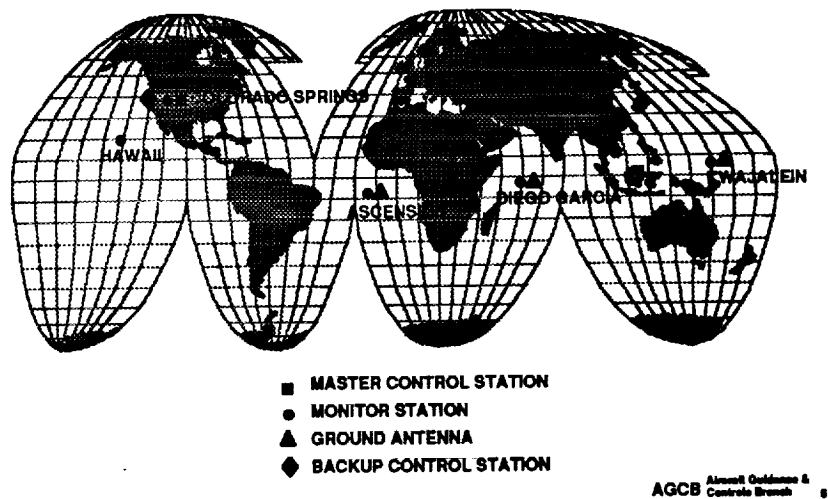AGCS Aircraft Guidance & Controls Branch

The GPS satellites will be contained in six 55° orbital planes 10,898 nautical miles above the earth which results in 12-hour orbits. Four satellites will be in each plane for a total of 24 satellites. Twenty-one of the satellites will be active and 3 will be spares for use in the advent of a satellite malfunction or failure.

The GPS provides two types of services. One is Precise Positioning Service (PPS) and the other is Standard Positioning Service (SPS). PPS is intended primarily for DOD or military operations while SPS is provided for civilian operations. The accuracy of the PPS is 15 meters SEP (spherical error precision – probability of errors within specification is 50%). This accuracy is met with a GPS receiver that acquires a satellite signal with the carrier-modulated Course Acquisition (C/A) code and then subsequently locks onto the carrier-modulated precision (P) code which provides higher accuarcy than the C/A code.

SPS is intended for civilian use and civilian receivers use the C/A code. The 2DRMS (twice the standard deviation of the circular standard error – probably of errors within specification is 96%) accuracy of this service is 100 meters horizontally and 150 meters vertically. The SPS accuracy results from an intentional degradation of the signal by the DOD which is referred to as Selective Availability (S/A). S/A can be turned on and off. When off the SPS accuracy would be on the order of 30 meters.

There are two communication downlinks to the user called L1 and L2. L1 operates at 1575.42 MHz and carries both C/A and P code plus system data. The DOD can encrypt the P code and when so done the P code is referred to as Y code. A key must be obtained from the DOD to decipher the encrypted code. L2 operates at a frequency of 1227.6 MHz and carries P or Y code plus system data. Tracking, telemetry, and control (TT&C) uses two S-band frequencies – 2222.5 MHz for downlink and 1783.74 MHz for uplink. TT&C also makes use of UHF crosslinks.

GPS CONTROL SEGMENT

- ■ MASTER CONTROL STATION
- ● MONITOR STATION
- ▲ GROUND ANTENNA
- ◆ BACKUP CONTROL STATION

AGCB Aircraft Guidance & Controls Branch

This viewgraph shows the location of the various ground stations and equipment for the GPS Control Segment. The master control station is located in Colorado Springs with a backup control station located in California. Monitor stations are located in Hawaii, Ascension Island, Diego Garcia, and Kwajalein.

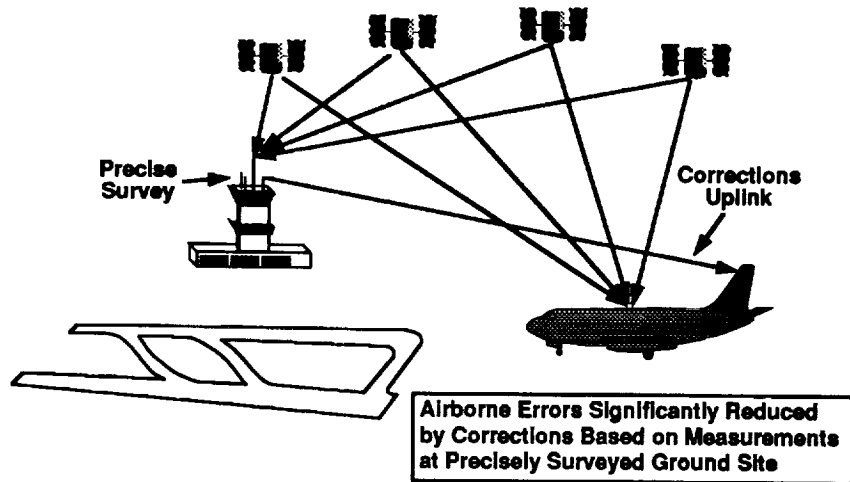## GNSS INITIAL OPERATIONAL CAPABILITY TARGETS
(NAVIGATION)

YEAR	Initial Operational Capability
93	GNSS Supplemental Means (Oceanic)
94	GNSS Sole Means (Oceanic)
94	GNSS Airport Surface Navigation (Requires augmentation; e.g., Differential GNSS & Low Speed Data Link)
95	GNSS Precision Approach (200 DH / 1800 RVR) (Requires augmentation; e.g., Differential GNSS & Low Speed Data Link)
95	GNSS Sole Means (Domestic)
97	GNSS-Based Autoland & Takeoff (300 RVR) (Requires augmentation; e.g., Differential GNSS & Low Speed Data Link)

AGCB Aircraft Guidance & Controls Branch

A GNSS task force under the direction of the RTCA was requested by the Federal Aviation Administration (FAA) to examine various applications of GNSS and to develop a series of basic technical system requirements to achieve various desired capabilities for early implementation of GNSS within the United States. The dates listed were obtained from the recently released task force report and are the earliest desired initial operational capabilities (IOC) for GPS. The GNSS Task Force believes that the technology will be in place to realize the initial operational capabilities by the dates shown. These capabilities would initially be approved by the FAA for certain areas and for use by properly equipped aircraft.

The GNSS Supplemental Means IOC is expected to occur this year. The definition of Supplemental Means navigation is the use of GPS in conjunction with some other navigation system such as Omega. Sole Means navigation is GPS navigation only without the availability of another on-board navigation system.

DIFFERENTIAL GPS

Precise Survey

Corrections Uplink

Airborne Errors Significantly Reduced by Corrections Based on Measurements at Precisely Surveyed Ground Site

AGCB Aircraft Guidance & Controls Branch

This viewgraph depicts the basic concept of differential GPS. The basic concept is to improve the airborne navigation solution by transmitting corrections to the airborne system based on GPS measurements made at a fixed site whose position is precisely known. The fixed ground site makes measurements of the satellites in view and computes corrections to the measurements based on its known location. These corrections are then transmitted to the airborne system (or ship, train, etc.) and processed in the airborne system to reduce the errors in the airborne measurements.

HONEYWELL/LARC DGPS/INS FLIGHT TESTS

- **Objectives of Tests were**
  - **Determine Potential of DGPS/INS for Use in Autoland Systems of Space Vehicles.**
  - **Record Extensive Data Base for Post-Flight Nav Accuracy Assessment**
- **Flight Tests Conducted Using HW Integrated DGPS/INS System (2-channel C/A code tracking GPS receiver)**
- **Data Gathered During Joint Flight Test Conducted by LaRC & HW Oct-Nov 1990 (S/A Off)**
- **Recorded DGPS/INS, MLS/INS, Autonomous GPS, Inertial Nav Data on Aircraft; Laser Tracking Position on the Ground**

AGCB Aircraft Guidance & Controls Branch

In early 1990, LaRC and Honeywell entered in to an agreement to flight test an integrated DGPS/Inertial Navigation System (INS) on Langley's Transport Systems Research Vehicle (TSRV) - a Boeing 737 research aircraft. The DGPS/INS had been developed by Honeywell. The system consisted of a GPS receiver, a GPS processor, and a laser gyro inertial reference unit.
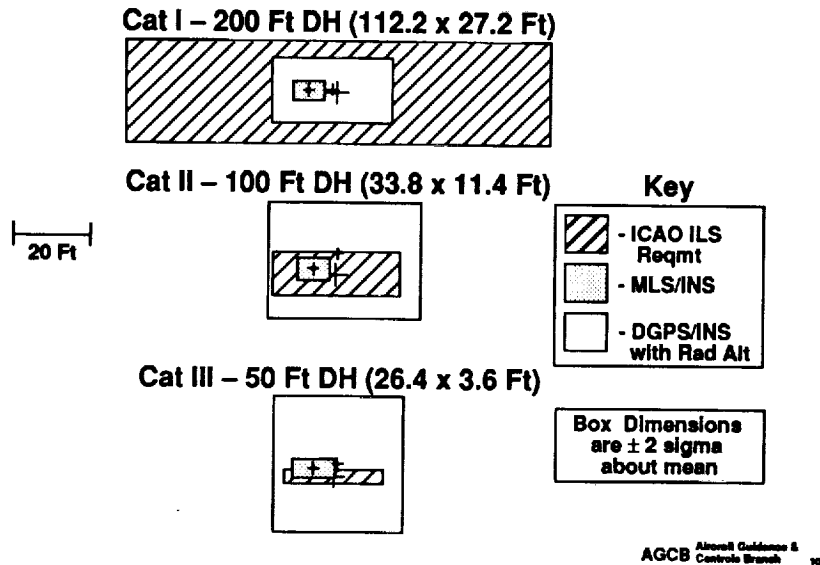
One objective of the test was to determine the potential of the DGPS/INS for use in autoland systems for space return vehicles - e.g. the shuttle and emergency return vehicle vehicles from the space station. A second objective was to record an extensive data base for post-flight evaluations and assessment of the navigation accuracy of the DGPS/INS.

The GPS receiver used in the Honeywell system was an early receiver design. The receiver was a 2-channel sequential C/A code tracking receiver. The technology has advanced rapidly making this design outdated. Typical receiver designs today have 6 to 10 channels and some have 12 channels for simultaneous tracking of several satellites.

The flight tests were conducted in October and November of 1990 during a time when the Selective/Availability (S/A) was turned off, that is, the intentional DOD corruption was not being added to the transmitted signals. The DOD had turned S/A off so that they could obtain good accuracy with the civilian GPS receivers they were using for their Desert Storm operations. There were not enough military GPS receivers available for their planned operations at that time. In any case, the navigation accuracy of the DGPS/INS should be the same even if S/A was on since differential GPS removes the corruption added by S/A.

The data that was recorded simultaneously on the TSRV for these tests included data from the DGPS/INS, a Microwave Landing System (MLS)/INS, Autonomous GPS (the basic measurements from the GPS receiver without inertial aiding), and aircraft inertial and air-data measurements. On the ground, the TSRV position was measured by a laser tracking and recorded along with a time tag for post-flight merging with the aircraft data.

NAV ERRORS VS LANDING SYSTEM REQUIREMENTS

Cat I – 200 Ft DH (112.2 x 27.2 Ft)

Cat II – 100 Ft DH (33.8 x 11.4 Ft)

Key

20 Ft

- ICAO ILS Reqmt
- MLS/INS
- DGPS/INS with Rad Alt

Cat III – 50 Ft DH (26.4 x 3.6 Ft)

Box Dimensions are ± 2 sigma about mean

AGCB Aircraft Guidance & Controls Branch

This viewgraph shows the results of a statistical analysis on the flight test data which was presented at the Institute of Navigation Conference in January 1992 and published in an ION paper by R. M. Hueschen and C. R. Spitzer of LaRC.

The cross-hatched boxes represent the performance windows established by the International Civil Aviation Organization (ICAO) for Category I, II, and III Instrument Landing Systems (ILS). The windows are centered about the ILS localizer and glideslope landing path (large plus signs) at specified decision heights. The width and height of the boxes represent, respectively, the required lateral and vertical performance. The top cross-hatched box is the required system performance an ILS system must meet to be certified for Category I operations. Data must show that the aircraft will be inside this box 95% of the time (statistically two standard deviations or 2σ) at 200 feet decision height. The middle cross-hatched box is the 2σ performance box for Category II performance at 100 feet decision height and the bottom one for Category III performance at 50 feet decision height.

The shaded boxes show the 2σ performance obtained from the MLS/INS. These boxes show that the MLS/INS met Category I, II, and III performance relative to the localizer (lateral deviation) and Category I and II performance relative to the glideslope (vertical deviation). The plus signs inside the boxes represent the mean of the lateral and vertical deviation, respectively, from the localizer and glideslope centerlines.

The white boxes represent the 2σ performance of the DGPS/INS with radar altimeter aiding. These boxes show that the DGPS/INS with radar altimeter aiding met the Category I performance requirement. This system was close to meeting the Category II lateral performance requirement and considerably exceeded the Category II and III vertical performance requirement. The vertical accuracy of DPGS/INS without radar altimeter aiding could not meet the Category I performance requirement.

107

OHIO UNIVERSITY GRANT

Three-Year Grant (Initiated April 6, 1992) from LaRC to Developed GPS
Interferometry Technology

Year 1

Demonstrate GPS Interferometry to Achieve Real-Time, 3-D
Relative Positioning Accuracies to 0.1 meter

Investigate Feasibility of GPS Interferometry for In-Flight
Reference System and Autoland Applications

Year 2

Continued Development of GPS Interferometry Core
Technology

Improvement of Aircraft Attitude and Heading Determination
from 1 mrad to 0.1 mrad

Year 3

Full Characterization of GPS Interferometry in Terms of
Accuracy and Robustness

Integration of GPS with Inertial Measurement Data

AGCB Aircraft Guidance & Controls Branch 11

A three-year grant (renewable on a yearly basis) was initiated with Ohio University on April 6, 1992 to develop GPS interferometry technology. A major purpose of the grant is to develop a differential GPS airborne in-flight reference system for the TSRV. In addition to serving as an in-flight reference system, this system is planned to be coupled to research guidance and control systems designed for GPS navigation in future flight tests.

The focus of the first year of the grant was to implement and flight test a DGPS navigation system using based on GPS interferometry techniques and demonstrate that the system could achieve real-time three-dimensional relative positioning accuracy of 0.1 meter. Also, this implementation was to determine the feasibility of using the system as an in-flight navigation reference and for autoland applications. As an in-flight reference system, it would be used to determine the performance of other research navigation systems such as a low-cost GPS or a GPS/low-cost IRU system. The feasibility for autoland applications is to be determined by assessing the performance of the inertially-aided TSRV autoland system when coupled to the DGPS during the flight tests.

The focus of the second year was continued development of the core GPS interferometry technology (e.g. developing algorithms to resolve carrier-phase integer ambiguity and developing methods to minimize multipath). During this year, the grant will continue some previous research by Ohio University on aircraft attitude and heading determination with GPS interferometry. The goal is to improve attitude and heading accuracy from previously demonstrated accuracy of 1 mrad to an accuracy of 0.1 mrad.

In year three the grant would complete the full characterization of GPS interferometry in terms of the system robustness and accuracy achievable under various conditions. Also, the grant would address the integration of the GPS data with inertial measurements focusing primarily on low-cost inertial systems.

GPS INTERFEROMETER

$$\Delta\phi = \phi_1 - \phi_2 = \underline{b}\cdot\underline{\hat{e}} + N\lambda + f\Delta t_{ue}$$
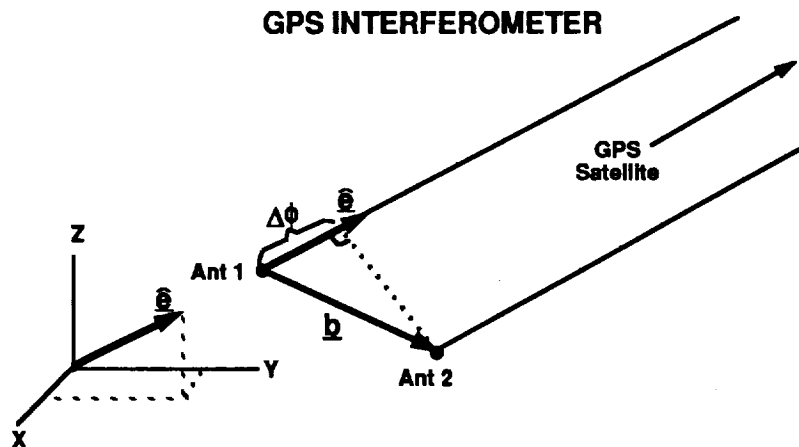
This viewgraph illustrates the fundamentals of GPS interferometry . A GPS interferometer consists of two GPS antennas separated by a baseline vector, $\underline{b}$, and connected to a GPS receiver. Each antenna receives signals from the same GPS satellite and the paths to the satellite from the antennas are consider parallel given the relatively short length of $\underline{b}$ compared to the distance to the satellite (approximately 11,000 nautical miles). In other words, the GPS carrier signal can be considered as a plane wave. The direction to the satellite is represented by the unit vector, $\underline{e}$. The phase of the GPS carrier signal is measured at each antenna resulting in phase measurements ϕ_1 and ϕ_2. Taking the difference of these measurements, called the single difference, represents the path length difference of the paths from the satellite to each antenna and is given by $\Delta\phi$ which is equal to the dot product of the baseline vector with the unit vector plus two additional terms. The term $N\lambda$ is a distance equal to the ambiguity in the number (N) of whole carrier cycles and is referred to as integer ambiguity. The term $f\Delta t_{ue}$ is a distance error due an unknown receiver clock offset from the satellite clock.
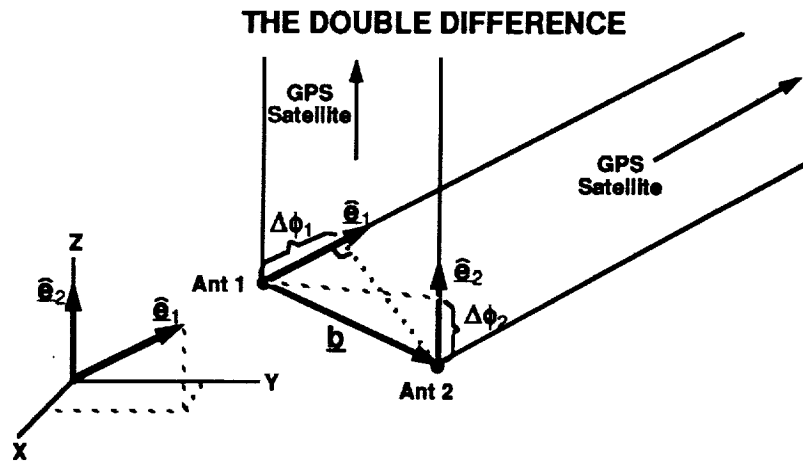
THE DOUBLE DIFFERENCE

$$DD = \Delta\phi_1 - \Delta\phi_2 = \underline{b} \cdot (\hat{\underline{e}}_1 - \hat{\underline{e}}_2) + N\lambda$$

If another single difference is determined from two more phase measurements from the carrier signal of another satellite, then taking the difference of two single differences forms the double difference (DD). The double difference eliminates the error due to receiver clock offset. However, the double difference will still contain an error dur to carrier cycle integer ambiguity.

BASELINE DETERMINATION

- Two Antennas
- Four Satellites
- Three Double Differences

$$\begin{bmatrix} DD_1 \\ DD_1 \\ DD_1 \end{bmatrix} = \begin{bmatrix} (\hat{e}_1 - \hat{e}_2)^T \\ (\hat{e}_1 - \hat{e}_3)^T \\ (\hat{e}_1 - \hat{e}_4)^T \end{bmatrix} \begin{bmatrix} b_1 \\ b_2 \\ b_3 \end{bmatrix} + \begin{bmatrix} N_1 \\ N_2 \\ N_3 \end{bmatrix} \lambda$$
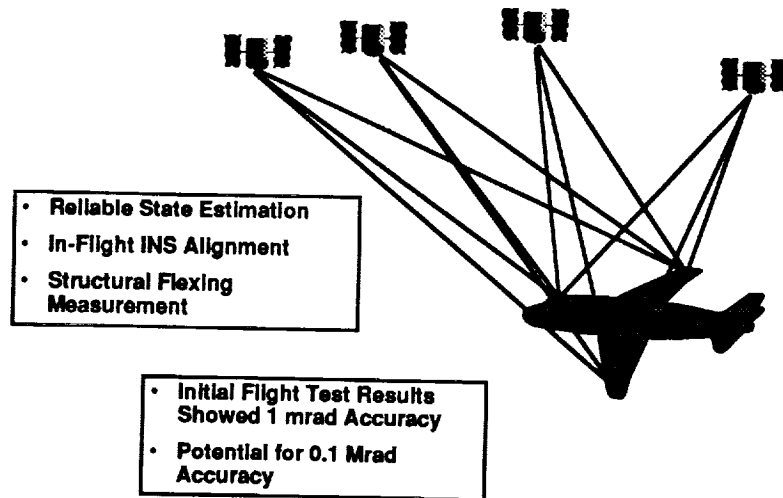
Double differences

Unit Vectors
to Satellites

Baseline Vector

Integer Ambiguities

Given two GPS antennas and four GPS satellite carrier signals, three independent double differences (DD) can be formed. The three double differences can be put into vector form as shown in the equation on the viewgraph. The baseline vector between the two antennas can be determined by solving this equation. This solution will contain the error due to carrier cycle integer ambiguity represented by the term on the right until the ambiguity can be resolved. In general, search methods can be used to quickly resolve the integer ambiguities when more than four satellites are available. Since the L1 carrier wave length is 19 cm and highly accurate phase measurements can be made in the GPS receiver, the baseline vector vector can be determined with high precision, especially when the carrier cycle integer ambiguity can be resolved. With the technology available in today's GPS receivers, the integer ambiguity is on the order of 5 cycles (approximately 1 meter) in the initial solution of the baseline vector. The time to resolve the integer ambiguity with current methods depends on the number of satellites available. A minimum of five satellites is required to resolved the integer ambiguity (four are required to obtain a three-dimensional solution). With five satellites available and current algorithms, the time to resolve the ambiguity can be on the order of 100 to 200 seconds. If six satellites are available, the time is less than 100 seconds. These times are based on the speed of a Intel 486 processor.

ATTITUDE AND HEADING DETERMINATION

- **Reliable State Estimation**
- **In-Flight INS Alignment**
- **Structural Flexing Measurement**

- **Initial Flight Test Results Showed 1 mrad Accuracy**
- **Potential for 0.1 Mrad Accuracy**

AGCB Aircraft Guidance & Controls Branch   16

If multiple antennas are installed on an aircraft and the distance between them is measured accurately, then GPS interferometry can be used to precisely determine aircraft attitude and heading. The GPS attitude and heading determination could be used in conjunction with an inertial reference unit (IRU) to provide reliable state estimation. It could also be used to align an inertial navigation system (INS) in flight (INS alignment normally requires 10 to 20 minutes sitting on the ground). The potential exists to determine aircraft structural flexing with the multiple antenna installation in conjunction with an IRU.

A GPS attitude and heading system was flight tested by Ohio University on their research DC-3 and the flight test results showed an accuracy of 1 mrad for attitude and heading determination. The heading accuracy is generally better than that obtained by IRU's. With further development, there is the potential to increase the accuracy of GPS attitude and heading determination to 0.1 mrad.

PRECISION DGPS NAVIGATION
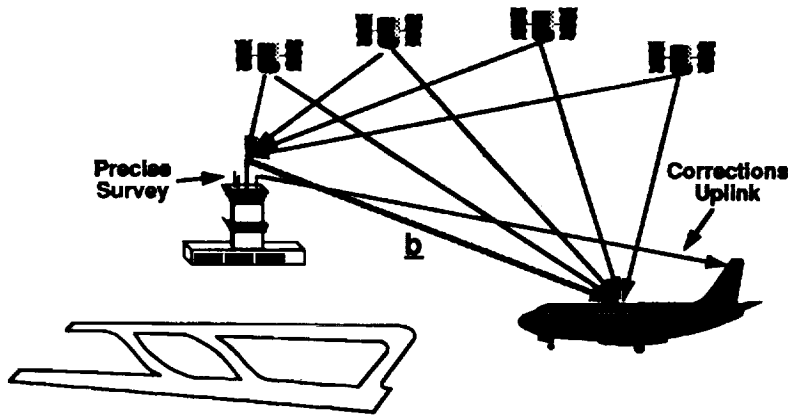
Determine Baseline **b** to within 0.1m in Real Time

AGCB Aircraft Guidance & Controls Branch

GPS interferometry can be used for precise position determination employing differential GPS (DGPS) techniques. For DGPS operation, one GPS antenna and receiver are located on the ground. This antenna is mounted at a precisely surveyed point. Another antenna and receiver are placed on the aircraft. The ground site then makes measurements on the GPS signals and determines corrections for the received signals based on its precisely known location. These corrections are then transmitted (uplinked) to the aircraft and applied to the GPS signals measured by the airborne receiver. Using the current computer technology, these corrections can be processed with the GPS receiver measurements and interferometry calculations to determine the baseline vector (the vector from the GPS ground antenna to the airborne GPS antenna) in real-time. The potential accuracy in the determination of the baseline vector is 0.1 meter. Achieving this accuracy is dependent on the success of developing robust processing techniques to minimize integer ambiguity and multipath errors. The minimization of multipath will also be dependent on hardware considerations such as ground and airborne antenna design and ground antenna siting.

PRECISION DGPS NAVIGATION STATUS

- Flight Tests on ATOPS TSRV (B737) Planned for Mid-April 1993 at Wallops Flight Facility
  - Open-Loop
  - Closed-Loop Autoland

- Potential Flight Test on TSRV at PAX River in Mid-May 1993
  - Different Environment for System Test
  - Process "Truth" Position Using Simultaneous Measurements from Multiple Trackers

AGCB Airsoft Guidance & Controls Branch 17

This viewgraph presents the status of the first-year effort of the grant with Ohio University. A DGPS navigation system has been developed and is planned to be flight tested on the TSRV in April 1993. The initial flight tests will consist of open-loop (not coupled to automatic G&C) approaches and landings to runways at Wallops Flight Facility. While performing these tests the aircraft will be tracked by a laser tracker at Wallops and the tracking will be recorded for post-flight processing with the airborne recorded data. After analyses show that the navigation system is performing properly and with acceptable accuracy, the system will be coupled to the autoland system of the TSRV and closed-loop approaches and landings will be performed (approximately forty are planned).

Potential flight tests are also planned at the Naval Air Warfare Center (NAWC) facilities at Patuxent River, Maryland. These tests will provide another environment in which to test the performance of the DGPS navigation system. Also, the NAWC will track the TSRV with multiple tracking facilities. NAWC will use the multiple tracking data and airborne navigation data to develop post-flight processing algorithms that are intended to provide a highly accurate position-reference determination. This post-flight processed tracking data will also be provided to LaRC for our own DGPS navigation system performance analyses.

Future Directions in Flight Simulation

- a user perspective -

Bruce Jackson
Aircraft Guidance and Controls Branch
18 March 1993

Motivation for this talk: I've been involved with aircraft simulations for eleven years (seven as a simulation support provider and four as a simulation user). I have rehosted several simulations from various sources in the first seven years, including the X-29A from Grumman/AFWAL, the AV-8B and F/A-18A from McDonnell-Douglas, and been involved in other simulation development efforts including the F-8 Oblique Wing Research Aircraft, the A-6F, X-31, V-22, F-4S, and F-14D. Since joining NASA I've been involved in developing and sharing a simulation model of the HL-20 with various sites.

It is obvious to anyone that has been involved in a shared simulation that an enormous amount of effort is expended in modifying the software and validating the result; and that there are as many ideas about how it should be done as there are Pratt & Whitney Aeronautical Vest Pocket Handbooks.

This proposal is a plea for help in resolving some of these issues; most of the ideas are not new. I've been encouraged and supported by the following people, whose help I would like to acknowledge: Bruce Hildreth of Systems Control Technology; Roger Burton, Buddy Denham and Jay Nichols of the Naval Air Warfare Center; Doug Sutton of SBE, Inc.; Tom Galloway of the Naval Training Systems Command; Larry Schilling, Marlin Pickett and Joe Pahle of NASA Dryden, who have at least taken an initial stab at solving this; Jerry Elliott, Carey Buttrill, Jake Houck and Dr. John McManus of NASA Langley; and W. A. Ragsdale of UNISYS.

Introduction

- Digital real-time aircraft flight simulations developed in late 1940s as training devices

- Reliance upon simulation-derived results has been growing, due to cost and safety advantages

- LaRC was early leader in sim technology

- Each facility developed own hardware/software architecture independently

- Emphasis has always been on hardware; software written as needed

Langley Research Center was an early leader in simulation technology, including a special emphasis in space vehicle simulations such as the rendezvous and docking simulator for the Gemini program and the lunar landing simulator used before Apollo.

In more recent times, Langley operated the first synergistic six degree of freedom motion platform (the Visual Motion Simulator, or VMS) and developed the first dual-dome air combat simulator, the Differential Manuevering Simulator (DMS).

Each Langley simulator was developed more or less independently from one another with different programming support. At present time, the various simulation cockpits, while supported by the same host computer system, run dissimilar software.

The majority of recent investments in Langley's simulation facilities have been hardware procurements: host processors, visual systems, and, most recently, an improved motion system. Investments in software improvements, however, have not been of the same order.

Concerns

- Simulation models of aircraft are increasing in number, detail, and importance

- Government, industry simulation facilities developed separate, dissimilar architectures

- Teaming arrangements require data exchange

- Few standards have been proposed to facilitate burgeoning simulation models

- Rehosting of flight dynamic models is tedious, labor-intensive, error-prone, inefficient

Reliance upon results from simulation experiments has become increasingly important as a result of improved simulation fidelity, increased flight hour costs, increased development time, and perceived safety-of-flight issues.

All aircraft manufacturing companies and most government agencies have their own simulation facilities. Unfortunately, due to historic reasons, most simulation facilities have evolved independently with dissimilar "architectures", or hardware/software environments - host computers, shared memory, variable names, sign conventions, iteration rates, real-time loop structures, and simulation control mechanisms and conventions.

Due to the immense risk and cost of developing new aircraft, and under economic pressure to reduce this cost, teaming arrangements between various manufacturers have become common, implying that these manufacturers share, to some degree, simulation models of the jointly-developed aircraft. Government oversight agencies likewise expect to receive simulation models of the aircraft during the development phase. However, due to the dissimilar architecture of the facilities, each exchange of a simulation model or software change requires a large manual effort to reformat data and code from one architecture to another, leading to the introduction of differences between the models. Resolving these differences is time consuming.

Technology Advancements

- CPU cost/performance improvements

- Data compression/interchange standards

- Internet access expansion

- Software engineering methods have matured

Driving the proliferation in simulation capability are rapid advances in computer technology. A laptop computer today has the power of yesterday's mainframe; a deskside or desktop computer of today outperforms last year's supercomputer. Desktop real-time high-fidelity simulation of rigid-body aircraft flight dynamics is now an actuality.

Moreover, the rapid interchange of large amounts of data, such as the aerodynamics model and dynamic check case data of a high-fidelity aircraft model, is common through wide area networks and data compression technology. Connections to world-wide pathways for data, in the form of the Internet, are growing at an ever-increasing rate. Same-day updates to simulation models are now possible, if the necessary standards for data exchange were in place.

Improvements in software design methods and languages - interface documentation, modular programming, object-oriented design, along with user friendly computer programming and execution environments - have improved the robustness and quality of most computer software. These modern software engineering methods are only now beginning to be applied to production real-time engineering simulation software.

Technology Advancements (cont'd)

CPU clock speed trend (Source: AvWST 3/1/93)
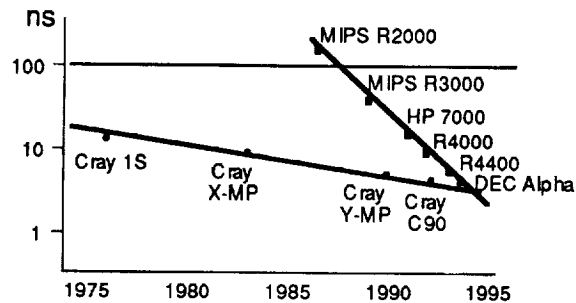
This graph depicts the improvements in RISC technology computers, leading to an apparent capture of the supercomputer CPU performance benchmark - 10 nanosecond clock time, or 100 MHz CPU clock rate. In general, one can expect to be able to run real-time on anything faster than 10 MHz clock rate (10 million instructions per second, or MIPS).

119

Simulation Requirements

- Real-time execution @ 30 Hz requires ~10 MIPS
- "Large" memory storage for data (> 4MB)
- Pilot interface - display, controls
- Dynamic system models
- Dynamic system data interpolation
- Time history data for validation

To provide real-time simulation capability, a processor with at least 10 MIPS capability is needed, a specification that is exceeded by most RISC machines today. Another requirement, easily met in any modern computer, is at least 4 MB of memory, although lower amounts have been successfully used. The capability to perform 64-bit "double precision" floating-point operations is usually expected.

Some sort of pilot interface is needed, of course, since real-time operation implies a pilot is in the loop with the simulation. While a mouse and simple line grahics might represent the minimum capability for pilot controls and displays, some sort of quasi-realistic control stick, throttle, rudder pedals, and other controls are needed, as well as a realistic out-the-window and primary flight instrument displays. This requires the capability for four to eight channels of analog input and color shaded 3D graphics, executing at 30 Hz or faster. Cell texturing has been found to improve the realism of the visual scene as well. No more that 100 to 150 millisecond transport delay, in addition to model dynamics, can be considered adequate for a realistic visual cue.

The aircraft model, in order to be considered high-fidelity, must include a fairly detailed model of the vehicle flight systems - aerodynamics, propulsion, sensors, control system, weight and inertia model, and equations of motion software models are needed. If takeoff and landings are to be performed, a realistic landing gear model is also required.

Supporting these models are usually large tables of data, arranged by flight condition, that are interpolated in real-time. Check case data is needed as well.

Rehost Costs

- Human serves as interface between computers
- One man-year minimum to rehost and validate new aircraft simulation model
- One to six man-months to incorporate changes - basically a two-person job per simulation per site
- V-22: five simulation sites, five years: 50 man-years to maintain rigid body flight dynamics models alone

When a simulation model is transferred from one site to another, the most common scenario requires a simulation engineer to convert the software from the original format into one that is compatible with the receiving facilities architecture. The involves, as a minimum, "rewiring" the software modules (e.g., adding FORTRAN COMMAND and EQUIVALENCE statements or function/subroutine arguments such that the correct input and output variables are passed to and from each module); it usually implies considerable restructuring of the code to meet architecture needs - changing variable names, "sense", and units of measure (radians to degrees, for example). It almost always involves converting the typical table lookup data from one format to another and executing appropriate precompilers to generate function table routines or real-time data files.

Verifying proper implementation is tedious as well, due to dissimilar check case data formats. It is not uncommon to receive hardcopy plots of time responses in lieu of digital data; these must either be matched "by eye" or redigitized for overplotting purposes. Rigor and criteria in matching this data is left up to the interpretation of the receiving facility, in general. Each new release of data or models requires some element of this manual process.

The experience of the Navy's Manned Flight Simulator was to expect at least 12 man-months of labor to rehost a complete simulation, and usually one or two people were assigned full-time as "model managers" for a particular simulation. It is estimated that the V-22 simulation support staff, given the five entities involved (Bell, Boeing, Navy, NAS, and Hughes), approached 10 people just to keep up with changes in data releases during the DT/OT (dvelopment/operational test) period.
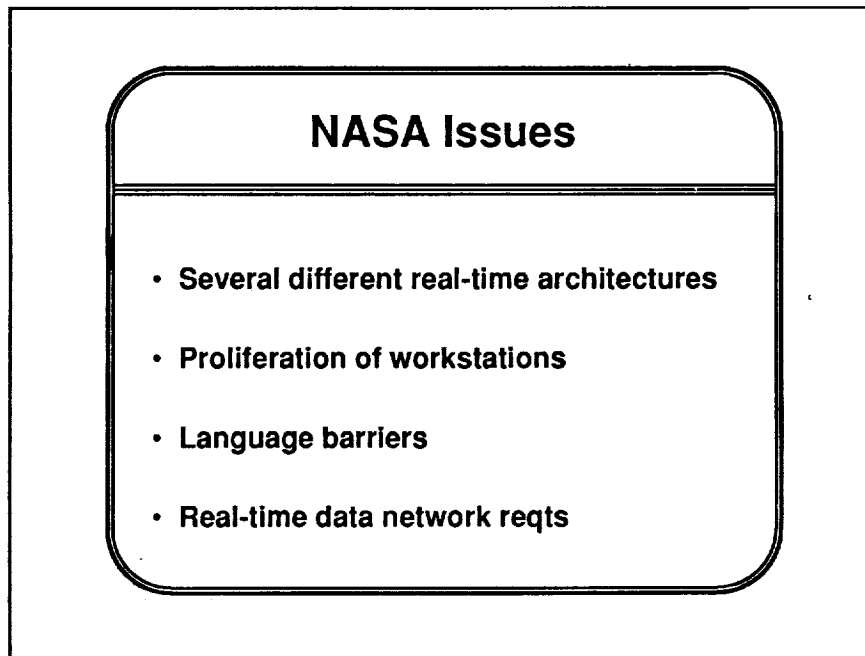
121

LaRC Issues

- **Multiple real-time architectures**
- **Introduction of high performance workstation computers**
- **Language barriers**
- **Opportunity for new technology development**
- **Real-time data network in place**

Due to historic reasons, Langley has three distinct simulation architectures running on two sets of host computers, leading to duplication of effort and cross-training of personnel. The equations of motion models are different, and have different variable names and units of measure.

Meanwhile, several user groups at Langley are developing independent real-time simulation capability with little or no commonality between them and the original real-time facility.

Language barriers exist: AGCB/FDB develops full vehicle simulations in Matrixx/Matlab; feeble autocode generators require nurture and constant attention to successfully generate real-time usable code. Hand generation of software from computer-generated wiring diagrams is common.

The opportunity to leapfrog into 21st century methods is here, if the needed resources are made available, resulting in potential industry benefit. Innovative cueing systems also being pursued by LaRC researchers.

NASA Issues

- Several different real-time architectures

- Proliferation of workstations

- Language barriers

- Real-time data network reqts

Langley is a microcosm of the simulation dissimilarity within NASA. Each NASA center has one or more simulation facilities, which are, by and large, dissimilar. Exchange of simulation models between any NASA facility requires manual rehosting.

National Issues

- Many real-time architectures

- Multiple host computers

- Language barriers

And the NASA problem is representative of the general industry problem: each simulation facility uses dissimilar architectures. Exchanging simulation models is not easily performed, with few exceptions.

Necessary Standards

- Standard data dictionary
  - Names
  - Sign convention
  - Units of measure
  - Precision (bytes)
- Equations of motion - standard inputs/outputs
- Standard partitioning of subsystem models
- Standard interfaces for other components
  e.g. cockpit display routines

What is needed are a set of standards for simulation data exchange. It is not anticipated that any existing facility will agree to adopt a simulation architecture developed elsewhere; too many resources have been expended in developing the existing architectures, and staff retraining is painful and expensive.

An evolutionary set of hierarchical standards would allow a gradual phase-in of the capability to exchange simulation models between facilities. The initial agreement would be on variable names, axis and sign conventions, and units of measure for commonly calculated variables, leading to a standard "data dictionary" that would be the basis for future simulation models, as well as an aid to translating to/from each facilities' variable name space. An agreement on where generic equations of motion and specific aircraft models would be delineated and how aircraft math models should be partitioned could lead to a standard set of inputs and outputs to/from the facility-supplied equations of motion and standard subsystem models (aero, engine, gear, controls, etc.) An agreement on headers for software modules would allow automated "wiring" of exchanged models into specific facility architectures; the ultimate would be to have a method of describing the math model that is not language specific.

To encourage commonality, a widely-accepted set of equations of motion that covers most forms of near-Earth flight could be made available to industry and academia that runs under most Unix platforms under X windows; these equations of motion would adhere to the standard, allowing easier mode interchange between existing simulation facilities and their support organizations and grantees.

125

Necessary Standards (cont'd)

- Dynamic system model interchange via ASCII
- Function data interchange standard
- Time history data
  - Large (>5 MB) files!
  - Should be self-documenting
  - Tied to flight test community/PID needs
- Memory mapping / real-time networking - SIMNET
- Automated validation - maneuver generator

The least common denominators in computer data interchange are 7-bit ASCII text files. An interchange standard for dynamic models and data should be based upon an agreement on how to encode and interprete dynamic systems in terms of ASCII characters. The resulting text file could be converted into facility-dependent real-time software or a number of block-based graphical editors.

Several attempts at this are underway to demonstrate this capability, including the Ames/Dryden SBIR contract with G & C Systems; at least one commerical control design software vendor has expressed an interest as well. Certainly a NASA-wide standard would be supported by major vendors of simulation and control design tools.

Necessary Standards (cont'd)

Wanted: Digital Aerospace Vehicle Exchange format:

- Self-documented, complete data package
- Human readable documentation
- Subsystem data
- Subsystem models
- Validation data
- Hooks to include specialized data such as display formats

The ultimate goal of this standardization effort would be the capability to easily transport complete simulations across the Internet between dissimilar real-time simulation facilities, and successfully implement and validate the rehosted simulation with a minimum effort and time.

Benefits of Standardization

- Increase confidence in simulation predictions

- Improve configuration control

- Increase productivity by factor of ten

By reducing or eliminating the human element in the digital exchange of digital simulation models, an increase in productivity will result; in addition, configuration control of simulation models across facilities will be enhanced, reducing paperwork. As the inevitable difficulties are resolved and multiple successes are experienced, confidence in imported simulations will grow, making the sharing of complete simulation models commonplace. This will undoubtedly raise some security questions, however.

Model Development

Wind Tunnel
CFD
Flight Test
Analysis
Validation Data
Controls

HOST CPU

Math Model
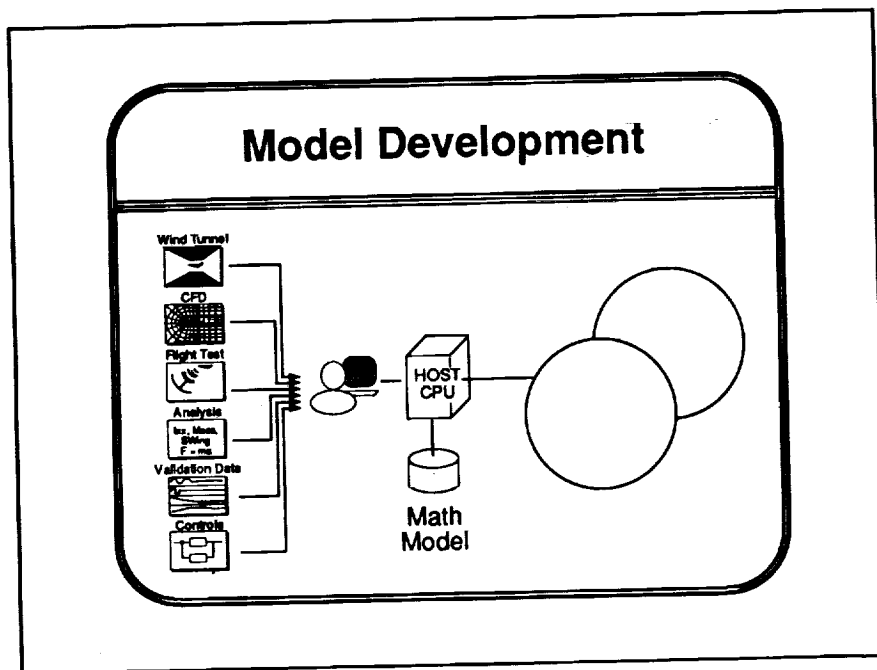
For reference, this is a simple-minded schematic of the current simulation development process, a very human-intensive operation. The only impact of the proposed standards would be to modify the end product to be amenable to exchange with other agencies.

Current Exchange Process

Transmitting facility:

Math Model and Check Case Plots

Digital Tape w/
FORTRAN models,
arbitrary data format
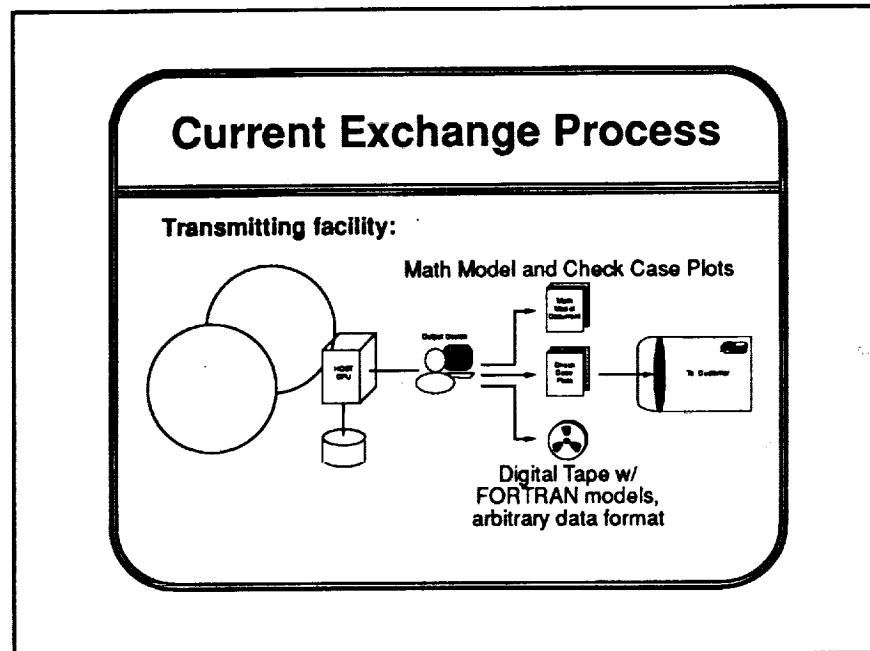
The current method of exchanging a simulation model is depicted in the next two figures. This shows the use of a human to generate, from the existing facility specific software, a set of listings, documentation, and a copy of the simulation "tape", although different media might be used. Dynamic check cases (time histories) are usually provided only in the paper documentation. Exchange of this data requires physical transport from one facility to another.

Current Exchange Process

Receiving facility:

Math Model and Check Case Plots

Digital Tape w/
FORTRAN models,
arbitrary data format
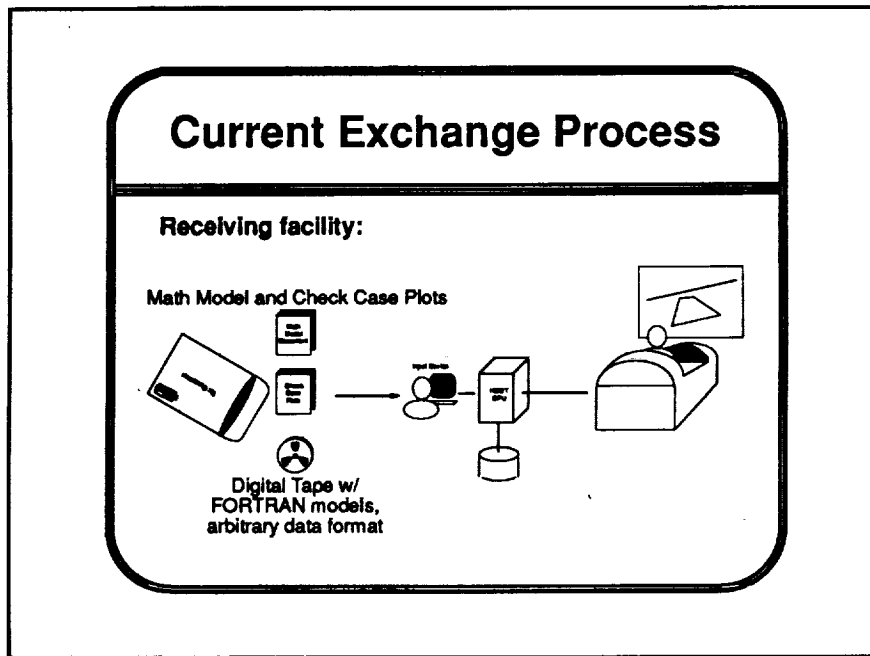
At the receiving end, another human is tasked with converting the software from the original facility architecture to that of the receiving facility, and validating the results. This is a six-to-twelve month process.

Desired Exchange Process

Transmitting facility:

Internet

HOST CPU
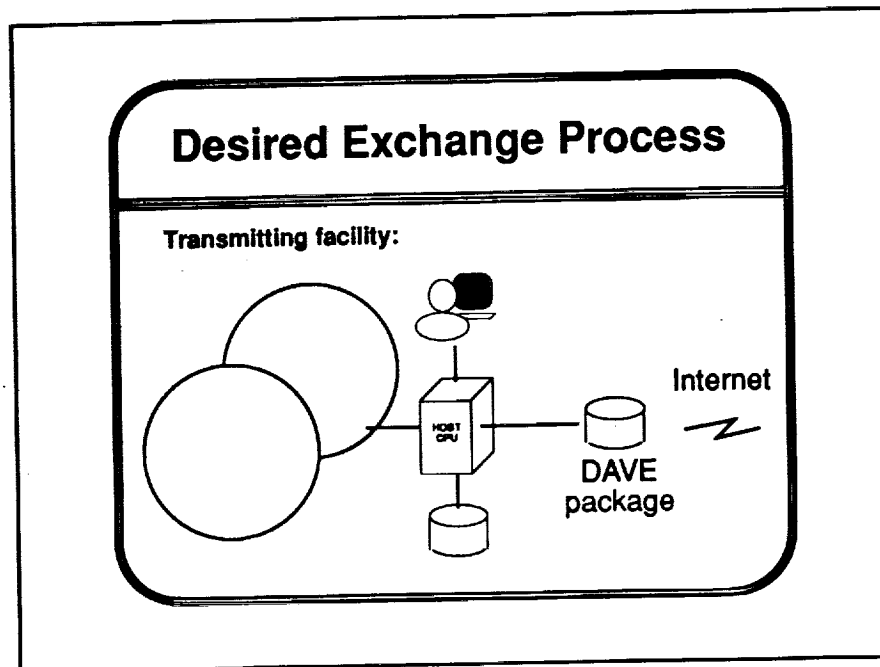
DAVE package

In the envisioned future, a post-processor converts the originating facility's model into a architecture-independent ASCII text file (or set of files). This package can be sent over the Internet to the receiving facility...

Desired Exchange Process

Receiving facility:

Internet

DAVE
package
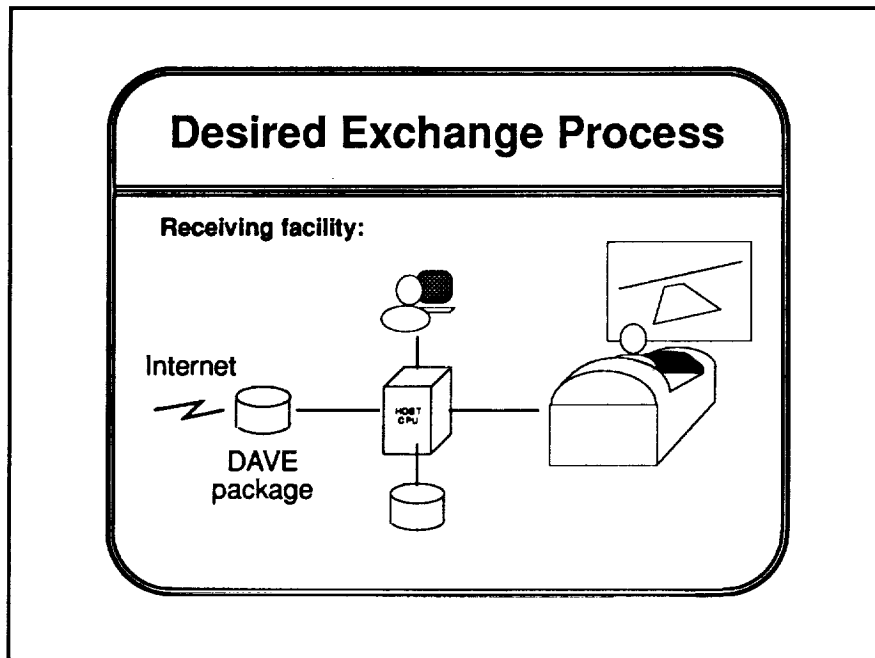
...where the package is run through another process to convert it into a model that can be run immediately on the new simulator facility. Some form of automated checkcase comparison should be a part of the exchanged data.

Implementation

- Langley community should develop Center-wide standards for data dictionary, wind tunnel data

- Solution for Langley could become NASA solution

- NASA solution would become Industry solution

- AIAA adoption as national standard would follow

- Method would be to have each site write a translation program. This would NOT REQUIRE the redesign of existing simulation architectures!

Langley is in a perfect position to simultaneously improve its simulation architecture, resolve a Langley data exchange problem, and lead an effort to vastly improved simulation model exchange capabilities for the United States aerospace industry, with minimal impact on existing software and facilities.

Conclusions

- Traditional spending emphasis is on hardware components (COF)

- Real payoff will be from software improvements

- Simulation modeling standards would be valuable contribution to American aerospace industry

- Langley should take lead in standards development

PRECISION INFLIGHT MEASUREMENT OF TURBULENT AIR MOTION USING A SOLID-STATE COHERENT LIDAR

Phase I SBIR study NAS1-19872 by

Coherent Technologies, Inc.
Boulder, Colorado

prepared for

John Ritter
NASA-Langley Research Center
Hampton, Virginia

CTI

OBJECTIVE:

Design an airborne, 2 micon pulsed, coherent solid-state lidar system that can accurately measure all three components of the turbulent velocity field at a point far enough in front of the aircraft to avoid its disturbance (i.e., 10 m or greater)

METHOD:

Use of a conical scan of the optical system focal point along a helical path traced out by the translation of the aircraft. Atmospheric aerosols or cloud droplets provide the desired air motion tracers.

APPROACH:

Design parameters will be determined using detailed lidar simulations. Doppler spectral analyses, time gating, and/or amplitude thresholding will be used to separate the desired returns from aerosols in the focal volume from interfering returns due to large hydrometeors (rain, snow, etc) which may not follow the local air motion.

139

PHASE I PROGRAM OBJECTIVES

- Performance and error analyses

- Airborne system requirements

- Preliminary design

- Experimental validation of error models

CTI

REQUIREMENTS FOR TURBULENT FLUX PROBE

o Measure relative wind vector just ahead of aircraft

o Measure in airflow undisturbed by aircraft body

o Achieve high measurement accuracy (0.05 m/s)

o Measure of all three vector components

o Sample at rate adequate to resolve 5 meter turbulence scale

o Altitude requirement : 0 to 1 km; 0 to 10 km desired

CTI

ERROR SOURCES

- photon shot noise

- aerosol inhomogeneities

- wind field inhomogeneities

- speckle

- platform vibration, flexing

- precipitation ' slip '

- backscatter from optics, distant objects

CTI

SYSTEM PARAMETERS

Focal length

Aperture

Wavelength

Pulselength

Pulse energy, repetition frequency

Doppler algorithm – radial component

Cone angle, PRF, vector retrieval algorithm

CTI

PULSE REPETITION FREQUENCY

o optimize to get best SNR consistent with minimum backscatter levels expected

o need at least 3 pulses per resolution element (5 meters at 100 m/sec ==> 60 Hz)

o Increase pulses per sample to verify wind homogeneity

o Increase pulses per sample to improve velocity precision

CTI

144

RELATED AVIONICS APPLICATIONS

o **Laser airdata probe to replace conventional pressure sensors**
  - precision measurement of TAS, AOA, AOS
  - rapid update for automatic flight control systems

o **Laser local wind shear sensor**
  - extension of airdata probe to measure local wind shear <u>rates</u>
  - input to pilot and/or control system

o **Laser local vortex wake sensor**
  - sensing of nearby wake vortex
  - warning to pilot, input to automatic control system during
    takeoff and landing

NAS802

CTI

145

A SIMULATION STUDY OF CONTROL AND DISPLAY REQUIREMENTS FOR ZERO-EXPERIENCE GENERAL AVIATION PILOTS

by

Eric C. Stewart

Flight Research Branch

presented at

NASA LaRC Workshop on

Guidance, Navigation, Controls, and Dynamics

for Atmospheric Flight

March 18, 1993

Purpose

To define basic human factor requirements for—
   Novices (non-pilots)
   Zero practice and training
   Precision, curved path, accelerated, complete maneuvers
   Instrument Meteorological Conditions (IMC)

Goal

To increase utility of General Aviation Airplanes by reducing training
   and proficiency requirements to safely access this segment of the
   transportation system

The purpose of this simulation study was to define the basic human factor requirements for operating an airplane in all weather conditions. The basic human factors requirements are defined herein as those for an operator who is a complete novice for airplane operations but who is assumed to have automobile driving experience. These operators thus have had no piloting experience or training of any kind. The human factor requirements are developed for a practical task which includes all of the basic maneuvers required to go from one airport to another airport in limited visibility conditions. The task was quite demanding including following a precise path with climbing and descending turns while simultaneously changing airpseed.

The ultimate goal of this research is to increase the utility of general aviation airplanes--that is, to make them a practical mode of transportation for a much larger segment of the general population. This can be accomplished by reducing the training and proficiency requirements of pilots while improving the level of safety. It is believed that advanced technologies such as fly-by-wire (or light) , and head-up pictorial displays can be of much greater benefit to the general aviation pilot than to the full-time, professional pilot.

Design Principles

- One mode of operation

- Pilot manually "closes the loop"

- Built-in safety features

Although the simulated systems continually evolved as the tests were conducted, the evolution was guided by the principle that the there would be only one mode of operation for the entire maneuver. It was believed that having multiple modes of operations would ultimately lead to "mode errors" in which the pilot would forget which mode he was operating in and make an inappropriate input. Such mode errors have proved to be catastrophic in other highly automated airplanes.

The second principle of design was that the pilot would actively be in control of the airplane. The level of augmentation required to produce satisfactory handling qualities for the novice is so high that without many changes a completely automatic system could be achieved. However, it was believed that in order to be acceptable to the public, the operator of the airplane must be in control of the airplane as it goes through the various maneuvers and not be merely a passive passenger.

Finally, the systems had to have built in safety features. For example, the control system was designed so that the airplane could not be stalled regardless of the inputs by the pilot. In addition, the airplane could not be maneuvered to extreme pitch and roll attitudes. This prevented the airplane from being flown too fast or to high load factors. Although these safety features reduce the maneuverability of the airplane so that it cannot perform some aggressive maneuvers, this was not considered to be a real handicap for an airplane used entirely for transportation.

```
┌─────────────────────────────────────────────────┐
│                                                 │
│           Decoupled Control System              │
│                  (E-Z Fly)                      │
│                                                 │
│                                                 │
│   Throttle Lever    ─────────►    Airspeed      │
│                                                 │
│                                                 │
│                                                 │
│   Long. Wheel       ─────────►    Vertical Speed│
│                                                 │
│                                                 │
│                                                 │
│   Lat. Wheel        ─────────►    Heading Rate  │
│   ━━━━━━━━━━━━━━━━━━━━━━━━━━━━━━━━━━━━━━━━━━━━   │
│                                                 │
│   R. Pedals         ─────────►    Sideslip      │
│                                                 │
└─────────────────────────────────────────────────┘
```

The E-Z Fly control system was designed to "decoupled" the airplane responses as shown here. The three primary cockpit controls (throttle, longitudinal wheel, and lateral wheel) individually and separately determine the three primary parameters (airspeed, vertical speed, and heading rate) needed to get from one point in space to another. In a conventional airplane the airspeed, vertical speed, and heading rate can all respond simultaneously to a single input on one of the cockpit controls--that is, the responses are coupled. The pilot must learn to suppress the unwanted responses in order to get the airplane to respond the way he wants it to. It is this coupling that makes an airplane hard to learn to fly for a novice.

The fourth cockpit control, the rudder pedals, was used to control the sideslip angle in the E-Z Fly control system. Ordinarily, the rudder pedals were left in the center position where they commanded a zero sideslip angle so that turns with the lateral wheel were naturally coordinated. However, in cross-wind conditions the rudder pedals could be used to align the nose of the airplane with the ground track.

Control System

(Vertical Speed Subsystem)
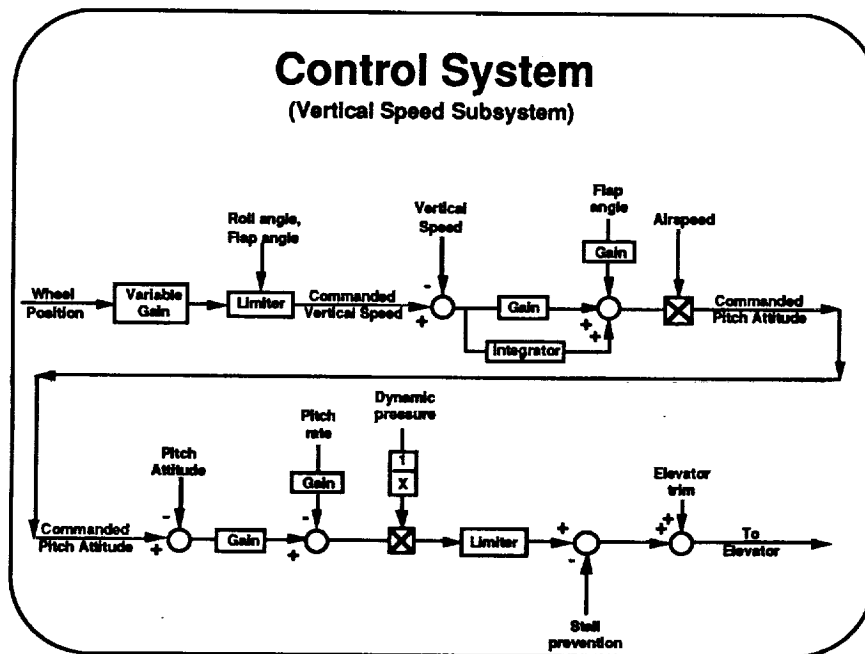
The E-Z Fly control system would probably require a fly-by-wire (or light) control system. The block diagram for the longitudinal-wheel-position-to-vertical speed subsystem is shown here. The wheel position was fed through a gain (which was decreased on final approach to provide fine control) and a limiter which kept the system from commanding a vertical speed the airplane could not sustain indefinitely. The heart of the control system was a simple proportional plus integral controller which was scheduled according to the airspeed and dynamic pressure. Pitch attitude and pitch rate were used to stabilize the system. Finally, a stall prevention feature based on angle of attack was added as a back-up to provide nose-down elevator. Ordinarily, this feature was never actuated because of the limiter on the commanded vertical speed mentioned earlier. However, the stall prevention feature was added insurance for extreme combinations of low airspeeds and large roll angles with the flaps and landing gear extended. These extreme conditions were never encountered if the pilot followed the pictorial head-up display.

Control System
(Airspeed Subsystem)
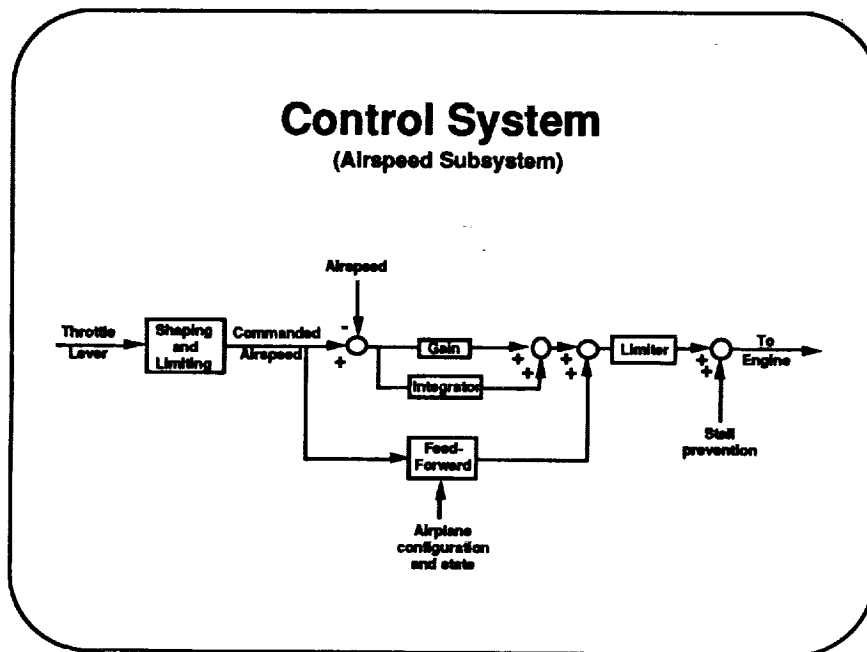
The block diagram for the second major component of the E-Z Fly control system is shown here. The average position of the throttle levers in the cockpit commanded the desired airspeed after passing through a shaping and limiting filter. This filter prevented the system from commanding unrealistic airspeeds which the airplane could not sustain safely. The commanded airspeed was directed through a feed-foward loop which defined a nominal throttle position as a function of the airplane configuration (flap and landing gear positions) and airplane state (vertical speed, roll attitude, and sideslip angle). The airspeed error was fed through a proportional path and an integral path. The integrator, of course, assured that the airspeed error was zero after the transients had died out. The final limiter function had a "sliding window" which allowed ±20% deviation of the throttle position from the nominal feed-forward throttle position. This "sliding window" was added to limit the amount of engine activity when large changes were made in the commanded airspeed. As a back-up, a stall prevention term driven by the angle of attack was added to commanded throttle position. As with stall prevention term for the vertical speed subsystem, this term was not needed except for extreme combinations of airplane configuration and state. These extreme conditions could not exist unless the airplane was completely off the desired trajectory.

Additional Control System Features

- Lateral wheel used to taxi
- Automatic control force trim
- Variable gain on final approach

Some additional features of the control system which do not appear on the previous slides are shown on this slide. The lateral wheel, rather than the rudder pedals, was used to steer the nose wheel on the ground. Whenever the airplane was on the ground the loop was opened in the usual lateral-wheel-to-roll-angle control system. Thus, the airplane was turned right or left by using the lateral wheel regardless of whether the airplane was in the air or on the ground. The second feature, automatic control force trim, was very helpful to the novices especially on their first simulated flight. Whenever there was a force on the longitudinal or lateral wheel, the control force was automatically reduced to a low level over a period of time. The novice pilots were completely unfamiliar with the concept of control force trim and almost never used the electric trim switch mounted on the control wheel. Without the automatic control force trim the novice test subjects often flew for long periods of time with steady control forces. These forces made it difficult to control the airplane precisely. The final feature was an automatic reduction of the gains on the longitudinal and lateral wheel during the final approach. The guidance (highway) was narrowing on final approach and unless the gains were reduced on the control wheel, the airplane appeared to be overly sensitive.

Highway in the Sky (HITS) Format

L 93-02043
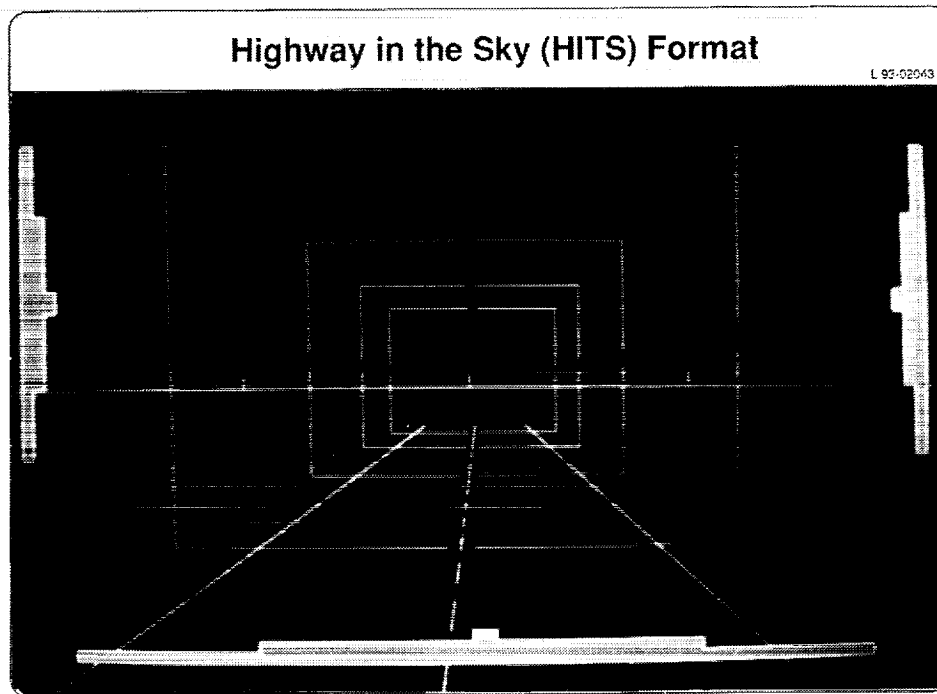
The second element of the E-Z Fly system was the Highway In The Sky (HITS). Although there were several variations of HITS, the basic format of this pictorial display is shown in this slide. The "surface" of the highway is marked by a solid white stripe on each side and a striped white line down the center as shown in the lower center of the slide. This highway was fixed in space and the airplane was flown above and past the highway. To provide increased vertical guidance green boxes were drawn on the road as shown. The green boxes and white stripes were ordinarily drawn about 6000 feet in the distance and had a nominal width of 1000 feet. As the airplane passed by a box or a section of the road, that box or section would pass out of view and a new box and road section would be added on at the far end of the road. This prevented the clutter of the display which would have resulted if the road was extended to the final destination. The 6000 feet of highway visible still provided some anticipation of when turns would have to be made in the future. The boxes had small gaps in the middle of each side which were used as aiming points for the red "trend mark." (Only the vertical trend marks are shown on the above slide).

A white horizon line was drawn across the display. Small vertical tic marks were placed every 10° of heading.

Finally, fixed green reference guides were added on either side and at the bottom of the display. The guides were fixed on screen regardless of the airplane maneuvering. They were ordinarily adjusted for each pilot so that they were at the very edge of his field of view. The guides on the sides could be used with the white horizon line to gauge pitch attitude. The guide at the bottom could be used to help in lateral steering.

HITS Display showing Trend Marks

L 92-00056
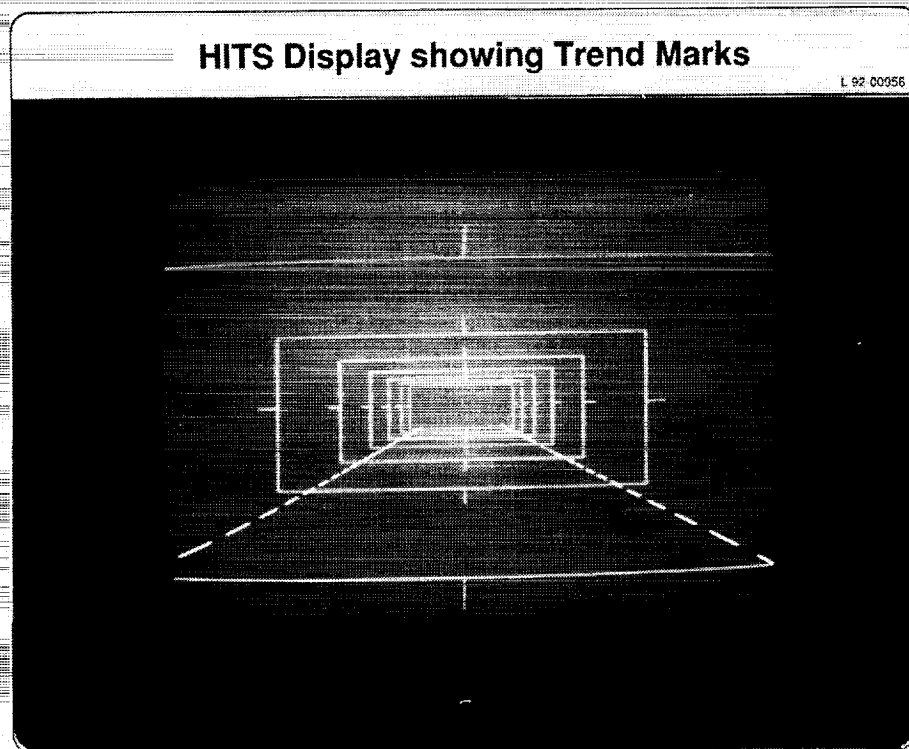
The vertical and lateral trend marks are shown in the center of the boxes of an earlier version of HITS in the above slide. The trend marks are used to provide linear rate information relative to highway. The perspective of the boxes and the lane stripes relative to one another seemed to provide adequate position guidance. However, the test subjects had trouble anticipating where they were going to be in the future because they had to mentally differentiate the time rate of change of the perspective of the highway. The trend marks helped by indicating where the airplane would pass through a given box if the controls were held in their present position. That is, an imaginary horizontal line drawn between the two red marks on the sides of the boxes would intersect a vertical line drawn between the red marks on the top and bottom of the boxes at the point the airplane trajectory would intersect the plane of the box. The trend marks responded very quickly to control inputs and thus gave much more rapid feedback than did the more slowly changing perspective of the pictorial highway.

Excess Downward Velocity
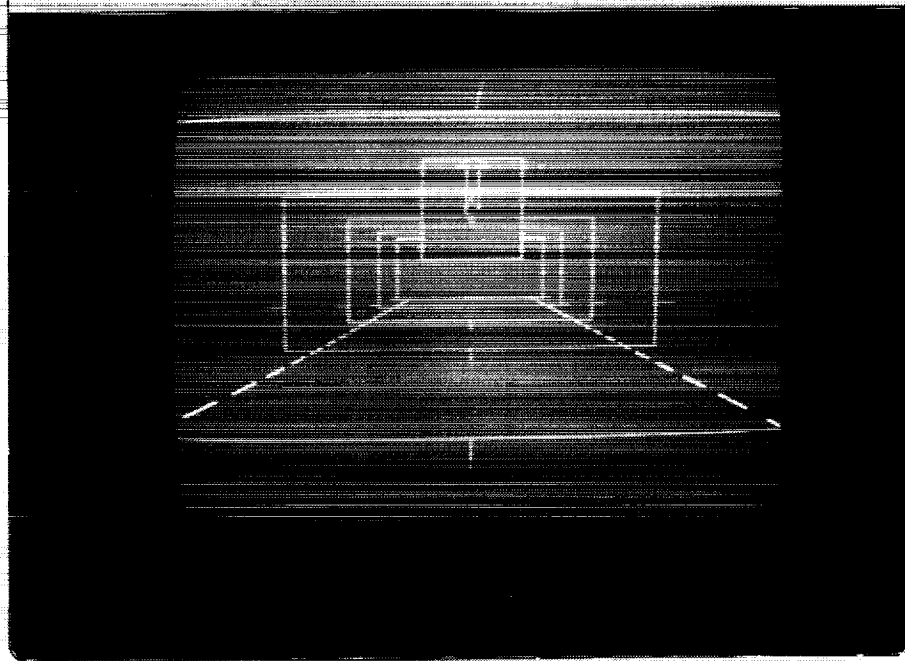
     This slide depicts the situation in which the airplane is in the correct position relative to the highway (the boxes are centered), but there is a downward velocity (the trend marks are progressively lower on more distant boxes). Also shown on this slide is the so-called "flight director" arrows in the white "sign" box. In this situation, the flight director arrows are indicating the pilot should pull up to arrest the downward velocity. In most situations where the pilot is properly following the HITS, the square white box and flight director arrows are removed to prevent clutter and provide a more intuitive display. More will be said about the flight director arrows later.

Left-ward Lateral Velocity
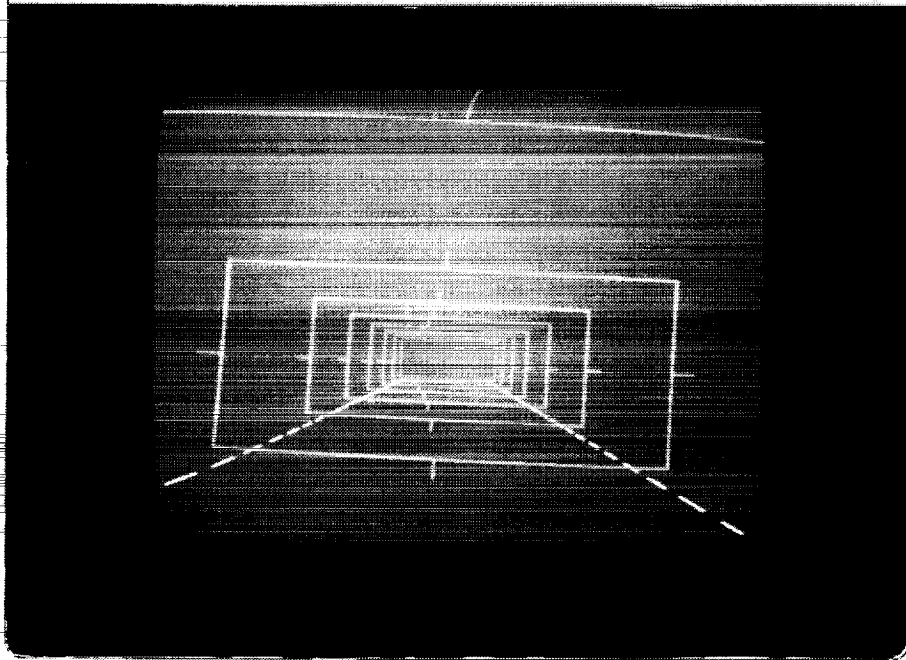
This slide shows what the display looks like when the airplane is on the centerline but is going to the left. As indicated by the lateral trend marks the present trajectory of the airplane will take the airplane off the side of the more distant boxes. The lateral trend marks were much more sensitive to lateral wheel inputs than the vertical trend marks were to longitudinal wheel inputs. This difference in sensitivity is due to fundamental physical differences in the airplane's responses in the two axes.

HITS Display showing Flight Director

L 93-02037
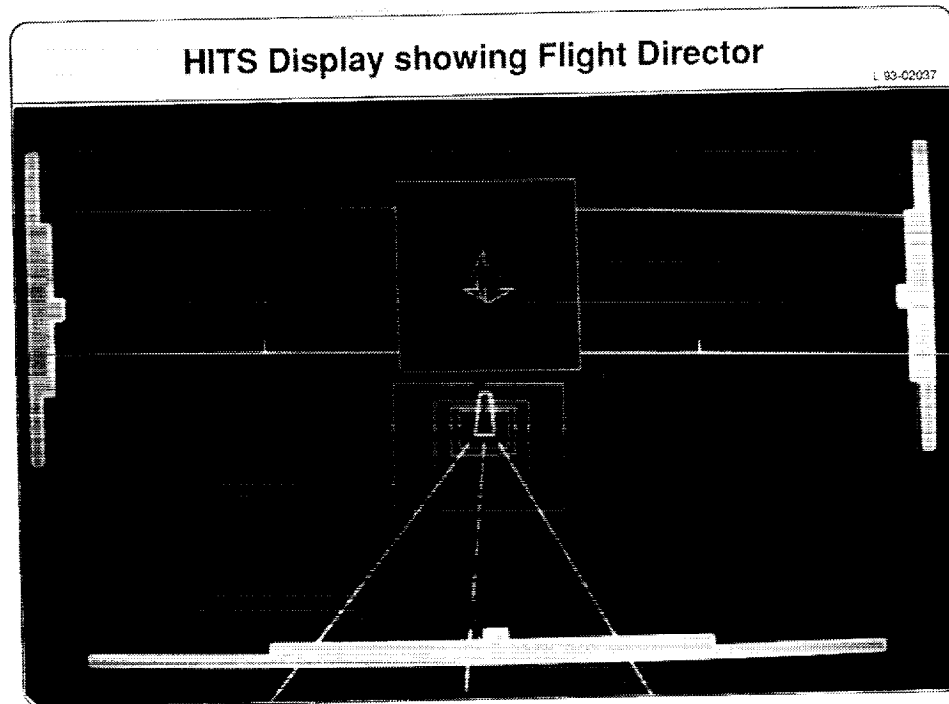
This slide shows the flight director arrows indicating that a slight push of the longitudinal wheel and left turn of the lateral wheel is needed. The flight director arrows were ordinarily not displayed when the pilot was close to the nominal trajectory. However, in this study the flight director arrows were used to indicate when it was time to rotate the airplane for takeoff and when to flare the airplane for landing. The flight director arrows usually disappeared shortly after takeoff when the pilot flew near the nominal trajectory. They remained off until the final approach as shown in the above slide. They were programmed to come on during the final approach even if the pilot was very close to the nominal trajectory. This was done because the vertical arrow was needed for the flare and it would probably have been too distracting for the arrows to appear suddenly at the flare point.

Flight Director Arrows When Completely off the HITS Trajectory

L 93-02C99
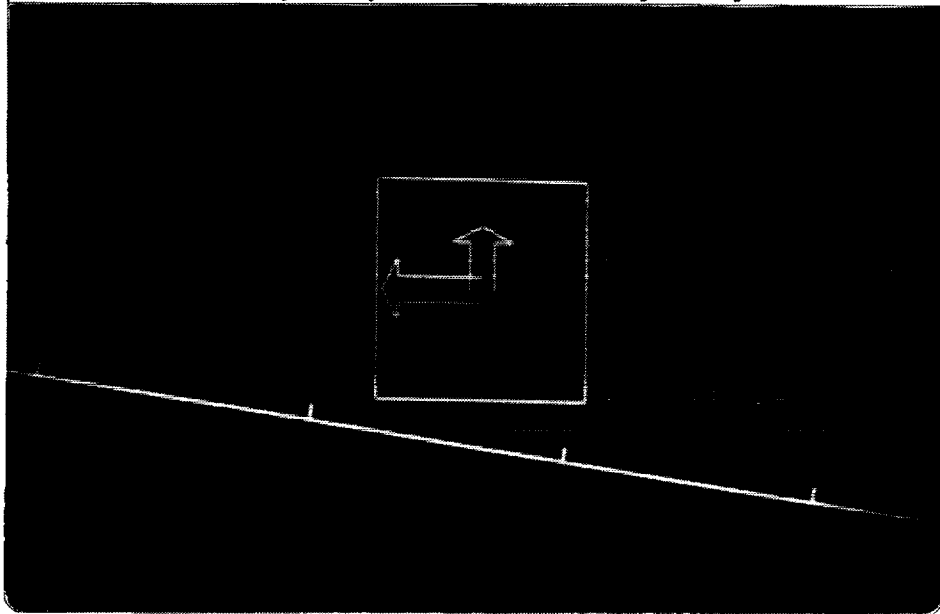
In addition to the rotation and the flare, the flight director arrows were needed when the pilot flew so far off the HITS trajectory that the highway could no longer be seen. This situation is depicted in the above slide where the pilot needs to pull up and turn to the left to re-acquire the pictorial part of the HITS display. A few of the novice pilots flew off highway during the first turn and had to use the flight director arrows to get back to the highway. In the majority of the cases, however, the test subjects always maintained visual contact with the pictorial highway.

HITS Display in a Turn
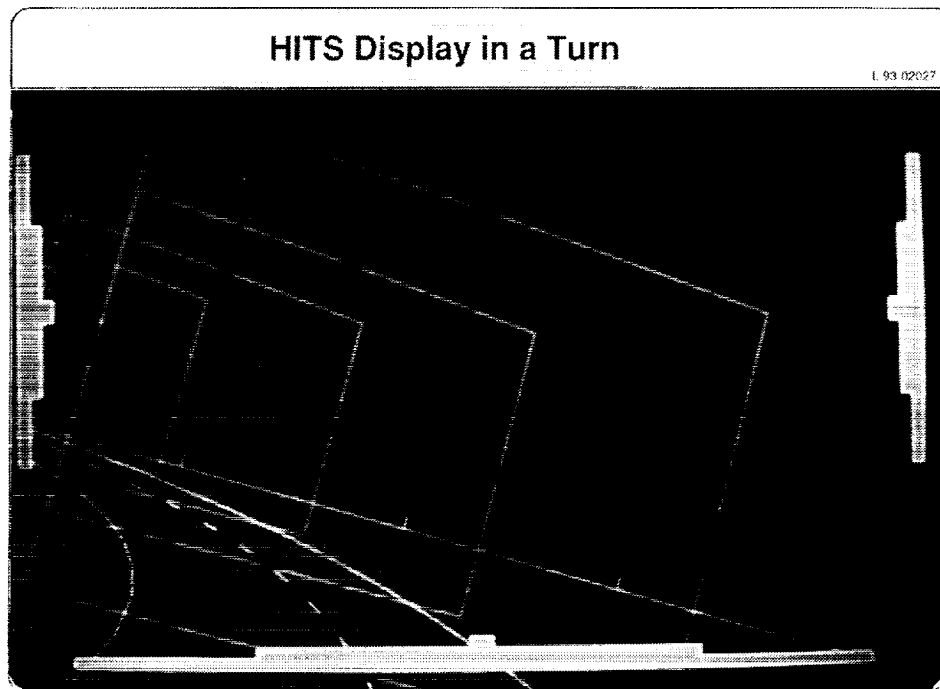
A sample of what the display looks like in a climbing turn is shown in the above slide. The "surface" of the highway was level in the turns and the boxes also remained vertically oriented (no bank). The airplane, of course, had to be banked to execute the turn; and this airplane bank can be seen by the angle between the fixed reference guide at the bottom of the display and either the horizon line or the sides of the boxes. In the turn, the geometry is such that the center of the reference guide does not line up with the center of the highway as it does in the straight segments. It appeared that placing the center of the reference guide on the outside (solid) highway stripe as shown above placed the airplane on a good trajectory. However, this technique had to be learned and thus did not satisfy the original goal of making the display completely intuitive.

Banked Highway on HITS Display

L S3-C2055
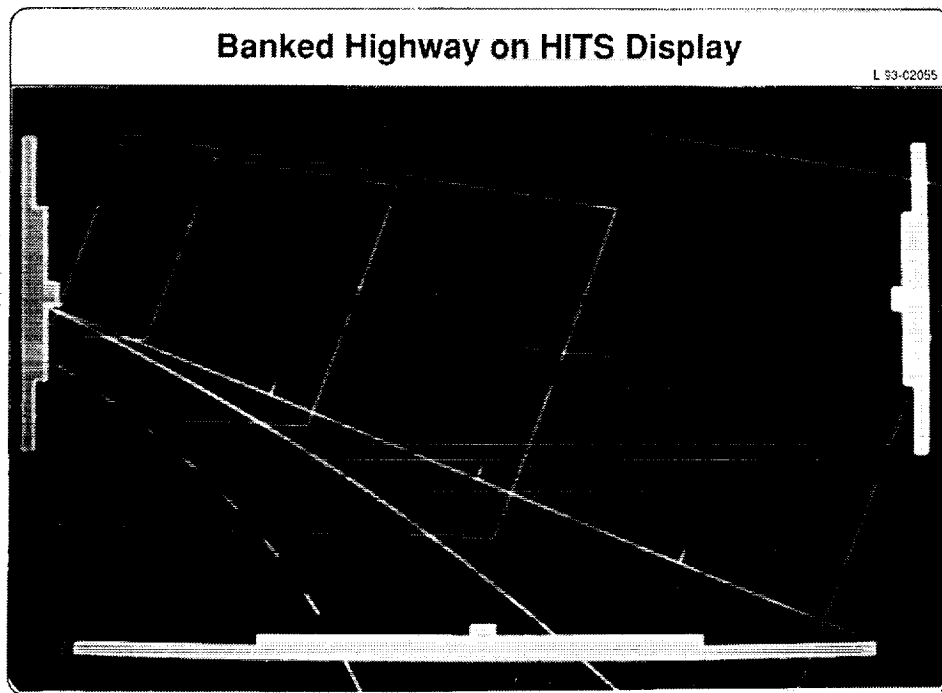
A limited number of runs were flown with a display in which the highway "surface" and the tops and bottoms of the boxes were banked as shown in the above slide. It was hoped this would be more intuitive than the unbanked display and that the reference guide could be aligned with the bottom (or top) of the boxes. However, most of the test subjects preferred the original display. The boxes appeared distorted and the transition from the straight segments to the turns and vice versa were confusing. It was discovered that the perspective in the climbing and descending turns was such that the bank of the highway had to be less than that of the airplane if the reference guide was to appear parallel to the bottom (or top) of the boxes.

161

Test Subjects

Subject	Piloting Experience	Occupation	Age	Sex
1	0 hours	Engineer	24	Female
2	0 hours	Enginerring Graduate Student	23	Female
3	8700 hours	Research Pilot	40	Male
4	0 hours	Secretary	29	Female
5	0 hours	Business Co-Op	20	Female
6	0 hours	Graphics Co-Op	24	Male
7	0 hours	Secretary	36	Female
8	800 hours	Engineer	43	Male
9	0 hours	Engineering Graduate Student	29	Male
10	6300 hours	Research Pilot	52	Male
11	800 hours	Engineer	45	Male
12	0 hours	Engineer	49	Male
13	0 hours	Engineering Co-Op	21	Male
14	0 hours	Library Science Co-Op	25	Female
15	0 hours	Engineering Co-Op	19	Male
16	400 hours	Engineer	45	Male
17	0 hours	Engineering Co-Op	19	Male
18	0 hours	Engineering Co-Op	20	Female

A wide variety of tests subjects was used in this study as can be seen from this slide. Only ten of the test subjects flew the initial series of test with a systematic set of research variables. The other eight test subjects flew only selected configurations such as the banked highway display.

Test Subject Summary

- Piloting Experience
  - 5 with at least some experience
  - 13 without any experience
- Background
  - 5 with non-technical backgrounds
  - 13 with technical backgrounds
- Sex
  - 7 females
  - 11 males
- Age
  - 19 to 52 years old
  - 31 years average age

Although all kinds of test subjects were used, most of the test subjects had no prior piloting experience. Since the test subjects were selected from the staff at the Langley Research Center most of the test subjects had a technical background. Also the test subjects were predominantly males. Only five of the test subjects were over 40 years old, and the average age was 31 years.

Maneuver
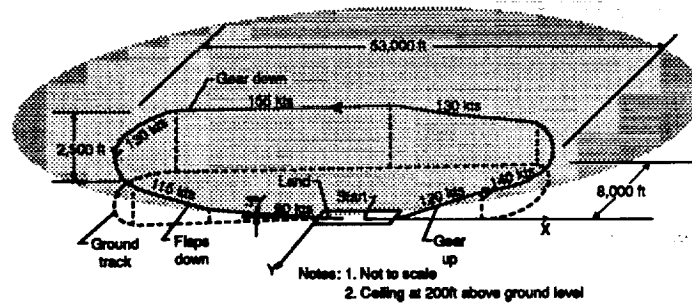
The same test maneuver was used for all the test subjects. The maneuver consisted of a racetrack-shaped maneuver including a takeoff and a landing. There were seven segments, each of which was flown at a different airspeed. Since the maneuver was only about 10 minutes long, the airplane was accelerating from one airspeed to another most of the time. The maneuver included complex tasks such as precision climbing (or descending) turns while accelerating from one airspeed to another. In addition, the landing gear and flaps were exercised. Perhaps the most significant factor was that most of the maneuver was conducted in reduced visibility conditions. That is, most of the maneuver was conducted above the simulated ceiling height of 200 feet.

Research Variables

- Control System (on or off)
- Automatic control force trim (on or off)
- Head-up or Head-down display
- Winds and turbulence
- Display format
  Trend marks
  Reference guides
  Banked turns

Several research variables were investigated as shown in this slide. Each of the variables was evaluated to see if it was necessary or helpful for the test subjects. The intent was to establish the minimum features to safely conduct the maneuvers.

Procedure

- Short briefing of test subjects~30 minutes
- Data taken on first run--no practice
- Limited number of total runs

  Repeat of baseline configuration to track
  learning curve

  One run with each research variable

The test subjects were given a short briefing to explain what the overall objectives of the research program were and to explain the fundamentals of what their task would be. The cockpit controls were identified and photographs of the display format were explained. After this introduction the tests subjects were allowed to fly the maneuver with almost no coaching from the researcher. For example, if the test subject failed to raise the landing gear or made some other obvious mistake this might be point out. But in general the researcher did not coach the subjects on when and how much control input to make. A limited number of runs was allowed for each test subject because they were learning so quickly. The first run(s) was considered to be the most important because the test subject's natural instincts readily came out then.

The default configuration of the simulation was: 1) E-Z Fly control system on, 2) Head-up pictorial display, 3) Automatic control force trim on, 4) Calm air conditions, 5) Vertical trend marks on, 6) Reference guides off, and 7) Unbanked highway turns. This was the first configuration flown by most of the test subjects. Then on alternate runs one of the research variables was altered. After one non-default variable conditions was tested, the default configuration was flown again. Thus, the default configuration was flown every other run throughout the sessions. This made it possible to track the test subjects' learning curves which were very steep because as mentioned earlier no prior training or practice was allowed. It also allowed the test subjects to directly compare one of the research variables to the default configuration.

Simulator Exterior
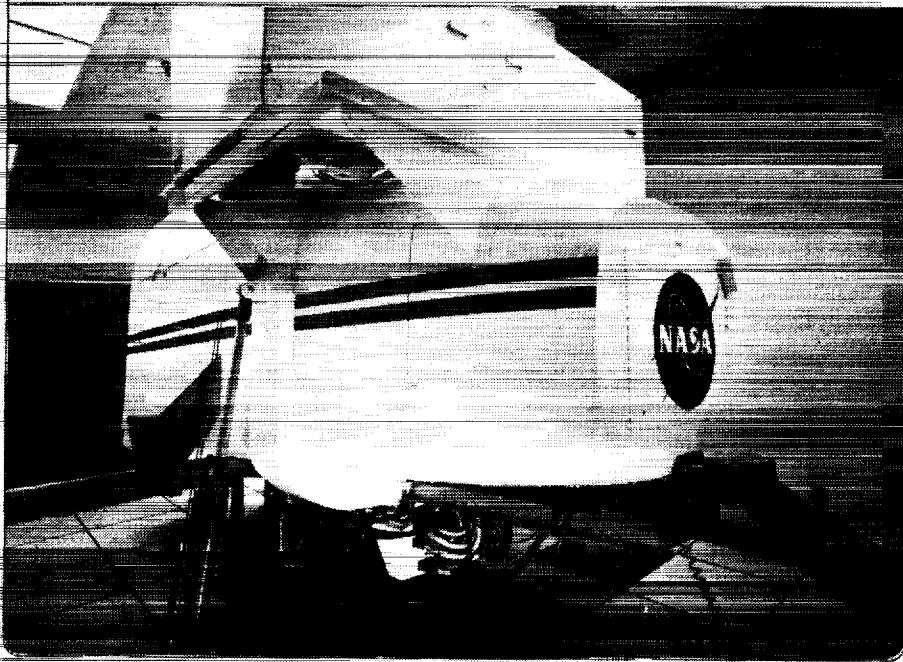
The Langley General Aviation Simulator was used in these tests. The simulation cockpit was mounted on a 3 DOF motion base which provided limited motion cues in pitch, roll, and heave. Of course, the equations of motion (and the visual system) had 6 degrees of freedom.

Simulator Interior

The cockpit was equipped with a computer generated image (CGI) visual scene out the front window. For the Head-up configuration, the line drawings of the HITS display were overlaid on the CGI image with a total field of view of about 38° laterally by 20° vertically. The cockpit also had a hydraulically-actuated control loader system to provide programmable force feel characteristics. Engine and windstream sounds were simulated by a series of speakers around the cockpit. A conventional instrument panel with mechanical displays was provided, but the test subjects almost never referred to these instruments.

Simulator Instrument Panel
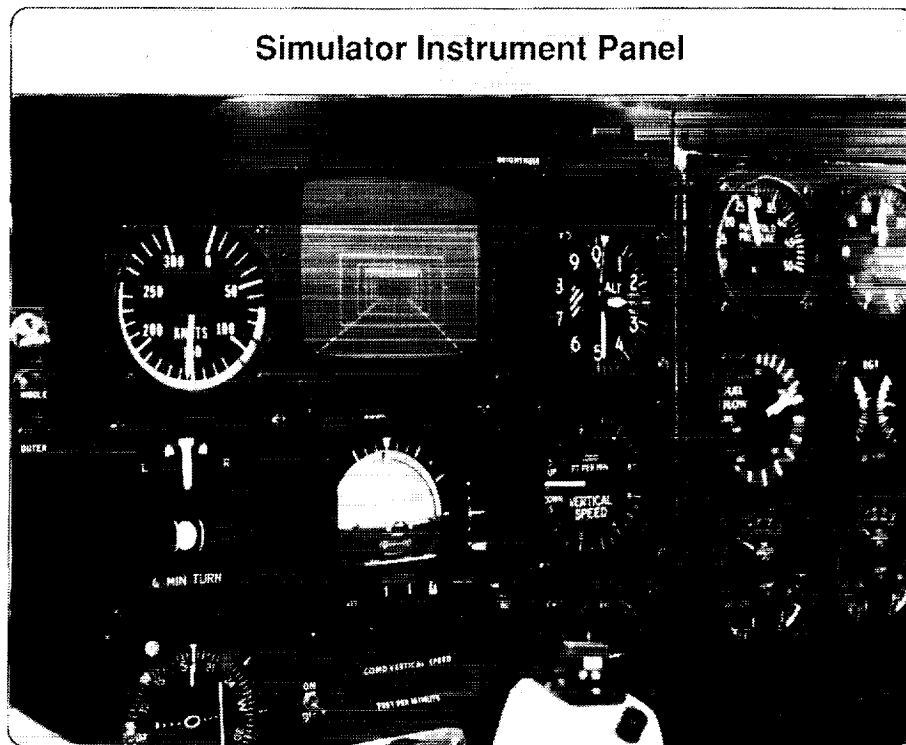
The instrument panel was modified as shown to evaluate the HITS in a head-down arrangement. A 5-inch black and white television monitor was mounted in the top center of the instrument panel. Unfortunately, the monitor had poor resolution. And because the monitor had a black and white format, the color distinctions of the HITS display could not be seen. Although the physical field of view of the monitor was small, the picture on the monitor represented a substantially larger field of view than did the head-up configuration. In the head-down configuration the simulated field of view was about 43° laterally by 25° vertically. This compares favorably to the 36° by 20° field of view in the head-up configuration.

Video

(4 minutes)

The video is a recording of the head-up visual scene during a maneuver flown by an experienced test subject. Selected portions of the maneuver are shown, including most of the final approach and landing.

First Trajectory by Zero-Experience Test Subject

(Compared to standard ILS glideslope accuracy)
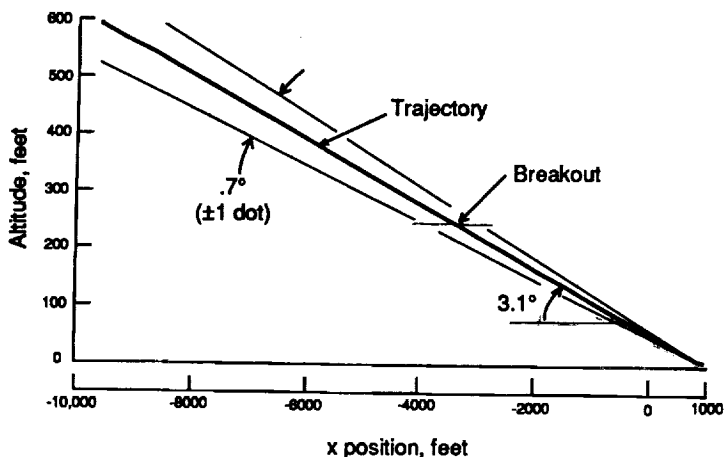
This slide shows the actual final approach trajectory flown by one of the zero-experience test subjects on his very first maneuver. The trajectory was flown with the default configuration (E-Z Fly control system and the head-up pictorial HITS display). For comparison purposes only a ±1 dot deviation on a standard ILS instrument is superimposed on the trajectory. The test subject was not flying an ILS approach. It is apparent that the test subject was able to very precisely control the flight path.

Pilot's Field of View
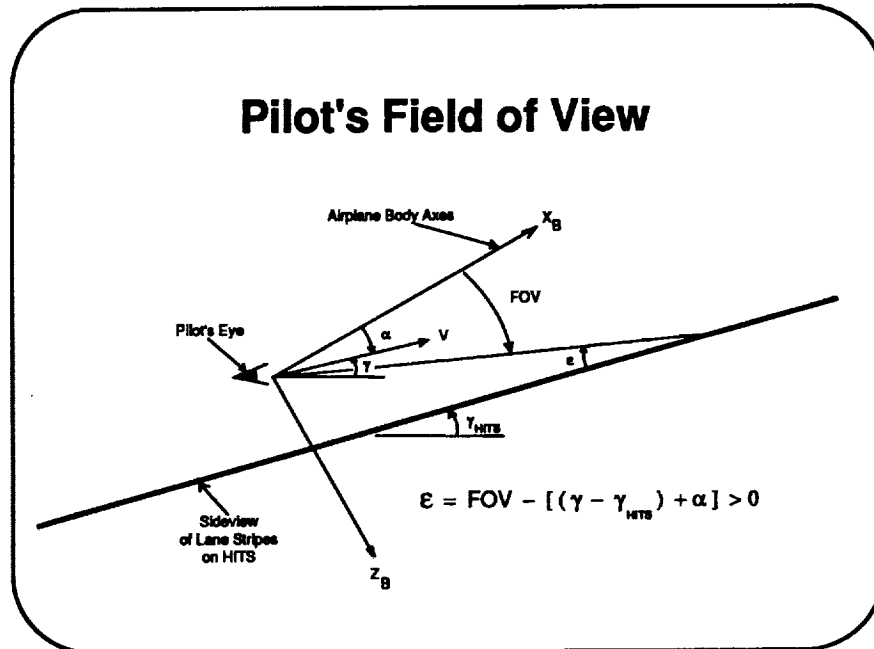
The amount of downward visibility (the angle FOV in the above slide) was critical to optimum performance. In order to see the lane stripes and the bottoms of the boxes the visual intercept angle, ε, had to be positive. In fact, the intercept angle has to be reasonably large, 3 or 4 degrees, if the highway is to be seen a reasonable distance ahead of the airplane. From the above formula it can be seen that if the airplane is climbing more steeply than the HITS path, ($\gamma - \gamma$ HITS) positive, or the angle of attack, α, is large; the intercept angle will be small. In this situation, the downward visibility, FOV, must be large. Immediately after takeoff when the airplane was climbing steeply at a low airspeed, the downward visibility was limited. This proved to be a critical time since the test subjects were not used to the display at all on their first run.

11° Downward Field of View
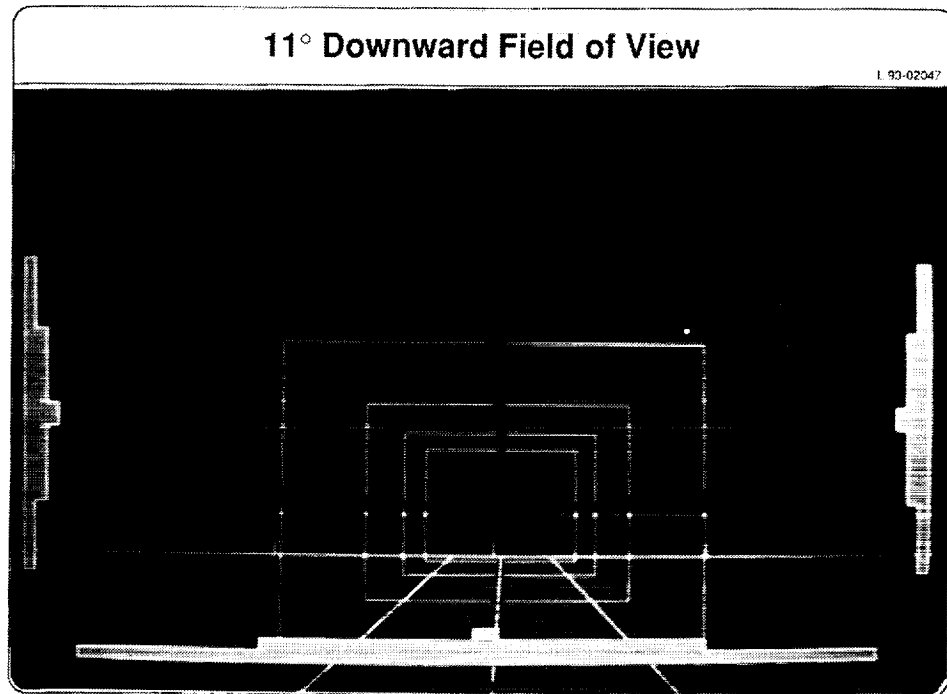
This slide illustrates the view for the default value of 11° for the downward field of view. The picture was taken on an ascending straight path. The fact that the HITS path is ascending can be ascertained by the fact that the vanishing point of the lane stripes is above the horizon.

16° Downward Field of View

L 93-02046
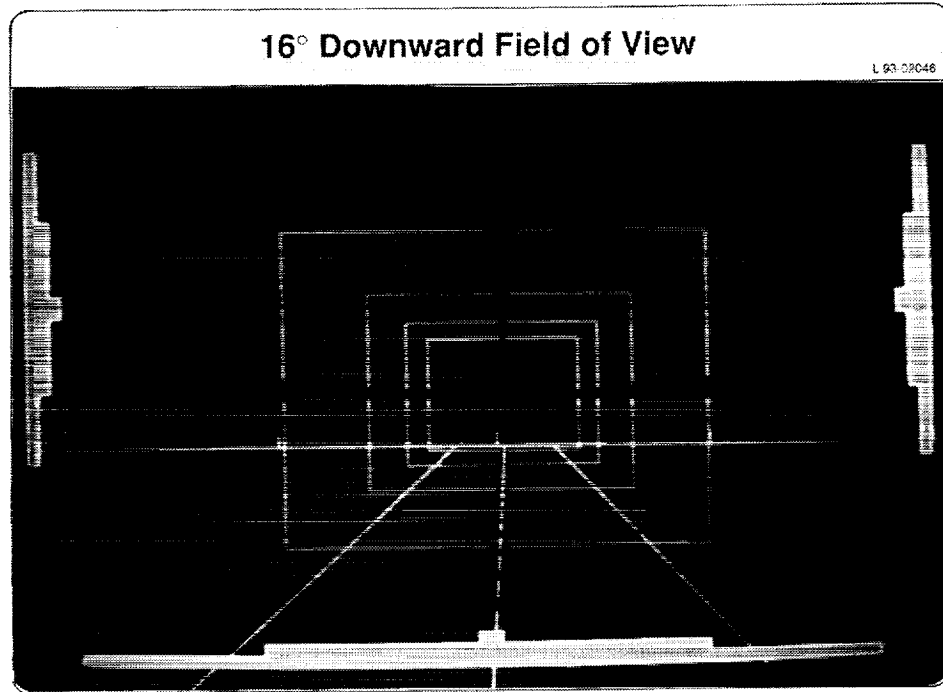
This picture was taken for same identical conditions as the previous slide except that downward field of view has been increased by 5° to 16°. The lane stripes are much more evident. The lane stripes can be aligned with the reference guide especially in the turns.

Results

- 100% of test subjects were able to complete IFR maneuver on first attempt without training or practice
- Automatic control force trim is very desirable
- Control system and display are synergistic
- Head-up display strongly preferred
- Downward field of view is critical
- Vertical trend marks are very helpful
- Lateral trend marks are helpful but extremely sensitive
- Reference guides are beneficial
- Turbulence and crosswinds are manageable
- Banked turn display was not helpful

Some of the results of this study are summarized in this slide. The latest tests were the most successful to data. All of the tests subjects were able to complete the entire maneuver on the first attempt without training or practice. The control system and display seem to complement one another, and the novices need to have both of them. Automatic control force trim made it possible to more precisely control the airplane because most of the novice test subjects never used the manual electric trim switch. The head-up display was universally preferred over the head-down display, but the comparison was not really fair because the head-down had poor resolution and no color. The downward field of view was critical especially in the first climbing turn. The trend marks were very helpful to the novices probably because of the immediate feedback they provided for pilot inputs. However, the lateral trend marks were overly sensitive to small inputs. The reference guides were also useful in helping to point the airplane in the proper direction. Turbulence and crosswinds degraded piloting performance, but caused no real problems. Most of the test subjects were able to track the HITS path even in the presence of a 14 knot crosswind. They usually recognized the misalignment of the airplane nose with HITS path, but this did not alter their basic flying technique. A short evaluation of a HITS with a banked roadway was made. Although it was hoped that using the angle of the bottom of the boxes to align the reference guides would be helpful, the banked turns were in general harder to fly than the basic unbanked display. The apparent distortion of the boxes and the reduction of vertical direction cues outweighed any improvement from the increased roll attitude guidance.

Parametric Uncertainty Modeling for Application to Robust Control

Christine M. Belcastro
AGCB
NASA Langley Research Center

B.-C. Chang & Robert Fischl
Drexel University
Philadelphia, PA

Presentation Outline

- *Parametric Uncertainty Modeling*

- *Multilinear Solution Framework*
  - *Results*
  - *Example*
  - *Extension to Rational Case*

- *Concluding Remarks*

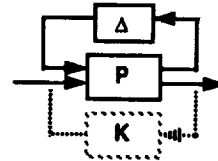- *Further Work*

Parametric Uncertainty Modeling

Motivation:

- **Robust Control Theory & Tools**

    - Required Uncertainty Model Structure:
        - ➤ Separated P-Δ Form:

    - Computational Efficiency Depends on Dimension of Δ Block
        - ➤ Minimal P-Δ Model Desired:

- **Practical Robust Control Applications**

    - P-Δ Model Difficult to Form for Real Parameter Variations

    - No General Systematic Approach for Minimal P-Δ Modeling

        - ➤ Multidimensional Minimal Realization Problem

            - ⇒ Problem to be Addressed in this Paper

Parametric Uncertainty Modeling (cont)

General Problem Definition:

Given State Space Model of Uncertain System:

$$\dot{x} = A(p)\,x + B(p)\,u$$
$$y = C(p)\,x + D(p)\,u$$

Any Element of A(p), B(p), C(p), D(p) ➤ Explicit Function* of p:

Uncertain Parameters: $p = [\,p_1,\,p_2,\,\cdots,\,p_m\,]$

$$p_{i_{min}} \le p_i \le p_{i_{max}} \longrightarrow p_i = p_{i_o} + \bar{\delta}_i = p_{i_o} + s_i \delta_i \ , \ |\delta_i| \le 1$$

Form a P-Δ Uncertainty Model:
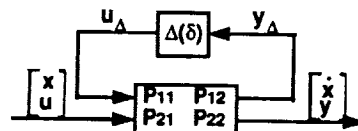
P - Constant Matrices

Δ(δ) - Uncertain Parameters

$$\Delta(\delta) = \text{diag}(\,\delta_1 I_1,\ \delta_2 I_2,\ \ldots,\ \delta_m I_m\,)$$

Parametric Uncertainty Modeling (cont)

General Problem (cont):

Any Element of A(p), B(p), C(p), D(p) $\longrightarrow$ __Explicit Function__* of p

__*Explicit Functional Forms__:	__Example__:
Linear Function**	$a_{ij}(p) = p_1 + p_2\, a_o$
Multilinear Function	$a_{ij}(p) = p_1 + p_1 p_2\, a_o$
Rational Function	$a_{ij}(p) = \dfrac{p_1 + p_2\, a_o + p_2^2\, p_3}{p_1\, p_3 + a_1\, p_4}$
$\vdots$	$\vdots$

** Formal Solution by Morton & McAfoos (1985 ACC & CDC)

$\Rightarrow$ **Many Practical Problems:**
Multilinear (Rational, ...)

Objective

__Develop__: *Systematic Method for Obtaining a P-Δ Model*
__Given__: *State-Space Model of a MIMO Uncertain System*
__such that__:

- Any Element of A(p), B(p), C(p), D(p) is a *Multilinear* Function of p:

$$a_{ij}(p) = p_1 + p_1 p_2\, a_o$$

- The Resulting P-Δ Model is *Minimal (or Near Minimal)*, i.e.:

$$\Rightarrow \quad \Delta(\delta) = diag(\, \delta_1 I_1,\ \delta_2 I_2,\ \ldots,\ \delta_m I_m\,)$$

has __Minimal Dimension__ for the Given State-Space Model

__Extend__: *Multilinear Results to Rational Case*

General Solution Framework

Block Diagram Perspective:

$$\begin{bmatrix} \dot{x} \\ y \end{bmatrix} = S(p)\begin{bmatrix} x \\ u \end{bmatrix} = \{S(p_o) + S_\Delta(\delta)\}\begin{bmatrix} x \\ u \end{bmatrix}$$

$$\begin{bmatrix} \dot{x} \\ y \end{bmatrix} = P_{22}\begin{bmatrix} x \\ u \end{bmatrix} + P_{21}\ u_\Delta$$

$$y_\Delta = P_{12}\begin{bmatrix} x \\ u \end{bmatrix} + P_{11}\ u_\Delta$$

$$u_\Delta = \Delta(\delta)\ y_\Delta$$
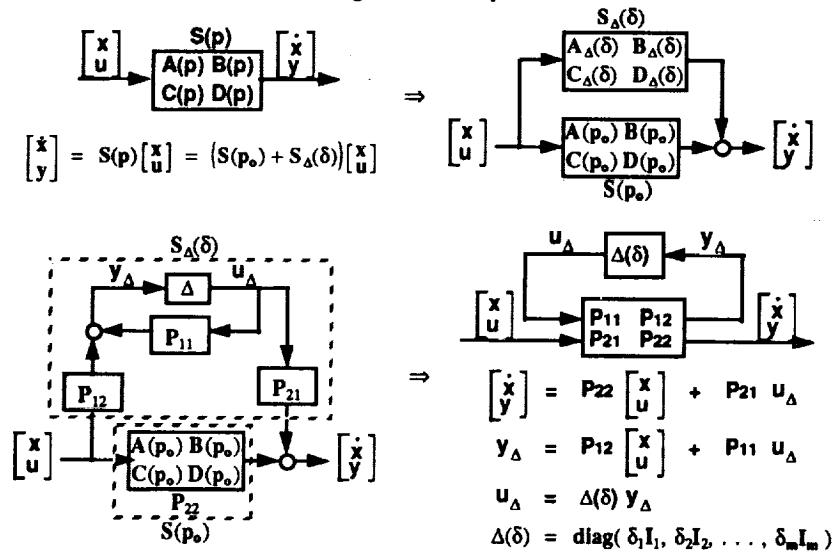
$$\Delta(\delta) = diag(\ \delta_1 I_1,\ \delta_2 I_2,\ \ldots,\ \delta_m I_m\ )$$

General Solution Framework (cont)

Equating Given & Desired Models:

$$P_{22} = S(p_o)$$

$$\Delta(\delta) = diag(\ \delta_1 I_1,\ \delta_2 I_2,\ \ldots,\ \delta_m I_m\ )$$

$$P_{21}(I - \Delta(\delta)P_{11})^{-1}\Delta(\delta)P_{12} = S_\Delta(\delta)$$

Solution of P_{21}, P_{12}, & P_{11} Matrices:

$$P_{21}(\ I - \Delta(\delta)\ P_{11})^{-1}\ \Delta(\delta)\ P_{12} = S_\Delta(\delta) = \begin{bmatrix} A_\Delta(\delta)\,B_\Delta(\delta) \\ C_\Delta(\delta)\,D_\Delta(\delta) \end{bmatrix}$$

Unknown Matrix Elements   Known Matrix Elements (Function of δ's)

General Solution Requires: Direct Matrix Inversion

$$(\ I - \Delta(\delta)\ P_{11}\ )^{-1}$$

$\Rightarrow$ Symbolic Matrix Inversion & Subsequent Solution
Difficult for Many Practical Problems

Multilinear Solution Framework

$$P_{21}(I - \Delta(\delta) P_{11})^{-1} \Delta(\delta) P_{12} = S_\Delta(\delta) = \begin{bmatrix} A_\Delta(\delta) B_\Delta(\delta) \\ C_\Delta(\delta) D_\Delta(\delta) \end{bmatrix}$$

Unknown Matrix Elements

Known Matrix Elements
(Multilinear Function of δ's)

Finite Power Series (Exact Solution):

$$(I - \Delta(\delta) P_{11})^{-1} = I + (\Delta(\delta) P_{11}) + (\Delta(\delta) P_{11})^2 + \ldots + (\Delta(\delta) P_{11})^r$$

such that: $\boxed{(\Delta(\delta) P_{11})^{r+1} = 0}$ $\Rightarrow$ **Requires Special Structure for P_{11}**

where: r - Determined by Maximum Crossterm Order in A, B, C, D

$$\Rightarrow \boxed{S_\Delta(\delta) = \begin{bmatrix} A_\Delta(\delta) B_\Delta(\delta) \\ C_\Delta(\delta) D_\Delta(\delta) \end{bmatrix} = P_{21} [I + \Delta(\delta) P_{11} + (\Delta(\delta) P_{11})^2 + \ldots + (\Delta(\delta) P_{11})^r] \Delta(\delta) P_{12}}$$

Uncertain Parameter Linear Terms **Uncertain Parameter Crossterms**

Note: 1.) nth Order Terms 2.) Inverse Terms
$\rightarrow$ Repeated Parameters $\rightarrow$ Redefine Parameters

Ex.: $p_i^2 = p_i p_{i+1}$ Ex.: $\dfrac{1}{p_i} = \bar{p}_i$

Uncertainty Modeling Procedure

To Obtain a *Minimal (or Near Minimal)*
P-Δ Uncertainty Model:

0. Determine P_{22} and Extract $S_\Delta(\delta)$:

$$P_{22} = S(p_o) = \begin{bmatrix} A(p_o) & B(p_o) \\ C(p_o) & D(p_o) \end{bmatrix} , \quad S_\Delta(\delta) = \begin{bmatrix} A_\Delta(\delta) B_\Delta(\delta) \\ C_\Delta(\delta) D_\Delta(\delta) \end{bmatrix}$$

1. Define Δ Matrix: $\Delta(\delta) = \text{diag}(\delta_1 I_1, \delta_2 I_2, \ldots, \delta_m I_m)$

Repeated Parameters *Only* for
nth Order Uncertain Parameters

2. Determine P_{21} and P_{12} Using Linear Terms (Morton & McAfoos):

$$P_{21} \Delta(\delta) P_{12} = [S_\Delta(\delta)]_0 = \begin{bmatrix} A_\Delta(\delta) B_\Delta(\delta) \\ C_\Delta(\delta) D_\Delta(\delta) \end{bmatrix}_0$$

Known Linear Uncertain Parameter Terms Only
(No Uncertain Parameter Crossterms)

181

Modeling Procedure (cont)

3. Determine P_{11} Using Uncertain Parameter Crossterms:

$$P_{21}\,(\Delta(\delta)\,\overline{P}_{11})^1\,\Delta(\delta)P_{12} \;=\; [S_\Delta(\delta)]_1 \;=\; \begin{bmatrix} A_\Delta(\delta)\,B_\Delta(\delta) \\ C_\Delta(\delta)\,D_\Delta(\delta) \end{bmatrix}_1 \quad\longleftarrow\; \begin{array}{l}\textbf{Known}\\ \textbf{First-Order}\\ \textbf{Crossterms}\end{array}$$

$$P_{21}\,(\Delta(\delta)\,\overline{P}_{11})^2\,\Delta(\delta)P_{12} \;=\; [S_\Delta(\delta)]_2 \;=\; \begin{bmatrix} A_\Delta(\delta)\,B_\Delta(\delta) \\ C_\Delta(\delta)\,D_\Delta(\delta) \end{bmatrix}_2 \quad\longleftarrow\; \begin{array}{l}\textbf{Known}\\ \textbf{Second-Order}\\ \textbf{Crossterms}\end{array}$$

$$\vdots$$

$$P_{21}\,(\Delta(\delta)\,\overline{P}_{11})^r\,\Delta(\delta)P_{12} \;=\; [S_\Delta(\delta)]_r \;=\; \begin{bmatrix} A_\Delta(\delta)\,B_\Delta(\delta) \\ C_\Delta(\delta)\,D_\Delta(\delta) \end{bmatrix}_r \quad\longleftarrow\; \begin{array}{l}\textbf{Known}\\ \textbf{rth-Order}\\ \textbf{Crossterms}\end{array}$$

with Nilpotency Condition Satisfied.

**If P_{11} Cannot be Found such that ALL of the above
Equations and Condition are Satisfied:**

**a.) Determine which Parameters Need to be Repeated
b.) Repeat Procedure from Step 1 Augmenting Δ Matrix**

**Once P_{11} has been Determined,
Minimal (or Near Minimal) P-Δ Model Has Been Found**

Example

Given Uncertain System Model :

$$A(p) = \begin{bmatrix} -\dfrac{V_a}{L_u} & 0 & 0 \\[2mm] 0 & -\dfrac{V_a}{L_u} & 0 \\[2mm] 0 & \dfrac{\sigma_w}{L_w}\sqrt{\dfrac{3V_a}{2\pi}} & -\dfrac{V_a}{L_w} \end{bmatrix} \qquad B(p) = \begin{bmatrix} \dfrac{\sigma_u}{L_u}\sqrt{\dfrac{V_a}{\pi}} & 0 \\[2mm] 0 & -\dfrac{V_a}{L_w}(1-\dfrac{1}{\sqrt{3}}) \\[2mm] 0 & \dfrac{\sigma_w}{L_w}\sqrt{\dfrac{3V_a}{2\pi}} \end{bmatrix}$$

$$C(p) = \begin{bmatrix} 1 & 0 & 0 \\ 0 & 0 & 1 \end{bmatrix} \qquad\qquad D(p) = \begin{bmatrix} 0 & 0 \\ 0 & 0 \end{bmatrix}$$

$$\Rightarrow\quad A(p) = \begin{bmatrix} -V_a\overline{L}_u & 0 & 0 \\[2mm] 0 & -V_a\overline{L}_u & 0 \\[2mm] 0 & \sigma_w\overline{L}_w^{2}\sqrt{\dfrac{3V_a}{2\pi}} & -V_a\overline{L}_w \end{bmatrix} \qquad B(p) = \begin{bmatrix} \sigma_u\overline{L}_u^{2}\sqrt{\dfrac{V_a}{\pi}} & 0 \\[2mm] 0 & -V_a\overline{L}_w(1-\dfrac{1}{\sqrt{3}}) \\[2mm] 0 & \sigma_w\overline{L}_w^{2}\sqrt{\dfrac{3V_a}{2\pi}} \end{bmatrix}$$

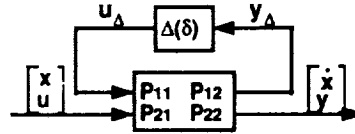**where:** $\quad \overline{L}_u = \dfrac{1}{L_u}\;,\;\; \overline{L}_w = \dfrac{1}{L_w}$

Example (cont)

P-Δ Model Solution:

$$\begin{bmatrix} \dot{x} \\ y \end{bmatrix} = P_{22} \begin{bmatrix} x \\ u \end{bmatrix} + P_{21}\, u_\Delta$$

$$y_\Delta = P_{12} \begin{bmatrix} x \\ u \end{bmatrix} + P_{11}\, u_\Delta$$

$$u_\Delta = \Delta(\delta)\, y_\Delta$$

where:

$$P_{22} = \left[\begin{array}{ccc:cc}
-V_a \tilde{L}_{u_o} & 0 & 0 & \sigma_{u_o} \tilde{L}_{u_o}{}^2 \sqrt{\tfrac{V_a}{\pi}} & 0 \\
0 & -V_a \tilde{L}_{w_o} & 0 & 0 & V_a \tilde{L}_{w_o}\left(1-\tfrac{1}{\sqrt{3}}\right) \\
0 & \sigma_{w_o} \tilde{L}_{w_o}{}^2 \sqrt{\tfrac{3V_a}{2\pi}} & -V_a \tilde{L}_{w_o} & 0 & \sigma_{w_o} \tilde{L}_{w_o}{}^2 \sqrt{\tfrac{3V_a}{2\pi}} \\ \hdashline
1 & 0 & 0 & 0 & 0 \\
0 & 0 & 1 & 0 & 0
\end{array}\right]$$

Example (cont)

P-Δ Model Solution (cont):

$$P_{21} = \left[\begin{array}{ccccccc}
-1 & \sigma_{u_o} \tilde{L}_{u_o} & 0 & 0 & 0 & \tilde{L}_{w_o} & 0 \\
0 & 0 & -V_a & V_a & 0 & 0 & 0 \\
0 & 0 & 0 & 0 & 1 & 0 & \tilde{L}_{w_o} \\ \hdashline
0 & 0 & 0 & 0 & 0 & 0 & 0 \\
0 & 0 & 0 & 0 & 0 & 0 & 0
\end{array}\right]$$

$$P_{12} = \left[\begin{array}{ccc:cc}
s\tilde{L}_{u_o} V_a & 0 & 0 & 0 & 0 \\
0 & 0 & 0 & 2s\tilde{L}_{u_o}\sqrt{\tfrac{V_a}{\pi}} & 0 \\
0 & s\tilde{L}_w & 0 & 0 & s\tilde{L}_w \\
0 & 0 & 0 & 0 & s\tilde{L}_w \tfrac{1}{\sqrt{3}} \\
0 & 2s\tilde{L}_w \sigma_{w_o}\tilde{L}_{w_o}\sqrt{\tfrac{3V_a}{2\pi}} & -s\tilde{L}_w V_a & 0 & 2s\tilde{L}_w \sigma_{w_o}\tilde{L}_{w_o}\sqrt{\tfrac{3V_a}{2\pi}} \\
0 & 0 & 0 & s\sigma_w\sqrt{\tfrac{V_a}{\pi}} & 0 \\
0 & s\sigma_w\sqrt{\tfrac{3V_a}{2\pi}} & 0 & 0 & s\sigma_w\sqrt{\tfrac{3V_a}{2\pi}}
\end{array}\right]$$

Example (cont)

P-Δ Model Solution (cont):

$$P_{11} = \begin{bmatrix} 0 & -\tilde{L}_u \frac{\sigma_u}{2} & 0 & 0 & 0 & 0 & 0 \\ 0 & 0 & 0 & 0 & 0 & \frac{2\tilde{L}_u}{\sigma_{w_o}} & 0 \\ 0 & 0 & 0 & 0 & 0 & 0 & \frac{\tilde{L}_w}{\sigma_{w_o}}\sqrt{\frac{2\pi}{3V_o}} \\ 0 & 0 & 0 & 0 & 0 & 0 & \frac{\tilde{L}_w}{\sigma_{w_o}}\sqrt{\frac{2\pi}{3V_o}} \\ 0 & 0 & \tilde{L}_w \sigma_{w_o}\sqrt{\frac{3V_o}{2\pi}} & 0 & 0 & 0 & 2s\tilde{L}_w \tilde{L}_{w_o} \\ 0 & 0 & 0 & 0 & 0 & 0 & 0 \\ 0 & 0 & 0 & 0 & 0 & 0 & 0 \end{bmatrix}$$

$$\Delta(\delta) \;=\; \mathrm{diag}\,[\; \delta_{\tilde{L}_u} I_2 \quad \delta_{\tilde{L}_w} I_3 \quad \delta_{\sigma_u} \quad \delta_{\sigma_w} \;]$$

Extension to Rational Case

$$\begin{bmatrix} S_{N_\Delta} \\ S_{D_\Delta} \end{bmatrix} = \begin{bmatrix} P_{21_N} \\ P_{21_D} \end{bmatrix} (I - \Delta P_{11})^{-1} \Delta P_{12}$$

(Multilinear Problem)

184
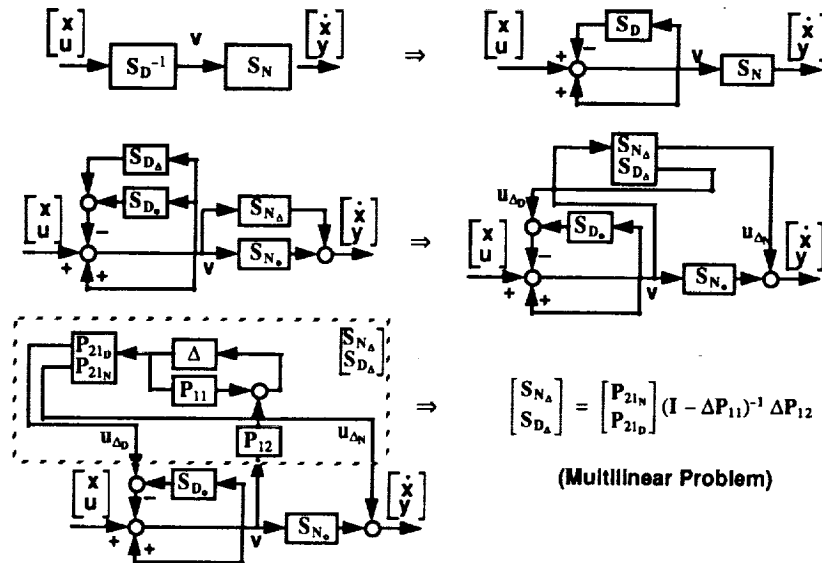
Extension to Rational Case (cont.)

System Equations:

$$\begin{bmatrix} \dot{x} \\ y \end{bmatrix} = S_{N_o} S_{D_o}^{-1} \begin{bmatrix} x \\ u \end{bmatrix} + \left(\begin{bmatrix} P_{21_{N_x}} \\ P_{21_{D_y}} \end{bmatrix} - S_{N_o} S_{D_o}^{-1} \begin{bmatrix} P_{21_{D_x}} \\ P_{21_{D_y}} \end{bmatrix} \right) u_\Delta$$

$$y_\Delta = [P_{12_x} \, P_{12_u}] S_{D_o}^{-1} \begin{bmatrix} x \\ u \end{bmatrix} + \left(P_{11} - [P_{12_x} \, P_{12_u}] S_{D_o}^{-1} \begin{bmatrix} P_{21_{D_x}} \\ P_{21_{D_y}} \end{bmatrix} \right) u_\Delta$$

$$u_\Delta = \Delta \, y_\Delta$$

where:

$$S_{N_o} S_{D_o}^{-1} = S_o = \begin{bmatrix} A_o \, B_o \\ C_o \, D_o \end{bmatrix} = P_{22}$$

$$S_{N_o} = \begin{bmatrix} A_{N_o} \, B_{N_o} \\ C_{N_o} \, D_{N_o} \end{bmatrix} \quad , \quad S_{D_o}^{-1} = \begin{bmatrix} A_{D_o} \, B_{D_o} \\ C_{D_o} \, D_{D_o} \end{bmatrix}^{-1}$$

Concluding Remarks

- ## *Multilinear Solution Framework*

  - *Solves Multilinear Parameter Case*
    - ⇒ *Accomodates nth Order and Inverse Terms*

  - *Eliminates Symbolic Matrix Inversion in Computation of P_{11}*
    - ⇒ **Computationally Tractable for Symbolic Solution**
      (Symbolic Algebra Tool Required)

  - *Can be Extended to Rational Parameter Case*
    - ⇒ *Preliminary Results*

- ## *Systematic Procedure for (Near) Minimal P-Δ Modeling*

  - *Minimality is Relative to Given State Space Realization*

    - ⇒ **A Lower Dimension P-Δ Model May Exist for Different Realization**

  - *(Near) Minimality by Construction*

    - ⇒ **Minimality may not Always be Assured**

Further Work

- _Evaluate/Refine/Generalize_ Procedure

    - *Wider Class of Problems*

    - *Multidimensional System Theory*

- _Automate_ Modeling Procedure

    - *Mathematica/Maple*

    - *Output Files to Matlab*

- _Apply_ to HSCT Problems

    - *Configuration Evaluation*

    - *Control System Analysis & Design*

Parametric Uncertainty Modeling for Application to Robust Control

Christine M. Belcastro
MS 489
NASA Langley Research Center
Hampton, VA 23665

B.-C. Chang
ME&M Dept.
Drexel University
Philadelphia, PA 19104

Robert Fischl
ECE Dept.
Drexel University
Philadelphia, PA 19104

Abstract

Advanced robust control system analysis and design is based on the availability of an uncertainty description which separates the uncertain system elements from the nominal system. Although this modeling structure is relatively straightforward to obtain for multiple unstructured uncertainties modeled throughout the system, it is difficult to formulate for many problems involving real parameter variations. Furthermore, it is difficult to ensure that the uncertainty model is formulated such that the dimension of the resulting model is minimal. This paper presents a procedure for obtaining an uncertainty model for real uncertain parameter problems in which the uncertain parameters can be represented in a multilinear form. Furthermore, the procedure is formulated such that the resulting uncertainty model is minimal (or near minimal) relative to a given state space realization of the system. The approach is demonstrated for a multivariable third-order example problem having four uncertain parameters.

1. Introduction

Advanced robust control system analysis and design is based on the availability of an uncertainty description which separates the uncertain system elements from the nominal system. More specifically, the uncertain system components are contained in a block-diagonal Δ matrix, which is connected to the nominal system, P(s), such that the closed-loop uncertain system is described by a linear fractional transformation (LFT). The idea of separating the uncertain part of a system from its nominal part in this manner, for use in robust control system analysis and design, was first posed by John Doyle (see [3] and [4]), and the robust control theory associated with this structured description of uncertainty continues to be an important area of research. A block diagram of this modeling structure can be depicted as follows in Figure 1:
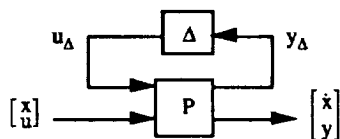
Figure 1. Block Diagram of General Uncertain System

where u contains all external inputs to the system (e.g., disturbances, control inputs, etc.), y contains all outputs from the system (e.g., controlled outputs, measured outputs, etc.) and u_Δ and y_Δ connect the uncertainties represented by Δ to the nominal system, P(s). Although this modeling structure is relatively straightforward to obtain for multiple unstructured uncertainties which occur throughout the system, it is difficult to formulate for many problems involving real parameter variations. Furthermore, it is difficult to ensure that the uncertainty model is formulated such that the dimension of the resulting model is minimal (i.e., the number of repeated parameters in Δ is minimized). Although formulating an uncertainty model is a requirement for utilizing the recently developed robust control analysis and design techniques mentioned above, very little research has been reported in the literature which addresses this problem, particularly for the real parameter uncertainty case. Results to date primarily apply to multiple uncertain parameters which enter the system model in a linear functional form, although some work involving nonlinear special cases have been worked [10]. The results for linear uncertain parameters were first presented in [8] (Morton & McAfoos, 1985) and [9]

(Morton, 1985). A later paper [10] (Steinbuch, et. al., 1991) summarizes the general uncertainty modeling problem and the results to date, and presents two simple scalar nonlinear uncertain parameter examples. However, no solution to the general minimal uncertainty modeling problem has been found. The objective of this paper is to present an important extension to these uncertainty modeling results. Specifically, a procedure is presented for obtaining a minimal (or near minimal) uncertainty model (having the form of Figure 1) given the state space realization of an uncertain system with multiple parametric uncertainties entering the model in a multilinear functional form. It should be noted that minimality here is relative to the given state space realization. As discussed in [1] and [2] (Belcastro, et. al., 1989 and 1991), the dimension of the uncertainty model (i.e., the dimension of the Δ matrix) is dependent on the state space realization of the system. Thus, one can consider the minimality of an uncertainty model for a particular state space realization, or one can consider the achievable minimality of the uncertainty model irrespective of the system realization. In this paper, we present a method of obtaining a minimal (or near minimal) uncertainty model relative to the given state space model of the uncertain system for multiple uncertainties entering the model in a multilinear functional form. The multilinear framework significantly reduces the computational complexity involved in obtaining a solution, as compared to solving the problem directly for the rational parameter case. Moreover, it can be shown that the multilinear solution framework can actually be used to solve the rational parameter case, as well. Thus, it provides a means of determining an uncertainty model for many difficult problems of practical interest.

The paper is organized in the following manner. Section 2 presents a formal problem definition for the general uncertain parameter case, briefly summarizes results for the special case of linear parametric uncertainty, and defines the problem to be addressed in this paper. Section 3 summarizes our results for this defined problem, and Section 4 presents an example problem which demonstrates these results. Section 5 briefly discusses the application of the multilinear solution framework to solve the rational uncertain parameter problem, and concluding remarks are given in Section 6.

2. Parametric Uncertainty Modeling: Problem Definition

2.1 General Problem Definition

Consider the state space model of an uncertain system:

$$\dot{x} = A(p) x + B(p) u , \quad x \in R^{n_x}, u \in R^{n_u} \qquad (1a)$$

$$y = C(p) x + D(p) u , \quad y \in R^{n_y} \qquad (1b)$$

where p represents a vector of real uncertain parameters:

$$p = [p_1, p_2, \cdots, p_m] \in R^m \qquad (2)$$

It is assumed that each entry of the model presented in equation (1) is a function of the parameters p. For the general rational case considered in this paper, the uncertain parameters can appear in a rational multivariate functional form within each element of the system model. For example, as given in [10] (Steinbuch et. al., 1991), the $(i,j)^{th}$ entry of the A matrix could have the form:

$$A_{ij}(p) = \frac{p_1 + p_2 \, a_o + p_2^2 \, p_3}{p_1 \, p_3 + a_1 \, p_4} \tag{3}$$

where a_o and a_1 are constants. It should be noted that n^{th}-order terms are included here because they can be handled within a multilinear framework by defining n-1 additional uncertain parameters which are equal to the parameter being raised to the nth power. For this example, a new uncertain parameter, $p_2' = p_2$, could be defined and p_2^2 would then be replaced by $p_2 p_2'$.

The uncertainty modeling problem consists of three components: scaling of the uncertain parameters, extraction of the uncertainties from the nominal system, and formulation of a linear fractional transformation (LFT) (see [5], Doyle, et. al., 1991 for a review of LFT's). These components are reviewed below.

Uncertainty Scaling:

Each uncertain parameter p_i in p can be bounded by an upper bound, p_{max_i}, and a lower bound, p_{min_i}, as follows:

$$p_{min_i} \leq p_i \leq p_{max_i} \tag{4}$$

Then the parameter can be written in terms of some nominal value within this range of uncertainty. One way to do this is shown below:

$$p_i = p_{nom_i} + \overline{\delta}_i = p_{nom_i} + s_i \, \delta_i \tag{5}$$

$$p_{nom_i} = \frac{p_{min_i} + p_{max_i}}{2} \tag{6}$$

$$s_i = \frac{p_{max_i} - p_{min_i}}{2} \tag{7}$$

$$|\delta_i| \leq 1 \tag{8}$$

Equations (4) - (7) can also be written in vector form by stacking each associated parameter quantity into vectors. The δ_i terms as defined in equations (5) and (8) are the uncertain terms that will be separated into the Δ matrix of Figure 1.

Uncertainty Extraction:

Using equation (5), the state space model of the uncertain system given in (1) can be rewritten in compact form as follows:

$$\begin{bmatrix} \dot{x} \\ y \end{bmatrix} = S(p) \begin{bmatrix} x \\ u \end{bmatrix} = S(p_{nom}) \begin{bmatrix} x \\ u \end{bmatrix} + S_\Delta(\delta) \begin{bmatrix} x \\ u \end{bmatrix} \tag{9}$$

where:

$$\delta = [\, \delta_1, \delta_2, \cdots, \delta_m \,] \in R^m \tag{10}$$

$$S(p) = \begin{bmatrix} A(p) & B(p) \\ C(p) & D(p) \end{bmatrix} = S(p_{nom}) + S_\Delta(\delta) \tag{11}$$

$$S(p_{nom}) = \begin{bmatrix} A(p_{nom}) & B(p_{nom}) \\ C(p_{nom}) & D(p_{nom}) \end{bmatrix} \tag{12a}$$

$$S_\Delta(\delta) = \begin{bmatrix} A_\Delta(\delta) & B_\Delta(\delta) \\ C_\Delta(\delta) & D_\Delta(\delta) \end{bmatrix} \tag{12b}$$

Separation of S(p) into nominal and uncertain parts, $S(p_{nom})$ and $S_\Delta(\delta)$, respectively, results in the extraction of the uncertainties from the nominal system.

Formulation of a Linear Fractional Transformation (LFT):

Equation (9) can be rewritten in the form of an upper (time domain) LFT by defining an input vector, u_Δ, and an output vector, y_Δ, associated with the uncertain part of the system as follows:

$$y_\Delta = P_{11} u_\Delta + P_{12} \begin{bmatrix} x \\ u \end{bmatrix} \tag{13}$$

$$\begin{bmatrix} \dot{x} \\ y \end{bmatrix} = P_{21} u_\Delta + P_{22} \begin{bmatrix} x \\ u \end{bmatrix} \tag{14}$$

$$u_\Delta = \Delta(\delta) y_\Delta \tag{15}$$

$$\Delta(\delta) = diag(\delta_1 I_1, \delta_2 I_2, ..., \delta_m I_m) \tag{16a}$$

$$\Delta(\delta) \in R^{n_\Delta \times n_\Delta} \tag{16b}$$

$$n_\Delta = \sum_{i=1}^{m} r_i \; , \; r_i = dim(I_i) \tag{17}$$

where P_{11}, P_{12}, P_{21}, and P_{22} are constant matrices with $P_{22} = S(p_{nom})$, and the matrices P_{11}, P_{12}, and P_{21} are related to $S_\Delta(\delta)$. The I_i terms in equation (16a) represent the identity matrix with dimension equal to the repeatedness of parameter δ_i. For example, the squared uncertain parameter of equation (3), i.e. p_2^2, results (after scaling) in the term δ_2^2. Thus, this example would require that both δ_2 and $\delta_2' = \delta_2$ (associated with the uncertain parameter p_2' discussed above) appear in Δ, which means that I_2 in equation (16a) would be a 2-dimensional identity matrix.

The objective of the uncertainty modeling problem is to find the matrices P_{11}, P_{12}, and P_{21} such that the system of equations represented by (13) - (16) is equivalent to the system represented by equation (9). To do this, equations (13) - (15) are combined such that u_Δ and y_Δ are eliminated, as follows:

$$\begin{bmatrix} \dot{x} \\ y \end{bmatrix} = [P_{22} + P_{21}(I - \Delta(\delta)P_{11})^{-1}\Delta(\delta)P_{12}] \begin{bmatrix} x \\ u \end{bmatrix} \tag{18}$$

Thus, the uncertainty modeling problem can be thought of as a multi-dimensional (minimal) realization problem defined by the following equation:

$$S_\Delta(\delta) = P_{21}(I - \Delta(\delta)P_{11})^{-1} \Delta(\delta)P_{12} \tag{19}$$

where δ represents the uncertain parameter vector defined in equation (10).

2.2 Summary of Results for Linear Parametric Uncertainties

As indicated previously in this paper, uncertainty modeling results have primarily focused on the special uncertainty case involving multiple uncertain parameters that enter the system model linearly. Results for this case were first presented by [8] (Morton & McAfoos, 1985), and involve solving equation (19) with $P_{11} = 0$. For this case, P_{21} and P_{12} can easily be found by expanding $S_\Delta(\delta)$ as a linear combination of the δ_i terms, and decomposing the resulting coefficient matrices. If any of the coefficient matrices has rank greater than one, then the associated δ_i term must be repeated in Δ a corresponding number of times in order to perform the decomposition. For example, if the coefficient matrix for δ_i is rank 2, then δ_i must appear twice in the Δ matrix. This is also discussed in [9] (Morton, 1985).

2.3 Specific Problem Definition for this Paper: Multilinear Parametric Uncertainties

In this paper, we consider the case of multiple uncertain parameters which enter any element of the system described in equation (1) in a multilinear manner. It should be noted that rational multivariate elements involving only one denominator term can be represented in a multilinear form directly. For example,

$$A_{ij}(p) = \frac{p_1 + p_2\, a_o + p_2{}^2\, p_3}{p_1\, p_3} \tag{21a}$$

$$= \tilde{p}_3 + \tilde{p}_1\, p_2\, \tilde{p}_3\, a_o + \tilde{p}_1\, p_2{}^2$$

where:

$$\tilde{p}_1 = \frac{1}{p_1} \quad , \quad \tilde{p}_3 = \frac{1}{p_3} \tag{21b}$$

The general multivariate rational uncertainty case containing multiple uncertain terms in the denominator (defined in Section 2.1) could be redefined. For example, an uncertain model element represented by equation (3) could be approximated in a multilinear form as follows:

$$A_{ij}(p) = \frac{p_1 + p_2\, a_o + p_2{}^2\, p_3}{p_1\, p_3 + a_1\, p_4} \tag{20a}$$

$$= \tilde{p}_4\, (p_1 + p_2\, a_o + p_2{}^2\, p_3)$$

where:

$$\tilde{p}_4 = \frac{1}{p_1\, p_3 + a_1\, p_4} \tag{20b}$$

Thus, in this formulation the fourth uncertain parameter, $\tilde{p}_4$, is dependent on the uncertain parameters p_1, p_3, and p_4. This approach therefore poses a slight restriction to the general case. However, a brief discussion of a technique for formulating the rational problem in such a way that the multilinear solution framework can be used is presented in Section 5.

2.4 Formal Problem Statement

A formal problem statement based on the above discussion can be summarized as follows:

Given: An uncertain system in state space form as in equation (1), i.e.:

$$\dot{x} = A(p)\, x + B(p)\, u , \quad x \in R^{n_x},\ u \in R^{n_u}$$
$$y = C(p)\, x + D(p)\, u , \quad y \in R^{n_y}$$

which can be rewritten as in equation (9), i.e.:

$$\begin{bmatrix} \dot{x} \\ y \end{bmatrix} = S(p)\begin{bmatrix} x \\ u \end{bmatrix} = S(p_{nom})\begin{bmatrix} x \\ u \end{bmatrix} + S_\Delta(\delta)\begin{bmatrix} x \\ u \end{bmatrix}$$

Find: The matrices P_{21}, P_{12}, and P_{11} such that the above system can be expressed as in equations (13-16), i.e.:

$$y_\Delta = P_{11}\, u_\Delta + P_{12}\begin{bmatrix} x \\ u \end{bmatrix}$$

$$\begin{bmatrix} \dot{x} \\ y \end{bmatrix} = P_{21}\, u_\Delta + P_{22}\begin{bmatrix} x \\ u \end{bmatrix}$$

$$u_\Delta = \Delta(\delta)\, y_\Delta$$

$$\Delta(\delta) = diag(\, \delta_1 I_1,\, \delta_2 I_2, \ldots,\, \delta_m I_m\,)$$

A detailed discussion of a solution to this problem for uncertainties which are represented within a multilinear framework, as discussed above, will be presented in the next section.

3. Parametric Uncertainty Modeling: A Multilinear Problem Solution

3.1 Multilinear Solution Framework

As indicated in Section 2, the solution to the uncertainty modeling problem posed above involves finding the matrices P_{21}, P_{12}, and P_{11} such that the $S_\Delta(\delta)$ matrices given by (12) and (19) are equal, i.e.:

$$S_\Delta(\delta) = \begin{bmatrix} A_\Delta(\delta) & B_\Delta(\delta) \\ C_\Delta(\delta) & D_\Delta(\delta) \end{bmatrix}$$

$$= P_{21}(I - \Delta(\delta)P_{11})^{-1}\, \Delta(\delta)P_{12} \tag{22}$$

$$= \begin{bmatrix} P_{21_x} \\ P_{21_y} \end{bmatrix}(I - \Delta(\delta)P_{11})^{-1}\, \Delta(\delta)\big[\, P_{12_x} \ \ P_{12_u}\,\big]$$

where the $A_\Delta(\delta)$, $B_\Delta(\delta)$, $C_\Delta(\delta)$, and $D_\Delta(\delta)$ terms in equation (22) are formed by scaling the uncertain parameters p and extracting the uncertain δ terms from the nominal system, as discussed in Section 2, and P_{21} and P_{12} are partitioned appropriately. Thus, the matrices $A_\Delta(\delta)$, $B_\Delta(\delta)$, $C_\Delta(\delta)$, and $D_\Delta(\delta)$ are known matrix functions of the δ parameters, and the matrices P_{21}, P_{12}, and P_{11} are the unknown matrix variables for which equation (22) is solved. This section presents the main result of the paper - namely a solution to the above problem for uncertainties that are represented within the multilinear framework described in Section 2.3.

As stated above, the solution to this problem involves solving equation (22) for P_{21}, P_{12}, and P_{11}. However, the inversion of the quantity $(I - \Delta(\delta)\, P_{11})$ in equation (22) for multiple parameter problems can become very cumbersome because P_{11} is of the same dimension as $\Delta(\delta)$, and the inversion has to be performed symbolically. Moreover, each element of P_{11} must be determined such that equation (22) is satisfied. Within the multilinear framework, however, this quantity can be replaced by a finite series. To see this, consider the matrix equation:

$$I - A^{n+1} = (I - A)(I + A + A^2 + A^3 + \ldots + A^n)$$

which can be written for any matrix A. Assuming that the matrix $(I - A)$ is invertible, this equation can be rewritten as:

$$(I - A)^{-1}(I - A^{n+1}) = I + A + A^2 + A^3 + \ldots + A^n$$

If matrix A is structured such that $A^{n+1} = 0$ (i.e., A is nilpotent), then:

$$(I - A)^{-1} = I + A + A^2 + A^3 + \ldots + A^n$$

This development is similar to the Neuman series expansion developed in [6] (Halmos, 1974) for a matrix A such that $\| A \| < 1$. For our problem, however, $A = \Delta(\delta)\, P_{11}$, where $\Delta(\delta)$ is a diagonal matrix and P_{11} is unknown. Although $\Delta(\delta)$ is norm-bounded by unity, P_{11} is not norm-bounded. However, since P_{11} is to be determined, requiring P_{11} to be structured such that:

$$(\Delta(\delta)\, P_{11})^{r+1} = 0 \tag{23}$$

yields:

$$(I - \Delta(\delta)\, P_{11})^{-1} = I + (\Delta(\delta)\, P_{11}) + (\Delta(\delta)\, P_{11})^2$$
$$+ \ldots + (\Delta(\delta)\, P_{11})^r \tag{24}$$

Substituting this into equation (22) results in:

$$S_\Delta(\delta) = \begin{bmatrix} A_\Delta(\delta) & B_\Delta(\delta) \\ C_\Delta(\delta) & D_\Delta(\delta) \end{bmatrix} \tag{25}$$

$$= P_{21}[I + \Delta(\delta)P_{11} + (\Delta(\delta)P_{11})^2 + \ldots + (\Delta(\delta)P_{11})^r]\Delta(\delta)P_{12}$$

which can be rewritten as:

$$S_\Delta(\delta) = P_{21}\Delta(\delta)P_{12} +$$
$$P_{21}[\Delta(\delta)P_{11} + (\Delta(\delta)\, P_{11})^2 + \ldots$$
$$\ldots(\Delta(\delta)P_{11})^r]\Delta(\delta)P_{12} \tag{26}$$

The first term on the right side of equation (26) represents the linear uncertain components of $S_\Delta(\delta)$, and the second term adds in the nonlinear terms. Furthermore, since the nonlinear terms of $S_\Delta(\delta)$ consist of cross terms and n^{th}-order terms (which can be represented as cross terms), the order, r, of the highest term in the series of equation (26) is defined by the highest cross term order required to realize $S_\Delta(\delta)$. Thus, r is defined by the order of the highest cross-term occurring in $A_\Delta(\delta)$, $B_\Delta(\delta)$, $C_\Delta(\delta)$, and $D_\Delta(\delta)$, i.e.:

$$r = \max(O_A, O_B, O_C, O_D) \qquad (27a)$$

and O_A, O_B, O_C, and O_D represent the order of the highest-order cross-product term in $A_\Delta(\delta)$, $B_\Delta(\delta)$, $C_\Delta(\delta)$, and $D_\Delta(\delta)$, respectively. That is, for a general uncertain m×n matrix M:

$$O_M = \max[\, order(m_{ij})\,;\; \text{for all } i = 1,2,...,m \\ \text{and } j = 1,2,...,n\,] \qquad (27b)$$

where the order of each m_{ij} is the order of its highest-order cross-product term, and cross-product term order is defined as:

$$order(\delta_1\,\delta_2\,\delta_3\,...\,\delta_i) = i - 1 \\ \text{for } i = 1, 2, \ldots, n_\Delta. \qquad (27c)$$

Thus, the maximum value of r is $r_{max} = n_\Delta - 1$, where n_Δ is the dimension of the Δ matrix and is given by equation (17). The nilpotent requirement of equation (23) for $(\Delta(\delta) P_{11})$ can be satisfied if the elements of P_{11}, p_{ij}, satisfy the following structure:

1.) $p_{ii} = 0$; $\qquad i = 1, 2, \ldots, n_\Delta$
2.) If $p_{ij} \neq 0$, then for
$\quad i = 1, 2, \ldots, n_\Delta$ and $j = 1, 2, \ldots, n_\Delta$:
$\quad$ a.) $p_{ji} = 0$;
$\quad$ b.) $p_{i\oplus1,j\oplus1} = 0$ or $p_{i\oplus2,j\oplus2} = 0$ or
$\quad \ldots$ or $p_{i\oplus(n_\Delta-1),j\oplus(n_\Delta-1)} = 0$

$\qquad (28)$

where the symbol "$\oplus$" represents "modulo n_Δ" addition [7] (Horowitz and Sahni, 1978) over the set $\{1, 2, \ldots, n_\Delta\}$, i.e.:

$$a \oplus b = \begin{cases} a+b & \text{if } a+b \leq n_\Delta \\ a+b-n_\Delta & \text{if } a+b > n_\Delta \end{cases}$$

$$1 \leq a \leq n_\Delta\,,\; 1 \leq b \leq n_\Delta$$

and n_Δ is the dimension of Δ (and, hence, P_{11}) as defined in equation (17). It should be noted that requiring P_{11} to satisfy the conditions of (28) does not impose a restriction in solving the uncertainty modeling problem, but rather it is a means of removing unnecessary freedom in determining P_{11} based on the uncertain system being modeled. Thus, (28) assists in the process of solving for P_{11}.

Using this multilinear framework, P_{21} and P_{12} can be found using the linear uncertain terms of $S_\Delta(\delta)$, and P_{11} can be found using the nonlinear terms of $S_\Delta(\delta)$ such that the conditions of (28) are satisfied. Thus, the procedure presented in [8] (Morton & McAfoos, 1985) (and briefly described in Section 2.2) for obtaining an uncertainty model for multiple linear uncertain parameters can be used to obtain P_{21} and P_{12}, and these matrices can be used in the second right-hand term of equation (26) so that P_{11} can be determined directly using equations (26) and (28). Details of the procedure for doing this are presented in [1] and [2] (Belcastro, et. al., 1989 and 1991), and an example problem is presented in Section 4 which demonstrates these results.

3.2 Uncertainty Modeling Procedure

Obviously, in order to reduce computational complexity in robust control system analysis and design, it is desired to obtain an uncertainty model of minimal dimension. As discussed in [1] and [2]

(Belcastro et. al., 1989 and 1991), the dimension of the uncertainty model is dependent on the system state space realization. These papers address the problem of obtaining a state space realization of an uncertain single-input single-output (SISO) system (given its transfer function) such that an uncertainty model of minimal dimension can be determined. For practical multivariable applications, however, it is usually desired to retain physical relevance to the problem being considered in assigning the states of the system, so that a particular state space realization may be preferred. Therefore, given a desired state space model of an uncertain system, one would like to be able to determine a minimal uncertainty model for this particular realization - which may or may not be an overall minimal uncertainty model for the system. A procedure to obtain a minimal (or near minimal) uncertainty model relative to a particular state space realization (based on the multilinear framework presented in Section 3.2) is therefore given in this section.

Given a state space realization of an uncertain system whose matrix elements are multilinear functions of the uncertain parameters of the system, it is desired to obtain an uncertainty model of the form of Figure 1, which has a minimal (or near minimal) number of repeated parameters in Δ. This can be done using the following approach:

1. Define a Δ matrix of the form of equation (16) which has only those repeated uncertain parameters necessary to realize the nth-order uncertain terms in the model, as discussed in Section 2.1.

2. Follow the procedure given in [8] (Morton & McAfoos, 1985) and [9] (Morton, 1985) for the linear uncertain parameter case to obtain P_{21} and P_{12} using equations (22) and (26). If problems with rank occur in defining P_{21} and P_{12}, go back to step 1 and add a repeated parameter to Δ, as described in Section 2.2.

3. Once P_{21} and P_{12} have been obtained, use the nonlinear uncertain terms in equations (22) and (26) to obtain P_{11} such that the conditions of (28) and, hence, equation (23) are satisfied. If P_{11} cannot be determined such that all of these equations and conditions are satisfied, the dimension of Δ is not large enough. If this occurs, it must be determined which parameter must be repeated (based on the specific problem encountered in trying to satisfy the above equations), and the process begins again at step 1 with the repeated parameter being added to the Δ matrix. Once P_{11} has been successfully determined such that all equations and conditions are satisfied, the minimal (or near minimal) uncertainty model for the given state space realization of the system has been determined, and equations (13) - (16) can be used to model the uncertain system as depicted in Figure 1.

It should be noted that the above procedure yields a minimal (or near minimal) uncertainty model by __construction__, since the initial Δ matrix defined in step 1 is of the smallest possible dimension required to model the given system, and additional parameters are added to this Δ matrix in steps 2 and 3 only if required. An example problem illustrating the above procedure is presented in Section 4.

4. Example

Consider the third-order multivariable system described in state space form as in equation (1) by the following realization:

$$A(p) = \begin{bmatrix} -\dfrac{V_a}{L_u} & 0 & 0 \\[2ex] 0 & -\dfrac{V_a}{L_w} & 0 \\[2ex] 0 & \dfrac{\sigma_w}{L_w{}^2}\sqrt{\dfrac{3V_a}{2\pi}} & -\dfrac{V_a}{L_w} \end{bmatrix} \qquad (29a)$$

$$B(p) = \begin{bmatrix} \frac{\sigma_u}{L_u{}^2}\sqrt{\frac{V_a}{\pi}} & 0 \\ 0 & -\frac{V_a}{L_w}(1-\frac{1}{\sqrt{3}}) \\ 0 & \frac{\sigma_w}{L_w{}^2}\sqrt{\frac{3V_a}{2\pi}} \end{bmatrix} \qquad (29b)$$

$$C(p) = \begin{bmatrix} 1 & 0 & 0 \\ 0 & 0 & 1 \end{bmatrix}, \quad D(p) = \begin{bmatrix} 0 & 0 \\ 0 & 0 \end{bmatrix} \qquad (29c)$$

where the uncertain parameters L_u, L_w, σ_u, and σ_w vary over the following ranges:

$$105.7 \le L_u \le 841.1 \qquad (30a)$$
$$10.4 \le L_w \le 795.5 \qquad (30b)$$
$$5.74 \le \sigma_u \le 9.69 \qquad (30c)$$
$$3.95 \le \sigma_w \le 13.4 \qquad (30d)$$

The elements of equation (29) can be expressed as multilinear functions of the uncertain parameters as follows:

$$A(p) = \begin{bmatrix} -V_a\tilde{L}_u & 0 & 0 \\ 0 & -V_a\tilde{L}_w & 0 \\ 0 & \sigma_w\tilde{L}_w{}^2\sqrt{\frac{3V_a}{2\pi}} & -V_a\tilde{L}_w \end{bmatrix} \qquad (31a)$$

$$B(p) = \begin{bmatrix} \sigma_u\tilde{L}_u{}^2\sqrt{\frac{V_a}{\pi}} & 0 \\ 0 & -V_a\tilde{L}_w(1-\frac{1}{\sqrt{3}}) \\ 0 & \sigma_w\tilde{L}_w{}^2\sqrt{\frac{3V_a}{2\pi}} \end{bmatrix} \qquad (31b)$$

$$C(p) = \begin{bmatrix} 1 & 0 & 0 \\ 0 & 0 & 1 \end{bmatrix}, \quad D(p) = \begin{bmatrix} 0 & 0 \\ 0 & 0 \end{bmatrix} \qquad (31c)$$

where:

$$\tilde{L}_u = \frac{1}{L_u}, \quad \tilde{L}_w = \frac{1}{L_w} \qquad (32)$$

$$.001189 \le \tilde{L}_u \le .009461, \quad .0013 \le \tilde{L}_w \le .00962$$

The first step is to extract the uncertain δ terms from the nominal system by scaling the uncertain parameters as in equation (5), as follows:

$$\tilde{L}_u = \tilde{L}_{u_o} + s_{\tilde{L}_u}\delta_{\tilde{L}_u} = \tilde{L}_{u_o} + \bar{\delta}_{\tilde{L}_u}$$

$$\tilde{L}_w = \tilde{L}_{w_o} + s_{\tilde{L}_w}\delta_{\tilde{L}_w} = \tilde{L}_{w_o} + \bar{\delta}_{\tilde{L}_w}$$

$$\sigma_u = \sigma_{u_o} + s_{\sigma_u}\delta_{\sigma_u} = \sigma_{u_o} + \bar{\delta}_{\sigma_u} \qquad (33)$$

$$\sigma_w = \sigma_{w_o} + s_{\sigma_w}\delta_{\sigma_w} = \sigma_{w_o} + \bar{\delta}_{\sigma_w}$$

so that, as in equation (12):

$$S(p_{nom}) = \begin{bmatrix} A(p_o)B(p_o) \\ C(p_o)D(p_o) \end{bmatrix}; \quad S_\Delta(\delta) = \begin{bmatrix} A_\Delta(\delta) & B_\Delta(\delta) \\ C_\Delta(\delta) & D_\Delta(\delta) \end{bmatrix} \qquad (34)$$

where:

$$A(p_o) = \begin{bmatrix} -V_a\tilde{L}_{u_o} & 0 & 0 \\ 0 & -V_a\tilde{L}_{w_o} & 0 \\ 0 & \sigma_{w_o}\tilde{L}_{w_o}{}^2\sqrt{\frac{3V_a}{2\pi}} & -V_a\tilde{L}_{w_o} \end{bmatrix} \qquad (35a)$$

$$B(p_o) = \begin{bmatrix} \sigma_{u_o}\tilde{L}_{u_o}{}^2\sqrt{\frac{V_a}{\pi}} & 0 \\ 0 & -V_a\tilde{L}_{w_o}(1-\frac{1}{\sqrt{3}}) \\ 0 & \sigma_{w_o}\tilde{L}_{w_o}{}^2\sqrt{\frac{3V_a}{2\pi}} \end{bmatrix} \qquad (35b)$$

$$C(p_o) = \begin{bmatrix} 1 & 0 & 0 \\ 0 & 0 & 1 \end{bmatrix}, \quad D(p_o) = \begin{bmatrix} 0 & 0 \\ 0 & 0 \end{bmatrix} \qquad (35c)$$

$$A_\Delta(\delta) = \begin{bmatrix} -V_a\bar{\delta}_{\tilde{L}_u} & 0 & 0 \\ 0 & -V_a\bar{\delta}_{\tilde{L}_w} & 0 \\ 0 & a_{\Delta_1}\sqrt{\frac{3V_a}{2\pi}} & -V_a\bar{\delta}_{\tilde{L}_w} \end{bmatrix} \qquad (36a)$$

$$B_\Delta(\delta) = \begin{bmatrix} b_{\Delta_1}\sqrt{\frac{V_a}{\pi}} & 0 \\ 0 & -V_a(1-\frac{1}{\sqrt{3}})\bar{\delta}_{\tilde{L}_w} \\ 0 & b_{\Delta_2}\sqrt{\frac{3V_a}{2\pi}} \end{bmatrix} \qquad (36b)$$

$$C_\Delta(\delta) = \begin{bmatrix} 0 & 0 & 0 \\ 0 & 0 & 0 \end{bmatrix}, \quad D_\Delta(\delta) = \begin{bmatrix} 0 & 0 \\ 0 & 0 \end{bmatrix} \qquad (36c)$$

where:

$$a_{\Delta_1} = 2\sigma_{w_o}\tilde{L}_{w_o}\bar{\delta}_{\tilde{L}_w} + \tilde{L}_{w_o}\bar{\delta}_{\sigma_w} + 2\tilde{L}_{w_o}\bar{\delta}_{\tilde{L}_w}\bar{\delta}_{\sigma_w}$$
$$+ \sigma_{w_o}\bar{\delta}_{\tilde{L}_w}{}^2 + \bar{\delta}_{\sigma_w}\bar{\delta}_{\tilde{L}_w}{}^2 \qquad (37a)$$

$$b_{\Delta_1} = 2\sigma_{u_o}\tilde{L}_{u_o}\bar{\delta}_{\tilde{L}_u} + \tilde{L}_{u_o}\bar{\delta}_{\sigma_u} + 2\tilde{L}_{u_o}\bar{\delta}_{\tilde{L}_u}\bar{\delta}_{\sigma_u}$$
$$+ \sigma_{u_o}\bar{\delta}_{\tilde{L}_u}{}^2 + \bar{\delta}_{\sigma_u}\bar{\delta}_{\tilde{L}_u}{}^2 \qquad (37b)$$

$$b_{\Delta_2} = 2\sigma_{w_o}\tilde{L}_{w_o}\bar{\delta}_{\tilde{L}_w} + \tilde{L}_{w_o}\bar{\delta}_{\sigma_w} + 2\tilde{L}_{w_o}\bar{\delta}_{\tilde{L}_w}\bar{\delta}_{\sigma_w}$$
$$+ \sigma_{w_o}\bar{\delta}_{\tilde{L}_w}{}^2 + \bar{\delta}_{\sigma_w}\bar{\delta}_{\tilde{L}_w}{}^2 \qquad (37c)$$

As can be seen by the last term in equation (37) (for either a_{Δ_1}, b_{Δ_1}, or b_{Δ_2}), $r = 2$ for this example problem (as defined by equation (27)). Since $S_\Delta(\delta)$ contains 2nd-order terms associated with L_u and L_w, the δ terms associated with these variables will have to appear twice in Δ. Thus, the dimension of Δ going into Step 1 of Section 3.2 is six. For a six-dimensional Δ, the matrices P_{21} and P_{12} can be determined, as described in Step 2 of Section 3.2. However, it is impossible to obtain a P_{11} matrix which satisfies all of the equations discussed in Step 3 of Section 3.2. Moreover, it is determined in that step that the δ term associated with L_w must be repeated a third time. Therefore, when steps 1 - 3 of Section 3.2 are repeated, the resulting uncertainty model can be expressed as in equations (13) - (16) and (22), where:

$$\Delta = \text{diag}[\begin{array}{ccccccc} \delta_{\tilde{L}_u} & \delta_{\tilde{L}_w} & \delta_{\tilde{L}_w} & \delta_{\tilde{L}_w} & \delta_{\tilde{L}_w} & \delta_{\sigma_u} & \delta_{\sigma_w} \end{array}]$$
$$= \text{diag}[\begin{array}{cccc} \delta_{\tilde{L}_u}I_2 & \delta_{\tilde{L}_w}I_3 & \delta_{\sigma_u} & \delta_{\sigma_w} \end{array}] \qquad (38)$$

$$P_{21_x} = \begin{bmatrix} -1 & \sigma_{u_o}\tilde{L}_{u_o} & 0 & 0 & 0 & \tilde{L}_{u_o} & 0 \\ 0 & 0 & -V_a & V_a & 0 & 0 & 0 \\ 0 & 0 & 0 & 0 & 1 & 0 & \tilde{L}_{w_o} \end{bmatrix} \qquad (39a)$$

191

$$P_{21_y} = \begin{bmatrix} 0 & 0 & 0 & 0 & 0 & 0 & 0 \\ 0 & 0 & 0 & 0 & 0 & 0 & 0 \end{bmatrix} \quad (39b)$$

$$P_{12_x} = \begin{bmatrix} s_{\tilde{L}_u}V_a & 0 & 0 \\ 0 & 0 & 0 \\ 0 & s_{\tilde{L}_w} & 0 \\ 0 & 0 & 0 \\ \\ 0 & 2s_{\tilde{L}_w}\sigma_{w_o}\tilde{L}_{w_o}\sqrt{\frac{3V_a}{2\pi}} & -s_{\tilde{L}_w}V_a \\ 0 & 0 & 0 \\ 0 & s_{\sigma_w}\sqrt{\frac{3V_a}{2\pi}} & 0 \end{bmatrix} \quad (39c)$$

$$P_{12_u} = \begin{bmatrix} 0 & 0 \\ 2s_{\tilde{L}_u}\sqrt{\frac{V_a}{\pi}} & 0 \\ 0 & s_{\tilde{L}_w} \\ 0 & s_{\tilde{L}_w}\frac{1}{\sqrt{3}} \\ \\ 0 & 2s_{\tilde{L}_w}\sigma_{w_o}\tilde{L}_{w_o}\sqrt{\frac{3V_a}{2\pi}} \\ s_{\sigma_u}\sqrt{\frac{V_a}{\pi}} & 0 \\ 0 & s_{\sigma_w}\sqrt{\frac{3V_a}{2\pi}} \end{bmatrix} \quad (39d)$$

$$P_{11} = \begin{bmatrix} 0 & P_{12} & 0 & 0 & 0 & 0 & 0 \\ 0 & 0 & 0 & 0 & 0 & P_{26} & 0 \\ 0 & 0 & 0 & 0 & 0 & 0 & P_{37} \\ 0 & 0 & 0 & 0 & 0 & 0 & P_{47} \\ 0 & 0 & P_{53} & 0 & 0 & 0 & P_{57} \\ 0 & 0 & 0 & 0 & 0 & 0 & 0 \\ 0 & 0 & 0 & 0 & 0 & 0 & 0 \end{bmatrix} \quad (40a)$$

$$P_{12} = -s_{\tilde{L}_u}\frac{\sigma_{u_o}}{2}$$

$$P_{26} = \frac{2s_{\tilde{L}_u}}{\sigma_{u_o}}$$

$$P_{37} = \frac{s_{\tilde{L}_w}}{\sigma_{w_o}}\sqrt{\frac{2\pi}{3V_a}}$$

$$P_{47} = \frac{s_{\tilde{L}_w}}{\sigma_{w_o}}\sqrt{\frac{2\pi}{3V_a}} \quad (40b)$$

$$P_{53} = s_{\tilde{L}_w}\sigma_{w_o}\sqrt{\frac{3V_a}{2\pi}}$$

$$P_{57} = 2s_{\tilde{L}_w}\tilde{L}_{w_o}$$

and the nominal system matrices are given above in equation (35). It should be noted that a certain amount of freedom exists in determining the above matrices, so that an uncertainty model obtained for a given uncertain system is not unique. It should also be noted that in the above uncertainty model development, the scaling terms s_{p_i} were incorporated into the model at the end so as to reduce the number of symbolic terms involved in the determination of the P_{21}, P_{12}, and P_{11} matrices.

5. Extension to Rational Case

The above procedure for solving the multilinear uncertainty modeling problem can in fact also be used to solve the more general rational uncertainty modeling problem. This is done by obtaining a matrix fraction description of the uncertain system, and representing the denominator matrix in a feedback loop so as to remove the inverse. The numerator and denominator matrices are then multivariate polynomial matrices which can be concatenated together and modeled using the multilinear techniques discussed above. Details of this approach will be presented in a subsequent paper.

6. Conclusions

This paper has summarized previous results in parametric uncertainty modeling, and has presented and demonstrated an important extension to these results. The extension consists of a framework for modeling multiple parametric uncertainties which can be represented in a multilinear functional form, and includes a procedure for obtaining a minimal (or near minimal) uncertainty model relative to a given state space realization of the uncertain system. As discussed in the paper, the multilinear framework can also be used to solve the more general rational uncertain parameter case, and provides a mechanism for significantly simplifying the computational complexity involved in determining an uncertainty model for a given uncertain system. Thus, many practical problems of interest can be solved within this framework. To demonstrate the results of the paper, an example problem was presented which consisted of a multivariable third-order uncertain system with four uncertain parameters. A minimal (or near minimal) uncertainty model was determined for the given state space realization of this system, and the resulting model had a dimension of seven. Although two of the uncertain parameters entered into the given model as squared terms and as fractions, they were easily modeled within the multilinear framework.

Further work being addressed in this area includes evaluating/refining/generaliziing this modeling procedure for a wider class of problems, automating the generalized modeling procedure, and applying the procedure to practical application problems.

References

[1] Belcastro, Christine M., Chang, B.-C., and Fischl, Robert: A Methodology for Formulating a Minimal Uncertainty Model for Robust Control System Design and Analysis, Proceedings of the 3rd Annual Conference on Aerospace Computational Control, Volume1, pp. 355 - 369, 1989.

[2] Belcastro, Christine M., Chang, B.-C., Fischl, Robert: On the Formulation of a Minimal Uncertainty Model for Robust Control with Structured Uncertainty; NASA TP-3094, September 1991.

[3] Doyle, John: Analysis of Feedback Systems with Structured Uncertainties; IEE Proc., Vol. 129, Pt. D, no. 6, pp 242 - 250, Nov. 1982.

[4] Doyle, John: Structured Uncertainty in Control System Design; Proceedings of the 1985 CDC, pp. 260 - 265.

[5] Doyle, John, Packard, Andy, and Zhou, Kemin: Review of LFT's, LMI's, and μ; Proceedings of the 1991 CDC, pp. 1227 - 1232.

[6] Halmos, Paul R.: Finite-Dimensional Vector Spaces, Springer-Verlag, 1974.

[7] Horowitz, E. and Sahni, S.: Fundamentals of Computer Algorithms, Computer Science Press, 1978.

[8] Morton, Blaise G., and McAfoos, Robert M.: A Mu-Test for Robustness Analysis of a Real-Parameter Variation Problem; Proceedings of the 1985 ACC, pp. 135 - 138.

[9] Morton, Blaise G.: New Applications of Mu to Real-Parameter Variation Problems; Proceedings of the 1985 CDC, pp. 233 - 238.

[10] Steinbuch, Maarten, Terlouw, Jan C., and Bosgra, Okko H.: Robustness Analysis for Real and Complex Perturbations Applied to an Electro-Mechanical System; Proceedings of the 1991 ACC, pp. 556 - 561.

Hypersonic Vehicle Control Law Development Using H_∞ and μ-Synthesis

Irene M. Gregory, John D. McMinn and John D. Shaughnessy
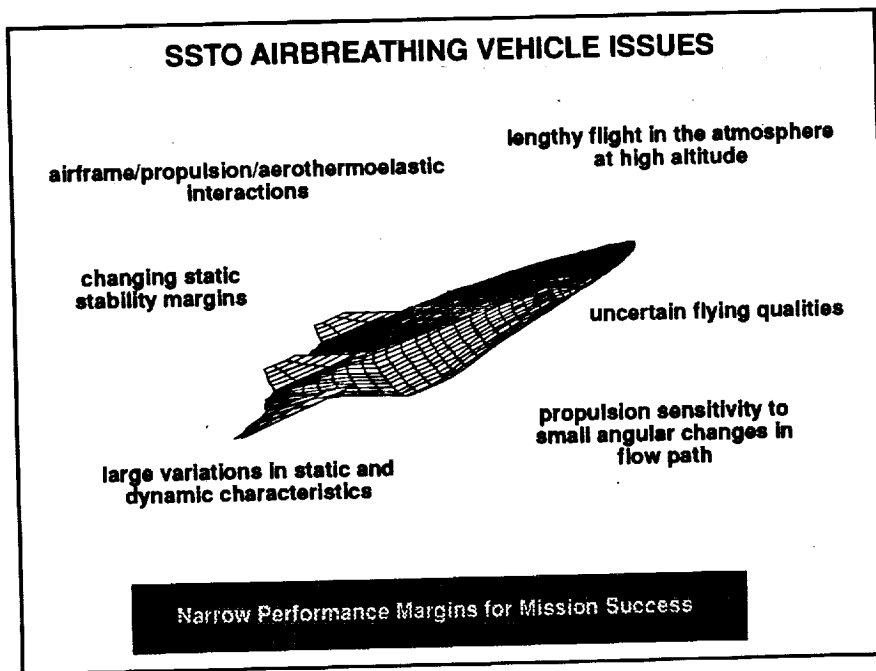
NASA Langley Research Center

and

Rajiv S. Chowdhry

Lockheed Engineering Sciences, Co.

Hypersonic Vehicle Control Law Development Using H_∞ and μ-Synthesis

Irene M. Gregory, John D. McMinn and John D. Shaughnessy

NASA Langley Research Center

and

Rajiv S. Chowdhry

Lockheed Engineering Sciences, Co.

Airbreathing SSTO vehicle has a multi facetted mission that includes orbital operations, as well as re-entry and descent culminating in horizontal landing. However, the most challenging part of the operations is the ascent to orbit. The airbreathing propulsion requires lengthy atmospheric flight that may last as long as 30 minutes and take the vehicle half way around the globe.

The vehicle's ascent is characterized by tight payload to orbit margins which translate into minimum fuel to orbit as the performance criteria.

SSTO AIRBREATHING VEHICLE ISSUES

lengthy flight in the atmosphere
at high altitude

airframe/propulsion/aerothermoelastic
interactions

changing static
stability margins

uncertain flying qualities

propulsion sensitivity to
small angular changes in
flow path

large variations in static and
dynamic characteristics

Narrow Performance Margins for Mission Success

The lengthy atmospheric flight and the minimum fuel to orbit performance requirement lead to a number of issues. Among these issues are:

- Large variations in static and dynamic vehicle characteristics that result from large and rapid mass change as well as aerodynamic heating.

- These variations lead to changing static stability margins as the aerodynamic center of pressure moves significantly with respect to c.g..

- Furthermore, since the undersurface of the vehicle serves as the compressing inlet and as the nozzle for the propulsion system, this vehicle experiences unprecedented degree of airframe/propulsion/aerothermoelastic interactions that lead to multiple and large parametric uncertainty.

- The lengthy atmospheric flight subjects the vehicle and the propulsion system to atmospheric turbulence which can excite vehicle dynamic modes as well as degrade propulsion performance through large density variations.

- Propulsion system itself is sensitive to small angular changes in the flow path that may be caused by interactions or atmospheric turbulence.

- Finally, flying qualities for hypersonic flight are not yet established.

All these issues lead to narrow margins for mission success making optimal vehicle performance absolutely essential.

```
┌─────────────────────────────────────────────────────────┐
│                                                         │
│              CONTROL SYSTEM PERFORMANCE                  │
│                    REQUIREMENTS                          │
│                                                         │
│                                                         │
│   - Tight Performance Margins For Reaching Orbital Speeds│
│                                                         │
│   - Closely Tracking Optimal Trajectory                 │
│                                                         │
│   - Tight Angle Of Attack Envelope - 0.5 Deg            │
│                                                         │
│   - Atmospheric Disturbance Rejection                   │
│                                                         │
│   - Robustness To Parameter Uncertainty                 │
│                                                         │
└─────────────────────────────────────────────────────────┘
```

In order to address these issues and enhance vehicle performance, the control system must satisfy the following requirements. It must :

- stabilize the vehicle,

- precisely track optimal fuel trajectory,

- attenuate atmospheric disturbances,

- while minimizing control effort since even moderate elevon deflections result in very large integrated drag penalty.

- All of these performance requirements must be satisfied in the presence of parametric uncertainty

And, as with all piloted vehicles, the flying qualities requirements must be met.

ROBUST CONTROL LAW FRAMEWORK

Airframe/Propulsion
Nonlinear Model with Multiple
Modelling Uncertainty

Linearized Uncertainty Model

Robust Control System
Design & Analysis

Framework for explicitly including parametric
uncertainty in control law synthesis and analysis

Robust Stability
& Performance
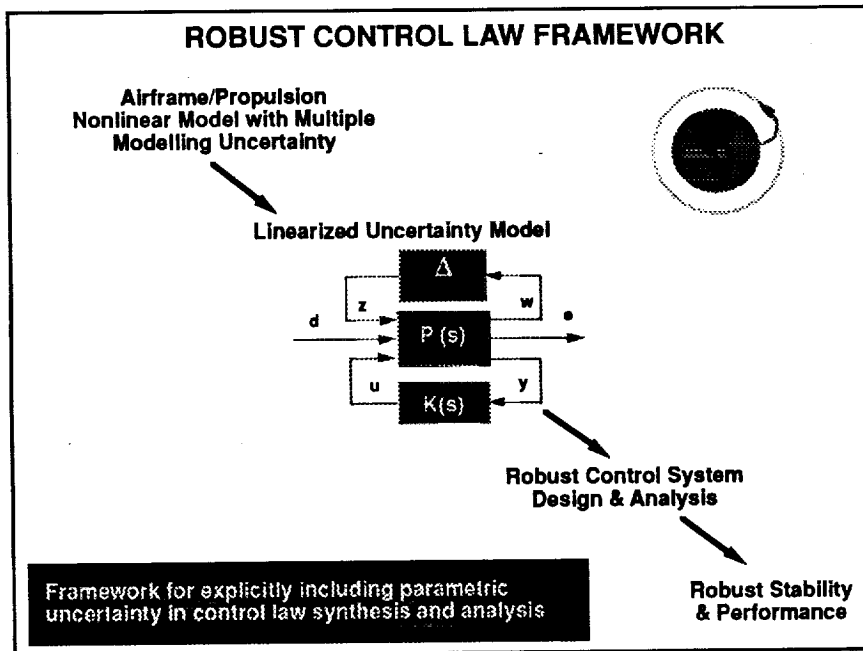
Recent advances in H∞/μ robust control theory provide a framework for explicitly including parametric uncertainty in control law design. The hypersonic vehicle ascent can be characterized in this framework as follows.

• We begin with aero/propulsion nonlinear model that includes multiple sources of uncertainty.

• This model is translated into a linearized uncertainty model illustrated by the diagram in the middle of the slide. The linear model itself is contained in plant P. All the uncertainty, with the physical relationship to the model preserved, is collected in block Δ. The controller K is then designed and analyzed for this linearized uncertainty model.

Once this process is successfully completed, the resulting control law provides robust stability and desired performance in the presence of specified uncertainty.

APPLICATION EXAMPLE

- **Flight condition**
  - 2000 psf q̄ trajectory
  - Mach 8

- **Plant - P (s)**
  - linear model of the vehicle
  - design specifications

- **Uncertainty block - Δ**
  - uncertainty in control effectiveness of elevon and fuel flow rate

- **Exogenous inputs - d**
  - commanded variables - velocity and altitude
  - atmospheric turbulence
  - sensor noise

- **Performance outputs - e**
  - velocity and altitude error
  - angle of attack
  - control effector - elevon and fuel flow rate
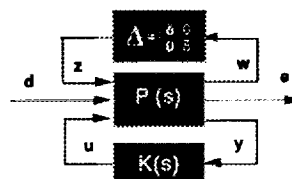
To explore this robust controls framework further, an example representing a number of issues we discussed has been selected. The vehicle is a conical configuration following a 2000 psf dynamic pressure trajectory and accelerating through Mach 8 at the design point.

We return to the Linearized Uncertainty Model diagram from the previous slide to illustrate how this example fits into the framework.

The plant P contains the linear model of the vehicle and the design specifications, which will be discussed in more detail later. All the uncertainty in the problem is relegated to the effectiveness of elevon and fuel flow rate, and is contained in the uncertainty block Δ. The physical inputs, d, into the system include the commanded variables, velocity and altitude, atmospheric turbulence, and sensor noise. The performance outputs, e, are velocity and altitude error, angle of attack, due to propulsion performance sensitivity to this quantity, and control effectors, both deflection and rate for elevon and fuel flow rate.

PROBLEM FORMULATION

- Applicability and effectiveness of H∞/μ controller
  - Performance
  - Stability
  - Changing flight conditions
  - Changing vehicle characteristics

- Performance metric
  - Velocity and altitude
    - 5 % steady state error
    - 10 % overshoot
    - 40 sec time constant
  - Angle of attack
    - limit to 0.5 deg peak-to-peak deflection
  - Elevon
    - limit deflections to 2 deg

H∞/μ controller designed for worst possible combination of inputs

We are interested in establishing how effective is each technique, that is H∞ and μ, in explicitly dealing with changing vehicle characteristics and flight conditions while providing performance and stability.

Performance on the global level refers to achieving minimum fuel to orbit. On the more immediate design level it encompasses a metric such as illustrated on this slide. The time domain response specifications, limits on the deflection and rate of the control effectors, and atmospheric turbulence attenuation are all serve as performance specifications.

It is important to point out that unlike other optimal robust control methods, H∞ based design results in a controller for the worse case input combination.

199

DESIGN SPECIFICATIONS

- **Time domain specs translated into frequency domain**
  - **steady state error, % overshoot, time constant --> transfer function**

- **Disturbance attenuation --> low frequency transfer function gain**

- **Rate and position limits on actuators --> transfer function**

- **Allowable uncertainty**
  - **% parameter variation**
  - **frequency dependent transfer function**

Design goals handled with frequency domain weightings

I like to spend a moment discussing how we fit design specifications discussed few slides back into the H∞ context. To fully exploit H∞ capabilities, design specifications must reflect the desired performance as closely as possible. Given the specifications on the time domain response, steady state error, percent overshoot, and time constant, translate directly into a transfer function that is utilized in H∞ context. The same can be said about performance specifications on alleviating atmospheric turbulence and limiting rate and position of actuators.

The allowable uncertainty in the system is also specified in frequency domain as a percent of nominal. It is either a constant across all frequency or varies depending on type of uncertainty.

At this juncture, we would like to examine how all this relates to a standard block diagram.

SYSTEM BLOCK DIAGRAM
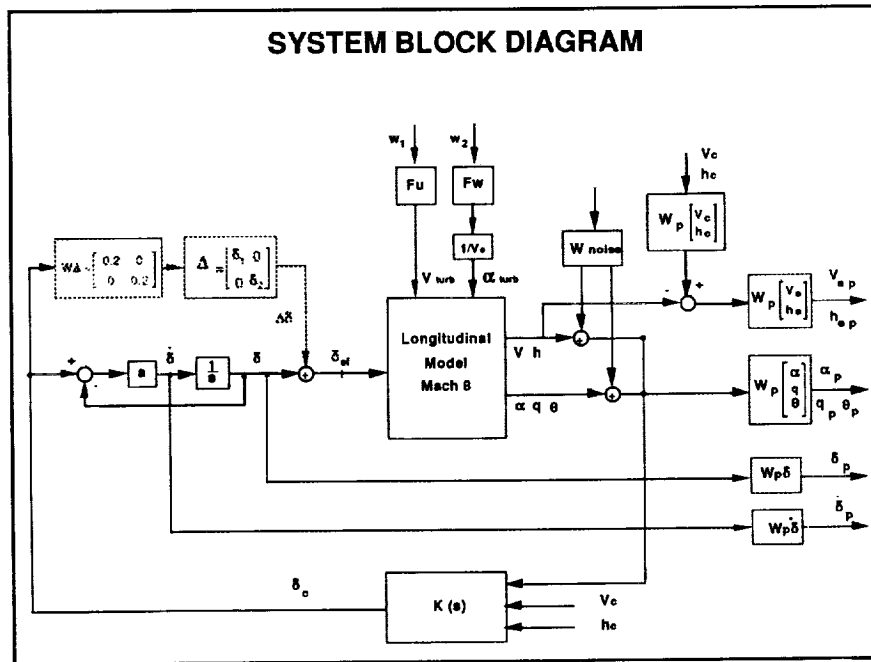
The three block general structure that you may recall from previous slides is expanded into this block diagram for our example. The dashed boxes, primarily on the right side of the diagram, represent the performance specifications. The dotted boxes, on the left, represent the uncertainty. The 20 percent uncertainty that was just discussed is expressed by the matrix WΔ and the diagonal structure of Δ reflects that each actuator effectiveness is independent of the other.

Now with problem formulated we design a controller which is analyzed in the following slides.

H∞ CONTROLLER FREQUENCY ANALYSIS
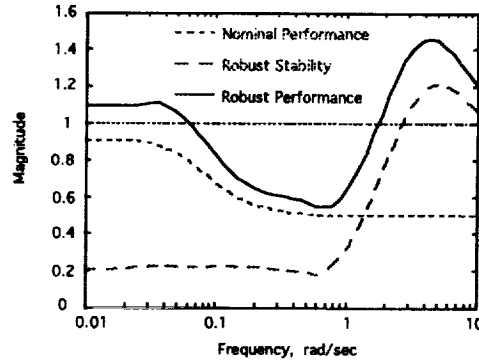
- **Nominal Performance**
  - performance of the nominal plant model

- **Robust Stability**
  - stability in the presence of allowable uncertainty

- **Robust Performance**
  - performance in the presence of allowable uncertainty

The first to be analyzed is the H∞ controller. Very briefly to provide you with a point of reference. 1 delineates the boundary between successfully passing a given test vs. failing it. We are interested in three metrics for this controller. The first is nominal performance which tells us whether the desired performance has been achieved under ideal conditions, in other words, we have no uncertainty in our system. As you can see from this plot, nominal performance is less than 1, therefore satisfying our desired performance requirements.

But since no realistic system model is ideal, we are really interested in its behavior in the presence of uncertainty. For this example it constitutes 20 percent control effectiveness uncertainty. The initial interest is in stability. This controller violates robust stability criteria around 4 rad/sec. As expected, the level of desired performance in the presence of this uncertainty is also not achieved.

At this point, we have two options - to relax the uncertainty and performance specifications or to see if μ controller can provide the desired robust performance.

μ CONTROLLER FREQUENCY ANALYSIS

Control system satisifes performance requirements in the
presence of 20 % control effectiveness uncertainty

The μ controller designed to handle 20 percent control effector
uncertainty satisfies all three metrics. The level of desired performance in the
presence of specified uncertainty is achieved with some margin to spare. We
would like to see how much uncertainty can be tolerated and still satisfy
robust performance.

μ CONTROLLER FREQUENCY ANALYSIS
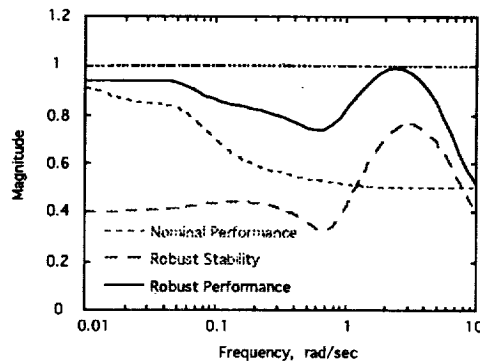
Control system satisfies performance requirements upto
40 % uncertainty in the control effectiveness

The maximum level is achieved at 40 percent uncertainty. In fact, this μ controller satisfied robust performance for up to 40 percent uncertainty in control effectiveness as indicated in this plot.

No analysis is complete without looking at the actual time histories. So to validate and to augment conclusions from frequency analysis, a sample of time responses is presented.

NOMINAL ELEVON RESPONSE

Commanded
  - Velocity (100 ft/sec)
  - Altitude (1000 ft)
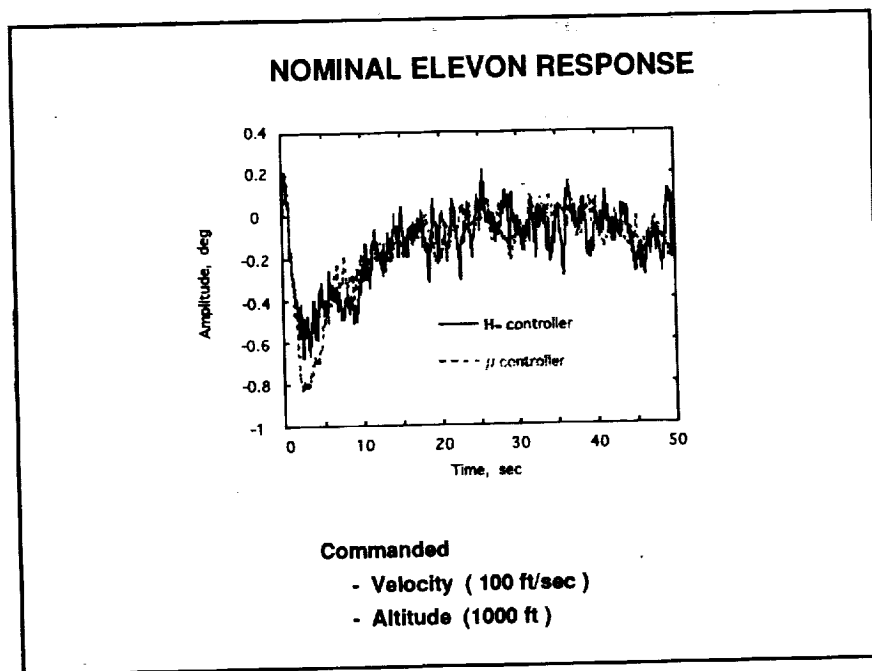
I like to point out that in all time responses you will see, the vehicle is commanded to simultaneously increase velocity and altitude while being subjected to moderate atmospheric turbulence.

The first plot is elevon response for both H∞ and μ controllers for an ideal system, i.e. no uncertainty present. Note that for both, initial deflection is less than one degree. Important fact is that both responses are very similar, indicating that improved robustness is achieved at a small loss in ideal performance as measured by the total deflection.

Introducing 20 percent uncertainty into the system drives H∞ controller unstable, which leaves us with μ controller response to consider.

WORST CASE PERFORMANCE ELEVON RESPONSE
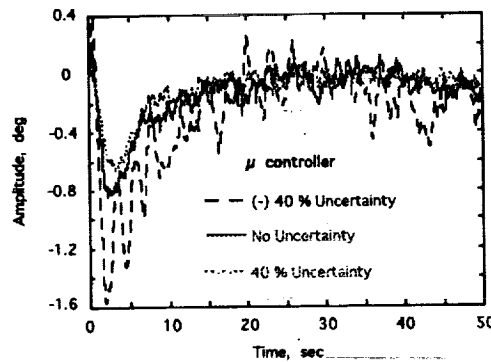
Commanded
- Velocity (100 ft/sec)
- Altitude (1000 ft)

Elevon and Fuel Flow Rate Uncertainty

If we look at worst case while the desired performance is still achieved, we get this plot. Recall that our performance specifications were still satisfied for 40 percent uncertainty. The amplitude of the response is dependent on the positive or negative uncertainty in the control effectiveness. In the worse case scenario when the actual effectiveness is 40 percent less than ideal, the elevon deflection is still less than 2 degrees which was the limit.

Well how does this behavior impact other performance variables of interest.

ALPHA NOMINAL AND WORST CASE RESPONSE
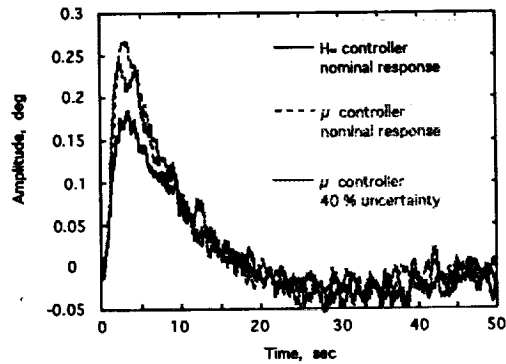
The commanded change in altitude which is facilitated by elevon deflection is unaffected by the uncertainty. In fact, it is faster and more precise for the μ controller than for the ideal H∞ one. But this performance improvement in altitude does have an adverse effect on another variable of importance - angle of attack.

The μ controller angle of attack peak is somewhat higher than that of the H∞ controller, though both responses are well within the specified limit of 0.5 degree. The uncertainty again has very small effect on the μ controller response

CONCLUSIONS

- Vehicle characteristics and control system requirements translate explicitly into H_∞ domain specifications

- H_∞ controller suffers performance degradation with introduction of control effectiveness uncertainty

- μ-synthesis results in an improved robust performance over H_∞ controller

Analysis And Synthesis Technique Provides A Systematic Approach To Explore Tradeoff Between Performance And Uncertainty Robustness

So what have we learned from this initial application of H∞ and μ to an airbreathing SSTO vehicle. The bottom line is that μ framework provides a systematic approach to include parametric uncertainty in design and to explore tradeoffs between performance and uncertainty robustness. This initial application of μ synthesis and analysis techniques to an airbreathing SSTO shows much promise.

ON-LINE EVALUATION OF MULTILOOP DIGITAL CONTROLLER PERFORMANCE

Carol D. Wieseman

NASA Langley Research Center

NASA LaRC Workshop on Guidance, Navigation,
Controls, and Dynamics of Atmospheric Flight
NASA Langley Research Center
March 18 - 19, 1993
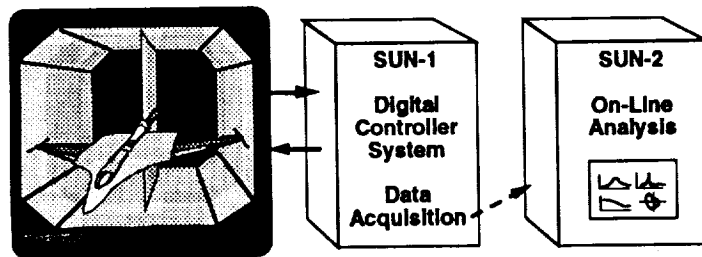
The purpose of this presentation is to inform the Guidance and Control community of capabilities which were developed by the Aeroservoelasticity Branch to evaluate the performance of multivariable control laws, on-line, during wind-tunnel testing. The capabilities are generic enough to be useful for all kinds of on-line analyses involving multivariable control in experimental testing. Consequently, it was decided to present this material at this workshop even though it has been presented elsewhere.

I want to acknowledge the other participants in the development of these capabilities. They were:

Sheri Hoadley and Vivek Mukhopadyay of NASA Langley Research Center and

Tony Pototzky and Sandra McGraw of Lockheed Engineering and Sciences Company

The capabilities are summarized for our application in the bottom figure. Our test involved a wind-tunnel model and two computers, the first was a digital controller where data acquisition was performed and then the data was transfered via eithernet to another computer where the on-line analyses were performed. I will be tell more about this on the next chart

BACKGROUND
AFW Controller Performance

- **Active Flexible Wing (AFW)**
- **Analysis During Test**
  - **Safety**
  - **Efficient Use of Test Time**
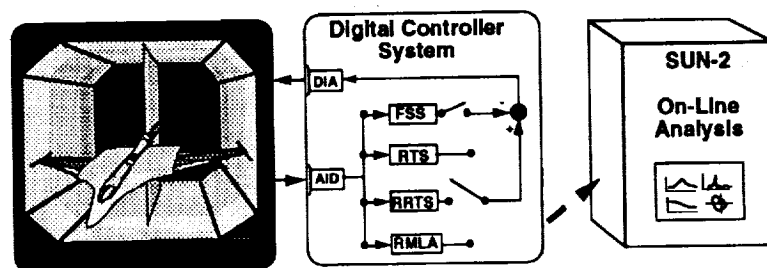
First, I want to provide you with some background for why we developed these analysis capabilities. One major objective of the Active Flexible Wing Program was to verify control law design methodologies by testing flutter suppression control laws in conjunction with rolling maneuver control laws. These are summarized in the middle box which represents the digital controller. FSS is flutter suppression. There were 3 roll control laws, any one of which could be operating at a time in conjunction with Flutter Suppression. These three control laws were Roll Trim System, Rolling Maneuver Load Alleviation and Roll Rate Tracking System.

The AFW had multiple control surfaces as well as multiple sensors, thus allowing for multivariable control laws.

In order to protect the model and tunnel from unnecessary damage and to make optimum use of limited wind-tunnel test time, it was essential to be able to evaluate the controller performance, on-line, during the wind tunnel test.

To provide this capability, necessary data was acquired by the digital controller and immediately sent to another computer for on-line analysis via ethernet.

210

ESSENTIAL ON-LINE ANALYSIS REQUIREMENTS

- **BEFORE AND DURING TESTING VERIFY**
  - **CONTROL LAWS**

- **BEFORE CLOSING LOOP PREDICT**
  - **IF CONTROL LAW WILL DESTABILIZE SYSTEM**
  - **STABILITY MARGINS**

- **AFTER CLOSING LOOP DETERMINE**
  - **STABILITY MARGINS**
  - **CONTROL SURFACE ACTIVITY**
  - **OPEN-LOOP FLUTTER BOUNDARY**
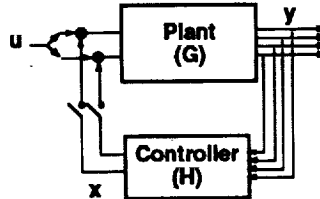
Specifically, there were three essential requirements. First, it was necessary to verify the correct execution of control laws both before and during testing. The diagram to the right depicts the controller/plant system in which the AFW plant is depicted by the rectangle labeled G and the Controller is depicted by the rectangle labeled H.

y are the outputs of the plant which correspond to accelerometer measurements and in some cases strain gauge measurements.

x are the control law outputs or the commands to the control surfaces which are sent to the model.

u are the excitations which can be added to the control law commands or to the sensors.

The second requirement was that during open-loop testing in which the control law commands are not sent to the model, it was essential to predict, before closing the loop, whether a control law would destabilize the system and what the margin of stability would be once the loop was closed. If the control law was predicted to destabilize the system or the margin of stability was predicted to be unsatisfactory, the loop on the control law would not be closed thus preventing the model and the wind-tunnel from damage.

The third requirement was that during closed-loop testing in which the control law commands are sent to the model, it was essential to evaluate the performance of the control law in order to guide the wind-tunnel test engineers in determining whether testing of that control law could continue to other test conditions. To do this, measures of stability margins and control surface activity were needed. It was also necessary to determine if the closed-loop system was above the open-loop flutter boundary.

ON-LINE ANALYSIS CAPABILITIES
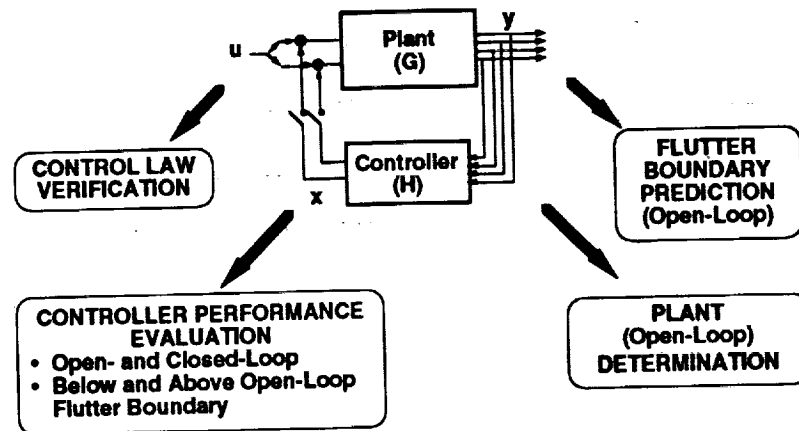
These three requirements were met with the development for four major areas of analyses capabilities depicted in this figure. They were:

first, control law verification by which correct execution of control laws could be assessed using both time and frequency domain analyses;

second, controller performance evaluation in both the time and frequency domain through which controller performance could be determined; performance was evaluated both open and closed-loop and both below and above the flutter boundary.

third, open-loop plant determination, and

fourth, open-loop flutter boundary predictions.

These last two analysis capabilities are performed using frequency domain techniques only and are by-products of frequency domain CPE.

All capabilities are for multi-variable or multi-loop control systems. Let me emphasize that the capabilites available are applicable to both stable and unstable plants as long as the overall system is stable, that is to say if we are testing open-loop the open-loop system must be stable, if closed-loop the closed-loop system must be stable. The capabilities were met by the software developed which will be described on the following slide

ON-LINE ANALYSIS SOFTWARE

	c	Fortran	Matlab script
• DATA INTERFACE PROGRAMS	√		
• TIME HISTORY PLOTS			√
• RMS CALCULATIONS		√	√
• FOURIER ANALYSIS		√	
• MATRIX OPERATIONS			√
• ASSOCIATED PLOTS			√

The following software modules were developed to support the analyses and are available for use by others:

- Data interface programs, coded in C, converted binary test data (from AID converters) to scaled and formatted data for use in Fourier Analysis codes and MATLAB, for plotting or other calculations. Additional data interface programs written in c converted the output of the Fourier analysis package to matlab format.

- MATLAB script files for plotting time history and frequency domain data.

- MATLAB script files for calculating RMS of time history data, and also plotting the RMS as a function of dynamic pressure

- Fourier Analysis Package, coded in Fortran, which calculates transfer functions of any of the outputs to the excitation. This software uses an array processor and has many capabilities of windowing and overlap averaging.

- MATLAB script files which perform all matrix operations needed to calculate stability margins and determine open-loop plant stability, as well as determine the plant transfer matrix from the open- or closed-loop system transfer matrices.

- MATLAB script files to generate all associated plots.

213

ON-LINE ANALYSIS CAPABILITIES

- DATA INTERFACE PROGRAMS
- TIME HISTORY PLOTS
- RMS CALCULATIONS
- FOURIER ANALYSIS
- MATRIX OPERATIONS
- ASSOCIATED PLOTS
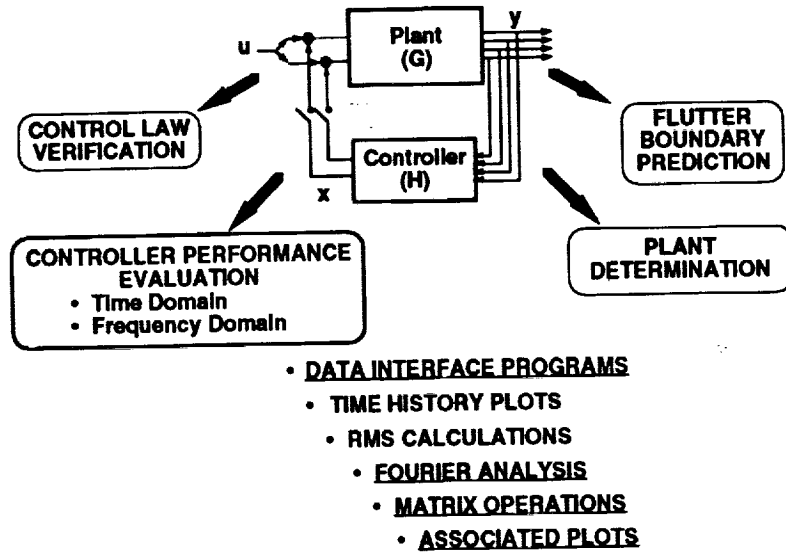
In this presentation, I am only going to elaborate on the frequency-domain controller performance and plant determination capabilities which use the data interface programs, the Fourier analysis package, and the MATLAB script files which performed required matrix operations and generated associated plots.

FREQUENCY DOMAIN CPE PROCEDURES

- Input Excitation, u, into each Control Surface

- Measure Time Responses of each Output x and y

- Perform Fast Fourier Transforms of u, x, and y

- Compute Power and Cross Spectra

- Compute Transfer Functions

- Construct Plant (G), Controller (H), and Return-difference Matrices (I+HG, and I+GH)

- Compute Singular Values for Evaluating Robustness to Multiplicative and Additive Uncertainties

- Compute Determinants for Plant Stability Evaluation
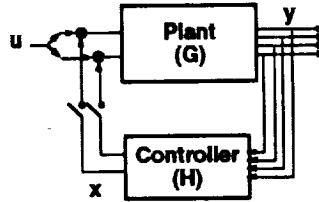
The following slide outlines the procedure to evaluate controller performance of a multi-loop controller in the frequency domain.

An excitation is input to one control surface at a time. The time responses of each output of the plant (accelerometers and strain gauges used by the controller) and controller commands are measured. The transfer functions of these outputs and commands with respect to the excitation are calculated by performing Fast Fourier transforms of u,x, and y and computing the power and cross spectra. The next and each control surface is excited in turn and the transfer functions are calculated for these signals. The transfer functions are then combined into transfer matrices. The Plant (G), Controller (H) and the return-difference matrices are constructed or computed. The singular values are computed in order to evaluate the robustness to multiplicative at the plant input and output points and additive uncertainties. The determinants are also computed to be used for evaluating plant stability.

The evaluation of the performance of multivariable controllers using excitations into the sensors instead of the control surface has also been developed and is available to handle the case of the overdetermined problem.

The following slide shows an example of actual results obtained during the wind-tunnel test.

215

CONTROLLER PERFORMANCE EVALUATION
FREQUENCY-DOMAIN FLUTTER SUPPRESSION

HEADER INFORMATION
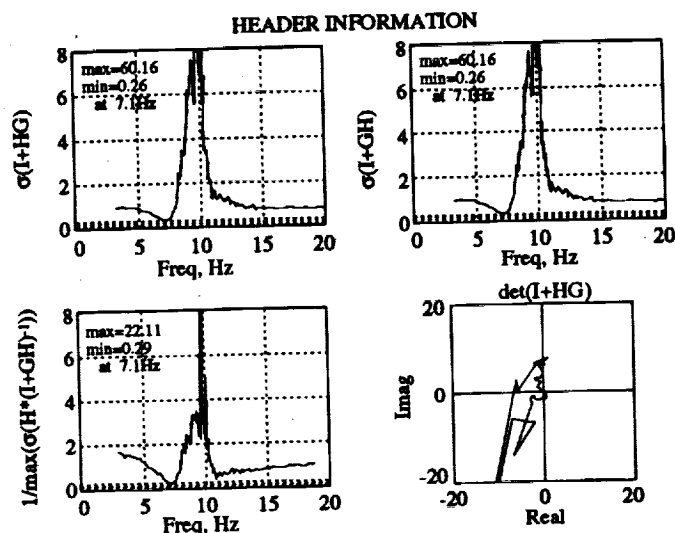
This slide is an example of the plot output from the CPE Analysis package. This is an actual plot of results that could be seen in the tunnel control room within about a minute from the completing the required data acquisition and could then be printed on a laserprinter in the control room. This data was used to aid in determining if we would go to the next test condition.

The top two plots are minimum singular values of the return-difference matrices. These provide measures of robustness to multiplicative uncertainties at both the plant input and plant output points. The closer the curve comes to zero, the closer the system is to being unstable. The minimum singular values are related to combined gain and phase margins for a multivariable system.

The dashed lines at the bottom of the plots display required levels of stability which allow a quick assessment of the stability margins due to multiplicative errors in the plant inputs or plant outputs.

The lower left depicts the margin of stability to an additive plant uncertainty. The lower right indicates whether the open-loop plant is stable or not. For these particular plots for a stable closed-loop system, the open-loop plant is unstable as indicated by an encirclement of the critical point at the origin which can be seen when the plot is magnified. The capability of enlarging this determinant plot to better identify encirclements was also available.

In all cases, the stability margins are the actual margins not conservative estimates because they are based on the actual plant. When performing open-loop analyses, if the method predicts that the closed-loop system is unstable, it is unstable.
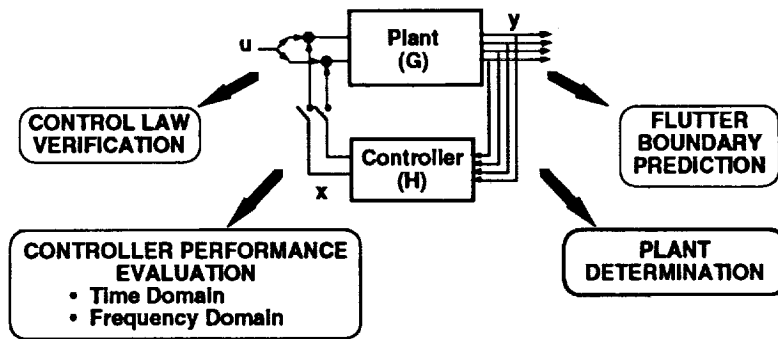
216

ON-LINE ANALYSIS CAPABILITIES

- **DATA INTERFACE PROGRAMS**
- **TIME HISTORY PLOTS**
- **RMS CALCULATIONS**
- **FOURIER ANALYSIS**
- **MATRIX OPERATIONS**
- **ASSOCIATED PLOTS**

Another capability that I wanted to elaborate on in this presentation was the determination of the open-loop plant. This capability also involved the data interface programs, the Fourier Analysis package, the matrix operations and associated plot routines.

PLANT DETERMINATION

$$G = \begin{bmatrix} G_{cc} & G_{ce} \\ G_{ec} & G_{ee} \end{bmatrix}$$

	System Open-Loop	System Closed-Loop
Plant **G**, Controller **H**	$G_{cc} = Y_{cc}$	$G_{cc} = ([I - X_{cc}^T]^{-1} Y_{cc}^T)^T$
	$G_{ec} = Y_{ec}$	$G_{ec} = ([I - X_{cc}^T]^{-1} Y_{ec}^T)^T$
	$G_{ce} = Y_{ce}$	$G_{ce} = Y_{ce} + G_{cc} X_{ce}$
	$G_{ee} = Y_{ee}$	$G_{ee} = Y_{ee} + G_{ec} X_{ce}$

* All matrices functions of ω
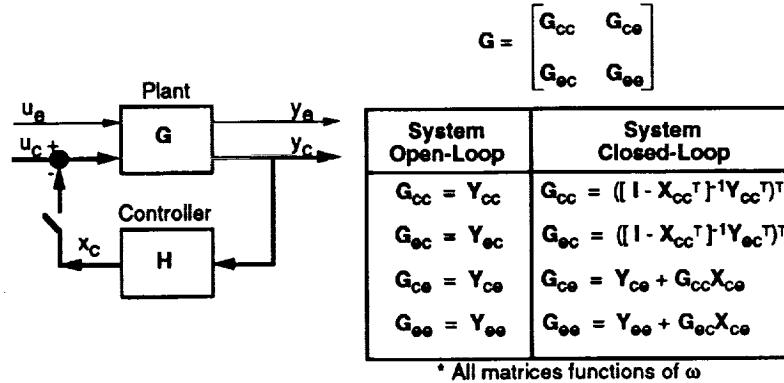
Part of the plant determination was a by-product of the CPE codes. This part is denoted as Gcc in the plant transfer matrix, G. Here the subscript c refers to the control surfaces actuated by the control laws and sensors used by the specified control law. The other control surfaces are denoted by a subscript e, for external. All of the control surfaces both used by the control law and those external to the control law were excited one at a time. The transfer functions of the outputs y and the control law commands x with respect to the excitation were calculated. The rest of the plant transfer matrix was then obtained using the equations in the lower right where the capital X and Y refer to transfer matrices of the control law outputs and plants with respect to the excitations.

When the system is open-loop, ie when the control law commands are not sent to the model, the equations are shown in the first column.

When the system is closed loop, the commands are sent to the model. The equations to obtain the entire plant transfer matrix are shown in the second column.

The transfer function calculations and matrix operations required to obtain the entire plant transfer matrix are also available in the on-line analysis package. The capital letters correspond to transfer matrices.

CONCLUDING REMARKS

**ON-LINE ANALYSIS CAPABILITIES FOR MULTI-VARIABLE
CONTROL**

- **Developed**
- **Available**

WHICH PERFORM DURING TESTING:

- **Control Law Verification**
- **Control Law Performance Evaluation**
- **Open-loop Plant Determination**
- **Stability Boundary (Flutter) Prediction**

The capability to evaluate the performance of multivariable control laws on-line during experimentation has been developed and is available. These capabilities perform during testing, control law verification, evaluation of performance of the control laws, determination of the open-loop plant and stability boundary prediction which in our application was flutter.

TECHNOLOGY TRANSFER

- **Presentations/Publications**

  American Control Conference, 1990

  4th Workshop on Comp. Control of Flex. Aerospace Systems, 1990

  Guidance and Control Conference, 1990

  Aerospace Flutter and Dynamics Council Meeting, 1991

  Dynamic Specialist Conference, 1992

  DSP Exposition and Symposium, 1992

  Journal of Guidance, Control and Dynamics, 1992

  FUTURE: ACAD Press Chapter, NASA Tech Brief, Journal of Aircraft

- **Spacecraft Dynamics Branch - Large Space Structures Application**

- **NASA Dryden Research Facility - X29 Flight Test**

There is no users manual for the software but both the theory and results for different aspects of the on-line analysis capabilities have been documented and presented at a variety of conferences over a period of 3 years from 1990-1992. These documents and the software are available to anoyne interested. The software has been provided to the Spacecraft Dynamics Branch for use in a large space structures application and the theory and equations were used by Dryden Flight Research Facility to support the X-29 flight test.

If you would like to obtain the software or more information, I'll give you my business card.

Fuzzy Logic Helicopter Control

By

Captain Gregory W. Walker

NASA Langley Research Center
Aeroflight Dynamics Directorate
U.S. Army Aviation Troop Command
Hampton, VA 23665-5225

Presented at the
First Annual LaRc Workshop on Guidance, Navigation, Controls, and
Dynamics for Atmospheric Flight
H.J.E. Reid Conference Center
March 18-19 1993

NASA / US Army

SLIDE 1: This work is an outgrowth of a project that is being jointly developed by the U.S. Army Aviation Troop Command's Aeroflight Dynamics Directorate and the NASA Langley Research Center.

OUTLINE OF PRESENTATION

- An Overview Of The Free Flight Rotorcraft Program

- Why This Program Is Looking At Fuzzy Logic Control

- Professor Sugeno's (Tokyo Institute of Technology) "Fuzzy Control of Unmanned Helicopters" Project

- Current Status

FFRRV

SLIDE 2: There is cooperating work going on between this project and Professor Sugeno. NASA nor the Army has Sugeno under any contract or grant, the cooperation is merely an exchange of ideas and flight data.

PROGRAM OBJECTIVE

Evaluate the use of wind-tunnel rotor systems on powered free-flying helicopter models to supplement full-scale flight testing.

- Reduce direct operating costs

- Elimination of manned-flight safety issues

- Reduced turn-around time

SLIDE 3: The program that this fuzzy logic work grew out of is the "Free Flight Rotorcraft Research Vehicle (FFRRV) Project". This is the objective of the FFRRV project, not specifically the "Fuzzy Logic" work.

THE TOOLKIT

Although motivated by maneuverability, agility, and detectability concerns, the free-flight rotorcraft test technique is being developed as a general research tool to supplement wind tunnel and simulation studies.

| WIND TUNNEL TESTS | → | ANALYSIS | ← | FREE-FLIGHT TESTS |

CORRELATION   PILOTED SIMULATION   CORRELATION

FULL-SCALE FLIGHT TESTS

OPERATIONAL READINESS
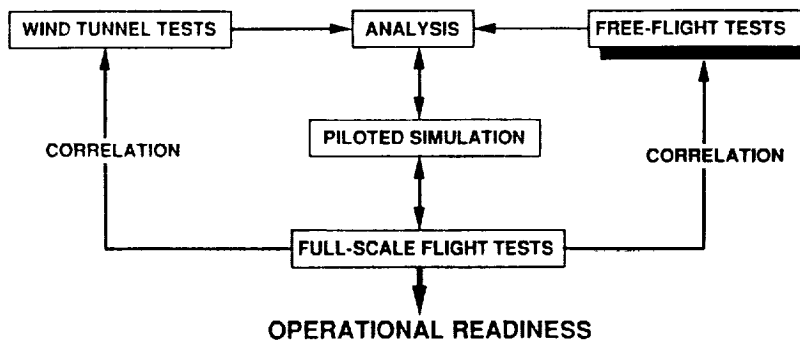
SLIDE 4: The FFRRV project will not supplant full scale flight testing, merely supplement it. The fixed wing community has had the ability to do dynamic studies at model scale for years, we are trying to bring such a capability to rotorcraft.

ROTORCRAFT FREE-FLIGHT TEST TECHNIQUE

(FFRRV)

Data Acquisition and
Processing System

Manned Digital Flight Control System
Ground Station

Vehicle Safety
Pilot
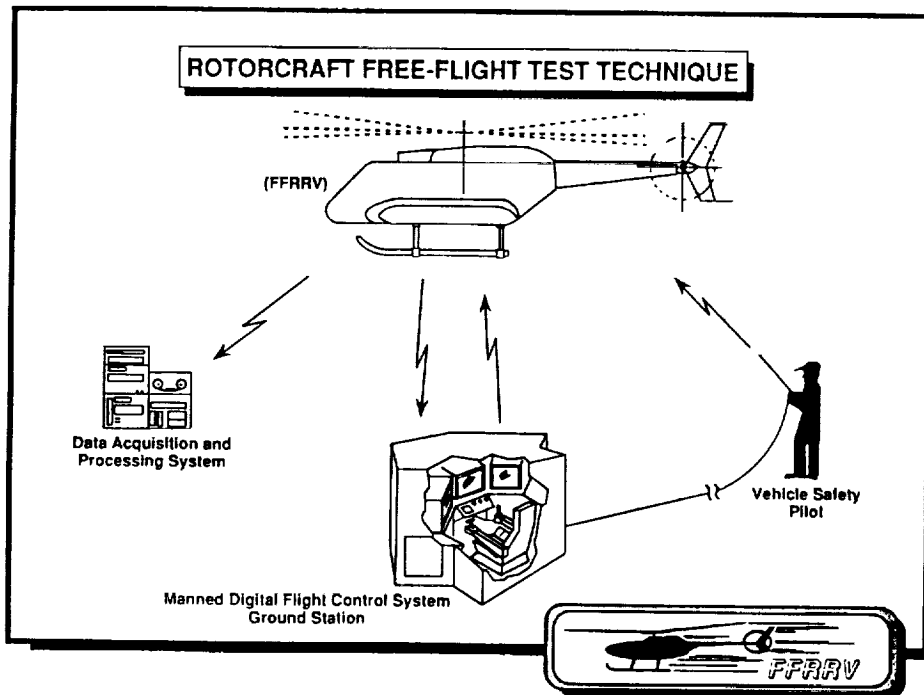
FFRRV

SLIDE 5: This slide depicts the test technique we are using to evaluate rotorcraft aerodynamics with FFRRV. The pilot sits in a ground based cockpit but perceives to be in the model via telepresence. The vehicle safety pilot has overall authority to interrupt the control system and terminate any experiment.

MANEUVERS INCLUDED IN AACT-III PROGRAM

Modified Lazy Eight

Hammerhead

Loop

Roll

One-Half Cuban Eight

Reverse One-Half Cuban Eight

Pushover

FFRRV
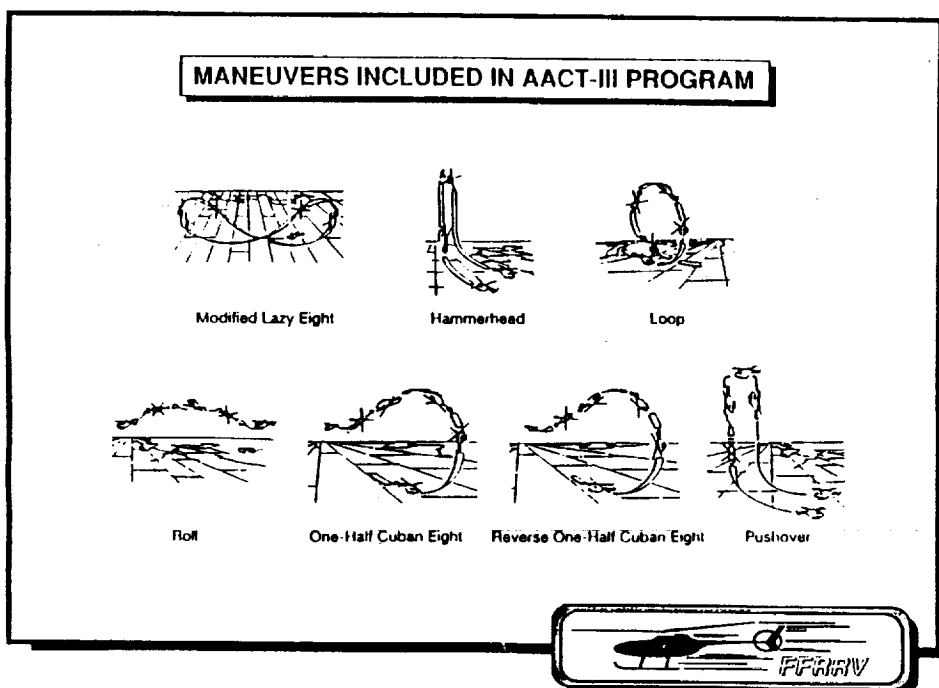
SLIDE 6: We want to look at aerodynamics in the "non-linear" world typical of air-to-air combat or nap-of-earth flying. This slide shows examples of maneuvering that characterize advanced combat rotorcraft. The researchers challenge is to quantify what makes a rotorcraft configuration more or less capable of such aggressive maneuvering.

223

OUTLINE OF PRESENTATION

- An Overview Of The Free Flight Rotorcraft Program

- Why This Program Is Looking At Fuzzy Logic Control

- Professor Sugeno's (Tokyo Institute of Technology)
  "Fuzzy Control of Unmanned Helicopters" Project

- Current Status

FFRHV

TRADITIONAL APPROACH

<u>Model The Aircraft</u> ➔ <u>Build</u> ➔ <u>A Stabilizer Of The System</u>

Attributes Of This Approach
- Non-linear dynamics -> often linearized for simplicity

- Requires a detailed knowledge of the physical system

- Overall performance directly related to the models accuracy

Strategy
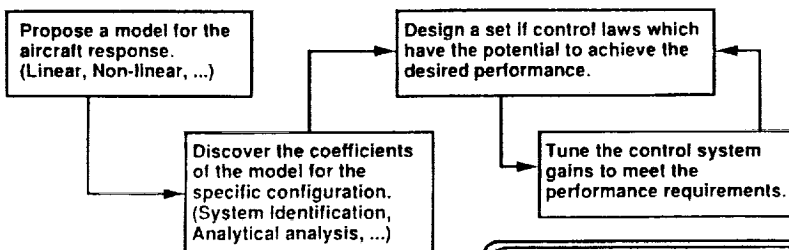
| Propose a model for the aircraft response. (Linear, Non-linear, ...) |
| Design a set If control laws which have the potential to achieve the desired performance. |
| Discover the coefficients of the model for the specific configuration. (System Identification, Analytical analysis, ...) |
| Tune the control system gains to meet the performance requirements. |

FFRHV

224

FFRRV UTILITY

ROTORS AND HUBS

COMPLETE CONFIGURATIONS

ANTI-TORQUE CONCEPTS
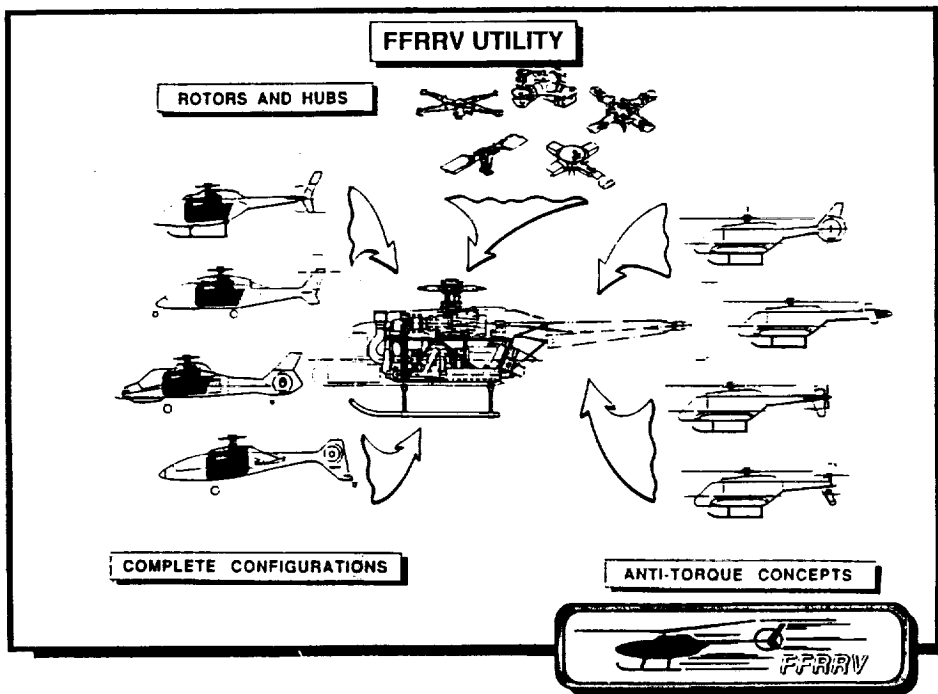
SLIDE 9: This slide shows how we intend to use FFRRV. These changes to the aircraft affect the dynamical model that a traditional control system approach requires. Some of these changes may require refining the models coefficients while other changes will force us to begin at the top, that of defining the mathematical model all over.

THE SYSTEM
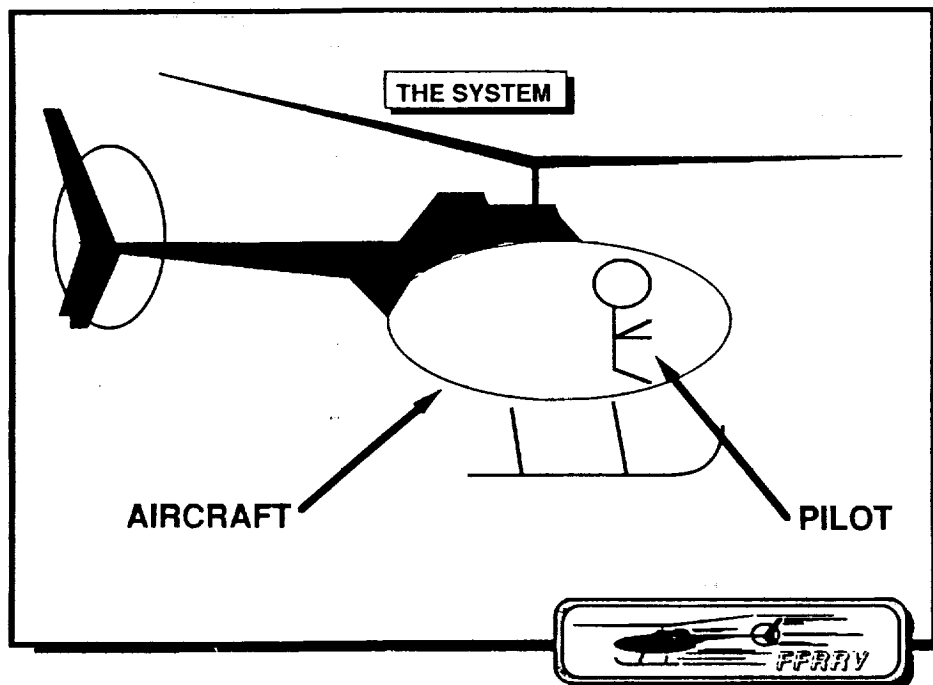
AIRCRAFT

PILOT

SLIDE 10: The system I am working with and trying to regulate has two portions: the aircraft and the pilot (where ever he/she resides). Instead of modeling the ever-changing aircraft I am modeling an adaptive pilot.
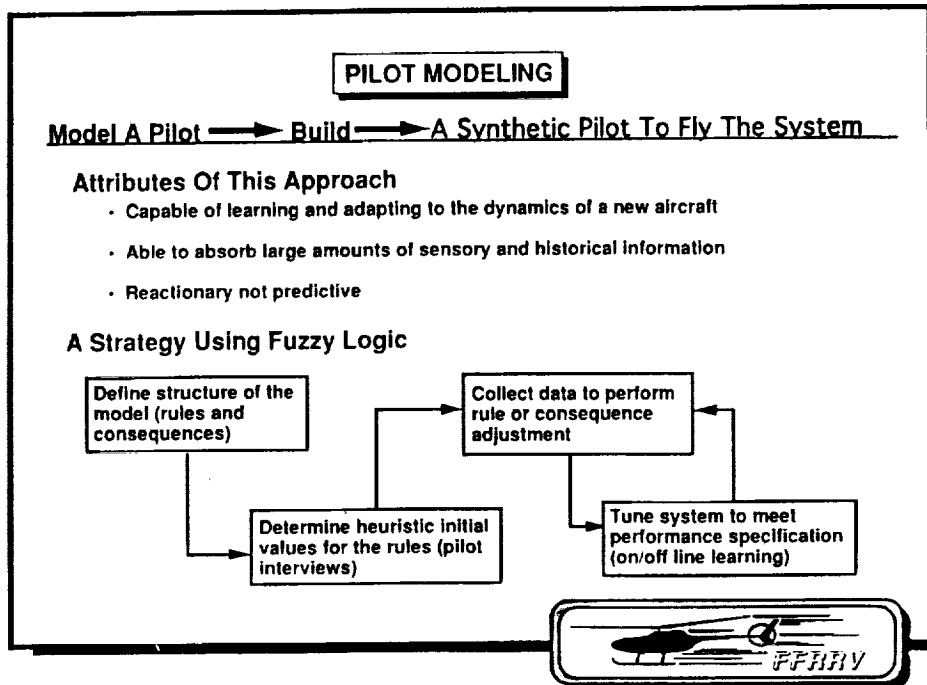
SLIDE 11: Good pilot
modeling should
incorporate these
attributes. This strategy
is the approach
Professor Sugeno at
Tokyo Institute of
Technology has used to
attack this problem.

PILOT MODELING

Model A Pilot ➡ Build ➡ A Synthetic Pilot To Fly The System

Attributes Of This Approach
- Capable of learning and adapting to the dynamics of a new aircraft

- Able to absorb large amounts of sensory and historical information

- Reactionary not predictive

A Strategy Using Fuzzy Logic

| Define structure of the model (rules and consequences) |
| Collect data to perform rule or consequence adjustment |
| Determine heuristic initial values for the rules (pilot interviews) |
| Tune system to meet performance specification (on/off line learning) |

FFRRV

SLIDE 12:

OUTLINE OF PRESENTATION

- An Overview Of The Free Flight Rotorcraft Program

- Why This Program Is Looking At Fuzzy Logic Control

- Professor Sugeno's (Tokyo Institute of Technology) "Fuzzy Control of Unmanned Helicopters" Project

- Current Status

FFRRV

Unmanned Hericopter for Sea Rescue

Satellite

Global positioning system

Mothership

control instruction
video information

Firing Ship

Remote Control of Helicopter by Oral Instructions

Fly Straight

Turn Left

Hover

Land

227

Automatic Autorotation Entry
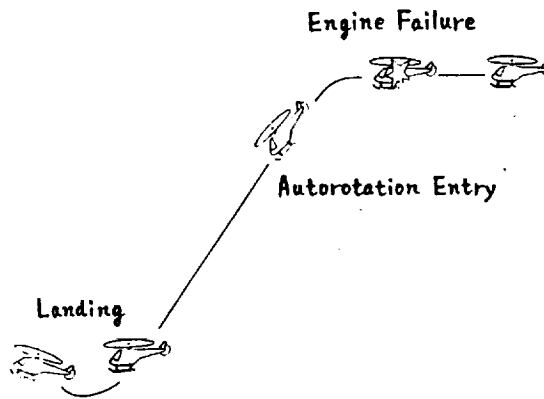
Engine Failure

Autorotation Entry

Landing

Linguistic Rules

Example For Hovering

1) If the body rolls, then control the lateral cyclic in reverse.

2) If the body pitches, then control the longitudinal cyclic in reverse.

3) If the nose turns, then control the tail rotor collective in reverse.

4) If the body moves sideways, then control the lateral cyclic in reverse.

5) If the body moves back and forth, then control the longitudinal cyclic in reverse.

6) If the body moves up or down, then control the main rotor collective in reverse.

Hierarchical Modular System

by M. Sugeno
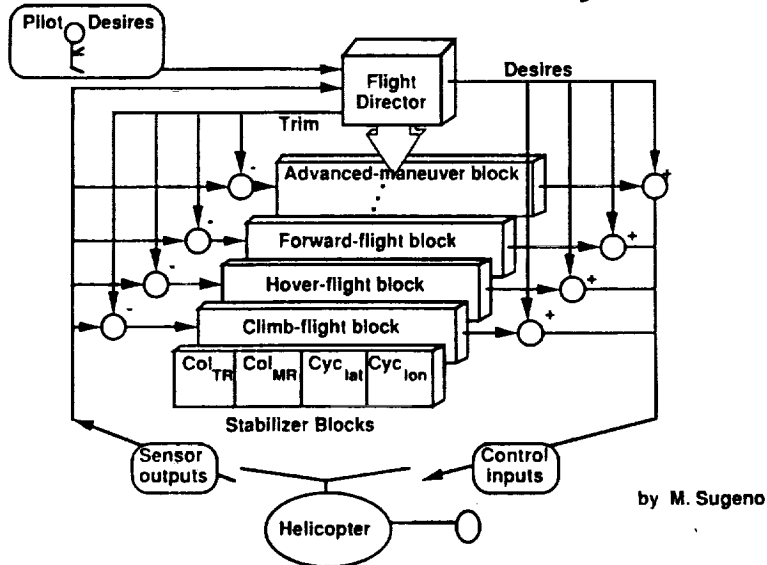
SLIDE 17: At first glance Professor Sugeno's controller appears like a simple gain scheduling controller. There are some significant differences: First, the lower level blocks are autonomous fuzzy logic controllers that can only perform their select mission. Secondly, the "gain scheduler" is not simply a mode switcher but is another fuzzy logic engine which blends the lower level blocks together to achieve a more abstract desire described by the pilot.

Lower Level Modules

Stabilizer Blocks

229
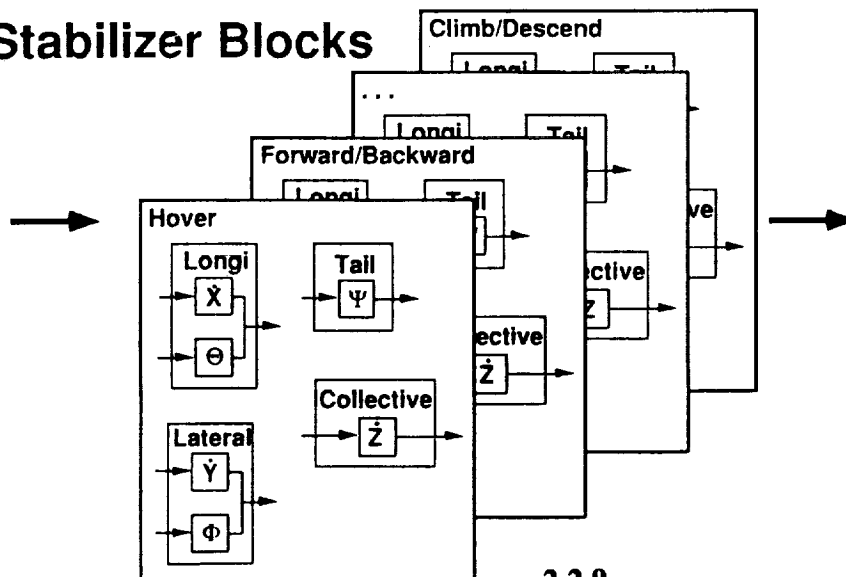
SLIDE 18: All the lower level stabilizer blocks have similar structure but each one is a unique multi-input/multi-output closed loop controller. The rule base and the fuzzy variable sets are different for each of these lower level blocks.

OUTLINE OF PRESENTATION

- An Overview Of The Free Flight Rotorcraft Program

- Why This Program Is Looking At Fuzzy Logic Control

- Professor Sugeno's (Tokyo Institute of Technology)
  "Fuzzy Control of Unmanned Helicopters" Project

- Current Status

FFRRV

SLIDE 19: In addition to building up the research vehicle the Free Flight Project is currently prototyping various systems using commercial and industrial model helicopters. This prototyping incudes: video check out, telemetry, sensor fusion including gps, and control strategies.

Tokyo Institute of Technology's work is ongoing and is currently focused on adding more flight capabilities to their industrial model. Some of these enhancements are: more aggressive flying, telemetry, gps.

CONCLUDING REMARKS

- A control system using fuzzy logic to model a pilot can provide stability to a helicopter.

- Prototyping efforts to demonstrate this are ongoing here at LaRC and in Japan.

- The design and use of such a controller requires a new focus.

FFRRV

SLIDE 20: The third bullet is the key. To really understand why fuzzy controller are proving successful requires a new focus on the problem. These fuzzy controllers model pilot response, not aircraft dynamics.

Reconfigurable Control

Hopfield Network Investigation

Phil Chandler, Meir Pachter

Mark Mears, Bob Smith

WRIGHT LABORATORY
FLIGHT CONTROL DIVISION

Hopfield Network Based Controller
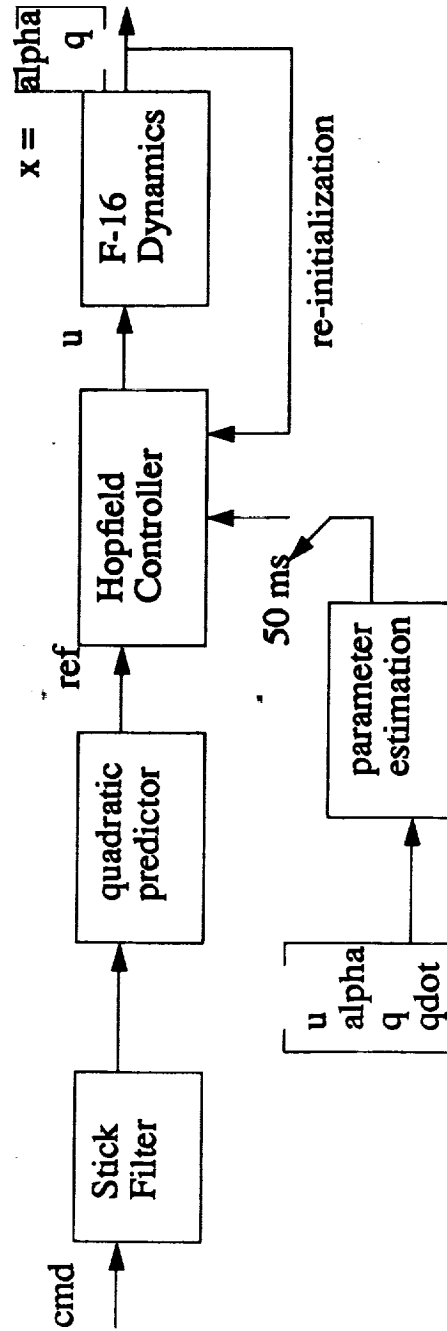
Control Optimization

- linear dynamics

$NV = C$

$V = [x_1, --x_k, u_1, --u_k]^T$

- quadratic cost

$V^T Q V + b^T V$

232

Algebraic Riccati Equation Based Controller

cmd

stick
filter

quadratic
predictor

ref

set point
equation

S

feedforward
gain

u

F-16
dynamics

gain

Riccati
Equation

u
q
alpha
qdot

Parameter
Estimation

50 ms
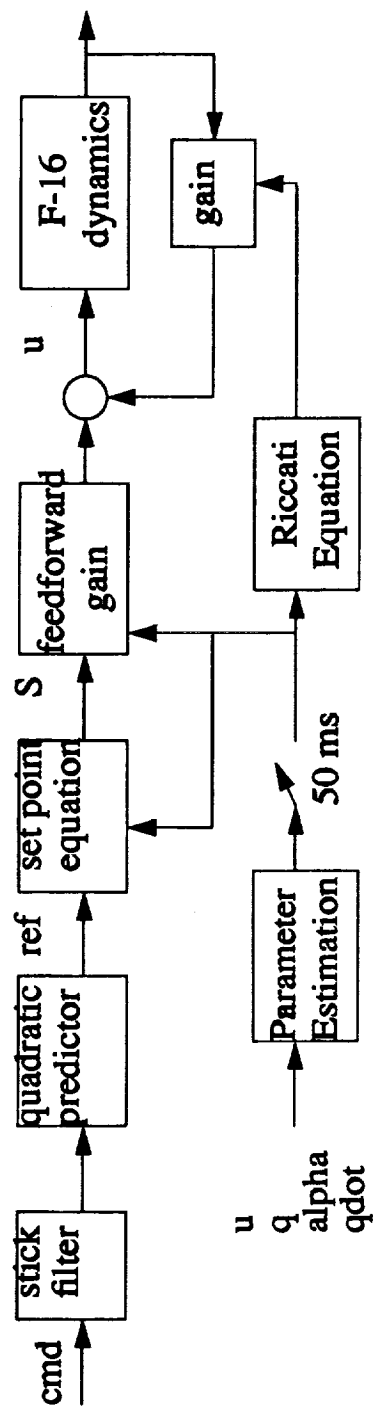
Control Optimization

$$A^T P + PA - PBR^{-1}BP + Q = 0$$

$$\dot{s} = [A^T - PBR^{-1}B^T]s + Qref$$

Estimation

$$Z = H\theta + v_1; M\theta = a + v_2$$

$$\hat{\theta} = \hat{\Theta}_{MV} + P_{MV}M^T \left(MP_{MV}M^T + R_2\right)^{-1} \left(a - M\hat{\theta}_{MV}\right)$$

233

Penalty Method

Direct Minimization

$$J(v) = \frac{1}{2}v^T Q v + v^T c + \frac{1}{2}\lambda(Av-b)^T(Av-b)$$

$$\frac{dJ}{dv} = Qv + c + \lambda A^T(Av-b)$$

$$v = [Q + \lambda A^T A]^{-1}(\lambda A^T b - c)$$

Hopfield Network (gradient descent)

$$J = \frac{1}{2}\sum_{k=1}^{M}[(Cx_k - ref)^T Q(Cx_k - ref) + u_k^T R u_k + \lambda\|x_{k+1} - Ax_k - Bu_k\|^2]$$

$M = C^T QC + \lambda A^T A + \lambda I_{hxn}$

$N = R + \lambda B^T B$

$S = \lambda(A^T - I_{hxn})B$

α == Gradient "step size"

$c^T Q\ ref$

x

u

M

N

S

S^T
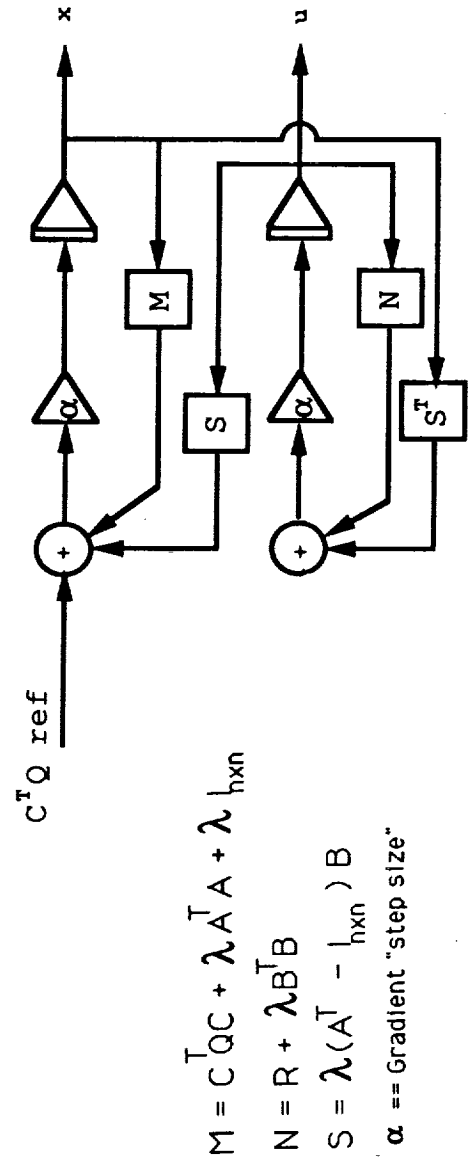
Lagrange Multiplier Approach

Hopfield Network

$$J = \frac{1}{2} \sum_{k=1}^{M} \left[(Cx_k - ref)^T Q (Cx_k - ref) + u_k^T R u_k + \lambda^T (x_{k+1} - Ax_k - Bu_k) \right]$$
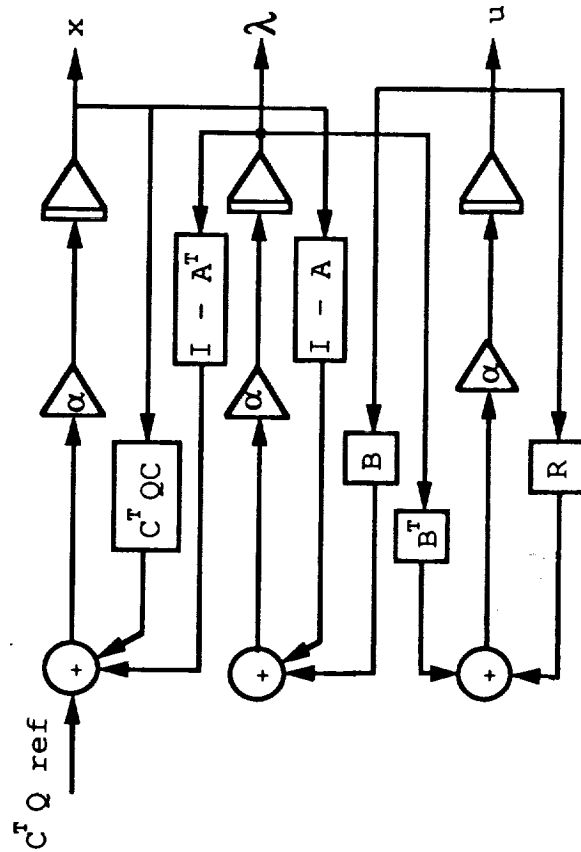
Equivalent Direct Optimization

$$J = \frac{1}{2} v^T M v + v^T b + \lambda^T (Av - c)$$

$$\begin{bmatrix} v \\ \lambda \end{bmatrix} = \begin{bmatrix} M & A^T \\ A & 0 \end{bmatrix}^{-1} \begin{bmatrix} -b \\ c \end{bmatrix}$$

Equivalency

1. Discrete-time dynamic problem tested

2. Discrete-time dynamic problem easily converted to equivalent static problem

3. Riccati is feedback form of Calculus of Variations optimization

4. Riccati eq. provides solution for dynamic problem

5. LaGrange multiplier approach provides solution to static optimization problem

6. Static problem = Dynamic problem = Riccati = LaGrange approach

So Why Hopfield Networks ?

(on a convex linear quadratic problem)

1. Speed a la massive parallelism

2. Analog hardware implementation

236

Plot of Riccati vs HNN

both traces, condition number = 360

alpha in deg

.08 .06 .04 .02 0

time steps (.01 sec)

difference

2.00E-17   1.00E-17   0

degrees

time steps (.01 sec)
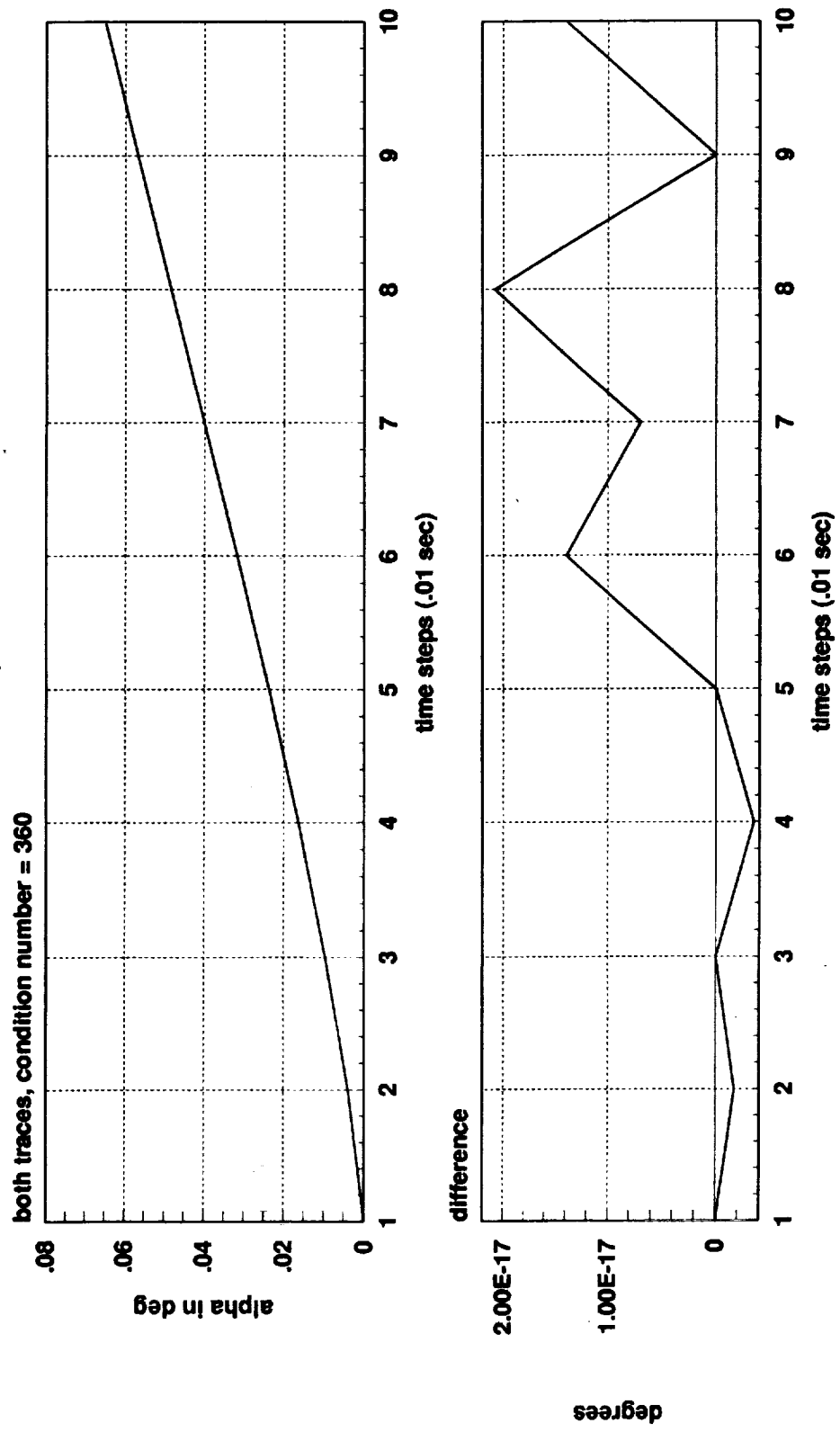
Example Problem w/failure (HNN penalty)

16:43:42   04-JAN-93
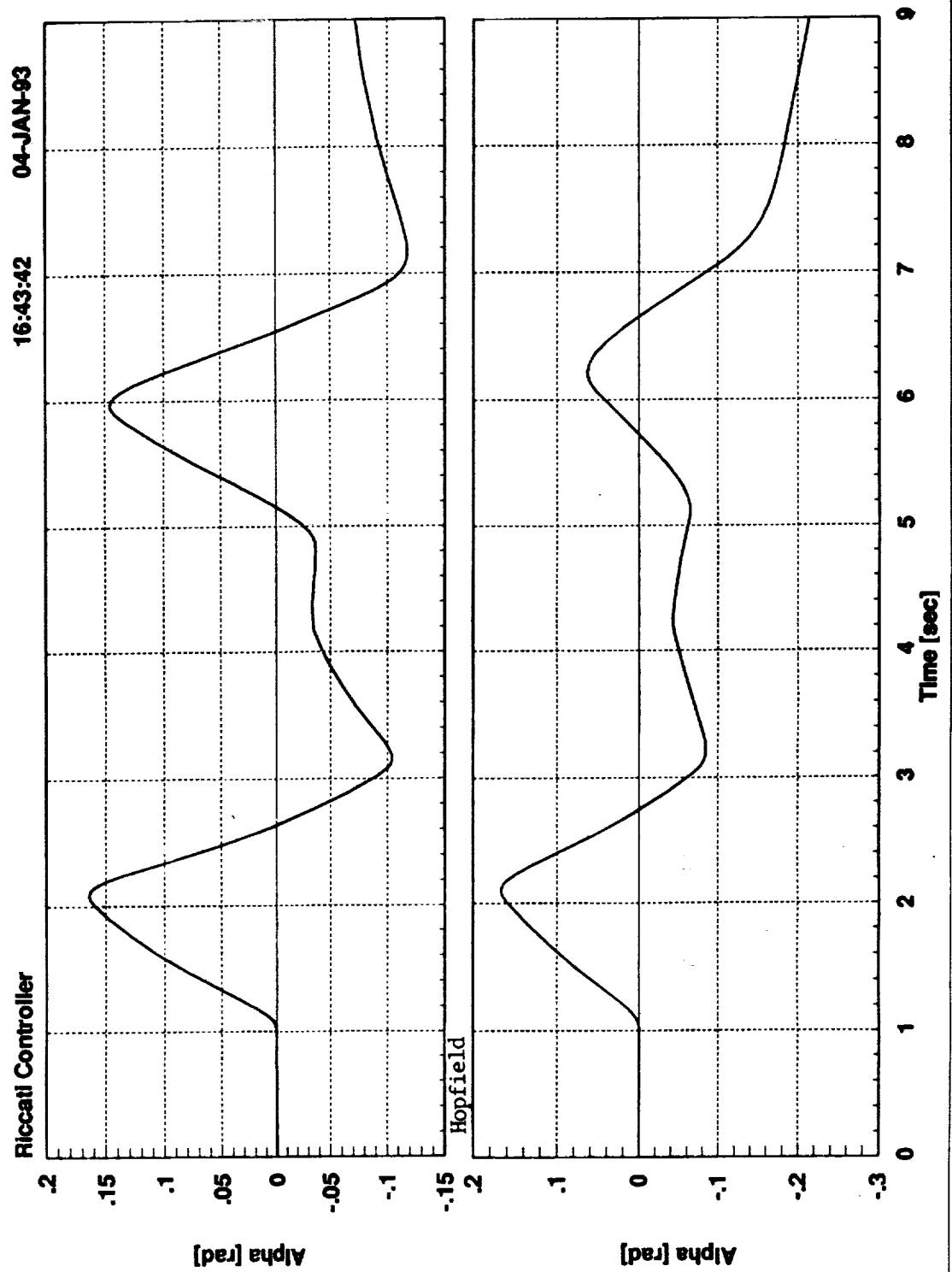
Example Problem ID Performance

Hopfield Controller   09:05:32   05-JAN-93

Actual

Min Var w/ Stoc

M-alpha

Time [sec]
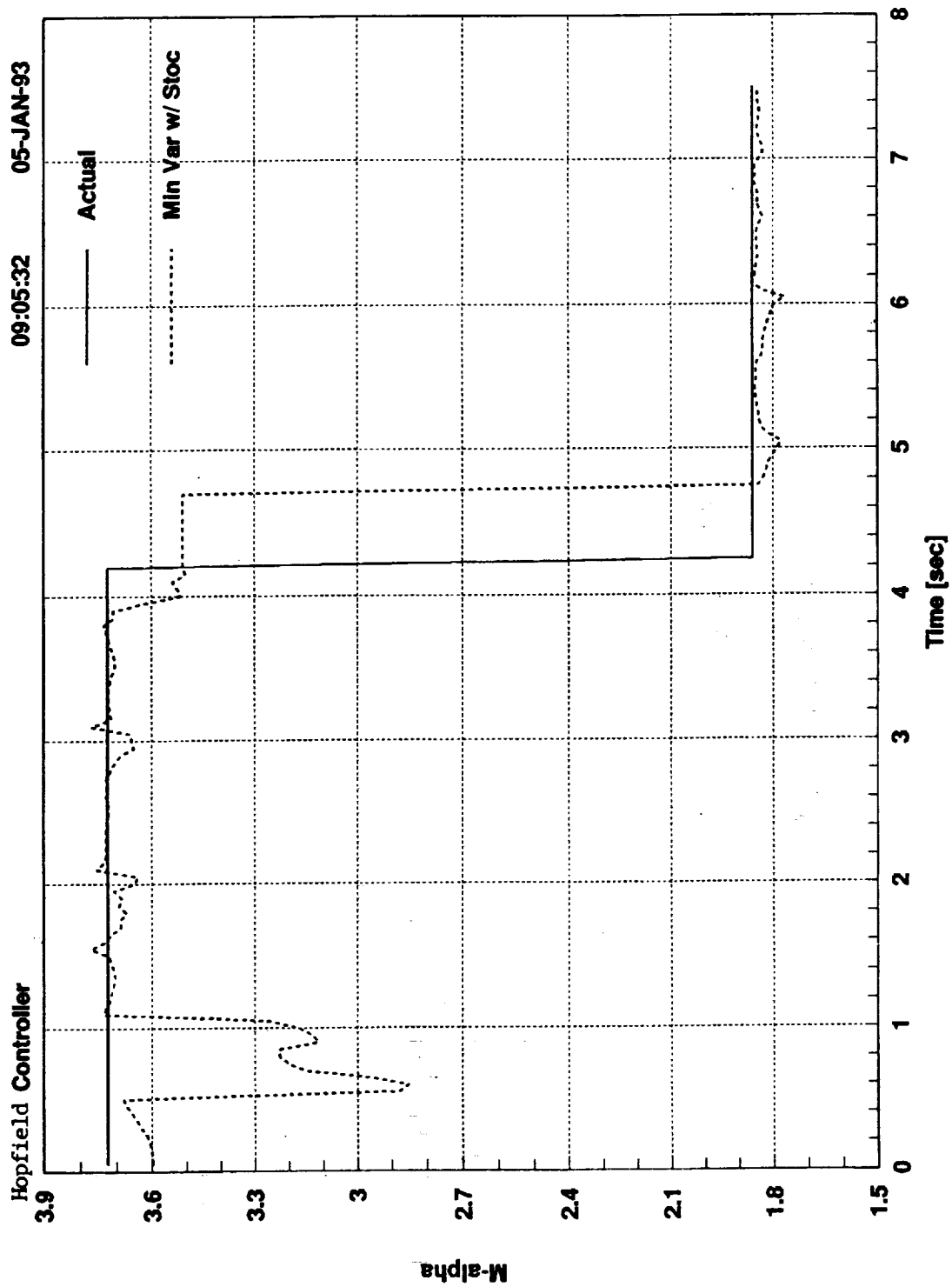
What about Nonlinear Constraints?

(non convex, non quadratic)

1.Linearize => LQ

2.Dynamic inversion => linear => LQ

3.Nonlinear Optimization

How? : pseudo simulated annealing a la HNN

1) HNN locates minimum (local)

2) hill climbing for x steps

3) Goto 1) and repeat N times

Summary

Hopfield Network equivalent to Riccati solution

Fast analog implementation possible if condition no. low enough, eg k=300

$$\left|\frac{\Delta\theta}{\theta}\right| \leq \kappa\left|\frac{\Delta y}{y}\right|$$

have approx. 60 db signal/noise ratio, then will yield acceptable results

Hopfield Networks appear suited for nonlinear (adaptive) control

Aircraft Digital Flight Control Technical Review

Otha B. Davenport, Technical Director
Directorate of Engineering & Technical Management
Headquarters Air Force Materiel Command
Wright-Patterson AFB OH

David B. Leggett
Flying Qualities Section
Wright Laboratory
Wright-Patterson AFB OH

Introduction

The Aircraft Digital Flight Control Technical Review was initiated by two pilot induced oscillation (PIO) incidents in the spring and summer of 1992. Maj Gen Franklin (PEO) wondered why the Air Force development process for digital flight control systems was not preventing PIO problems. Consequently, a technical review team was formed to examine the development process and determine why PIO problems continued to occur. The team was also to identify the "best practices" used in the various programs they looked at.

The charter of the team was to focus on the PIO problem, assess the current development process, and document the "best practices". A multi-agency, multi-disciplinary team was established with members from Air Force Material Command/Engineering (AFMC/EN), Wright Laboratory/Flight Dynamics Directorate (WL/FIG), Aeronautical Systems Center/Engineering (ASC/EN) (both engineers and managers were represented), and Air Force Flight Test Center (AFFTC) (both engineers and pilots were represented). The team conducted the review in July and August of 1992 and prepared the final report and briefing for Gen Yates, the AFMC commander, in August and September 1992.

The team reviewed all major USAF aircraft programs with digital flight controls, specifically, the F-15E, F-16C/D, F-22, F-111, C-17, and B-2. The team interviewed contractor, System Program Office (SPO), and Combined Test Force (CTF) personnel on these programs. The team also went to NAS Patuxent River to interview USN personnel about the F/A-18 program. The team also reviewed experimental USAF and NASA systems with digital flight control systems: the X-29, X-31, F-15 STOL and Maneuver Technology Demonstrator (SMTD), and the Variable In-Flight Stability Test Aircraft (VISTA). The team also discussed the problem with other experts in the field, including Ralph Smith and personnel from Calspan. The following are the major conclusions and recommendations of that review.

Findings: Digital Mechanization

First of all, a review of aircraft that have experienced PIO problems in the past indicates that PIO is not a problem caused by digital mechanization per se. PIOs have been encountered with all kinds of control system mechanizations. Mechanical, hydromechanical, electromechanical, and analog electronic systems have all encountered PIOs in the past. Table 1, from Reference 1, shows several PIO problems that have occurred in the past.

However, digital electronic flight control systems have allowed us to break the space, weight,

and power barriers that effectively limited the flight control complexity that could be achieved with other control system mechanizations. With digital flight mechanization we can tailor the flight control system for a far wider variety of flight conditions and flight tasks than was possible before. This added complexity adds some additional risk that may require a more disciplined, more structured process to manage in the development process.

Findings: Development Process

All of the programs we looked at used pretty much the same development process. A simple schematic of that process is shown in Figure 1. This process is inherently iterative. Each step is intended to better identify the system and reevaluate the system based on the latest identification. When problems are encountered the design should be modified, re-identified and reevaluated. When problems are overcome the process moves on to the next step. This process is intended to reduce risk as the uncertainty decreases. Our conclusions about the process were that the process had the right steps, but the execution varied from program to program.

In some programs, the twin constraints of cost and schedule sometimes drove the process to run "open-loop" when flying qualities problems (including possible PIO problems) were encountered. For example, if a design did not meet the quantitative requirements in the specification and the necessary fix significantly impacted cost or schedule, some programs discounted the applicability of the requirements and decided to proceed with simulation to see if the problems existed. If problems were encountered in simulation and the necessary fix significantly impacted cost or schedule, some programs discounted the fidelity of the simulator and decided to proceed with flight test to see if the problems existed.

Findings: PIO

Figure 2 shows a simplified schematic of the pilot-vehicle system. The pilot can be viewed as a feedback system that closes the outer-loop around the airframe-sensor-flight control system. The feedback path for the pilot is a multi-channel path that includes the pilot's visual cues (outside and inside the cockpit), motion cues, aural cues, tactile cues (force and displacement) from his controllers, and others. A PIO occurs when this outer loop becomes dynamically unstable or neutrally stable. In the most general sense, a PIO is the result of a disharmony between the pilot's action and the expected aircraft reaction. This occurs when one or more of these feedback cues provide confusing or even conflicting information to the pilot and his gain is high enough to drive the outer-loop system unstable. PIO susceptibility is when the aircraft possesses certain characteristics that make it prone to get into a PIO in flight conditions and tasks in which it must frequently fly. The typical causes of PIO susceptibility are well known: high stick sensitivity, excessive system phase lag, large system nonlinearities, lightly damped response modes, unstable response modes, coupled response modes, etc. Each of these problems causes some kind of disharmony in one or more of the pilot's feedback channels.

However, the presence of such characteristics does not mean that the aircraft will PIO all the time. There are other factors involved as well. First of all, a PIO is more likely to occur when the pilot is performing a "high gain" task, that is, he is trying hard to minimize an error in aircraft attitude or rate. Such "high gain" tasks include precision landing, carrier landing, aerial refuelling (particularly probe-and-drogue), LAPES, close formation flying, target tracking, etc. A PIO is more likely to occur in these kinds of tasks than in tasks where the pilot is only loosely monitoring aircraft attitude or rate and making occasional corrections.

244

The pilot is a factor in the probability of a PIO occurence because a pilot can learn to avoid PIOs in a specific airplane by learning the tasks and the conditions in which that airplane is PIO prone, and learning to avoid it by lowering his gain in those tasks and conditions. Thus a PIO is less likely with a pilot who is experienced with the airplane's PIO tendencies and has learned the appropriate technique to avoid it. PIO is more likely with a pilot who is unfamiliar with the airplane or is unaware of its PIO tendencies. The fact that the pilot is a factor in a PIO should not be interpreted to mean that the pilot is at fault. PIO susceptibility is a design flaw because the aircraft is supposed to be designed such that a pilot can command the necessary degree of precision to do the task without fear of driving the outer loop unstable. An aircraft can and should be designed such that it is not PIO prone in tasks or conditions in which it must commonly operate. The team struggled with the perception that such a design might be impractical from a cost, weight or performance perspective until a very high performance front-line fighter was considered that had never had a PIO and was clearly in the "good" handling qualities regime. This aircraft had set the standard in cost, weight and performance. It was not designed specifically for PIO but careful attention had been paid during it's design to the characteristics that cause good handling qualities.

Sometimes a PIO is initiated by a discrete event, commonly called a "trigger event". A trigger event is not necessary for a PIO to occur, nor will the identical trigger event initiate a PIO every time. This is because the trigger event is not the cause of a PIO, it is only a catalyst. A trigger event could be something related to the aircraft such as a discontinuity in the control system (e.g. a sudden failure or a large discontinuity in the control law gain schedule), or it could be something totally unrelated to the aircraft such as a large, abrupt atmosperic disturbance or a pilot distraction. In a PIO prone aircraft, the trigger event will initiate the PIO by causing the pilot to make abrupt corrections, and the PIO tendencies (due to whatever factors) will provide the "confusion" that sustains the PIO. If the aircraft is not PIO prone to begin with, the trigger event will probably not cause a PIO because the pilot can apply sudden corrections without becoming "confused".

Of all of these factors, only the aircraft susceptibility and certain trigger events are within the control of the designer. Mission requirements may demand that certain "high gain" tasks be done. The aircraft will be flown by pilots with a wide range of experience (the only way to gain experience with an aircraft is to start learning without any). Certain trigger events are random events with a high probability that they will happen to someone sometime in the aircraft's service life. In order to design an aircraft that is not PIO prone the designer must control those well-known factors that cause PIO susceptibility. The difficult question for the designer is "What values of these factors provide the appropriate level of PIO resistance?"

The reason that this is a difficult question is that, like all sciences that involve the human element, flying qualities issues, including PIO susceptibility, have the characteristics of a "soft" science. That is, since a human being's appraisal is the measure of merit, it is very subjective in nature, and highly variable depending on what human being is doing the evaluating. This variability exists in both the research end, where you are trying to develop criteria to address the problem, and on the verification end, where you are trying to prove that your delivered product is satisfactory. Thus, there is not necessarily an absolute answer, but instead a certain probability based on evaluation by a number of human beings.

The nature of the problem is illustrated in Figure 3. Cooper-Harper pilot ratings are the most common quantitative measure used in flying qualities evaluations. For a typical handling qualities experiment, the correlation curve of a parameter that correlated with Cooper-Harper ratings would

typically look something like that shown in Figure 3. At the "good" end of the curve, there is a certain point up to which, in a typical experiment, all of the pilots will agree that the aircraft is good, and the diversity of Cooper-Harper ratings will be small. At the "bad" end of the curve, there is a certain point beyond which all of the pilots will agree that the aircraft is bad, and the diversity of Cooper-Harper ratings will be small. Between these two points is an area where it is more difficult to say precisely how bad the aircraft is because the diversity of pilot ratings will be much greater at any point in this region than at the ends (References 2 and 3). Consequently, the objective, open-loop requirements derived from handling qualities research must be considered inferential in nature. That is, meeting them will provide a high probability of having good handling qualities, but it does not guarantee good handling qualities.

Findings: Flying qualities specifications

The quantitative PIO criteria available in the current flying qualities specification, MIL-STD-1797, and from other sources, are based largely on data generated in experiments conducted on ground-based and in-flight simulators in the 1960s and 1970s. The review team found that of all the available criteria, no one criteria seems to be universally accepted by the community at large. In the flying qualities specifications, most of the quantitative PIO requirements resided in paragraphs that were intended to assure good overall flying qualities, not just to preclude PIO. For example, in MIL-STD-1797 requirements on phase lag in the pitch response reside in paragraph 4.2.1.2 Short-term Pitch Response. In the specifications, paragraphs intended explicitly to preclude PIO problems have been largely qualitative in nature ("there shall be no tendency for PIO"). Finally, the verification requirements in MIL-STD-1797 do not specifically call for testing for PIO characteristics. The lack of a strong tie between the requirements and the verification at each stage of the process has led some programs to defer critical actions at a time when small changes could have precluded a much more significant change later on.

Findings: Flight Test Phase

The final test of the flying qualities and the PIO tendencies of an aircraft is in the flight test phase. The problem with waiting until the flight test phase to determine the degree of PIO susceptibility is that by this point in the development the number of realistic options to resolve problems is dramatically reduced, and design changes at this stage have a greater impact on cost and schedule than at earlier stages. Often a cheaper and easier solution at this stage is to train the pilots to avoid the PIO if they can. Consequently, a system with a PIO tendency sometimes does not get fixed unless the pilots cannot find a technique to avoid the PIO or it prevents mission accomplishment.

Conclusions

As a result of these findings, the Review Team concluded that the process, as currently implemented, had the the following flaws:

1) The available criteria and analysis methods are inferential in nature, they lack universal acceptance, and the current test techniques are not rigorous for PIO problems.

2) Because of this, the current process lacks firm go/no-go criteria at each step in the process for the manager to assess the risk of PIO and decide whether to proceed or whether further iteration is necessary.

3) Consequently, with regard to flying qualities in general and PIO in particular, the development process tends to be driven "open-loop" instead of as an iterative process.

4) Finally, the decision of what is good enough is typically left until the flight test phase, where many options that were available in previous development phases are now precluded by cost and schedule constraints, and changes are made only if the pilots cannot be trained to avoid the PIO or the task cannot be modified and retain it's military utility.

Recommendations

The Review Team made the following recommendations to resolve these problems in the process.

First, establish an Integrity Approach for flight control similar in nature to those established for structures and propulsion. The intent of this program would be to change the paradigm from one of "proceed unless a PIO problem is proven to exist" to one of "proceed only when a PIO problem is proven not to exist". This would be done through establishment of firm go/no-go criteria for each step in the development process. At the design stage it would consist of improved flying qualities criteria. However, since these would still be inferential in nature, further "gates" would be established at other steps in the process. Rigorous demonstration maneuvers, such as Handling Qualities During Tracking (HQDT) would be required in early stages of the development process, such as ground simulation. In-flight simulation would be recommended, perhaps even required if results were inconclusive in the earlier stages. Finally, the verification of adequate PIO resistance would not just be compliance with the inferential requirements, but also satisfactory handling qualities in the demonstration maneuvers during flight test. With the requirements and verification agreed to between the Air Force and the contractor, this process provides a relevant measure of the capability of the aircraft to be operated by the vast majority of the pilot corps.

The second recommendation was to establish a Flying Qualities Working Group in each SPO that has an aircraft under development. The initial purpose of this group is to conduct an assessment of the system and attempt to achieve the appropriate balance between design, pilot-training and military utility. This working group consists of engineers from the SPO, the contractor, the laboratories, and the Flight Test Center, and the test pilots from the contractor and the Flight Test Center. The purpose of the Flying Qualities Working Group is to monitor the progress of the flying qualities of the design through the development stages, help resolve problems, and insure that potential problems are communicated to all the agencies involved.

The third recommendation was to enhance the flying qualities research program to improve the criteria and analysis methods available. The objective is to resolve the conflicts between existing criteria, develop a more comprehensive analysis method, and, hopefully, reduce the region of uncertainty in the present predictive methodology. Another objective would be to develop criteria and analysis methods for new flight regimes (such as high angle of attack) and unconventional response modes (such as direct lift).

The fourth recommendation was to incorporate the "Best Practices" into a new tool being developed for the SPO engineer called the Air Force Acquisition Model (AFAM). The Review Team identified 22 "Best Practices". Space limitations preclude listing all of them here, but they are summarized below:

1) In the requirements definition stage, use quantitative PIO requirements in the specifications, with specific verification requirements.

2) In the design stage, use multiple analysis methods and criteria to assess the flying qualities of the design.

3) Keep the needs of flight test in mind during the design. For example, include a means to change control system gains during the flight test phase in anticipation of the need to adjust them in order to resolve problems.

4) Ground test with hardware in the loop to identify system characteristics.

5) Use full-up ground simulation and in-flight simulation to assess handling qualities and PIO tendencies and use well-defined "high gain" pilot-in-the-loop tasks.

6) In the flight test stage, use well-defined "high gain" pilot-in-the-loop handling qualities testing (HQDT, etc.) as part of the envelope expansion process.

On 5 Feb 1993, the findings and recommendations of the Review Team were briefed to the Commander of Air Force Materiel Command. He has directed that AFMC implement the recommendations.

As a result of these and previous briefings to the senior leadership of the Air Force, the "best practices" are being included in the AFAM for use in current and future Air Force programs. The SPO's either have or are now forming the working groups and conducting assessments to be reviewed by the Program Director. The Air Force Science and Technology program funding for flying qualities has been increased by over 100%. Finally, the Commander of Aeronautical Systems Center through the Directorate of Engineering is planning to release a draft Integrity Program standard by the end of 1993. The focus of the Air Force on the total system requirements for affordable, capable and sustainable aircraft that meet the users needs has been improved by the contributions of all of the team members.

References

1. Ashkenas, Irving L., Henry R. Jex, and Duane T. McRuer, Pilot-Induced Oscillations: Their Cause and Analysis, Norair Report NOR-64-143 and STI Report TR-239-2, 20 Jun 1964.

2. Wilson, David J. and David R. Riley, Cooper-Harper Pilot Rating Variability, AIAA Paper 89-3358, 14-16 Aug 1989.

3. Riley, David R. and David J. Wilson, More on Cooper-Harper Pilot Rating Variability, AIAA Paper 90-2822, 20-22 Aug 1990.

4. Military Standard, Flying Qualities of Piloted Aircraft, MIL-STD-1797A, 30 Jan 1990.

TABLE I. Some Past PIO Problems (Taken from NOR-64-143)

Examples shown as: SPECIES (Aircraft): Critical Subsystem: Critical Flight Condition : Remarks

CLASS	TYPE		
	I. LINEAR	II. SERIES NONLINEAR ELEMENTS	III. SUBSIDIARY FEEDBACK NONLINEAR ELEMENTS
PITCH	IMPROPER SIMULATION: D, V: a: Abnormally high value of $1/T_{\theta2}$ and low ζ_{sp} led to zero ζ_{sp} when regulating large disturbances. GCA-INDUCED PHUGOID (C-97): D, c: b: Lag from radar-detected error to voice command led to unstable closed-loop phugoid mode. ARM ON STICK (A4D-1, T-38A): F: a: Arm mass increases feel system inertia; leads via H feedback to unstable coupling with short-period dynamics if pilot merely hangs loosely onto stick after a large input.	PORPOISING (SB2C-1): F: c: Hysteresis in stick versus elevator deflection resulted in low frequency speed and climb oscillations. L.C. MANEUVER (F-86-D, F-100C): F,S: a: Valve friction plus compliant cabling resulted in large oscillations at short period. PITCH-UP (XF-104, F-101B, F-102A): V: c: Unstable kink in M(α) curve led to moderate-period oscillations of varying amplitudes (depending on extent and nature of the kink) during maneuvers near the critical angle of attack. LANDING PIO (X-15): S: b: Closed-loop around elevator rate-limiting caused moderate oscillations at short period.	BOBWEIGHT BREAKOUT (A4D-1, T-38A): F, B: a: At high-g maneuvers the bobweight overcomes system friction and reduces apparent damping of the aircraft in response to force inputs, resulting in large oscillations at short period. LOSS OF PITCH DAMPER
LATERAL-DIRECTIONAL	u_β/u_ϕ EFFECT (X-15, T-33VSA, F-101B, F-106A, KC-135A, B-58): V: c: Zeros of roll/aileron transfer function are higher than dutch roll frequency, $|u_\beta/u_\phi| > 1.0$, leading to closed-loop instability at low ζ conditions. BORESIGHT OSCILLATIONS (F-5A): D, V: c: Spiral roll mode driven unstable if roll information is degraded during gunnery.		LOSS OF YAW DAMPER
YAW	FUEL SLOSH SNAKING (KC-135A, T-37A): V: c: Fuel slosh mode couples with dutch roll mode when rudder used to stop yaw oscillations.	TRANSONIC SNAKING (A3D): V, F: a, c: Separation over rudder causes control reversal for small deflections, leading to limit cycle if rudder used to damp yaw oscillations.	
ROLL	NONE KNOWN	PILOT-INDUCED CHATTER (F-104B): A: c: Small limit cycle due to damper aggravated whenever pilot attempted to control it.	

*Critical Subsystems:
D = Display
F = Feel system (except B)
B = Bobweight
S = Power servo actuator
V = Vehicle (airframe)
A = Augmenter (damper)

**Critical Flight Conditions:
a = Low altitude, near-sonic Mach
b = Landing approach and takeoff
c = Cruise
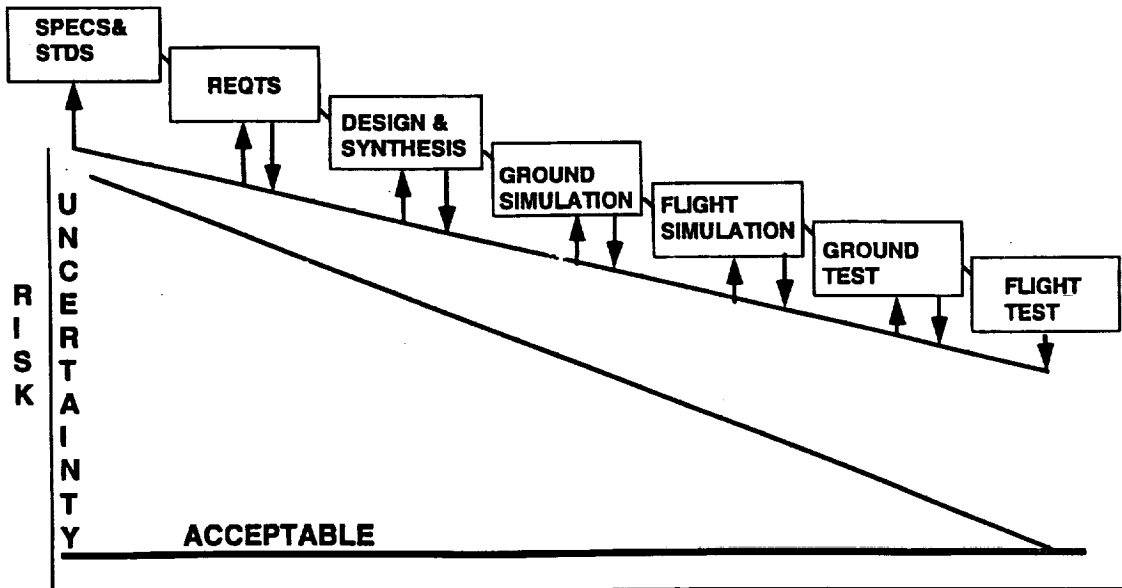
FIGURE 1. Simple Schematic of the Development Process

249

FIGURE 2. Simplified Schematic of Pilot-Vehicle System

FIGURE 2. Simplified Schematic of Pilot-Vehicle System
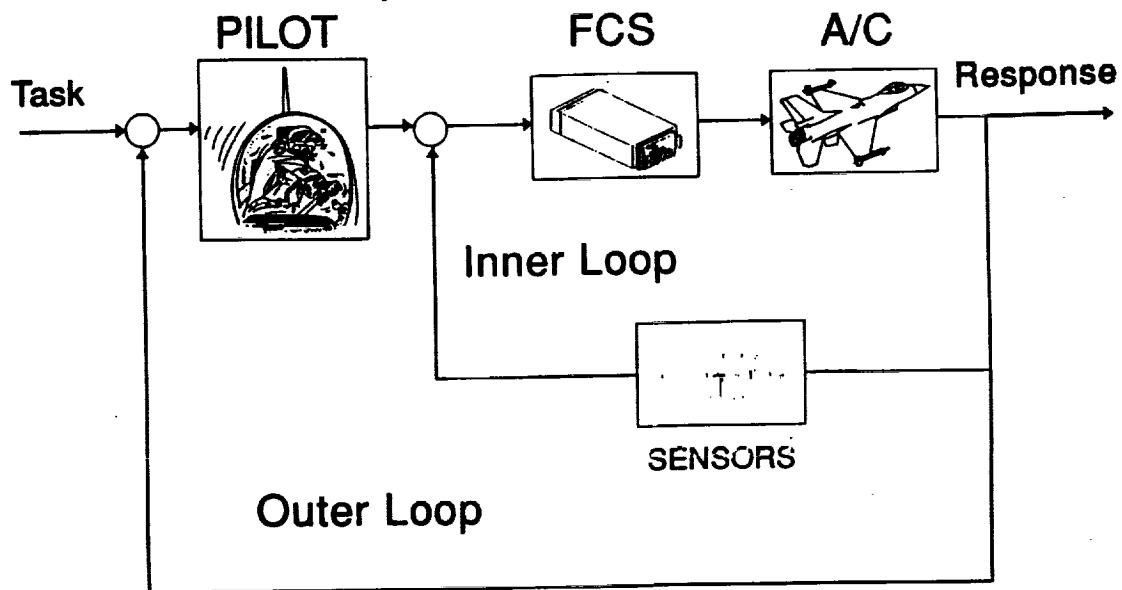
FIGURE 3. Pilot Rating Correlation With a Flying
Qualities Parameter
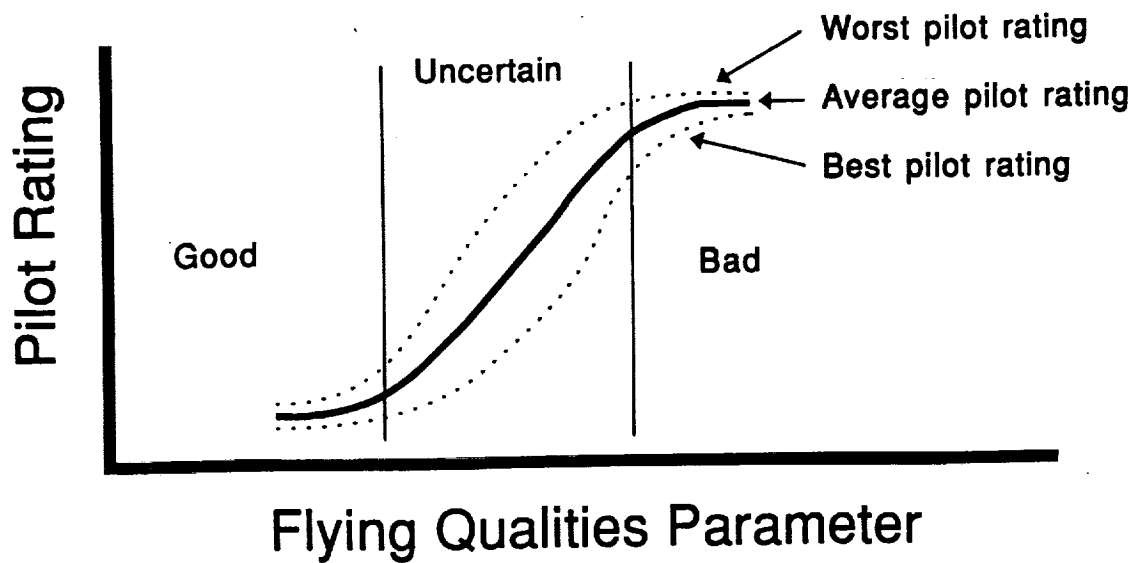
FIGHTER/ATTACK AIRCRAFT GROUP

NASA AGILITY DESIGN STUDY:
PROJECT DESCRIPTION AND STATUS

NASA LaRC Workshop on Guidance, Navigation, and Controls

March 18, 1993

Michael J. Logan, P.E.
Group Leader, Fighter/Attack Aircraft, Vehicle Integration Branch
NASA Langley Research Center, Hampton VA

The NASA Agility Design Study Project was started in late 1991 in response to a request from NASA Headquarters to assess the impact of "agility" requirements and related technology research projects on fighter aircraft. The study is currently being conducted through the Vehicle Integration Branch within the Advanced Vehicles Division. The Project Engineer is Mike Logan of VIB.

FIGHTER/ATTACK AIRCRAFT GROUP

AGILITY DESIGN STUDY

¤ PROJECT OVERVIEW

¤ INTERIM RESULTS

¤ IN-HOUSE CONFIGURATION STUDIES

¤ CONCLUDING REMARKS

This presentation will provide a brief project overview, provide some preliminary results, discuss in-house activities and show the future plans for the activity.

FIGHTER/ATTACK AIRCRAFT GROUP

PROJECT DESCRIPTION

¤ **OBJECTIVE:**

» *TO ASSESS THE IMPACT OF AGILITY BASED REQUIREMENTS ON AIRCRAFT DESIGN DECISIONS*

¤ **APPROACH:**

» *IDENTIFY AGILITY REQUIREMENTS*

» *DEVELOP ASSOCIATED DATA BASES AND PREDICTIVE METHODOLOGY*

» *CONDUCT DESIGN TRADE STUDIES*

» *OPERATIONAL IMPACT ANALYSES*

¤ **ANTICIPATED RESULTS:**

» *QUANTIFIED AGILITY METRICS*

» *BALANCED DESIGN TRADE DATA*

» *MISSION EFFECTIVENESS vs. COSTS OF VARYING LEVELS OF AGILITY*

256

The purpose of this project is to assess the impact of "agility" requirements on aircraft design decisions and technology requirements. The approach being taken is to divide the effort into four distinct phases. These are to a) Identify agility requirements, b) develop a data base and predictive requirements, c) conduct design trade studies using these levels and predictive methods and d) perform an operational analysis to determine the impact on the combat effectiveness of the vehicles. Each of thse task areas will be explained further. Out of this effort will come quantified agility metrics, design trade data, and mission effectiveness vs. costs of varying the levels of agility.

FIGHTER/ATTACK AIRCRAFT GROUP

PROJECT OVERVIEW

PARTICIPANTS:

- **NASA:**
  Langley
  Dryden
  Ames
- **INDUSTRY:**
  Boeing
  Eidetics
  General Dynamics
  McDonnell-Douglas
  Others
- **AIR FORCE:**
  ASD/XR
  Wright Labs
- **NAVY:**
  NAWC

TASK AREAS:

Task 1 - Requirements ID

Task 2 - DB & Methodology

Task 3 - Config. Studies

Task 4 - Ops. Analysis

WORK EFFORTS:

- IN-HOUSE RESEARCH
- CONTRACTED STUDIES
- WORKING GROUP MEETINGS

NEEDS — DISCIPLINE RESEARCH — DESIGN METHODOLOGY — FLIGHT VALIDATION — FOCUS

The effort is being conducted using a combination of in-house research, contracted studies, and working group meetings to accomplish the tasks. The participants include NASA, industry, and the military services, both Air Force and Navy.

FIGHTER/ATTACK AIRCRAFT GROUP

TASK 1- REQUIREMENTS IDENTIFICATION

¤ "METRIFICATION":

- Review of existing metrics research
- Operator input
- Definition/selection of appropriate metrics

¤ QUANTITATIVE ASSESSMENT OF CURRENT CAPABILITIES

¤ EVALUATION OF AGILITY GOALS FOR FUTURE AIRCRAFT

Task 1 involved identifying an appropriate set of agility requirements. This was done by conducting reviews of existing metrics research, gathering operator input from the Air Force Figher Weapons School, and developing a consensus from the working group on which "metrics" to use. As part of this phase, current capability was also assessed and goal levels assigned.

FIGHTER/ATTACK AIRCRAFT GROUP

METRIC SELECTION RESULTS

¤ **WORKING GROUP CONSENSUS**

- Government Inputs: NASA, AF
- Industry Inputs: Boeing, Eidetics, General Dynamics, McDonnell-Douglas

¤ **METRICS SELECTED:**

METRIC	CONDITIONS
1. Maximum Negative Ps	0.6M @ 15,000 ft., max inst. $\dot{\psi}$ 450kts. @ sea level, max inst. $\dot{\psi}$
2. Time-to-bank 90°	0.6M @ 15,000 ft., max inst. Nz 450kts. @ sea level, 5g
3. Minimum nose-down pitch acceleration	Condition for C_m^*
4. Max. achievable, departure-free, trimmed angle-of-attack	Subsonic
5. Maximum lateral acceleration	Max. inst. Nz (Air-to-Air) 1g wings level (Air-to-ground)

The first working group meeting included representatives from NASA, industry, and the Air Force. Five metrics were selected and flight conditions for both air-to-air and air-to-ground were assigned. Note that thse metrics were not selected because they "define" agility but rather because they are readily computable in the conceptual design phase of the aircraft's development and because taken together they can reasonably "categroize" the potential agility of the aircraft when it is built.

FIGHTER/ATTACK AIRCRAFT GROUP

TASK 2- DATA BASE & METHODOLOGY DEVELOPMENT

¤ COLLECTION OF SUPPORTING DATA

- Current fleet capabilities
- Technology research reports

¤ ALGORITHM DEVELOPMENT / VALIDATION

- Identifying appropriate techniques
- Computerization
- Benchmarking

¤ INTEGRATION INTO DESIGN SYNTHESIS PROCESS

- Code integration into FLOPS
- Data generation

The second phase of the activity was oriented towards developing the necessary predictive methodology for the effort. In addition, a limited data base was developed to assess current fleet capabilities with regards to the chosen metrics. The prediction codes have been developed and will be integrated into the VIB aircraft sizing/synthesis program, FLOPS when they have been validated against the collected data.

FIGHTER/ATTACK AIRCRAFT GROUP

TASK 3- CONFIGURATION TRADE STUDIES

¤ **DEFINE MISSIONS AND REQUIREMENTS/CONSTRAINTS**

¤ **DEVELOP CONCEPTUAL DESIGNS OF CONFIGURATION MATRIX:**

OBSERVABLES	AGILITY		
	Low	Medium	High
Conventional			
Reduced			
Low			

¤ **IDENTIFY TECHNOLOGY EXPLOITATION OPPORTUNITES**

¤ **DOCUMENT FUTURE RESEARCH NEEDS**

- Flight research
- Wind tunnel testing
- Methodology development

The third phase of the activity seeks to define the design and configuration related tradeoffs necessary to achieve given levels of agility. The approach here is to define a common set of missions and "conventional" range/payload/mission requirements and apply agility constraints to vehicles of differing observables classes. These studies will provide both design information as well as identifying technology needs. The effort is being done with contracted studies with airframers as well as in-house systems studies by VIB.

267

FIGHTER/ATTACK AIRCRAFT GROUP

TASK 4 - OPERATIONAL ANALYSIS

¤ DETERMINISTIC + MAN-IN-LOOP SIMULATION

¤ STUDY MATRIX FROM TASK 3

¤ AIR-TO-AIR EVALUATION

- Exchange ratios
- 1 v 1, M v N

¤ AIR-TO-GROUND EVALUATION

- Pk (Lethality)
- Ps (Survivability)

The fourth phase of the activity would identify the operational benefits associated with increasing levels of agility. This would be accomplished by means of simulation and combat effectiveness evaluations in both an air-to-air and air-to-ground context.

FIGHTER/ATTACK AIRCRAFT GROUP

PROJECT STATUS

TASK 1 STARTED NOVEMBER 1991

Metric evaluation conducted
Group meeting consensus on 5 metrics
Current fleet evaluation underway
Completion of task scheduled for late '92

TASK 2 UNDERWAY

Task Order issued to Boeing 9/92
Data/methods selection meetings held
"Validated" methods available 1Q '93

TASK 3 GETTING STARTED

Configuration study task assignments defined
Task Order mods issued to 2 of 3 contractors (GD, McAir)
Studies to be completed by 3Q 93

The project is presently only one and a half years old. The Phase I activity has been completed. Phases II and III are currently in work with Phase II nearly complete. Phase III is expected to be complete by the end of the third quarter of '93. Phase IV has not yet received a funding decision from NASA HQ.

FIGHTER/ATTACK AIRCRAFT GROUP

IN-HOUSE CONFIGURATION STUDIES

¤ **OBJECTIVE:**

» *WORK IN PARALLEL TO INDUSTRY TO DEVELOP AGILITY-CONFIGURATION DECISION RELATIONSHIPS*

¤ **APPROACH:**

» *CONDUCT CONVENTIONAL CONCEPTUAL DESIGN USING STUDY MATRIX*

» *APPLY AGILITY CONSTRAINTS TO VEHICLES*

» *ANALYZE IMPACT ON PROCESS AND DESIGN DECISIONS*

272

The Phase III design trade studies activity involves both contracted and in-house systems studies. The objective of the in-house studies is to help develop agility vs. configuration decision relationships. The approach is to develop a set of configurations which are sized to "conventional" range/payload/mission requirements using the same observables matrix as the airframers. Agility constriants will then be applied to these vehicles. The results of this imposition will be studied in terms of both its change on the configuration process as well as the designs themselves.

273

FIGHTER/ATTACK AIRCRAFT GROUP

SYSTEM STUDY PROCESS
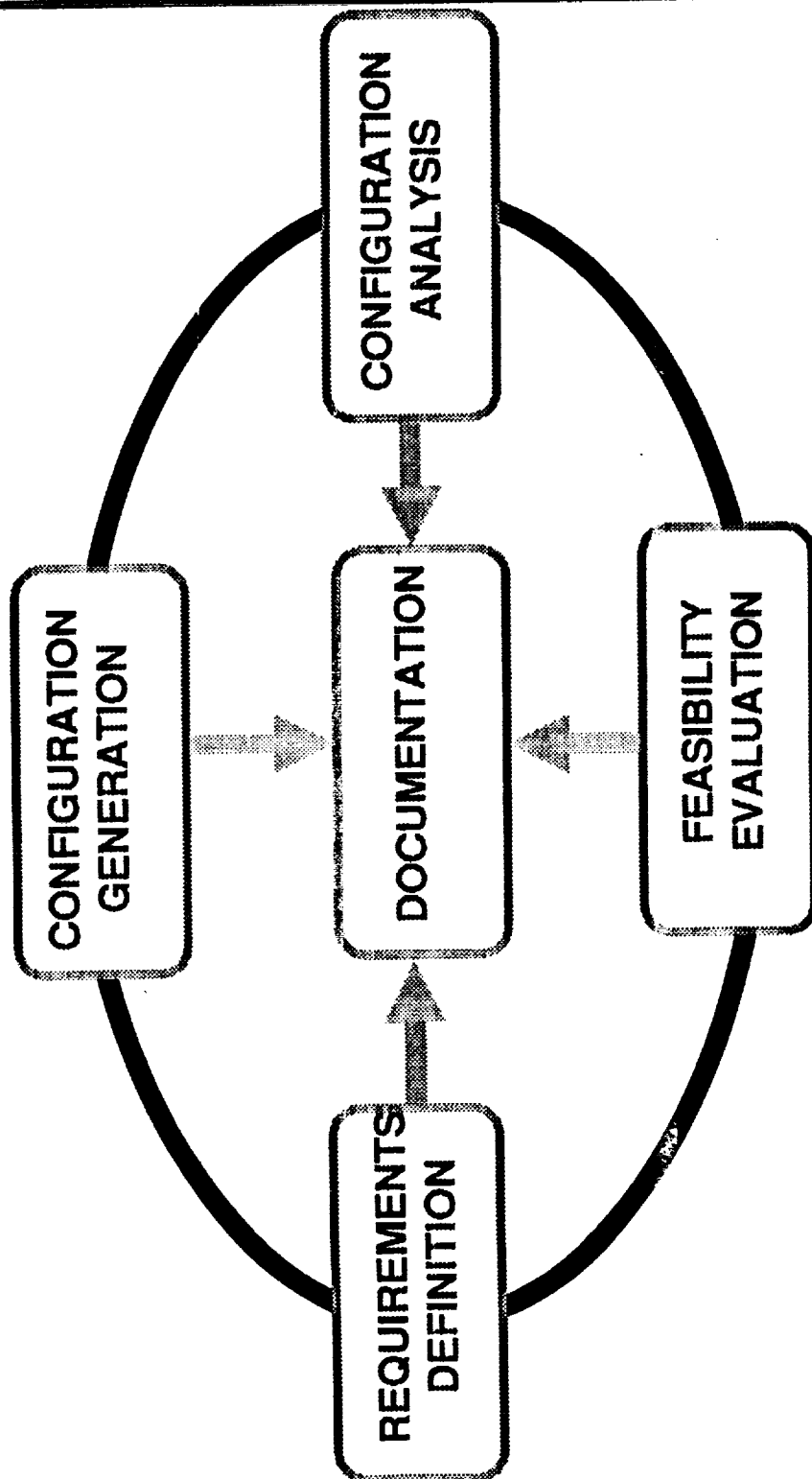
The system study process being followed is similar to that being used by the airframers. VIB developed the range/payload/mission requirements using input provided by the Air Force in terms of an aircraft of practical interest, namely a multi-role fighter class vehicle. A set of configurations was generated using the study matrix. Each of these configurations was analyzed and trade studies of variations in initial assumptions and technology sets was conducted. Each baseline configuration was subjected to a feasibility evaluation to determine it suitability to the mission and its strengths/weaknesses relative to existing configurations and each other. As part of the study, documentation of the results and methods used is being produced.

FIGHTER/ATTACK AIRCRAFT GROUP

MISSION DEFINITIONS

¤ **AIR-TO-GROUND:**

BATTLEFIELD AIR INTERDICTION (BAI) PROFILE

LOITER
20 min

CRUISE <= 15000ft., best Mach
450nmi

LOW LEVEL
TF/TA - 50nmi

COMBAT

WUTO
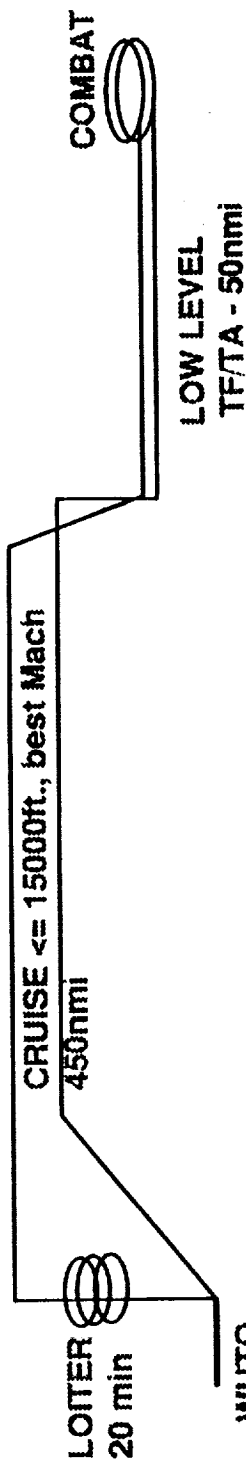
¤ **AIR-TO-AIR:**

DEFENSIVE COUNTER AIR (DCA) PROFILE

LOITER
20 min

CRUISE - const. alt, best Mach
150nmi

SUPERSONIC
M=1.5, 50nmi

DASH

COMBAT

LOITER, M=.8
30 min

WUTO

276
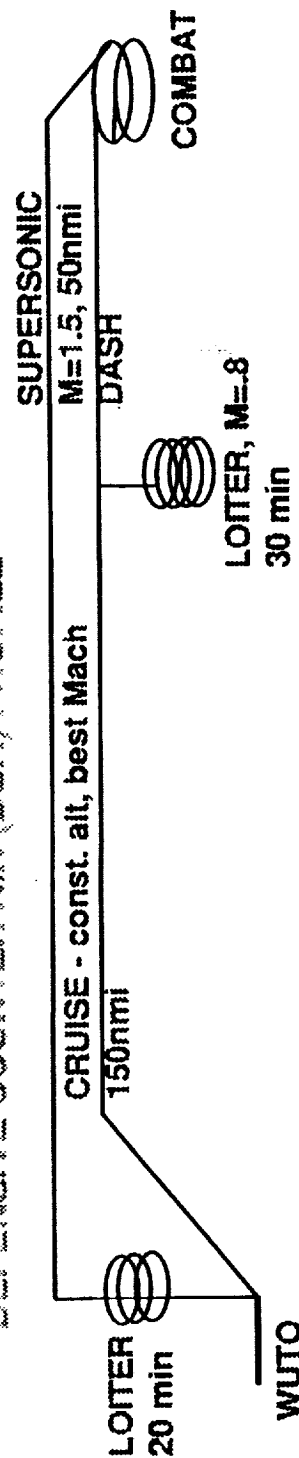
These missions are the ones being used for the Agility Design Study project. They are similar to the Air Forces Multi-Role Forces baseline missions and are representative of this class of vehicle. Note that there is both an air-to-air as well as an air-to-ground requirement.

FIGHTER/ATTACK AIRCRAFT GROUP

SIZING CONSTRAINTS AND ASSUMPTIONS

¤ TECHNOLOGY AVAILABILITY DATE: 2000-2010

¤ PERFORMANCE:

- $Nz \geq 6.5$ (Air-to-ground load, SL, $M=0.9$)
- ACCEL $M=0.8-1.5 \leq 60$ sec. (Air-to-air load, after hold)
- $Nz \geq 3.5$ (Air-to-air load, 35k', $M=0.9$)
- $Nz \geq 6.5$ (Air-to-air load, 20k', $M=0.9$)

¤ PAYLOAD:

- Basic Air-to-ground: 2xMk84 (LGB), 2xAim-9, 20mm/500 rd.
- Basic Air-to-air: 2xAim-120, 2xAim-9, 20mm/500 rd.

¤ SYSTEMS

- Avionics: 1800 lb. installed
- Engine: 100 HP, 1% Bleed extraction

A common set of initial assumptions were made regarding technology timeframe, performance, payload, and potential variations to use in trade studies.

FIGHTER/ATTACK AIRCRAFT GROUP

CONFIGURATION CONCEPTS
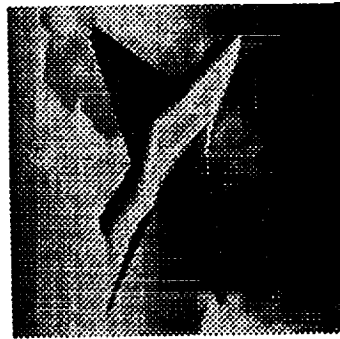
Single Engine Stealthy (SES)
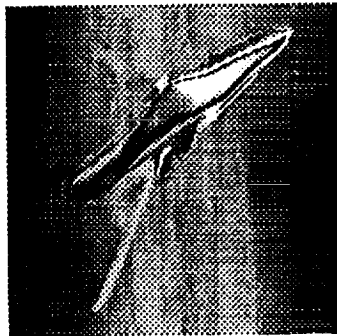
F-16XL

Single Engine Grey (SEG)

Swing Wing Fighter (SWF)

Single Engine White (SEW)
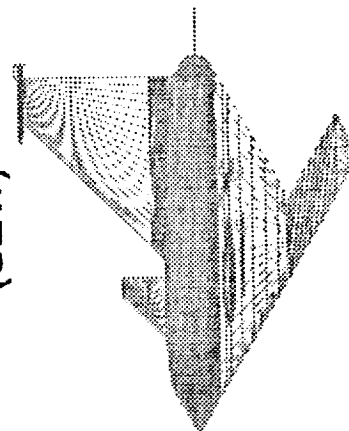
Advanced Reconfigurable Fighter (ARF)
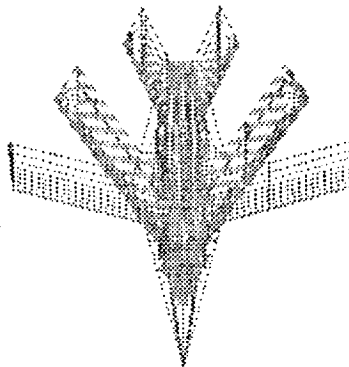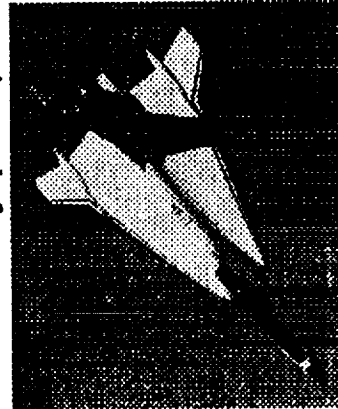
Several configuration concepts were evaluated for this effort. Three configurations were generated which correspond to the three levels of "observables" used in the study matrix. Two alternate configurations were also reviewed for applicability. These were an advanced reconfigurable fighter which has common fuselage, engine, cockpit, etc. and removable empennage. This concept would in theory provide less of a compromise for the differing roles the aircraft must perform, namely, air-to-air combat and ground attack. A less radical approach is represented by a variable sweep concept which will be used to determine both its conventional performance benefits and its agility benefits (if any). As a reference to existing aircraft capable of performing the basic mission the F-16XL is being used (although it cannot meet the desired performance levels unmodified).

281

C-4

FIGHTER/ATTACK AIRCRAFT GROUP

SINGLE ENGINE WHITE- BASELINE SUMMARY

¤ **GEOMETRY:**

Sw=390 sq ft.
AR=2.31
t/c=0.06
L=50.5

¤ **FEATURES:**

"Conventional" shaping
V-tail, all-flying
Thrust vectoring
External weapons carriage

¤ **WEIGHTS:**

GTOW: 38650 (F110 29k#)
Empty: 19250

282
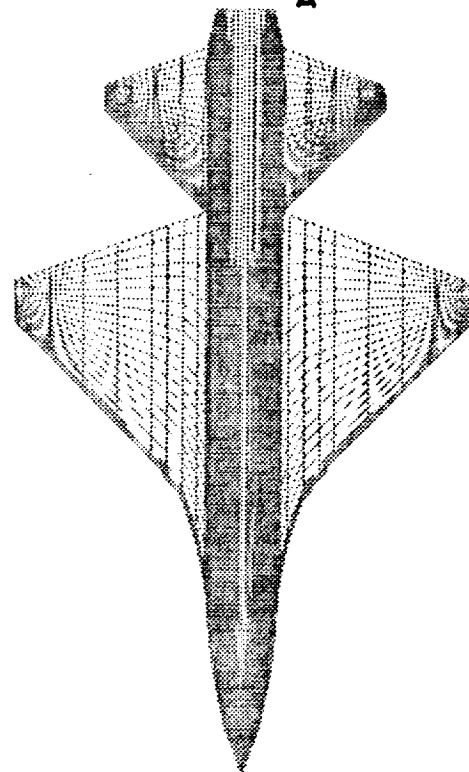
This summarizes the salient characteristics of the "conventional" observable level concept. It is a wing-body-tail configuration (although it is a V-tail) with thrust vectoring a potential option. All weapons are carried externally.

FIGHTER/ATTACK AIRCRAFT GROUP

SINGLE ENGINE GRAY - BASELINE SUMMARY

¤ GEOMETRY:

Sw=560 sq. ft.
AR=3.15
t/c=0.06
L=59'10"
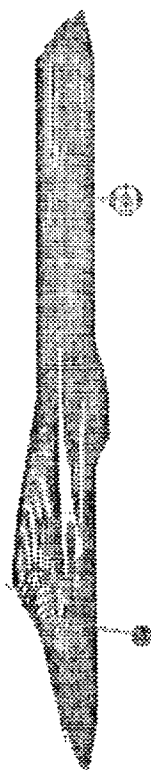
¤ FEATURES:

Internal Weapons Carriage
50 Deg. Wing Sweep
Small Canard
Fixed Inlets Underwing
P/Y Thrust Vectoring
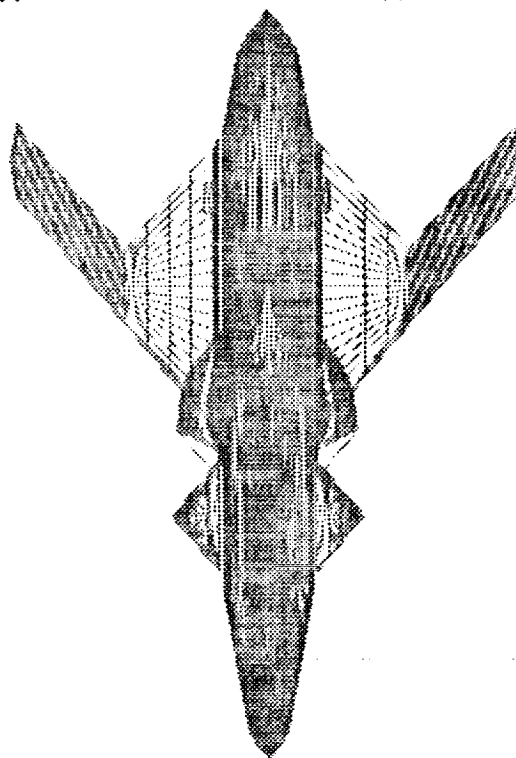
¤ WEIGHTS:

GTOW: 38120 (F110 29k#)
Empty: 21340

This is the configuration developed by the Dryden engineer who was on-site at LaRC to participate in the study. It assumes pitch and yaw thrust vectoring with internal carriage weapons.

FIGHTER/ATTACK AIRCRAFT GROUP

SINGLE ENGINE STEALTHY - BASELINE SUMMARY

¤ **GEOMETRY**

Sw=740 sq. ft.
AR=2.16
I/c=10-15-6 (Large Bay)
6-8-4 (Small Bay)
L=46'4"
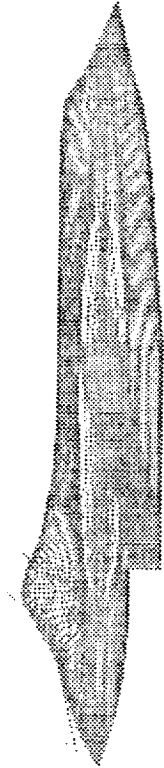
¤ **FEATURES:**

Internal Weapons Carriage
Blended 50° Wing-Body
"L.O. Vectoring Nozzle"
Several TE Devices

¤ **WEIGHTS:**

GTOW: 35600 (SB,M1.4)
36400 (LB,M=1.05)
39200 (SB, F110 @ 33k#)
Empty: 19500-21100
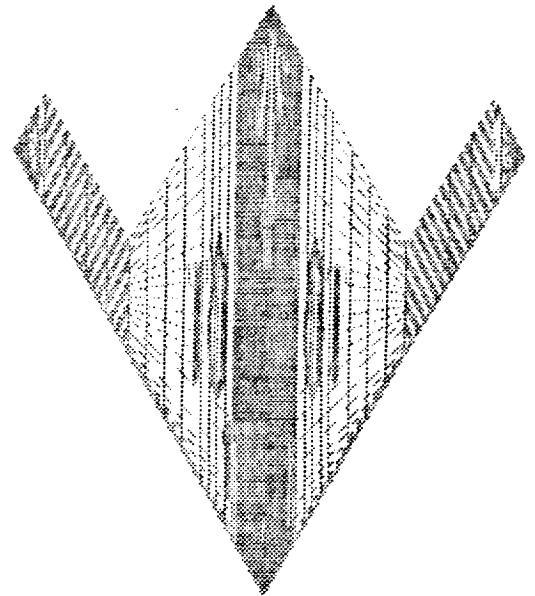
This is a "flying wing" concept designed to incorporate low observable features. All weapons are acrried internally and it has an aligned edge planform.

FIGHTER/ATTACK AIRCRAFT GROUP

CONFIGURATION STUDIES NEEDS

¤ **AERO PREDICTION METHODS FOR CONCEPTUAL DESIGN:**

- HIGH-α PREDICTION CURRENTLY NOT SUITABLE
- SEMI-EMPIRICAL METHOD NECESSARY
- PARAMETRIC TEST PROGRAM TO GENERATE DATA BASE
- INDUSTRY RECOGNIZES NEED, LOOKS TO NASA

¤ **WEIGHT PREDICTION:**

- STATISTICAL METHODS INSENSITIVE TO TECHNOLOGY
- UNIQUE CONFIGURATIONS FALL OUTSIDE DATA BASE
- SEMI-ANALYTICAL STRUCTURES/SYSTEMS METHODS NEEDED
- ISSUES BEING ADDRESSED AS PART OF CRITICAL DISCIPLINES
- INDUSTRY WILLING TO PARTICIPATE

One of the important "by-products" of this study is the identification of critical needs in terms of methodology necessary to support the application of NASA developed technology into future or existing vehicles. Two of the areas of current need include aerodynamics prediction for the non-linear region simple and fast enough to use during conceptual design and advanced, second level weight prediction. Note that in both cases, industry is looking to NASA to help develop this capability.

FIGHTER/ATTACK AIRCRAFT GROUP

CONCLUDING REMARKS

AGILITY DESIGN STUDY UNDERWAY

First phase nearly complete
Second phase in work
Third phase starting

IN-HOUSE CONFIGURATION STUDIES

Three basic configurations developed
Trade study data base generated
Needs for predictive methodology identified

FUTURE PLANS

Incorporate agility prediction into synthesis (1Q '93)
Re-evaluate in-house configurations (2Q '93)
Compile industry results (3Q '93)
Conduct operational effetiveness (Phase IV)

In conclusion, the NASA Agility Design Study is underway with current work in Phases II and III. Near term plans include completing the validation of the metric prediction algorithms and incorporation of them into the vehicle sizing system. The airframer design studies will be completed by 3Q '93. Far term plans are to conduct operational effectiveness studies.

DEVELOPMENT OF
HIGH-ANGLE-OF-ATTACK
NOSE-DOWN PITCH CONTROL MARGIN
DESIGN GUIDELINES FOR COMBAT AIRCRAFT

Marilyn E. Ogburn
John V. Foster

*Workshop on Guidance, Navigation, Controls, and
Dynamics for Atmospheric Flight*

NASA Langley Research Center
Hampton, VA

March 18, 1993

BBi-24 Ogburn

OUTLINE

- Background and objectives

- Approach

- Development of preliminary guidelines

- Experimental and flight results

- Summary and Plans

BBI-11 Ogburn

OUTLINE

A broad research program to identify maneuvering requirements for advanced fighters and the corresponding design criteria to aid in making critical design tradeoffs is being conducted under the NASA High-Angle-of-Attack Technology Program (HATP). As part of this activity, NASA and the U.S. Navy are conducting cooperative research to develop high-angle-of-attack control margin requirements. This paper will summarize the status of this program. Following some background information, the simulation study conducted to develop a set of preliminary guidelines for nose-down pitch control is reviewed and the results of some very limited flight tests are described.

CONTROL EFFECTIVENESS REQUIREMENTS FOR MULTI-AXIS RELAXED STABILITY COMBAT AIRCRAFT

Maneuvering Requirements

Performance Considerations

- Relaxed stability in pitch and yaw
- Reduced control surface size

Design Criteria Required

Advanced Control Effectors

- Forebody controls
- Ailerons as flaps
- Conventional horizontal tails
- Canards
- Trailing edge flaps
- Body flaps

Aerodynamic

Propulsive

BBD-6 Ogburn
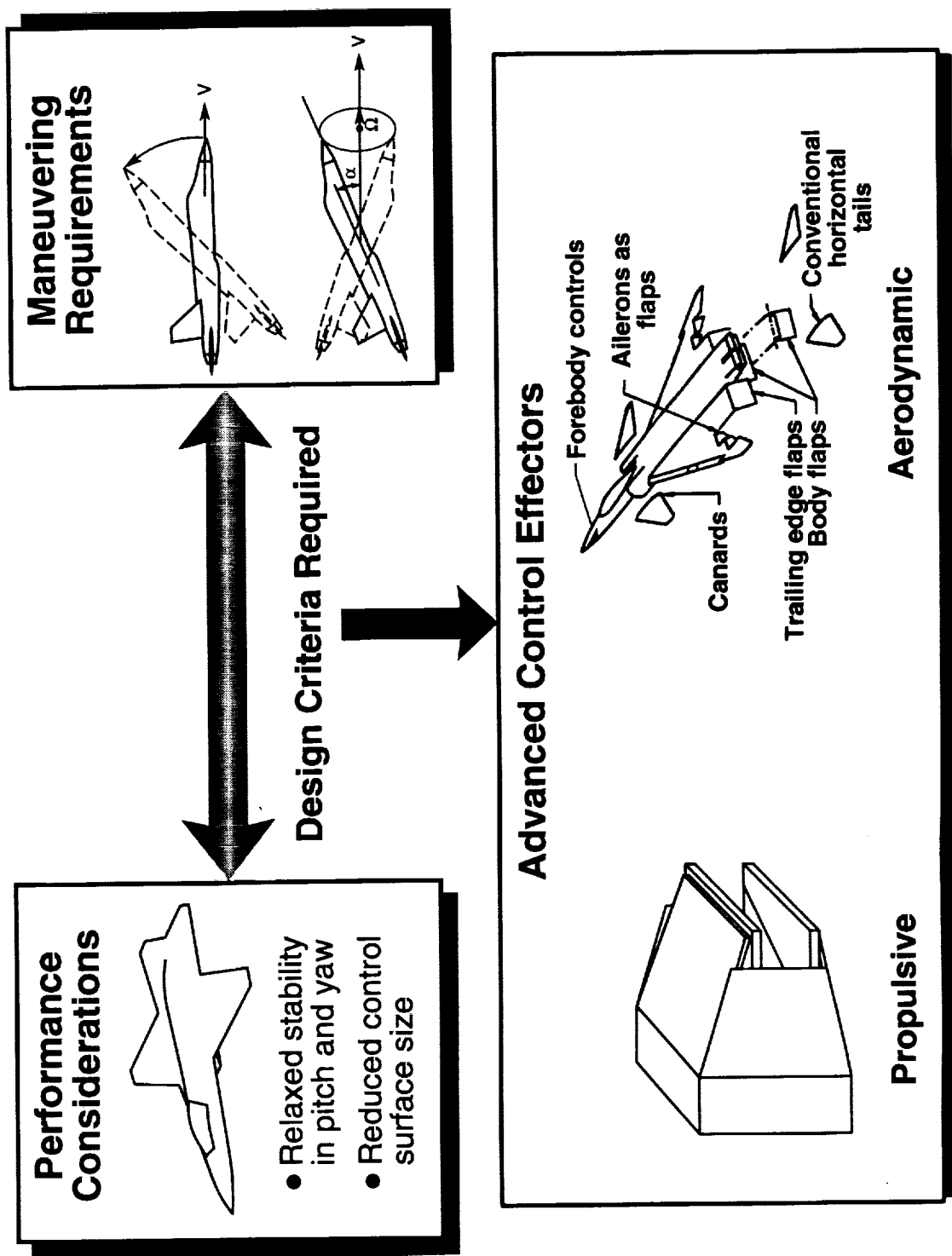
CONTROL EFFECTIVENESS REQUIREMENTS FOR
MULTI-AXIS RELAXED STABILITY COMBAT AIRCRAFT

A well-defined set of criteria exists and has been used for the design of combat aircraft for performance considerations. These criteria address the use of concepts such as relaxed stability in pitch and yaw and reduced control surface size to enhance performance characteristics. However, detailed, validated design criteria to define minimum maneuvering requirements, particularly for flight at low speeds and high angles of attack, do not currently exist. These criteria are needed to aid in making the critical design tradeoffs between performance and maneuvering requirements, which often result in conflicting design characteristics. The use of advanced propulsive and aerodynamic control effectors will aid in achieving the control moments to meet enhanced maneuvering requirements; however, these control concepts cannot be utilized most effectively for making design tradeoffs until design criteria for maneuvering are determined.

KEY DESIGN ISSUE

Nose up

Nose down

Full nose-down aerodynamic control

① "Unacceptable"

② "Desirable"

Pitching moment coefficient C_m

Angle of attack

0

298
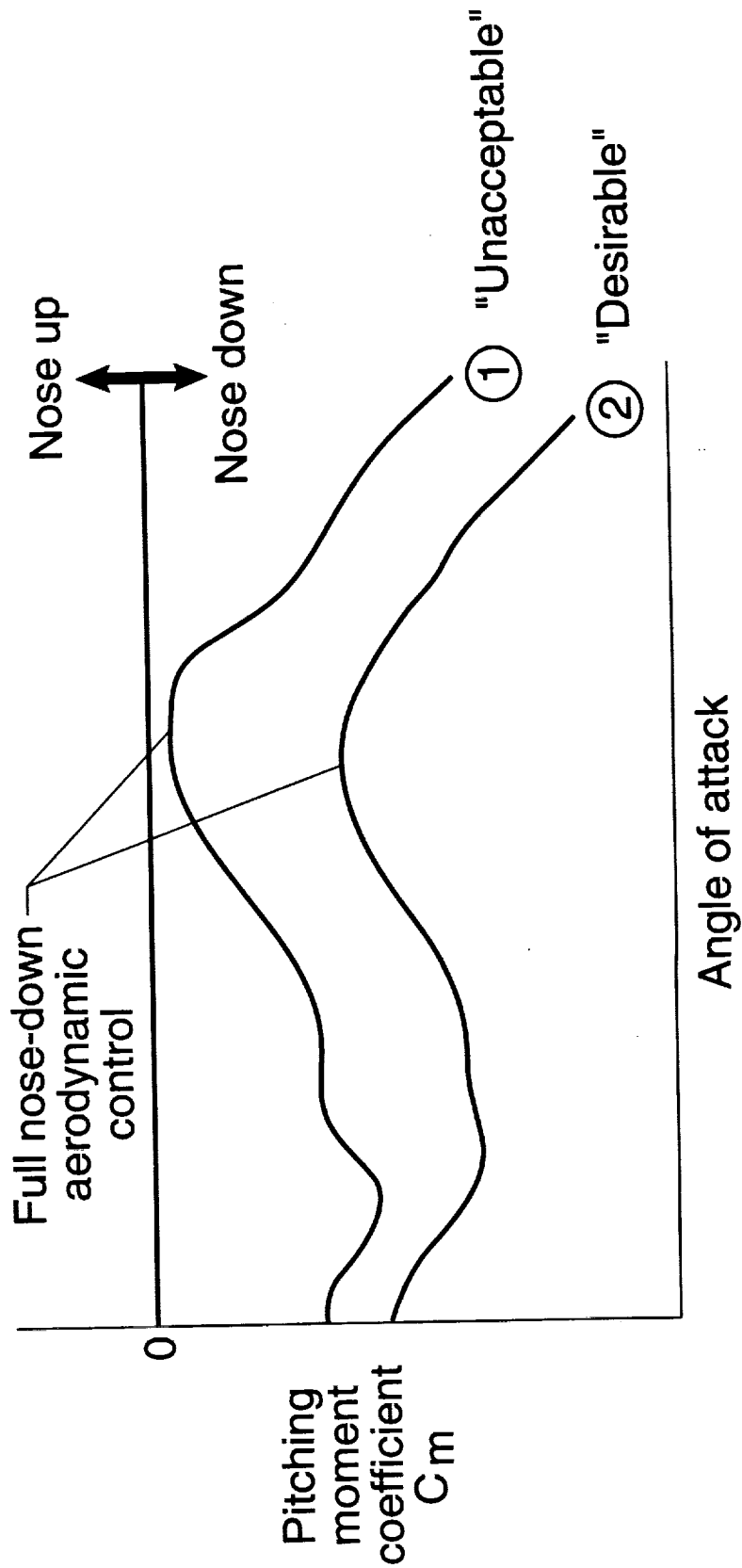
KEY DESIGN ISSUE

The first element in the development of control margin requirements is nose-down pitch control at high angles of attack. The key design issue is the level of nose-down pitching moment required for tactical maneuvering and for safety of flight. Guidelines are needed to help the designer determine that, for his particular airplane, the C_m characteristics illustrated by curve 1 are unacceptable whereas the curve 2 characteristics are desirable.

SCOPE OF ACTIVITY

Analysis and simulation → Preliminary guidelines → Flight testing → Flight validated design criteria/specifications

Preliminary guidelines → Near term applications

BBA-44 Ogburn
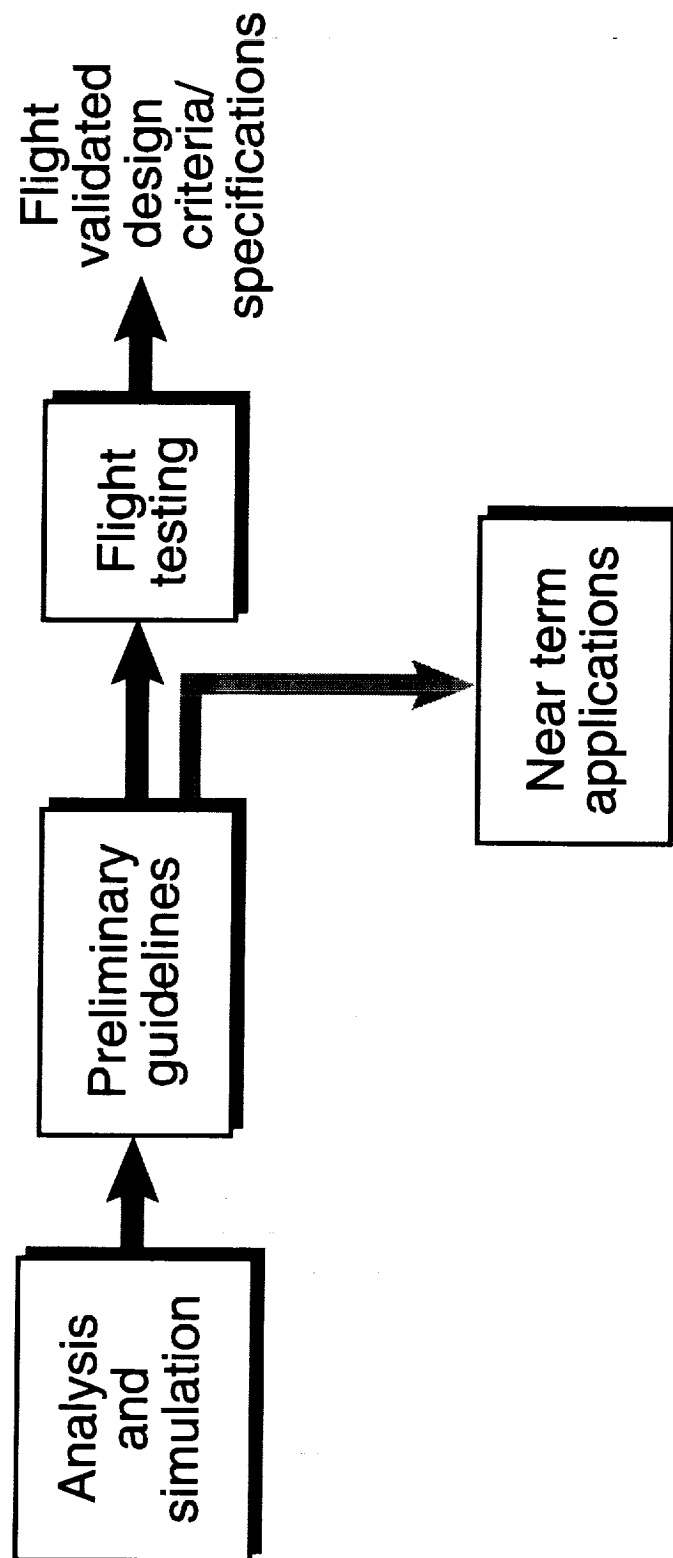
SCOPE OF ACTIVITY

A cooperative program was formed by NASA and the Navy to address this design issue and is often referred to by the acronym HANG (high-angle-of-attack nose-down guidelines). This chart shows the overall outline of the activity. The first step involved analysis and a simulation study which were used to develop a set of preliminary guidelines. Flight testing for validation of these guidelines has been initiated. The final output of this work will be a set of flight-validated design criteria and specifications for flight test demonstration.

301

APPROACH TO DEVELOPMENT OF PRELIMINARY GUIDELINES

- Examine existing data base for relaxed stability aircraft

- Conduct manned simulation on DMS

  - Systematic parametric variation of key nose-down C_m characteristics

  - Anchored to baseline F-18 model

  - Specific evaluation methodology

    ◆ Maneuvers

    ◆ Pitch recovery rating scale

    ◆ Figures of merit

BBE-31 Ogburn

302

APPROACH TO DEVELOPMENT OF PRELIMINARY GUIDELINES

The set of preliminary guidelines was developed in two steps. The first involved analysis of information from previous simulation and flight tests of relaxed static stability aircraft to correlate aircraft response in recoveries to available nose-down aerodynamic pitching moment. The next step comprised a more detailed systematic study on the Langley Differential Maneuvering Simulator.

PRELIMINARY GUIDELINE
BASED ON EXISTING AIRCRAFT

BBJ-19 Ogburn
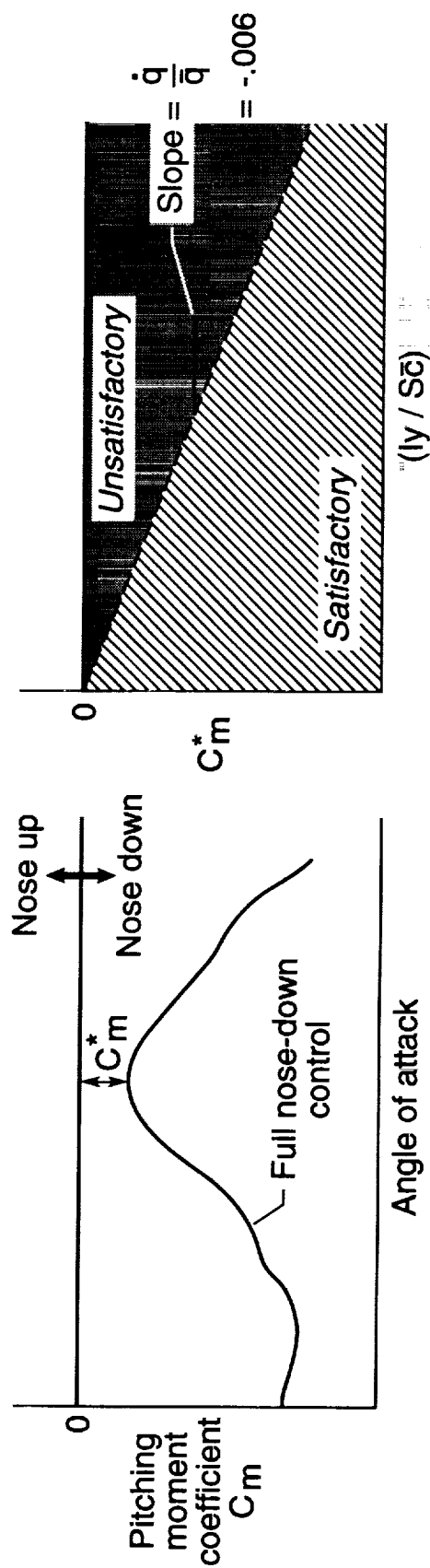
PRELIMINARY GUIDELINE BASED ON EXISTING AIRCRAFT

A key parameter for the definition of required nose-down pitching moment is the value of C_m at the minimum point (C_m^*), as illustrated in the figure. Determination of the smallest value of C_m^* that is acceptable from a pitch recovery point of view is important in making critical configuration design tradeoffs. Because C_m can be related to a first-order definition of pitch acceleration by using the aircraft inertia and geometry information, these characteristics were examined for some existing aircraft and correlated with the known high-α nose-down capabilities of these aircraft. The results were used to generate the plot shown which defines a preliminary guideline for C_m^* based only on the airplane mass and geometry characteristics. For a given configuration, the designer needs only to calculate the value of ($I_y/S\bar{c}$) and use the chart to determine the minimum levels of C_m^* required for "satisfactory" and "unsatisfactory" nose-down control characteristics. Although this result provides a useful, easy-to-apply guideline, particularly during very preliminary design studies, it was felt that a more comprehensive criterion that applies to more than just one point on the C_m curve is needed. As a result, a systematic, parametric study using piloted simulation was conducted as the first step in developing such a design guide.

306
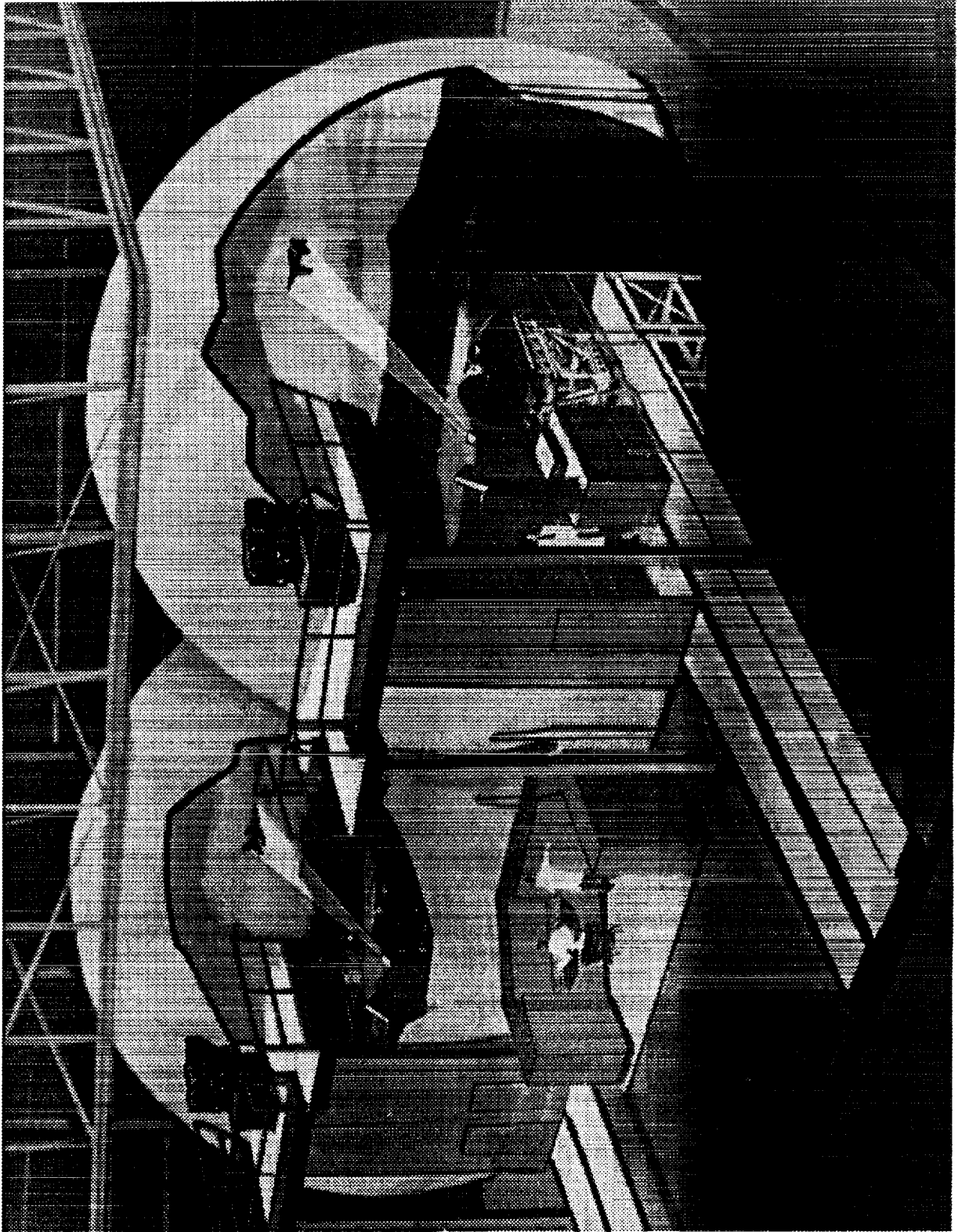
DIFFERENTIAL MANEUVERING SIMULATOR

The Langley Differential Maneuvering Simulator (DMS) was used for the simulation study. As illustrated in the drawing, the DMS is a domed facility with extensive state-of-the-art features that make it a very effective tool for air combat research and high-angle-of-attack flight dynamics studies. These features include a visual scene produced by a computer-generated imaging system, programmable displays and force-feel systems, and artificial "g" cues. A key aspect of the subject simulation study was the systematic variation of the key parameters which define the nose-down pitching moment capability. The parametric variations were anchored to an existing comprehensive F-18 math model, and a specific evaluation methodology was developed to determine the relative merits of the pitch response as the parametric variations were made.

PRELIMINARY DESIGN GUIDELINE

308

BBJ-18 Ogburn
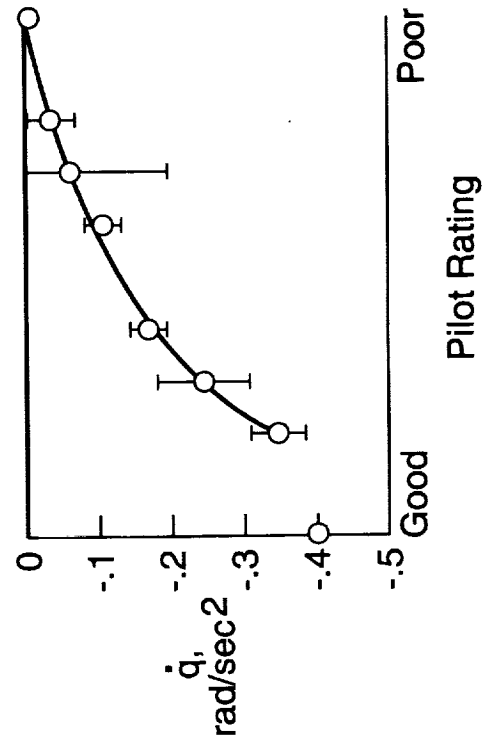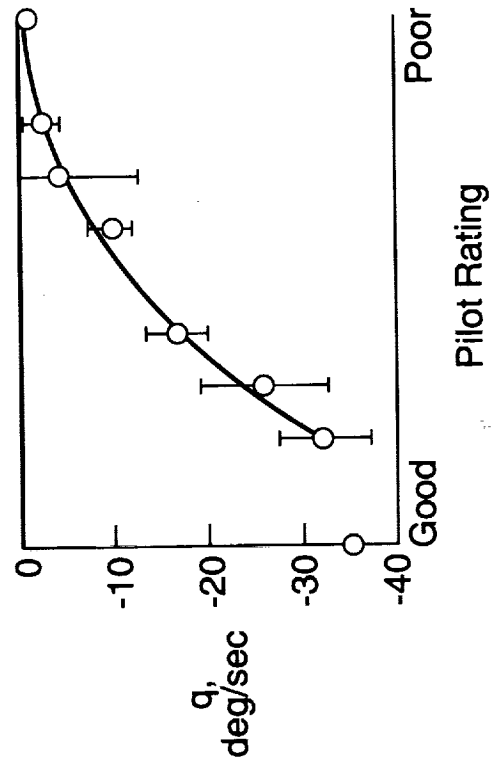
PRELIMINARY DESIGN GUIDELINE

The results of the simulation evaluation showed clearly that the pilots were evaluating the short-term pitch response. A simple pushover maneuver starting from 1g stabilized trim at high angles of attack to recover to low angles of attack was used as the primary evaluation maneuver. It was determined that two primary figures of merit were needed because the pilots said that they judged two response characteristics during the recovery: (1) the pitch acceleration almost immediately following the forward stick input and (2) the pitch rate buildup over the initial part of the recovery. The two figures of merit that best correlated the pilots' ratings and comments with the airplane response were the maximum pitch acceleration achieved within one second of the initiation of forward stick movement and the pitch rate at two seconds into the recovery. The pilot ratings covered a range of values that indicated good to poor response. Confidence levels are shown about the mean value for several pilot ratings. The pitch acceleration results generally agree well with the preliminary guideline discussed earlier that was based on previous flight and simulation experience and with the results from other related work. The current results have also been checked using piloted simulations of several relaxed static stability configurations besides the F-18, and full-scale flight validation has been initiated.

FLIGHT TESTS

- Objectives
  - Validate/refine research test methodology
  - Validate simulation results and refine design guidelines as necessary

- Approach: Conduct two phase flight program
  - Phase I: Limited study emphasizing *test methodology*
    - ◆ Navy F-18
    - ◆ NASA HARV
  - Phase II: Detailed study emphasizing *guideline validation*
    - ◆ NASA HARV with thrust vectoring controls

BBE-10 Nguyen

3 1 0

FLIGHT TESTS

The objectives of the flight tests are to validate and refine the test methodology used in the development of the guidelines and the numerical guideline values. A two-phase flight program is being conducted. Phase I, a very limited study to validate the test methodology using a Navy F-18 and the NASA HARV, has been completed. The second phase, which is in progress, is a much more detailed study to validate the guideline values, using the HARV with thrust vectoring controls to provide a wide range of nose-down pitch response.

NATC FLIGHT TEST RESULTS
Two Pilots - Preliminary
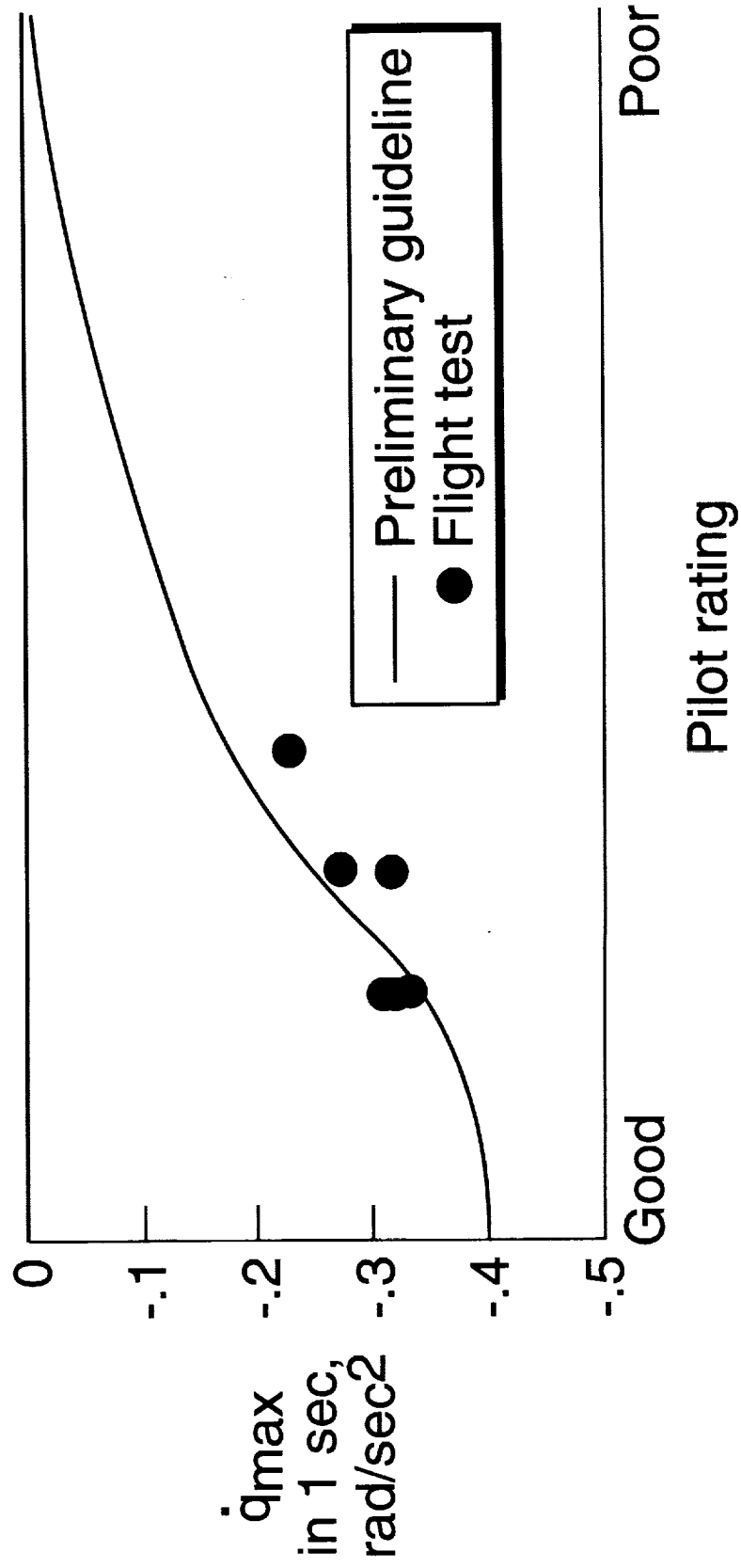
NATC FLIGHT TEST RESULTS

Flight tests of a Navy F-18 were conducted at the Patuxent River Naval Air Test Center. Two Navy pilots performed and rated 32 pushover maneuvers. The center of gravity was varied using a fuel-transfer c.g. control system. The flight program was very successful in achieving its primary objective which was the verification of the fundamental simulation methodology and validation of the key figures of merit ($\dot{q}$ and q). As a very limited, preliminary check of the guidelines developed in the simulation study, the results from flight for the maneuvers with the most linear pitch acceleration response (similar to the simulation responses) were compared with the simulation data shown earlier. The plot shows fairly good correlation for the $\dot{q}_{max}$ in 1 second metric. A comparison of the flight results with the preliminary guideline values for the initial pitch acceleration response shows good agreement between flight and simulation.

NATC FLIGHT TEST RESULTS
Two Pilots - Preliminary

Legend:
— Preliminary guideline
● Flight test

Y-axis: q at 2 sec, deg/sec (0, -10, -20, -30, -40)

X-axis: Pilot rating (Good ... Poor)

BBJ-17 Ogburn
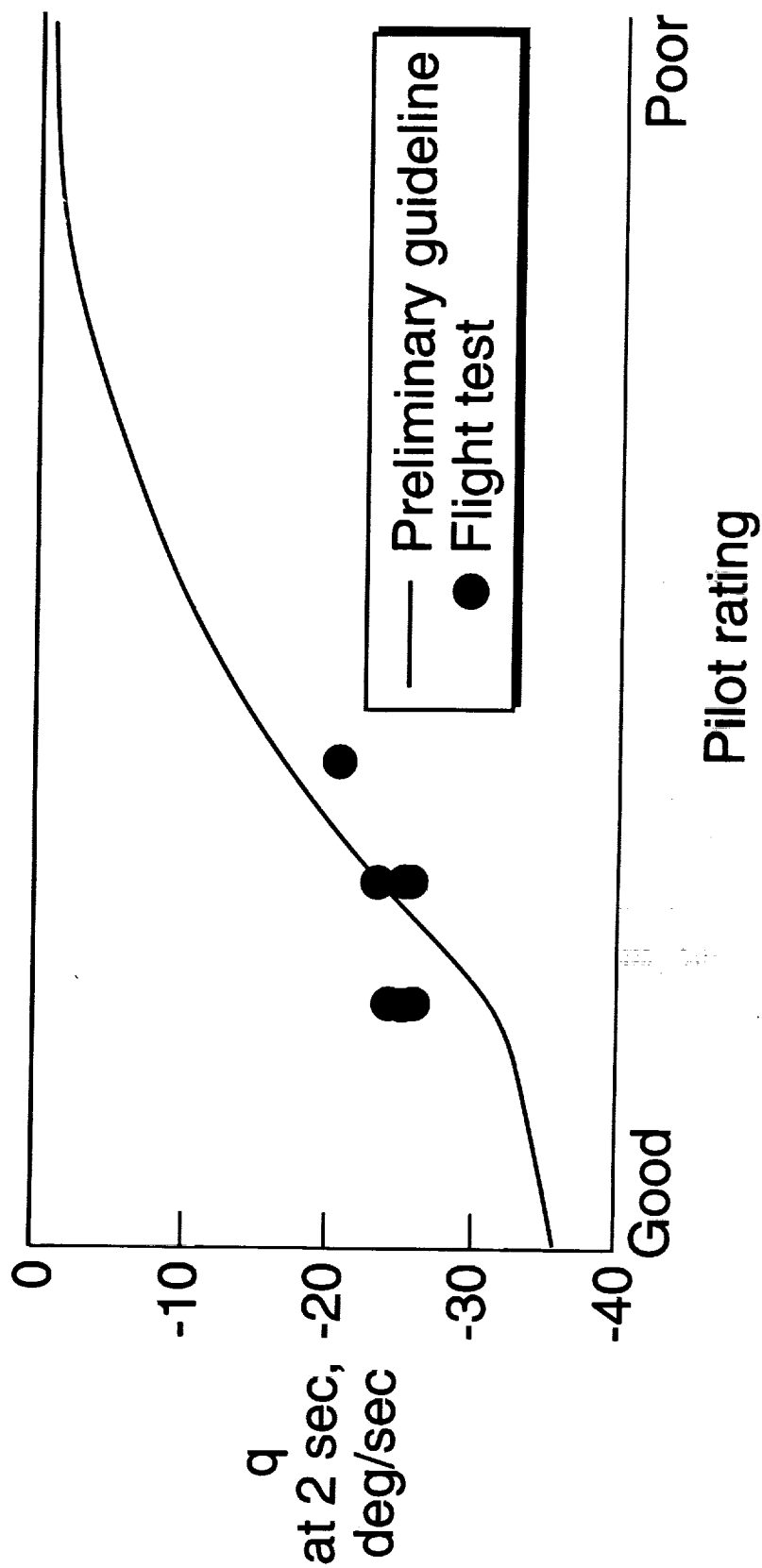
NATC FLIGHT TEST RESULTS

Similarly, the correlation for the pitch rate in 2 seconds metric was also fairly good. Again, it should be noted that this flight data base is very small so that no conclusions can be drawn based on this data alone. Definitive refinement and validation of the guidelines will be accomplished in the second phase of the flight test program which is currently in progress.

SUMMARY OF
FLIGHT TEST RESULTS TO DATE

- Flight tests validated simulation study methodology
  - Pushover maneuver
  - Rating scale

- Results verified that short-term response is primary figure of merit
  - $\dot{q}$ and q are appropriate figures of merit

- Good correlation obtained between simulation and flight for comparable maneuvers

BBJ-8 Ogburn

316

SUMMARY OF FLIGHT TEST RESULTS TO DATE

The limited amount of flight testing that was completed in the first phase of these tests satisfied the primary objective which was to validate the simulation study methodology by confirming the suitability of the pushover as the primary evaluation maneuver and the utility of the rating scale. These preliminary flight tests also provided much information that has been very valuable in the preparation for further tests. The results verified that the pilots' opinions of the recoveries are based on the short-term pitch response, and good agreement for the numerical response values was obtained between the individual pilots' simulation and flight results for maneuvers in which the character of the response was comparable.

NOSE-DOWN PITCH CONTROL DESIGN GUIDELINE

Out-of-control pitch recovery requirements

Recovery from rolling maneuver requirements

Pushover maneuver requirements

Largest value

max nose-down control

C_m

α

318
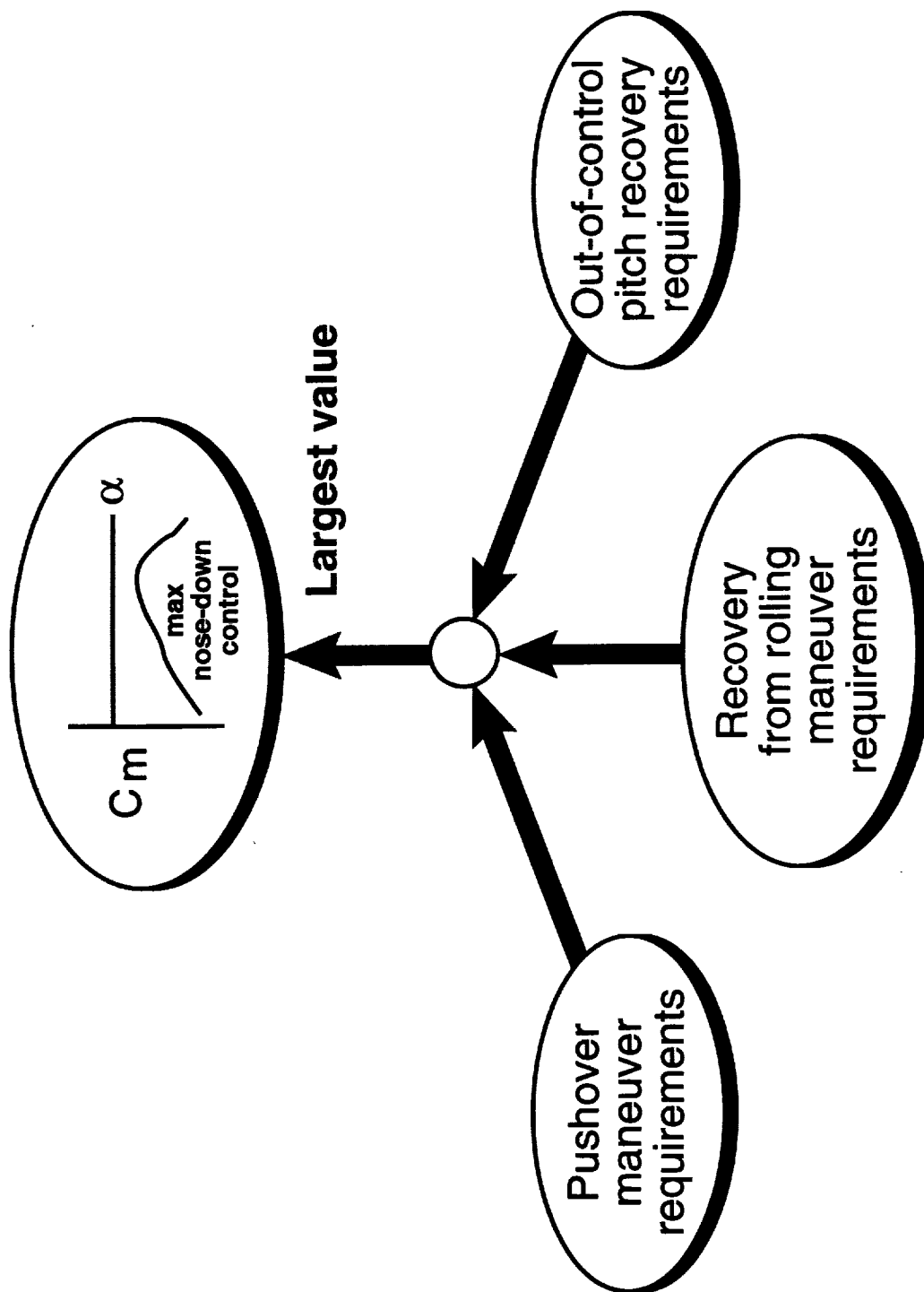
TOTAL C_m REQUIREMENT

A method for designing the C_m versus angle of attack curve was developed using the preliminary guideline values. The overall design process is accomplished in four steps, the first three of which require separate calculations of the C_m required at each angle of attack. The first step, which satisfies the requirements for the pushover maneuver, is described in a previous publication on this work. The second and third steps involve the calculation of C_m values based on the nose-down pitch control power needed to oppose the inertia coupling generated during commanded roll maneuvers and uncommanded roll/yaw motions. The final step is to select the largest value of Cm computed for any of the first three steps at each angle of attack.

SUMMARY AND PLANS

- Preliminary pitch control guidelines developed
  - Test and analysis methodology developed
  - Extensive simulation results obtained
  - Simulation study methodology validated by first phase of flight tests and additional simulation

- Follow-on activities in progress
  - Continue analysis of existing flight and simulation data
  - Complete systematic HARV experiments with thrust vectoring
    - Parametric variation of nose-down capability
    - Perform variety of maneuvers
    - Analyze flight/simulation results
  - Develop guidelines for roll/yaw axes

BBi-15 Ogburn

320

SUMMARY AND PLANS

In summary, the research activity described in this paper has resulted in the development of preliminary nose-down pitch control guidelines. The appropriate study methodologies were developed and validated by limited flight test programs and extensive simulation results have been obtained from which the guidelines were derived. There is still much work to be done to reach the final goal of a complete set of fully-validated design criteria and specifications for demonstrating in flight that the criteria have been met. The analysis of existing data will continue, but the main activity will be to complete experiments in progress using the HARV with thrust vectoring, primarily to validate the numerical guidelines. Using the HARV with thrust vectoring controls enables the evaluation of a wide range of nose-down response. The capability to vary the level of pitch vectoring that is obtained for forward stick inputs means that the character and the level of the pitch response during recoveries from high angles of attack can be specified. A systematic parametric variation of nose-down response is being made and a large number and variety of maneuvers including the pushover maneuver are being performed, rated, and analyzed. In addition, a complementary effort is underway to develop similar design guidelines for the roll/yaw axes.

322
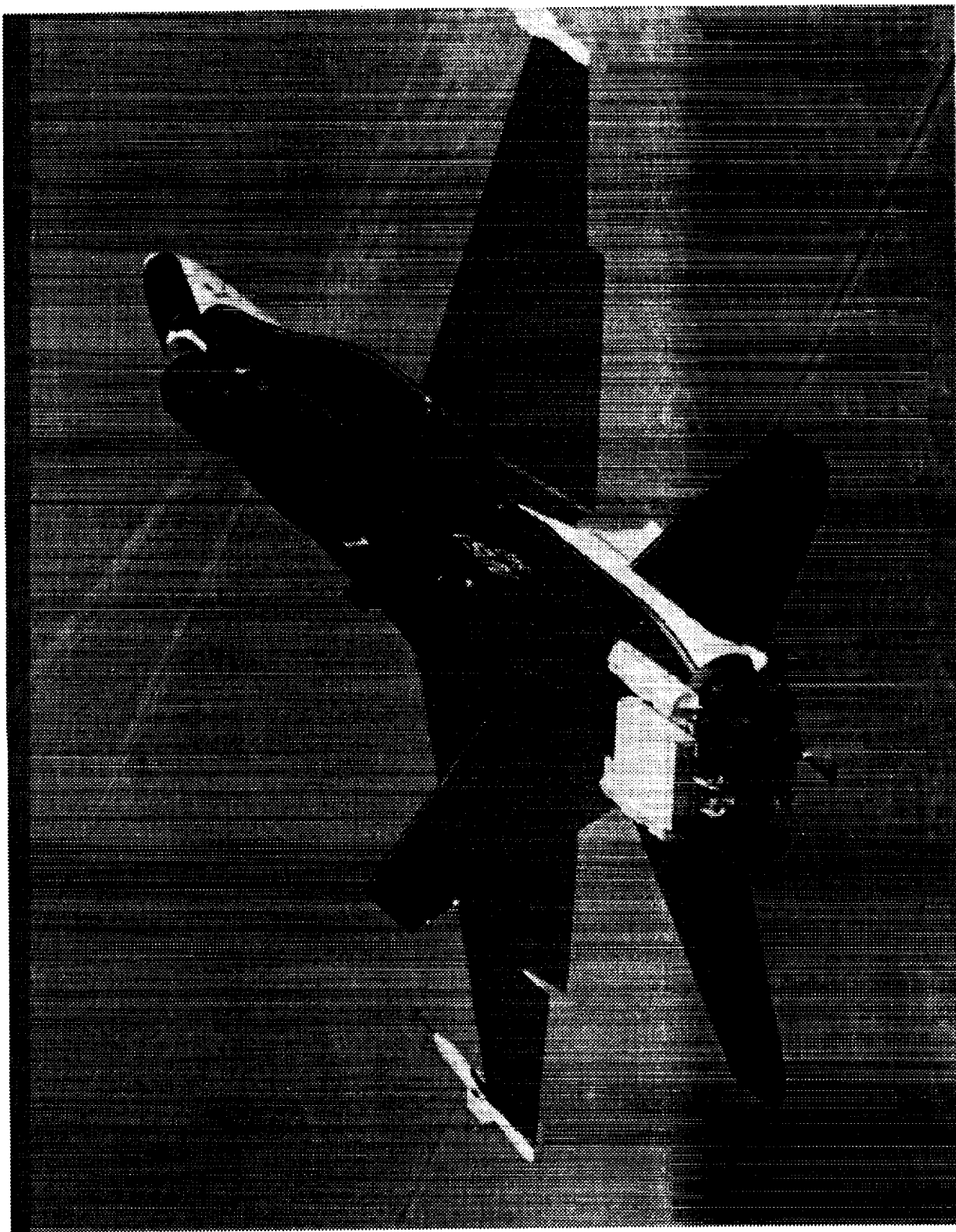
Robust, Nonlinear, High Angle-of-Attack Control Design for a Supermaneuverable Vehicle

1LT Richard J. Adams
WL/FIGC
Wright-Patterson AFB, OH

NASA LaRC GNC Workshop
18 March 1993

Introduction

Key Technical Challenges:

High Angle-of-Attack Flight
Flying Qualities
Robustness
Multiple/Redundant Control Effectors

Solutions:

Dynamic Inversion
Structured Singular Value Synthesis
Control Selector/Command Limiting/Daisy Chaining

324

Supermaneuverable Vehicle

Variable geometry inlet

F404 - Generation II engine

2D-CD TV/TR Gimballed nozzle

Equations of Motion

rotational dynamics of the aircraft in the body axis

$$\dot{q} = 1/I_y \left[m_{aero} + m_{thrust} + pr (I_z - I_x) + I_{xz}(r^2 - p^2) \right]$$

$$\begin{bmatrix} \dot{p} \\ \dot{r} \end{bmatrix} = \begin{bmatrix} I_x & -I_{xz} \\ -I_{xz} & I_z \end{bmatrix}^{-1} \begin{bmatrix} l_{aero} + l_{thrust} + pqI_{xz} + qr (I_y - I_z) \\ n_{aero} + n_{thrust} - qrI_{xz} + pq (I_x - I_y) \end{bmatrix}$$

aircraft motion with respect to its velocity vector

$$\dot{\alpha} = q - (p \cos\alpha + r \sin\alpha) \tan\beta - (\cos\mu/\cos\beta)\dot{\gamma} - \sin\mu(\cos\gamma/\cos\beta)\dot{\chi}$$

$$\dot{\beta} = p \sin\alpha - r \cos\alpha - \sin\mu \, \dot{\gamma} + \cos\mu \, \cos\gamma\dot{\chi}$$

$$\dot{\mu} = (\cos\alpha/\cos\beta)p + (\sin\alpha/\cos\beta)r + \tan\beta\cos\mu \, \gamma + [\sin\gamma + \tan\beta \, \sin\mu \, \cos\gamma] \, \dot{\chi}$$

Control Law Structure
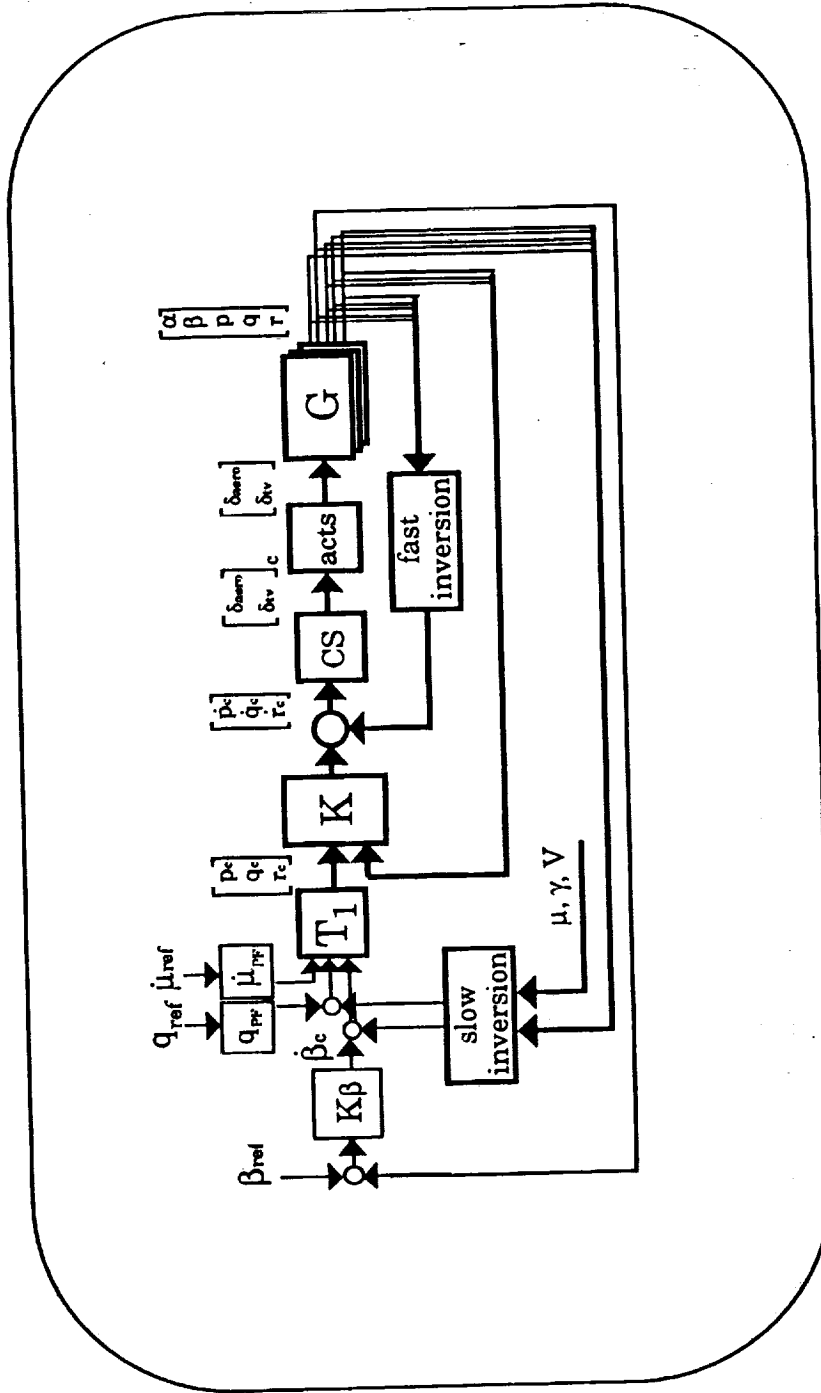
Fast Inversion

the rotational dynamics are broken into a linear parameter varying part and a nonlinear part

$$\begin{bmatrix} \dot{p} \\ \dot{q} \\ \dot{r} \end{bmatrix} = \begin{bmatrix} 0 & L_\beta & L_p & 0 & L_r \\ M_\alpha & 0 & 0 & M_q & 0 \\ 0 & N_\beta & N_p & 0 & N_r \end{bmatrix} \begin{bmatrix} \alpha \\ \beta \\ p \\ q \\ r \end{bmatrix} + \begin{bmatrix} I_x & 0 & -I_{xz} \\ 0 & I_y & 0 \\ -I_{xz} & 0 & I_z \end{bmatrix}^{-1} \begin{bmatrix} pq\,I_{xz} + qr(I_y - I_z) \\ pr(I_z - I_x) + I_{xz}(r^2 - p^2) \\ -qr\,I_{xz} + pq(I_x - I_y) \end{bmatrix}$$

$$+ \begin{bmatrix} 0 & L_{\delta DT} & L_{\delta A} & L_{\delta R} \\ M_{\delta E} & 0 & 0 & 0 \\ 0 & N_{\delta DT} & N_{\delta A} & N_{\delta R} \end{bmatrix} \begin{bmatrix} \delta_E \\ \delta_{DT} \\ \delta_A \\ \delta_R \end{bmatrix} + \begin{bmatrix} 0 & L_{\delta RTV} & L_{\delta YTV} \\ M_{\delta PTV} & 0 & 0 \\ 0 & N_{\delta RTV} & N_{\delta YTV} \end{bmatrix} \begin{bmatrix} \delta_{PTV} \\ \delta_{RTV} \\ \delta_{YTV} \end{bmatrix}$$

by assuming that a control selector is in place the control contribution can be rewritten

$$\begin{bmatrix} \dot{p} \\ \dot{q} \\ \dot{r} \end{bmatrix} = \cdots + \begin{bmatrix} 1 & 0 & 0 \\ 0 & 1 & 0 \\ 0 & 0 & 1 \end{bmatrix} \begin{bmatrix} \dot{p}_c \\ \dot{q}_c \\ \dot{r}_c \end{bmatrix}$$

Fast Inversion (cont)

cancel linear parameter varying dynamics   cancel nonlinear inertial coupling

$$\begin{bmatrix} \dot{p}_c \\ \dot{q}_c \\ \dot{r}_c \end{bmatrix} = \begin{bmatrix} \dot{p}_{des} \\ \dot{q}_{des} \\ \dot{r}_{des} \end{bmatrix} - \begin{bmatrix} 0 & L_\beta & L_p & 0 & L_r \\ M_\alpha & 0 & 0 & M_q & 0 \\ 0 & N_\beta & N_p & 0 & N_r \end{bmatrix} \begin{bmatrix} \alpha \\ \beta \\ p \\ q \\ r \end{bmatrix} - \begin{bmatrix} I_x & 0 & -I_{xz} \\ 0 & I_y & 0 \\ -I_{xz} & 0 & I_z \end{bmatrix}^{-1} \begin{bmatrix} pq\,I_{xz} + qr(I_y - I_z) \\ pr(I_z - I_x) + I_{xz}(r^2 - p^2) \\ -qr\,I_{xz} + pq(I_x - I_y) \end{bmatrix}$$

add desired dynamics

$$\begin{bmatrix} \dot{p}_{des} \\ \dot{q}_{des} \\ \dot{r}_{des} \end{bmatrix} = \begin{bmatrix} 0 & L'_\beta & L'_p & 0 & L'_r \\ M'_\alpha & 0 & 0 & M'_q & 0 \\ 0 & N'_\beta & N'_p & 0 & N'_r \end{bmatrix} \begin{bmatrix} \alpha \\ \beta \\ p \\ q \\ r \end{bmatrix} + \begin{bmatrix} 1 & 0 & 0 \\ 0 & 1 & 0 \\ 0 & 0 & 1 \end{bmatrix} \begin{bmatrix} \dot{p}_c \\ \dot{q}_c \\ \dot{r}_c \end{bmatrix}$$

μ-Synthesis

robust performance/tracking
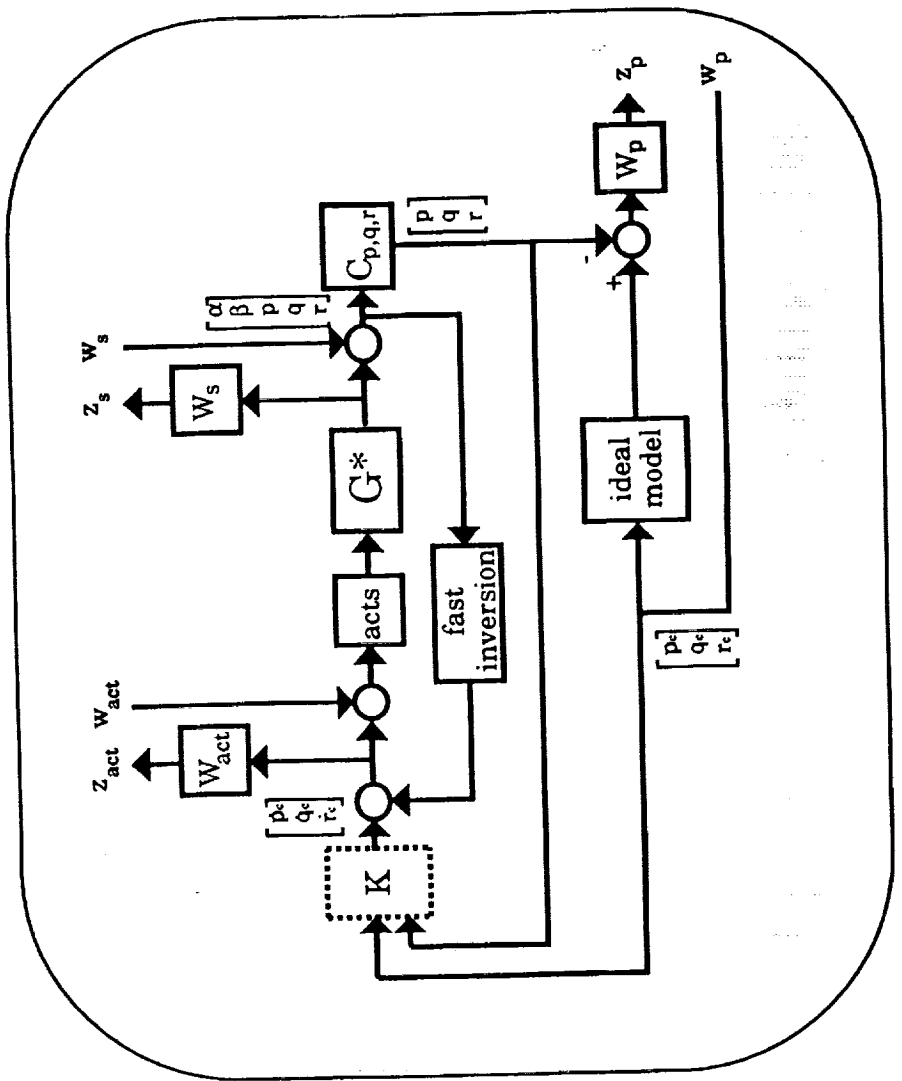
ideal model

$$\begin{bmatrix} \dfrac{p}{p_c} \\[2mm] \dfrac{q}{q_c} \\[2mm] \dfrac{r}{r_c} \end{bmatrix} = \begin{bmatrix} \dfrac{3}{s+3} & 0 & 0 \\[2mm] 0 & \dfrac{3}{s+3} & 0 \\[2mm] 0 & 0 & \dfrac{3}{s+3} \end{bmatrix}$$

Slow Inversion

create new stability axis inputs

$$\begin{bmatrix} p_c \\ q_c \\ r_c \end{bmatrix} = \begin{bmatrix} \cos\alpha & 0 & \sin\alpha \\ 0 & 1 & 0 \\ \sin\alpha & 0 & -\cos\alpha \end{bmatrix} \begin{bmatrix} \dot{\mu}_c \\ \dot{\alpha}_c \\ \dot{\beta}_c \end{bmatrix}$$

rewrite α and β equations with new inputs

$$\dot{\alpha} = q - (p\cos\alpha + r\sin\alpha)\tan\beta - (\cos\mu/\cos\beta)\dot{\gamma} - \sin\mu(\cos\gamma/\cos\beta)\dot{\chi} + \dot{\alpha}_c$$

$$\dot{\beta} = p\sin\alpha - r\cos\alpha - \sin\mu\,\dot{\gamma} + \cos\mu\,\cos\gamma\,\dot{\chi} + \dot{\beta}_c$$

cancel gravitational terms and add sideslip compensation

$$\dot{\alpha}_c = q_c' - \cos\mu\,\cos\gamma/\cos\beta\;(g/V)$$

$$\dot{\beta}_c = K_\beta(\beta_{ref} - \beta) - \sin\mu\,\cos\gamma\;(g/V)$$

Control Selector

control effectors

generalized controls

$$\delta_{aero} = \begin{bmatrix} \delta_E \\ \delta_{DT} \\ \delta_A \\ \delta_R \end{bmatrix} \qquad \delta_{tvec} = \begin{bmatrix} \delta_{PTV} \\ \delta_{RTV} \\ \delta_{YTV} \end{bmatrix} \qquad \delta^* = \begin{bmatrix} \dot{p}_c \\ \dot{q}_c \\ \dot{r}_c \end{bmatrix}$$

$$B_{aero} = \begin{bmatrix} 0 & L_{\delta DT} & L_{\delta A} & L_{\delta R} \\ M_{\delta E} & 0 & 0 & 0 \\ 0 & N_{\delta DT} & N_{\delta A} & N_{\delta R} \end{bmatrix} \qquad B_{tvec} = \begin{bmatrix} 0 & L_{\delta RTV} & L_{\delta YTV} \\ M_{\delta PTV} & 0 & 0 \\ 0 & N_{\delta RTV} & N_{\delta YTV} \end{bmatrix} \qquad B^* = \begin{bmatrix} 1 & 0 & 0 \\ 0 & 1 & 0 \\ 0 & 0 & 1 \end{bmatrix}$$

$$B_{aero}\delta_{aero} = B^*\delta^* \qquad \delta_{aero} = T_{aero}\delta^* \qquad T_{aero} = N_{aero}(B_{aero}N_{aero})^{\#}$$

$$B_{tvec}\delta_{tvec} = B^*\delta^* \qquad \delta_{tvec} = T_{tvec}\delta^* \qquad T_{tvec} = N_{tvec}(B_{tvec}N_{tvec})^{\#}$$
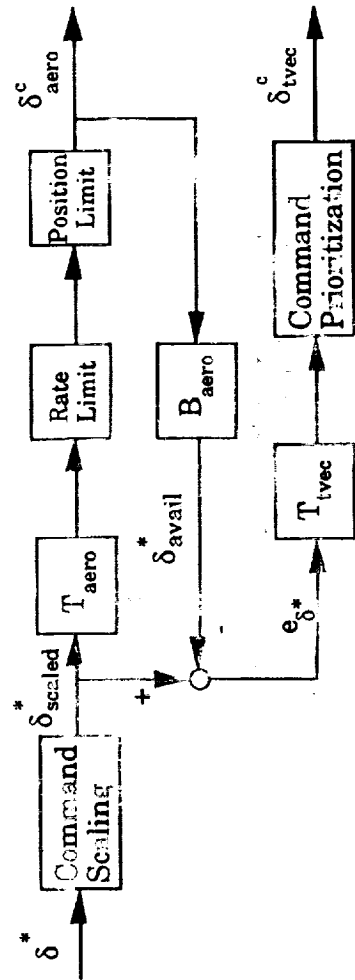
Command Scaling
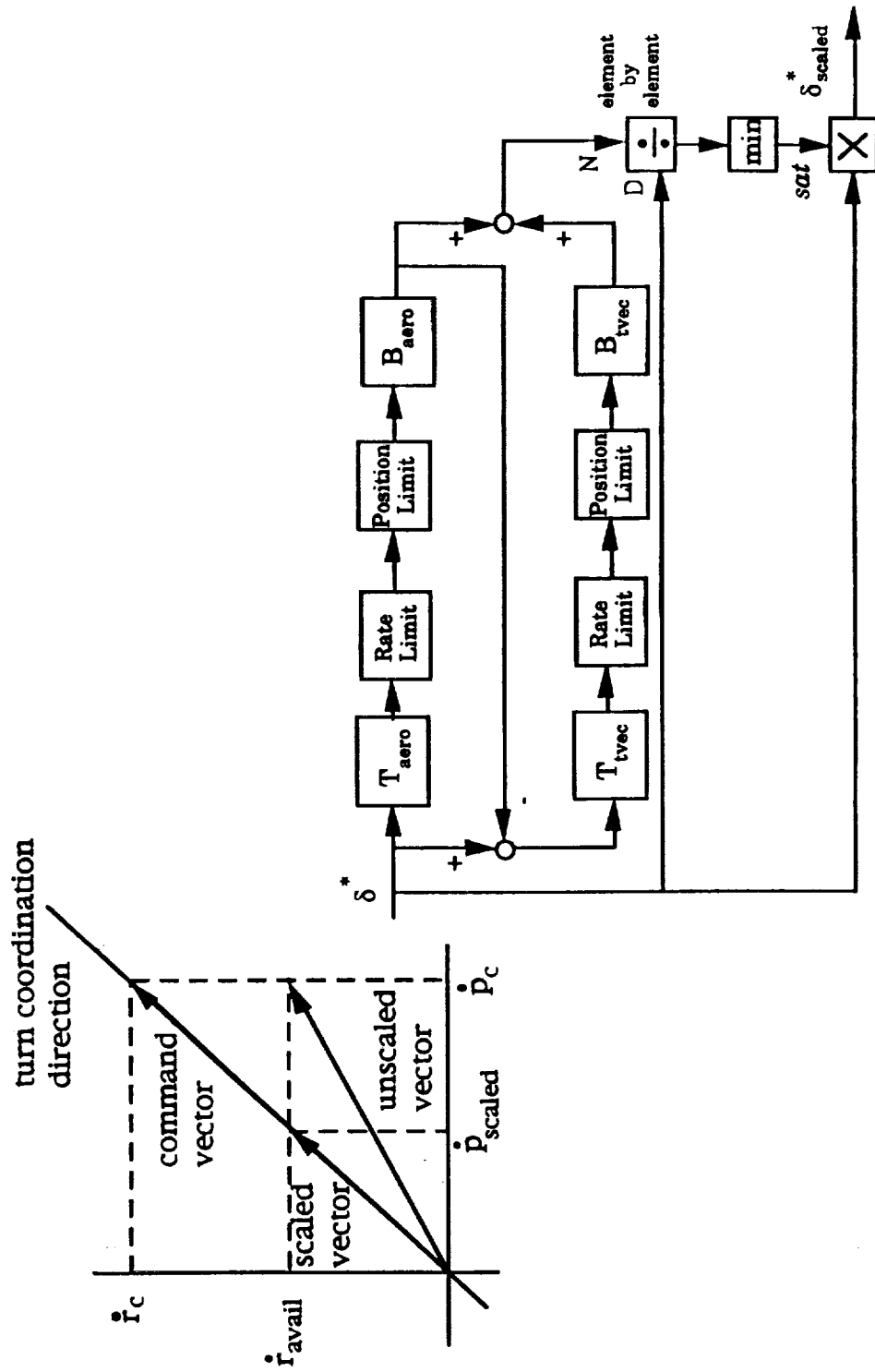
Structured Singular Value Analysis

μ

dashed-longitudinal
solid-lat/directional

freq (rad/sec)

$\Delta\delta_E$
$\Delta\delta_{DT}$
$\Delta\delta_A$
$\Delta\delta_R$

$\Delta\beta$
$\Delta\alpha$

$\Delta p, \Delta q, \Delta r$

$\Delta Y_\beta = 0.15 Y_\beta$
$\Delta L_\beta = 0.10 L_\beta$
$\Delta L_p = 0.30 L_p$
$\Delta L_r = 0.30 L_r$
$\Delta M_q = 2.00 M_q$
$\Delta N_\beta = 0.30 N_\beta$
$\Delta N_p = 0.50 N_p$
$\Delta N_r = 0.15 N_r$

$\Delta Z_{\delta E} = 0.22 Z_{\delta E}$
$\Delta Y_{\delta R} = 0.15 Y_{\delta R}$
$\Delta L_{\delta DT} = 0.15 L_{\delta DT}$
$\Delta L_{\delta DF} = 0.10 L_{\delta DF}$
$\Delta L_{\delta R} = 0.40 L_{\delta R}$
$\Delta N_{\delta DT} = 0.15 N_{\delta DT}$
$\Delta N_{\delta DF} = 0.20 N_{\delta DF}$
$\Delta N_{\delta R} = 0.15 N_{\delta R}$
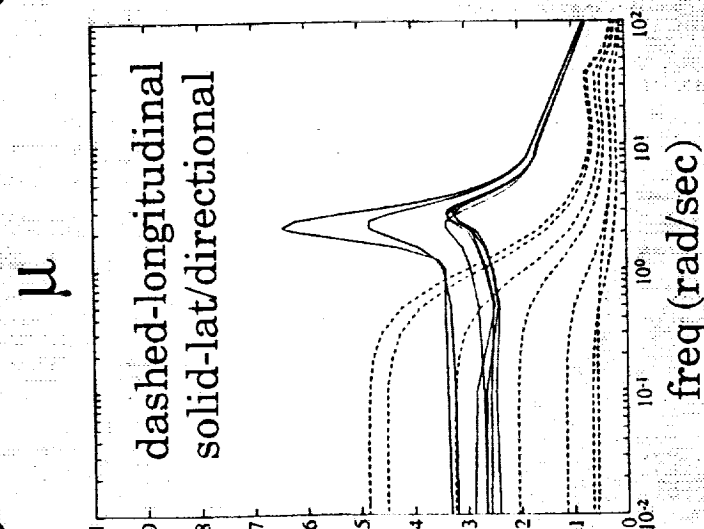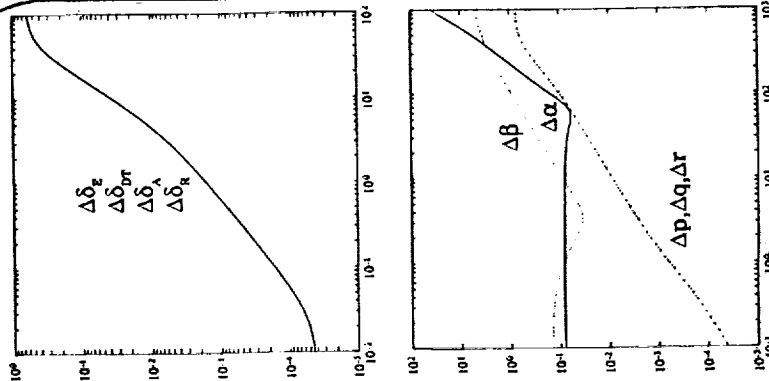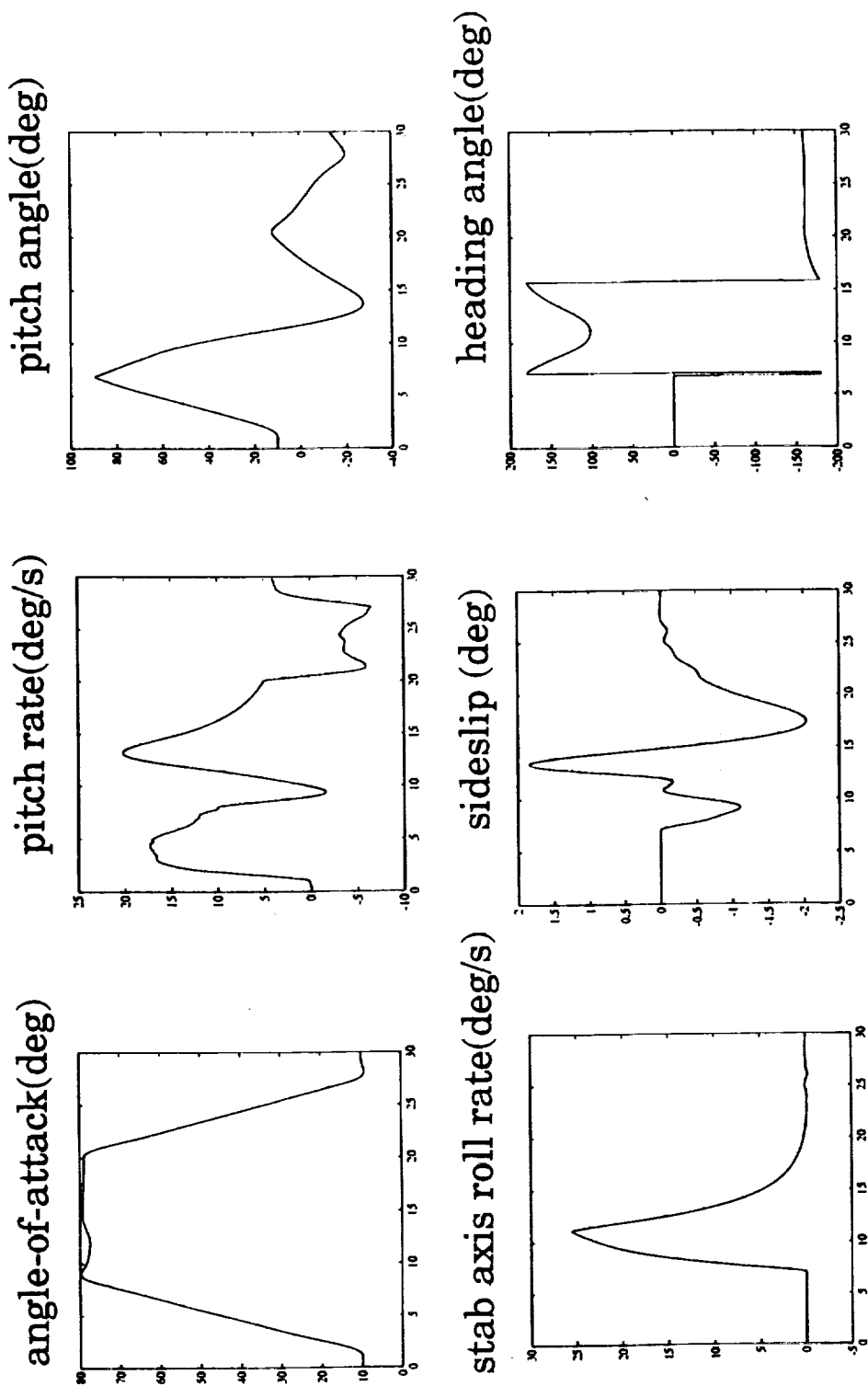
Herbst-like Maneuver

angle-of-attack(deg)

pitch rate(deg/s)

pitch angle(deg)

stab axis roll rate(deg/s)

sideslip (deg)

heading angle(deg)

Herbst-like Maneuver (cont)

altitude (feet)

horiz tail (deg)

aileron (deg)

rudder (deg)

pitch thrust vect(deg)

yaw thrust vect(deg)
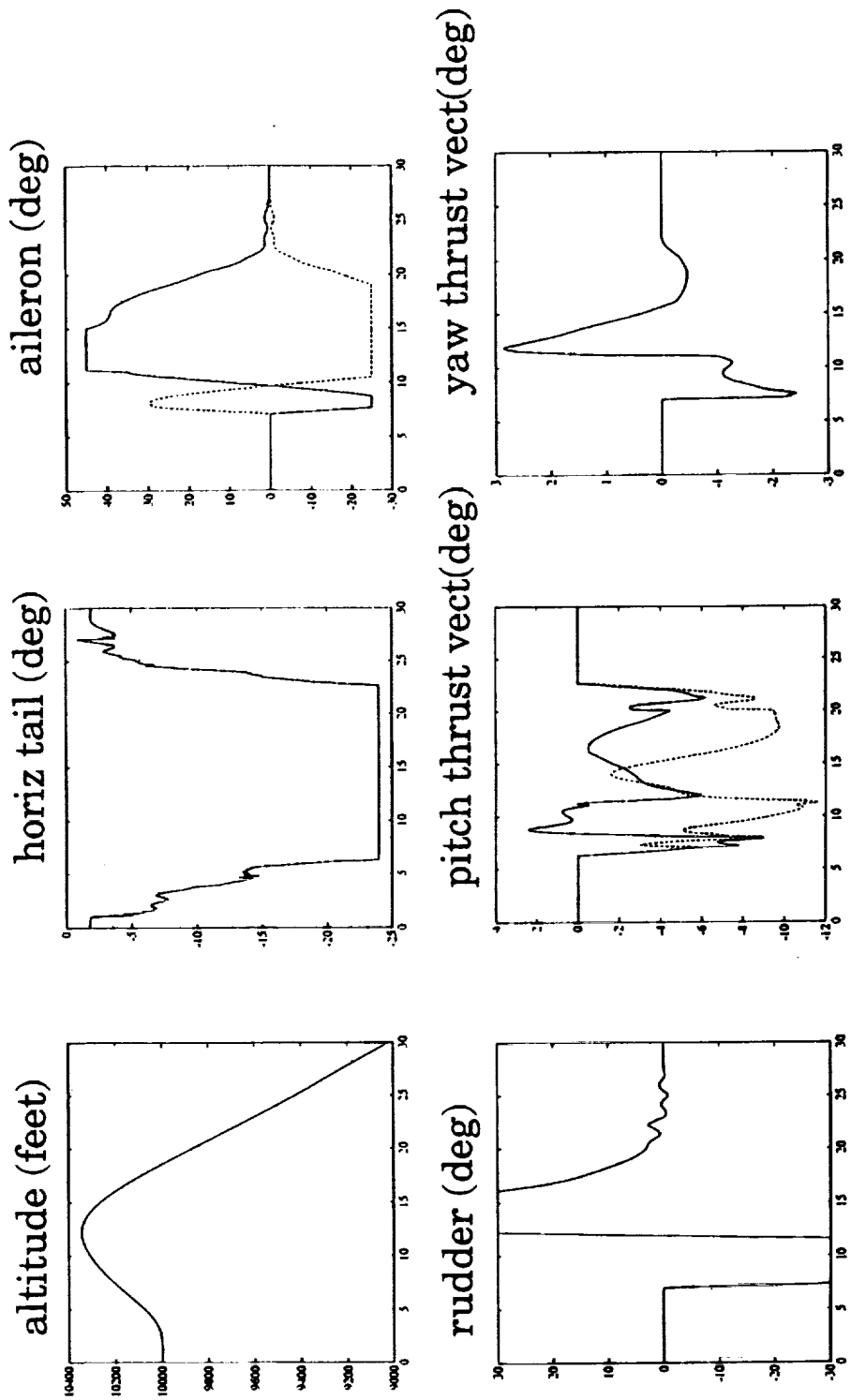
ROBUST, NONLINEAR, HIGH ANGLE-OF-ATTACK CONTROL DESIGN FOR A SUPERMANEUVERABLE VEHICLE

Richard J. Adams[†], James M. Buffington[*], and Siva S. Banda[‡]

WL/FIGC Bldg 146
2210 Eighth St. Ste 21
Wright-Patterson AFB, OH 45433-7531
Tel: (513) 255-8678, Facsimile: (513) 476-4000
adams@falcon.flight.wpafb.af.mil

ABSTRACT

High angle-of-attack flight control laws are developed for a supermaneuverable fighter aircraft. The methods of dynamic inversion and structured singular value synthesis are combined into an approach which addresses both the nonlinearity and robustness problems of flight at extreme operating conditions. The primary purpose of the dynamic inversion control elements is to linearize the vehicle response across the flight envelope. Structured singular value synthesis is used to design a dynamic controller which provides robust tracking to pilot commands. The resulting control system achieves desired flying qualities and guarantees a large margin of robustness to uncertainties for high angle-of-attack flight conditions. The results of linear simulation and structured singular value stability analysis are presented to demonstrate satisfaction of the design criteria. High fidelity nonlinear simulation results show that the combined dynamic inversion/structured singular value synthesis control law achieves a high level of performance in a realistic environment.

† Stability and Control Engineer
* Aerospace Engineer
‡ Aerospace Engineer

INTRODUCTION

Supermaneuverablity is defined as the ability to maneuver an aircraft up to and beyond the stall angle-of-attack. Some tactical payoffs of high angle-of-attack maneuvering include superior survivability, confusion of adversary pilots, and the ability to increase first-shot opportunities[1]. Additional control power in the form of forebody vortex flow control and thrust vectoring can allow fighter aircraft to operate in the post-stall flight regime. Therefore, advanced control law design techniques must be found for robust high angle-of-attack stability augmentation and maneuvering. The resulting controllers must provide for the integration of both conventional and unconventional control effectors.

Modern robust multivariable design methods provide an efficient means of developing linear controllers for aircraft. Since the flight control problem is inherently multivariable, and the linear aircraft model has associated uncertainties, robust multivariable methods are a good choice for flight control design when nonlinearities are not too severe. In a Flight Dynamics Directorate contracted effort[2,3], a robust H_∞ controller within an inner/outer loop framework was designed for a supermaneuverable aircraft at a single flight condition, and robust performance was demonstrated for a Herbst-like maneuver. A robust controller for this same vehicle was designed by Sparks[4] for a single flight condition using μ-synthesis in a model-following framework to simultaneously incorporate flying qualities specifications and account for structured uncertainty. A recent Wright Laboratory technical report[5] describes the design of a μ-synthesis controller for a supermaneuverable vehicle that is integrated into an inner/outer loop control structure to provide full-envelope robust stability and performance for angles-of-attack up to 25 degrees.

Traditionally, flight control law development for low to moderate angle-of-attack flight regimes has been accomplished using linear design methods on linearized models of the aircraft. However, the advantages of supermaneuverability dictate that future air combat will venture into high angle-of-attack, nonlinear flight regions. Purely linear controllers are not able to effectively control supermaneuverable aircraft for more than very limited flight envelopes. This limitation has motivated a number of researchers to explore nonlinear techniques such as dynamic inversion. Bugajski and Enns[6] have used nonlinear dynamic

inversion to control the HARV aircraft across a wide, high angle-of-attack flight envelope. Huang[7] has used a dynamic inversion approach to develop high angle-of-attack control laws for the X-29.

High angle-of-attack maneuvering is still a relatively new area in flight controls. Venturing into the regions of post-stall flight can and should elicit serious questions about safety issues such as control effector saturation and departure susceptibility. Different methods have been successfully demonstrated that assist in preventing the destabilizing effects of control saturations. In an approach used by Bugajski and Enns[6], loop bandwidths are reduced so that a scaled projection of the desired control vector is achieved and the control surfaces lie on the boundary of an achievable subspace. A method of allocating control effectors such that the maximum possible moment is generated within a constrained set of achievable values has been suggested by Durham[8]. Another approach introduces thrust vectoring controls when saturations occur in aerodynamic surfaces[5].

The main contribution of the work presented in this paper is the integration of some the most promising approaches described above into a detailed design approach for achieving robust high angle-of-attack flight control designs. The most notable advancement is the integration of dynamic inversion and structured singular value synthesis. Linearization of the vehicle dynamics is accomplished through a nonlinear dynamic inversion scheme. A robust compensator is designed around the linearized plant using μ-synthesis in a model-following framework. The μ-synthesis design satisfies flying qualities requirements and robustness goals throughout the design envelope. A control allocation scheme is used which uses the pseudo-inverse of the control distribution matrix to allocate controls based on body axis rotational acceleration commands. A method known as daisy-chaining is used to generate thrust vectoring commands when aerodynamic control effector saturation occurs. Adverse control power saturation effects are minimized by scaling lateral commands based on an achievable control vector. Control effector prioritization is implemented through a daisy-chain technique that limits lateral control power demands that compete with longitudinal power requirements.

In the following sections, a description of a modified F-18 aircraft model is given followed by the definition of design requirements. A brief theoretical background is presented on nonlinear dynamic inversion and μ-synthesis. The

controller architecture and design is described followed by the control allocation scheme and departure resistance logic. Finally, linear robustness analysis results and the results of a high fidelity nonlinear simulation of a supermaneuver are presented.

AIRCRAFT MODEL

The aircraft model described in this paper is based upon a modified version of the F-18 aircraft. The vehicle is a twin engine fighter aircraft with a moderately swept wing, twin canted vertical tails, and a large leading edge root extension. The aircraft model is augmented with two dimensional thrust vectoring nozzles that provide pitch and yaw moments when deflected symmetrically and a roll moment when deflected asymmetrically. The aerodynamic control inputs to the aircraft dynamics are the elevators, the ailerons, the rudders, and the leading and trailing edge flaps. The aerodynamic surfaces are useful at normal flight conditions, where there is adequate aerodynamic control surface effectiveness. The thrust vectoring inputs are useful at high angle-of-attack, low dynamic pressure operating conditions, where the traditional aerodynamic control effectiveness is inadequate. The pilot inputs include a control stick and rudder pedals.

A nonlinear simulation model of this aircraft exists as modular FORTRAN code. The model consists of separate modules describing the atmosphere, nonlinear equations of motion, aerodynamics, engines, thrust vectoring nozzles, variable geometry inlets, sensors, and actuators which include rate and position limits. The high-fidelity model was developed as part of a previous effort which gives more detail than that presented here[9]. There are five pairs of aerodynamic surfaces: three pairs for active control and two pairs scheduled for optimum performance. The ailerons, rudders, and elevators are used for stability augmentation and flight path manipulation. The leading and trailing edge flaps are scheduled to maximize airframe performance across the flight envelope. The aerodynamic data are contained in tabular format and linear interpolation is used for traditional force and moment aerodynamic coefficient build-up. Thrust vectoring-induced aerodynamic effects are added to static and dynamic baseline aerodynamic coefficients to obtain total aerodynamic coefficients.

The dynamics of this vehicle can be described by the following set of first order nonlinear differential equations [6,10]. The first three equations describe the rotational dynamics of the aircraft in the body axis.

$$\dot{q} = \frac{1}{I_y} [m_{aero} + m_{thrust} + pr(I_z - I_x) + I_{xz}(r^2 - p^2)] \tag{1}$$

$$\begin{bmatrix} \dot{p} \\ \dot{r} \end{bmatrix} = \begin{bmatrix} I_x & -I_{xz} \\ -I_{xz} & I_z \end{bmatrix}^{-1} \begin{bmatrix} l_{aero} + l_{thrust} + pqI_{xz} + qr(I_y - I_z) \\ n_{aero} + n_{thrust} - qrI_{xz} + pq(I_x - I_y) \end{bmatrix} \tag{2}$$

q, p, and r are the body axis pitch, roll, and yaw rates respectively. I_x, I_y, I_z, and I_{xz} are the moments of inertia. The m, l, and n terms are the aerodynamic and thrust moment contributions to the rotational equations of motion.

The next three equations describe the evolution of aircraft motion with respect to its velocity vector.

$$\dot{\alpha} = q - (p \cos\alpha + r \sin\alpha) \tan\beta - \frac{\cos\mu}{\cos\beta} \dot{\gamma} - \sin\mu \frac{\cos\gamma}{\cos\beta} \dot{\chi} \tag{3}$$

$$\dot{\beta} = p \sin\alpha - r \cos\alpha - \sin\mu \dot{\gamma} + \cos\mu \cos\gamma \dot{\chi} \tag{4}$$

$$\dot{\mu} = \frac{\cos\alpha}{\cos\beta} p + \frac{\sin\alpha}{\cos\beta} r + \tan\beta \cos\mu \dot{\gamma} + [\sin\gamma + \tan\beta \sin\mu \cos\gamma] \dot{\chi} \tag{5}$$

α, β, and μ are the angle-of-attack, sideslip angle, and roll angle about the velocity vector.

The last three equations describe the orientation of the velocity vector with respect to inertial space.

$$\dot{\gamma} = \frac{\cos\mu}{mV} L - \frac{\cos\beta \sin\mu}{mV} Y - \frac{\cos\gamma}{V} g + \frac{1}{mV} F_{thrust\,\gamma} \tag{6}$$

$$\dot{\chi} = \frac{1}{mV \cos\gamma} [\sin\mu L + \cos\beta \cos\mu Y] + \frac{1}{mV} F_{thrust\,\chi} \tag{7}$$

$$\dot{V} = -\frac{D}{m} - g \sin\gamma + \sin\beta Y + \frac{1}{m} F_{thrust\,V} \tag{8}$$

γ is the flight path angle, χ is the ground track angle, and V is the velocity. The F_{thrust} terms are the linear contributions of vehicle thrust to the aircraft equations of motion , resolved into the respective vectors. L, D, and Y are lift, drag, and side force, respectively. The parameter m is vehicle mass, and g is gravitational acceleration.

DESIGN REQUIREMENTS

Flying qualities are the primary measures of performance for a manual flight control system. For conventional flight, specifications for flying qualities can be found in MIL-STD-1797A[11]. While these requirements are not valid for high angle-of-attack flight, enough guidance is given to provide a basis for extrapolation. A rigorous study of new flying qualities measures is beyond the scope of this paper. The following high-α requirements are defined here only as baselines for this design study.

Requirements for the short period mode include constraints on the frequency and damping of a low order fit of the transfer function between pilot inputs and aircraft pitch response. Appropriate forms for this low order transfer function and methods for deriving the low order fit are described in MIL-STD-1797A. Short period frequency, ω_{sp} , should be a function of equivalent airspeed, V_{eq}. An appropriate guideline for short period frequency is:

$$\omega_{sp} \text{ (rad/s)} \approx 1.0 \times \frac{V_{eq} \text{ (ft/s)}}{100} \tag{9}$$

Therefore, the desired pitch response speed to pilot commands should increase with equivalent airspeed. At flight conditions above 30 degrees angle-of-attack, short period damping should be at the high end of the military standard's level 1 and 2 requirements. For these conditions, the acceptable range for ζ_{sp} is between 0.7 and 2.0 .

The primary roll subsidence mode flying quality parameter is roll mode time constant, T_R. The roll mode time constant is found from a first order fit of the transfer function between pilot input and roll rate response. Past experience with fighter aircraft has shown that desired values for T_R are a function of angle-of-

attack. MIL-STD-1797A level 2 requirements are used as a baseline range of acceptable roll mode time constants. The target values used in this study are: T_R = 0.30 at α = 0 deg, T_R = 0.75 at α = 30 deg, and T_R = 1.40 at α = 60 deg.

The desired directional response to pilot inputs can be derived from requirements on the Dutch roll mode. Dutch roll frequency, ω_D, and damping, ζ_D, can be derived from a second order fit of the transfer function between pilot input and sideslip response. Because of the danger of departure susceptibility at high angles-of-attack, the Dutch roll damping is required to be greater than 0.8. The Dutch roll frequency requirement is taken directly form MIL-STD-1797A, $\omega_D \geq 1.0$ rad/s.

DYNAMIC INVERSION

The purpose of dynamic inversion is to develop a feedback control law that linearizes the plant response to commands. In general the nonlinear aircraft dynamics can take the form

$$\dot{x} = f(x,u), \qquad y = Cx \tag{10}$$

where x is an n-dimensional state vector, u is an m-dimensional input vector, C is a $p \times n$ matrix, and y is a p-dimensional vector of output variables. A transformation is necessary to put the equations in a form from which the inverse dynamics can be constructed. Each controlled output, y_i, is differentiated until an input term from u appears[12]. Only m outputs can be controlled independently by the m available inputs, therefore p must equal m. As shown by Lane and Stengel[13], the output equations may now be written in the form,

$$y^{[d]} = \begin{bmatrix} y_1^{[d_1]} \\ y_2^{[d_2]} \\ \vdots \\ y_p^{[d_p]} \end{bmatrix} = h(x) + G(x)u \tag{11}$$

where $y_i^{[d_i]}$ represents the d_ith derivative of the output y_i. The inverse dynamics control law can be written as

$$u = G(x)^{-1}(v - h(x)) \tag{12}$$

h(x) represents the nonlinear output dynamics and G(x) represents the nonlinear control distribution. The parameter v represents the desired linear dynamics of the closed loop system. With the inverse dynamics control law implemented, the closed loop system now has the form,

$$y^{[d]} = v \tag{13}$$

If the system is observable and $\sum_{i=1}^{p} d_i = n$, then all of the closed loop poles may be placed. If $\sum_{i=1}^{p} d_i < n$, then closed loop stability cannot be proven. In this case the unobserved dynamics or the *internal dynamics* of dynamic inversion must be checked at local operating points to insure stability[13].

STRUCTURED SINGULAR VALUE SYNTHESIS

The structured singular value (μ) framework provides a unifying measure which can be used to simultaneously address stability and performance robustness specifications[14,15]. If μ is less than unity for a properly scaled system, then the specifications are met. It is desirable to be able to address these multiple objectives directly within a design method. μ-synthesis provides for the direct incorporation of robust stability and performance goals into a design by combining H_∞ design with structured singular value analysis[16,17]. The μ-synthesis problem is described by the attempt to find a controller that minimizes an upper bound on the structured singular value,

$$\min_{K} \inf_{D \in D} \sup_{\omega} \bar{\sigma}(DM(K)D^{-1}). \tag{14}$$

M(K) is the weighted closed loop transfer function shown in Fig. 1.

One approach to this problem is the DK-iteration; it calls for alternately minimizing sup $\bar{\sigma}(DM(K)D^{-1})$ for either K or D while holding the other constant. First the controller synthesis problem is solved using H_∞ design on the nominal design model, G_w. μ-analysis is then performed on the closed loop transfer function M(K), producing values of the D scaling matrices at each frequency. The resulting

frequency response data are fit with an invertible, stable, minimum phase transfer function which becomes part of the nominal synthesis structure. With D fixed, the controller synthesis problem is again solved by performing an H_∞ design on the augmented system. The DK-iterations are continued until a satisfactory controller is found or a minimum is reached. Fig. 2 shows a flow diagram for the DK-iteration. The resulting controller order is the order of the design plant and weighting matrices, in addition to the order of the D-scale transfer function fits. With each iteration, the D-scale frequency response data from the previous iteration is combined with the current values, and then the transfer function fit is performed on the combined data. This approach avoids a built-in increase in controller order that would result if at each iteration new D-scale fit transfer functions were augmented into the synthesis model from the previous step. It is important to note that the DK-iteration is not guaranteed to converge to a global minimum, but practical experience has shown that the method works well for a broad class of problems[17].

CONTROL LAW DEVELOPMENT

Dynamic inversion and structured singular value synthesis are combined to achieve robust manual control for high angle-of-attack flight. The controller structure is shown in Fig. 3. Pilot pitch stick inputs command a pitch rate, q_{ref}, roll stick inputs command a stability axis roll rate, $\dot\mu_{ref}$, and pedal inputs command a sideslip, β_{ref}. The following sections describe each element of the control design.

Fast Inversion

The aerodynamic and thrust induced moments in eqs. (1) and (2) determine the classical linear stability and control characteristics of the aircraft. These terms may be expanded into derivative form.

$$m_{aero} = [\, C_{m\alpha} V \alpha + \frac{\bar c}{2} C_{mq} q + C_{m\delta_E} \delta_E \,] \frac{1}{2}\rho V S \bar c \tag{15}$$

$$l_{aero} = [\, C_{l\beta} V \beta + \frac{\bar b}{2} C_{lp} p + \frac{\bar b}{2} C_{lr} r + C_{l\delta_{DT}} \delta_{DT}$$
$$+ C_{l\delta_A} \delta_A + C_{l\delta_R} \delta_R \,] \frac{1}{2}\rho V S \bar b \tag{16}$$

$$n_{aero} = [\, C_{n\beta} \, V \, \beta + \frac{\bar{b}}{2} C_{np} \, p + \frac{\bar{b}}{2} C_{nr} \, r + C_{n\delta_{DT}} \, \delta_{DT}$$
$$+ C_{n\delta_A} \, \delta_A + C_{n\delta_R} \, \delta_R \,] \frac{1}{2} \rho V S \bar{b} \quad (17)$$

$$m_{thrust} = [\, C_{m\delta_{PTV}} \, \delta_{PTV}] \quad (18)$$

$$l_{thrust} = [\, C_{l\delta_{RTV}} \, \delta_{RTV} + C_{l\delta_{YTV}} \, \delta_{YTV} \,] \quad (19)$$

$$n_{thrust} = [\, C_{n\delta_{RTV}} \, \delta_{RTV} + C_{n\delta_{YTV}} \, \delta_{YTV} \,] \quad (20)$$

where S is the wing area, $\bar{c}$ is the mean aerodynamic chord, and $\bar{b}$ is the wing span. δ_E is the symmetric elevator position, δ_{DT} is the asymmetric elevator position, δ_A is the aileron position, δ_R is the rudder position, δ_{PTV} is the symmetric pitch thrust vectoring nozzle position, δ_{RTV} is the asymmetric pitch (roll) thrust vectoring nozzle position, and δ_{YTV} is the yaw thrust vectoring nozzle position. The derivatives in eqs. (15-20) can be represented in dimensional form where:

$$M_q = \frac{\rho V S \bar{c}^2}{4 I_y} \, C_{m_q} \,, \qquad M_{\alpha,\delta} = \frac{\rho V^2 S \bar{c}}{2 I_y} \, C_{m\alpha,\delta} \quad (21)$$

$$L^*_{p,r} = \frac{\rho V S \bar{b}^2}{4 I_x} \, C_{l_{p,r}} \,, \qquad L^*_{\beta,\delta} = \frac{\rho V^2 S \bar{b}}{2 I_x} \, C_{l\beta,\delta} \quad (22)$$

$$N^*_{p,r} = \frac{\rho V S \bar{b}^2}{4 I_z} \, C_{n_{p,r}} \,, \qquad N^*_{\beta,\delta} = \frac{\rho V^2 S \bar{b}}{2 I_z} \, C_{n\beta,\delta} \quad (23)$$

$$L_{\beta,p,r,\delta} = (L^*_{\beta,p,r,\delta} + \frac{I_{xz}}{I_x} N^*_{\beta,p,r,\delta}) \frac{I_z I_x}{(I_z I_x - I_{xz}^2)} \quad (24)$$

$$N_{\beta,p,r,\delta} = (N^*_{\beta,p,r,\delta} + \frac{I_{xz}}{I_z} L^*_{\beta,p,r,\delta}) \frac{I_z I_x}{(I_z I_x - I_{xz}^2)} \quad (25)$$

$$Z_{\alpha,\delta} = \frac{\rho V^2 S}{2m} \, C_{z\alpha,\delta} \quad (26)$$

$$Y_{\beta,\delta} = \frac{\rho V^2 S}{2m} \, C_{y\beta,\delta} \quad (27)$$

The rotational equations of motion can now be written as a combination of linear and nonlinear contributions.

$$
\begin{bmatrix} \dot{p} \\ \dot{q} \\ \dot{r} \end{bmatrix} = \begin{bmatrix} 0 & L_\beta & L_p & 0 & L_r \\ M_\alpha & 0 & 0 & M_q & 0 \\ 0 & N_\beta & N_p & 0 & N_r \end{bmatrix} \begin{bmatrix} \alpha \\ \beta \\ p \\ q \\ r \end{bmatrix} +
$$

$$
\begin{bmatrix} I_x & 0 & -I_{xz} \\ 0 & I_y & 0 \\ -I_{xz} & 0 & I_z \end{bmatrix}^{-1} \begin{bmatrix} pqI_{xz} + qr(I_y - I_z) \\ pr(I_z - I_x) + I_{xz}(r^2 - p^2) \\ -qrI_{xz} + pq(I_x - I_y) \end{bmatrix} + \begin{bmatrix} 0 & L_{\delta DT} & L_{\delta A} & L_{\delta R} \\ M_{\delta E} & 0 & 0 & 0 \\ 0 & N_{\delta DT} & N_{\delta A} & N_{\delta R} \end{bmatrix} \begin{bmatrix} \delta_E \\ \delta_{DT} \\ \delta_A \\ \delta_R \end{bmatrix}
$$

$$
+ \begin{bmatrix} 0 & L_{\delta RTV} & L_{\delta YTV} \\ M_{\delta PTV} & 0 & 0 \\ 0 & N_{\delta RTV} & N_{\delta YTV} \end{bmatrix} \begin{bmatrix} \delta_{PTV} \\ \delta_{RTV} \\ \delta_{YTV} \end{bmatrix} \quad (28)
$$

At this point, it is assumed that a generalized control scheme has been implemented in the form of a control selector, described later in this paper. Eq. (28) can be rewritten in terms of the generalized controls: roll, pitch, and yaw acceleration commands.

$$
\begin{bmatrix} \dot{p} \\ \dot{q} \\ \dot{r} \end{bmatrix} = \begin{bmatrix} 0 & L_\beta & L_p & 0 & L_r \\ M_\alpha & 0 & 0 & M_q & 0 \\ 0 & N_\beta & N_p & 0 & N_r \end{bmatrix} \begin{bmatrix} \alpha \\ \beta \\ p \\ q \\ r \end{bmatrix} +
$$

$$
\begin{bmatrix} I_x & 0 & -I_{xz} \\ 0 & I_y & 0 \\ -I_{xz} & 0 & I_z \end{bmatrix}^{-1} \begin{bmatrix} pqI_{xz} + qr(I_y - I_z) \\ pr(I_z - I_x) + I_{xz}(r^2 - p^2) \\ -qrI_{xz} + pq(I_x - I_y) \end{bmatrix} + \begin{bmatrix} 1 & 0 & 0 \\ 0 & 1 & 0 \\ 0 & 0 & 1 \end{bmatrix} \begin{bmatrix} \dot{p}_c \\ \dot{q}_c \\ \dot{r}_c \end{bmatrix} \quad (29)
$$

The first step in control law development is the implementation of a dynamic inversion loop that replaces the existing rotational aircraft dynamics with some set of desired dynamics. This step is called the fast inversion.

$$\begin{bmatrix} \dot{p}_c \\ \dot{q}_c \\ \dot{r}_c \end{bmatrix} = \begin{bmatrix} \dot{p}_{des} \\ \dot{q}_{des} \\ \dot{r}_{des} \end{bmatrix} - \begin{bmatrix} 0 & L_\beta & L_p & 0 & L_r \\ M_\alpha & 0 & 0 & M_q & 0 \\ 0 & N_\beta & N_p & 0 & N_r \end{bmatrix} \begin{bmatrix} \alpha \\ \beta \\ p \\ q \\ r \end{bmatrix} -$$
$$\begin{bmatrix} I_x & 0 & -I_{xz} \\ 0 & I_y & 0 \\ -I_{xz} & 0 & I_z \end{bmatrix}^{-1} \begin{bmatrix} pqI_{xz} + qr(I_y - I_z) \\ pr(I_z - I_x) + I_{xz}(r^2 - p^2) \\ -qrI_{xz} + pq(I_x - I_y) \end{bmatrix} \quad (30)$$

Eq. (30) is the application of the dynamic inversion step in eq. (12) to the outputs p, q, and r. The stability derivatives and inertial properties in eq. (30) are found through linear interpolation of values stored in a tabular database. The desired dynamics contain a set of linear stability derivatives that provide satisfactory modal frequency and damping characteristics.

$$\begin{bmatrix} \dot{p}_{des} \\ \dot{q}_{des} \\ \dot{r}_{des} \end{bmatrix} = \begin{bmatrix} 0 & L'_\beta & L'_p & 0 & L'_r \\ M'_\alpha & 0 & 0 & M'_q & 0 \\ 0 & N'_\beta & N'_p & 0 & N'_r \end{bmatrix} \begin{bmatrix} \alpha \\ \beta \\ p \\ q \\ r \end{bmatrix} + \begin{bmatrix} 1 & 0 & 0 \\ 0 & 1 & 0 \\ 0 & 0 & 1 \end{bmatrix} \begin{bmatrix} \dot{p}_c' \\ \dot{q}_c' \\ \dot{r}_c' \end{bmatrix} \quad (31)$$

Structured Singular Value Synthesis

The fast inversion control law provides equalization of the dominant dynamics across the flight envelope. This equalization effectively eliminates the requirement for gain scheduling. A robust controller may now be designed around the linearizing fast inversion loop to provide command tracking performance. Robust tracking of body axis rotational rate commands is achieved with a μ-synthesis controller. The structured singular value of two uncertainty and one performance block is minimized using a DK-iteration. As shown in Fig. 4, three frequency dependent weights are chosen to balance performance and robustness considerations.

The design plant is defined by $G^* = C^*(sI - A^*)^{-1}B^*$. A^* is the system dynamics matrix at some flight condition which is considered to be central to the flight envelope in terms of modal frequencies and damping. B^* is the normalized

control effectiveness matrix in eq. (29). C^* produces the outputs α, β, p, q, and r. The fast inversion block represents the body axis rate inversions shown in eq. (30).

W_{act} defines the uncertainty at the actuator input, W_s defines the uncertainty at the sensor output, and W_p weights the error between the complementary sensitivity function of the closed loop system and an ideal model of the system response. The actuator and sensor uncertainty models are taken from Haiges, et al.[18]. Wp is chosen such that the closed loop system follows the ideal model closely at frequencies below 10 rad/s. The ideal model represents the desired transfer function between body axis rate commands and roll, pitch, and yaw rate responses. For this problem it is defined as

$$
\text{Ideal Model} = \begin{bmatrix} \dfrac{p}{p_c} \\ \dfrac{q}{q_c} \\ \dfrac{r}{r_c} \end{bmatrix} = \begin{bmatrix} \dfrac{3}{s+3} & 0 & 0 \\ 0 & \dfrac{3}{s+3} & 0 \\ 0 & 0 & \dfrac{3}{s+3} \end{bmatrix} \tag{32}
$$

A successful μ-synthesis design will achieve this first order tracking response to body axis rotational rate commands. The diagonal structure of the ideal model will also force the response to be decoupled in roll, pitch, and yaw.

Slow Inversion

Because only three generalized controls are available, the first step in dynamic inversion ignores the dynamics associated with angle-of-attack and sideslip. These *internal dynamics* can be accounted for in a second application of dynamic inversion to these slower state dynamics. A simple unitary transformation can be made to translate stability axis rate commands into the body axis rate commands that are available to the μ-synthesis controller.

$$\begin{bmatrix} p_c \\ q_c \\ r_c \end{bmatrix} = T_1 \begin{bmatrix} \dot{\mu}_c \\ \dot{\alpha}_c \\ \dot{\beta}_c \end{bmatrix}, \qquad T_1 = \begin{bmatrix} \cos\alpha & 0 & \sin\alpha \\ 0 & 1 & 0 \\ \sin\alpha & 0 & -\cos\alpha \end{bmatrix} \qquad (33)$$

Notice that q_c is equal to $\dot{\alpha}_c$. Eqs. (3) and (4) can be rewritten with these stability axis rate commands.

$$\dot{\alpha} = q - (p\cos\alpha + r\sin\alpha)\tan\beta - \frac{\cos\mu}{\cos\beta}\dot{\gamma} - \sin\mu\frac{\cos\gamma}{\cos\beta}\dot{\chi} + \dot{\alpha}_c \qquad (34)$$

$$\dot{\beta} = p\sin\alpha - r\cos\alpha - \sin\mu\,\dot{\gamma} + \cos\mu\cos\gamma\,\dot{\chi} + \dot{\beta}_c \qquad (35)$$

If sufficient frequency separation exists between the body axis rate command responses and a contribution to the $\dot{\alpha}$ and $\dot{\beta}$ equations, then that contribution can be canceled by a slow inversion loop. The inversion control law for $\dot{\alpha}_c$ includes only the nonlinear effect of gravitational acceleration due to vehicle orientation. The other terms in the $\dot{\alpha}$ equation are either considered negligible or too fast to be controlled.

$$\dot{\alpha}_c = q_c{'} - \frac{\cos\mu\cos\gamma}{V\cos\beta}g \qquad (36)$$

The inversion control law for the sideslip equation includes the nonlinear term representing gravity induced sideslip due to non-zero roll angle. Again all other terms are considered negligible or too fast to control.

$$\dot{\beta}_c = K_\beta(\beta_{ref} - \beta) - \sin\mu\cos\gamma\frac{g}{V} \qquad (37)$$

The addition of a sideslip feedback term to this equation provides sideslip command tracking and increased turn coordination. The gain K_β is selected to provide a second order response that satisfies the frequency and damping requirements for the Dutch roll mode. Assume that the closed loop system exactly matches the desired first order response in eq. (32). Then it can be assumed that

$$\frac{\dot{\beta}}{\dot{\beta}_c} \approx \frac{3}{(s+3)} \quad \text{and} \quad \frac{\beta}{\dot{\beta}_c} \approx \frac{3}{s(s+3)} \qquad (38)$$

With the addition of the sideslip feedback gain K_β, the simplified transfer function from β_c to β can be written as

$$\frac{\beta}{\beta_{ref}} \approx \frac{\frac{K_\beta}{s}\frac{3}{(s+3)}}{(1 + \frac{K_\beta}{s}\frac{3}{(s+3)})} \approx \frac{3\,K_\beta}{s^2 + 3s + 3K_\beta} \qquad (39)$$

A value of 0.5 is selected for K_β, so the sideslip response to commands should be second order with a frequency of 1.2 rad/s and a damping of 1.2.

Command Shaping

The desired flying qualities for the pitch and roll axis are achieved through the use of prefilters. By scheduling these prefilters, the response to pilot inputs can be shaped appropriately with flight condition. As described earlier, the desired roll response is first order with a time constant that is a function of angle-of-attack. With the μ-synthesis compensator implemented, we can assume that the stability axis roll rate transfer function is:

$$\frac{\dot{\mu}}{\dot{\mu}_c} \approx \frac{3}{(s+3)} \qquad (40)$$

so the response with a first order prefilter with gain K_μ is:

$$\frac{\dot{\mu}}{\dot{\mu}_{ref}} = [\dot{\mu}_{PF}]\frac{\dot{\mu}}{\dot{\mu}_c} \approx \frac{3K_\mu}{(s+3)(s+K_\mu)} \approx \frac{3K_\mu}{(s^2 + (3+K_\mu)s + 3K_\mu)} \qquad (41)$$

A schedule for the roll prefilter gain that achieves the desired equivalent system response with angle-of-attack is:

$$K_\mu = 3.65 - 0.0433\,\alpha \quad \text{and} \quad \min(K_\mu) = 0.5. \qquad (42)$$

The desired pitch response to pilot inputs is second order with a short period frequency that is a function of equivalent airspeed. The transfer function representing the pitch response to pilot commands is:

$$\frac{q}{q_c} = \frac{3}{(s + 3)} \tag{43}$$

The pitch response with a first order prefilter with gain K_q is:

$$\frac{q}{q_{ref}} = [q_{PF}] \frac{q}{q_c} = \frac{3K_q}{(s + 3)(s + K_q)} = \frac{3K_q}{(s^2 + (3+K_q)s + 3K_q)} \tag{44}$$

The prefilter gain, K_q, is scheduled to provide the desired level of damping and increase in short period frequency with equivalent airspeed.

$$K_q = \frac{1}{3}\left(\frac{V_{eq}\ (ft/s)}{100}\right)^2 \tag{45}$$

CONTROL LIMITING AND PRIORITIZATION

The control selector, sometimes referred to as pseudo-controls, has two functions. The first is to normalize control effectiveness by transforming generalized rotational rate commands into actuator position commands. The second is to take advantage of available control redundancy by allowing for control redistribution without changing the linear closed loop performance. The basic idea of the control selector is in redefining the control contribution to the state equation (28,29),

$$B\delta = B^*\delta^* \tag{46}$$

B and δ are the actual control effectiveness matrix and control vector. B^* and δ^* are the generalized control effectiveness matrix and control vector. The actual control can now be defined in terms of the generalized control,

$$\delta = T\delta^* \tag{47}$$

The transformation, T, is the control selector. It is defined simply by

$$T = N(BN)^{\#}B^{*} \qquad \text{(48)}$$

The operation $(\ )^{\#}$ is a pseudo-inverse and N is a matrix that may be used to combine controls or emphasize/de-emphasize a control channel in the case of redundant effectors. Because the B matrix in eq. (48) is a function of flight condition and aircraft state, the control selector is a function of parameters such as Mach number, altitude, angle-of-attack, and engine power level angle.

The generalized and actual controls for the supermaneuverable vehicle are given by

$$\delta^{*} = \begin{bmatrix} \dot{p}_c \\ \dot{q}_c \\ \dot{r}_c \end{bmatrix}, \qquad \delta = \begin{bmatrix} \delta_E \\ \delta_{DT} \\ \delta_A \\ \delta_R \\ \delta_{PTV} \\ \delta_{RTV} \\ \delta_{YTV} \end{bmatrix} \qquad \text{(49)}$$

Consider the following partitioning of the control effector vector as shown in eq. (28)

$$\delta = \begin{bmatrix} \delta_{aero} \\ \delta_{tvec} \end{bmatrix}, \quad \text{where} \quad \delta_{aero} = \begin{bmatrix} \delta_E \\ \delta_{DT} \\ \delta_A \\ \delta_R \end{bmatrix}, \quad \delta_{tvec} = \begin{bmatrix} \delta_{PTV} \\ \delta_{RTV} \\ \delta_{YTV} \end{bmatrix} \qquad \text{(50)}$$

resulting in

$$B_{aero} = \begin{bmatrix} 0 & L_{\delta DT} & L_{\delta A} & L_{\delta R} \\ M_{\delta E} & 0 & 0 & 0 \\ 0 & N_{\delta DT} & N_{\delta A} & N_{\delta R} \end{bmatrix}$$

$$B_{tvec} = \begin{bmatrix} 0 & L_{\delta RTV} & L_{\delta YTV} \\ M_{\delta PTV} & 0 & 0 \\ 0 & N_{\delta RTV} & N_{\delta YTV} \end{bmatrix} \qquad \text{(51)}$$

353

With the above partitions, eq. (46) is written as:

$$[B_{aero} \quad B_{tvec}]\begin{bmatrix} \delta_{aero} \\ \delta_{tvec} \end{bmatrix} = B^* \delta^* \text{, where } \quad B^* = \begin{bmatrix} 1 & 0 & 0 \\ 0 & 1 & 0 \\ 0 & 0 & 1 \end{bmatrix} \qquad (52)$$

A daisy-chain method is used to generate thrust vector commands. Thrust vectoring is used only when the aerodynamic surfaces are not able to generate the necessary forces and moments required for commanded maneuvers. Therefore, the computation of aerodynamic control commands is independent of thrust vectoring control commands. The control selector is defined by

$$\delta_{aero} = T_{aero} \delta^* \qquad\qquad \delta_{tvec} = T_{tvec} \delta^* \qquad (53)$$

and

$$T_{aero} = N_{aero}(B_{aero}N_{aero})^\# \qquad T_{tvec} = N_{tvec}(B_{tvec}N_{tvec})^\# \qquad (54)$$

where N_{aero} and N_{tvec} are used to weight the redundant control effectors. Since the ailerons contribute more to the roll acceleration and the first priority of the horizontal tail should be pitch control, the differential horizontal tail command is reduced by weighting the command to be a quarter of the other aerodynamic commands. There is no redundancy for the thrust vectoring control effectors, and thus, the weighting matrices become

$$N_{aero} = \begin{bmatrix} 1 & 0 & 0 & 0 \\ 0 & .25 & 0 & 0 \\ 0 & 0 & 1 & 0 \\ 0 & 0 & 0 & 1 \end{bmatrix} \quad N_{tvec} = \begin{bmatrix} 1 & 0 & 0 \\ 0 & 1 & 0 \\ 0 & 0 & 1 \end{bmatrix} \qquad (55)$$

Computation of the control selector eq. (53) depends on flight condition. Therefore, the elements of B_{aero} and B_{tvec} are found using linear interpolation of stored table values.

Nonlinear elements, such as position and rate limits, are required to implement the daisy-chain. Fig. 5 shows the structure of the nonlinear control selector. A limited aerodynamic surface command (δ^c_{aero}) is generated from a

354

rotational acceleration command (δ^*) via the aerodynamic control selector (T_{aero}), the aerodynamic surface limits, and command scaling logic. An achievable aerodynamic rotational acceleration vector (δ^*_{avail}) is computed from the limited aerodynamic surface command using the control distribution (B_{aero}). The difference of the commanded and achievable rotational acceleration vectors (e_{δ^*}) is transformed to a thrust vector command (δ^c_{tvec}) using the thrust vector control selector (T_{tvec}) and command prioritization logic.

The command scaling logic limits the acceleration command in the event of control effector saturation. The lateral/directional generalized control command that is generated by the control system can be thought of as a vector. This concept is illustrated in Fig. 6. When saturation occurs in one axis, the resulting control vector loses both the magnitude and the direction of the desired control. By scaling the command vector in both axis, an achievable control vector can be realized that preserves the direction of the desired command and holds the limiting controls on their limits. A block diagram of the command scaling logic is shown in Fig. 7. The figure shows that the scaled vector is the product of the commanded vector and the minimum ratio of available and commanded acceleration, $\delta^*_{scaled} = \delta^* \times sat$. The scaling parameter, sat, is always less than or equal to unity. It can be argued that when saturations occur, control bandwidth is too high. An interpretation can be made that this scaling logic acts to reduce the control bandwidth in the event of control power saturation[6].

The command prioritization logic limits the amount of commanded differential pitch (roll) thrust vectoring. By using models of rate and position limiters within a daisy-chain, roll thrust vectoring is commanded only when the thrust vectoring nozzles are not saturated due to symmetric pitch thrust vectoring commands. For commanded rolls at high angles-of-attack, it can be interpreted that rolls commands correspond to performance and pitch commands correspond to stability. Therefore, the pitch thrust vectoring command, and thus stability, has top priority.

ROBUSTNESS ANALYSIS

A range of flight conditions must be selected for the purpose of linear analysis. Table 1 describes the seven conditions that span a broad range of Mach numbers, altitudes, and angles-of-attack. Linearized models of the vehicle dynamics at these points are used for robustness analysis.

Table 1 Flight Conditions for Linear Analysis

Flight Condition	Mach	Altitude (ft)	Angle-of-Attack (deg)	Equivalent Airspeed (ft/s)
1	0.2	10,000	30	109.7
2	0.2	10,000	45	109.7
3	0.2	10,000	60	109.7
4	0.2	30,000	75	72.09
5	0.4	30,000	50	144.2
6	0.6	30,000	20	216.3
7	0.6	30,000	30	216.3

The linear analysis models at each of these test conditions include high order actuator models, vehicle dynamics, and control elements shown in Fig. 3.

The robustness of the closed loop system is tested to simultaneous structured and unstructured uncertainties. The structured uncertainties consist of perturbations in aerodynamic stability and control derivatives. They are shown in Table 2. The structured uncertainties are presented in additive form because uncertainty percentages can vary greatly with flight condition, especially when the nominal value of a parameter approaches zero. The values shown in parentheses in Table 2 are the uncertainty percentages at flight condition 1. These are presented to show the relative degree of uncertainty in the different coefficients. Uncertainties in thrust vectoring are not included because the control distribution logic dictates that those effectors are only used at conditions where linear analysis is no longer appropriate. The dimensional form of these uncertainties can be found using eqs. (21-27).

Table 2 Structured Uncertainty Levels

stability derivatives	control derivatives
$\Delta C_{Z\alpha} = 0.150$ (20%)	$\Delta C_{Z\delta E} = 0.0100$ (21%)
$\Delta C_{y\beta} = 0.0150$ (12%)	$\Delta C_{y\delta R} = 0.0016$ (10%)
$\Delta C_{l\beta} = 0.0030$ (10%)	$\Delta C_{l\delta DT} = 0.0015$ (2%)
$\Delta C_{lp} = 0.3000$ (66%)	$\Delta C_{l\delta DA} = 0.0010$ (2%)
$\Delta C_{lr} = 0.1000$ (31%)	$\Delta C_{l\delta R} = 0.0010$ (40%)
$\Delta C_{m\alpha} = 0.150$ (40%)	$\Delta C_{m\delta E} = 0.0200$ (5%)
$\Delta C_{mq} = 6.0000$ (86%)	$\Delta C_{n\delta DT} = 0.0015$ (6%)
$\Delta C_{n\beta} = 0.0030$ (10%)	$\Delta C_{n\delta DA} = 0.0015$ (6%)
$\Delta C_{np} = 0.1250$ (140%)	$\Delta C_{n\delta R} = 0.0020$ (5%)
$\Delta C_{nr} = 0.0750$ (24%)	

Unstructured uncertainties include uncertain actuator and sensor dynamics. Fig. 8 shows the levels of multiplicative uncertainty that must be tolerated for each actuator and sensor channel. The quantities were derived as part of the work presented by Haiges, et al.[18]. The same level of unstructured uncertainty is assumed for all of the aerodynamic control effectors.

The results of structured singular value analysis indicate that the closed loop system is robust to the levels of uncertainty considered. Fig. 9 shows the upper bounds for the structured singular values at each of the linear test points. The fact that these bounds are less than unity at all frequencies provides a sufficient condition for robust stability. The peak in the lateral/directional bounds at 2-3 rad/sec indicates that Dutch roll mode is the most sensitive to plant uncertainties.

NONLINEAR RESULTS

In order to test the nonlinear performance of the flight control system, batch simulations are run on a high fidelity six degree-of-freedom simulation of the supermaneuverable vehicle. A challenging supermaneuver that tests the performance of the control laws and the control distribution logic is a very high angle-of-attack velocity vector roll. Fig. 10 shows such a maneuver where the aircraft is pitched up to 80 degrees angle-of-attack and then rolled 180 degrees about the velocity vector. This supermaneuver creates a rapid 180 degrees change

in heading angle. The solid arrows represent the aircraft's velocity vector. Fig. 11 shows the time histories for this maneuver. Actuator positions are given in terms of left and right tail (δ_{TL}, δ_{TR}), left and right aileron (δ_{AL}, δ_{AR}), rudder (δ_R), left and right pitch thrust vectoring (δ_{PTVL}, δ_{PTVR}), and yaw thrust vectoring (δ_{YTV}). The left and right convention is used in place of symmetric and asymmetric so that control effector saturations are properly represented.

The 180 degree change in roll and heading angle is achieved by holding a 30 deg/sec stability axis roll rate command for six seconds. The performance of the dynamic inversion/μ-synthesis control system is demonstrated by the smooth, well damped stability axis roll rate response and the excellent turn coordination at 80 degrees angle-of-attack. Less than 2 degrees of sideslip is generated during the supermaneuver. Notice that all of the aerodynamic surfaces saturate during this maneuver, forcing the control distribution, scaling, and prioritization logic to be activated. Command scaling comes into effect due to rate saturations in yaw thrust vectoring at the application and removal of the stability axis roll rate command. The pitch thrust vectoring prioritization logic is activated when symmetrical horizontal tail saturates, causing a requirement for symmetrical pitch thrust vectoring.

CONCLUSIONS

High angle-of-attack control laws have been developed for a supermaneuverable vehicle with thrust vectoring capability. The methods of dynamic inversion and structured singular value synthesis are successfully integrated into a design approach which achieves desired performance and robustness levels. An advanced generalized controls approach is demonstrated for the allocation of redundant aerodynamic and thrust vectoring effectors. Command scaling and prioritization are implemented to minimize the destabilizing effects of saturations during demanding supermaneuvers. The design goals are achieved across a broad range of airspeeds, altitudes, and angles-of-attack. High fidelity simulations show that the nonlinear aspects of the control laws perform well in a highly dynamic, nonlinear environment.

REFERENCES

[1] Gal-Or, B., *Vectored Propulsion, Supermaneuverability and Robot Aircraft*, Springer-Verlag, New York, NY, 1990.

[2] Haiges, K.R., Chiang, R.Y., Madden, K.P., Emami-Naeini, A., Anderson, M.R., and Safonov, M.G., "Robust Control Law Development for Modern Aerospace Vehicles, Final Report," WL-TR-91-3105, Wright Laboratory, Wright-Patterson AFB, OH, Aug. 1991.

[3] Chiang, R.Y., Safonov M.G., Haiges, K.R., Madden, K.P., and Tekawy, J.A., "A Fixed H_∞ Controller for a Supermaneuverable Fighter Performing a Herbst Maneuver," *Automatica*, vol. 29, No. 1, pp. 111-127, 1993.

[4] Sparks, A.G., and Banda, S.S., "Application of Structured Singular Value Synthesis to a Fighter Aircraft," *Proc. 1992 American Control Conf.*, Chicago, IL, June 1992, pp.1301-1305.

[5] Adams, R.J., Buffington, J.M., Sparks, A.G., and Banda, S.S., "An Introduction to Multivariable Flight Control System Design," WL-TR-92-3110, Wright Laboratory, Wright-Patterson AFB, OH, Oct. 1992.

[6] Bugajski, D. J., and Enns, D. F., "Nonlinear Control Law with Application to High Angle-of-Attack Flight," *Journal of Guidance, Control, and Dynamics*, Vol.15, No.3, 1992, pp.761-767.

[7] Huang C., Knowles, G., Reilly, J., Dayawansa, M., and Levine, W., "Analysis and Simulation of a Nonlinear Control Strategy for High Angle-of-Attack Maneuvers," presented at the 1990 AIAA Guidance, Navigation, and Control Conf., Portland, OR, Aug. 1990.

[8] Durham, W. C., "Constrained Control Allocation," *Proc. 1992 AIAA Guidance, Navigation, and Control Conf.*, Hilton Head, SC, Aug. 1992, pp.1147-1155.

[9] Haiges, K.R., Tich, E.J., and Madden, K.P., "Robust Control Law Development for Modern Aerospace Vehicles, Task 1: Model Development," WRDC-TR-89-3080, Wright Laboratory, Wright-Patterson AFB, OH, Aug. 1989.

[10] Miele, A., *Flight Mechanics: Theory of Flight Paths, Vol. 1*, Addison-Wesley, Reading, MA, 1962

[11] "Military Specification - Flying Qualities of Piloted Vehicles," MIL-STD-1797A, March 1987.

[12] J.E. Slotine and W. Li, *Applied Nonlinear Control*, Prentice Hall, Englewood Cliffs, 1991.

13 S. H. Lane and R.F. Stengel, "Flight Control Design Using Non-linear Inverse Dynamics," *Automatica*, vol. 24, pp. 471-483, 1988.

14 J. C. Doyle, "Analysis of Feedback Systems with Structured Uncertainties," *IEEE Proceedings*, vol. 129, Part D, No. 6, Nov. 1982, pp. 242-250,.

15 J.C. Doyle, J. Wall, and G. Stein, "Performance and Robustness Analysis for Structured Uncertainty," *Proc. 21st IEEE Conf. Decision Contr.*, Dec. 1982, pp.629-636

16 J. C. Doyle, "Structured Uncertainty in Control System Design," *Proc. 24th IEEE Conf. Decision Contr.*, Ft. Lauderdale FL, Dec. 1985, pp.260-265.

17 G. J. Balas, A. K. Packard, J. C. Doyle, K. Glover, and R. S. R. Smith, "Development of Advanced Control Design Software for Researchers and Engineers," *Proc. 1991 American Control Conf.*, Boston MA, June 1991, pp.996-1001.

18 Haiges, K.R., et al., "Robust Control Law Development for Modern Aerospace Vehicles, Task 2: Control System Criteria and Specifications," WRDC-TR-90-3005, Wright Laboratory, Wright-Patterson AFB, OH, Aug. 1989.
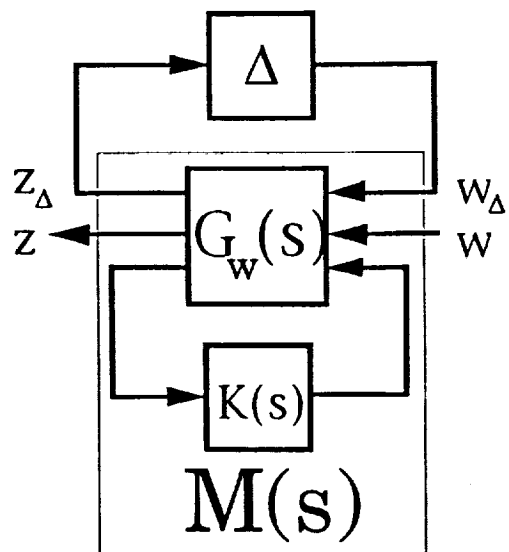
Fig. 1 MΔ Form for μ-synthesis

Richard J. Adams, James M. Buffington, and Siva S. Banda
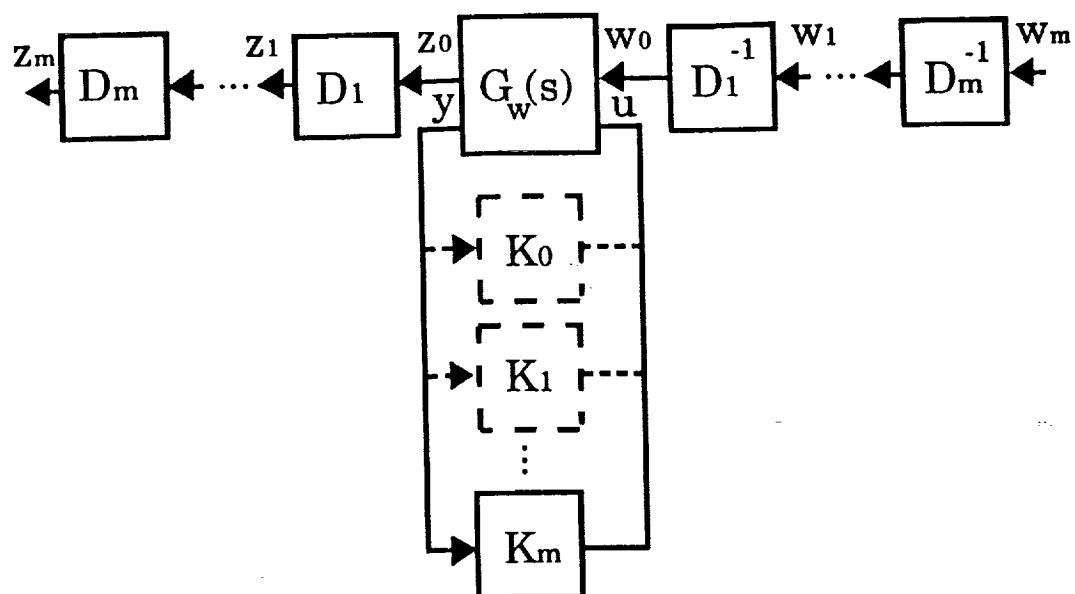
Fig. 2 DK-iteration Process

Richard J. Adams, James M. Buffington, and Siva S. Banda
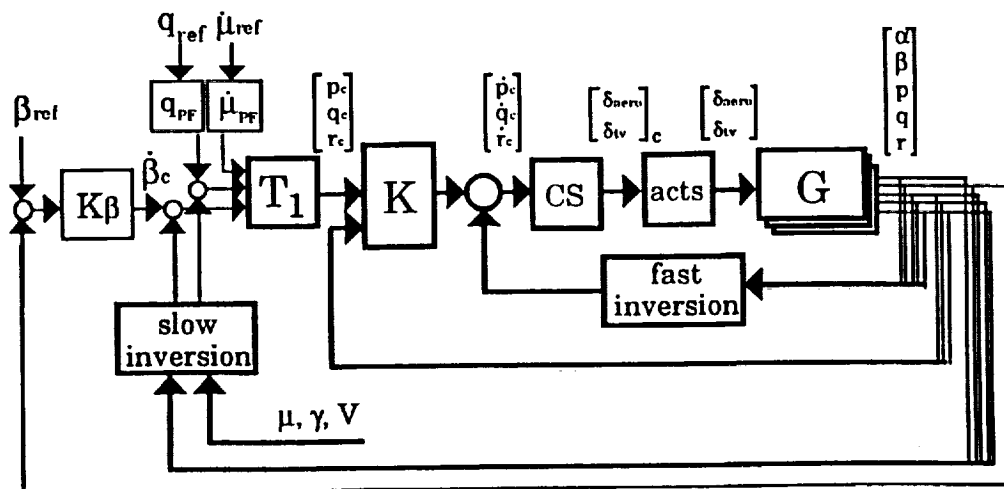
Fig. 3 Closed Loop System
Richard J. Adams, James M. Buffington, and Siva S. Banda
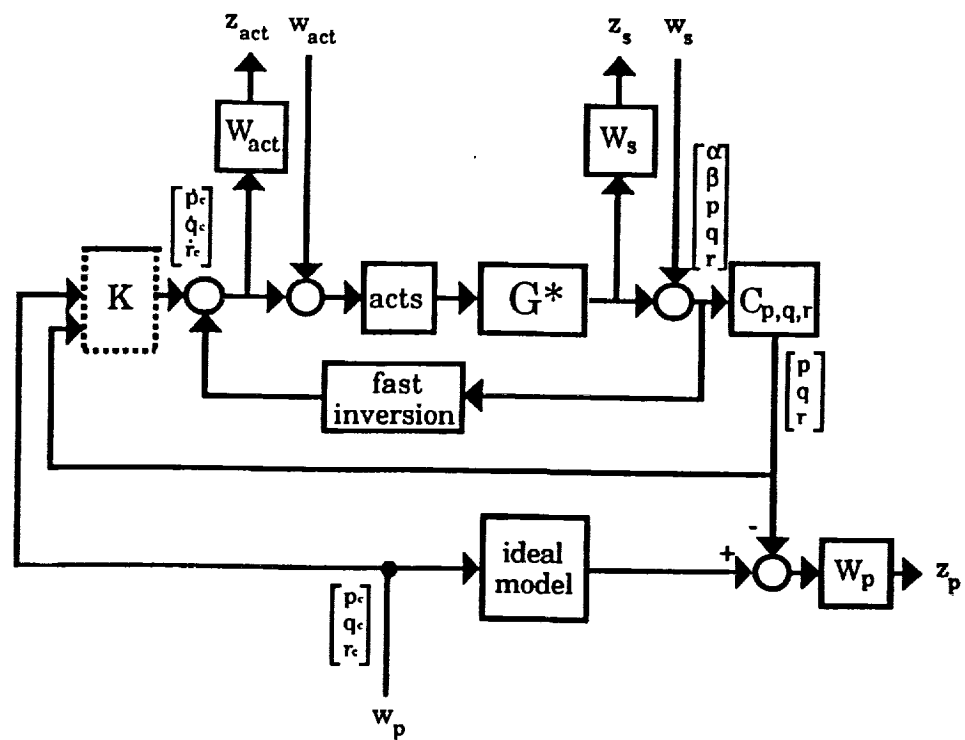
Fig. 4 Design Model for μ-synthesis

Richard J. Adams, James M. Buffington, and Siva S. Banda
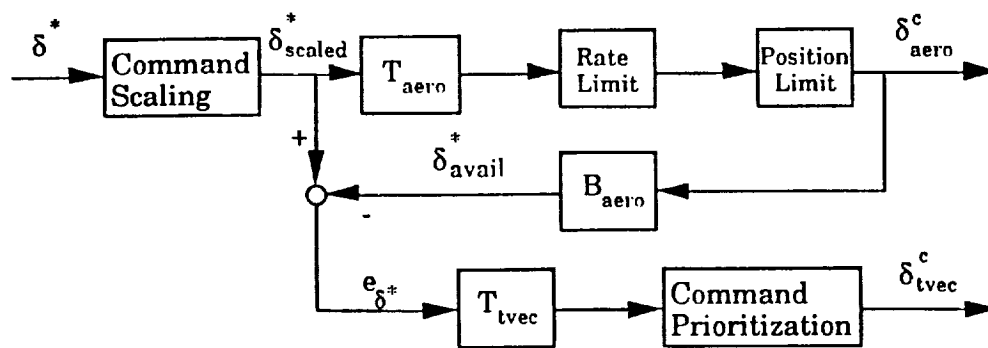
Fig. 5 Nonlinear Control Selector
Richard J. Adams, James M. Buffington, and Siva S. Banda
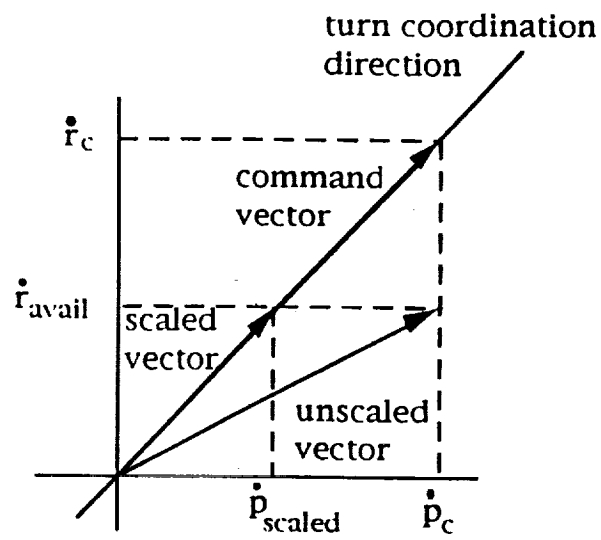
Fig. 6 Lateral/Directional Command Scaling

Richard J. Adams, James M. Buffington, and Siva S. Banda
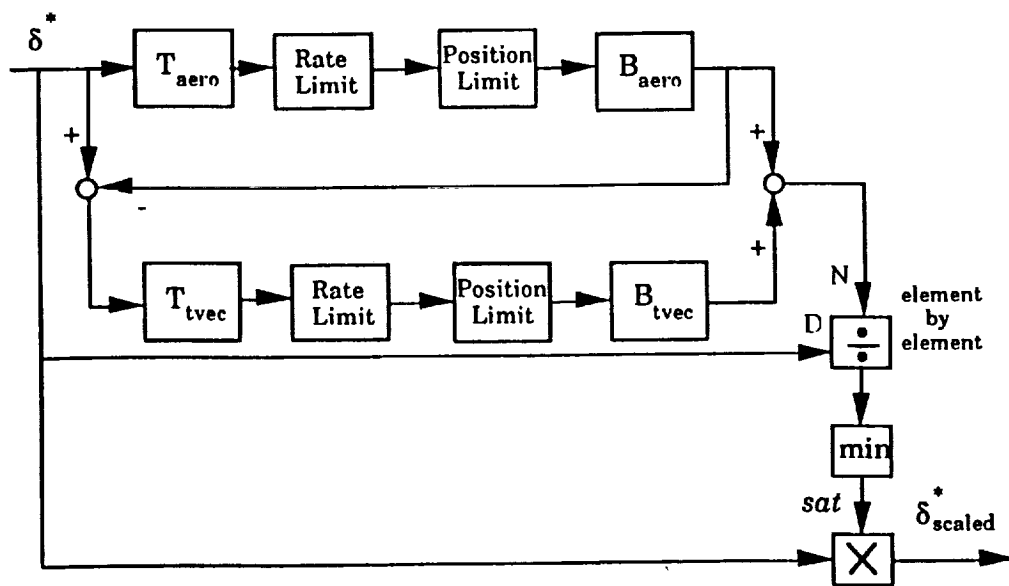
Fig. 7 Command Scaling Logic

Richard J. Adams, James M. Buffington, and Siva S. Banda
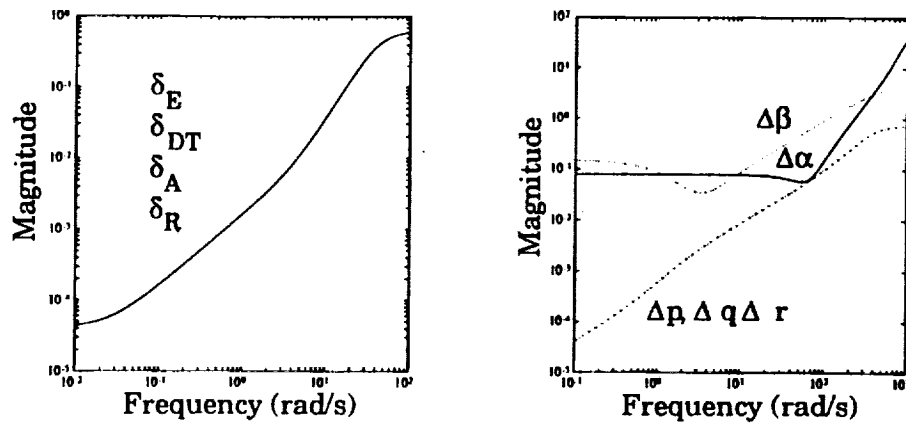
Fig. 8 Magnitudes of Unstructured Uncertainties
Richard J. Adams, James M. Buffington, and Siva S. Banda
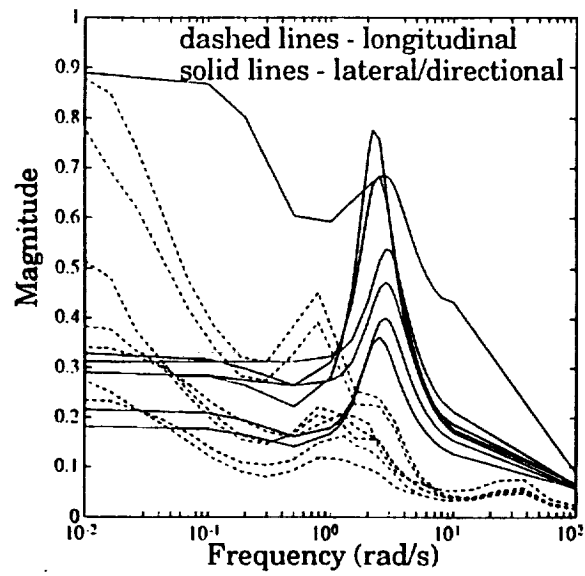
Fig. 9 Upper Bounds on Structured Singular Value
Richard J. Adams, James M. Buffington, and Siva S. Banda
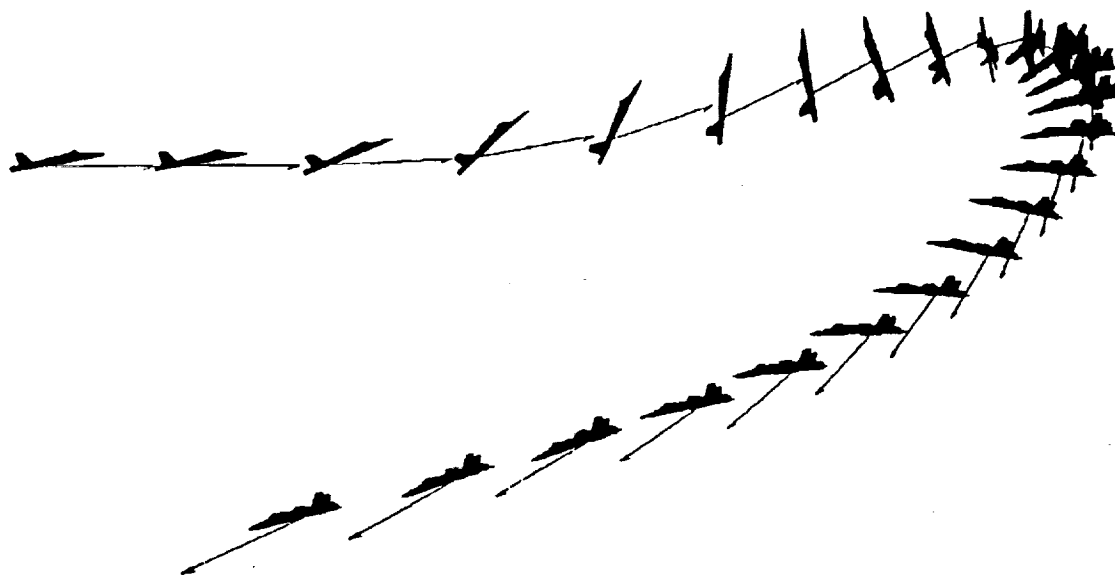
Fig. 10 High Angle-of-Attack Supermaneuver
Richard J. Adams, James M. Buffington, and Siva S. Banda
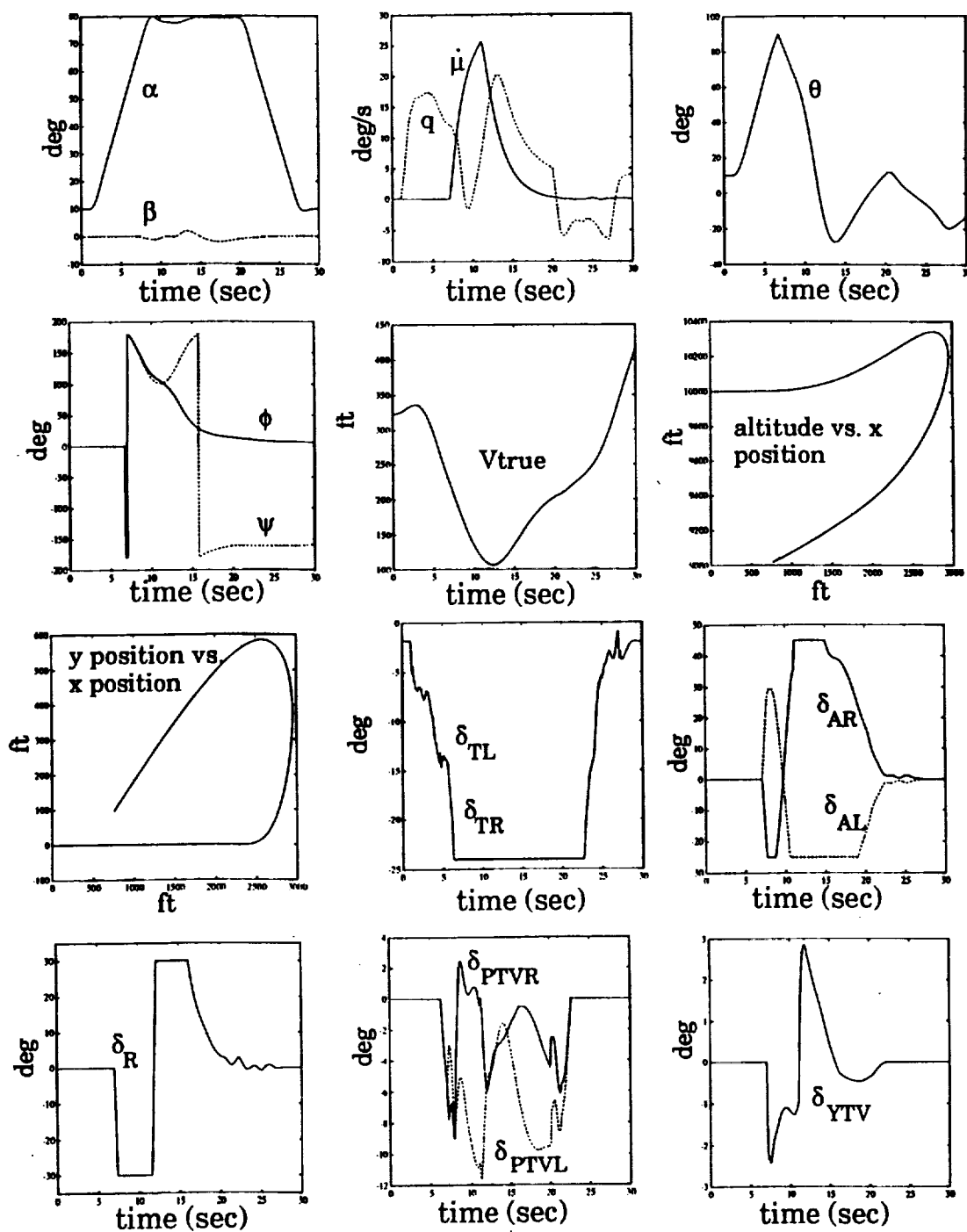
Fig. 11 Nonlinear Time Responses

Richard J. Adams, James M. Buffington, and Siva S. Banda

X-31 AERODYNAMIC CHARACTERISTICS DETERMINED FROM FLIGHT DATA

ALEX KOKOLIOS

JOINT INSTITUTE FOR THE ADVANCEMENT OF FLIGHT SCIENCES

AIRCRAFT GUIDANCE AND CONTROLS BRANCH

NASA LANGLEY RESEARCH CENTER

Abstract

The lateral aerodynamic characteristics of the X-31 were determined at angles of attack ranging from 20 to 45 degrees. Estimates of the lateral stability and control parameters were obtained by applying two parameter estimation techniques, linear regression and the extended Kalman filter, to flight test data. An attempt to apply maximum likelihood to extract parameters from the flight data was also made but failed for reasons given within. An overview of the System Identification process is given, including a listing of the more important properties of all three estimation techniques that were applied to the data. A comparison is given of results obtained from flight test data and wind tunnel data for four important lateral parameters. Finally, future research to be conducted in this area is discussed.

SYSTEM IDENTIFICATION

EXPERIMENT

FLIGHT DATA →

DATA COMPATIBILITY CHECK

CORRECTED DATA →

MODEL IDENTIFICATION

MODEL →

MODEL VERIFICATION
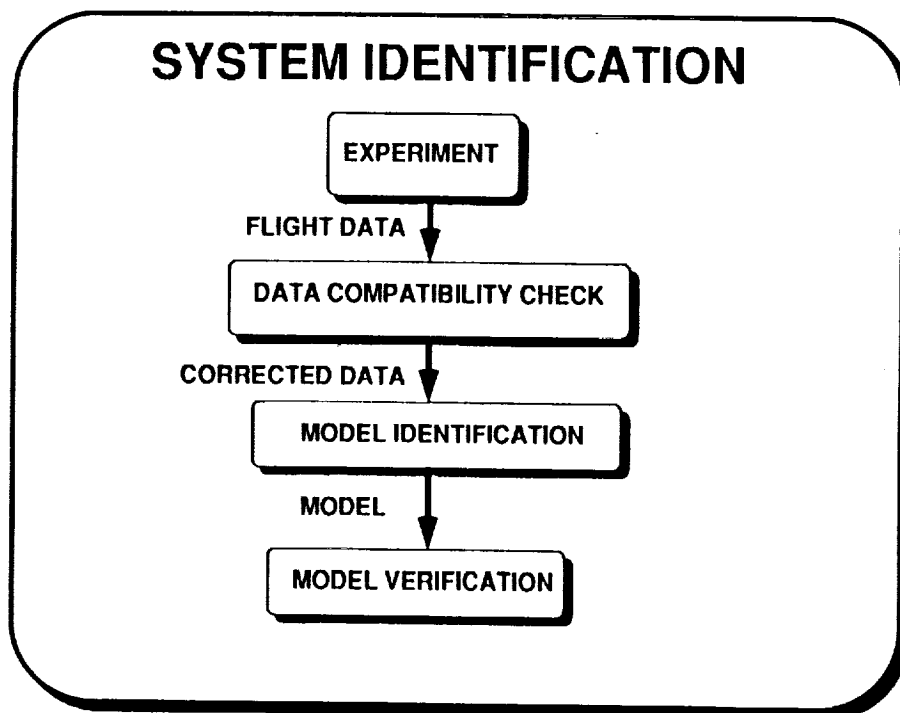
Overview of System Identification

System Identification is a complex process involving several steps. It begins with the experiment, or flight test, which yields the flight data. The flight data must then be subjected to a data compatibility check to check for the presence of any scale factor or bias errors. Once any such errors have been found and accounted for, the process known as model identification may then be applied to the corrected data. More will be said about this process later, as it is in itself a complex process. Once a model has been determined, it must then be verified either by comparing the estimates to results obtained from other experiments, or by the application of other estimation techniques to the same set of data. When a model has been verified, it may then be used to update the data-base or simulator or to refine the existing control laws of the aircraft.

MODEL IDENTIFICATION

The Process of Model Identification can be separated into two distinct

steps:

      (1) Model Structure Determination; and

      (2) Parameter Estimation.

The Model Identification Process

The identification of a particular model can be broken down into two separate steps: that of determining the structure of the model; and that of estimating the parameters in this particular model. In the case of aircraft aerodynamic analysis the parameters are often the stability and control parameters as is the case in the present study.

MODEL STRUCTURE DETERMINATION

The Model Structure is determined through the use of Stepwise

Regression, a generalization of linear regression, as follows:

a) An adequate model is determined from postulated terms

    (the postulated terms may include linear as well as nonlinear

    terms);

b) The parameters associated with the selected terms are

    estimated, using the Least Squares method, by minimizing

    the following cost function:

$$J = \sum_{i=1}^{N} \left(C_{a_i} - \theta_o - \sum_{j=1}^{I} x_{ji}\theta_j \right)^2$$

Model Structure Determination

For this particular study, the structure of the model was determined through the use of a technique known as stepwise regression, a generalization of linear regression which works as follows. First, an adequate model is determined by choosing the so-called regressors from a pool of postulated terms. These postulated terms may include the states and inputs, as well as any combinations of the two. Thus, the regressors may be linear or nonlinear. Once these regressors have been chosen, the parameters associated with these regressors are estimated using a Least Squares method, which minimizes the given cost function. The cost function minimizes the sum of squares of the difference between the measured aerodynamic force or moment coefficient, C_{ai}, and the model-predicted coefficient, given by the remaining expression within the parentheses (x represents the chosen regressor and θ the associated parameter to which an estimate is sought; θ_o estimates the steady state value of the coefficient). Note that this summation is carried out over N, the number of data points collected during the maneuver.

The Parameter Estimation Process

Three different parameter estimation techniques were applied to the X-31 drop model for this particular study: the least squares method in the form of stepwise regression (as discussed in the previous slide); the maximum likelihood method; and the extended Kalman filter method. Results obtained by applying the least squares and extended Kalman filter methods to X-31 drop model flight test data will be presented. First, however, some of the important properties of each of these techniques is discussed. Also, an explanation is given as to why the application of maximum likelihood to flight test did not yield any results.

C-5

Linear Regression Estimation

Parameter estimation through linear regression has several desirable properties. First, linear regression is a simple, linear estimation problem. The regression is applied to each aerodynamic force or moment coefficient individually, thereby keeping the number of unknowns in each equation small. Finally, linear regression can be applied to an unstable system without any difficulties. The drawback to using linear regression however, is that the estimates obtained with this technique are, in general, biased. Thus, the motivation exists to apply a second estimation technique to the flight test data, one that yields unbiased estimates of the parameters. Two such methods are maximum likelihood, and the extended Kalman filter. Generally, the estimates obtained from linear regression are used as the initializations for the second estimation technique.

MAXIMUM LIKELIHOOD METHOD

- Optimizes Parameter Estimates by fitting Outputs predicted by the Model to the measured Outputs

- In the absence of process noise an Output Error Method, but with continual Update of the Measurement Noise Covariance Matrix

- Cost Function:
$$J = \sum_{i=1}^{N} [z_i - y_i(\theta)]^T \hat{R}^{-1} [z_i - y_i(\theta)]$$

- Parameter Estimates are unbiased

- Nonlinear Estimation Technique (thus requiring iterative approach)

- Requires Integration of the Aircraft Equations of Motion (will cause problems if aircraft is unstable)

Maximum Likelihood Estimation

Maximum likelihood optimizes parameter estimates by fitting the model-predicted outputs to the measured outputs. In the absence of any process noise, it is an output error method but more general because it continually updates the measurement noise covariance matrix. In the given cost function, z_i represents the measurement, y_i the prediction (which is a function of θ, the parameters to which an estimate is sought), and R represents the measurement noise covariance matrix. As in the case of the least squares cost function, the maximum likelihood cost function sums over N, the number of data points collected during the maneuver. The estimates obtained in this manner are unbiased. Note that maximum likelihood is a nonlinear estimation technique and thus requires an iterative approach such as the Newton-Raphson method. The difficulty in applying the maximum likelihood method lies in the fact that it requires integration of the aircraft equations of motion, which will cause problems if the aircraft is unstable. Since the X-31 is open-loop laterally unstable at high angles of attack, application of the maximum likelihhod method to X-31 flight data failed to produce reasonable estimates. Thus, another estimation technique had to be found.

EXTENDED KALMAN FILTER

- A Nonlinear Estimation Problem, with the aircraft model defined as:

$$\dot{x}(t) = f[x(t), u(t)] + w(t)$$

$$z_i = h_i[x(t_i), u(t_i)] + v_i$$

$$w(t) \sim N(0, Q(t))$$

$$v_i \sim N(0, R_i)$$

Note that x contains the states as well as the parameters (I.e., the stability and control derivatives).

- Given the model of the aircraft as described above, form an algorithm for calculating the minimum variance estimate of x(t) :

I.e., minimize:

$$J = E\{(\hat{x} - x)^T (\hat{x} - x)\}$$

The Extended Kalman Filter

A second method that was used to refine the parameter estimates obtained through linear regression was the extended Kalman Filter. The extended Kalman filter, like maximum likelihood, is also a nonlinear estimation problem, with the aircraft model defined as shown above. The time derivative of the state is assumed to be a function of the states and inputs plus a process noise term, $w(t)$, assumed to be of normal distribution with zero mean and variance given by $Q(t)$. Similarly, the measured output is assumed to be some function of the states and inputs plus a measuremnt noise term, v_i, also assumed to be of normal distribution with zero mean and variance given by R_i. It should be noted that x may contain the states as well as the parameters (i.e., the state vector is augmented with the stability and control parameters to which estimates are sought). Given the model as described above, the extended Kalman filter cost function is formed by determining the minimum variance estimate of the state. Here, x represents the true value of the state, $\hat{x}$ the estimate, and E{ } represents the expected value operator.

DIAGRAM OF THE KALMAN FILTER
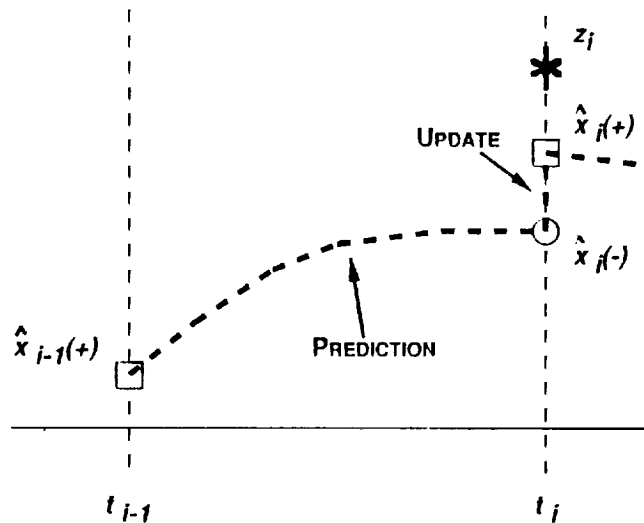
Timing Diagram of the Kalman Filter

A timing diagram of the extended Kalman filter is shown, illustrating how an estimate is obtained. Basically, a two-step process is carried out at each data point. Given that an estimate $\hat{x}_{i-1}(+)$ is known at time t_{i-1}. The estimate is then propagated to the next time t_i by simply integrating the equations of motion across one time step. This estimate, $\hat{x}_i(-)$, is then updated by the extended Kalman filter equations, which take into account the new measurement, z_i as well as information about the assumed statistics of the measurement and process noise terms. The updated estimate is denoted by $\hat{x}_i$ (+), the (+) indicating it is the value of the estimate after the update has been carried out (similarly, a (-) indicates the value of an estimate prior to an update). It is this update step which stabilizes the integration scheme where maximum likelihood failed. Note that the updated value of the estimate will always lie between the predicted value and the measured value.

381
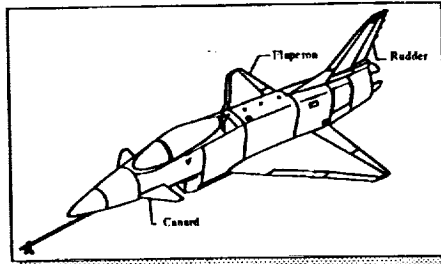
THE X-31 DROP MODEL

- Delta wing, canard configuration intended to serve as a high-alpha
  test vehicle
- Unpowered, 27% dynamically-scaled model of the full-scale aircraft.
- Laterally Unstable in high angle-of-attack flight regime.

Application to the X-31 Drop Model

An isometric of the X-31 drop model is shown above. The X-31 is a delta wing, canard configured aircraft intended to demonstrate enhanced maneuverability at high angles of attack. The drop model, currently undergoing flight testing at the Plum Tree test site, is a 27% dynamically-scaled model of the full-scale aircraft. The X-31 is known to be laterally unstable at high angles of attack.

382
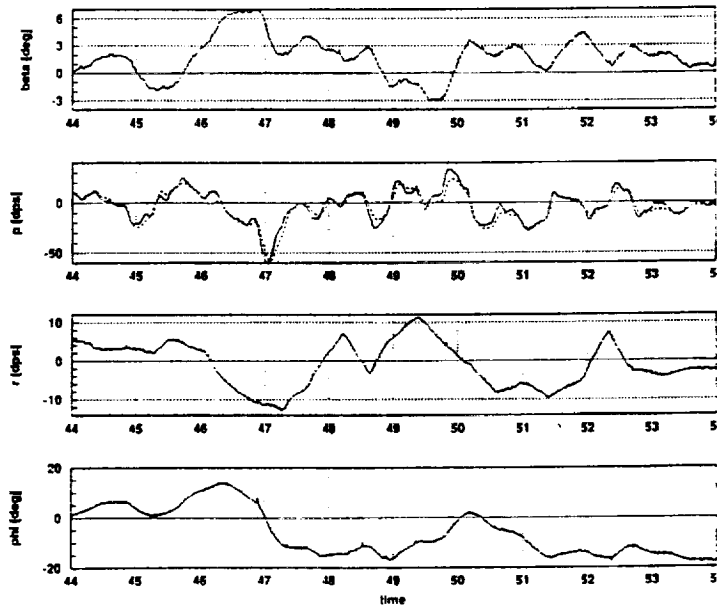
State Estimation

An algorithm using the extended Kalman filter method was applied to X-31 drop model flight test data. The results of the application to one maneuver is shown above. The plots show the time history of four lateral states, including the sideslip angle, the roll-rate, the yaw-rate, and the bank-angle, during a lateral maneuver. The solid lines represent the measured data and the dashed lines represent the estimates as obtained using the extended Kalman filter algorithm. As seen, the algorithm predicts the states very accurately, with the exception of the roll-rate. The exact reason why the algorithm is able to predict all the states accurately with the exception of the roll-rate is not yet fully understood.

PARAMETER ESTIMATION RESULTS
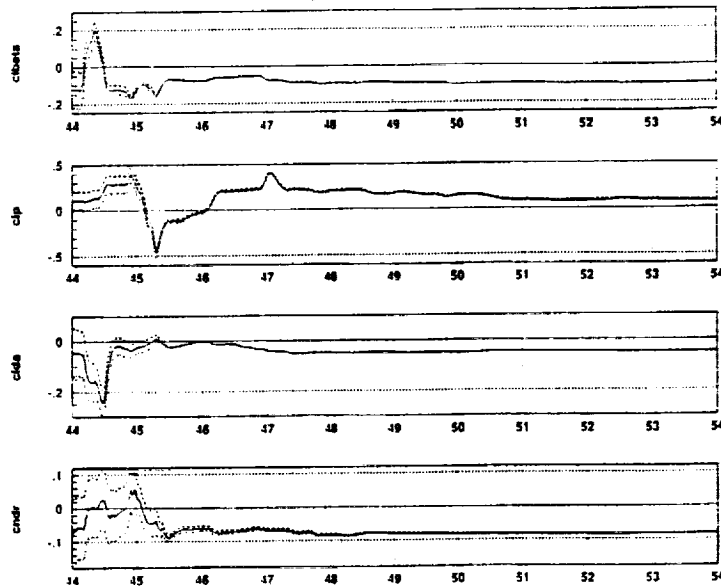
Parameter Estimation

The above plots show the results for the parameter estimation as obtained by applying the extended Kalman filter algorithm to the same maneuver discussed in the previous slide. Shown are the estimates for the dihedral effect, the roll-damping, the aileron effectiveness, and the rudder effectiveness. The solid lines represent the estimates while the accompanying dotted lines represent the standard errors associated with those estimates. The estimates were initialized at the values obtained from applying linear regression to the same maneuver. As seen from the plots, all four estimates return to values that are close to the initial values, indicating that the extended Kalman filter estimates are in close agreement with the linear regression estimates.
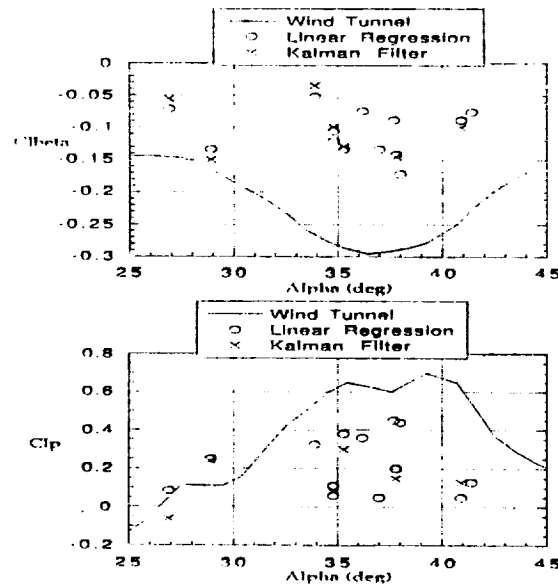
Comparison of Results

Shown are the comparison of the estimates obtained for the dihedral effect and the roll-damping as obtained from wind tunnel data and from the application of linear regression and extended Kalman filter methods to flight test data. Notice first that the estimates obtained using linear regression and the extended Kalman filter algorithm agree well with each other for the flight regime under study. The apparent scatter in the estimates may be attributed to the fact that each estimate was obtained from a different maneuver and it ispossible that the estimates are sensitive to the particular maneuver. It appears, however, that there are some significant differences between estimates obtained from wind tunnel data and those obtained from flight data. Several comments may be made about this. First, the estimates obtained from wind tunnel data were obtained from static wind tunnel testing and thus were not subject to the dynamic effects encountered during the flight tests. Thus, the estimates obtained from flight data can be said to embody the dynamics of the aircraft, whereas those obtained from wind tunnel data do not. In addition, for the case of the roll-damping, the wind tunnel estimates are known to be extremely sensitive to the oscillation amplitude as well as the canard setting of the model during the wind tunnel testing. Further investigations to fully explain these differences are currently underway.

COMPARISON OF RESULTS
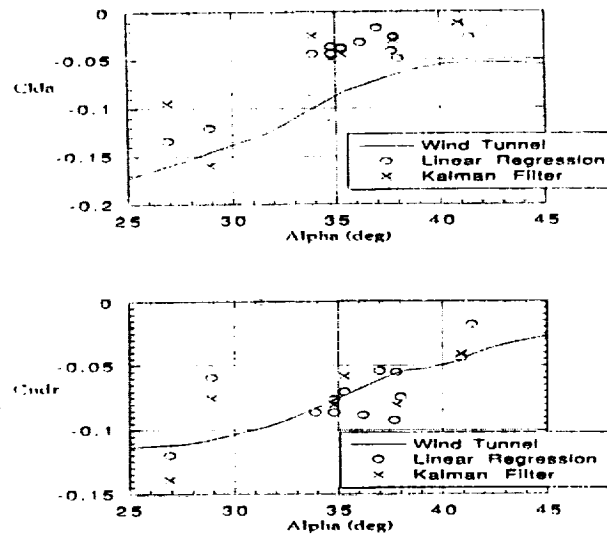
Comparison of Results

Similar plots shown in the previous slide are shown in this slide for the aileron effectiveness and rudder effectiveness. Note again that the estimates obtained from flight data through linear regression and extended Kalman filter methods are in good agreement with each other. Note also that estimates obtained from wind tunnel data seem to be in better agreement for the two control derivatives than for the previous two stability derivatives. A systematic difference is seen between flight data estimates and wind tunnel estimates for the aileron effectiveness. Preliminary results obtained from X-31 full-scale flight tests seem to favor the estimates obtained from flight data. All estimates seem to be in good agreement for the rudder effectiveness. Note that both the rudder and the aileron have decreased effectiveness with increasing angle of attack, as would be expected.

FUTURE WORK

Future Research will likely include the following:

- **Comparison of Wind Tunnel, Drop Model, and Full Scale Aircraft Results.**

- **Explanation of possible differences in results using various Experiments and/or Estimation Techniques.**

- **Extension of research to longitudinal data.**

Future Research

Future research to be conducted in this area will likely include a comparison of wind tunnel, drop model, and full-scale aircraft results. An attempt will be made to explain any differences that may appear in the results obtained using these various experiments and estimation techniques. And finally, an extension of this research will be made to determine the longitudinal aerodynamic characteristics of the X-31.

Nonlinear Aerodynamic Modeling using Multivariate Orthogonal Functions

by

Eugene A. Morelli

Lockheed Engineering and Sciences Co.

Aircraft Guidance and Control Branch

NASA Langley Research Center

March 19, 1993

Complete details can be found in:

Morelli, E.A., *Nonlinear Aerodynamic Modeling using Multivariate Orthogonal Functions*, AIAA paper 93-3636, Atmospheric Flight Mechanics Conference, Monterey, CA, August 1993.

The problem to be addressed in this work is that of modeling nondimensional force and moment aerodynamic coefficents over the entire subsonic envelope. The particular application discussed here is the Z force coefficient for the F-18 High Angle of Attack Research Vehicle (HARV).

System Identification for Aircraft

A priori knowledge:

Rigid Body Dynamics

Aerodynamics

Wind Tunnel Data

Flight Test Data

High Fidelity
Mathematical
Description
of the
Aircraft Dynamics
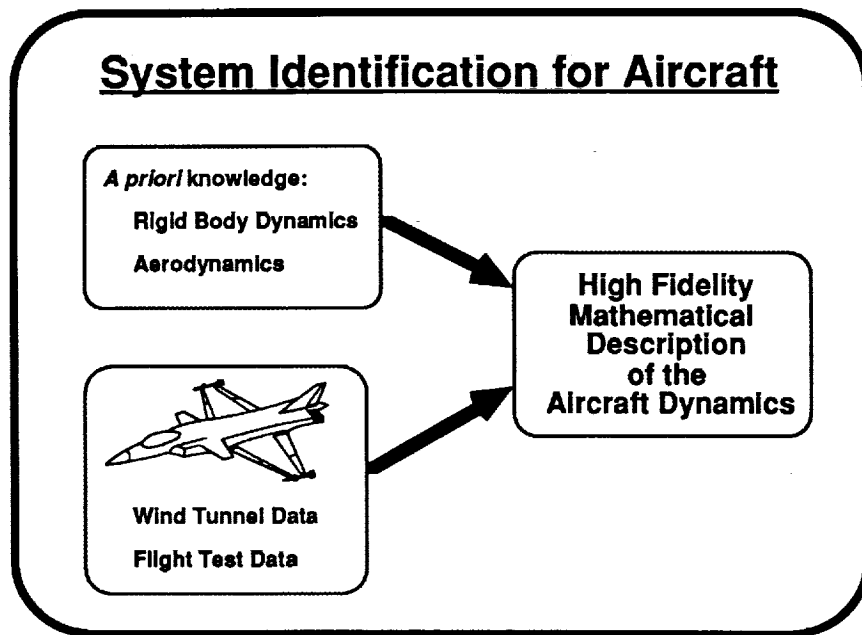
In general for high fidelity math models of aircraft dynamics, some a priori knowledge is combined with experimental data. The experimental data generally supplies the information on the aerodynamics particular to the aircraft under study.

Aircraft Equations of Motion

Force
Equations

$$\dot{U} = -QW + RV + g_x + \frac{\bar{q}\,S\,C_x + T}{m}$$

$$\dot{V} = -RU + PW + g_y + \frac{\bar{q}\,S\,C_y}{m}$$

$$\dot{W} = -PV + QU + g_z + \frac{\bar{q}\,S\,C_z}{m}$$

Shown here are the three nonlinear equations of motion for translational motion of an aircraft. Moment equations are omitted for simplicity, but the same discussion can be applied to them as well. The objective is to find a model for the aerodynamic coefficients, like Cz, in terms of the aircraft states and outputs and their derivatives, and the controls. This would allow prediction of dynamic behavior when such models are substituted into the equations above, along with a model for the thrust.

Aerodynamic Modeling

$$C_z = C_z \left(\alpha, \ M, \ \overline{Q}, \ \widehat{\alpha}, \ \delta_s, \ \delta_n, \ \delta_r \right)$$

where $\overline{Q} = \dfrac{Qc}{2V}$, $\widehat{\alpha} = \dfrac{\dot{\alpha}\,c}{2V}$

$$\overline{C}_z = c_0 + c_1 \, \alpha + c_2 \, M + c_3 \, \overline{Q} + c_4 \, \widehat{\alpha} + c_5 \, \delta_s + c_6 \, \delta_n + c_7 \, \delta_r$$
$$+ c_8 \, \alpha \, M + c_9 \, \alpha^2 \, \overline{Q} + \ldots \, ?$$

Key Questions:

- What terms should be included ?

- What are the parameter values ?

- When is a given expansion valid ?

Part of the a priori knowledge is the functional dependence shown on the first line of this slide. Using this information, a polynomial model is postulated which is analogous to a truncated multivariable Maclaurin series expansion for Cz. This approach gives rise to the three questions posed at the bottom of the slide.

Aerodynamic Coefficient Expansion

$$\overline{C}_z = c_0 + c_1\,\alpha + c_2\,M + c_3\,\overline{Q} + c_4\,\hat{\overline{\alpha}} + c_5\,\delta_s + c_6\,\delta_n + c_7\,\delta_f$$
$$+ c_8\,\alpha\,M + c_9\,\alpha^2\,\overline{Q}$$

**Usually difficult to accurately estimate parameters
in this expansion from experimental data because:**

- Experimental data does not contain sufficient information

- Control system or the experiment correlates the regressors

- The model structure is in question

Assuming now that the number of terms to be included has been determined somehow (perhaps using stepwise regression), and the range of validity of this expansion has also been determined, there remain further difficulties in accurately estimating the parameter values (the c's) in the model. These difficulties are listed on this slide.

Aerodynamic Coefficient Expansion in Terms of Orthogonal Functions

$$C_z = a_1 \xi_1 + a_2 \xi_2 + \ldots + a_n \xi_n$$

where in general

- $\xi_i = \xi_i(\alpha, M, \widehat{Q}, \widehat{\alpha}, \delta_s, \delta_n, \delta_r)$ for $i = 1, 2, \ldots, n$

- $\xi_i^T \xi_j = 0$ for $i \neq j$

- $a_i = \dfrac{\xi_i^T C_z}{\xi_i^T \xi_i}$ $\longrightarrow$ the ith term in the model depends only on C_z and ξ_i

If instead of ordinary polynomials in the expansion for Cz, orthogonal polynomials with the properties shown on this slide were used, the difficulties in accurately estimating the model parameters disappear. This is because the computation of the value of the model parameter for term i depends only on the measured data (Cz) and orthogonal function i. This follows from the expansion for Cz in terms of orthogonal polynomials and the properties of orthogonal polynomials.

394

Model Structure Determination

- Minimum predicted square error is the criterion for which orthogonal functions should be included in the model :

$$PSE = \frac{1}{N} \sum_{i=1}^{N} (C_{z_i} - \overline{C}_{z_i})^2 + 2\sigma_p^2 \frac{n}{N}$$

where

$$\sigma_0^2 = \frac{1}{N} \sum_{i=1}^{N} (C_{z_i} - \overline{C}_z)^2 \quad ; \quad \overline{C}_z = \frac{1}{N} \sum_{i=1}^{N} C_{z_i}$$

$$\sigma_p^2 = \frac{\sigma_0^2}{2}$$

The orthogonal functions to be included in the model can be determined in a straightforward way using the predicted square error (PSE) criterion, where n is the number of terms in the model and N is the number of data points. Since each term in the orthogonal function expansion is independent of all the others, the decision of whether or not to include each individual orthogonal function term can be made based on whether or not its inclusion reduces PSE. This can be done for each term sequentially and without regard to any other terms already in the model.

Finding Ordinary Polynomial Models

$$C_z = a_1\,\xi_1 + a_2\,\xi_2 + \ldots + a_n\,\xi_n$$

It is possible to :

- Generate orthogonal functions based on the data using a technique similar to Gram-Schmidt orthogonalization

- Determine the orthogonal function expansion by decrease in fit error vs. additional terms

- Decompose each orthogonal function without ambiguity in terms of ordinary polynomials, e.g.

$$\xi_1 = b_1\,\alpha + b_2\,M + b_3\,\alpha\,\delta_s$$

- Arrive at an ordinary polynomial model with adequate structure and accurately estimated parameters

Details of how to generate multivariate orthogonal functions based on the data can be found in the reference given on the first slide. In that reference, it is also shown that each orthogonal function can be decomposed precisely into an expansion in terms of ordinary polynomials. Once the model structure determination is done in terms of orthogonal functions, the expansions for each included orthogonal function in terms of ordinary polynomials is substituted and common terms are combined, resulting finally in an ordinary polynomial model with adequate model structure and accurately estimated model parameters

Full Envelope Expansion for the F-18 HARV from Wind Tunnel Data

$$C_z = c_1 + c_2\alpha + c_3\alpha^2 + c_4\delta_s + c_5\alpha^3 + c_6\alpha\delta_s + c_7\alpha^2\delta_s + c_8 M$$
$$+ (c_9 + c_{10}\alpha + c_{11}M + c_{12}\alpha^2 + c_{13}\alpha M + c_{14}\alpha^2 M$$
$$+ c_{15}\alpha^3 + c_{16}\alpha^4 + c_{17}\alpha^3 M + c_{18}\alpha^4 M)\ \bar{Q}$$
$$+ (c_{19} + c_{20}\alpha + c_{21}M + c_{22}\alpha^2$$
$$+ c_{23}\alpha M + c_{24}\alpha^2 M + c_{25}M^2 + c_{26}\alpha^3)\ \hat{\alpha}$$
$$+ (c_{27} + c_{28}\alpha)\ \delta_n + (c_{29} + c_{30}\alpha + c_{31}M)\ \delta_r$$

Valid for:

-4.0 deg $\leq \alpha \leq 90$ deg	
$0.2 \leq M \leq 0.9$	
-24.0 deg $\leq \delta_s \leq 10.5$ deg	
-3.0 deg $\leq \delta_n \leq 33.0$ deg	
-8.0 deg $\leq \delta_r \leq 45.0$ deg	

This is the result of using the technique developed here to model the Z aerodynamic force coefficient for the F-18 HARV over the entire subsonic flight envelope, based on a wind tunnel database.

Flight Test Maneuver
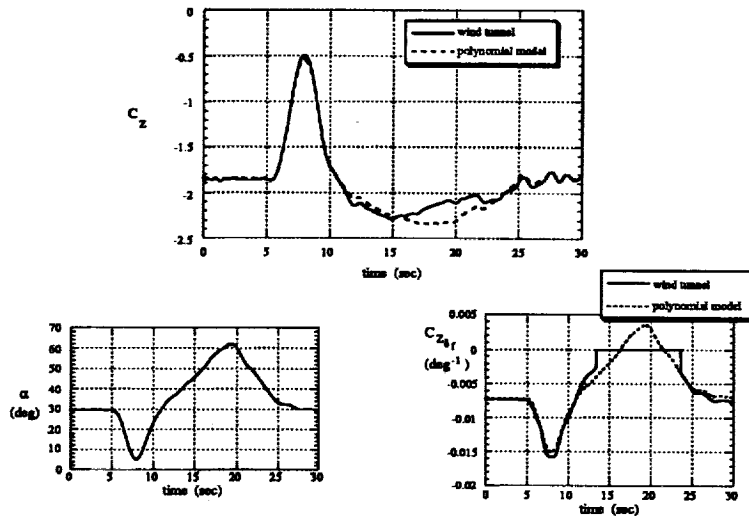
A prediction case for the polynomial model is shown here, using independent variable time histories taken from flight data. The prediction is excellent, with slight error in the time period from 13 to 23 seconds. This was traced to the fact that the wind tunnel database zeroed certain components of the Z force coefficient when angle of attack exceeded 40 degrees, because of lack of data. The polynomial model, on the other hand, extrapolated reasonably, as shown on the lower right plot.

Features of the Model

- Large tables of aerodynamic data reduced to
  a small number of parameters

- Smooth aerodynamic functions and partial derivatives

- Better insight on the aerodynamic functional dependence

- Potential for automated simulator updates

- One model for the entire flight envelope

Along with the improved accuracy
of model parameters and excellent
prediction capability inherent in
the modeling approach discussed here,
this slide outlines the some features
of nonlinear aerodynamic models
generated with this technique.

Conclusion

Accomplishment

- Developed and demonstrated a full envelope nonlinear aerodynamic modeling technique

Applications

- Flight Simulators

- Global Stability and Control Analysis

- Dynamic Analysis

- High Angle of Attack Control Design

The fact that the aerodynamic model for a full subsonic envelope can be made compact and smoothly differentiable while retaining excellent predictive capability has potential utility in a wide range of activities.

A Study Of Roll Attractor And Wing Rock of Delta Wings at High Angles Of Attack

T.Niranjana, D.M.Rao and Bandu N. Pamadi
Vigyan Research Associates Inc.,

NASA LaRC Workshop on GNC, Dynamics
For Atmospheric Flight
NASA Langley Research Center
Hampton, Va

March 18,19, 1993.

Wing Rock

• What is Wing Rock?

Wing rock is a high angle of attack dynamic phenomenon of limit cycle motion predominantly in roll. One of the earliest observation of wing rock was made by Mckinney and Drake (NACA RM No. L7k07 (1948)) in free flight model tests. The wing rock is one of the limitations to combat effectiveness of the fighter aircrafts. Interest in wing rock has picked up considerably following the study of Nguyen et.al (AIAA Paper No.81-1883 (1981)).

• Causes of Wing Rock

• Nonlinearities in static rolling and yawing moments at high alpha.
• Static hysterisis of rolling moment with roll/sideslip angles.
• Dependence of roll damping on roll/sideslip angle such that negative damping occurs at small angles and positive damping at high angles.
• Nonlinear variation in roll damping with roll rate.

Roll Attractor

- What is Roll Attractor?

The steady state or equilibrium trim angle (ϕ_{trim}) attained by the free-to-roll model, held at some angle of attack, and released from rest at a given initial roll (bank) angle (ϕ_0).

- Multiple Roll Attractors.

Model attains different trim angles (ϕ_{trim}) depending on initial roll angle (ϕ_0)

Previous Studies of Roll Attractor Phenomenon

- Hanff and Ericson, Paper 31, AGARD CP-494, 1990

- Jenkins, Myatt and Hanff (AIAA 93-0621)

- Model Tested: $65deg$ Delta Wing.

$\alpha \leq 20deg, \phi_{trim} = 0$

$\alpha = 20deg, \phi_{trim} = \pm 1.5deg$

$\alpha = 30deg, \phi_{trim} = 0, \pm 21.0deg$

$\alpha = 35deg, \phi_{trim} = \pm 11.0deg$

$\alpha \geq 40deg, \phi_{trim} = 0$

Hanff and Ericson (1990)

α = 30deg
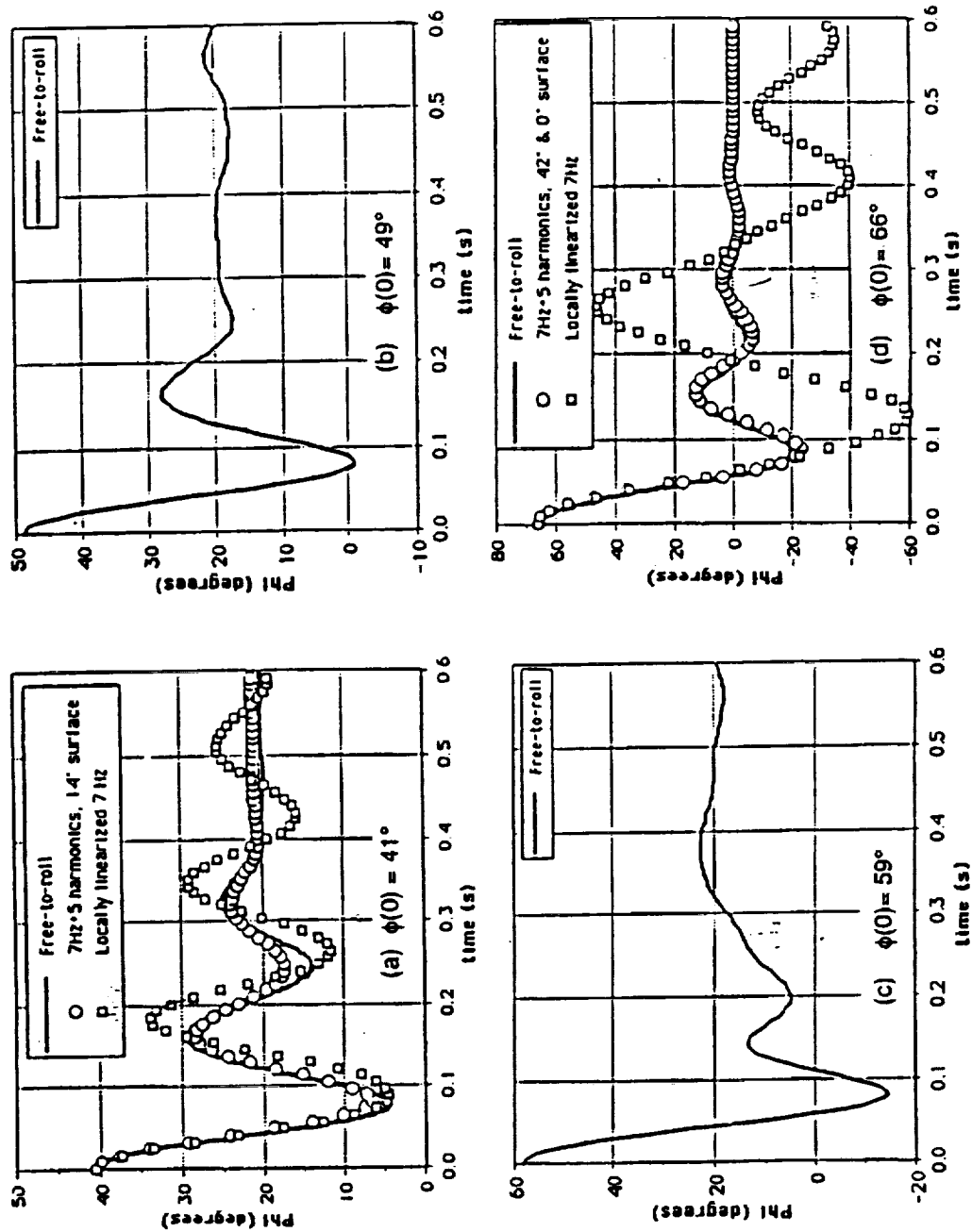
Fig.5 Free-to-roll motion histories.

Outline Of Presentation

- Test Facility and Experimental Work.

- Mathematical Modelling Of Roll Attractor Phenomenon.

- Analysis And Comparison Of Predictions With Experimental Data.

- Concluding Remarks.

Experimental Work

● Test Models:

(1) 80 Deg. Delta Wing (Wing Rock Studies and Effect of Fences on Wing Rock)
(2) 60 Deg. Delta Wing (Roll Attractor Studies)
(3) Aircraft Model With 60 Deg. Delta Wing (Wing Rock And Roll Attractor Studies)

● Test Facility:
Vigyan's Low Speed Wind Tunnel, 3ft x 4ft, Maximum speed = 175 ft/sec

● Sensors:
Rate Gyro for Roll Rate and Accelerometer for Roll Angle

80 Deg Delta Wing

Model Geometry
View of The Model Mounted in Wind Tunnel
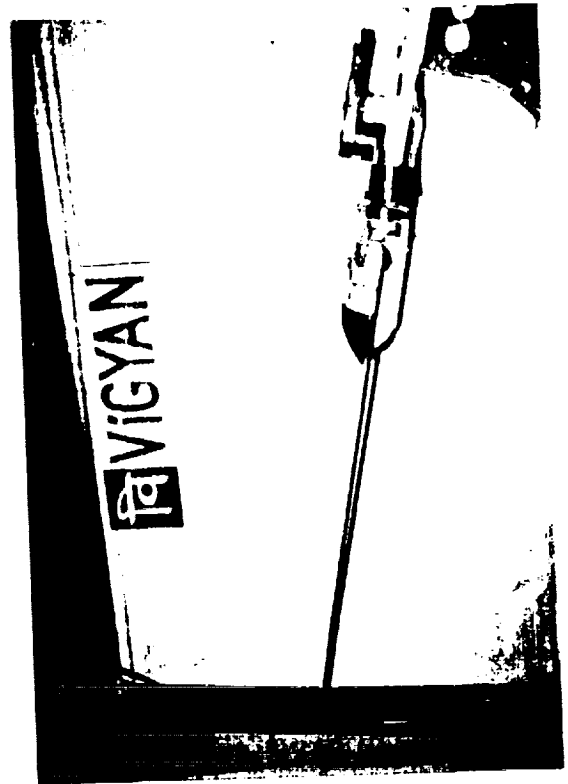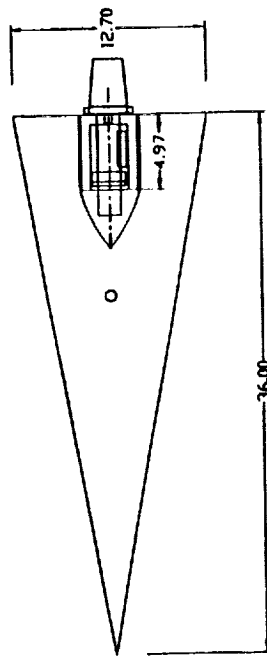
Geometry of Various Fences Employed
For 80 Deg Delta Wing

Apex fence

Leading edge fence

Chordwise fence

Spanwise fence
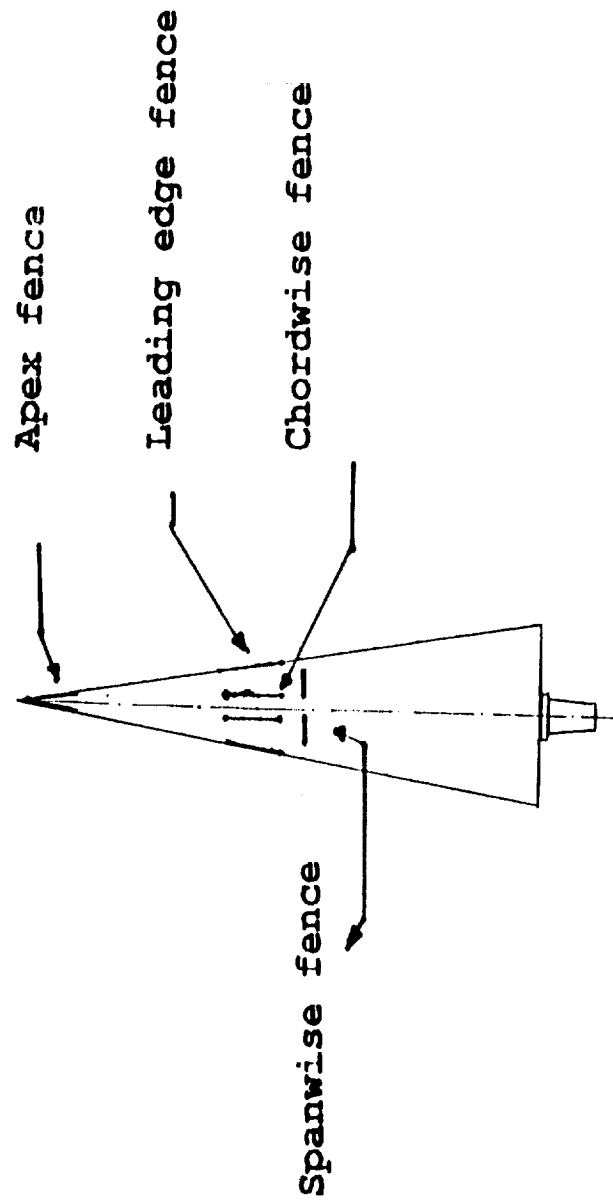
60 Deg Delta Wing Model

Model Geometry
View of The Model Mounted in Wind Tunnel
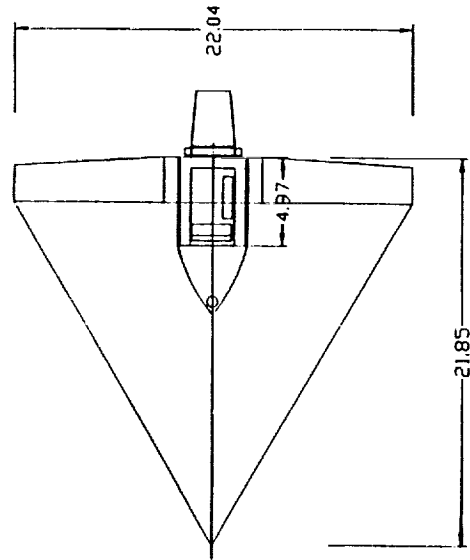
Aircraft Model With 60 Deg Delta Wing

Model Geometry
View of The Model Mounted in Wind Tunnel

411
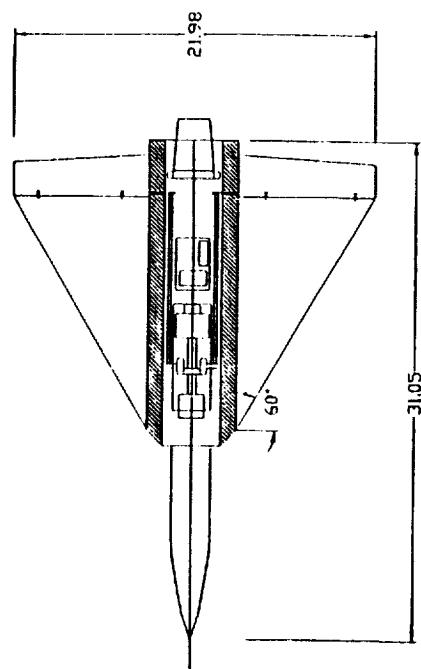
Wing Rock Buildup of 80 Deg Delta Wing

$\alpha = 25$ Deg

We observed that the value of α for the onset of wing rock was around 25 Deg, which is consistent with pre-vious studies.

$\alpha = 25$ deg. Phase plane

Roll rate

Roll angle

Wing rock buildup

Roll angle

Time.. sec

412
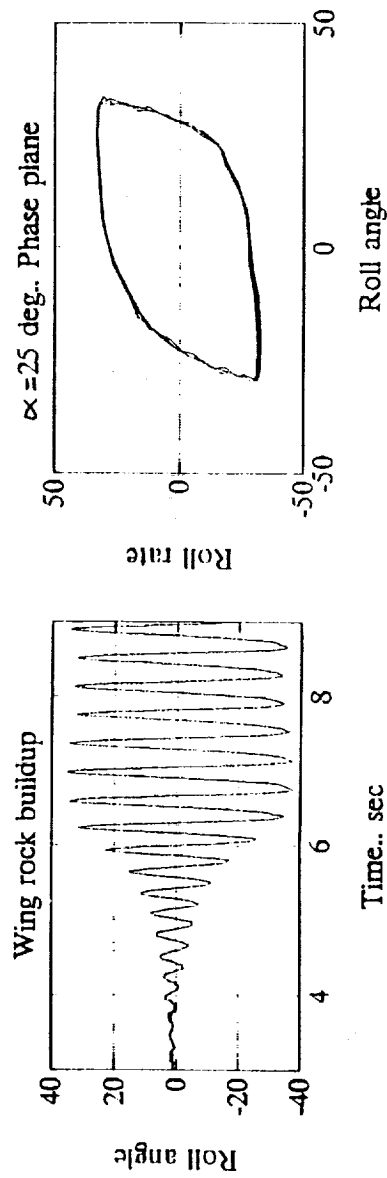
Effect of Various Fences on Wing Rock of 80 Deg Delta Wing

For $\alpha \leq 25$ Deg, we observed that the fences donot have any major effect on the roll damping. Typical results obtained at $\alpha = 20 Deg$ are presented below.

413
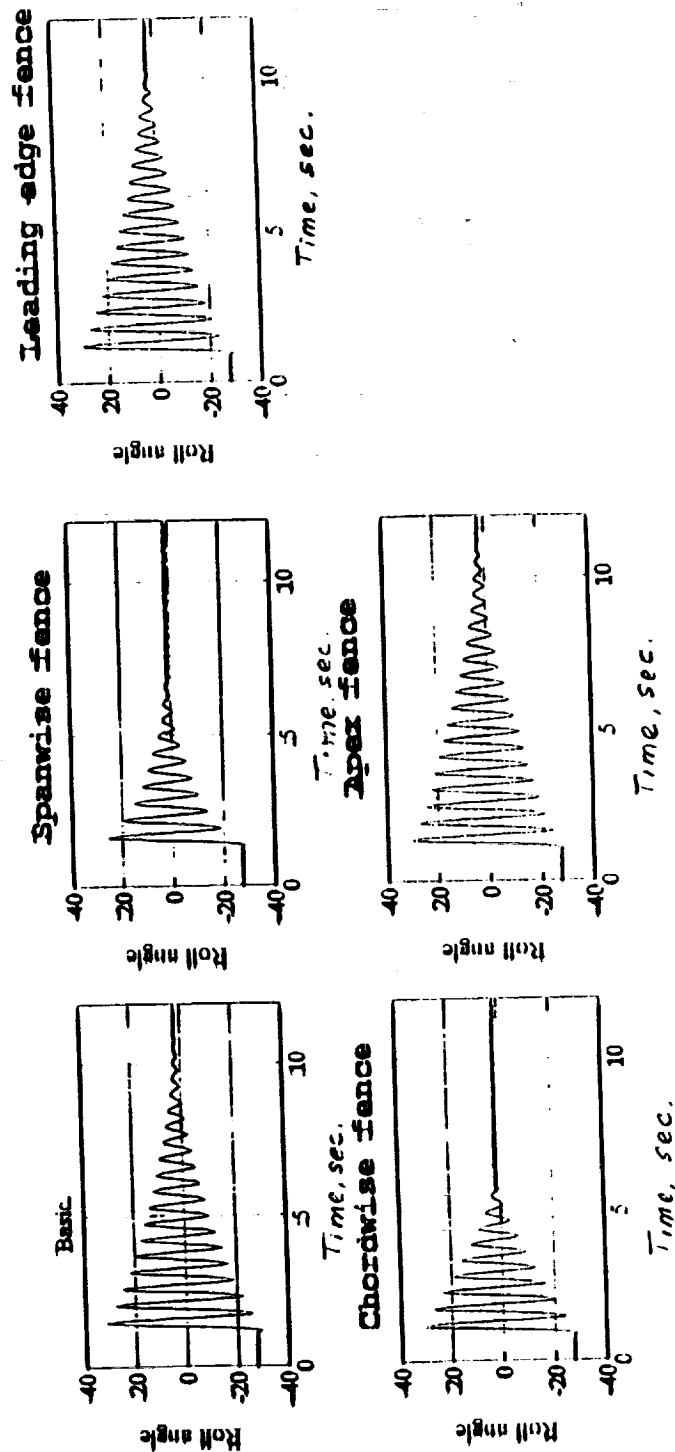
Effect of Various Fences on Wing Rock
of 80 Deg Delta Wing
(Continued....)

Spanwise fences are found to be effective in suppressing the wing rock motion.

$$\alpha = 30deg$$
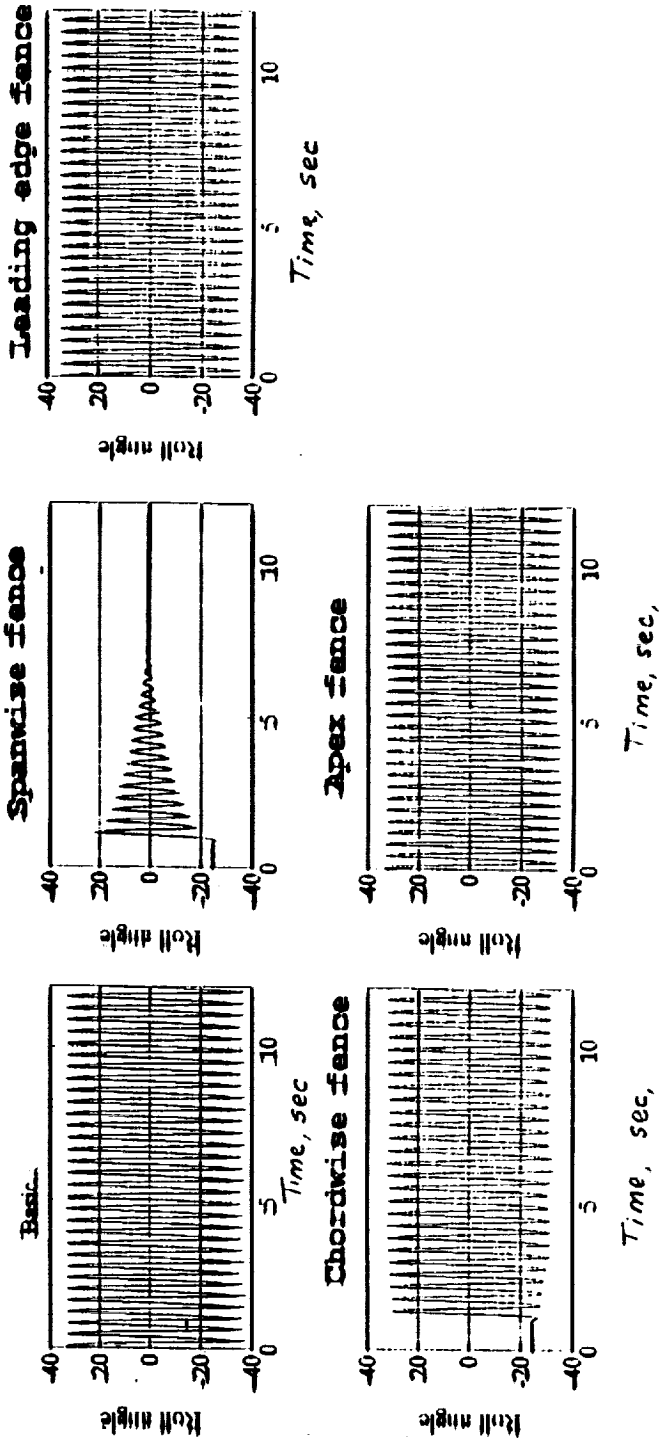
Present Roll Attractor Experimental Results

60 deg Delta Wing Model
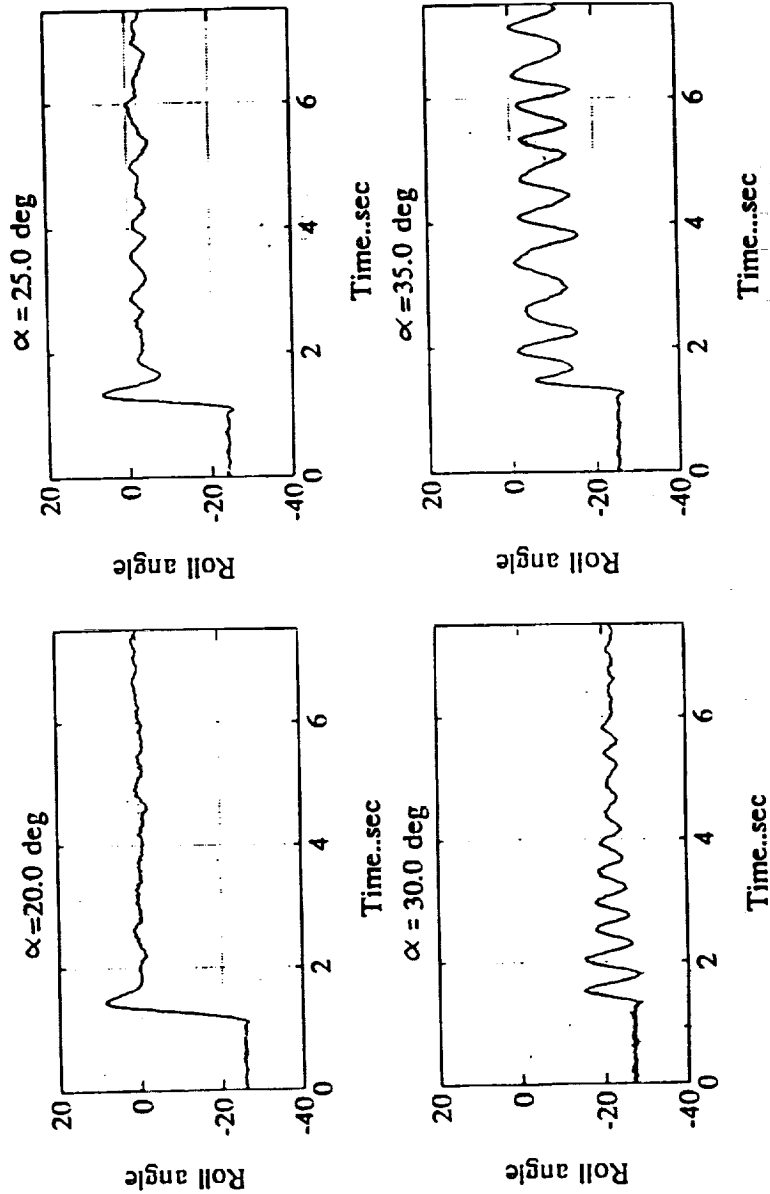
Present Roll Attractor Experimental Results (Continued..)

60 deg Delta Wing

$\alpha = 40.0$ deg
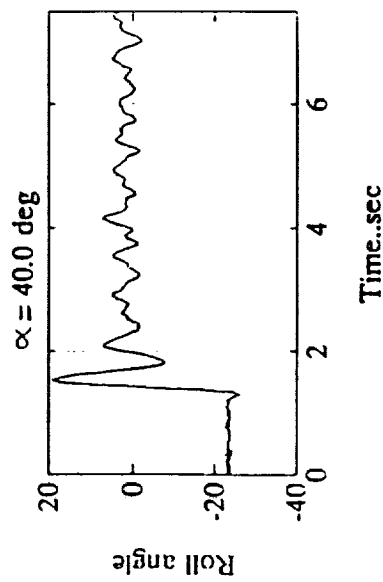
Summary of Roll Trim Angles

$\alpha \leq 20deg,\ \phi(trim) = 0$

$\alpha = 25deg,\ \phi(trim) = \pm3.5deg$

$\alpha = 30deg,\ \phi(trim) = 0, \pm21.0deg$

$\alpha = 35deg,\ \phi(trim) = \pm11.0deg$

$\alpha \geq 40deg,\ \phi(trim) = 0$

Experimental Results of Aircraft Model With 60 Deg Delta Wing

This generic aircraft model with 60 deg delta wing exhibits "one sided" wing rock. It may be noted that the 60 deg delta wing alone does not exhibit wing rock but has non zero roll trim angles as noted earlier. Hence it is evident that the forebody must be responsible for creating wing rock since tail apparently has no effect.

$\alpha = 26.5$ deg

417
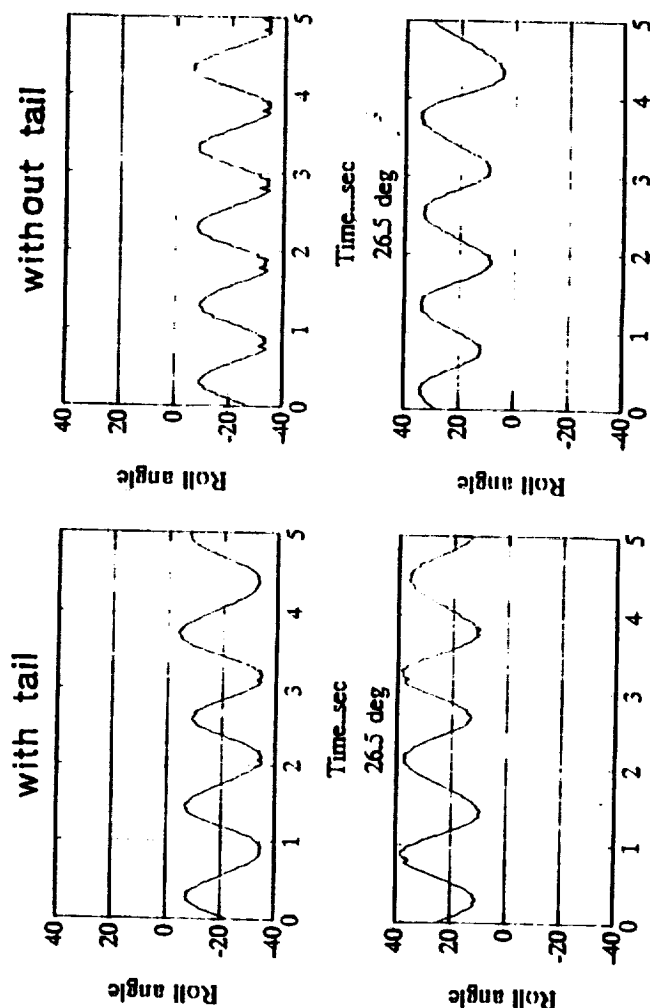
Simulation Of Model Motion In Roll Attractor Studies

- Single DOF Free-To-Roll Motion

$$I_x \ddot{\phi} = L_{\dot{\phi}} \dot{\phi} + L(\phi)$$

$$\ddot{\phi} = \frac{L_{\dot{\phi}} \dot{\phi}}{I_x} + \frac{L(\phi)}{I_x}$$

$$\ddot{\phi} = C_{lp} \dot{\phi} + C_l(\phi)$$

- Method of Solution:

(i) Use $C_l(\phi)$ from experimental data of Hanff (1993).

(ii) Use C^2 cubic splines to interpolate data

(iii) Assume C_{lp} constant

(iv) Do Numerical integration using Matlab

418

Experimental Static Rolling Moment
Coefficient, Hanff et.al (1993)
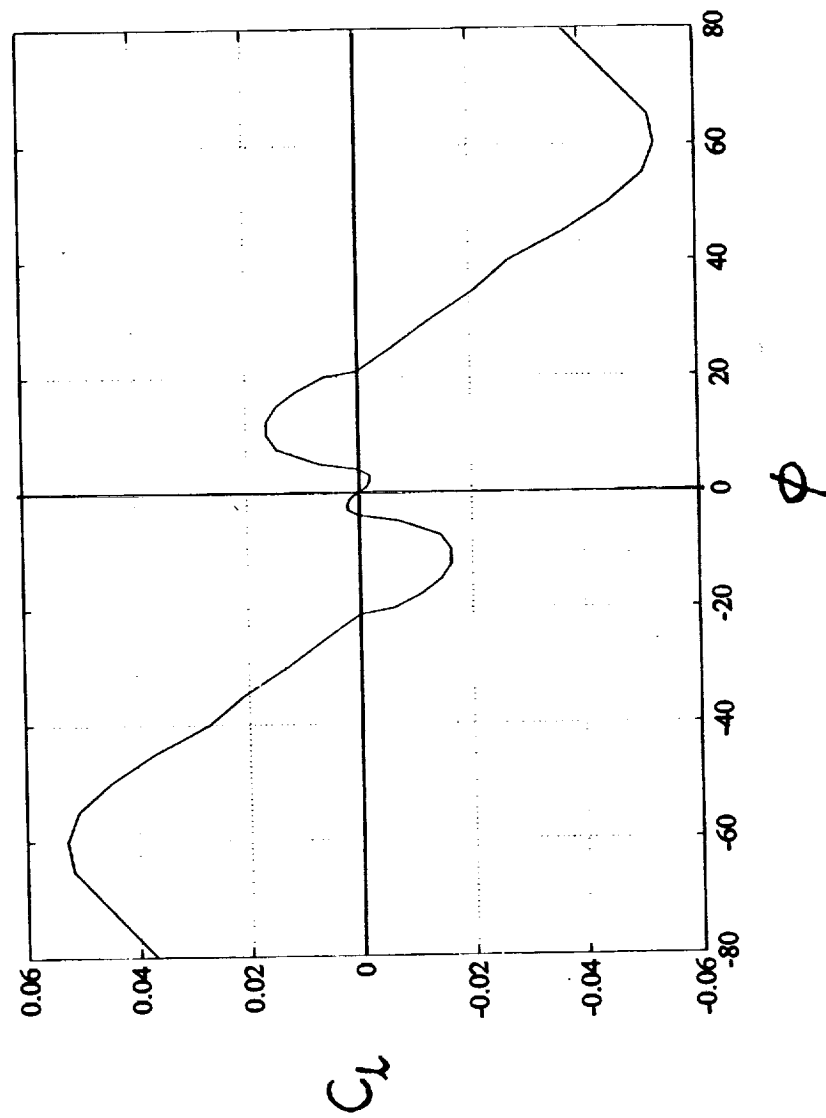
Solution Structure

- Represent the plant model in state-space form

$$\dot{x} = F(x)$$

where $x \varepsilon R^2$, $x_1 = \phi$ and $x_2 = \dot{\phi}$.

$$F(x) = \begin{bmatrix} x_2 \\ -C_{lp} x_2 + C_l(x_1) \end{bmatrix}$$

- Attractor:

The set of all trajectories starting from different initial conditions but ending in the same subspace of the given state-space as $t \to \infty$

- Fixed points/Equilibrium solutions can form elements of attractor set.

420

Fixed Points/Equilibrium Solutions

For Fixed Points, $F(x) = 0$.

i.e, $x_2 = 0$ and $C_l(x_1) = 0$

From Experimental C_l vs $\phi(x_1)$ graph,

$x_{10} = 0, \pm 4deg, \pm 21deg.$ (3 Attractors)

● Stability Of Fixed Points

Let $x(t) = x_0 + y(t)$. Assume $F(x)\epsilon C^2$.

Ignoring second and higher order terms, we get,

$\dot{y} = Ay$

A is the Jacobian matrix of first partials of $F(x)$.

Stability of Fixed Points

● Stable Node - If Eigen Values Of A are real and negative.

● Unstable Node - If Eigen Values Of A are real and positive.

● Saddle Point - If Eigen Values Of A are real, some and positive and others negative.
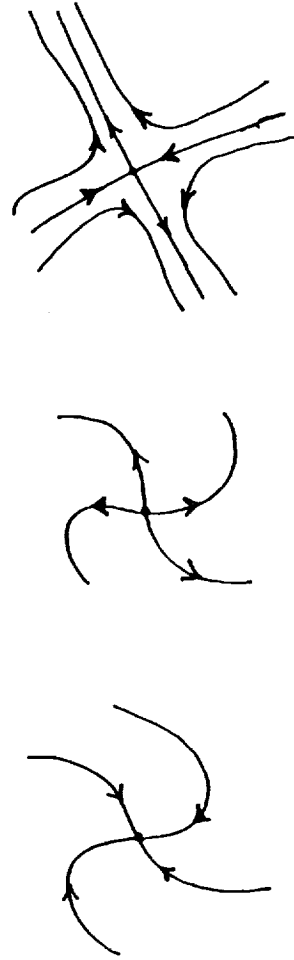
Stable Node   Unstable Node   Saddle Point

Fixed Points

We have three fixed points. The associated eigen values and the nature of the fixed point (node) are as follows,

(a) $x_{10} = 0, x_{20} = 0, \lambda_1 = -0.009166, \lambda_2 = -0.1908338$; (Stable Node)

(b) $x_{10} = \pm 4, x_{20} = 0, \lambda_1 = 0.021854, \lambda_2 = -0.221854$; (Saddle Point)

(c) $x_{10} = \pm 21, x_{20} = 0, \lambda_1 = -0.03558369, \lambda_2 = -0.1645416$; (Stable Node)

Results Of Simulation
(Phase Plane Trajectories)

Phase Plots With Different Initial Roll Angles
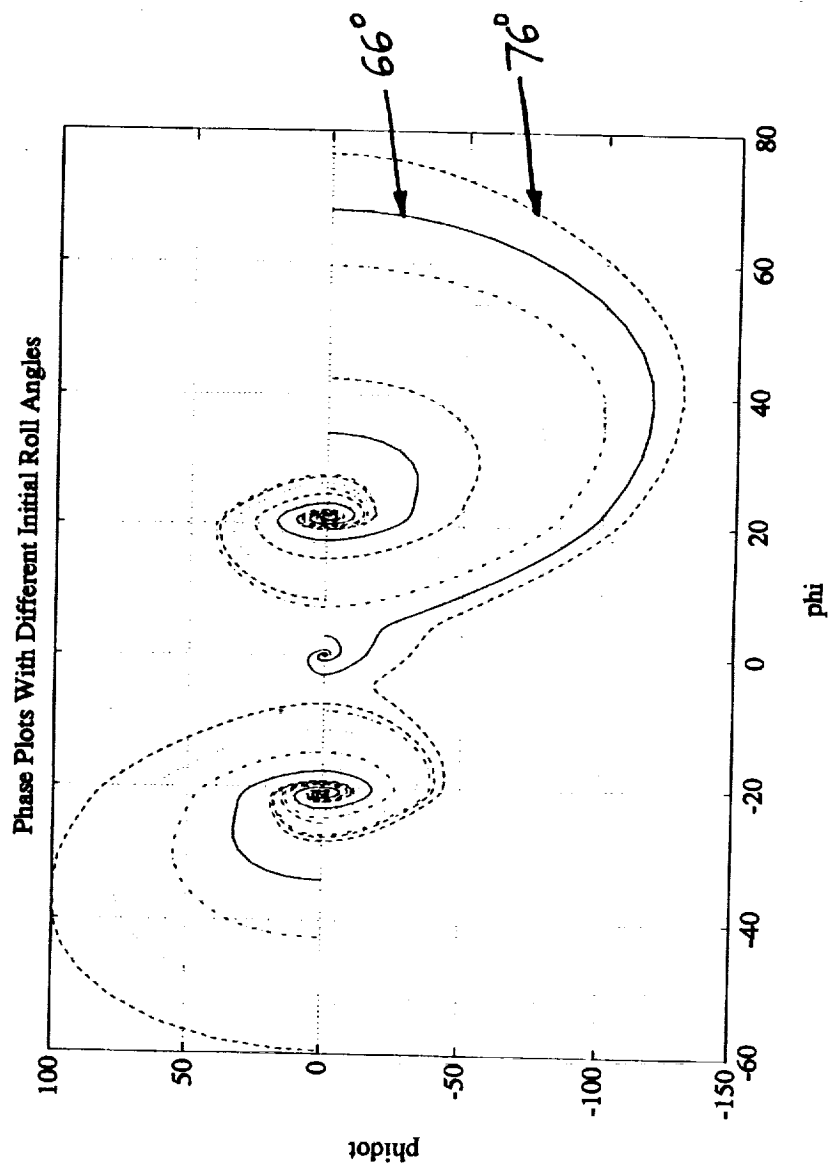
Results Of Simulation (Time Histories)

Time Histories With Different Initial Roll Angles
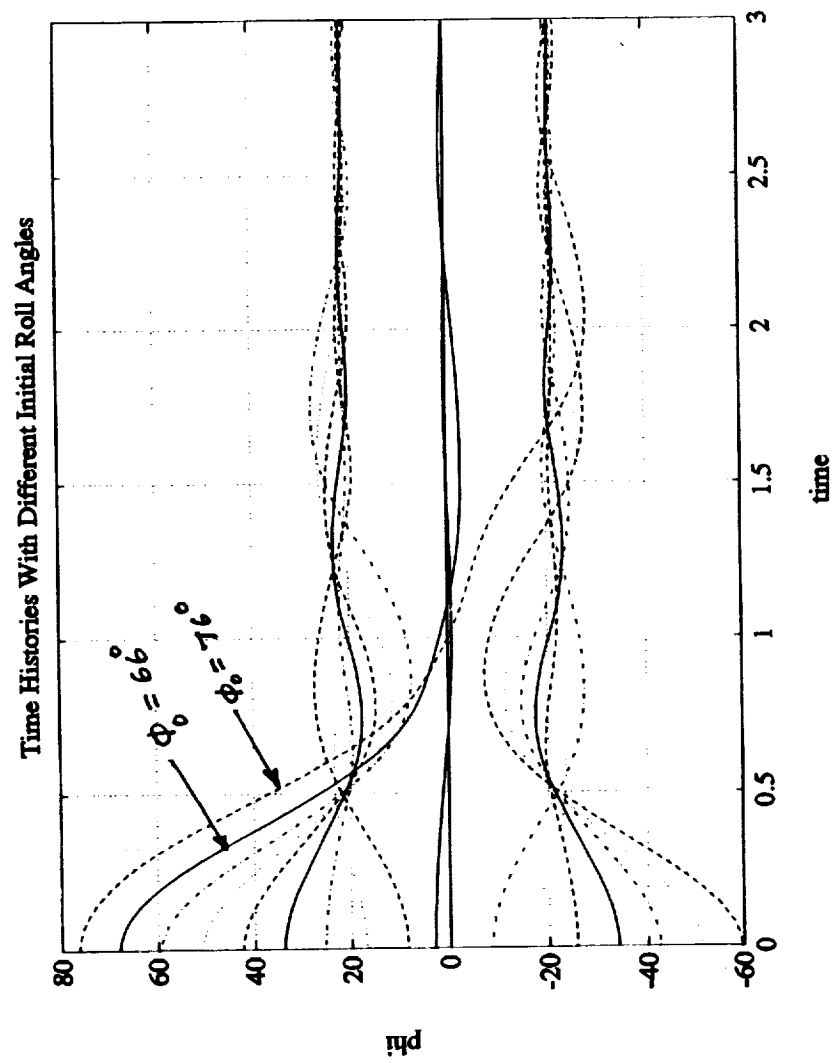
Predicted And Measured Time Histories
(First 3 Seconds)
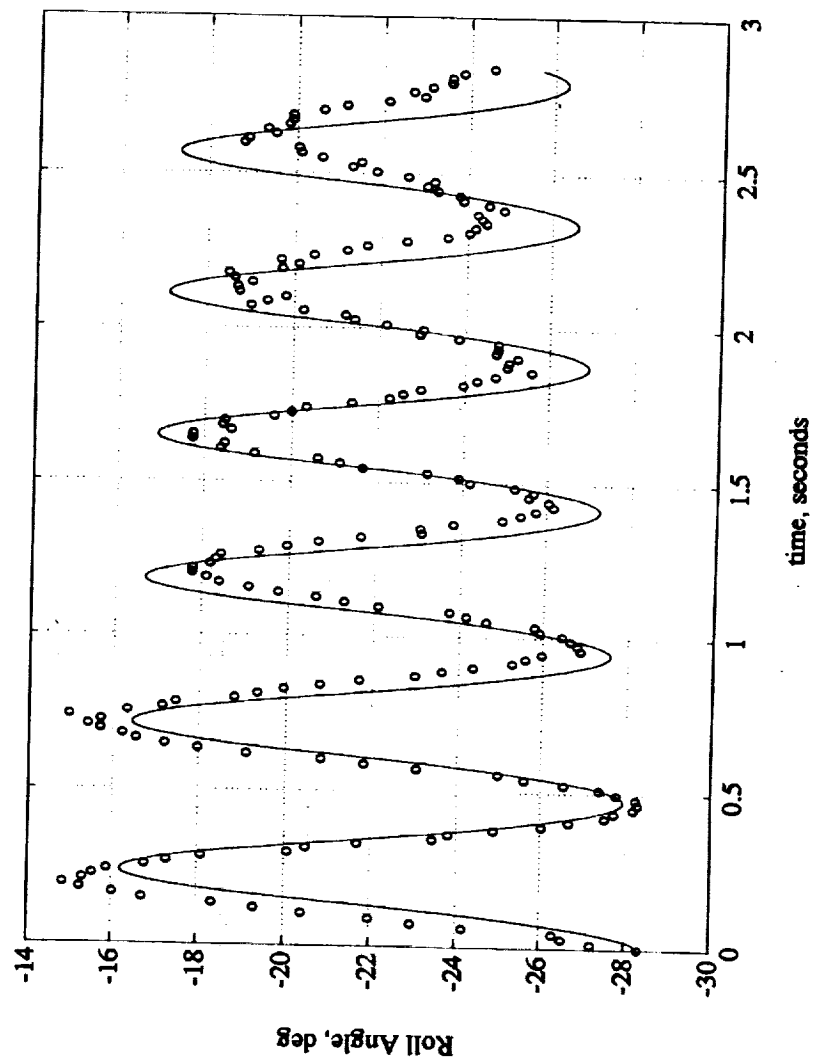
Comparison Of Predicted And Measured Time Histories (Present Experiments)

It may be noted that the present simulation based on assuming constant roll damping and nonlinear experimental data on rolling moment coefficient predicts the multiple roll trim angles of 60 deg delta wing correctly. The difference in the transients especially at lower roll angles could be due to nonlinearity in roll damping which is ignored here.

427
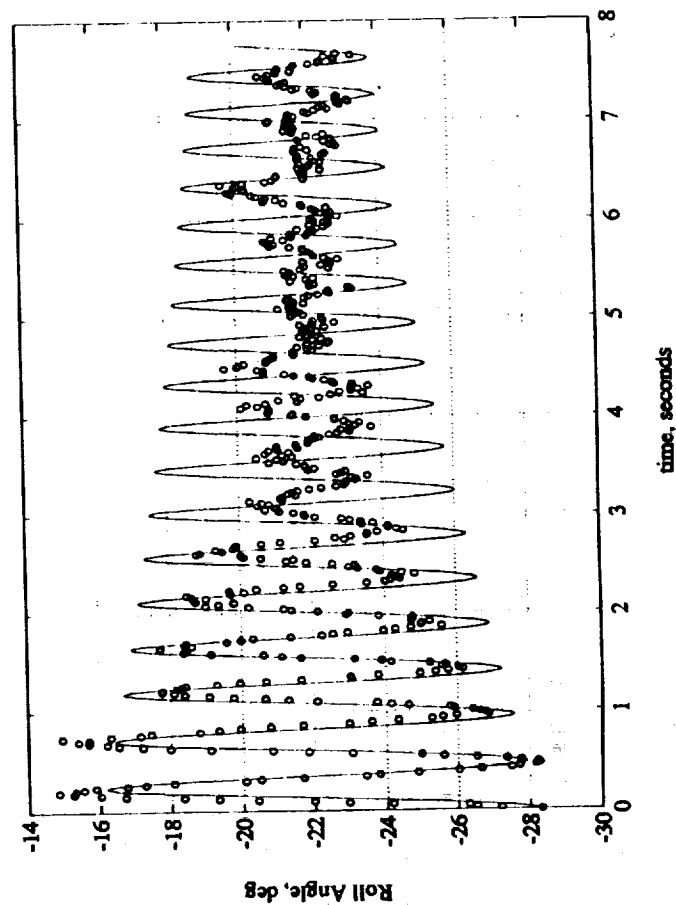
Comparison Of Predicted And Measured Time Histories (Hanff and Ericson)

From this figure we observe that the present simulation predicts all the roll trim angles of Hanff and Ericson. As mentioned previously, the locally linearized simulation of Hanff and Ericson fails to predict the roll trim angle for $\phi(0) = 66deg.$
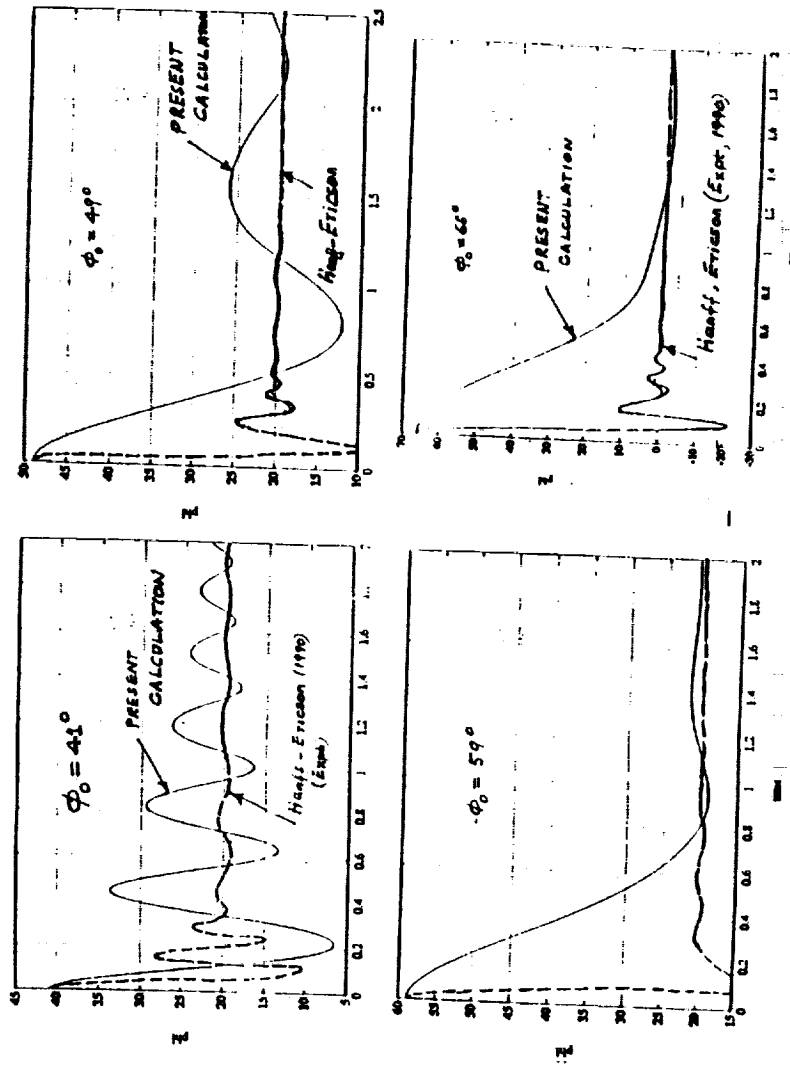
Concluding Remarks

- Experimental Test Facility For Dynamic Semi-Free Flying Models Developed.
- Single DOF, Free-To-Roll Tests Conducted on 80 and 60 deg Delta Wings and Aircraft Model.
- Wing Rock Observed For 80 deg Delta Wings.
- Wing Rock Not Observed For 60 deg Delta Wing, Multiple Roll Attractor Observed.
- Aircraft Model (60 deg Delta Wing) Exhibits One Sided Wing Rock.
- The Simple Math Model Successfully Predicts Multiple Roll Attractors Recorded by Hanff and Ericson. However, The Transients Donot Match.
- Hanff and Ericson Failed To Predict The Roll Attractor For For $\phi_0 = 66 deg.$
- Predicted Transient Is In Better Agreement With Present Experimental Data.

429

Further Work

- Conduct Free-To-Roll Roll Attractor Tests For 60 deg Delta Wing For All the Initial Values Of Hanff and Ericson.
- Consider Nonlinear Damping in Math Model.
- Use Parameter Identification Techniques For Better Matching Of Math Model And Experimental Data.

MODELING TRANSONIC AERODYNAMIC RESPONSE USING NONLINEAR SYSTEMS THEORY FOR USE WITH MODERN CONTROL THEORY

Walter A. Silva
Aeroelastic Analysis and Optimization Branch
Structural Dynamics Division
NASA Langley Research Center
Hampton, VA 23681-0001

Title Chart

This presentation addresses the application of a nonlinear systems theory to the modeling of nonlinear unsteady aerodynamic responses. In particular, transonic aerodynamic responses, such as those computed using CFD codes, will be modeled.

OUTLINE

- Motivation and Approach

- Volterra Theory of Nonlinear Systems

- CAP-TSD Code

- Application to a CFD Model
  (NACA 0012 rectangular wing)

- Concluding Remarks

Outline Chart

The presentation begins with a brief description of the motivation and approach that has been taken for this research. This will be followed by a description of the Volterra Theory of Nonlinear Systems and the CAP-TSD code which is an aeroelastic, transonic CFD (Computational Fluid Dynamics) code. The application of the Volterra theory to a CFD model and, more specifically, to a CAP-TSD model of a rectangular wing with a NACA 0012 airfoil section will be presented. Finally, some concluding remarks will be made.

MOTIVATION FOR RESEARCH

```
┌─────────────────────────────────────────────┐
│      Modern Control Theory (time domain)      │
└─────────────────────────────────────────────┘
```

Current
Approach

Future
Approaches

```
┌──────────────────┐              ┌──────────────────┐
│ Time-domain      │              │ Nonlinear        │
│ Approximate      │              │ Aerodynamics     │
│ Aerodynamics     │              └──────────────────┘
└──────────────────┘
          ↑ RFAs                                • Transonic
┌──────────────────┐            CFD <             behavior
│ Linear           │
│ Frequency-       │
│ Domain Aero      │                              • High alpha
└──────────────────┘
```
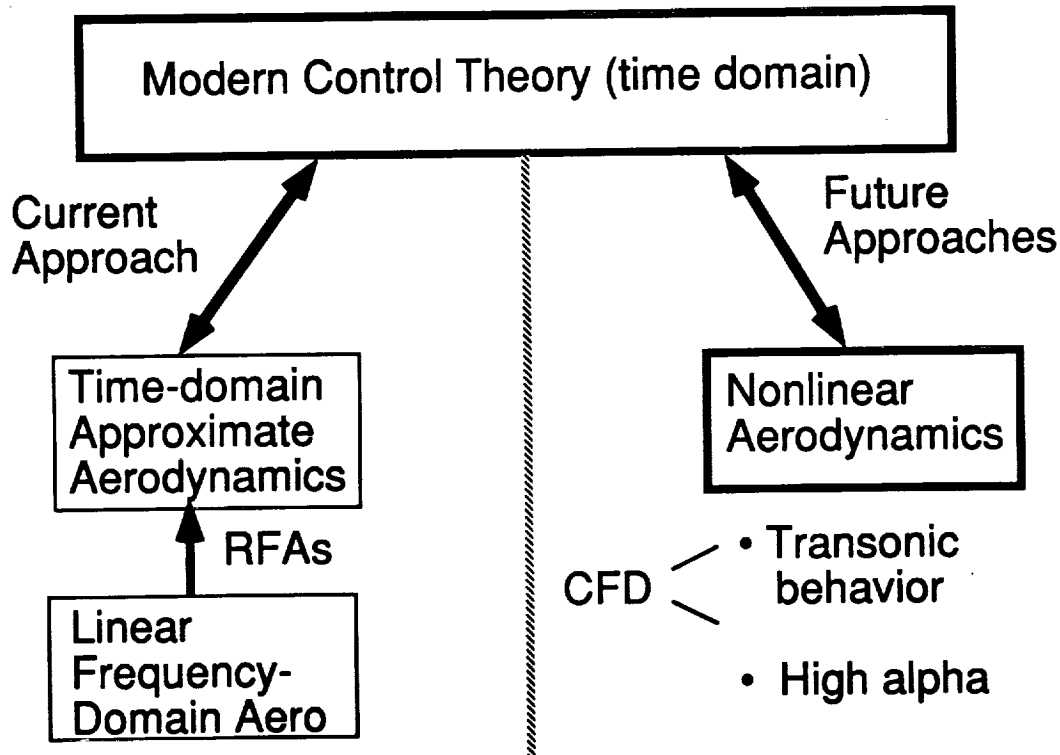
Motivation For Research

The current approach for performing aeroservoelastic analysis and design, in the preliminary design stage, begins with the generation of linear, frequency-domain aerodynamics such as those obtained using doublet lattice theory. Using the concept of rational function approximations, a time-domain model of the linear aerodynamics is generated which is then amenable for use with modern control theory. In the future, however, it is highly desirable to be able to design control laws that can account for nonlinearities in the flow such as the nonlinearities created by transonic flows and high alpha motions. Many of these complex behaviors are currently modeled using CFD codes but there is, currently, no practical method for using the information generated by CFD codes in modern control theory.

BASIC APPROACH

- To model unsteady nonlinear aerodynamic responses as a Volterra nonlinear system

VOLTERRA THEORY OF NONLINEAR SYSTEMS
Volterra Series

$$y(t) = \int_0^t h_1(t-\tau)\, u(\tau)\, d\tau +$$

$$\int\int_0^t h_{2s}(t-\tau_1, t-\tau_2)\, u(\tau_1)\, u(\tau_2)\, d\tau_1\, d\tau_2 + \dots +$$

$$\int_0^t \dots \int_0^t h_{ns}(t-\tau_1, \dots, t-\tau_n)\, u(\tau_1) \dots u(\tau_n)\, d\tau_1 \dots d\tau_n + \dots$$

- Assumes system is causal and time invariant
- Symmetric higher-order kernels: $h_{2s}(t_1, t_2) = h_{2s}(t_2, t_1)$
- Higher-order kernels are measure of nonlinearity
- Theory also referred to as the Volterra-Wiener Theory

Volterra Theory of Nonlinear Systems, Volterra Series

The basic premise of the Volterra theory of nonlinear systems is that the response of a nonlinear system, y(t), due to an arbitrary input, u(t), can be predicted by an infinite series of multidimensional convolution integrals. This is known as the Volterra series. Each convolution integral has a kernel associated with that particular order. That is, the first integral, also referred to as the first-order integral, has the standard one-dimensional kernel or unit impulse response. The second integral, or the second-order convolution, has the second-order kernel which is a two-dimensional unit impulse response, and so on. This particular formulation assumes that the system is causal and time invariant. The higher-order kernels, of order two and above, are symmetric. These kernels are also a measure of nonlinearity. This can be clearly seen when the higher-order kernels are zero and the response of the system is linear. Therefore, when the higher-order kernels are non-zero valued, they represent a deviation from linear response or a nonlinear response. Due to the contributions of Norbert Wiener, the theory is also referred to as the Volterra-Wiener theory of nonlinear systems.

VOLTERRA THEORY OF NONLINEAR SYSTEMS
Volterra Series

For a "weakly" nonlinear system,

$$y(t) \cong \int_0^t h_1(t\text{-}\tau)\, u(\tau)\, d\tau \; +$$

$$\iint_{00}^{tt} h_{2s}(t\text{-}\tau_1, t\text{-}\tau_2)\, u(\tau_1)\, u(\tau_2)\, d\tau_1\, d\tau_2$$

- Many physical systems accurately modeled as weakly nonlinear

- The basic problem is one of kernel identification

Weakly Nonlinear Systems

  The assumption of a weakly nonlinear system can be made in order to simplify the present analysis. This assumption simply states that kernels of order three and above are negligible and the response of the system can be modeled using only second-order nonlinearities. There exist many physical systems that have been accurately modeled as weakly nonlinear in the fields of biology, chemistry, and robotics. The basic problem, then, is one of kernel identification. If the first- and second-order kernels can be identified, then the response of the nonlinear system to arbitrary inputs can be computed.

VOLTERRA THEORY OF NONLINEAR SYSTEMS
Kernel Definition and Identification
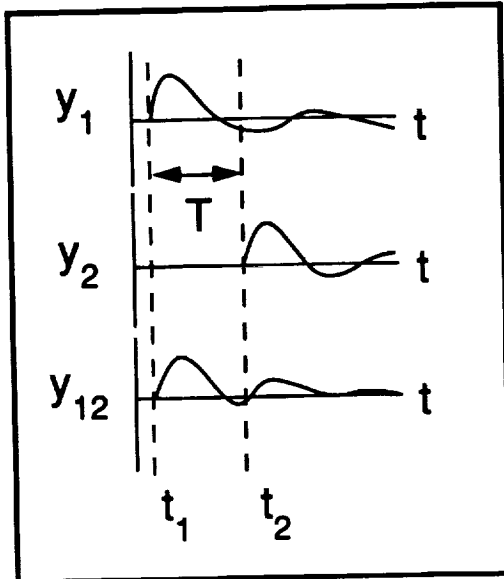
$$h_{2s} = (1/2)\ (y_{12}\text{-}y_2\text{-}y_1)$$

$$h_{2s} = f\ (\ t\ ,\ T\ )$$

- For a linear system, second- (and higher-) order kernels are identically zero

- Nature of nonlinear kernels depends on the nature of the system being investigated

Kernel Definition and Identification

One method for identifying kernels is the method of unit impulse responses. Shown in this chart is the definition of the second-order kernel, for a weakly nonlinear system, using unit impulse responses. The y1 response is the response of the nonlinear system to a unit impulse input at time t1; y2 is the response of the nonlinear system to a unit impulse input at time t2; and y12 is the response of the nonlinear system to a unit impulse input at time t1 and a unit impulse input at time t2. Since the system is time invariant, y2 is y1 shifted in time. The second-order kernel is then computed as one-half the difference of these responses. As the time lag, T, between the two unit impulse inputs is varied, additional terms of the second-order kernel are generated. As can be seen, the second-order kernel is a two-dimensional function of time, t, and time lag, T. It is clear from this definition that for a purely linear system, the second-order kernel is identically zero by the principle of superposition. When this secon-order kernel is non-zero, this implies a deviation from linearity, or a nonlinear response. The nature, or character, of the nonlinear kernels depends on the system being investigated and no assumptions can be made a priori to the actual computation of the kernel.

VOLTERRA THEORY OF NONLINEAR SYSTEMS
State-Space Realization

- Linear

$$\dot{x} = Ax + Bu$$
$$y = Cx$$

and $h(t) = C [\exp(At)] B$

- Nonlinear (Bilinear State Equation)

$$\dot{x} = Ax + Nxu + Bu$$
$$y = Cx$$

and $h(t_1, t_2) = C[\exp(At_2)(N)\exp(At_1)]B$

- **If kernels are known, then A, B, C, and N matrices can be computed.**

State-Space Realization

A truly powerful characteristic of the Volterra theory of nonlinear systems is shown in this chart. It is well known that for a linear system described as shown here that the unit impulse response of that system is defined as shown. If the unit impulse response of the system is known, then using realization techniques one can compute the A, B, and C matrices. The analogous situation exists for a Volterra nonlinear system where the second-order kernel is defined as shown. Therefore, if the second-order kernel of a system can be identified, the A, B, C, and N matrices of a bilinear state-space equation can be realized. This is then a nonlinear, state-space description of the nonlinear unsteady aerodynamic system.

CAP-TSD CODE

- Computational Aeroelasticity Program - Transonic Small Disturbance

- Uses time-accurate, approximate factorization finite-difference algorithm

- Applicable to realistic configurations

CAP-TSD Code

The CFD code used for this research is the CAP-TSD code. CAP-TSD is an acronym that stands for Computational Aeroelasticity Program - Transonic Small Disturbance. The code solves the nonlinear, general-frequency transonic small disturbance equation using a time-accurate, approximate factorization algorithm developed by Dr. Jack Batina and a team from the Unsteady Aerodynamics Branch. The code is applicable to realistic configurations.

APPLICATION TO A CFD MODEL

- Theory -- Continuous systems -- unit impulse function

    CFD codes -- Discrete systems -- unit pulse function

    (example in paper and Ref. 23)

    unit pulse function u(t) = 1.0 for t = t0

    0.0 for t ≠ t0

- Unsteady Aerodynamic System

    input -- downwash function

    output -- lift or moment response

Application to a CFD Model

The Volterra theory discussed thus far addresses continuous systems for which the unit impulse function is defined. CFD codes, however, are discrete systems. Therefore, the unit pulse function, which is the discrete equivalent of the unit impulse input for continous systems, should be used. The unit pulse function is defined as having a value of unity at one point in time and being zero at all other times. The unsteady aerodynamic system is defined as having the downwash function as the input and lift, moment, or any other force as its output. Definition of the input and output depends on the system to be investigated.

APPLICATION TO CAP-TSD

- Downwash function in CAP-TSD for any modeshape

$$f(x,y,t)^{\pm} = \frac{dz^{\pm}}{dx} + A_1(t)\frac{d\phi(x,y)}{dx}$$

$$+ A_2(t)(\frac{1}{L_{ref}})\phi(x,y)$$
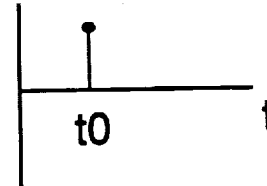
Apply unit pulse to $A_1(t)$ and $A_2(t)$

- Exponential pulse capability (NOT unit pulse)

$$p(t) = \delta_0 \exp(-w(t-t_c)^2)$$

$$\dot{p}(t) = -2w(t-t_c)p$$
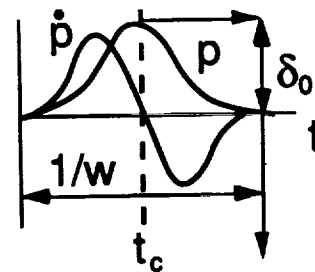
For arbitrary pitching motion,

$$A_1(t) = p(t) \quad \text{and} \quad A_2(t) = \dot{p}(t)$$

Application to CAP-TSD

More specifically, the application of the Volterra theory to the CAP-TSD code is shown in this chart. The downwash function is defined as shown where the plus and minus signs represent the upper and lower surfaces of the airfoil. The dz/dx term are the slopes of the upper and lower surfaces of the airfoil. The A1 term represents the rate of change of motion since it is multiplied by the modal slopes and the A2 term represents the actual motion. A unit pulse is applied to A1 and A2 separately to obtain the unit pulse response due to each of these terms of the downwash. The CAP-TSD code has a capability referred to as the exponential pulse capability which should not be confused with the unit pulse input. The exponential pulse capability is defined as shown and for arbitrary motions, the A1 term is replaced with the p(t) function and the A2 term is replaced with the rate-of-change of p(t) function.

RESULTS FOR NACA0012 RECTANGULAR WING
Computational Model

- NACA0012 rectangular wing with pitch and plunge degrees of freedom

- Semi-span model (panel AR=2.0)

- Grid dimensions: 140 x 40 x 92

Computational Model

  The CAP-TSD model consists of a rectangular wing with a NACA 0012 airfoil and with pitch and plunge degrees of freedom. It is a semi-span model with a panel aspect ratio of 2.0. The grid is dimensioned 140 by 40 by 92 grid points in the x-, y-, and z-directions respectively.

RESULTS FOR NACA0012 RECTANGULAR WING
Analysis

- Lift-coefficient response due to pitch about the mid-chord

- All responses at M = 0.8

- Nonlinear responses about a converged steady-state solution

Analysis

The results that will be presented consist of lift coefficient due to a pitching motion about the mid-chord of the wing. All results are for a Mach number of 0.8, for which a shock exists so that differences between the linear (flat plate) and nonlinear (thickness) solutions should be noticeable. All nonlinear CAP-TSD solutions were computed about a converged steady-state solution.

LINEAR (FLAT PLATE) UNIT PULSE RESPONSE IN LIFT DUE TO FIRST COMPONENT OF PITCHING MOTION
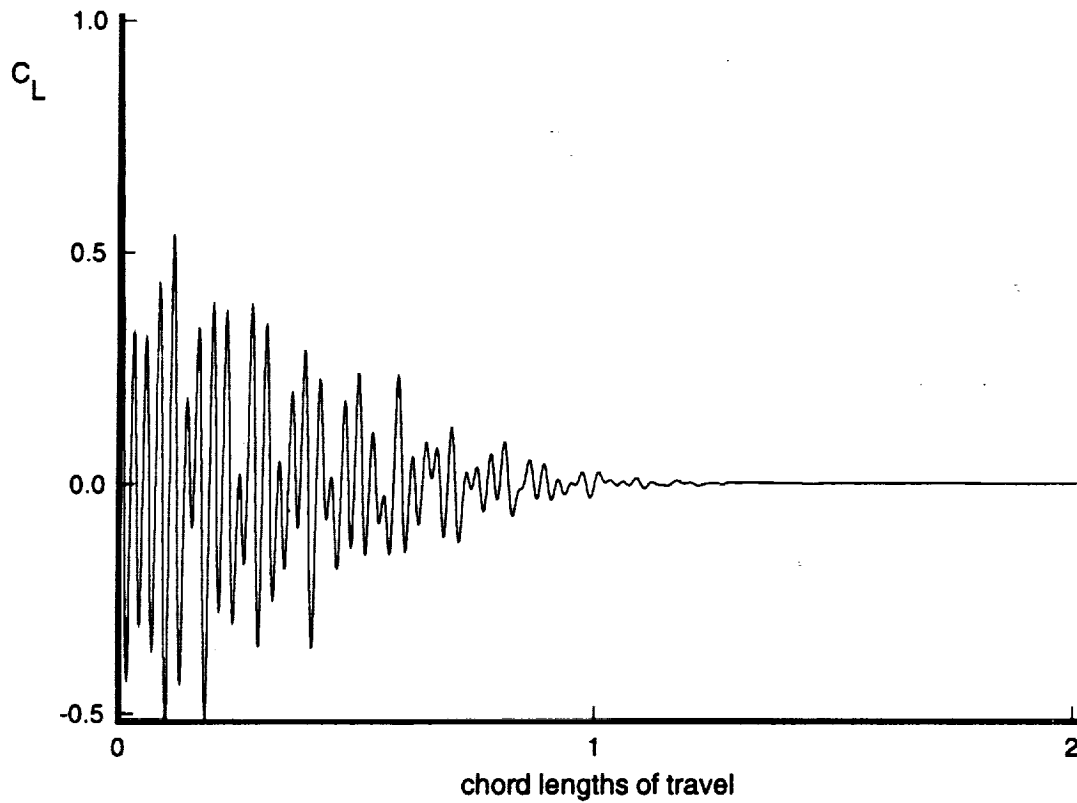
Linear (flat plate) Unit Pulse Response in Lift Due to First Component of Pitching Motion

This is the unit pulse response in lift due to the first component of the pitching motion, or the downwash. The response is stable, or square integrable, as would be expected.

LINEAR (FLAT PLATE) UNIT PULSE RESPONSE IN LIFT DUE TO SECOND COMPONENT OF PITCHING MOTION
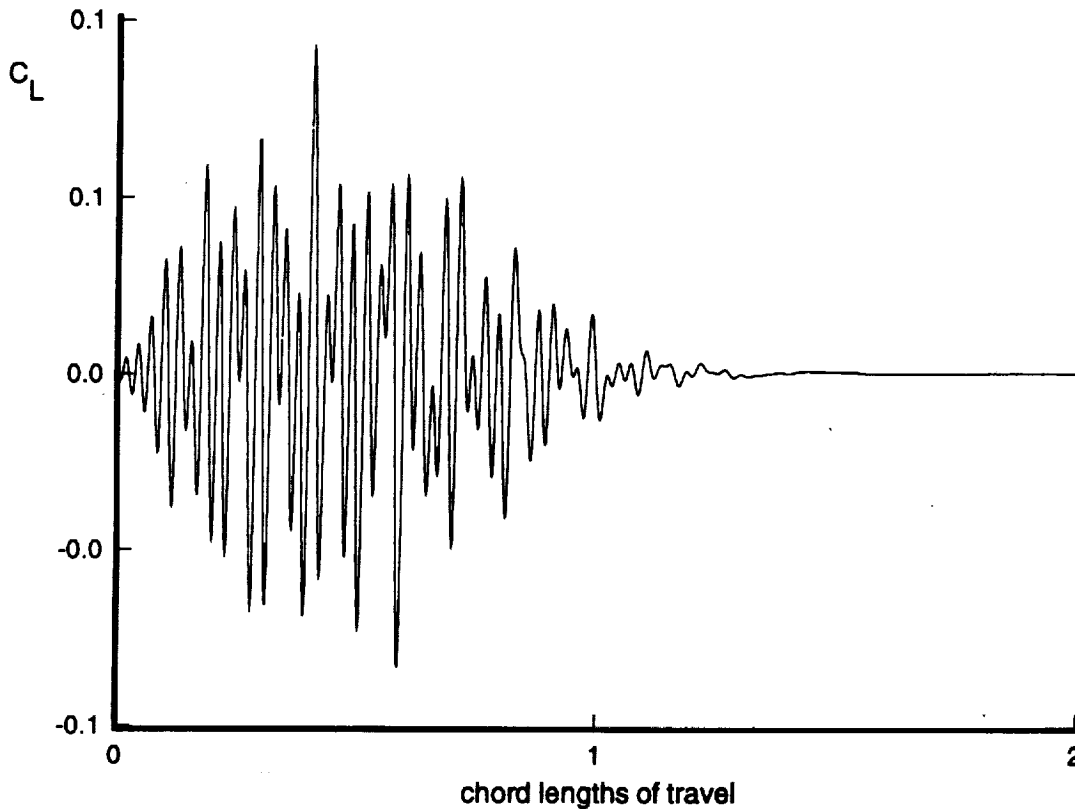

Linear (flat plate) Unit Pulse Response in Lift Due to Second Component of Pitching Motion

This is the unit pulse response in lift due to the second component of the pitching motion, or the downwash. Again, this response is stable, or square integrable. In order to validate that these responses are indeed unit pulse responses, an arbitrary pitching motion was generated.

LOW FREQUENCY PITCHING MOTION
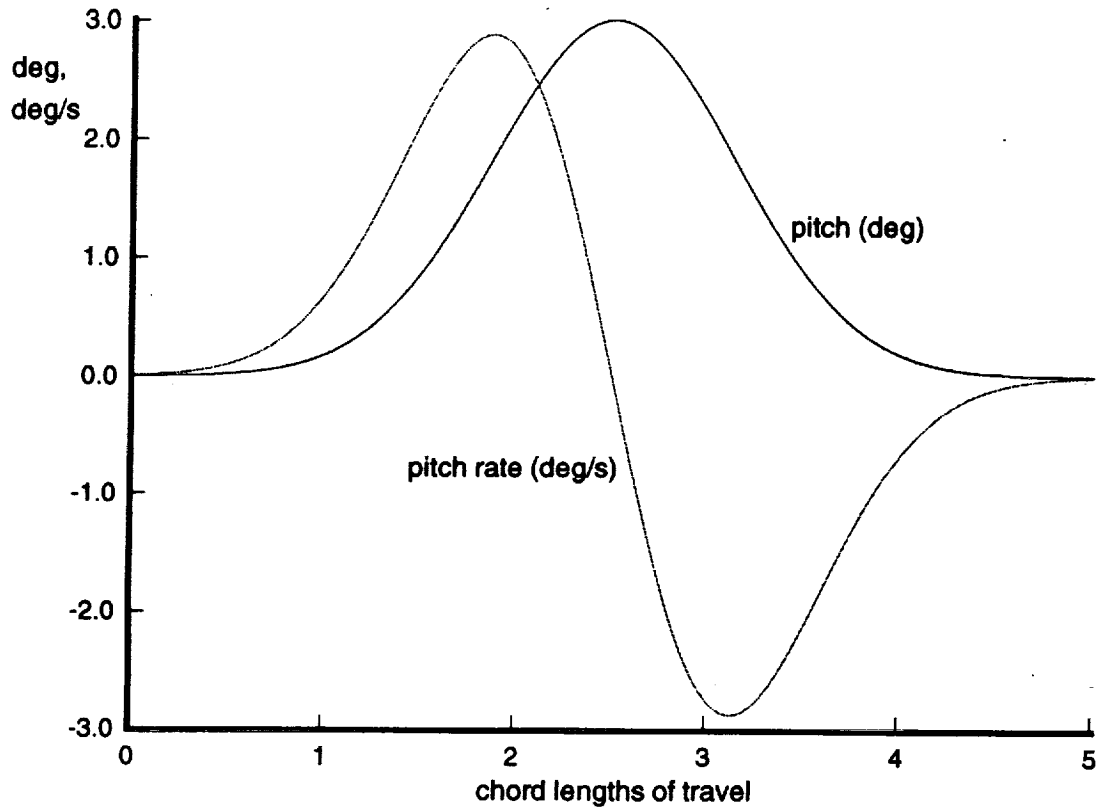
Low Frequency Pitching Motion

This is the pitching motion that was generated. It consists of a positive pitch up to 3 degrees and then back down to 0 degrees. The corresponding rate-of-change of motion is also presented. This motion was then processed through the CAP-TSD code to obtain the CAP-TSD flat plate solution. The pitching motion was convoluted with the first unit pulse response presented and the rate-of-change of pitching motion was convoluted with the second unit pulse response presented. These two convolutions were then added to obtain the total linear convolution response.

LIFT DUE TO LOW FREQUENCY PITCHING MOTION

Legend:
— □ — CAP-TSD flat plate (6000s,40million,1day)
— ◇ — linear convolution (10s,200k,15s)

C_L (vertical axis, 1.0 to 5.0)

chord lengths of travel (horizontal axis, 0 to 5)
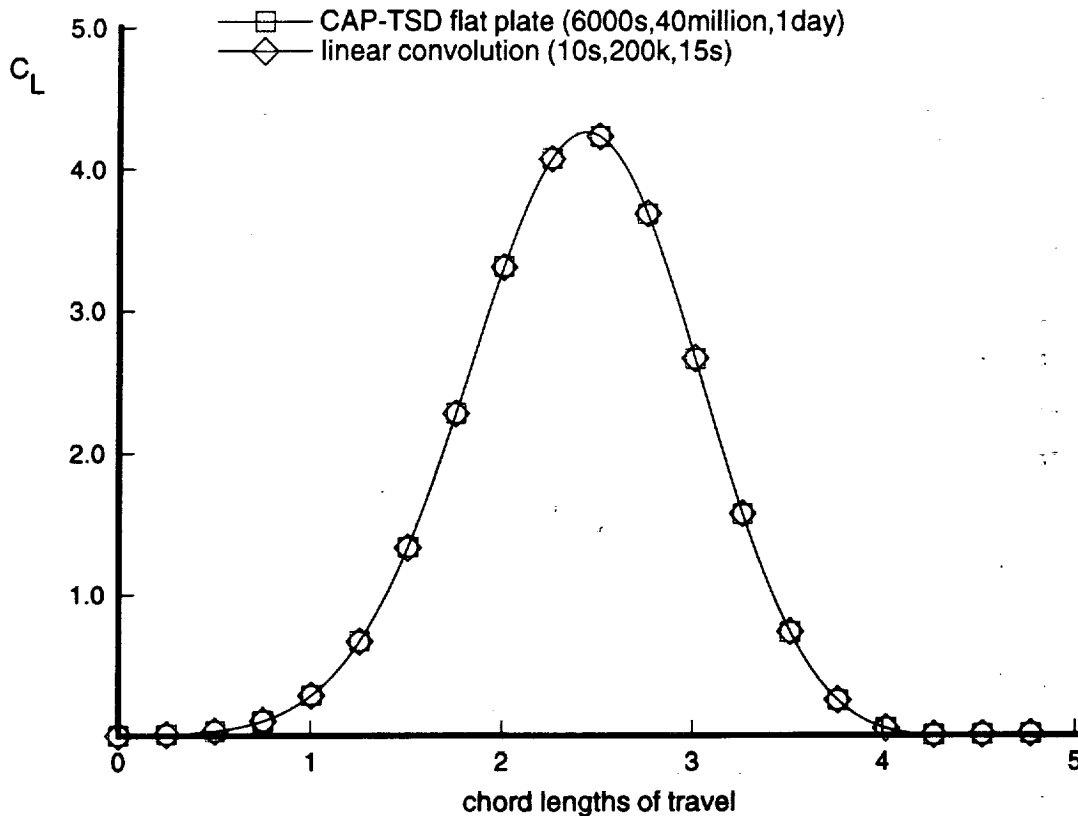
Lift Due to Low Frequency Pitching Motion

This is a comparison of the CAP-TSD flat plate solution and the linear convolution solution for the low frequency pitching motion. As can be seen, the comparison is excellent yielding identical responses to plotting accuracy. It is important to note the savings in cost that was obtained by using the convolution procedure. The CAP-TSD solution cost 6000 cpu seconds, required 40 million words of memory, and was available the next day. The convolution solution cost 10 cpu seconds, required 200 thousand words of memory, and was available in 15 seconds. For linear results this is, of course, of minimal importance since linear problems are readily solved by more efficient means than a complex CFD code. The implication, however, is that similar cost savings may be achieved for nonlinear solutions. It should also be mentioned that the cost of computing the unit pulse responses should be added to the total cost of the convolution solution, but that cost was only 2400 cpu seconds. The real benefit to be obtained from the Volterra, or convolution approach, however, is that once the unit pulse responses (or kernels) are available, the same kernels can be used to predict the response to other inputs.

HIGH FREQUENCY PITCHING MOTION
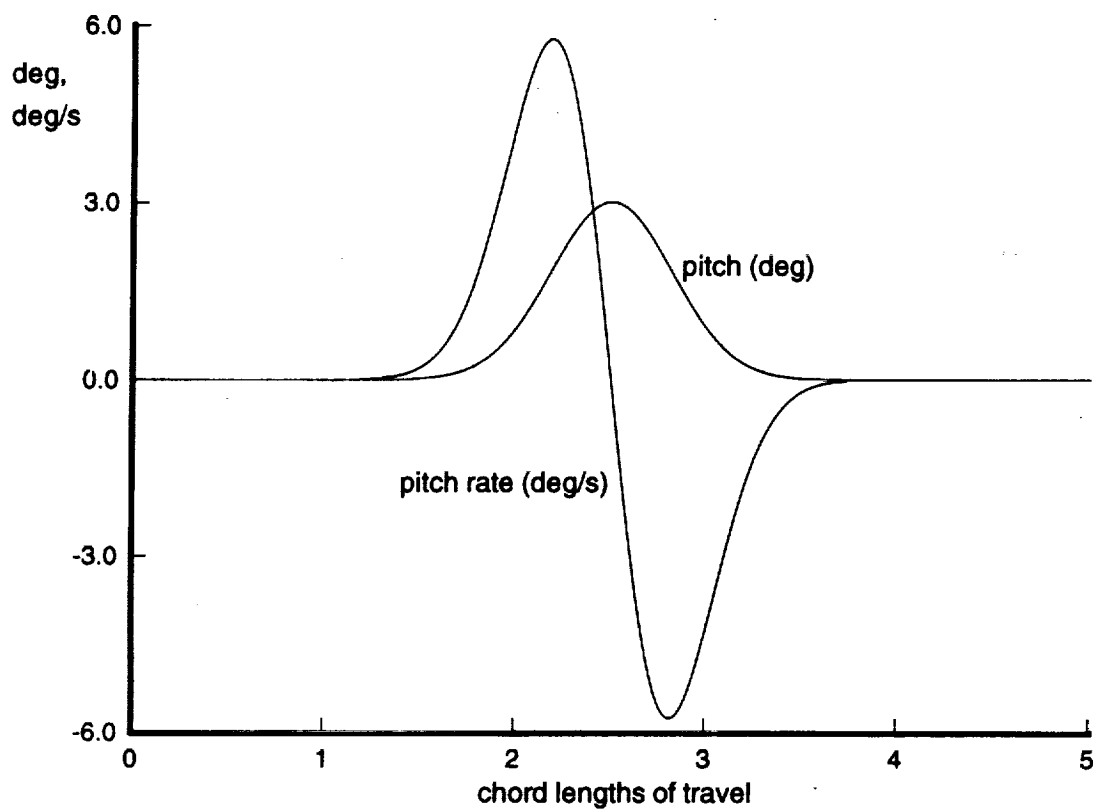
High Frequency Pitching Motion

For example, if the input is now a high frequency input such as shown in the chart, convolution of this input with the corresponding unit pulse responses yields....

LIFT DUE TO HIGH FREQUENCY PITCHING MOTION
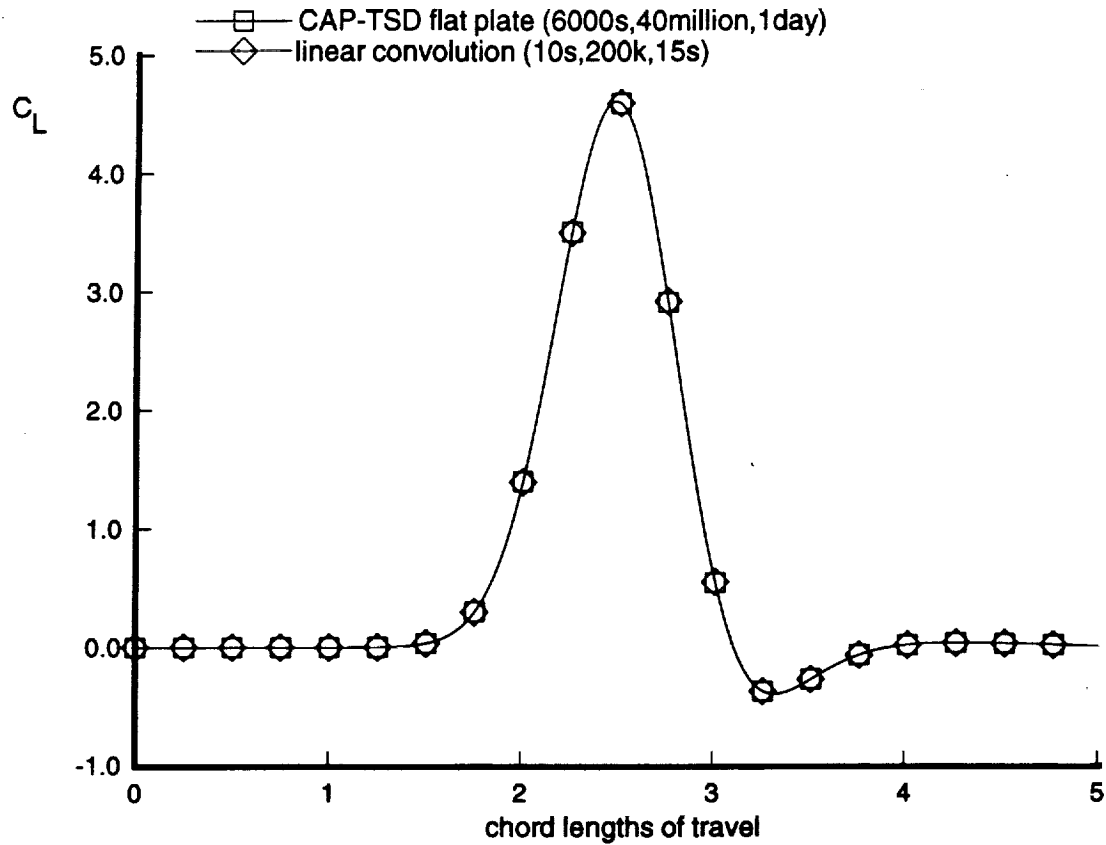
Lift Due to High Frequency Pitching Motion

... this result. Again, the comparison between the CAP-TSD flat plate solution and the linear convolution is excellent. Although the cost of the CAP-TSD solution is once again the same as that of the previous low-frequency result, the cost of the convolution is as shown on the chart. The cost of the kernel computation was paid initially and is not paid again.

FIRST-ORDER UNIT PULSE RESPONSE IN LIFT
DUE TO FIRST COMPONENT OF PITCHING MOTION
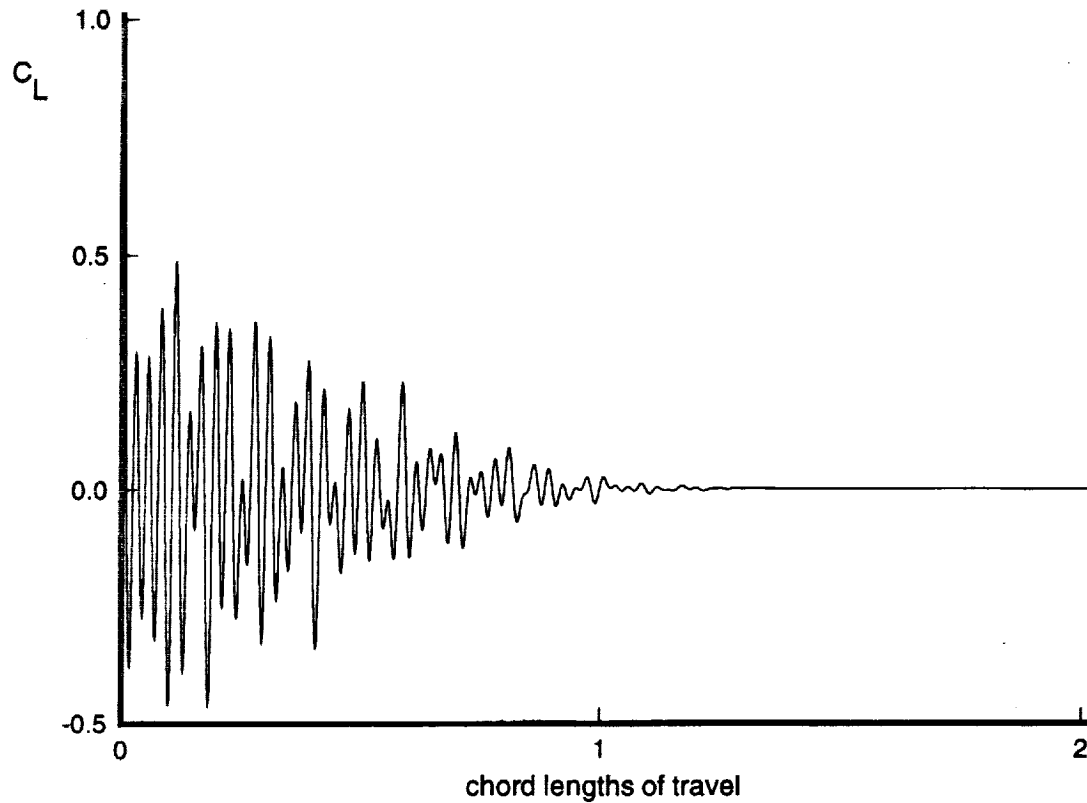
First-Order Unit Pulse Response Due to First Component of Pitching Motion

Investigation of the nonlinear responses begins with the computation of the first-order kernel. It is important to realize that the first-order kernel is the linear portion of the nonlinear response which is not, in general, equivalent to the purely linear response. Shown in this chart is the first-order unit pulse response due to the first component of the pitching motion. Although this response has a similar characteristic to the purely linear unit pulse response shown previously, when plotted together noticeable differences are noticeable.

FIRST-ORDER UNIT PULSE RESPONSE IN LIFT
DUE TO SECOND COMPONENT OF PITCHING MOTION
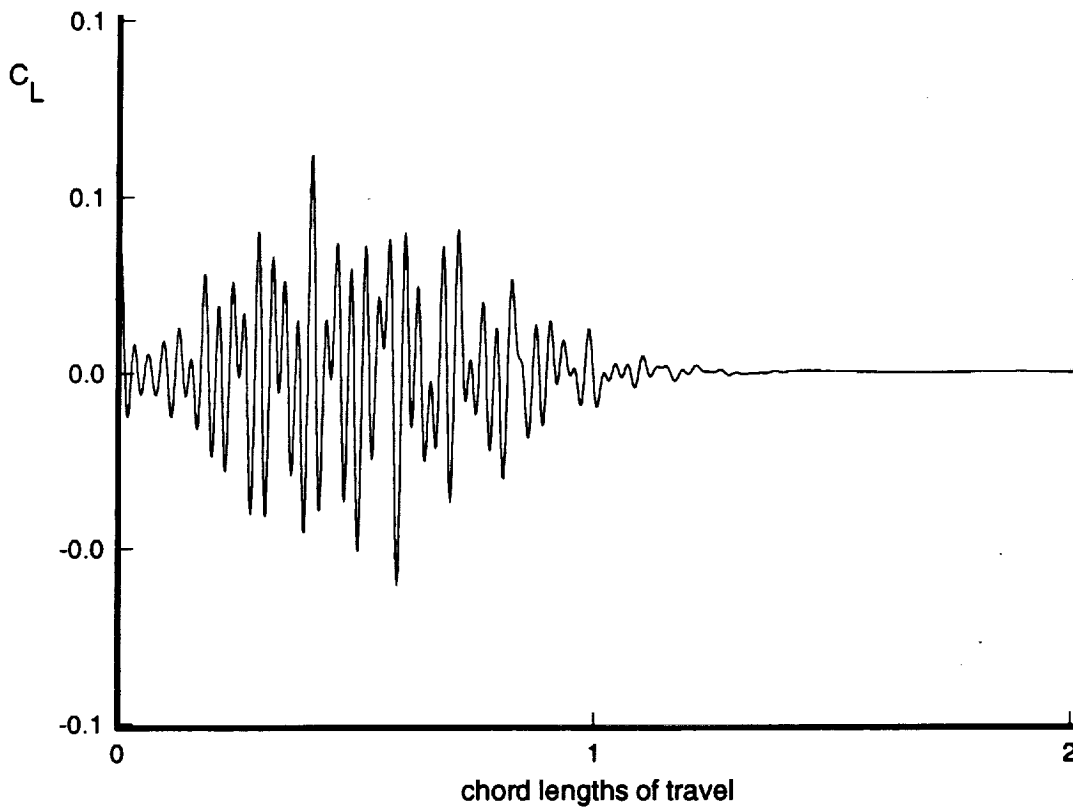
First-Order Unit Pulse Response Due to Second Component of Pitching Motion

This is the first-order unit pulse response due to the second component of the pitching motion. Again, a similar characteristic to the linear, or flat plate, response but it is different.

LIFT DUE TO FORCED HARMONIC PITCHING MOTIONS
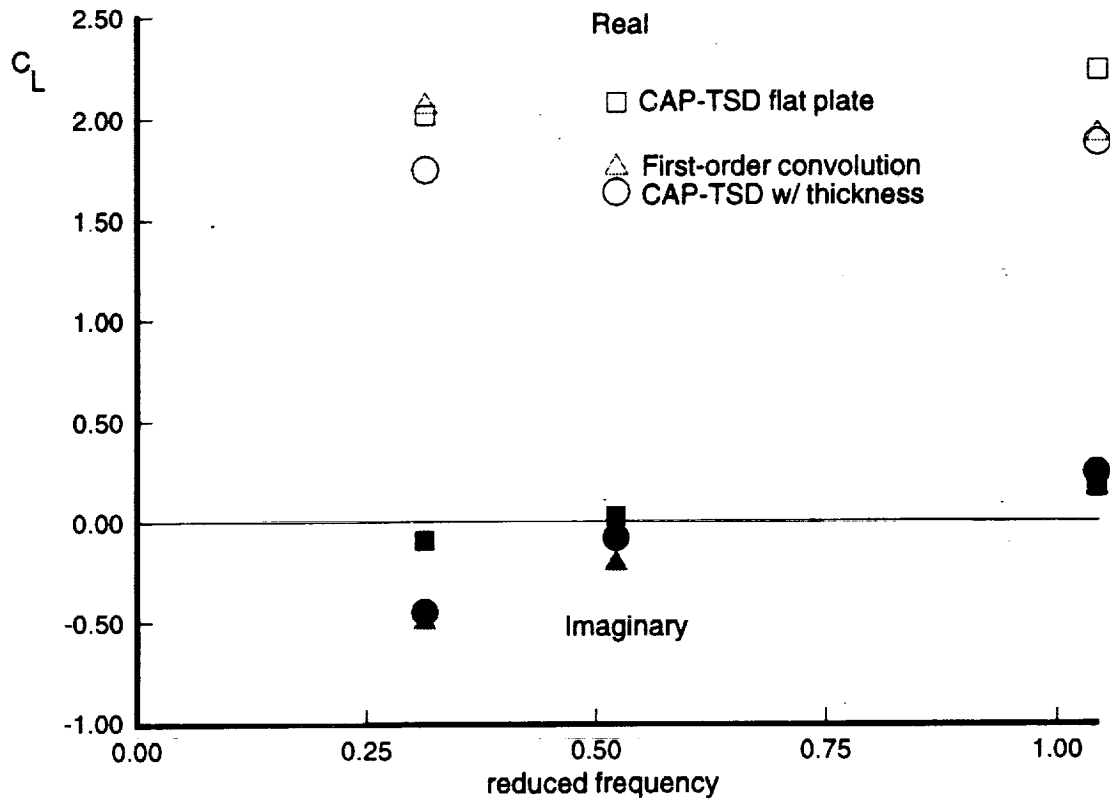
Lift Responses Due to Forced Harmonic Pitching Motions

The first-order kernel was evaluated using forced harmonic pitching motions at three reduced frequencies of motion and compared with CAP-TSD flat plate and CAP-TSD with thickness results. The data indicates that the first-order kernel predicts the CAP-TSD nonlinear (with thickness) result at the high frequency. This comparison is degraded as reduced frequency is lowered which is to be expected since the transonic nonlinearities become more dominant as frequency is reduced. This indicates a need for the second-order kernel responses. Of interest is once again the cost savings. The three first-order responses were generated in about half an hour whereas the CAP-TSD results lasted several days and cost significantly more in CPU and memory.

SECOND-ORDER (NONLINEAR) UNIT PULSE RESPONSE IN LIFT DUE TO FIRST COMPONENT OF PITCHING MOTION
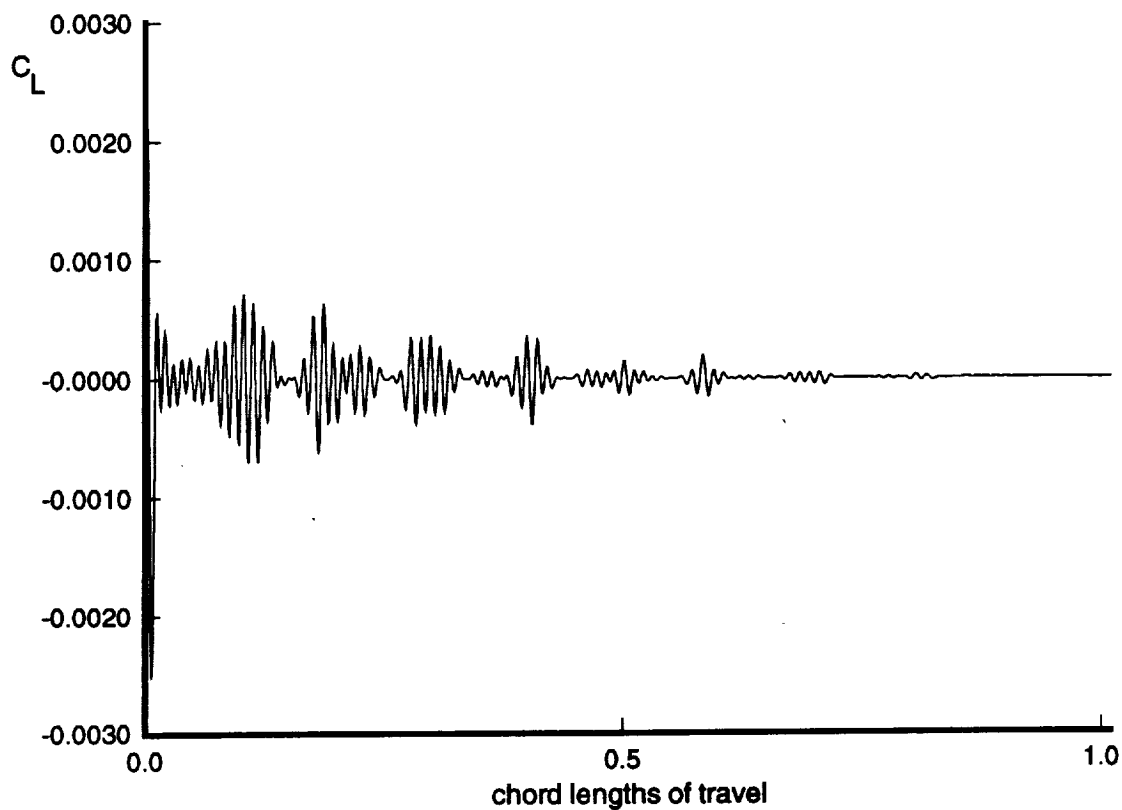
Second-Order Nonlinear Unit Pulse Response Due to First Component of Pitching Motion

Shown here is the first term of the second-order kernel, or unit pulse response, due to the first component of the pitching motion. Note the noticeably different characteristic of this response as compared to the two previously shown responses. A total of four terms of the second-order kernel were computed for the present analysis.

LIFT DUE TO LOW FREQUENCY PITCHING MOTION
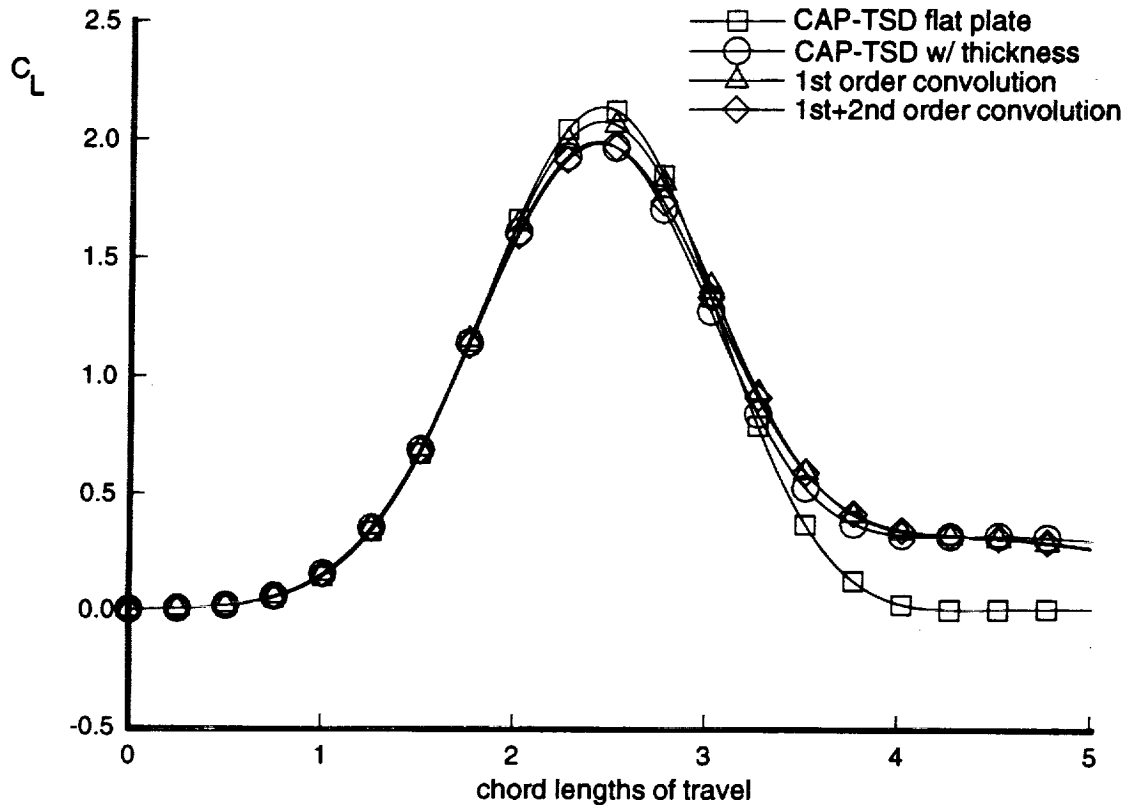
Lift Due to Low Frequency Pitching Motion

Shown here is a comparison of the responses obtained for the low frequency pitching motion: the CAP-TSD flat plate solution, the CAP-TSD with thickness solution, the first-order convolution, and the summation of the first- and second-order convolutions. It is obvious that the purely linear response, the CAP-TSD flat plate response, is quite different from the CAP-TSD with thickness response. The first-order solution, however, although it overshoots the CAP-TSD nonlinear solution (with thickness), is an improvement over the linear response. This is most notable in the latter part of the responses. The addition of the second-order terms provides the necessary difference to the first-order solution to accurately predict the peak of the CAP-TSD nonlinear solution, with very slight discrepancies near the latter part of the responses.

454

ADVANTAGES OF METHODOLOGY

- CFD code used initially to define kernels

- Once kernels are defined, CFD code NOT USED AGAIN

- Linear and nonlinear responses computed using simple convolution subroutine (negligible cost)

- Kernels can be used to generate linear and nonlinear state-space matrices that define the unsteady response of the aerodynamic system

Advantages of Methodology

The advantages of the methodology are as follows. First, the CFD code is used initially to define the necessary kernels. Once the kernels are defined, the CFD code need not be used again. This is where the potential for significant cost savings becomes obvious. Second, once the kernels are defined, linear and nonlinear responses can be computed using simple convolution routines at a negligible computational cost. Finally, from the kernels, linear and nonlinear state-space matrices can be generated that define the unsteady response of the aerodynamic system.

CONTINUED DEVELOPMENT (PLANS)

- Second-order kernel definition, application, limitations

- DAVINCI (Definition of Aerodynamic Volterra Integrals for Nonlinear Control Interactions) Team formed with Aeroservoelasticity Branch (Mukhophadyay, Wieseman)

- System realization, bilinear equations

- Apply methodology to Euler/Navier-Stokes code(s)

Continued Development (Plans)

Current efforts are aimed at additional second-order kernel definition and validation, applications, and limitations. The DAVINCI (Definition of Aerodynamic Volterra Integrals for Nonlinear Control Interactions) Team has been formed with Dr. Vivek Mukhophadyay and Carol Wieseman of the same branch. Additional work is being performed in understanding the system realization issues for bilinear systems and bilinear equations. It is also planned to apply kernel identification techniques to higher-level fluid dynamics equations such as the Euler and Navier-Stokes equations.

CONCLUDING REMARKS

- Linear and nonlinear discrete aerodynamic unit pulse response functions (kernels) defined for arbitrary frequencies

- Linear (flat-plate) results : excellent

- Nonlinear results

  - First-order term provides "linearized" result

  - Second-order term provides nonlinear effect

  - Additional validation/development underway

- Cost savings (CPU, memory and turnaround time)

Concluding Remarks

In conclusion, linear and nonlinear discrete aerodynamic unit pulse response functions (kernels) were defined for arbitrary frequencies. The fact that these functions exist is of significance as it represents an approach different to the indicial method. Linear, or flat plate, results were excellent in comparison with the CAP-TSD flat plate generated results. The linear results validate the use of unit pulse responses for aerodynamic systems. The nonlinear results are very encouraging in that, for the responses investigated, the first-order term provides the "linearized" result and the second-order term captures the nonlinear effect. There is, of course, additional validations and development work that needs to be performed to fully understand the effectiveness and the limitations of the methodology. As was shown, the cost savings is significant for the cases shown, which would make CFD codes practical for preliminary analysis and design.

EFFECT OF AEROELASTIC-PROPULSIVE INTERACTIONS ON FLIGHT DYNAMICS OF A HYPERSONIC VEHICLE

David L. Raney and John D. McMinn
NASA Langley Research Center
Hampton, VA 23681

Anthony S. Pototzky
Lockheed Engineering Sciences Co.

Christine L. Wooley
University of Cincinnati

Outline

Motivation and Objectives

Model Description

Propulsion Sensitivities

Impact on Flight Dynamics

Concluding Remarks

Motivation and Objectives
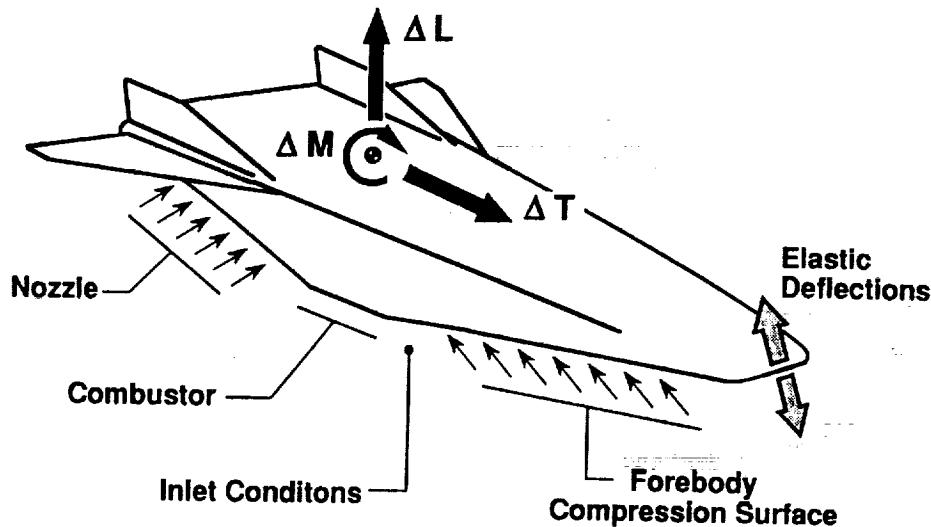
- **Assess magnitudes of propulsive force and moment perturbations**
- **Examine impact on longitudinal flight dynamics**

MOTIVATION AND OBJECTIVES

The desire to achieve orbit-on-demand access to space with rapid turn-around capability and aircraft-like processing operations has given rise to numerous hypersonic aerospace plane design concepts which would take off horizontally from a conventional runway and employ air-breathing scramjet propulsion systems for acceleration to orbital speeds. Most of these air-breathing hypersonic vehicle concepts incorporate an elongated fuselage forebody to act as the aerodynamic compression surface for a scramjet combustor module. This type of airframe-integrated scramjet propulsion system tends to be highly sensitive to inlet conditions and angle-of-attack perturbations. Furthermore, the basic configuration of the fuselage, with its elongated and tapered forebody, produces relatively low frequency elastic modes which will cause perturbations in the combustor inlet conditions due to the oscillation of the forebody compression surface. The flexibility of the forebody compression surface, together with sensitivity of scramjet propulsion systems to inlet conditions, creates the potential for an unprecedented form of aeroelastic-propulsive interaction in which deflections of the vehicle fuselage give rise to propulsion transients, producing force and moment variations that may adversely impact the longitudinal flight dynamics and/or excite the elastic modes. These propulsive force and moment variations may have an appreciable impact on the performance, guidance, and control of a hypersonic aerospace plane. The objectives of this research are (1) to quantify the magnitudes of propulsive force and moment perturbations resulting from elastic deformation of a representative hypersonic vehicle, and (2) to assess the potential impact of these perturbations on the vehicle's longitudinal flight dynamics.

Vehicle Geometry
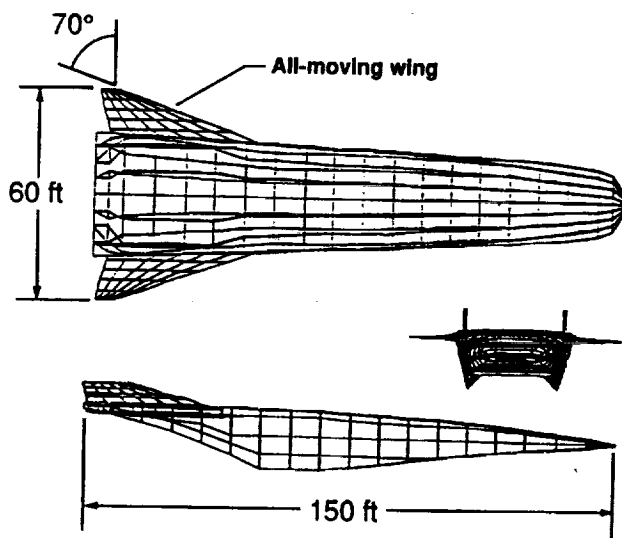
VEHICLE GEOMETRY

A three-view finite element representation of the vehicle concept used in this modeling effort is shown in the figure. It is a hypersonic lifting body with underslung engine nacelles, very similar in configuration to the proposed X-30 research vehicle. The vehicle length is 150 ft. The wingspan is 60 ft, with a wing sweep angle of 70 degrees. Vertical fins project from the upper surface of the aft fuselage near the wing root. The configuration is equipped with all-moving wing control effectors. At hypersonic speeds, the lower surface of the elongated fuselage forebody acts as a compression wedge for the scramjet combustor unit, and the lower surface of the aft portion of the vehicle acts as a nozzle. The weight of the vehicle used in this study was 300,000 lb. The configuration was analyzed at two hypersonic flight conditions: Mach 6 at 75,000 feet and Mach 10 at 95,000 feet, representing two points along a typical ascent trajectory. The dynamic pressures at these two flight conditions are 1,840 psf and 2,010 psf, respectively.

461

Aeroelastic Model

2.9 Hz   3.8 Hz   5.5 Hz   5.7 Hz

7.7 Hz   8.9 Hz   10.9 Hz
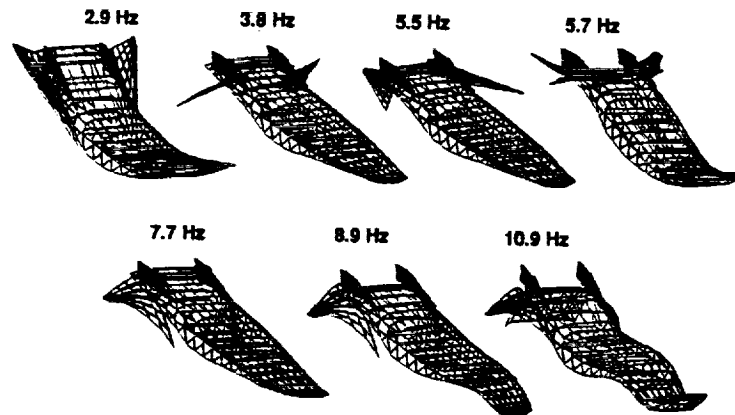
- 2 Rigid Body Modes, 7 Elastic Modes, 3rd Order Actuator

- General form of model:

$$\dot{x} = [A]\,x + [B]\,u$$

$$y = [C]\,x$$

$$x = \left\{ \begin{array}{l} \text{rigid body states} \\ \text{elastic states} \\ \text{actuator states} \end{array} \right\} \qquad y = \left\{ \begin{array}{l} \text{fuselage deflections} \\ \text{angle of attack} \end{array} \right\}$$

$$u = \left\{ \text{control command} \right\}$$

AEROELASTIC MODEL

The aeroelastic state-space model used in this study is a longitudinal approximation. The model includes seven symmetric bending modes and two rigid body modes. The rigid body degrees of freedom are pitch and vertical translation (plunge). No translational degree of freedom along the vehicle's longitudinal axis is included. The general form of this aeroelastic model is shown in equations (1) and (2).

$$\dot{x} = [A]\,x + [B]\,u \qquad (1)$$
$$y = [C]\,x \qquad (2)$$

The state vector, x, contains a total of 21 elements; two for each of the nine second-order dynamic modes, and three states for an actuator model associated with the all-moving wing. The input vector, u, corresponds to the all-moving wing control command. The output vector, y, includes the rigid body angle of attack and pitch rate, as well as displacements, slopes, and accelerations at various locations throughout the fuselage and wing.

Numerical values for the matrices [A], [B], and [C] appearing in equations (1) and (2) were generated using the Interaction of Structures, Aerodynamics, and Controls code, ISAC. Second-order piston theory was used to model the unsteady aerodynamic effects at the two selected hypersonic flight conditions. The shapes and in-vacuo frequencies of the seven elastic modes are shown in the figure. Mode shapes which strongly impact the fuselage geometry are of particular importance, since they are likely to have the greatest influence on the propulsion system. The in-vacuo frequencies of the elastic modes are relatively low and closely spaced.

Propulsion Model
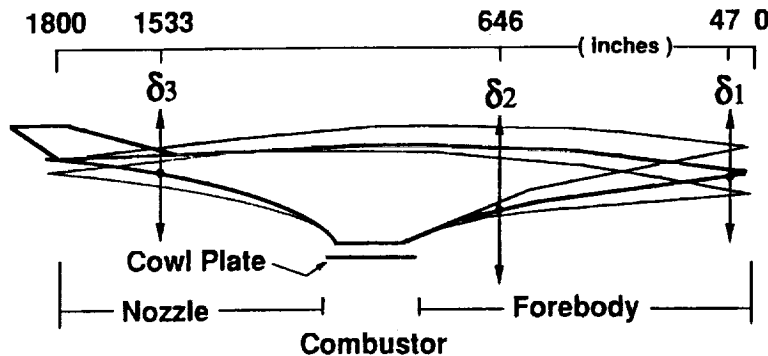
Undersurface geometry analyzed by SRGULL

Assumptions:
2-d forebody and nozzle
1-d combustor
no unsteady propulsion aerodynamics

General form of model:

$$\begin{Bmatrix} F_A \\ F_N \\ M \end{Bmatrix} = f(\delta 1, \delta 2, \delta 3, \alpha)$$

PROPULSION MODEL

The propulsion model was developed using the SRGULL code for hypersonic propulsion systems. The SRGULL code uses a two-dimensional inviscid Forebody and inlet analysis, and a one-dimensional combustor analysis to address the entire propulsion system flowpath shown in the figure. A variable grid is used to analyze the vehicle nose-to-tail stream tube control volume, determining mass capture, forebody and inlet drag, and combustor and nozzle performance. The nose-to-tail propulsion flowpath consists of the undersurface of the fuselage forebody, the combustor module, and the undersurface of the fuselage afterbody (serving as the nozzle). Using SRGULL, a database was produced which allows the interpolation of propulsive axial and normal force and pitching moment perturbations resulting from a given structural deflection at a given angle of attack.

To produce the propulsive force and moment database, the SRGULL code was first run at both flight conditions (Mach 6 and Mach 10) for the undeflected vehicle geometry over an angle-of-attack range from -1 to 3 degrees in one-degree increments. Structural deflections were then generated at selected stations along the fuselage centerline by calculating the RMS elastic responses to a Von Karman spectra turbulence input. Three stations along the fuselage centerline, designated as δ1, δ2, and δ3 in the figure were chosen to parameterize a set of perturbation geometries. The three stations are located 47 inches, 646 inches, and 1,533 inches back from the nose of the vehicle. The RMS deflections were then used to produce a collection of 27 perturbation geometries consisting of the set of all possible combinations of the upward, zero, and downward deflection positions at each of the three selected fuselage stations, assuming that the combustor section was rigid. Each of the perturbation geometries was then analyzed using SRGULL over the angle-of-attack range from -1 to 3 degrees at both Mach Numbers to produce a database of axial force, normal force, and pitching moment perturbations as a function of fuselage deflections and angle of attack. The data was then combined into a 4-dimensional interpolation table using angle of attack and the deflections at the three fuselage stations as the independent variables. Curve fits to the data were used to increase the number of breakpoints in the interpolation table. In this way, a database was produced which could be used to estimate the propulsive forces and moments for any deflected geometry by interpolating from the table based on angle of attack and the deflections at the three selected fuselage stations.

Propulsive Force and Moment Data
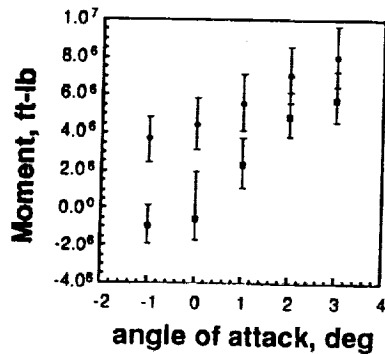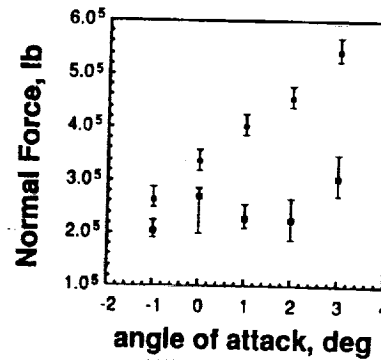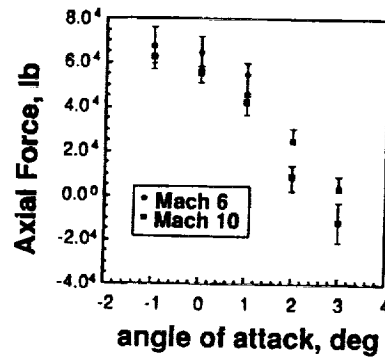
- Large variation with alpha
- Symbols: data for undeflected geometry
- Brackets: range of variation due to perturbed geometries

PROPULSIVE FORCE AND MOMENT DATA

The force and moment database produced using SRGULL is plotted against angle of attack in the figure. The solid symbols represent the data for the undeflected vehicle geometry at Mach Numbers of 6 and 10. The brackets about each symbol indicate the range of variation in axial force, normal force, or moment that resulted from the analysis of the 27 perturbation geometries.

464

Simulation Layout

Aeroelastic Model   Propulsion Model
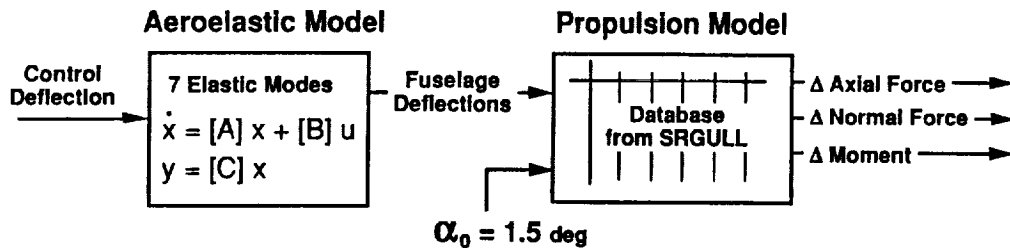
- **Removed rigid body modes from aeroelastic model**
- **Excited elastic modes with control doublet**
- **Examined magnitudes of elastically-induced propulsive perturbations**

SIMULATION LAYOUT

In order to ascertain the approximate magnitudes of elastic deflections and resulting propulsive perturbations which can be expected in response to a typical control input, a simulation was constructed incorporating the aeroelastic and propulsion models in the general structure shown in the figure. In this simulation, the aeroelastic model is driven by control surface deflections to yield an output vector, y, consisting of angle-of-attack perturbations and elastic deflections which are then fed into the propulsive interpolation database to produce time histories of the resulting force and moment perturbations. The rigid body dynamics of the aeroelastic model are unstable at both flight conditions and were removed so that these time histories could be produced in the absence of the divergent rigid body motion. The time histories were generated using the propulsive force and moment interpolation database at an angle of attack of 1.5 degrees. This angle of attack did not change during the time histories, since the angle-of-attack perturbations did not occur in the absence of the rigid body modes. Therefore, the propulsive perturbations produced by the control doublet are entirely the result of elastic fuselage deformations and not of angle-of-attack variations. Also, the perturbations do not include the aerodynamic lift, drag, or moment acting on the control surface itself. The responses do not represent worst case perturbations, but rather are intended to provide insight into the magnitude of the propulsion system sensitivity to elastic deformation of the vehicle.

Perturbation Time Histories

max = 2.4 inches

max = 2% from nominal
(about 0.02 g)
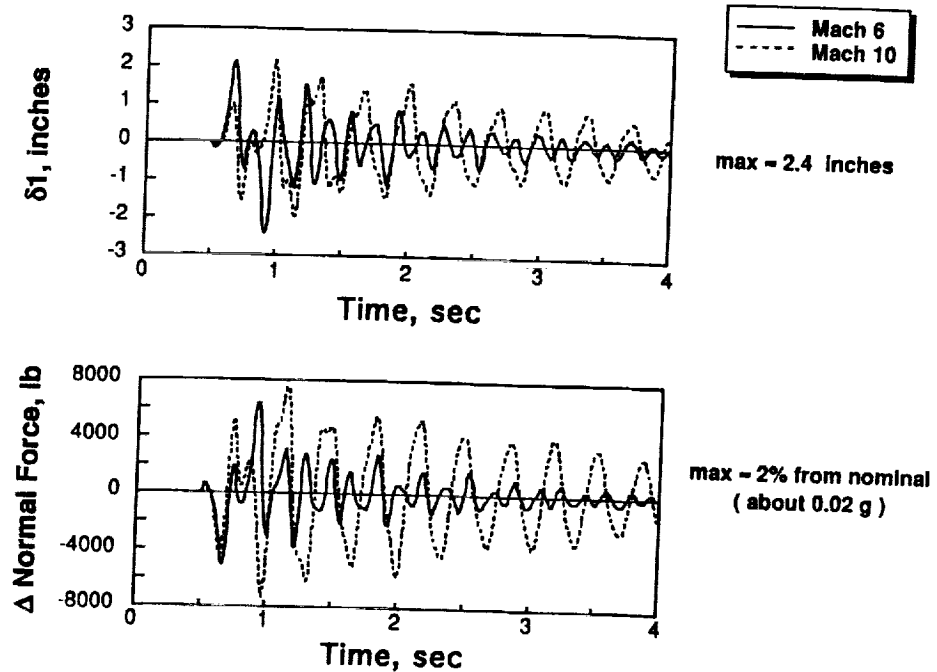
PERTURBATION TIME HISTORIES

Time histories of the elastic deflections at the first station along the fuselage centerline designated as δl (47 from the nose of the vehicle) are shown in the figure for the Mach 6 and Mach 10 flight conditions. The doublet was initiated 0.5 seconds into the run. The largest fuselage deflections reach about 2.4 inches at this fuselage station. These deflections appear to represent relatively minor distortions of the aerodynamic compression surface of the integrated airframe-propulsion system. The deflections did not produce appreciable accelerations at the pilot station.

Time histories of the propulsive force and moment perturbations resulting from the elastic deflections are also shown. The largest normal force perturbations range from 6,390 lbs for the Mach 6 case to 7,580 lbs for Mach 10 case.

Perturbation Time Histories

max ~ 4% from nominal
(about 0.01 g)

max > 10% from nominal
trim moment
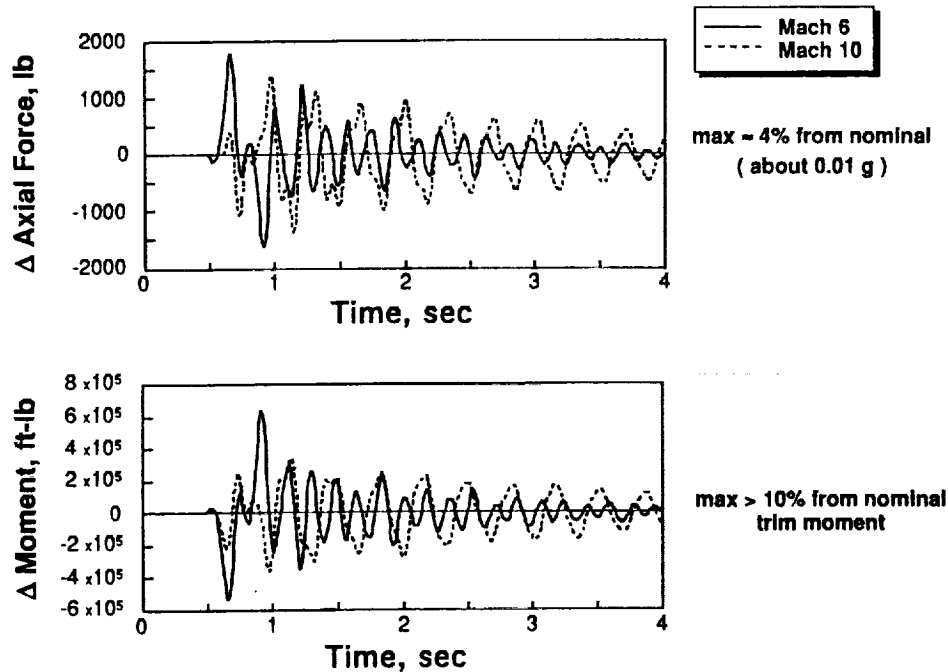
PERTURBATION TIME HISTORIES (continued)

The largest axial force perturbations range from 1,770 lbs to 1,410 lbs, and the pitching moment perturbations range from 6.32 x 10^5 ft-lbs to 3.60 x 10^5 ft-lbs in the Mach 6 and Mach 10 cases, respectively. The maximum normal force perturbations represent approximately 2 percent variations from nominal and would produce vertical acceleration transients of about 0.02 g's for a vehicle weighing 300,000 lb. The maximum axial force perturbations represent approximately 4 percent variations from nominal and would produce longitudinal acceleration transients of less than 0.01 g's for a vehicle weighing 300,000 lb. The maximum moment perturbations, however, represent greater than 10 percent variations from the nominal trim moment and may require substantial control deflections to maintain stable trimmed flight. It is important to remember that these force and moment perturbations are due solely to propulsion system sensitivity to elastic deflections. They do not include the effect of angle-of-attack perturbations on the propulsion model. The large pitching moment variation is due mainly to the aerodynamic contribution of the forebody. Maintaining trim in presence of the large pitching moment perturbations may require excessive control activity in hypersonic flight, which could translate into a substantial drag increment when integrated over the duration of a mission, implying reduced fuel efficiency and decreased payload capacity.

Simulation Layout
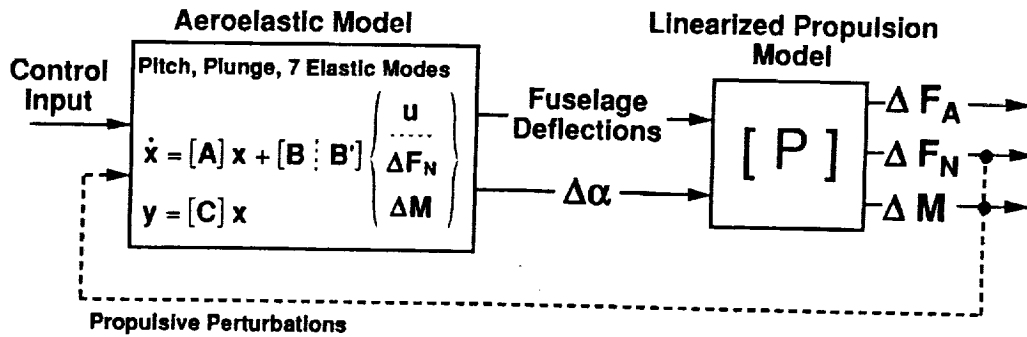
Examine impact of propulsive perturbations on aeroelastic model.

Equates to augmenting the stability matrix:

$$\dot{x} = [A]\,x + [B]\,u + [B']\,[P]\,[C]\,x \;,\; or$$

$$\dot{x} = [A + A']\,x + [B]\,u \quad \text{where} \quad A' = [B']\,[P]\,[C]$$

Propulsive force and moment perturbations treated as "virtual inputs" applied at cg.

SIMULATION LAYOUT

The simulation was used to assess the impact of the propulsive perturbations on the dynamics of the combined aeroelastic-propulsive system. This was accomplished by feeding the propulsive force and moment perturbations back into the aeroelastic model as indicated by the dashed line in the figure. As shown in the figure, this simply equates to augmenting the stability matrix with the effect of the linearized propulsion sensitivities. The model contains a further approximation in that the propulsive force and moment perturbations are applied at the cg, rather than being distributed over the aft nozzle area and cowl structure of the vehicle. Application of forces and moments to the aeroelastic model at the cg produces acceptable results regarding the impact of the propulsive perturbations on the vehicle's rigid body dynamics (pitch and plunge), but should not be used to assess the impact of propulsive perturbations on the elastic modes. In order to achieve the latter, it would be necessary to apply the propulsive perturbation loads to the structure using an appropriate load distribution function.

468

Impact on Rigid Body Modes

Mach 6

Mach 10
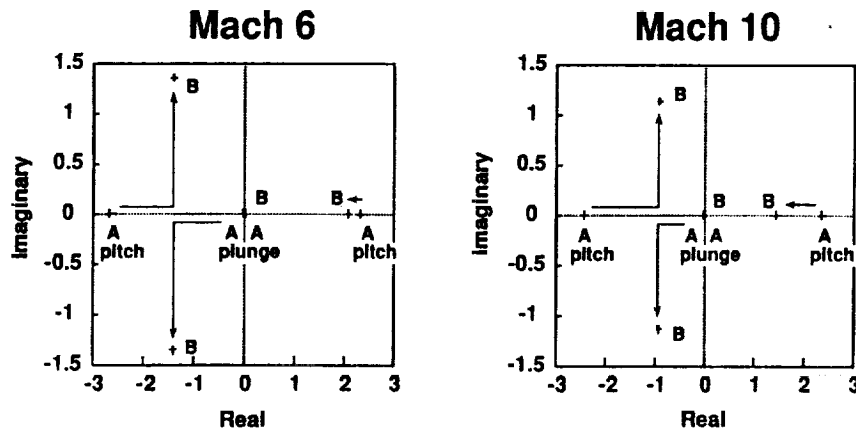
- Illustrates Impact on rigid body modes due to augmenting stability matrix with propulsion system sensitivities.

- Propulsion linearization conditions: $\alpha_0 = 1.5$ deg, $\delta_0 = 0$

- Final position of eigenvalues was strongly dependent upon linearization conditions of propulsion model.

IMPACT ON RIGID BODY MODES

The figure illustrates the effect of the propulsive perturbations on the rigid body dynamics for the Mach 6 and Mach 10 flight conditions. The roots labeled "A" in the figure represent the statically unstable pitch and plunge modes when the propulsive perturbations are not being fed into the aeroelastic model. When the propulsive perturbations are fed into the aeroelastic model, two of the poles associated with the rigid body modes are observed to couple, producing a new oscillatory mode. The frequency of the unstable pole associated with the pitch mode is also observed to vary. The final position of the rigid body roots is indicated by the points labeled "B" in the figure. The Mach 10 case exhibits a slightly greater variation in the frequency of the unstable root of the pitch mode.

469

Eigenvalue Dispersion Caused by Varying Linearization Conditions

Mach 6

Mach 10
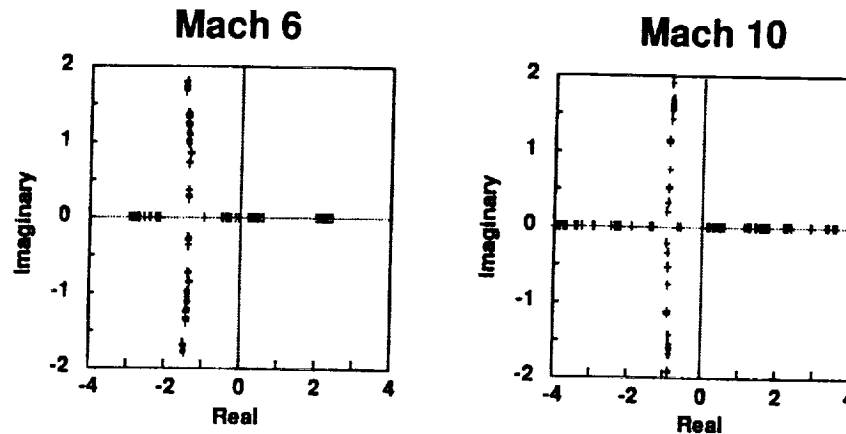
- Varied α_0 and δ_0 used to linearize propulsion sensitivities.

- Illustrates range of possible dynamic characteristics due to nonlinear propulsion database.

- Can be viewed as uncertainty associated with rigid body flight dynamics.

EIGENVALUE DISPERSIONS

It was found that the final position of the poles of the augmented stability matrix varied depending on the angle of attack and nominal fuselage deflections about which the propulsion model was linearized. This variation is a direct result of nonlinearities in the propulsive force and moment database. The nonlinearities introduce uncertainty into the system regarding the position of the rigid body poles, because the pole locations vary as the structure deforms and as angle of attack varies. In order to chart the pole variation resulting from nonlinearities in the propulsive force and moment database the propulsion linearization conditions were varied and corresponding eigenvalues of the augmented stability matrix were plotted. The angle of attack was varied over the range of -1 to 3 degrees, and nominal fuselage deflections were simultaneously varied according to the deflection time history shown in the previous figures. The resulting eigenvalue dispersions are shown in this figure. The variation of linearization conditions caused a wide range of dynamic characteristics to be observed at both flight conditions. This variation in dynamic characteristics due to the propulsion nonlinearities may be viewed as uncertainty associated with the rigid body modes.

Future Research

Robust Control Law
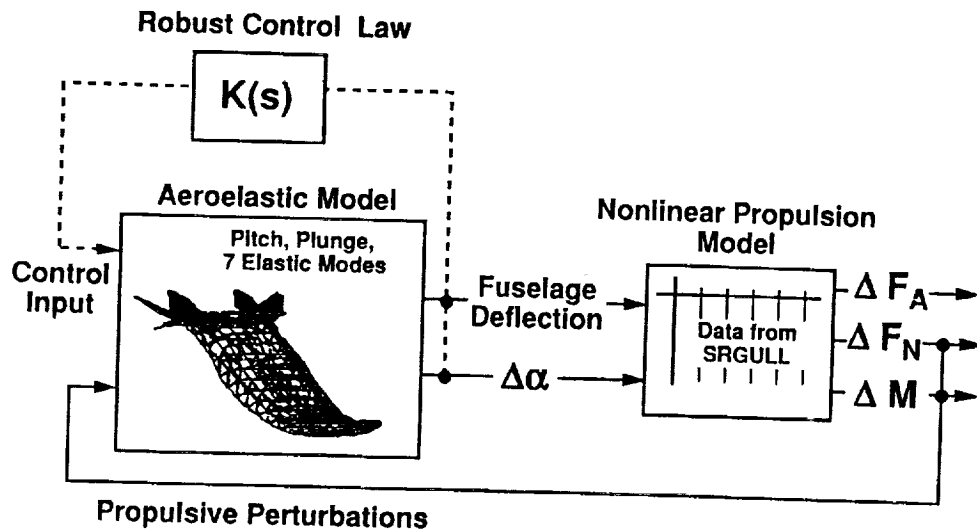
- **Improve integration of aeroelastic/ propulsion models.**
- **Investigate control solutions for robust performance in the presence of ASPE interactions.**

Concluding Remarks

- **Quantified propulsion sensitivities to angle-of-attack and fuselage elasticity.**

- **Elastically-induced propulsive perturbations did not cause excessive accelerations.**

- **Propulsive moment perturbations may require excessive control deflection to maintain stable trimmed flight.**

- **Propulsion sensitivities significantly alter rigid body flight dynamics.**

- **Nonlinearities in propulsion sensitivities may be viewed as uncertainty in rigid body dynamics.**

CONCLUDING REMARKS

A study has been conducted to investigate the impact of aeroelastic-propulsive interactions on the longitudinal flight dynamics of an air-breathing hypersonic vehicle. A model was developed based on a finite element representation of a hypersonic configuration at two flight conditions of Mach 6 and Mach 10. The model included rigid body pitch and plunge modes and seven elastic modes, as well as propulsion system sensitivities to angle-of-attack variations and structural deflections. The model was incorporated into a simulation to produce time histories of propulsion force and moment perturbations in response to elastic deflections. The force and moment perturbations were then fed back into the aeroelastic model to allow their impact on the dynamics of the combined aeroelastic-propulsive system to be assessed.

The propulsion model exhibited a pronounced sensitivity to angle-of-attack variations and elastic fuselage deflections. Significant nonlinearities were observed in the propulsion system sensitivities. Elastic responses to a representative control input appeared acceptable. The normal and axial force perturbations induced by the elastic deflections were appreciable, but did not produce excessive vertical or longitudinal acceleration transients for the subject configuration. Moment perturbations induced by the elastic deflections, however, appeared quite large and might require significant control activity to maintain stable trimmed flight. A high level of control activity at hypersonic speeds could compromise fuel efficiency, thereby reducing payload capacity or range.

A significant impact on the rigid body flight dynamics was observed when the propulsive force and moment perturbations were fed back into the aeroelastic model. At both flight conditions, the propulsive perturbations caused a coupling of two poles associated with the rigid body flight dynamics. It was also found that the eigenvalues of the rigid body modes were highly sensitive to the angle of attack and nominal fuselage deflections chosen as the linearization condition of the model. This sensitivity is a direct result of nonlinearities in the propulsive force and moment database, and can be thought of as uncertainty associated with the vehicle's rigid body stability coefficients. Considerable variation in the rigid body modes was observed, emphasizing robustness as a critical factor in the design of flight control laws for air-breathing hypersonic vehicles.

C-6.

Launch-Vehicle Trajectory Solutions with Dynamic-Pressure Constraints Via Finite Elements and Shooting

Robert R. Bless*, LESC

Hans Seywald*, AMA

Dewey H. Hodges, Georgia Tech

*Guidance Group, Spacecraft Controls Branch

Outline

- Optimal Control Problem Definition
- State Constraints
- Methods of Solution
  - Multiple Shooting
  - Finite Elements
- Launch-Vehicle Model
- Results
- Summary

Problem Definition

$$\text{minimize} \quad J = \phi[x(t_f), t_f] + \int_0^{t_f} L(x, u, t)\, dt$$

subject to state equations $\quad \dot{x} = f(x, u)$

boundary conditions $\quad \psi[x(t_f), t_f] = 0$

control constraints $\quad C(x, u, t) \leq 0$

and state constraints $\quad S(x, t) \leq 0$

Result is a nonlinear multi-point boundary-value problem

State Constraints

Consider active state constraint for $t_1 \leq t \leq t_2$

$$S(x) = 0$$

is equivalent to

$$S[x(t_1)] = 0$$

$$\vdots$$

$$\frac{d^{(q-1)} S[x(t_1)]}{dt^{(q-1)}} = 0$$

and

$$\frac{d^q S}{dt^q} = S^{(q)}(x, u) = 0 \quad \text{for} \quad t_1 \leq t \leq t_2$$

Multiple Shooting Method

- Initial guesses chosen for states and costates
- Differential equations integrated forward
- Guesses updated via zero-finding method
- Process repeats until all boundary conditions are satisfied

Finite Element Method

- Discretization of continuous-time necessary conditions
- Set of nonlinear algebraic equations generated
- Initial guesses required for each element along trajectory
- Nonlinear equations can be solved by Newton-Raphson method

Comparison of Methods

- Shooting
  - Sensitive to initial guesses
  - Slow iteration process due to integration
  - Numerically exact answer is found
- Finite Element
  - Initial guesses more easily obtained
  - Fast iteration process (sparse Jacobian)
  - Second-order accuracy

Finite element solutions can provide guesses for shooting

Launch-Vehicle Model

- NLS two-stage rocket (point-mass model)
    - States are mass, altitude, velocity, and flight-path angle
    - Scalar control is angle-of-attack
    - Fixed staging time; change in thrust and mass
    - Exponential atmosphere
    - Piecewise constant aerodynamic coefficients

Launch-Vehicle Model (continued)

- Mission
    - Maximize final mass
    - Perigee injection of 80×150 NM orbit
- Constraint on maximum dynamic pressure
- Engine out on pad

Results

Results

478
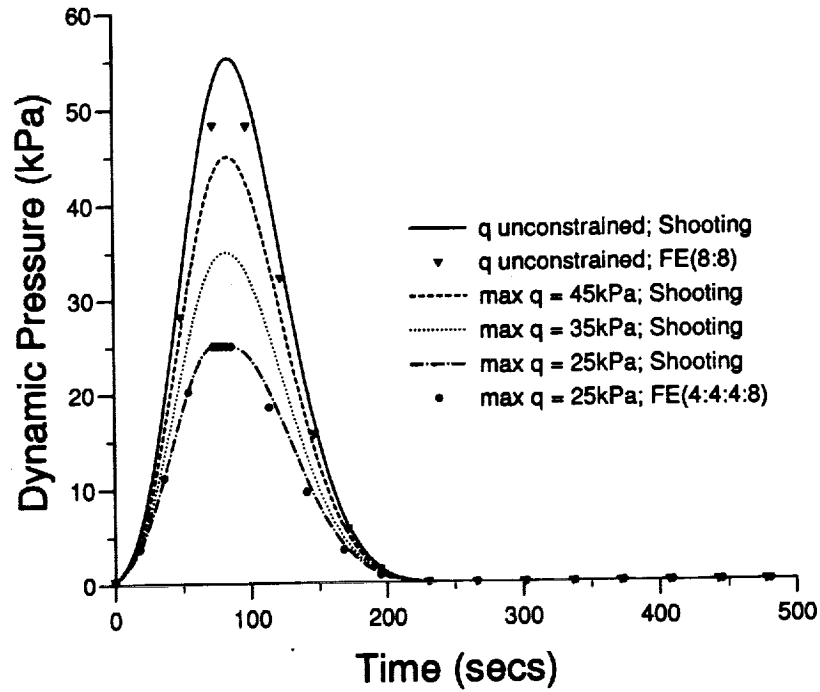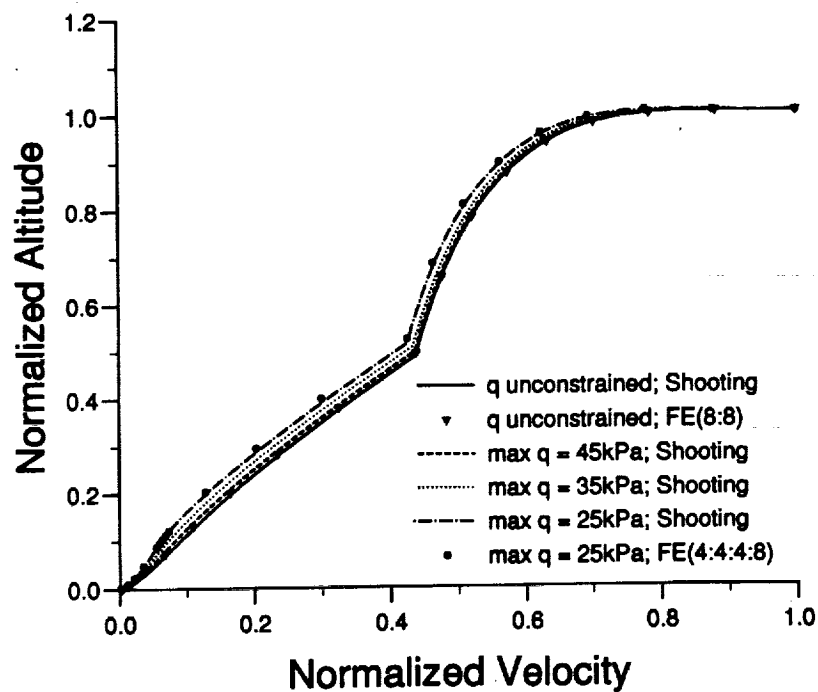
Results

Results
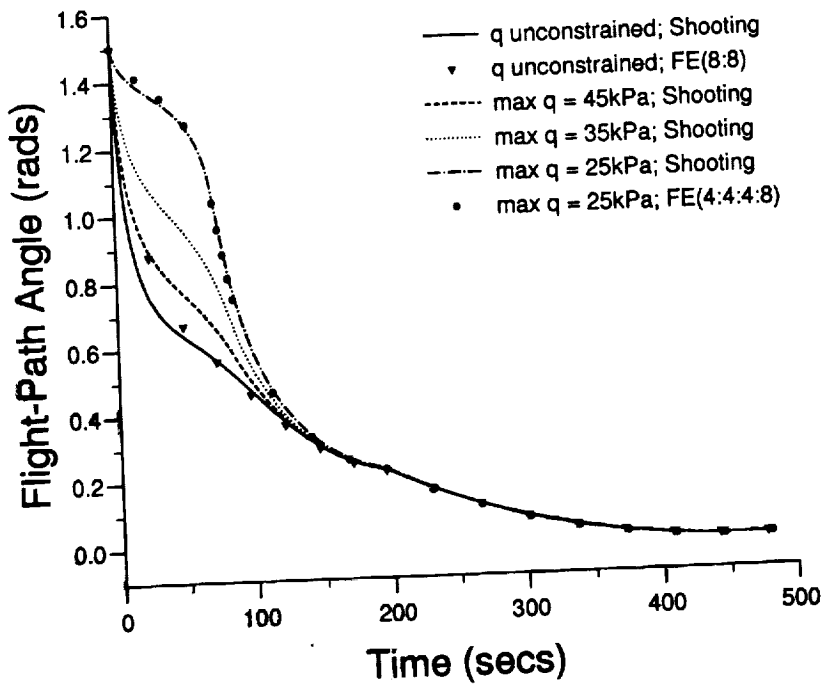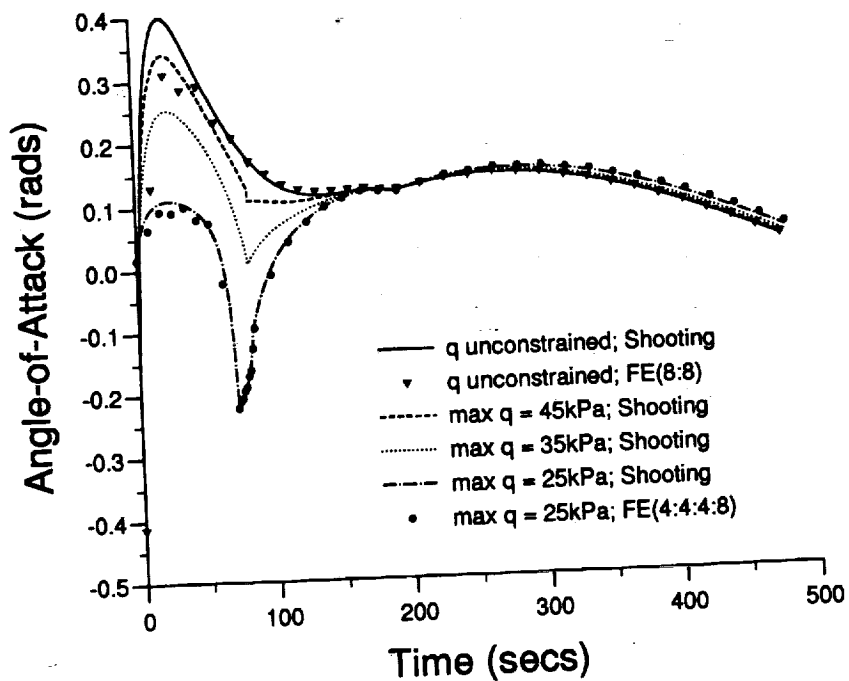
Results
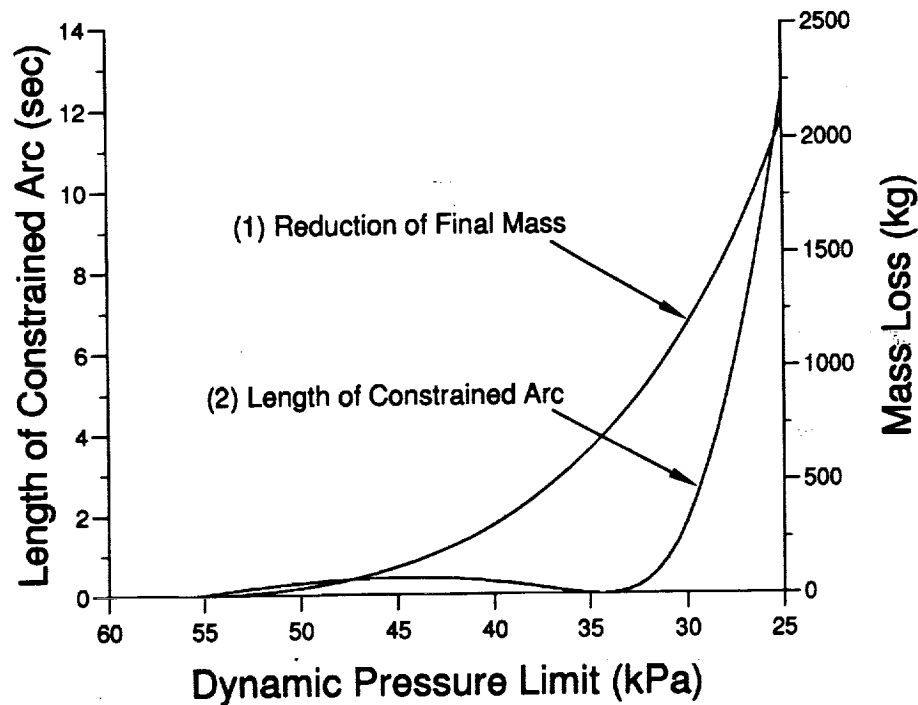
Summary

(1) The finite element and shooting methods are complementary algorithms

(2) The work has produced a family of dynamic-pressure constrained solutions

(3) An uncommon first-order touch-point solution has occurred (not observed in literature yet)

(4) This work will be reported on at the AIAA GNC Conference in August

    (a) Derivation of finite element method

    (b) Discuss touch-point behavior

Optimal RTLS Abort Trajectories for an HL-20 Personnel Launch Vehicle

Kevin Dutton
Spacecraft Controls Branch

Outline

- Objective of study
- HL-20 Vehicle and Mission
- Modelling Information
- Problem Formulation
- Solution Method
- Results
- Concluding Remarks

Objective

**Primary: Determine whether RTLS abort at
T seconds along launch trajectory is
possible using optimal control theory**

**Secondary: Assess effects of bank angle
constraint, lift coefficient constraint, free
and fixed final boundary conditions, etc.**

HL-20 PLS BASELINE DESIGN

23.5 ft

29.5 ft

	Weight, lb
Dry (with 22% margin)	19,777
Landed	22,057
On-Orbit	26,186
Launch Escape System/Adapter	8,420
Gross Launch on NLS	34,607

Removeable panels

OMS

Aluminum pressure vessel

RCS

Subsystem attachment areas

Shuttle-derived tiles

Fighter technology landing gear
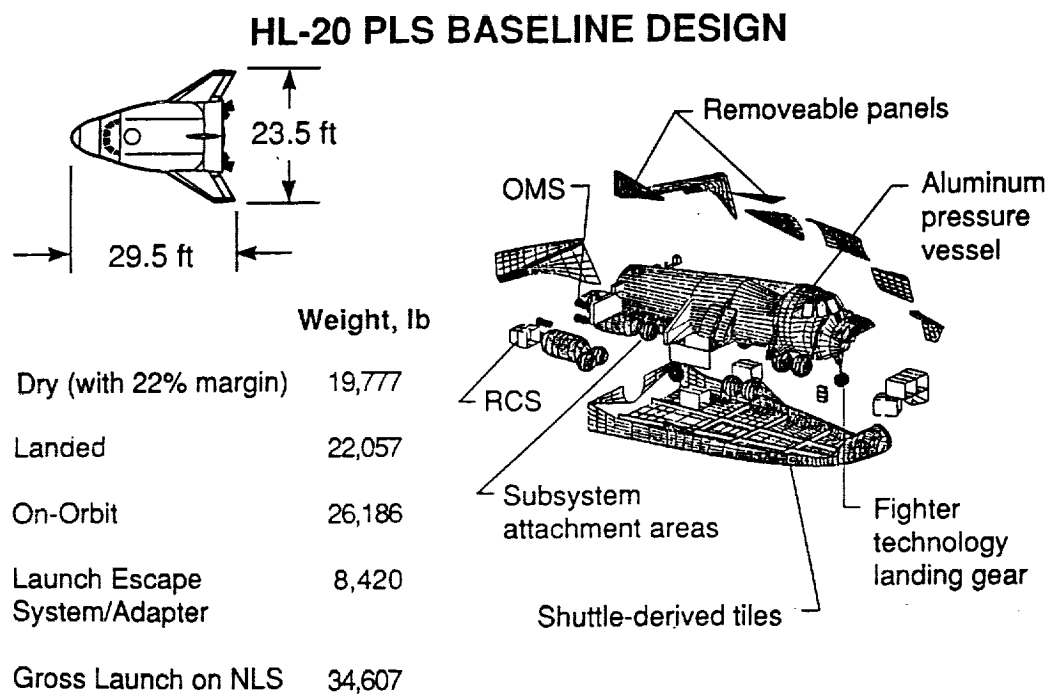
HL-20 PLS CURRENT TECHNOLOGY DESIGN

482

THE PERSONNEL LAUNCH SYSTEM (PLS)

Complementary System to Space Shuttle

- Space Station crew transfer
- Alternate access to/from space for people/priority cargo

Space Station Reference Mission

- Transfer and return up to 8 Space Station personnel and/or priority cargo
- 72-hour mission duration
- 1,100 ft/sec on-orbit propulsive capability
- Placed in orbit by existing or future booster system
- Kennedy Space Center launch/landing site
- Alternate landing site capability
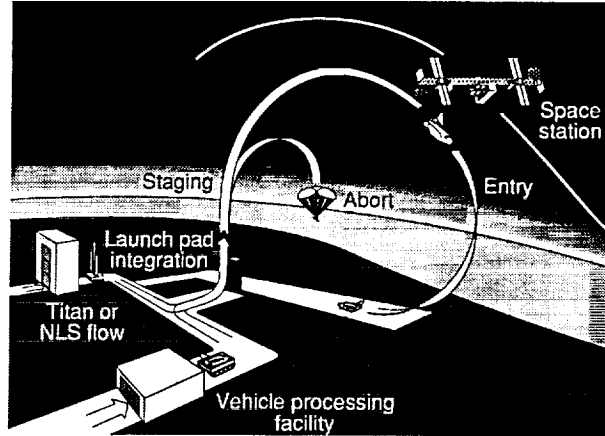
Talay 34

HL-20 Aborts

VAB Analysis

- **On the pad**
- **0-20 sec**   Return to Launchsite (Shuttle landing facility)
- **20-65 sec**   RTLS (Skid strip)
- **65-403 sec**   Ocean landing by parachute
- **403-478 sec**   Transatlantic abort landing
- **478+ sec**   Abort to orbit

Vehicle Aerodynamic Model

- Aerodynamic data from Jackson and Cruz

- At each angle of attack and Mach number, find $\delta_E, \delta_L, \delta_U$ that trim vehicle and minimize drag; calculate Cl and Cd here

- For each Mach number, determine coefficients for Cd expression

$$C_D = C_{D_0}(M) + C_{D_1}(M) \, C_L + C_{D_2}(M) \, C_L^2$$

Optimal Control Theory

- **Cost** $\min\limits_{\bar{u}} J = \Phi[\bar{X}(t_0), \bar{X}(t_f)]$

- **Plant** $\dot{\bar{X}} = f(\bar{X}, \bar{u})$

- **Constraints:**

	Control	State
	$\bar{g}(\bar{X}, \bar{u}) = 0$	$\bar{c}(\bar{X}) = 0$
	$\bar{h}(\bar{X}, \bar{u}) \leq 0$	$\bar{d}(\bar{X}) \leq 0$

- **Boundary conditions** $\psi[\bar{X}(t_0), \bar{X}(t_f)] = 0$

Cost Function and Plant

- $J = -h(t_f)$ (final altitude)
- States $\bar{X} = [h\ x\ y\ V\ \gamma\ \psi]^T$
  - x,y   Cartesian system, x east, y north, origin at point runway centerline extended
  - ψ 0 for easterly flight, increases CCW
- Controls $\bar{u} = [C_L\ \sigma]^T$
  - σ negative for right bank
- Equations of motion: flat earth, non-thrusting, aerospace vehicle

Control/State Constraints

- Bank angle can be constrained (40 deg. nominal)

$$-\sigma_{max} \leq \sigma \leq \sigma_{max}$$

- Lift coefficient is constrained between upper and lower trim limits (function of Mach)

$$C_{L_{min}}(M) \leq C_L \leq C_{L_{max}}(M)$$

- Normal and axial load factor constraints (3 g units nominal)

485

Lift Coefficient Constraint
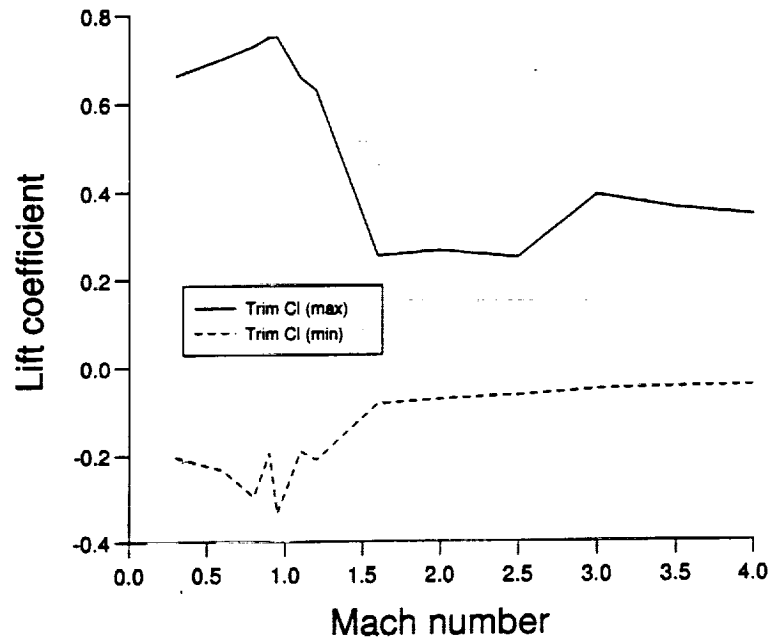
Initial Conditions

- Initial conditions for abort at T seconds are
  conditions at T along ascent trajectory
  followed by primary solid rocket motor (srm)
  burn, followed by sustainer srm burn

- Example: Initial conditions for abort at T=30

h(t0) = 32882 ft	V(t0) = 1565 ft/sec
x(t0) = - 7409 ft	γ(t0) = 79.7 deg
y(t0) = 45357 ft	ψ(t0) = - 2.0 deg

486

Final Conditions

For all cases:

$x(tf) = 0.0$ ft

$y(tf) = 0.0$ ft

$V(tf) = 521.0$ ft/sec

$\gamma(t_f) = -19.0$ deg

$\psi(t_f) = -220.7$ deg
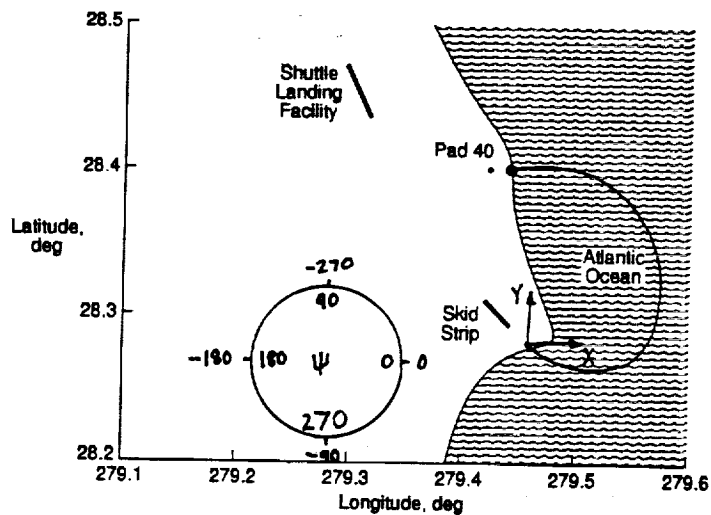
Solution Method

Trajectory Optimization by Differential Inclusion (TODI)

- eliminates controls from problem by constraining state rates

- leads to nonlinear programming problem where parameters are state values at user defined nodes (NPSOL)

The Differential Inclusion Approach Explained on a Simple Example

$$\min \; - x(1)$$
$$\dot{x} = u, \quad 0 \le u \le 1$$
$$x(0) = 0$$

pick states at equidistantly chosen node points
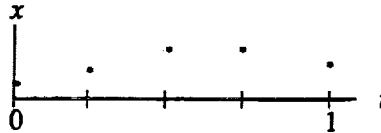
neighboring states have to satisfy either

(differential equation approach)

$$\frac{x_{i+1} - x_i}{\Delta t} = u_i, \quad 0 \le u_i \le 1$$

or

(differential inclusion approach)

$$\frac{x_{i+1} - x_i}{\Delta t} \ge 0 \quad and \quad \frac{x_{i+1} - x_i}{\Delta t} \le 1$$

General Discretization Scheme

Optimal control problem

$$\min_{u \in (PWC[0,1])^m} \Phi(x(0), x(1))$$

$$\Psi(x(0), x(1)) = 0$$

$$\dot{x} = f(x(t), u(t))$$
$$g(x(t), u(t)) = 0$$
$$h(x(t), u(t)) \le 0$$

$$c(x(t)) = 0$$
$$d(x(t)) \le 0$$

Finite dimensional discretization

$$\min_{[x_0 \dots x_N] \in R^{n \times N}} \Phi(x_0, x_N)$$

$$\Psi(x_0, x_N) = 0$$

for $i = 0, \dots, N-1$:
$$p\left(\frac{x_{i+1} - x_i}{N}, x_i\right) = 0$$
$$q\left(\frac{x_{i+1} - x_i}{N}, x_i\right) \le 0$$

for $i = 0, \dots, N$:
$$c\left(x_i\right) = 0$$
$$d\left(x_i\right) \le 0$$

Solution for 30 Second Abort Case
Altitude vs. Time
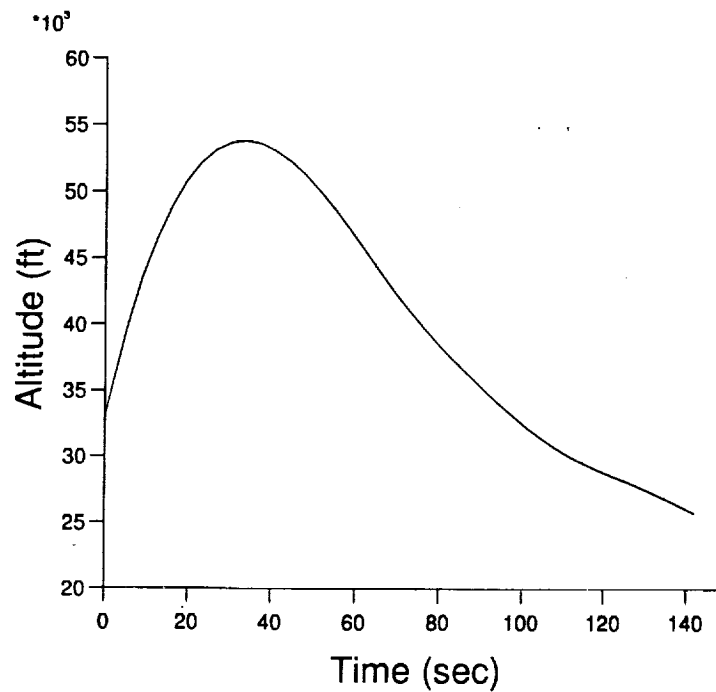
Solution for 30 Second Abort Case
Groundtrack

489
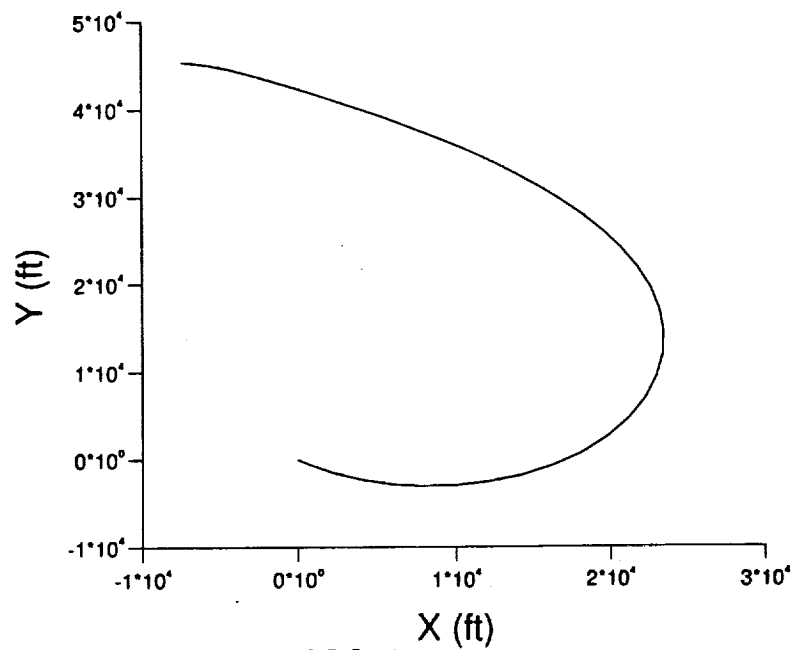
Solution for 30 Second Abort Case
Velocity vs. Time
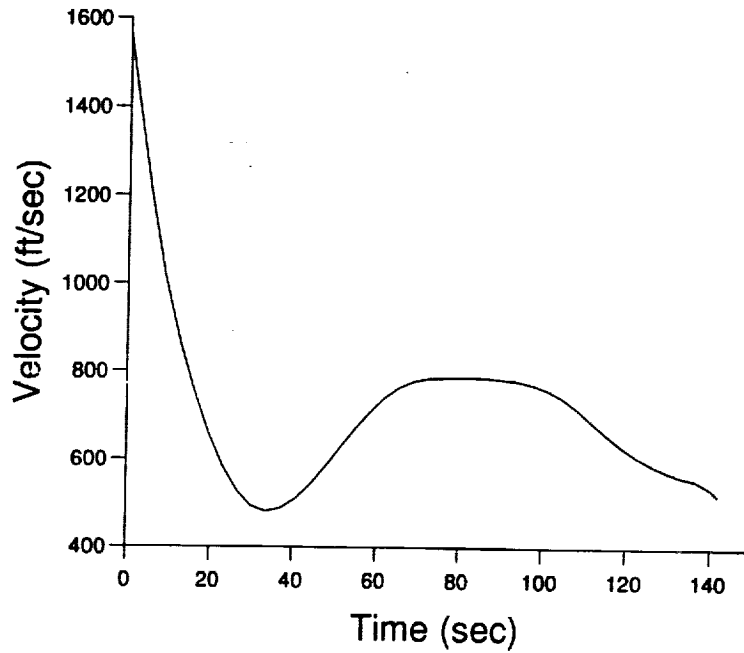
Solution for 30 Second Abort Case
Flight Path Angle vs. Time

490
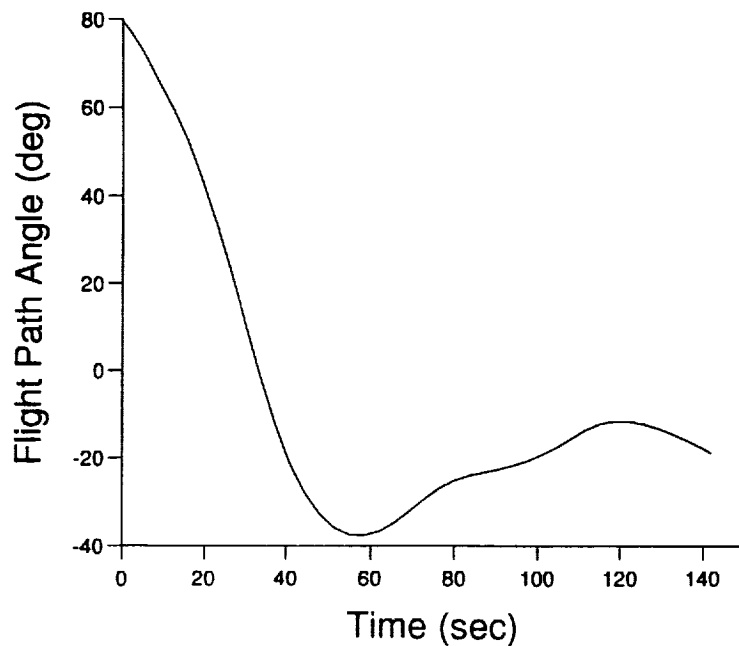
Solution for 30 Second Abort Case
Heading vs. Time
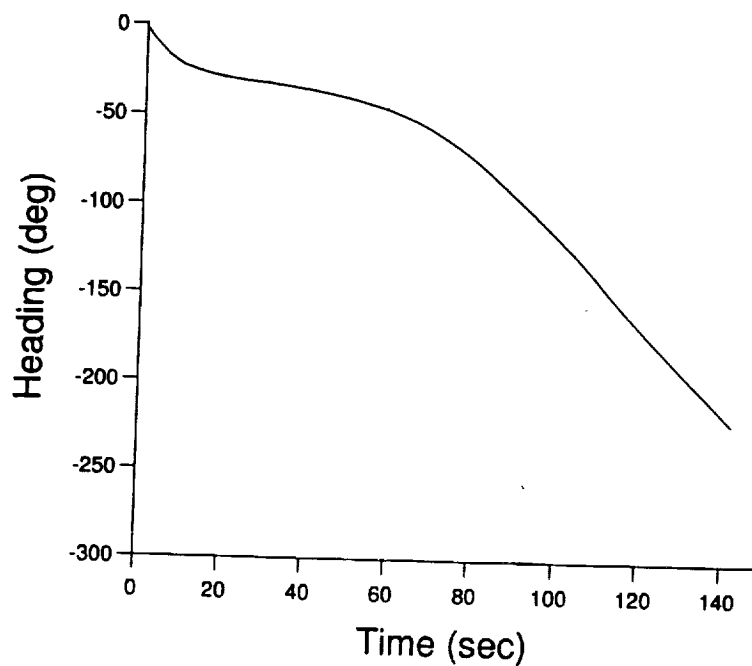
Solution for 30 Second Abort Case
Lift Coefficient vs. Time

491
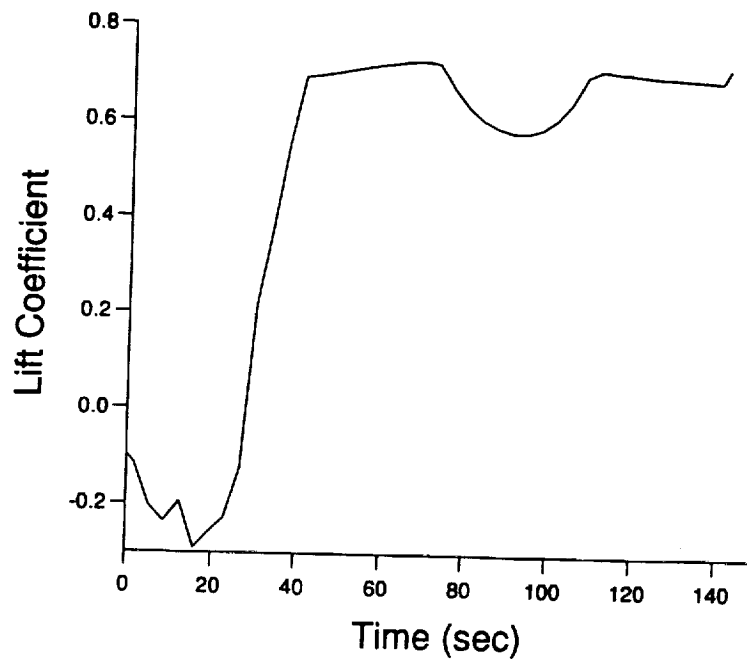
Solution for 30 Second Case
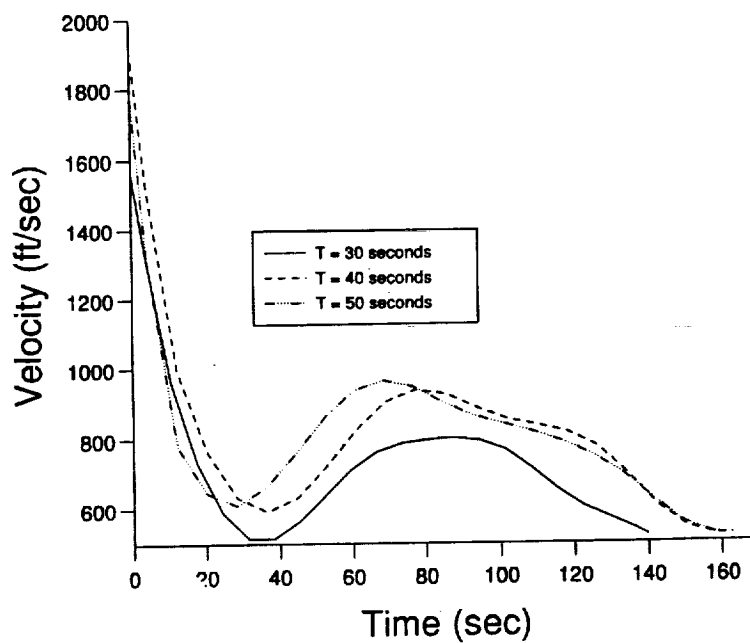## Bank Angle vs. Time
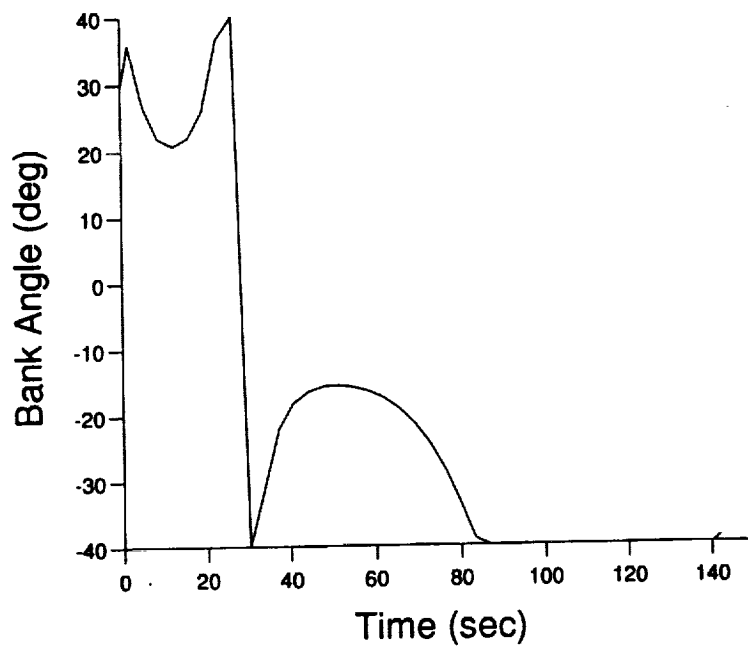
Comparison of T=30,40,50 Sec. Aborts
Altitude vs. Time

492
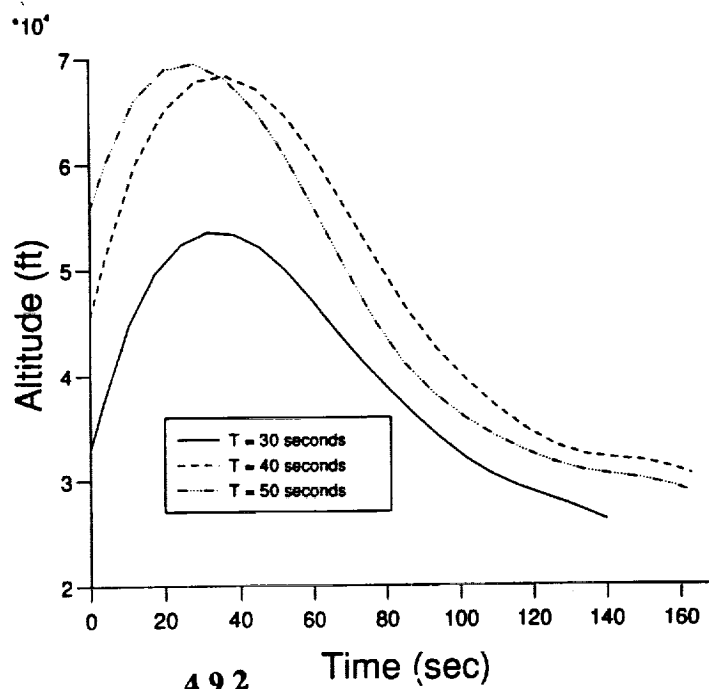
Comparison of T=30,40,50 Sec. Aborts
Groundtrack
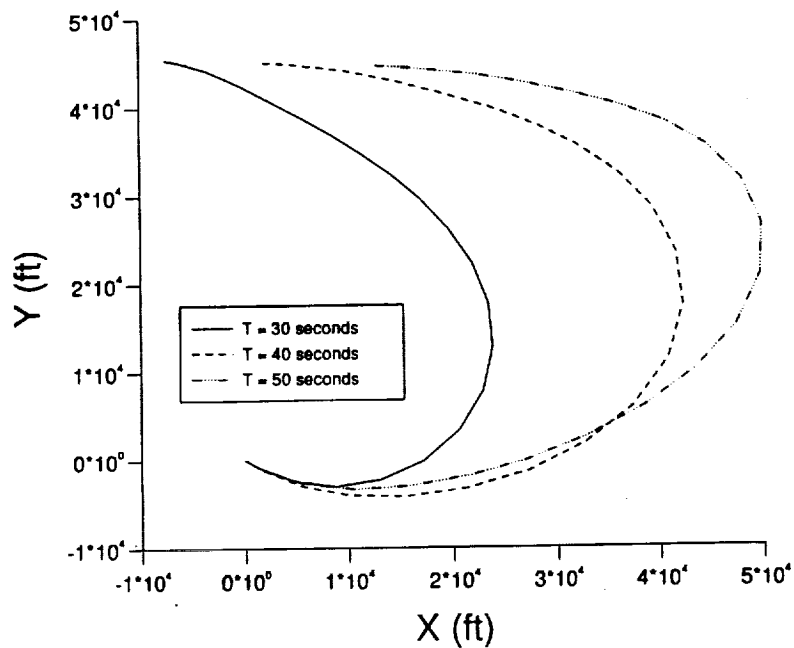
Comparison of T=30,40,50 Sec. Aborts
Velocity vs. Time

493

Comparison of T=30,40,50 Sec. Aborts
Flight Path Angle vs. Time
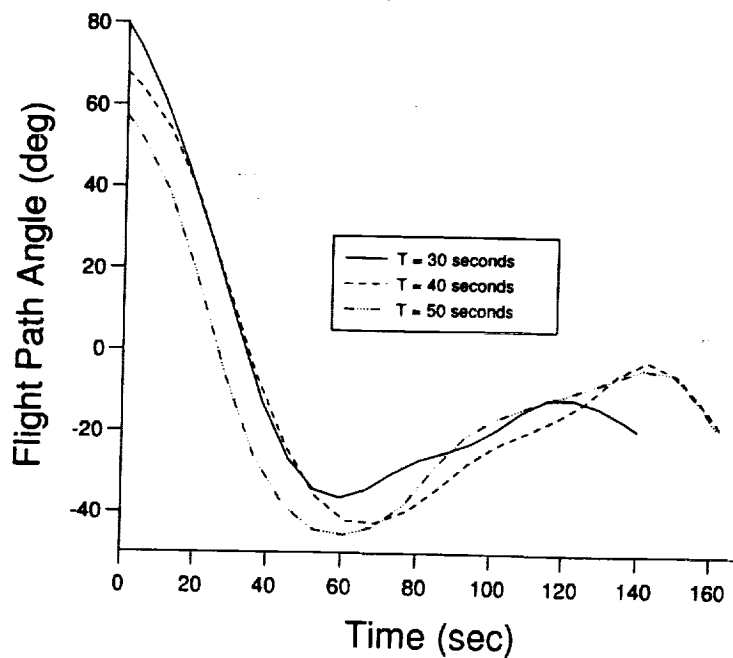
Comparison of T=30,40,50 Sec. Aborts
Heading vs. Time

494
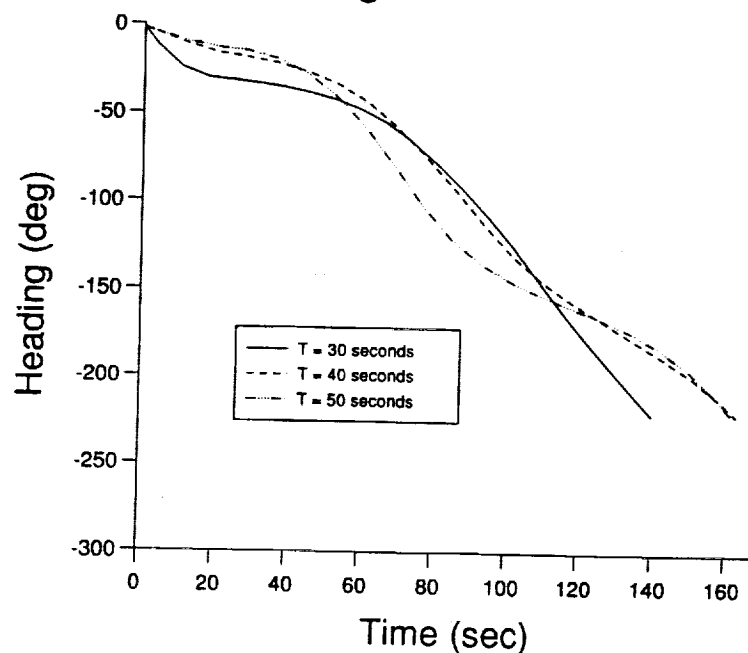
Comparison of T=30,40,50 Sec. Aborts
Lift Coefficient vs. Time
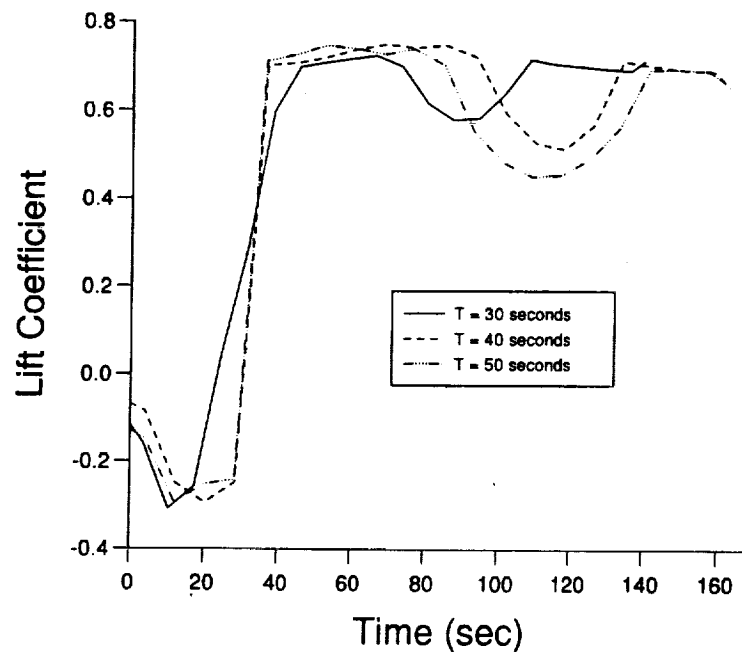
Comparison of T=30,40,50 Sec. Aborts
Bank Angle vs. Time

495
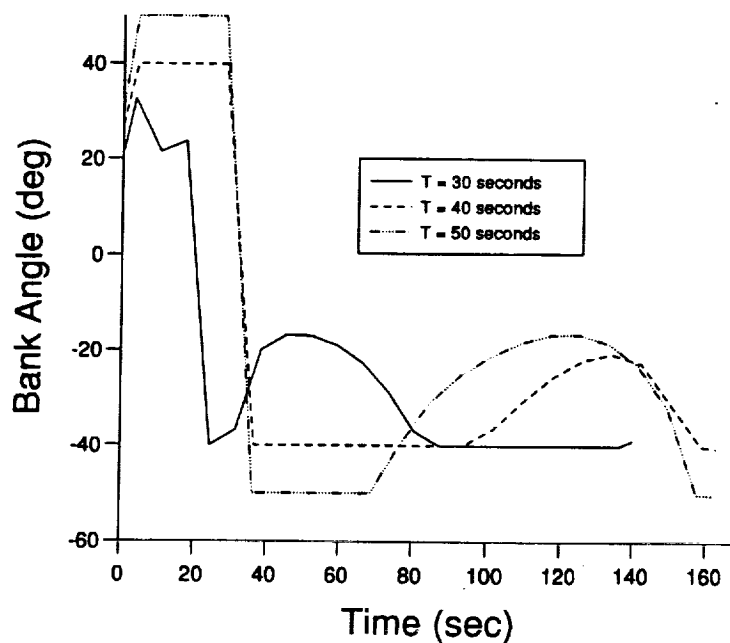
Concluding Remarks

- When final V is fixed, maximizing final h is nearly same as maximizing final energy ==>calculation of minimum energy trajectories

- Choice of cost function for abort (and reentry) not obvious

- Future work:

  - Single Stage Vehicle (?)

  - experiment to assess "power" of TODI approach compared to traditional shooting

Range Optimal Atmospheric Flight Vehicle Trajectories in Presence of a Dynamic Pressure Limit

BY

Hans Seywald

Analytical Mechanics Associates Inc. (AMA)

Spacecraft Control Branch, NASA LaRC

PURPOSE OF THIS TALK

- Explore nature of range–optimal flight

- Present techniques for identifying temporal structure of optimal control

- Demonstrate in application to an aircraft example

PROBLEM FORMULATION

Cost Function:

$$J [u] = - x (t_f)$$

Initial Conditions:

$E(0) = 38,029.[m]$
$h(0) = 12,119.[m]$
$\gamma(0) = 0.°$
$x(0) = 0.[m]$

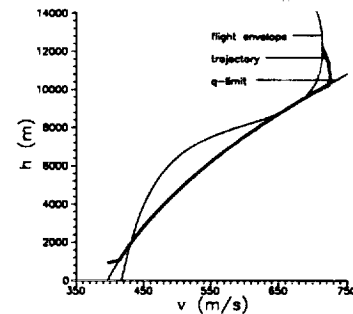**Control constraint:**

$0 \leq \eta \leq 1$
$|n| \leq n_{max}$

State Equations:

$\dot{E} = (\eta T - D) \dfrac{v}{W}$
$\dot{h} = v \sin \gamma$
$\dot{\gamma} = \dfrac{g}{v}(n - \cos \gamma)$
$\dot{x} = v \cos \gamma$

Final Conditions:

$E(t_f) = 9000.[m]$
$h(t_f) = 942.[m]$
$\gamma(t_f) = -11.5°$
$x(t_f)$ be maximized

State constraint:

$v \leq v_{max}(h)$

Final time:

$t_f = 60[sec]$

SIGNIFICANCE FOR PRACTICAL APPLICATION

- Validate optimality of solutions obtained with other methods

- Use optimal solutions to develop guidance laws based on neighboring optimal control

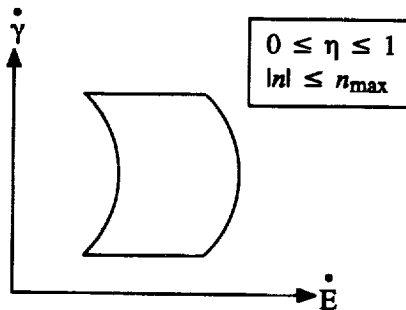- Decide on choice of discretization (e.g. finite elements)

OUTLINE

- Hodograph analysis

- Possible control logics / Optimal switching structures

- Numerical procedures and results

- Summary and Conclusions

HODOGRAPH ANALYSIS

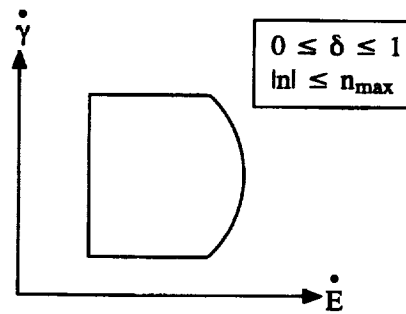| Original formulation: |
| --- |

$$\dot{E} = (\eta T - D)\frac{V}{W}$$
$$\dot{\gamma} = \frac{g}{V}(n - \cos\gamma)$$

$$0 \leq \eta \leq 1$$
$$|n| \leq n_{max}$$

New formulation:

$$\dot{E} = [\delta(T - D + D_{max}) - D_{max}]\frac{V}{W}$$
$$\dot{\gamma} = \frac{g}{V}(n - \cos\gamma)$$

$$0 \leq \delta \leq 1$$
$$|n| \leq n_{max}$$

POSSIBLE CONTROL LOGICS / OPTIMAL SWITCHING STRUCTURE

1) $v - v_{max} < 0$, $\delta = 1$, $\qquad \dfrac{\partial H}{\partial n} = 0$

2) $v - v_{max} = 0$, $\delta = 1$, $\qquad n > 0$ *from* $\dfrac{d}{dt}(v - v_{max}) = 0$

3) $v - v_{max} = 0$, $\delta = 1$, $\qquad n < 0$ *from* $\dfrac{d}{dt}(v - v_{max}) = 0$

4) $v - v_{max} = 0$, δ *from* $\dfrac{d}{dt}(v - v_{max}) = 0$, n *singular*

5) $v - v_{max} = 0$, δ *from* $\dfrac{d}{dt}(v - v_{max}) = 0$, $n = n_{max}$

6) $v - v_{max} < 0$, $\qquad\qquad \delta = 0$, $n = n_{max}$

THOROUGH ANALYSIS YIELDS

- 12 different possible control logics are obtained

  6 cases with v_{max}–limit not active
  1 first–order singular case with v_{max} –limit not active
  6 cases with active v_{max}–limit
  1 first–order singular case with v_{max}–limit active
 1 second order singular case with v_{max}–limit active

- To perform higher order optimality tests the Generalized Legendre–Clebsch condition has been extended to the case of singular control in presence of state/control constraints

REMARKS

- Switching structure is non–intuitive

- Dynamic pressure constraint makes problem very ill–conditioned

      (i)   standard shooting codes fail
      (ii) developed flexible shooting code
      (iii) trick: start integration at the end of singular control
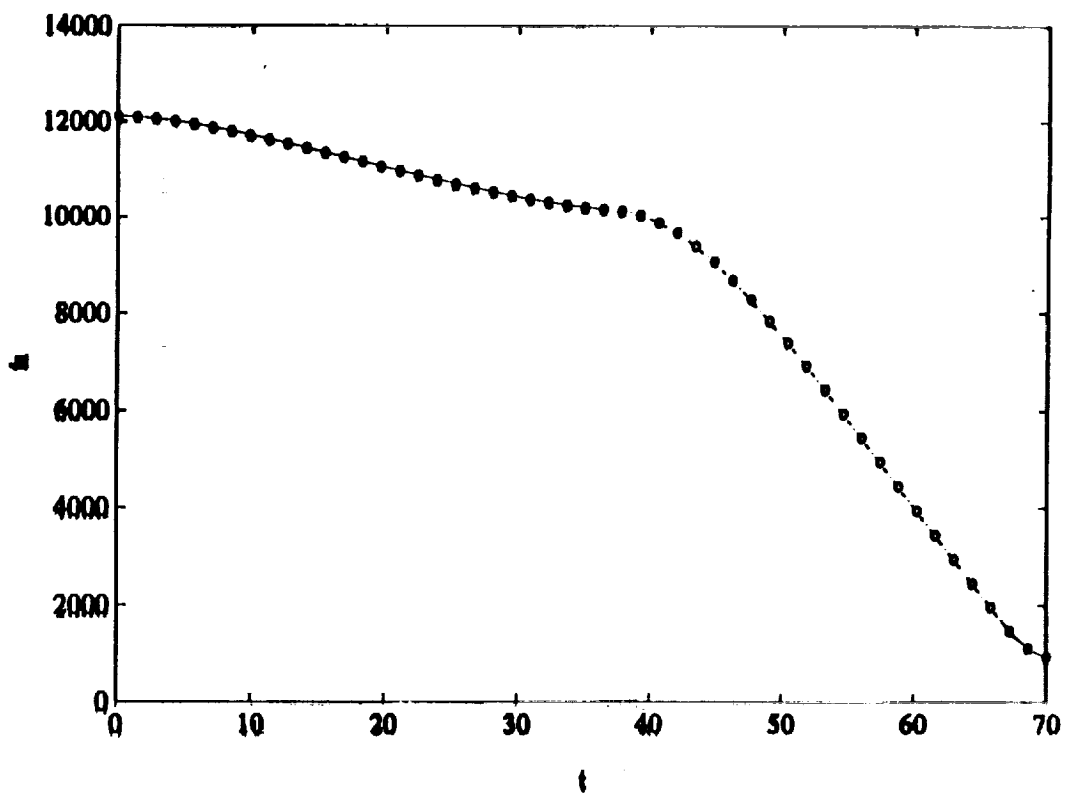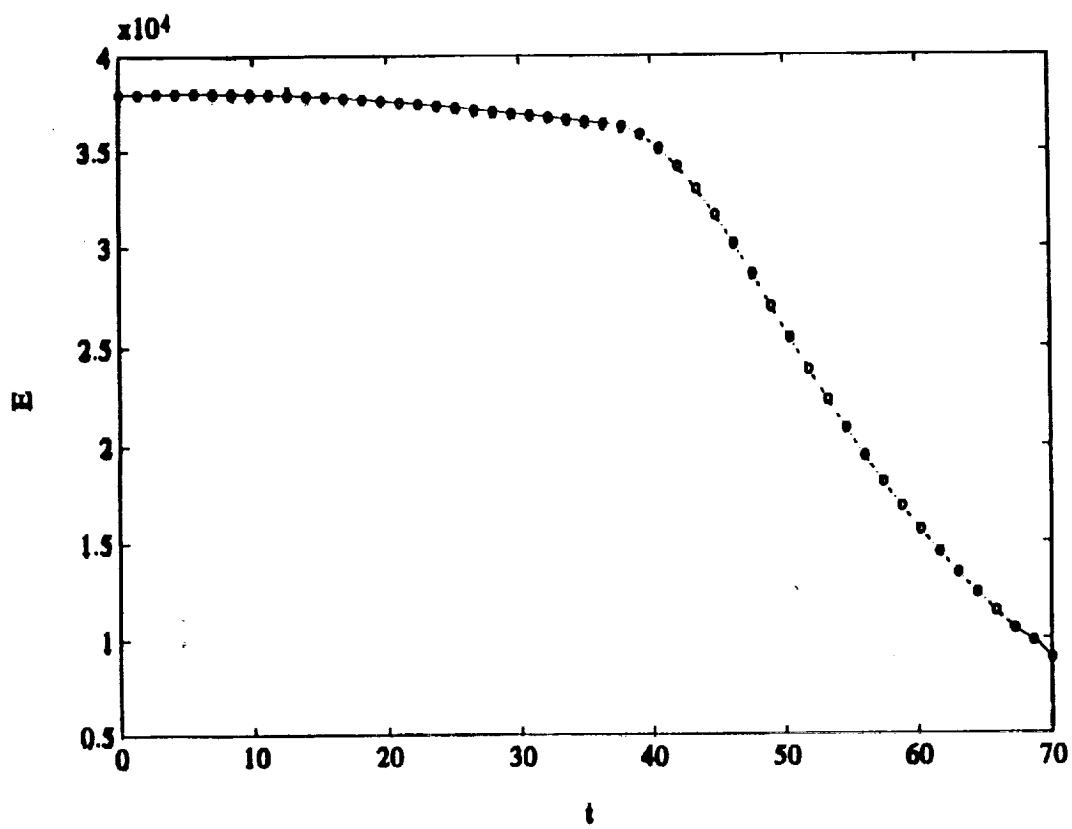
STRUCTURE OF SHOOTING CODE
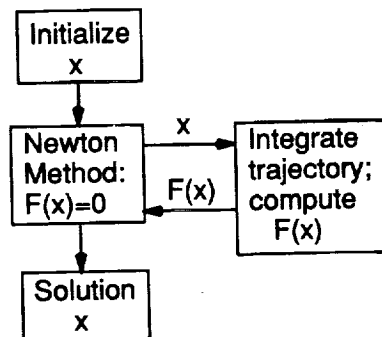
- Boundary value problem: find x such that $F(x)=0$

- User completely determines function F

- Simple structure allows independent debugging of $F(x)$

flight envelope

trajectory

q-limit

504
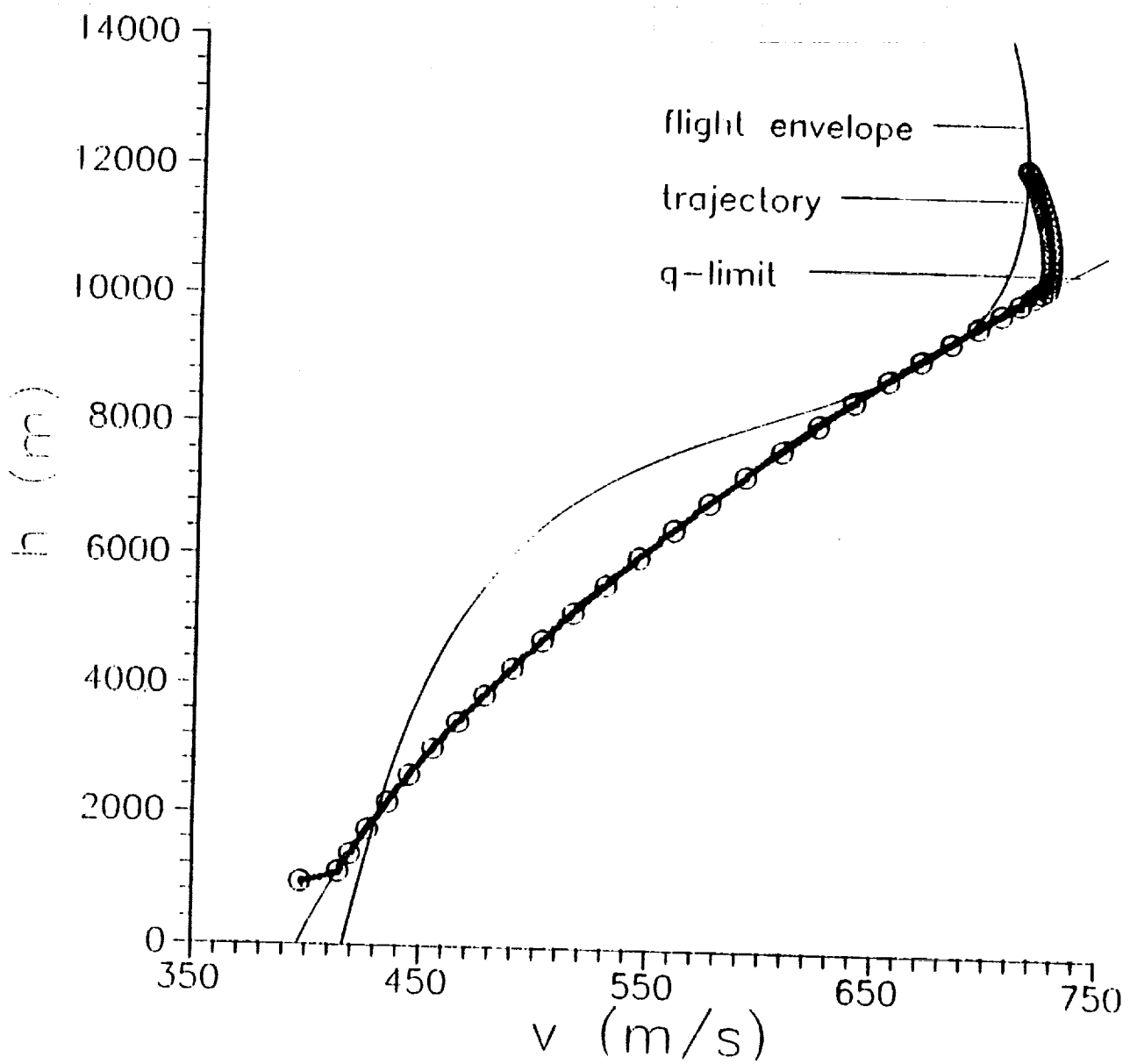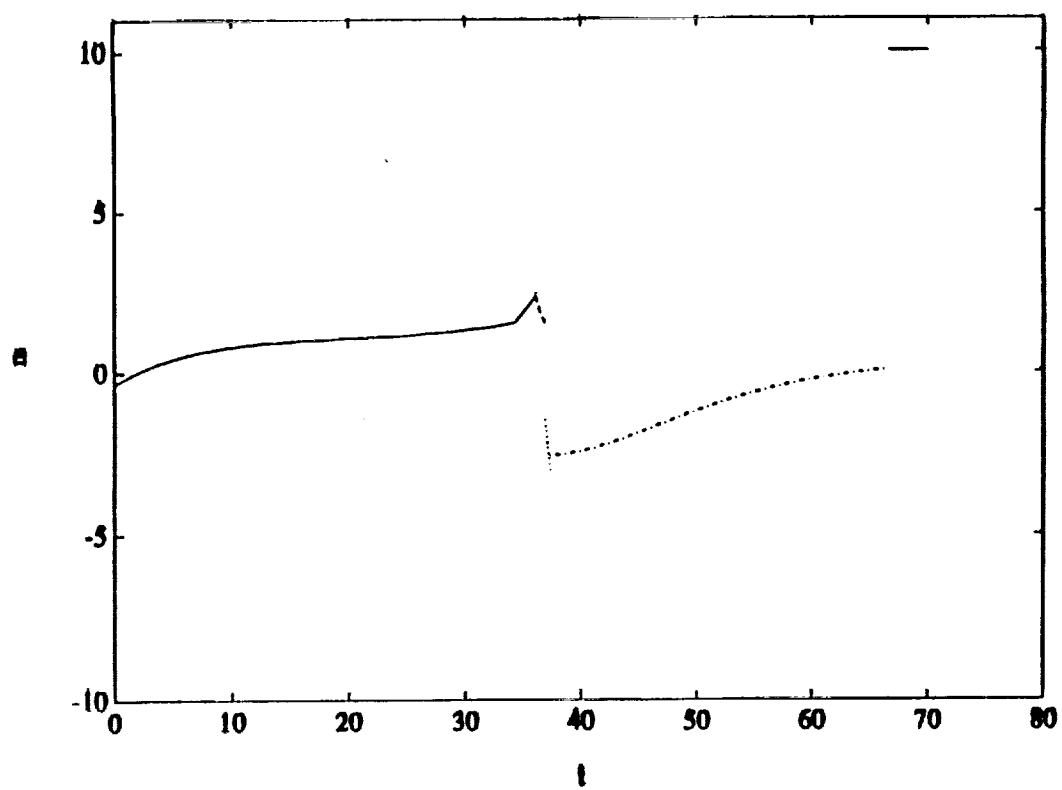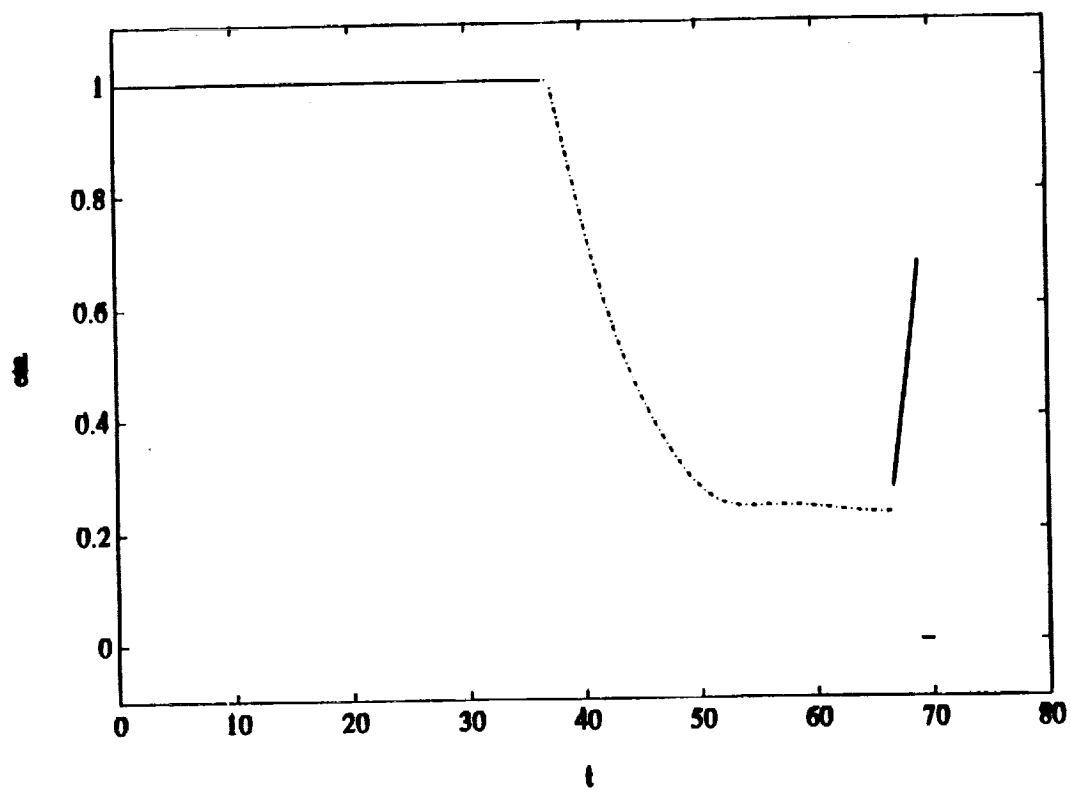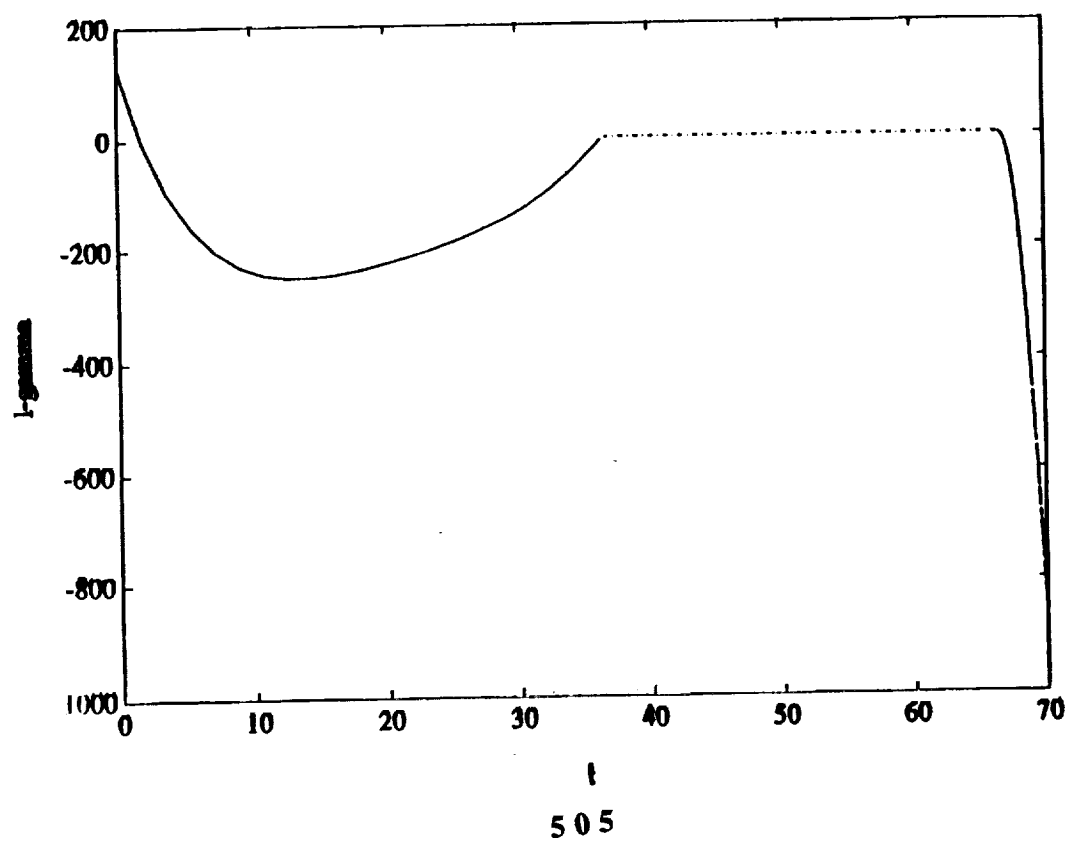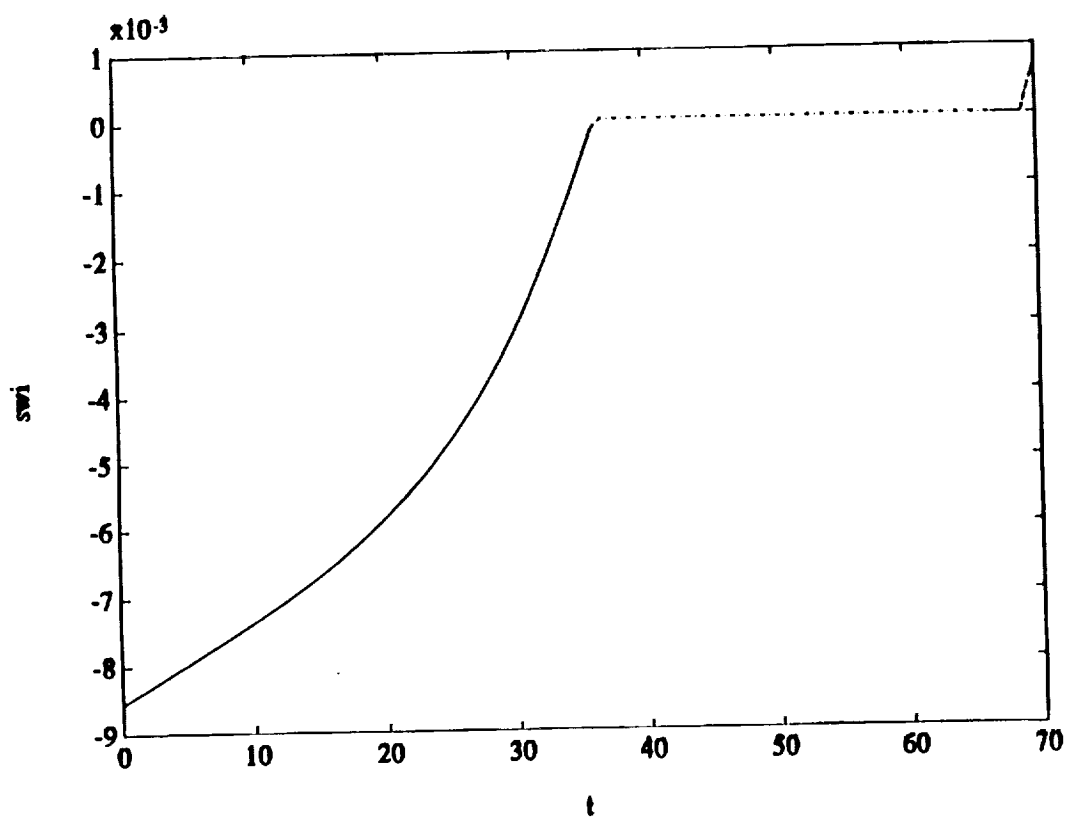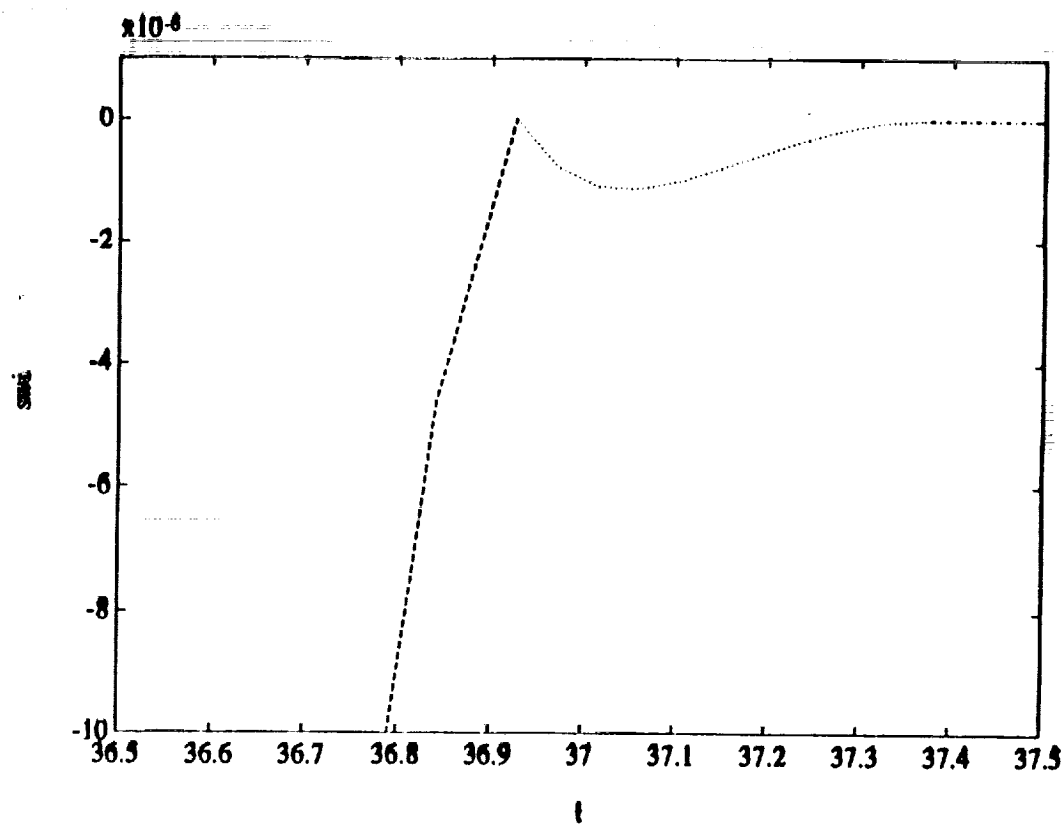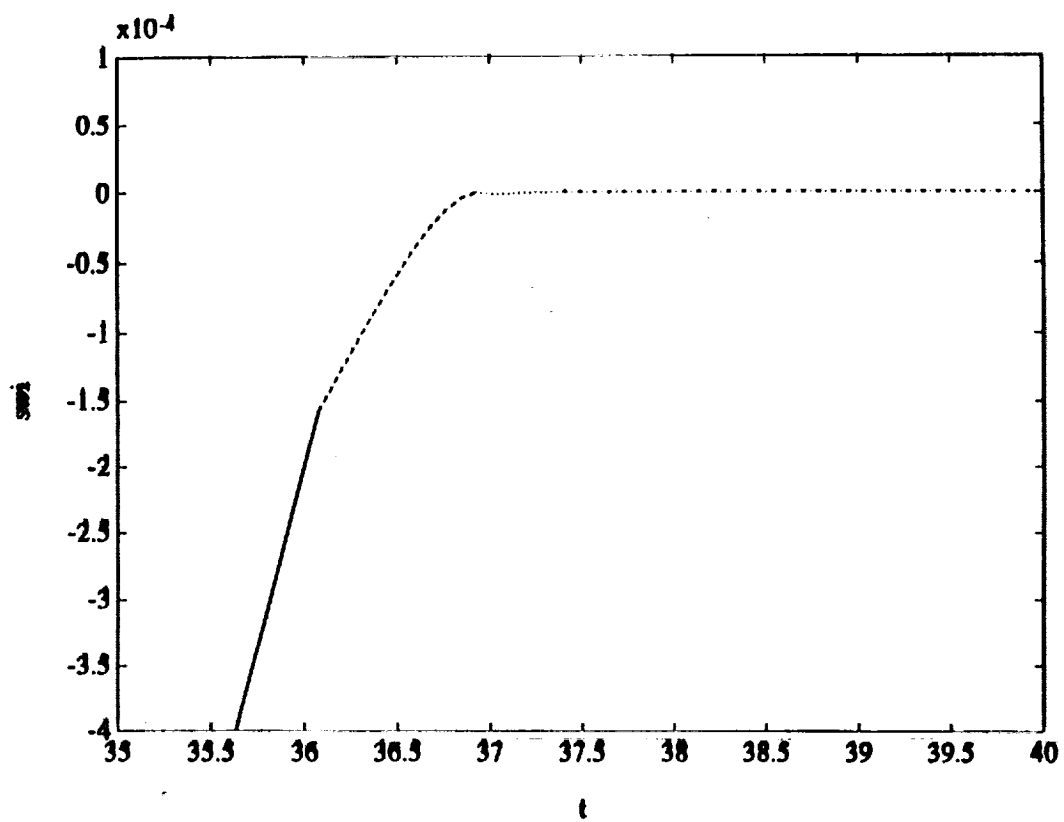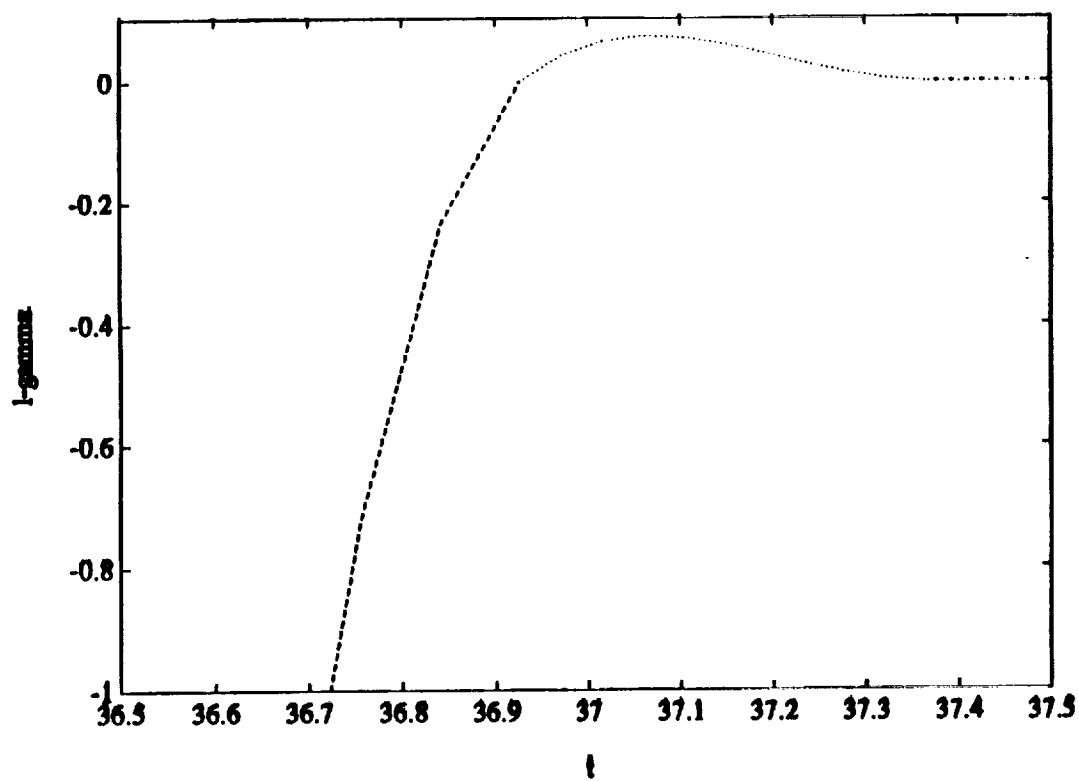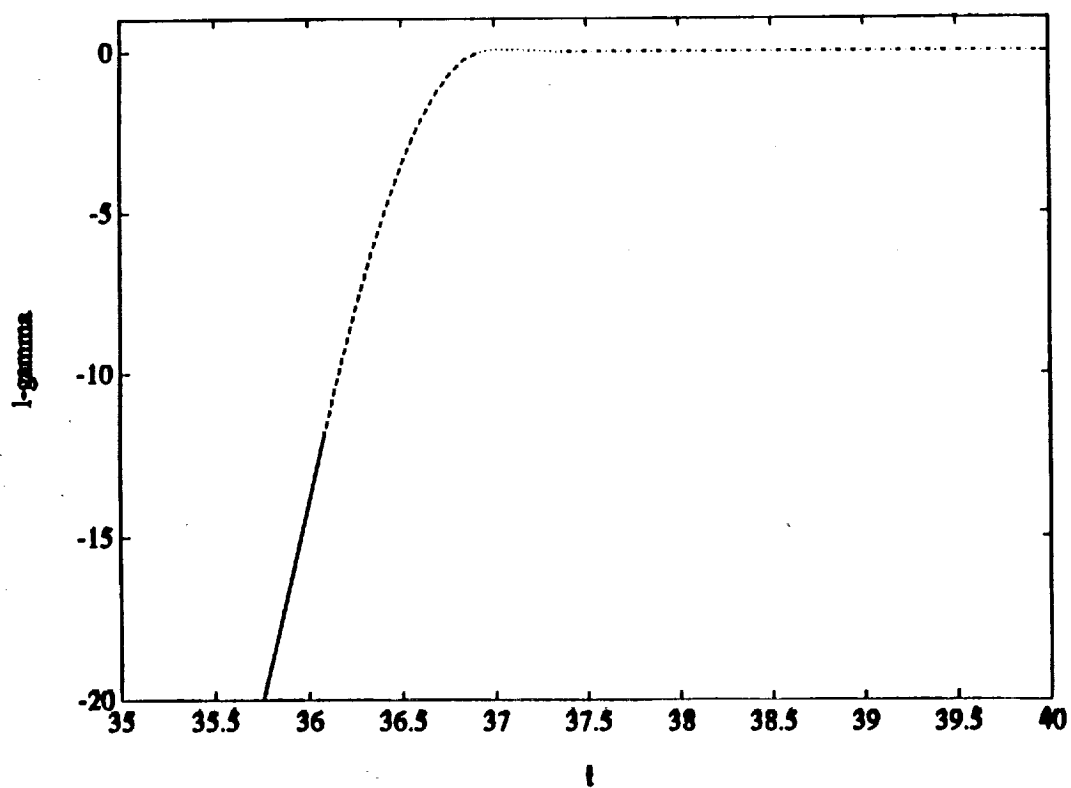
SUMMARY

- All possible control logics are analyzed

- Optimal switching structures are identified.
  Solutions involve singular control along state constrained arcs

- A flexible multipoint shooting code was developed and applied successfully

- TODI was used to perform sanity check and to guess the optimal switching structure

slides_NASA_workshop

3-D Air-to-Air Missile Trajectory Shaping Study

by

Renjith Kumar, Hans Seywald
Analytical Mechanics Associates Inc., Hampton, Virginia

and

Eugene Cliff, Late Henry Kelley
Department of Aerospace Engineering, VPI&SU, Blacksburg, Virginia

HISTORICAL BACKGROUND

- Sir Francis Drake and "Manouevre Board"

- World War II
    - Pure-Pursuit
    - Deviated Pursuit
    - Command to Line-of-sight
    - Collision course
    - Proportional Navigation

- Singular Perturbation (Reduced-Order Modeling)

THE GUIDANCE PROBLEM
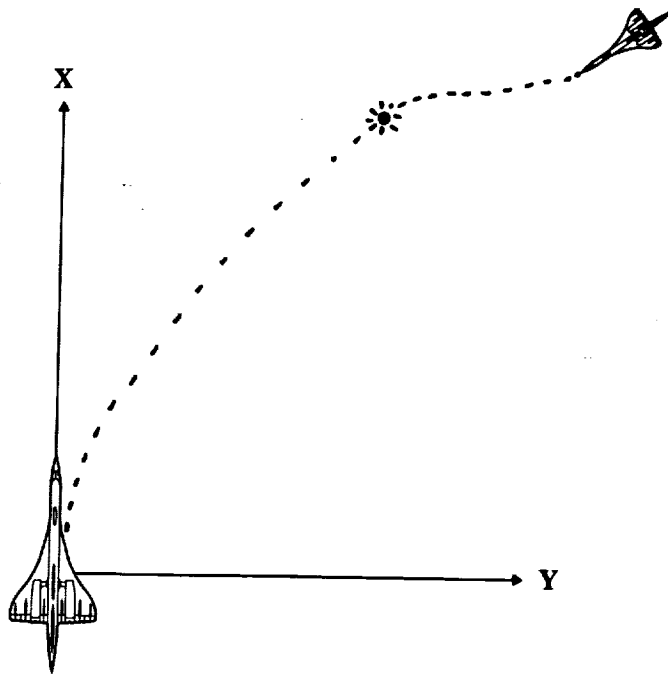
PROBLEM FORMULATION

Cost

$$\min \ -x(t_f)$$

Differential Constraints

$$\dot{x} = V \cos\gamma \ \cos\chi$$

$$\dot{y} = V \cos\gamma \ \sin\chi$$

$$\dot{h} = V \sin\gamma$$

$$\dot{E} = \frac{V}{W(t)} \ (T(t) - D(h,M,n))$$

$$\dot{\gamma} = \frac{g}{V} \ (n_v - \cos\gamma)$$

$$\dot{\chi} = \frac{g}{V} \ \frac{n_h}{\cos\gamma}$$

Initial and Final Conditions

$x(0) = 0$	$x(t_f)$ to be optimized
$y(0) = 0$	$y(t_f) = y_f$
$h(0) = h_0$	$h(t_f) = h_0$
$E(0) = E_0$	$E(t_f) \geq E_f$
$\gamma(0) = \gamma_0$	$\gamma(t_f)$ free
$\chi(0) = \chi_0$	$\chi(t_f)$ free

Controls

$$n_v \ , \ n_h$$

Control Constraints

$$\sqrt{n^2_v + n^2_h} \leq 30$$

$$\sqrt{n^2_v + n^2_h} \leq \frac{qS}{W} C_{Lmax}(M)$$

DRAG, THRUST & WEIGHT MODEL

Drag Model

$$D = qS \left[C_{D_0}(M,h) + C_{Di}(M) \left(\frac{W}{qS}\right)^{1.8} n^{1.8} \right] \qquad \text{where} \qquad n = \sqrt{n^2_v + n^2_h}$$

Thrust Model
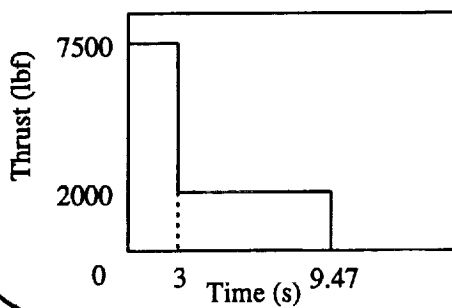
Weight Model
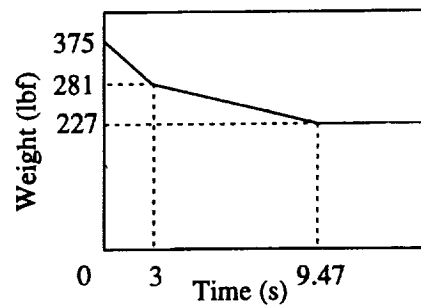
INDIRECT METHOD

Optimal control problem

$$\min \quad \Phi(x(t_f), t_f)$$

$$\dot{x} = f(x, u, t)$$

$$x(t_0) = x_0$$

$$\psi(x(t_f), t_f) = 0$$

if solution does exist then it satisfies ⇨

Boundary value problem

$$\dot{x} = f(x, u, t)$$

$$\dot{\lambda} = -\frac{\partial H}{\partial x} \quad \text{where} \quad H \doteq \lambda^T f$$

$$\min_{u \in \Omega} \quad H(x, \lambda, u, t)$$

$$x(t_0) = x_0$$

$$\psi(x(t_f), t_f) = 0$$

$$\lambda(t_f) = \frac{\partial \Phi}{\partial x(t_f)} + v^T \frac{\partial \Psi}{\partial x(t_f)}$$

$$H(t_f) = \frac{\partial \Phi}{\partial t_f} + v^T \frac{\partial \Psi}{\partial t_f}$$

5 1 1

OPTIMAL TRAJECTORY IN 3-D
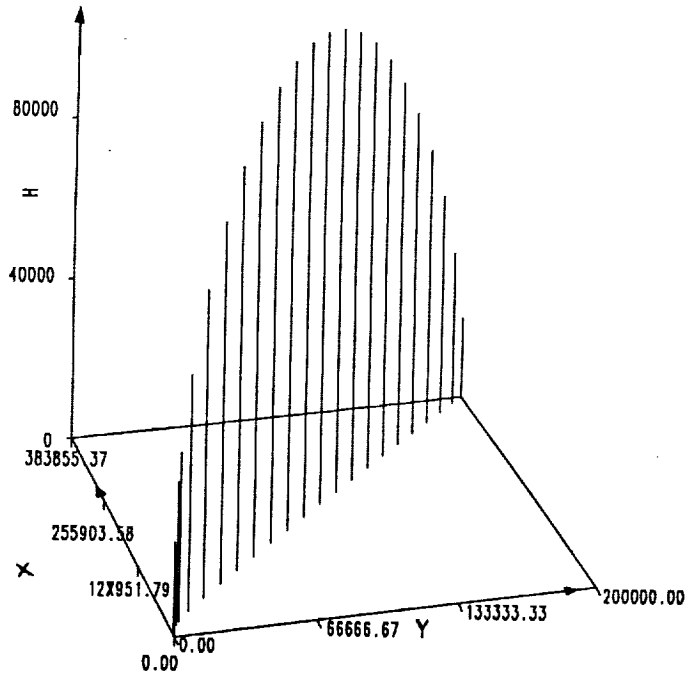
VERTICAL LOAD-FACTOR TIME HISTORY

512
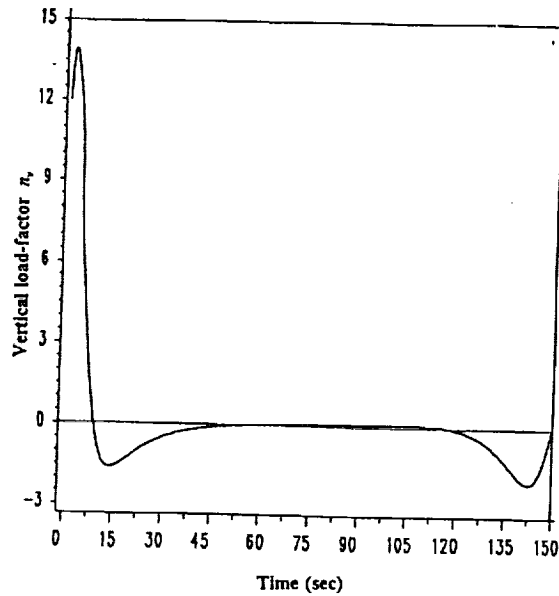
HORIZONTAL LOAD-FACTOR TIME HISTORY
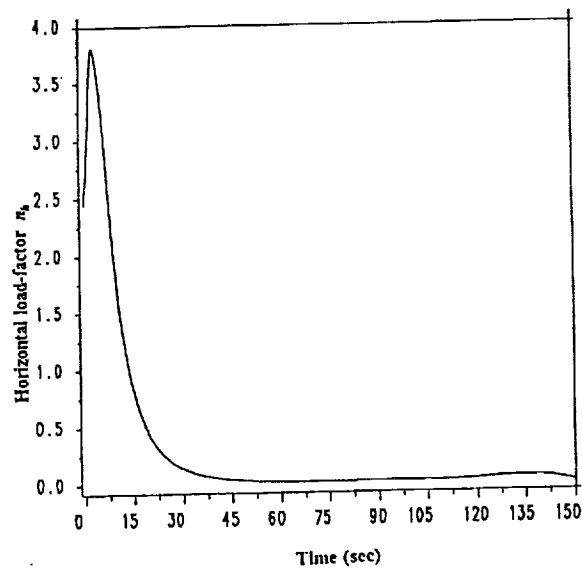
ATTAINABILITY SET FOR FINAL TIME 150s
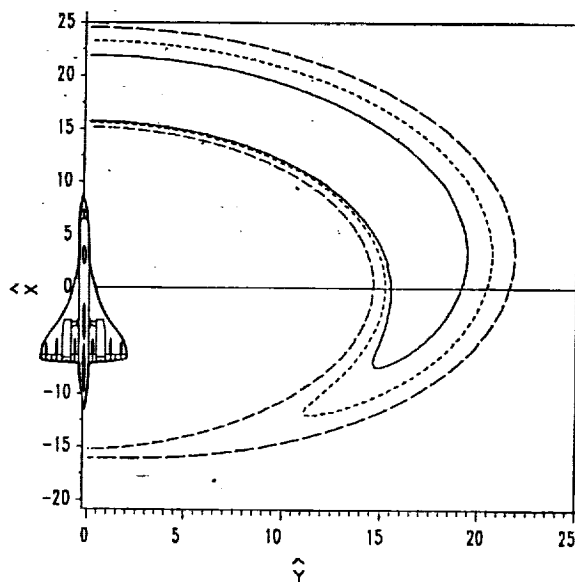
ACCESSORY MINIMUM PROBLEM

$$\min \; \tfrac{1}{2} x(t_f)^T S_f x(t_f) \; + \; \tfrac{1}{2} \int_{t_0}^{t_f} [x^T, u^T] \begin{bmatrix} A_{11} & A_{12} \\ A_{21} & A_{22} \end{bmatrix} \begin{bmatrix} x \\ u \end{bmatrix} \; dt$$

$$\dot{x} = Fx + Gu$$

$x\,(t_0) = x_0$	t_0 fixed	$A^T = A$	$A_{22} > 0$
$Bx(t_f) - b = 0$	t_f fixed	$S_f^T = S_f$	$S_f \geq 0$

ACCESSORY MINIMUM PROBLEM (contd.)

$$u = A_{22}^{-1} [(-A_{21} - G^T(S - RQ^{-1}R^T))x - G^TRQ^{-1}b]$$

$$\dot{S} = D_{21} + D_{22}S - SD_{11} - SD_{12}S \qquad ; \qquad S(t_f) = S_f$$

$$\dot{R} = D_{22}R - SD_{12}R \qquad ; \qquad R(t_f) = B^T$$

$$\dot{Q} = -R^TD_{12}R \qquad ; \qquad Q(t_f) = 0$$

⇩

!! new !!

$$H \doteq S - RQ^{-1}R^T$$
$$\dot{H} = D_{21} + D_{22}H - HD_{11} - HD_{12}H$$

THREE PHASE GUIDANCE

- BOOST PHASE GUIDANCE

- MIDCOURSE GUIDANCE

- TERMINAL GUIDANCE

IDENTIFY REFERENCE SOLUTION
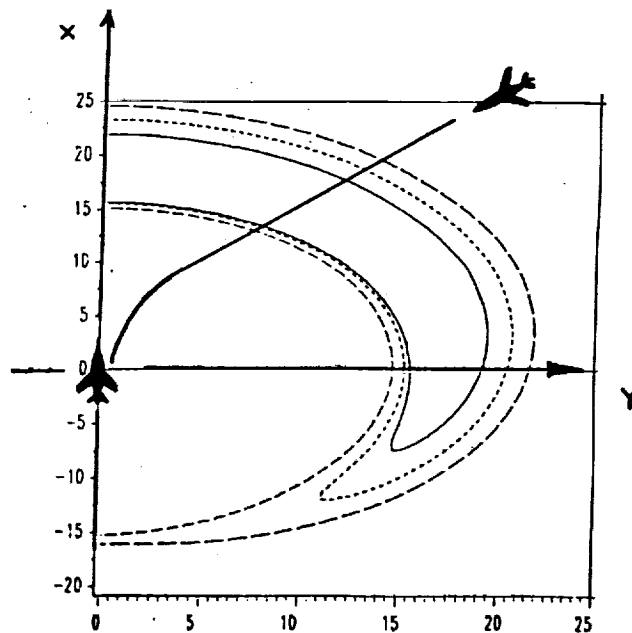
MIDCOURSE GUIDANCE (NEIGHBORING SOLUTION)

Closed-loop Control

$$u_{CL}(t) = u_{ref}(t) + \delta u(t)$$

$$\delta u(t) = G_1(t)\, \delta X(t) + G_2(t)\, d\psi(t)$$

Change in final time (cost)

$$dt_f = K_1(t)\, \delta X(t) + K_2(t)\, d\psi(t)$$

5 1 6
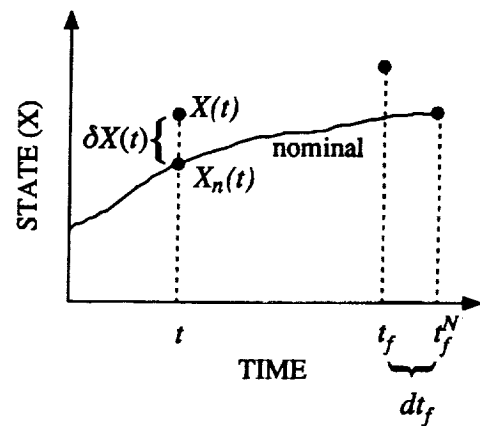
MIDCOURSE GUIDANCE (TRANSVERSAL COMPARISON)

$$t_f' = t_f - t = t_f^N - t_I$$

$$t - t_I = \frac{K_1(t_I)[X(t) - X_N(t_I)] + K_2(t_I)[d\psi(t)]}{[1 + K_1(t_I)\dot{X}^N(t_I)]}$$

Closed-loop Control

$$u(t) = u^N(t_I) + G_1(t_I)[X(t) - X^N(t_I)]$$
$$+ [G_1(t_I)\dot{X}^N(t_I) + \dot{u}^N(t_I)][t - t_I] + G_2(t_I)d\psi(t)$$
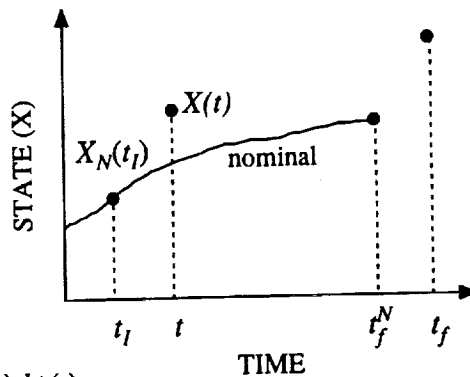
MIDCOURSE GUIDANCE (HORIZONTAL PROJECTION) AGGRESSIVE TARGET

517
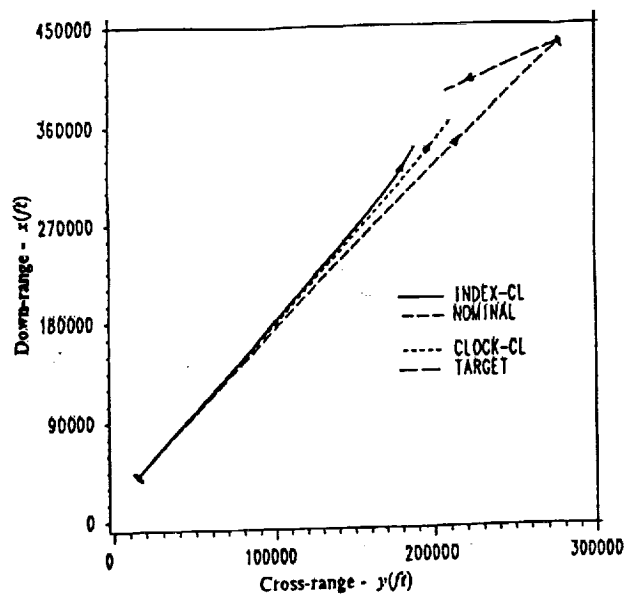
MIDCOURSE GUIDANCE (HORIZONTAL PROJECTION)
RUN-AWAY TARGET
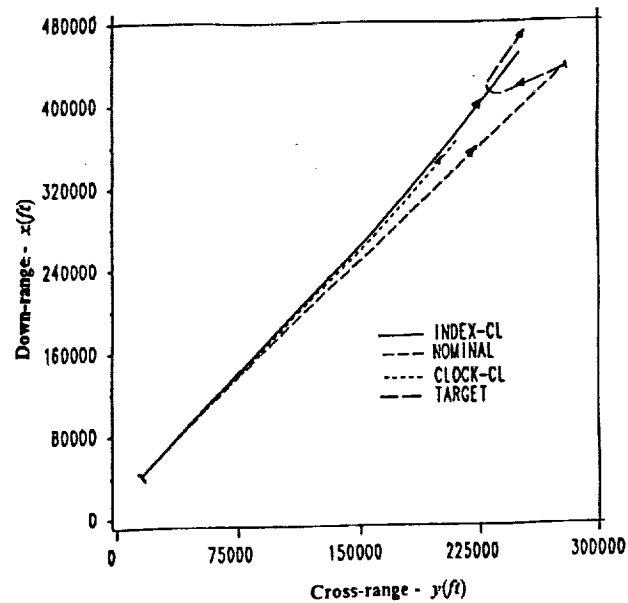
MIDCOURSE GUIDANCE (ALTITUDE)
RUN-AWAY TARGET

518
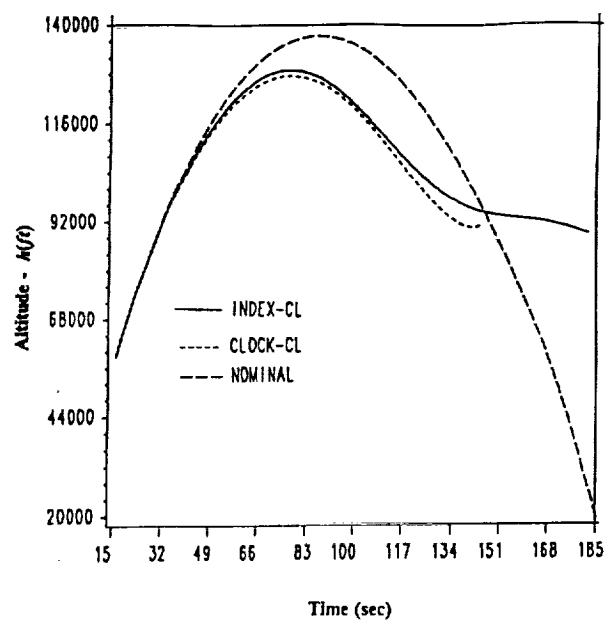
NEAR-OPTIMAL GUIDANCE (HORIZONTAL PROJECTION) SHINAR'S TARGET
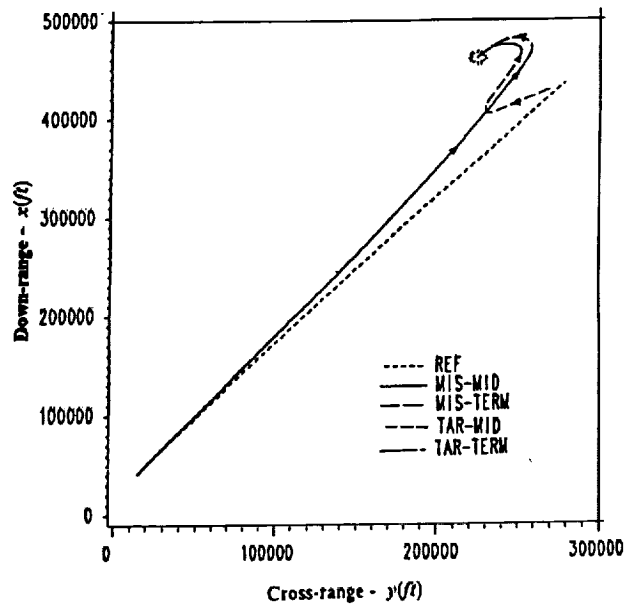
HALF-PN GUIDANCE (HORIZONTAL PROJECTION) SHINAR'S TARGET
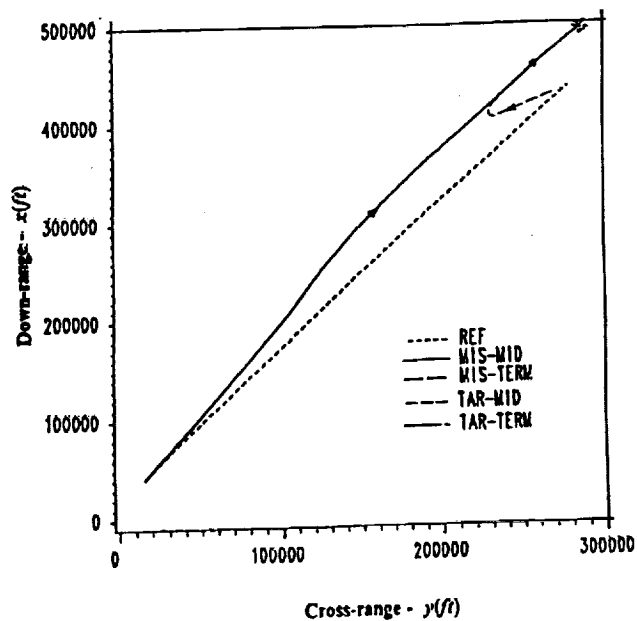
SALIENT CONTRIBUTIONS

- Identified attainable sets via intricate homotopy procedures.

- Checked sufficiency conditions for weak local optimality.
  - Derived a new matrix differential equation for conjugate point testing.

- Developed an efficient method of optimal gain evaluation.

- Developed a composite midcourse guidance strategy (half-pn) which saves on-board storage.

Constrained Minimization of Smooth Functions Using A Genetic Algorithm

Lynda J. Foernsler, SCB
Dr. Daniel D. Moerder, SCB
Dr. Bandu N. Pamadi, Vigyan

Purpose

- Discuss the use of a simple genetic algorithm for constrained minimization of differentiable functions with differentiable constraints.

- Assess the performance of this approach

Outline

- Genetic Algorithms (GA)

- Problem Formulation for GA

- Numerical Experiment

- Comparison to Penalty Function Approach

- Conclusions

- Future Work

Genetic Algorithms

- Nonderivative, nondescent, random search procedures for unconstrained functional minimization

- Algorithmic structure is based on notions from biology with "survival of the fittest" search heuristic

- Operations performed on successive generations of a population represented by binary coded strings (DNA-analog)

GA Operations

M = population
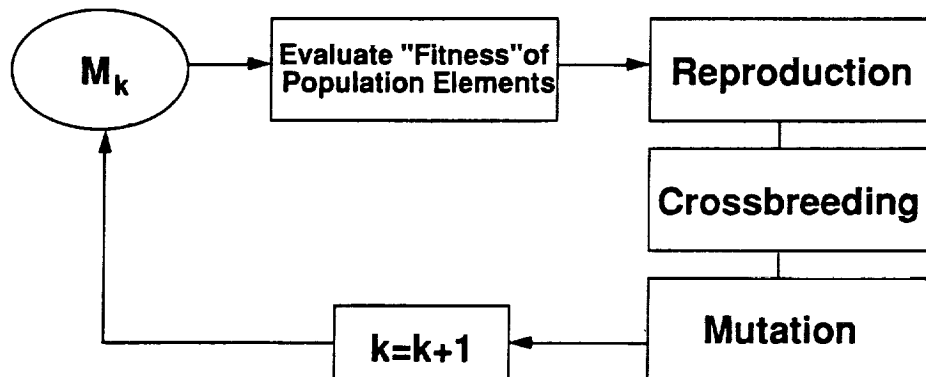
• Initial population, M_0, is randomly generated

Constrained Function Minimization

$$x^* = \min_{x \in \Re^n} c(x)$$

subject to

$$f_i(x^*) = 0 \quad i \in E$$

$$f_j(x^*) \geq 0 \quad j \in I$$

Kuhn-Tucker (KT) Conditions

$$\left.\frac{\partial \mathcal{L}(x, \lambda)}{\partial x}\right|_{x^*, \lambda^*} = 0$$

$$\lambda_j^* \geq 0 \qquad j \in I$$

$$\lambda_k^* f_k(x^*) = 0 \qquad k \in E \cup I$$

$$f_k = 0 \qquad k \in E$$

$$f_k \geq 0 \qquad k \in I$$

where

$$\mathcal{L}(x, \lambda) = c(x) - \sum_{k \in E \cup I} \lambda_k^* f_k(x^*)$$

Problem Formulation For GA

- Convert the solution of the necessary conditions for a constrained minimum into an unconstrained function minimization

- Solve the resulting unconstrained minimization problem

$$x^* = \arg \min_{x \varepsilon X} g(x)$$

where X is the user-specified bounded volume over which the GA takes place.

Unconstrained Minimization Problem Formulation

$$g(x, \lambda^*) = \sum_{i=1}^{n} |\mathcal{L}_{x_i}(x, \lambda^*)| + \sum_{j \in E} |f_j(x)| + \sum_{k \in I} |\min\{0, f_k(x)\}|$$

- estimate λ^* by setting $\mathcal{L}_x(x, \lambda) = 0$

$$\nu(x^*) = (f_x^T(x^*))^+ c_x(x^*)$$

$$\nu_i(x) = \begin{cases} \nu_i(x) & f_i = 0 & i \in E \\ |\nu_i(x)| & f_i < 0 & i \in I \\ 0 & f_i > 0 & i \in I \end{cases}$$

- KT conditions are satisfied by solving the nonsmooth equation

$$g(x, \nu(x)) = 0$$

Genetic Algorithm Function Minimization

$$x^* = \arg \min_{x \in \mathcal{X}} g(x, \nu(x))$$

where $\mathcal{X}$ is the user-specified bounded volume over which the genetic search takes place:

$$\mathcal{X} = \{x : (x_i)_{min} \le x_i \le (x_i)_{max}; \ i = 1, \ldots, n\}$$

GA Function Minimization

$$x^* = \arg\min_{x \in \mathcal{X}} g(x, \nu(x))$$

where $\mathcal{X}$ is the user-specified bounded volume over which the genetic search takes place:

$$\mathcal{X} = \{x : (x_i)_{min} \le x_i \le (x_i)_{max}; \; i = 1, \ldots, n\}$$

Numerical Experiment (1)

- Mission: Determine control settings for an energy-state approximation of minimum-fuel ascent to orbit for the Langley Accelerator

- Control variables:

$$\bar{x} = \begin{cases} \alpha, & \text{angle of attack (deg)} \\ h, & \text{altitude (ft)} \\ \delta_E, & \text{elevon deflection (deg)} \\ \delta_T, & \text{thrust vector angle (deg)} \\ \eta, & \text{fuel equivalence ratio} \end{cases}$$

5 2 6

- Cost:

$$c(x) = -\frac{dE}{dm}$$

subject to

   - vertical acceleration balance equality constraint

   - pitch moment balance equality constraint

   - dynamic pressure inequality constraint

- Monte Carlo Experiment

   - 100 GA runs

   - 600 generations/run

- Used final generation $\bar{x}$ values from GA runs as initial guesses for Newton-Raphson (NR) method

Distribution of KT Error
for Aerospace Plane Model

one outlier at 4.47
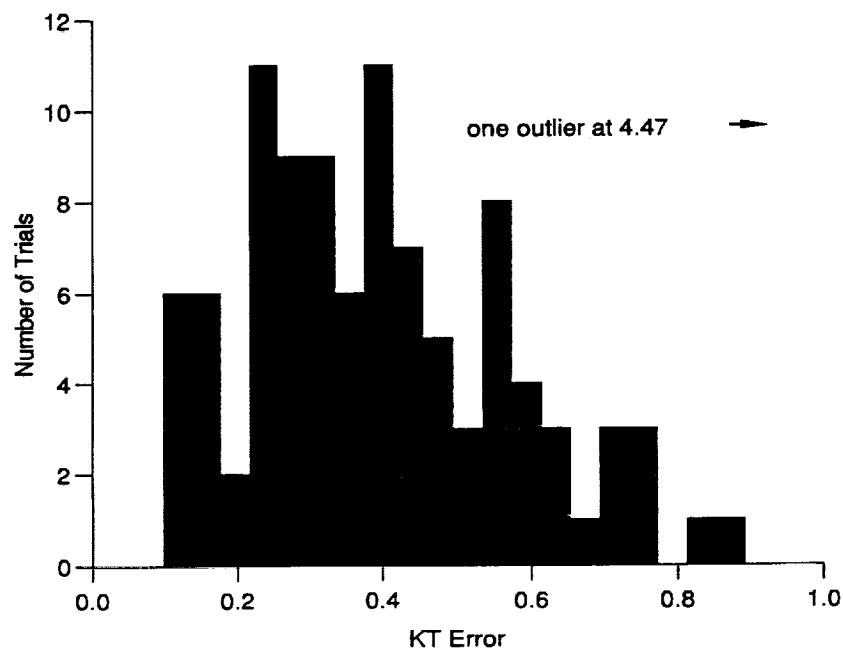
Distribution of Control Settings
for KT Approach

elevon deflection (deg)

thrust vector angle (deg)

thrust vector angle (deg)

optimum

optimum

optimum

alpha (deg)

alpha (deg)

elevon deflection (deg)

KT Error Thresholds

total number of runs meeting KT error threshold
minimum number of generations
median number of generations

Number of Generations to KT Error Thresholds
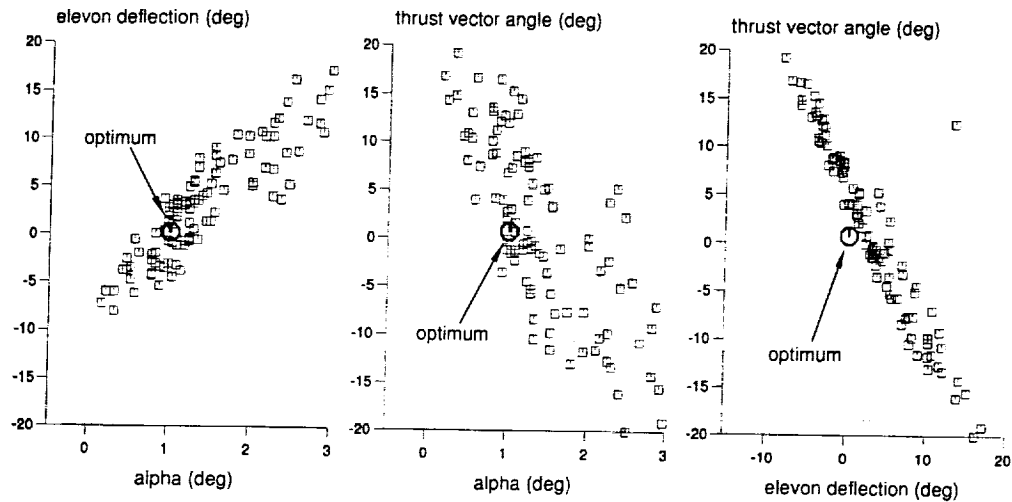
Number of Runs Satisfying KT Error Thresholds
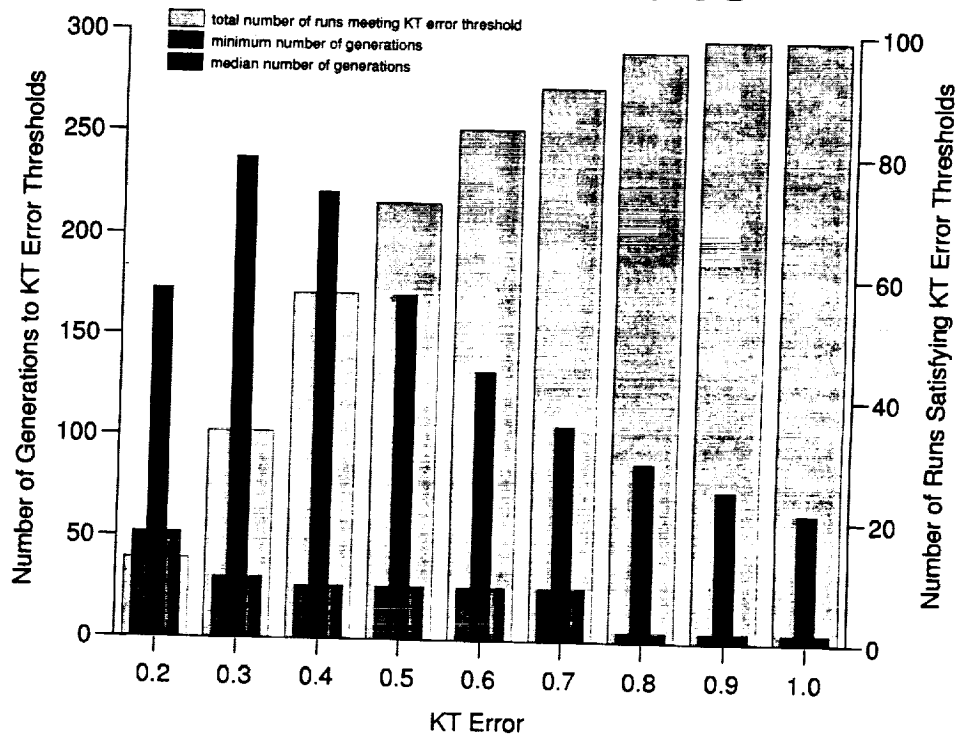
KT Error

KT Formulation Results

- 82 of the NR runs converged

- 99/100 runs converged within a KT
  error threshold of .9

- Fewer number of generations/run would
  have sufficed

Comparison To Penalty Approach

- Penalty function form:

$$x^*_{pen} = \arg \min_{x \in \mathcal{X}} \left\{ c(x) + \sum_{k \in \mathcal{E} \cup \mathcal{I}} p(x, f_k(x)) \right\}$$

- Monte Carlo Experiments

  - 100 GA runs

  - 600 generations/run

  - various penalty-weighting combinations

- Initial Guesses for NR method

Best Penalty Function Histogram
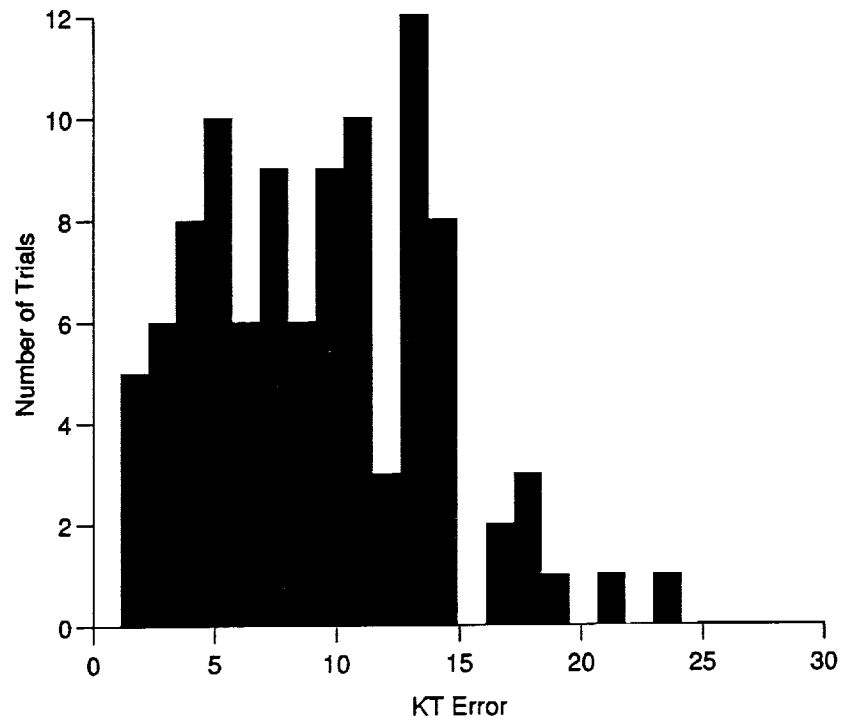
Best Penalty Function Scatter Plots
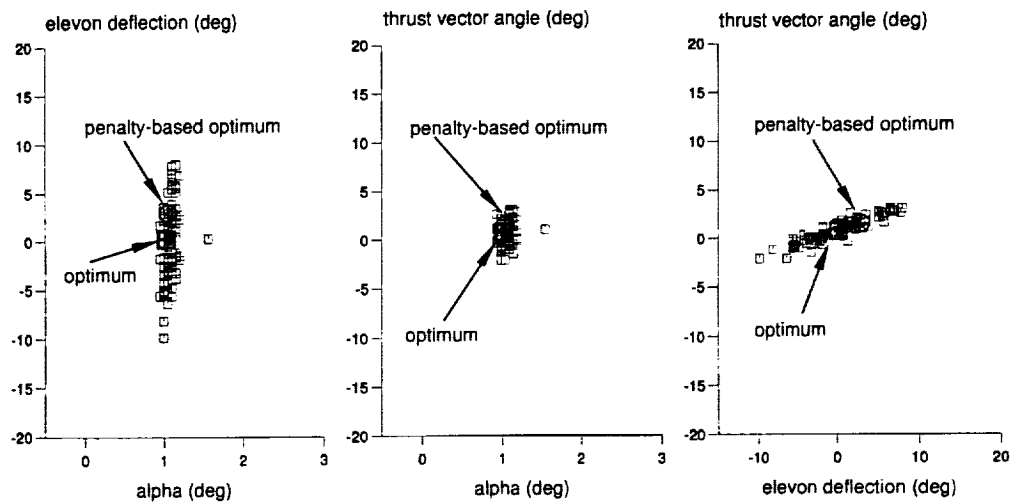
Penalty Function Results

- 74 of the NR runs converged for the best case

- fine tuning of penalty-weighting combinations is problem specific

Conclusions (1)

- Discussed search characteristics and algorithmic operations of a simple genetic algorithm.

- Discussed method of adapting the KT conditions for a constrained minimization problem to formulate an unconstrained minimization function to be used by a genetic algorithm.

- Demonstrated KT method formulation numerically on an aerospace plane model of the Langley Accelerator

Conclusions (2)

- For this study, KT approach provides reliable initial guesses for Newton-Raphson method

- Unlike the penalty approach, the KT approach

  - minimizes a function whose optimum value is known a priori

  - provides a measure of the constrained stationarity of the solution

Future Work

- Exploit stopping criterion of KT approach

- Extend GA algorithm to include non-smooth cost function and non-smooth constraints

ADVANCED INFORMATION PROCESSING SYSTEM

AIPS

Felix L. Pitts

NASA Langley Research Center

Workshop on Guidance, Navigation, Controls, and
Dynamics for Atmospheric Flight

March 19, 1993

OUTLINE

- Background and Description
- Program Accomplishments
- Current Focus
- Applications
- Technology Transfer
- FY92 Accomplishments
- Funding

NEED FOR VALIDATED ARCHITECTURES

A need exists for architectural concepts that have been <u>validated</u> such that their physical implementation in hardware and software will meet the <u>quantitative missions requirements</u> such as

cost

weight, volume, power

throughput performance

transport lag

mission success probability

mission availability

•

and also be responsive to <u>qualitative requirements</u> such as

expandability

graceful degradation

technology insertion

damage tolerance

•

AIPS IS

* A COMPUTER SYSTEMS PHILOSOPHY
* A SET OF VALIDATED HARDWARE BUILDING BLOCKS
* A SET OF VALIDATED SERVICES AS EMBODIED IN SYSTEM SOFTWARE

TO ACHIEVE

* DISTRIBUTED FAULT-TOLERANT SYSTEM ARCHITECTURES FOR A BROAD RANGE OF APPLICATIONS

534

GOAL

- **PROVIDE THE KNOWLEDGEBASE** which will allow achievement of **VALIDATED** fault-tolerant distributed computer system architectures, suitable for a broad range of applications, having failure probability requirements to 10E-9 at 10 hours

AIPS PROGRAM HISTORY

Phase I 1983-1984

Requirements Survey	(NASA, JPL, Airframers)
Technical Survey	(NASA, DoD, Industry, Academe)
Architecture Synthesis	(CSDL monitored by Peer Review Group)

Phase II 1986-1986

Functional & Detailed Design of Building Blocks
Reliability & Performance Modeling of Building Blocks

Phase III 1986-1993

Emphasize Validation to Verify AIPS Attributes
Focus on: Engineering Model for ALS
High Throughput/Highly Reliable Army Fault Tolerant Architecture

AIPS BUILDING BLOCKS: HARDWARE

FAULT TOLERANT PROCESSORS — Simplex, Duplex, Triplex, Quadruplex, FTPP

INTERCONNECTION NETWORKS — MESH, BRAIDED MESH, REDUNDANT BUSES, RING, REDUNDANT RINGS

INTERFACES

[IOS] Input/Output Interfaces

[ICIS] Inter-Computer Interface Sequencer
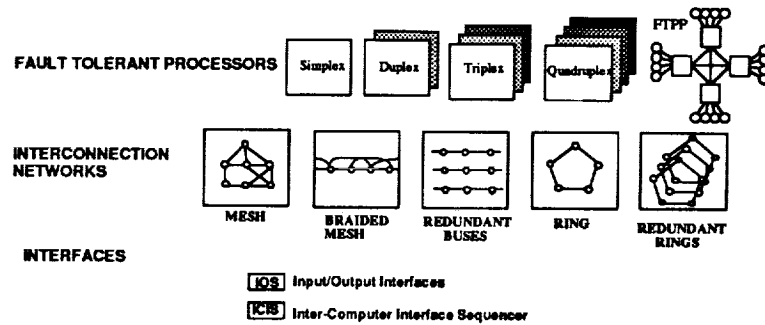
AIPS BUILDING BLOCKS: SOFTWARE

LOCAL SYSTEM SERVICES:
  Ada Real Time Operating System
  FTP Redundancy Management
  Local Time Management

INPUT/OUTPUT (I/O) SYSTEM SERVICES:
  I/O User Communications
  I/O Redundancy Management

INTERCOMPUTER (IC) SYSTEM SERVICES:
  Ada Distributed Synchronous
  Communications
  IC User Communications
  IC Redundancy Management

SYSTEM MANAGER:
  Function Allocation & Migration
  System Redundancy Management
  Global Time Management

AIPS EXAMPLE CONFIGURATION

FTPP   I/O NETWORKS

TRIPLEX FTP

I/O NETWORKS

DUPLEX FTP

INTER- COMPUTER NETWORK

TRIPLEX FTP

I/O NETWORKS

SIMPLEX PROCESSOR

FEATURES: APPROPRIATE FUNCTION RELIABILITY
LOW FAULT TOLERANCE OVERHEAD
GROWTH CAPABILITY
Ada OPERATING SYSTEM
REDUNDANCY TRANSPARENT TO USER
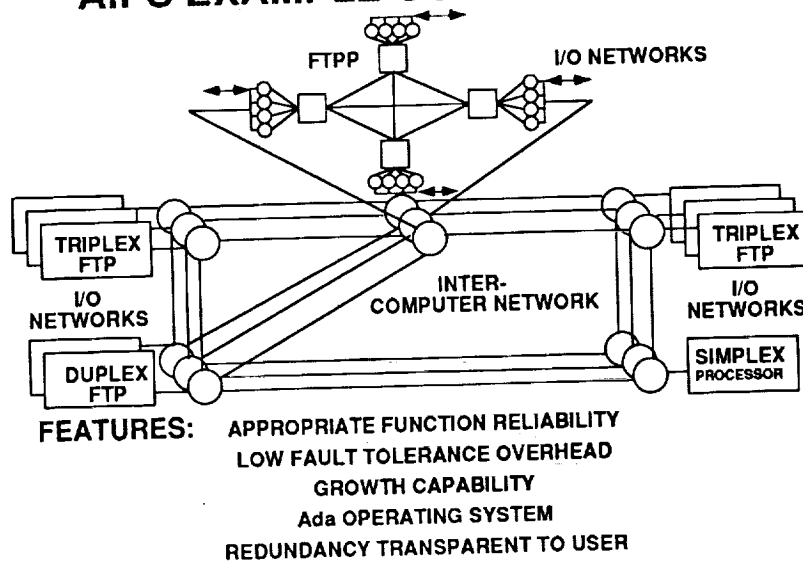
DISTRIBUTED SYSTEM CONTROL

- AIPS Operates in an overall framework that can be characterized as a limited form of a fully distributed multicomputer system

  - Each GPC has the Resources to Operate Autonomously

  - Each GPC in Steady State is Assigned to a Unique Set Of Functions

  - Local Operating System in Each GPC Provides Local System Services of Initialization, Task Scheduling and Dispatching, I/O Service, and Local Redundancy Management

SYSTEM COMPLEXITY MANAGEMENT

- AIPS Architecture Designed to Hide System Complexity from Applications

- System Services, as Implemented in Hardware and Software, Manage Distributed Resources and Hardware Redundancy

- Distributed Computation Deliberately Separated from Fault Tolerance

- Exact Consensus Between Processes and Exact Consensus Between Bus Transmissions Simplifies Fault Detection and Isolation

- Hardware Mechanization of Fault Detection and Isolation Simplifies Redundancy Management

- AIPS Architecture Designed to Facilitate Congruent Data Flow in Redundant Processors and Between GPCs

PROGRAM ACCOMPLISHMENTS

- Produced an Analytical and Empirical Knowledgebase for Validation of AIPS Architecture and Building Blocks

- Architecture Design Rules and Guidelines
- Analytical Reliability, Performance, Availability and Cost Models
- Empirical Reliability and Performance Data

- Developed and Demonstrated Distributed Engineering Model

- Validatability, Distributed computation, Mixed redundancy, Fault tolerance (processors, networks, interfaces), Damage tolerance, Graceful degradation, Expandability, Transparency of fault tolerance to applications programmer, Low fault tolerance overhead, Performed Laboratory Test and Evaluation

- Demonstrated AIPS Building Blocks
  - 3 Triplex FTPs and 1 Simplex Processor
  - Triplex Intercomputer Network, Mesh I/O network
  - System Services Software (>100,000 Lines of Ada Code)

ACCOMPLISHMENTS (cont'd)

- COMPLETED MULTIPATH REDUNDANT AVIONICS SUITE MPRAS 2102 AIPS TASK FOR ADVANCED LAUNCH SYSTEM
  - AIPS ENGINEERING MODEL OPERATIONAL
  - GOVT/INDUSTRY REVIEW 10/89
  - 4 REPORTS PUBLISHED SEPT. 1991
  - SUBMITTED AIPS/ALS UPDATE FOR ALS/ADP REVISION D PLAN
  - PRODUCED A 20 MINUTE AIPS VIDEO

- COMPLETED "HANDS OFF" CASE / AIPS DEMO FOR CODE GENERATION AND EXECUTION OF ATOPS 737 AUTOPILOT

- PUBLISHED NUMEROUS REPORTS AND PAPERS
  - ATTACHED 29 REPORT BIBLIOGRAPHY

AIPS CURRENT FOCUS

- **Base Program**
  - **AG&C/CASE/AIPS Demo (NASA Funding)**
  - **Develop Authenticated Protocols for Inter-System Communication (SDI Funding)**

- **Army Fault Tolerant Architecture (Army Funding)**
  - **Fault Tolerant Parallel Processor Development**
  - **Common-Mode Fault Study**
  - **Optical Fault Tolerant Interconnection Networks**

- **Terminate CSDL/ AIPS Contract**
  - **Contract Completed 9/30/92; All Tasks Completed by 9/30/93**

AG&C/CASE/AIPS DEMONSTRATION

FLIGHT SIMULATION

AIPS

Code
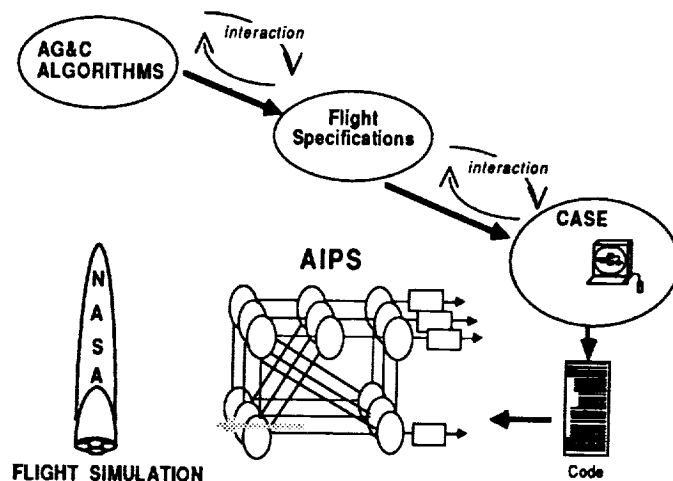
Army Fault-Tolerant Architecture (AFTA)

- Helicopter Night-Time Nap of the Earth Operations
- Integrated Flight Controls and Image Processing
- High Throughput/Ultra Reliable Fault-Tolerant Parallel Processor (FTPP)

FTPP

- Supports Variety of Redundancy Management Modes
- Allows Mixed Redundancy
- Heterogenous Processing
- Can Trade Throughput for Reliability in Real-Time
- Byzantine Resilient Operation is Inherent to the Architecture
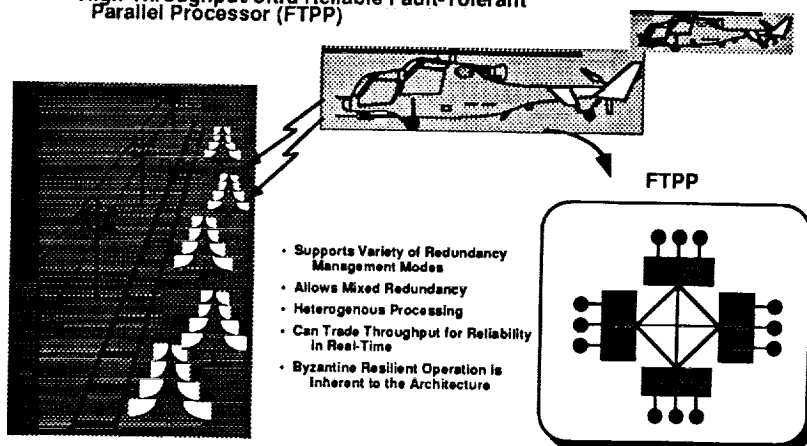
Fault Tolerant Parallel Processor

High Performance Voting Architecture. Fully connected fiber optic network between processor groups.

Tolerates arbitrary failure modes (Asymmetrical faults).

Uses many Processing Elements (PE's) for high throughput.

Uses redundant PE's for high reliability. Data Voting Architecture

Can trade Throughput for reliability or availability in real-time.

Uses Non Development Items (NDI) PEs, backplanes, power supplies, I/O for improved suportability

Allows mixed redundancy and heterogeneous processing resources.

AFTA Characteristics

❏ Processing Elements

Support for 3 to 40 PE's per Cluster (FTPP).

680x0's, 80960's, MIPS R3000's, TMS320x0, etc...

PE's in the AFTA are grouped into redundant Virtual groups to achieve fault tolerance.

Virtual groups can be simplex, triplex, quadraplex, or quintuplex.

Static Virtual group configuration determined by reliability and availability analysis.

❏ Network Elements provides:

100 Mbit/sec fiber optic interchannel links.

Standard bus interface to Processing Elements.
(Mil-STD-344, Pi-bus, Futurebus, Safebus, etc...)

Time management primitives for architecture (synchronization).

Reliable data Communication services (Voting, Source congruency).

Maps physical processing sites into virtual groups (VIDs).

AFTA Characteristics cont'd

□ Software main components:

XD Ada-based operating system with real-time extensions.
Preemptive rate group scheduler.

Periodic task communication between Virtual groups. Pre-defined communication services.

Performance Penalties from Redundancy Management and Operating systems functions minimal. (10% - 15%)

POSIX Real-time operating system interface standard (IEEE P1003).
LynxOS Version being evaluated now (FY93).

□ I/O controllers

Fault-Tolerant Data bus (Auth. protocols)

1553, JIAWG FT data bus, VME, etc....

AFTA Physical Architecture

AFTA Virtual Architecture

Quadruplex	Simplex	Triplex with I/O	Quadruplex	Triplex with I/O	Triplex	Simplex	Simplex with I/O	Simplex

Network Element Virtual Bus
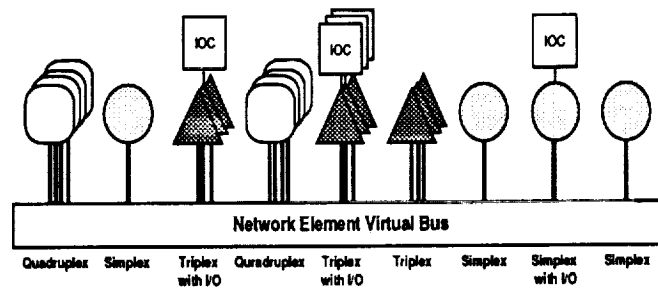
AFTA Program Status

Three phase program:

I. Conceptual study - Completed in FY91. Analytical modeling, feasibility studies, requirements acquisition, preliminary design.

II. Detailed design. FY92. Design hardware and software architectures.

III. Detail design and evaluation. FY93. Complete HW and SW architecture designs, begin performance evaluation activities of AFTA in relation to TF/TA application.

Major deliverables:

1. All procured hardware and software.

2. All software and hardware documentation

3. Final written comprehensive report.

4. CECOM will receive an AFTA for evaluation in FY95. (Loan from CSDL)

SELECTED APPLICATIONS OF AIPS

- **Unmanned Undersea Vehicle (UUV) - DARPA**

  - Under DARPA sponsorship, Draper designed and built two UUVs, each of which is autonomously controlled by a triplex FTP based on the AIPS architecture

  - Both vehicles have undergone extensive sea trials without any significant FTP related problems

- **Seawolf SSN-21 Ship Control System - US Navy (NavSea)**

  - A quadruply redundant FTP, based on the AIPS architecture, has been militarized and packaged in SEM-E modules to perform the "swim-by-wire" functions onboard the SSN-21 Seawolf nuclear attack submarine

SELECTED APPLICATIONS OF AIPS (Cont.)

- SDIO Battle Management / C3   - US Army (SDC)

  - A quadruply redundant FTP with attached processors (FTP/AP) was delivered to Army Strategic Defense Command for evaluation as a Battle Management Computer

- Army Fault Tolerant Architecture - US Army CECOM

  - An AIPS-based Army Fault Tolerant Architecture (AFTA) has been developed for the helicopter terrain avoidance/terrain following flight control application for the Army Communications and Electronics Command

SELECTED APPLICATIONS OF AIPS (Cont.)

- GPALS Engagement Planner - US Army (SDC)
  - The brassboard of Army Fault Tolerant Architecture is being fabricated for the GPALS (Global Protection Against Limited Strikes) Engagement Planner application for the Army SDC

- MAGLEV Command and Control Computer - DOT
  - A fault-tolerant, fail-safe computer architecture using the AIPS-developed design for validation methodology was developed for the US Maglev (magnetically levitated) transportation system under DOT sponsorship

AIPS TECHNOLOGY TRANSFER

- Tech Aerojet FTP
  - Under a contract from NASA MSFC Tech Aerojet selected the AIPS Fault Tolerant Processor architecture for the engine control application on the National Launch System
  - Under a subcontract from Tech Aerojet , Draper helped them define an Intel i960-based triplex FTP's fault tolerance related hardware for fabrication by Tech Aerojet

- Martin Marietta Astronautics FTPP
  - A study was done by Draper to apply AIPS technology to Martin's aerospace needs under a contract from MM
  - Following the study, a quadruply redundant Fault Tolerant Parallel Processor (FTPP) was delivered to Martin for use in various IR&D and sponsored projects

5 4 5

FY92 ACCOMPLISHMENTS

During FY92, three major tasks were active:

• Army Fault Tolerant Architecture (AFTA)

- Detailed design of the AFTA hardware and software was completed.

- The Network Element, the only hardware development item in AFTA, which is responsible for fault tolerance related functions and message passing between processors, was designed and breadboarded.

- Breadboard of the NE was fabricated and tested; the Scoreboard, one of the two NE cards which was designed using VHDL, worked the first time without any errors.

- A 2-volume report documenting the conceptual study phase of AFTA was published.

FY92 ACCOMPLISHMENTS

• Authenticated Protocols-Based Inter-Computer and I/O Networks

- A detailed design of the Transport Layer, patterned after the Open Systems Interconnect (OSI) model, of the inter-computer communication software was completed.

- Key generation, signaturing and message authentication algorithms were produced, coded and optimized in C and Assembly languages.

• Hosting of AGN&C Algorithms using CASE on AIPS/FTPP

- Martin Marietta Astronautics, Denver produced Matlab scripts of advanced guidance algorithms designed at NASA LaRC.

- Draper Lab, in collaboration with Martin, chose a subset of Matlab scripts for interfacing with the CASE tool.

- Modification of the CASE tool to accept Matlab scripts was started.

FUNDING

	FY92 and Prior	FY93	TOTAL
• SDIO/ALS	$3.23 M		
• SDIO/BMC3	$1.22 M	$150 k (Authen Proto)	
• ARMY/AVRADA	<u>$2.30 M</u> $6.75 M		
• NASA RC FUNDING	$1.45 M	$50 k (AG&C Demo) $403 k (CASE)	
• TOTALS	$8.2 M	$830 k	$9.03 M

Automated Code Generation

for GN&C Applications

Carrie K. Walker
Information Systems Division
carrie@csab.larc.nasa.gov
804-864-1704

March 19, 1993

Outline

- ASTER

- Applications

- GN&C Demonstration

- Matlab Integration

- Summary

Automatic Programming Subsystem

- Accepts functional specifications

- Generates source code (Ada, C)

- Generates documentation

- System architecture:
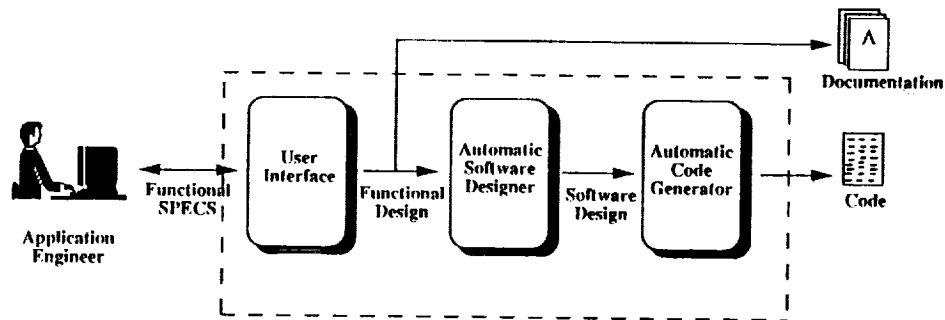
Automatic Testing System

550

Data Flow Diagram

CSDL CASE
Computer-Aided Software Engineering
Automated Programming
Subsystem
Sponsored By
The NASA Langley Research Center
Developed By
The Charles Stark Draper Laboratory, Inc.

Major Menu Options	
Load Project File	Choose Transform
Save Project Transform	Clear Transform
Describe Transform	Change Size
Edit Superior	List Inferiors
Generate Document	Generate Code
Execute	Check Consistency
Show Free Nodes	Delete Transform
Hierarchy	Edit Signal Types
Suggestion Box	

Create component transform from the user defined transform: First Order Lag

---

Data Flow Diagram

CSDL CASE
Computer-Aided Software Engineering
Automated Programming
Subsystem
Sponsored By
The NASA Langley Research Center
Developed By
The Charles Stark Draper Laboratory, Inc.

Major Menu Options	
Load Project File	Choose Transform
Save Project Transform	Clear Transform
Describe Transform	Change Size
Edit Superior	List Inferiors
Generate Document	Generate Code
Execute	Check Consistency
Show Free Nodes	Delete Transform
Hierarchy	Edit Signal Types
Suggestion Box	

L: Create Terminal   M: Create Transform   R: Screen To Point

Benefits of the ASTER Approach

- Reduce development time

- Reduce errors

- Code and documentation always agree

- Decouple engineering design and software design

- Reuse engineering designs

- Facilitate and reduce testing

- Provide an open, extensible architecture

Software Development Techniques

Conventional Approach

Engineering Design — Software Design — Code

ASTER

Engineering Design — Documentation & Code
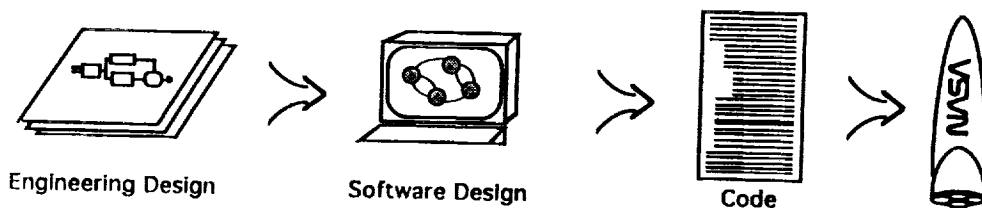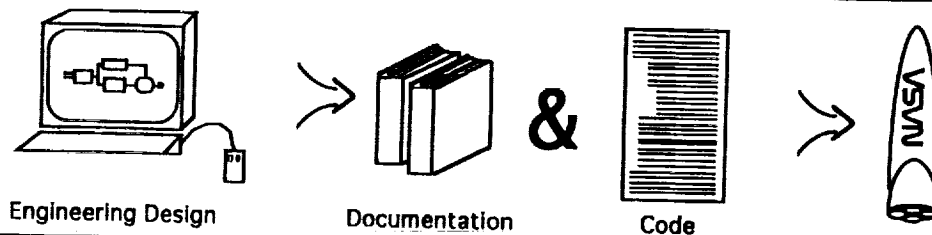
Demonstrations

- **Large Gap Magnetic Suspension System (LGMSS)**
  - C code running on an embedded Silicon Graphics workstation
  - Passed CDR and delivered to customer

- **B737 Autoland Flight Control System**
  - Ada running on Draper's Fault Tolerant Processor in conjunction with a FORTRAN simulator on a MicroVAX
  - Ada running on Draper's Fault Tolerant Parallel Processor in conjunction with a FORTRAN simulator on a MicroVAX
  - C currently being hosted on Draper's Transputer FTP

- **Guidance and Control System for a Mars Lander**
  - Ada running on VAX in conjunction with FORTRAN simulator

- **Inertial Fiber Optic Gyro/Standy Attitude Indicator (IFOG/SAI)**
  - Ada running on a MIPS R3000

- **Inertial Reference System for Deep Submergence Rescue Vehicle**
  - Model upgrade from FORTRAN to Ada on a VAX

Demonstrations (cont.)

- **Space Station Control System**
  - Applied for documentation purposes
  - Ada and C code generated

- **General Dynamics Electromechanical Actuator**
  - Ada and C code generated

- **Martin Marietta Load Relief Filter**
  - Ada code running on SUN and VAX
  - C code running on a variety of workstations, PC's & computers

- **Boeing B737 Yaw Damping System**
  - Ada running on Draper FTP for N-version software experiment
  - C running on Draper FTPP

- **Autonomous Exploration Vehicle**
  - Ada running on SUN workstation
  - C running on SUN workstation

- **Shuttle's Ascent First Stage Guidance**
  - Implemented by Martin Marietta under IR&D
  - Ada executed and tested on two environments, including a shuttle software simulator

Objectives of AGN&C Demonstration

- Demonstrate the cooperative use of complimentary technologies within the Flight Systems Directorate

- Drive the development of ASTER

    - Vector/Matrix/Quaternion Operations
    - MATLAB™ Integration
    - Libraries

Systems Architecture Branch

Approach

- Develop Finite Element Numerical Optimal Control (FENOC) Algorithm

- Develop flight software specification (MATLAB)

- Input specification into ASTER

- Generate Ada code

- Test code

- Execute on target architecture

Systems Architecture Branch

Integrated AGN&C Demonstration
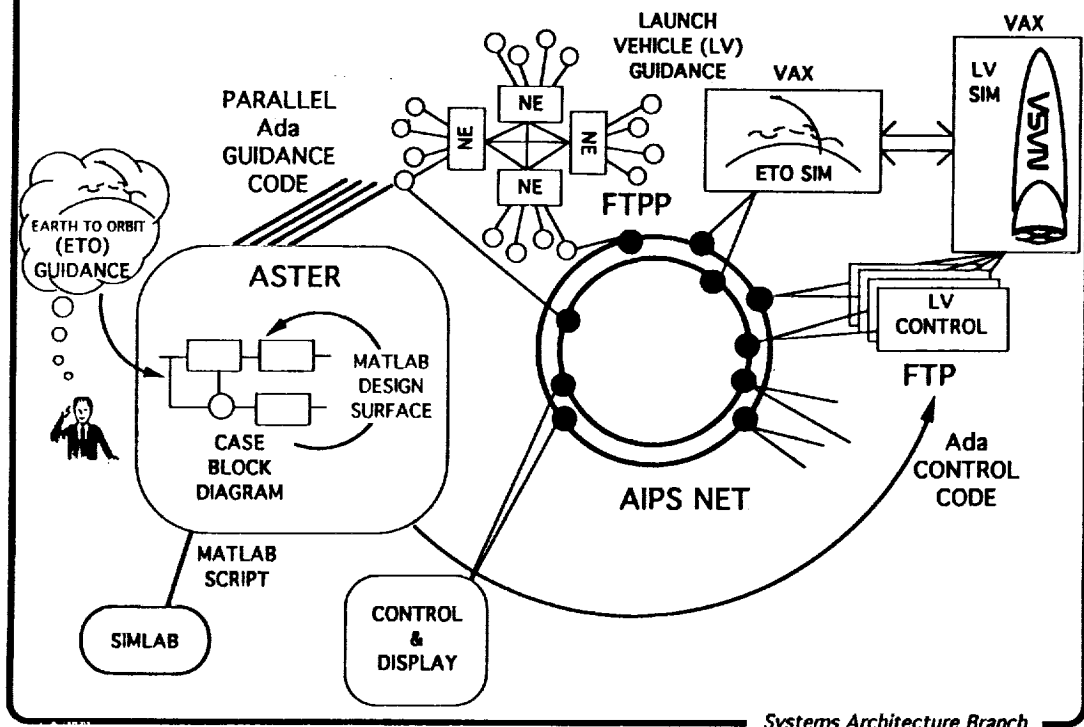
Summary

- ASTER is a production quality code generation system.

- ASTER has been demonstrated on a variety of "real" applications.

- The AGN&C demonstration has identified ASTER enhancements.

- The AGN&C demonstration will illustrate the cooperative use of complimentary technologies within the Flight Systems Directorate.

Related Publications

1. McDowell, M. E.: *Computer-Aided Software Engineering at The Charles Stark Draper Laboratory*. CSDL-P-2802, The Charles Stark Draper Laboratory, Inc., April 1988.

2. Walker, Carrie K.; and Turkovich, John J.: Computer-Aided Software Engineering: An Approach to Real-Time Software Development. *AIAA Computers in Aerospace 7*, October, 1989.

3. Turkovich, John J.: Automated Code Generation for Application Engineers. *AIAA/IEEE 9th Digital Avionics Systems Conference*, October, 1990.

4. *AIS CASE User's Guide*. The Charles Stark Draper Laboratory, Inc., Cambridge, MA, June, 1991.

5. Walker, Carrie K.; Turkovich, John J.; and Masato, T.: Applications of an Automated Programming System. *AIAA Computers in Aerospace 8*, October, 1991.

6. Jones, Denise R..; Walker, Carrie K.; and Turkovich, John J.: Automated Real-Time Software Development. *Technology 2002 Conference*, December, 1992.

7. *ASTER User's Guide*. The Charles Stark Draper Laboratory, Inc., Cambridge, MA, March 1993.

557

PANEL DISCUSSION

Howard Stone

I would like to have the panelists come up and be seated. While the panelists are coming let me add that we [the GNCTC] are going to be compiling the presentation material of this workshop into a NASA CP [conference publication]. We plan to send a copy of that CP to all who are interested in receiving a copy. If you are interested in receiving that publication please sign in on one of the yellow pads out in the lobby. We will also attempt to pick up the essence of this panel discussion for inclusion in the CP. To do that we are going to be videotaping the panel discussion. We do invite audience participation and to facilitate the taping process, we need to have everybody use a mike. If you have a question or a comment, wait for a mike to get to you. These mikes that are on the table are portable and we can move them around the room. Also, we have invited people to feel free to come up and use the view graph projectors in this discussion. If you do that, then please put on the lapel mike.

Let me now introduce our panel. Your participation is very much appreciated and the GNCTC at LaRC would like to thank each one of you [the panelists] for coming and being willing to participate.

From right to left, our first panelist is Tom Richardson from Boeing Defense and Space Group in Seattle. Tom has worked in control systems synthesis, aircraft stability and control, aeroelastic modeling, and flight control architecture designs. He has been responsible for developing techniques to achieve highly reliable digital flight control systems using advanced architectures, fault detection, and redundancy management techniques. He is currently manager of Boeing's Defense and Space Group flight control technology organization and is the program manager for the Air Force Strategic Flight Management Contract and the NASA fly-by-wire contract that Felix [Pitts] discussed earlier. Tom we appreciate you coming.

Our second panelist is Clint Browning from Honeywell in Clearwater, Florida. He is the Head of the Engineering Department for Space Shuttle Flight Control and is technical director for Honeywell on the ACRV program. Clint started out at Vought years ago. He worked Scout, something near and dear to us at Langley. He worked on the Small Spinning Upper Stage and the shuttle program. Also he worked with Boeing on a roll channel automatic landing system for the Boeing 727. Clint, we do appreciate you coming very much.

Next to Clint is John Hodgkinson from McDonnell Douglas Aerospace West in Long Beach. He is currently manager of Stability, Control, and Flying Qualities Technology and is responsible for methods development and research in these areas. Formerly he managed the YF-23 flight controls development at Northrop and was Director of Engineering Technology at Eidetics. He has served on two AGARD G&C working groups and the AIAA Atmospheric Flight Mechanics and GN&C technical committees. He teaches flying qualities at Northrop University where he is an Adjunct professor and is a lecturer in flight mechanics and stability and control at UCLA. Thank you, for taking time to be here.

Our final panel member is Dave Leggett from Wright Laboratory. Dave graduated from Georgia Tech and the Air Force Institute of Technology where he got his masters degree. He has been with the Flying Qualities Group for the last twelve years and has worked on aircraft projects such as the NT-33, F15/STOL, the Maneuver Technology Demonstrator, and the Variable In-Flight Stability Test Aircraft (VISTA). He now has the awesome task of directing the research supporting the revision of MIL-STD-1797. Dave, we thank you for being here and I will go ahead and turn the session over to you now.

Dave Leggett

The subject of this discussion is the direction of guidance navigation, and controls research needed to insure US competitiveness and leadership in aerospace technologies. I want to start off by saying one of our biggest challenges right now is the fact that research budgets are shrinking for absolutely everyone. One of the good things I heard in the last two days is talk of exchanging information and trying to set up channels of communication between different organizations. I think that we need to do more than just talk to one another. We are going to have to find ways to pool our resources and do joint research programs together -- that is the only way we are going to be able to put enough resources, enough mass on a given problem to solve it. I am going to focus just on the Air Force, I will let some of my compatriots here talk about the civil side of things.

I will start with where I think flying qualities needs some research. One of the areas we are particularly interested in is the development of standardized evaluation maneuvers for evaluating aircraft handling qualities. The lack of a standard set of evaluation maneuvers is part of the reason we have some discrepancies in our different flying qualities criteria and analysis methods. Another reason to develop standardized evaluation maneuvers was discovered by the review team during the digital flight control system development process review. We found out that, in a lot of cases, handling qualities testing has basically just become parameter ID. They just go up and do parameter ID and compare the numbers to the numbers in the spec. That was never the intent of the spec. We still intended aircraft handling qualities evaluation to be done using closed-loop evaluation by getting the pilot to really do some tasks and evaluate the aircraft for those tasks. In order to put that into the spec., as it seems now we are going to have to, we have to have some means of defining a standard task that we can use to compare all aircraft against. I think in the next few years we are going to be interested in developing a list of possible tasks to use as well as guidance to the SPO's on how to do those tasks.

Another area we are going to be interested in is in resolving a lot of the discrepancies in the current handling qualities criteria and the handling qualities analysis methods. Although there is a good bit of agreement among a many of the different criteria and analysis methods, there are also areas where they disagree. It seems like everybody has their favorite criteria and that leads to a lot of people mistrusting the other criteria. I think we need to resolve that to make a better flying qualities spec.

I will now move on to some other areas the Air Force is interested in. We seem to be expanding the envelopes of flight here and the Air Force is interested in what kind of capabilities those things will give them. A hot buzz word in recent years has been agility. I think Air Force interest in agility per se is kind of waning, there are a lot of reasons for that; however, I am not going to go into those now. There is one area of agility I think the Air Force is still very much interested in and that is high angle of attack. I think we are interested in trying to find out what we can do in that regime, how we can do it, and how we can control the airplane at high angles of attack. Another region of the expanding envelope that the Air Force is interested in is high-speed flight, or hypersonic flight. That is an area where if you just look at the budget, the Air Force budget for doing hypersonic research is shrinking. I do not think that is because of lack of interest, it is largely because of priorities and the overall budget is shrinking. That is an area where we have little data and we would like to know what can we do with that capability, how do we get it [the capability], and how do we control it.

Another area of interest which is not really a flight regime, is new control responses and unconventional flight modes. Examples are a direct speed control or a speed hold mode, or a level turn mode. When the AFTI F-16 or the F-16 CCV flew, we tried a bunch of unconventional modes and in the case of several of them, the pilots could not find any particular need for them at the time. Interestingly, some F-117 pilots came to talk to us about a year ago

560

and mentioned that they'd love to be able to turn without banking the airplane so I think there are opportunities for these kind of unconventional modes opening up.

Another area that the Air Force is definitely interested in is application of multi-input/multi-output control design methods and other modern control methods. All those things go over my head so I do not think I will say too much about them other than to say that I know there are several offices in the Air Force that are definitely interested in pursuing these kinds of design methods.

The Air Force is definitely interested in areas of research to reduce pilot workload. I saw a lot of things here in the last two days that were looking in that area, in particular the use of displays to help reduce the pilots workload. One of the things the Air Force is working on getting some standardization in display symbols and in display formats -- we have been sponsoring some research in that area. I think it would help pilots as they transition from one aircraft to another if they did not have to learn a whole new HUD whenever they go to another airplane.

Another area in displays that I think might be being overlooked is display dynamics. If we are going to use displays to help the pilots do the tasks, if he is going to be depending on that display to do the job, then display dynamics are going to play a role in here too. In a lot of cases the displays depend on data from sensors which is filtered and that filter introduces dynamics that we are going to have to deal with.

Another item in the area of reducing pilot workload is automatic flight modes. More and more of what the airplane is going to be doing in the future is going to be done automatically. We have had automatic landing systems for some time, though the Air Force is even interested in making them autonomous automatic landing systems. There are other automatic systems that we are putting the aircraft now too: automatic collision avoidance systems and so forth. Those help in one way, to reduce pilot workload, but I think we also need to give some consideration on what is going to be the pilot's role in a system where he is less and less the pilot and more and more the system manager. I think there is some things we are going to have to deal with and explore about how the pilot is going to interface with this system.

Another thing the Air Force is interested in is new means and methods of generating forces and moments on the aircraft. Forebody vortex control is an example of that sort of thing. That is an area I do not know too much about but I do know that there are offices in the Air Force, particularly at Wright Lab, that are interested in that area.

Finally, I think virtually every combat aircraft from here on out is going to pay a lot of attention to stealth technology, and for the guidance and control folks that is a new challenge. A lot of these Stealth airframes have some really nasty aerodynamic characteristics and yet at the same time they put restrictions on control surfaces: how many, the shape, the size, and how much we can move them. We are being asked to do a lot more with a lot less with these configurations and I think that is another challenge for us.

At this point I think I will pass it onto you, John. I did manage to fill up the five minutes, did I not?

John Hodgkinson

We have a saying where I work that when, for example, we have to give a briefing to the vice president or something, it is time to raise the level of ambiguity of the discussion. That is really what I'm going to do for a minute. I'm going to talk on very ambiguous terms.

In asking what the direction of our research should be, we need to recognize that we [the aerospace industry] are a small analogue of what is happening in this country. So when you look at what comprises U.S. competitiveness and what is U.S. leadership, you think of certain categories of things that we do well, and things that we do not do so well. The things that we do not do so well are the things that are the focus of total quality management, such as cranking out products that are good, reliable, and on schedule, and talking to the customer. That kind of scheduled activity is one thing that, we are working very hard to do better and to compete better on.

In the other category of things that we well, and which we do not focus sufficiently on, because it is much more difficult to quantify, is the unforeseen breakthrough research that proceeds from a brilliant insight. This nation, by virtue of its culture, has repeatedly provided such breakthroughs over the decades. It is a very difficult thing to manage, and it is a very difficult thing to fund. I know we all draw research schedules. We have five year plans - and I think my friends at St. Louis have ten year plans - for the research we are doing. It is very hard to imagine any breakthroughs happening on a ten year plan of that kind. However, *the inspirational, exploratory research is something that we -- and I believe this very, very strongly -- should preserve in this country.*

Okay, I will be a little more specific now. Some statistics that I heard from Bruce Holmes really interested me. I think one of the statistics was that 83.7 percent of general aviation accidents had human factors as a contributing factor. I think that was the number -- I wrote it down. It is certainly a very dramatic one [number]. We look very carefully at the statistics where I work and in the last thirty years of commercial airplane operations fifty percent of airplane losses have involved primary flight crew error. So it seems to me that we are doing an excellent job of making sure that control systems, structures, and so on are safe. Fail-safe technology twenty-or-so years ago dramatically improved airplane safety. I know we have experts here (at LaRC) on redundancy management and work is needed to insure that kind of thing continues. It seems to me, however, that the *human element is the one area where the real pay dirt is in assuring further advances.* Furthermore, we are fortunate in this country, because of a culture that encourages people to speak out, to have the kind of excellent test pilots (like Lee Person and Rob Rivers here, for example) that could be a big help to us. *We [the engineers] need to listen to those folks and they need to continue talking to us.*

Bottom line -- NASA and its partners need to focus on the inspirational kinds of research, the exploratory kinds of research and, furthermore, I'd suggest that we look at the human interfaces being an area that has a lot of payoff.

Clint Browning

I really appreciate the opportunity to be here and participate with these distinguished panel members and to be a part of this workshop program. I have just a few charts that I want to use to emphasize the area that we are addressing. I want to present the priority needs from the space standpoint and our overall aerospace industry [see figure 1]. I realize this list is not complete and the more people I talk to within my company, the longer the list kept getting. I'm sure you can think of others that are important to competitiveness and leadership. The first item, which Howard mentioned this in his opening talk, is *the need to reduce launch operations cost.* About this there can be no doubt. There is also, I think a great pay back to be gained from applying the so-called dual use technologies, the kinds of things that the military and commercial industry are working, that have application in space and sometimes vice versa. Shortening the design cycle is a critical area that we are all facing; the kind of time lines that we have been dealing with in the past, from both the schedule and resources standpoint just cannot continue. We have got to find ways to do it faster, quicker, and cheaper as well as with increased quality. [We need to]

increase fault tolerance. [We need to] promote cooperative government /industry joint research -- which we heard some of these gentlemen already refer to.

```
┌─────────────────────────────────────────────────────────┐
│                                                          │
│        Space Vehicle GN&C - Priority Needs               │
│        ─────────────────────────────────────             │
│                                                          │
│   • Reduce Launch Operations Cost                        │
│   • Apply "Dual Use" Commercial and Military Technologies│
│   • Shorten the Design Cycle                             │
│   • Increase the Fault Tolerence                         │
│   • Promote Cooperative Govt/Industry Joint Research     │
│                                                          │
└─────────────────────────────────────────────────────────┘
```

Figure 1 - First Vu-Graph of Clint Browning's Talk

To insure U. S. aerospace leadership, we must focus technology dollars to reduce the operations cost. One area that I believe would have benefits is to reduce the complexity. Systems like the space shuttle have a tremendous amount of complexity to them. On a system like the shuttle there may be sixty or eighty subcontractors providing LRU'S for the avionics. Reducing the actual number of LRU'S, the interfaces, simplifying the certification/verification/check out process, and improving the system reliability and availability all potentially reduce launch delays due to system complexity. We need to make avionics cheaper. Using commercial off the shelf components may be the way to go. One area for space that has to be a concern is the radiation effects, the SEU tolerance has to be considered. I might also mention an area that needs, I believe to be seriously looked at, is the S level parts requirement that has been imposed upon space avionics components. With today's total quality management, perhaps the thing that needs to be done is to certify a process and a company that is producing very high quality parts and not impose the S level in all areas. Also lets get vehicle health management out of the talking stage, integrate and demonstrate the use of sensors, the diagnostics, and the processing for self monitoring. The expected pay-off is to reduce the army that required to launch these vehicles. These areas are not new to anyone but I think they are certainly areas that need dollars and technology research applied.

In navigation a lot of work is being done in integrated autonomous navigation, particularly related to the GPS inertial navigation systems and particularly in the terminal phases of the missions where the differential mode has added high accuracy to the GPS approach. There is a lot of work going on in avionics companies with highly fault tolerant INS/GPS combinations. I think these are areas that navigation can help in terms of competitiveness, and even the part that the GPS might play in the attitude determination.

I might just break right here and say, personally, and I think from our standpoint at Honeywell, I'm very impressed with the research this is going on throughout this organization from what we heard over the last two days and we are relating to some of what has been said here.

In automation, the cockpit displays and hand controls is an important area. Do you go on up to the six degree of freedom hand controls? This whole area of the role of the crew versus automation has been mentioned, and that applies not only to the cockpit crew but to the ground crews. What is the role of those that are working on the preparation for the launch? What is the role of those that are on board the vehicle and the impact on autoland and safety. Due to physical deterioration in space, autoland becomes more and more critical the longer people stay in space. It will be more of a consideration for the sixteen day orbiter, moving on up to a twenty eight day orbiter, and perhaps longer for moon and Mars missions. It is generally felt that autoland is an absolute necessity. Advanced guidance concepts are required to expand flight envelopes, and therefore not be so dependent upon the weather, both for launch and return.

A high level of functional integration and fewer boxes has been a focus in the military arena. Flight control, navigation, the processors, air data, radar altimeter, and perhaps terrain following can be combined into a single small avionics box. I think there is a lot of promise there, in terms of reducing the complexity and the number of interfaces to be dealt with. A lot of good work is going on in these areas. We do need a practical application and demonstration in some real life examples.

Reducing the design, test, verification, and integration cycle is very important. Integrated product development using integrated product teams can be cost effective by bringing different disciplines together, cutting down the time for serial functions, and performing parallel functions. I this believe ought to be encouraged and has great potential and we see many companies beginning to adopt this approach. Rapid prototyping, going all the way from the requirements/specifications through the analysis and design and the automatic code generation to the hardware and the integration, testing, and check out, has a tremendous opportunity to offer a competitiveness advantage which ought to all be encouraged. We have seen some indications of a three to five hundred percent productivity increase. What normally might take two hundred dollars as an industry standard to generate a line of ADA code is reduced to the twenty dollar range, which I think ought to continually be explored.

The Tagutchi design of experiments approach should be applied not only to the front end of the development process but as the systems analysis progresses application to the production manufacturing area and tests will reduce the test matrices associated with all the combinations and the parameters that have to be tested. Even application into the wind tunnel testing should reduce the amount of tunnel time required.

The need for increased fault tolerance in some ways flies in the face of the need to reduce complexity. The Space Shuttle quad system is tremendously complex and expensive, yet many of the unmanned launch vehicles have had a single string failure point in which a single failure will ruin the mission. Now we are seeing more and more of the launch vehicle companies begin to look at the increased fault tolerance because the cost of the payloads is becoming prohibitive to lose. There is a balance that must be found. The use of the standard buses and the open architecture's using modular approaches to help make the avionics easier to integrate.

The last direction is to actively promote joint government research where government in many cases does provide some study funds or in the cases of memorandums of understanding where both put up some funds for proof of concept. We had an excellent cooperative arrangement with NASA/Langley on the 737 INS/GPS autoland test. This helps get some things started that if industry or just the government kept them to themselves, it might not flourish. I must say on the other side of that coin though that industry is in business to make money and if this is all that ever happens, there is no pay back and there is no way that we can survive. There has to be some hope of a program or project, a way to sell something and to make some money. Many times companies are penalized for doing this. It might be best, from a business standpoint, to stand back and let somebody invest their money waiting for the proof of the concept and then step in and build something. There is another side of this that we really must watch and be careful because by the time the government gets ready to deploy a system, anybody could come and figure out how to do it and build it. Many companies started out on the INS/GPS research years ago. By the time that it is deployed or certified for flight, there is fifty competitors out there that can build and market the system. How do you help make it attractive for companies to do this kind of research? It is not the subject for a technical audience but you may find some companies are reluctant to engage in this research so I raise it as an issue. Thank you very much.

564

Tom Richardson

First of all, I want to thank you for inviting me. This has been very interesting and illuminating to see the whole of guidance/navigation/control at NASA/Langley and some the Air Force effort. Second of all, I want to thank all of you hard-core attendees for staying around on a Friday afternoon. I looked at panel discussion on the program and I thought, well my goodness, there is going to be about five people out there on Friday afternoon -- so thanks for sticking in. I think it is worthwhile. None of us [on the panel] collaborated on what we were going to say but a lot of the themes are similar and I think the big drivers are the shrinking budgets and also the need to do better. These two factors are somewhat at odds, but I think we (in the research community) have got to do better and can do better. We do that by improving efficiency and by focusing our research.

One of the things I want to hit on in particular is focusing our research. We saw a lot of tremendous papers today and it is good to see all this basic research going on and I think that it ought to continue. When I look at the way aerospace research is defined, I see two basic varieties. There is basic research, which is far term, and applied research, which always has a near term payoff and has some other attributes. It is kind of gray as to where near term and far term is, but some things people at LaRC work with are clearly far term. Often you can't see where the research is going and maybe only twenty five percent of those efforts will be successful. But that basic research should go on -- because of that twenty five percent. I'd like to direct my subsequent comments more to what I would call *applied research*, things that have more of a near term payoff and that are going to be applied to our critical national needs. The application could be military or civilian.

I made a list! I made a list [see figure 2] of some of the big things. I may have missed some things, but I think it is important to develop a list to kind of categorize things. You have to market the research we do to the folks that control the money and I do not see how you can do it without prioritizing things.
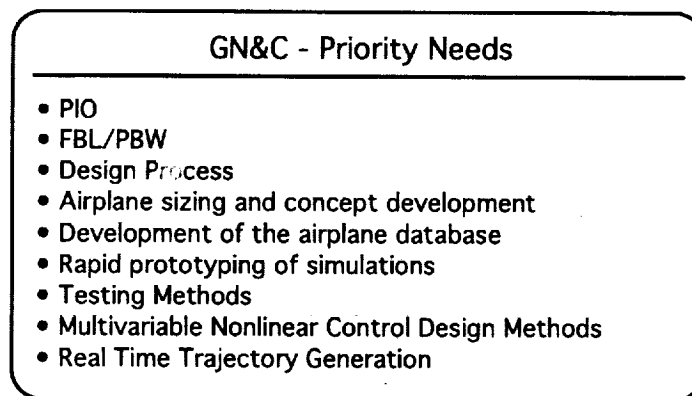
GN&C - Priority Needs

- PIO
- FBL/PBW
- Design Process
- Airplane sizing and concept development
- Development of the airplane database
- Rapid prototyping of simulations
- Testing Methods
- Multivariable Nonlinear Control Design Methods
- Real Time Trajectory Generation

Figure 2 - First Vu-Graph of Tom Richardson's Talk

Pilot Induced Oscillation (PIO)

It keeps coming up. It has been known for years and my feeling is, the reason it is never solved, is that every time it happens the program manager gets by it somehow and says "Well, that is it, we have gotten that out of the way," and hopes that it will never happen again. Of course it does happen again and it is a big thing. *It is probably one of the biggest problems we have in flight controls.* If you want to focus problems in the controls area, pilot induced oscillation is a choice with which I agree wholeheartedly. We need some standards, we need to agree on what the criteria is that we are working towards, and we need to agree on some kind of design process. If

you are talking PIO, then pretty soon you see the need for a better simulation of a pilot and their dynamic response. There is a lot to be done in this area (PIO) but it is a very important area.

Fly by Light/Power by Wire

This term may be a little bit constrictive, as it really should be something like *Advanced Vehicle Management Systems*. That is the title the Air Force gives it. There is a real need for research in this area, which addresses the question of how do you implement these complex systems that are feasible now. The guidance/navigation/control function at NASA Langley is kind of the way we organize thing. In my area, we focus more the algorithm development. However we work very closely with the people that do the actual implementations and are concerned with system architecture aspects. I think that is important, so I look along this Fly by Light/Power by Wire task as addressing the overall system architecture. There are many issues. What is the best way to blend photons and electricity? How do you best do it, how do you get by with the minimum amount of equipment to achieve redundancy or are you just going to go QUAD every time? There is a lot of weight involved and there is a lot of cost. In fact, one of the big drivers now in the work we do is cost.

Design Process

Everybody is mentioning the design process. It is very important that we have a good understanding of what our process is. It is hard to quantify. The reason it is hard [to quantify] is because it is not only events that happen, it is they happen in certain times in the design process and there is a lot of feedback. Getting that [the design process] nailed down where everybody understands what is to happen is crucial. It is got to be done faster. We have to figure out ways to automate things. Things like automatic code generation will help.

Airplane sizing and concept development

There is lots of other issues in airplane sizing and concept development. We have mentioned agility. I do not know if everybody appreciated what they are talking about in the agility study but what is important is more of the up front work when you are sizing the airplane, that you do not just size it to performance. You should size it for maneuvering and I think that is very important. Even if it is done very simplistically, it needs to be done up front. Otherwise they are going to give you an airplane and say, "Okay there it is, go make it fly, ... by the way we want to go zero to ninety degrees bank angle in a quarter of a second." So, there is a lot of work, there is a lot of activity that is done in the early sizing and concept development. *If the flight controls people do not participate in that, or if we are too slow, we get left in the dust.* I have been on a lot of programs where you just got a new program, you are all happy and settling in and they say "Oh, the flight control systems spec. has to be out in three weeks" and you barely have time to type it in that time and they say "Well, put it out and we'll fix it later on when we get a little bit smarter" and you know how that goes.

Development of the Airplane Database

This is very critical and it kind of goes in with airplane concept development [,which is discussed above]. I think we need more analytical methods and less dependence on a wind tunnels. We have some very good panel methods. There is the PANAIR code [at Boeing], there is vortex lattice, there is things can give you a quick answer -- not the best answer maybe, but codes that can give you a quick answer to get you going. We have to think about ways to do database development more quickly and have less reliance on the big ticket items. Wind tunnel testing is still a big ticket item. In a major program like the F22, the relative cost of wind tunnel testing is not so high. Testing is especially a big ticket item when you are in the some R&D program where you have got some limited funds to put some things together. Here, the cost of wind tunnel testing can wipe out your entire program.

Rapid Prototyping

This is important in all areas, and in simulation in particular, There is a lot of comment about the portability of software, and I strongly feel that we ought to be able to run our simulations at our work bench and have that same code run in the real time environment. That give is you two things. One, it gives you speed. You can transition more quickly, you do not have to go back and recheck the thing out in real time, with everybody sitting around watching you. Two, it lets you control the database. You have got the database in your area, and you do not have to worry because you have one [database] and somebody else has another and you can never figure out who has the right one. Code portability puts more of the focus [of database control] on the people doing the work. This is critical. All of the technology for creating this good situation is there. It is a matter of organizing it [the technology] and figuring out how to make it work. There is a lot of near term payoff here. We have done a lot of work in this area at Boeing and it has been very fruitful.

Testing Methods

A paper presented earlier described flutter testing and procedures used to come up on the flutter point, an unstable situation. The techniques described in that presentation can be applied to any test situation, particularly of something that has conditional stability. The investigation of PIO comes to mind. We need more formalized methods. This is an area that can have important near term payoffs if worked.

Multivariable Nonlinear Control Design methods

Many of the methods at technologies in this area are mature. We have some excellent methods. For the near term, they [the methods] need to be packaged. I am excited about an Air Force program , "Design Guidelines for Multivariable Control", that will attempt to systematize this area. They [the Air Force] are going to apply modern methods to some Air Force aircraft.

Real Time Trajectory Generation

We need real fast algorithms that work reliably and automatically. They [the algorithms] need to be robust. They really need to work in real time. The need occurs all the time, particularly in military aircraft. Something happens on a mission and the pilot must replan. This is a big problem. The pilot is faced with a 4D navigation and optimization problem with N constraints. The constraints may be involve survivability, fuel state, and wind conditions. Something to give a quick, not necessarily completely optimal, answer is required. Genetic algorithms may be fruitful here.

Well, that is my list. It is not an exhaustive list, it just the ones I know about. I should mention that the order of the list is not intended to reflect priority. The order is simply the order that these issue occurred to me.

The final chart [figure 3] I have labeled "Panel Action", but the action is really for everyone. Come up with a [prioritized] list of the applied research to be done.

567

```
┌─────────────────────────────────────────────────┐
│                  Panel Action                   │
│  ─────────────────────────────────────────────  │
│                                                 │
│  • Priority list of applied research - problem statement │
│                                                 │
│  • Objective - vision of the future             │
│                                                 │
│  • Plan for validating technology               │
│                                                 │
└─────────────────────────────────────────────────┘
```
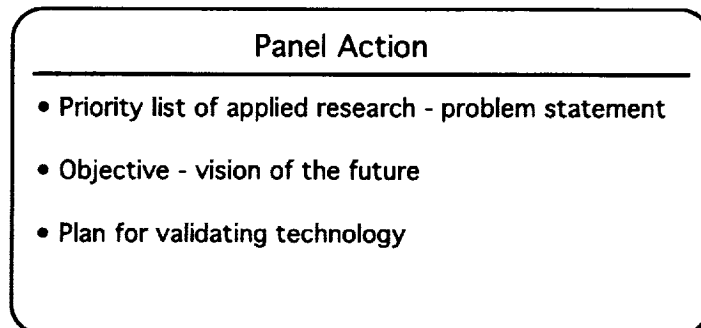
Figure 3 - Second Vu-Graph of Tom Richardson's Talk

Problem Statement

Creating the list must proceed from the problem statement. One should start with the question, "What are the problems we have with aerospace vehicle design?"

Objective - vision of the future

We need to ask: "What is the objective? What are we trying to get out of all this?" We need to have some vision of the future, of what we want to exist 3-5 years from now. We might say, "We want to have the ability to quickly do these simulations and not have to fool around with these ways that we have always done them in the past."

Plan for validating technology.

We need a plan for validating the technology developed. Some of the work required here is in place, some needs help.

That is pretty much all I had. Thank you very much.

[The panel then moved to a question and answer period that was not readily transcribed. However, the videotape of the entire panel discussion, including the question and answer period, is easily followed by someone with a technical background and a copy may be obtained from the LaRC GNCTC. - Editor]

REPORT DOCUMENTATION PAGE

1. AGENCY USE ONLY (Leave blank)	2. REPORT DATE	3. REPORT TYPE AND DATES COVERED
	December 1993	Conference Publication

4. TITLE AND SUBTITLE	5. FUNDING NUMBERS
NASA LaRC Workshop on Guidance, Navigation, Controls, and Dynamics for Atmospheric Flight 1993	WU 505-64-52-01

6. AUTHOR(S)

Carey S. Buttrill (Editor)

7. PERFORMING ORGANIZATION NAME(S) AND ADDRESS(ES)	8. PERFORMING ORGANIZATION REPORT NUMBER
NASA Langley Research Center Hampton, VA 23681-0001	

9. SPONSORING / MONITORING AGENCY NAME(S) AND ADDRESS(ES)	10. SPONSORING / MONITORING AGENCY REPORT NUMBER
National Aeronautics and Space Administration Washington, DC 20546-0001	NASA CP-10127

11. SUPPLEMENTARY NOTES

12a. DISTRIBUTION / AVAILABILITY STATEMENT	12b. DISTRIBUTION CODE
Unclassified - unlimited Subject category - 01	

13. ABSTRACT (Maximum 200 words)

This publication is a collection of materials presented at a NASA workshop on Guidance, Navigation, Controls, and Dynamics (GNC&D) for Atmospheric Flight. The workshop was held at the NASA Langley Research Center on March 18-19, 1993 and was sponsored by the Aircraft Working Group of the Langley Guidance, Navigation, and Controls Technical Committee. The workshop presentations describe the status of current research in the GNC&D area at Langley Research Center over a broad spectrum of research branches. The workshop was organized in 8 sessions: (1) Overviews, (2) General, (3) Controls, (4) Military Aircraft, (5) Dynamics, (6) Guidance, (7) Systems, and (8) a Panel Discussion.

A highlight of the workshop was the panel discussion which addressed the following issue: "Direction of Guidance, Navigation and Controls research to insure U.S. competitiveness and leadership in aerospace technologies." The panel consisted of representatives from Wright Labs, Honeywell, Boeing, and McDonnell Douglas that are respected in the GNC&D field. A transcript of the discussion is included in these proceedings.

14. SUBJECT TERMS	15. NUMBER OF PAGES
Guidance, control, dynamics, and atmospheric flight	579
	16. PRICE CODE
	A25

17. SECURITY CLASSIFICATION OF REPORT	18. SECURITY CLASSIFICATION OF THIS PAGE	19. SECURITY CLASSIFICATION OF ABSTRACT	20. LIMITATION OF ABSTRACT
unclassified	unclassified	unclassified	

C-7.